CARDIO-VASCULAR DYSFUNCTION AND PHYSIOLOGICAL MANIFESTATIONS INDUCED BY ENVIRONMENTAL CONDITIONS

EDITED BY: Marc-Antoine Custaud, Ronan Padraic Murphy, Olga Vinogradova, Claude Gharib, François Guerrero and Michael D. Delp

PUBLISHED IN: Frontiers in Physiology

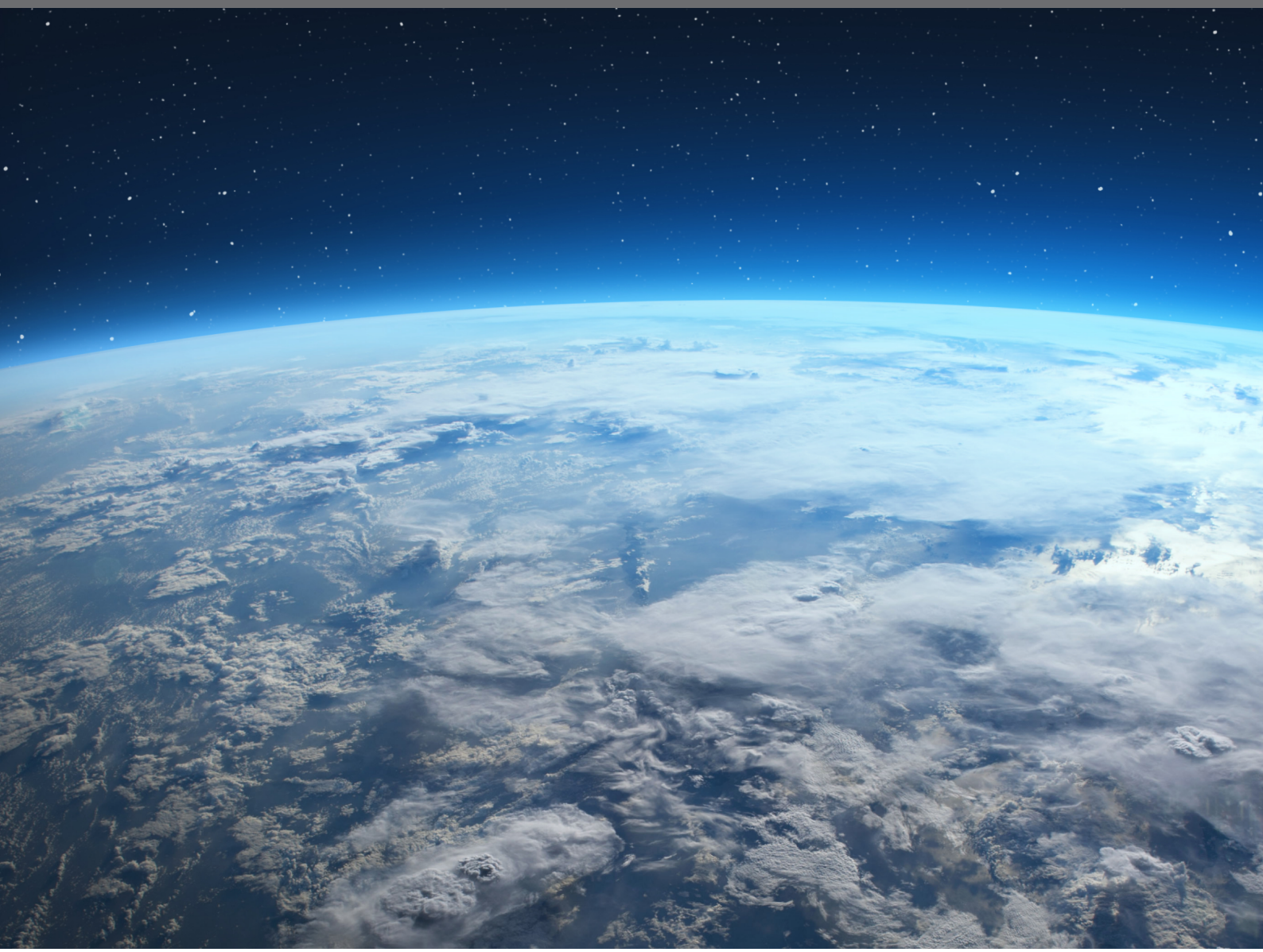

frontiers Research Topics

frontiers

ISSN 1664-8714
ISBN 978-2-88974-808-2
DOI 10.3389/978-2-88974-808-2

About Frontiers

Frontiers is more than just an open-access publisher of scholarly articles: it is a pioneering approach to the world of academia, radically improving the way scholarly research is managed. The grand vision of Frontiers is a world where all people have an equal opportunity to seek, share and generate knowledge. Frontiers provides immediate and permanent online open access to all its publications, but this alone is not enough to realize our grand goals.

Frontiers Journal Series

The Frontiers Journal Series is a multi-tier and interdisciplinary set of open-access, online journals, promising a paradigm shift from the current review, selection and dissemination processes in academic publishing. All Frontiers journals are driven by researchers for researchers; therefore, they constitute a service to the scholarly community. At the same time, the Frontiers Journal Series operates on a revolutionary invention, the tiered publishing system, initially addressing specific communities of scholars, and gradually climbing up to broader public understanding, thus serving the interests of the lay society, too.

Dedication to Quality

Each Frontiers article is a landmark of the highest quality, thanks to genuinely collaborative interactions between authors and review editors, who include some of the world's best academicians. Research must be certified by peers before entering a stream of knowledge that may eventually reach the public - and shape society; therefore, Frontiers only applies the most rigorous and unbiased reviews.
Frontiers revolutionizes research publishing by freely delivering the most outstanding research, evaluated with no bias from both the academic and social point of view. By applying the most advanced information technologies, Frontiers is catapulting scholarly publishing into a new generation.

What are Frontiers Research Topics?

Frontiers Research Topics are very popular trademarks of the Frontiers Journals Series: they are collections of at least ten articles, all centered on a particular subject. With their unique mix of varied contributions from Original Research to Review Articles, Frontiers Research Topics unify the most influential researchers, the latest key findings and historical advances in a hot research area! Find out more on how to host your own Frontiers Research Topic or contribute to one as an author by contacting the Frontiers Editorial Office: frontiersin.org/about/contact

CARDIO-VASCULAR DYSFUNCTION AND PHYSIOLOGICAL MANIFESTATIONS INDUCED BY ENVIRONMENTAL CONDITIONS

Topic Editors:
Marc-Antoine Custaud, Université d'Angers, France
Ronan Padraic Murphy, Dublin City University, Ireland
Olga Vinogradova, Institute of Biomedical Problems, Russian Academy of Sciences (RAS), Russia
Claude Gharib, Université de Lyon, France
François Guerrero, Université de Bretagne Occidentale, France
Michael D. Delp, Florida State University, United States

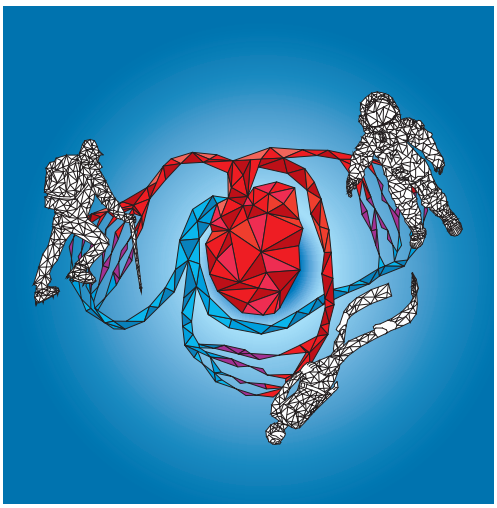

This Research Topic eBook comprises Volume I and Volume II of Cardio-vascular Dysfunction and Physiological Manifestations Induced by Environmental Conditions.

Citation: Custaud, M.-A., Murphy, R. P., Vinogradova, O., Gharib, C., Guerrero, F., Delp, M. D., eds. (2022). Cardio-vascular Dysfunction and Physiological Manifestations Induced by Environmental Conditions.
Lausanne: Frontiers Media SA. doi: 10.3389/978-2-88974-808-2

Table of Contents

SIMULATED WEIGHTLESSNESS – DRY IMMERSION

SIMULATED WEIGHTLESSNESS – HDBR

OTHER ENVIRONMENTAL CONDITIONS RELATED TO GRAVITY

DIVING

ANIMAL AND CELLS MODELS

frontiers in Physiology

EDITORIAL
published: 17 March 2022
doi: 10.3389/fphys.2022.870917

Editorial: Cardio-vascular Dysfunction and Physiological Manifestations Induced by Environmental Conditions

Marc-Antoine Custaud[1]*, *Olga Vinogradova*[2], *Claude Gharib*[3], *Michael Delp*[4], *François Guerrero*[5] and *Ronan Murphy*[6]

[1] University of Angers, CHU Angers, CRC, INSERM, CNRS, MITOVASC, Equipe CarMe, SFR ICAT, Angers, France, [2] Institute of Biomedical Problems, Russian Academy of Sciences, Moscow, Russia, [3] Institut NeuroMyoGène, Université de Lyon, Lyon, France, [4] Department of Nutrition, Food and Exercise Sciences, Florida State University, Tallahassee, FL, United States, [5] Laboratoire ORPHY, EA 4324, Université de Bretagne Occidentale, Brest, France, [6] Cell and Molecular Physiology Group, Faculty of Science and Health, School of Health and Human Performance, Dublin City University, Dublin, Ireland

Keywords: weightlessness, diving, deconditioning, gravity, extreme environment

Editorial on the Research Topic

Cardio-vascular Dysfunction and Physiological Manifestations Induced by Environmental Conditions

OPEN ACCESS

Edited and reviewed by:
Hanns-Christian Gunga, Charité Universitätsmedizin Berlin, Germany

***Correspondence:**
Marc-Antoine Custaud
macustaud@chu-angers.fr

Specialty section:
This article was submitted to Environmental, Aviation and Space Physiology, a section of the journal Frontiers in Physiology

Received: *07 February 2022*
Accepted: *09 February 2022*
Published: *17 March 2022*

Citation:
Custaud M-A, Vinogradova O, Gharib C, Delp M, Guerrero F and Murphy R (2022) Editorial: Cardio-vascular Dysfunction and Physiological Manifestations Induced by Environmental Conditions. Front. Physiol. 13:870917. doi: 10.3389/fphys.2022.870917

INTRODUCTION

Interactions between living organisms and their environment are complex, being generationally, spatially, and temporally regulated. Genetic adaptations occur and persist over many generations which confer both a survival and reproductive advantage in the context of a particular environment, a condition of evolution known as Darwinism. Acclimatization involves a constellation of integrative adaptive responses which confer functional compensation. This biological and physiological phenomenon may extend over a period of hours to months to years, even trans generationally, in response to a complex set of environmental factors. Within the bounds of the principle of parsimony, acclimation may be referred to as the functional compensation in response to a single environmental factor. Studies of acclimation are ordinarily performed in the laboratory where only one variable is manipulated at a time (Fregly, 1996). As our understanding of biological systems advance, and the contribution of growing disciplines such as epigenetics, the integrative research studies, technological platforms, modeling systems, and experimental approaches have become pivotal to elucidating functional physiological adaptations at the molecular and cellular level.

Gravity, a constant environmental condition that exists over a continuum, plays an indispensable role in maintaining normal and healthy physiological function, regulating tissue, and organ homeostasis, including that of the skeletal, muscle, neuro-vestibular, and importantly, cardiovascular system. Moreover, it plays a crucial role in the regulation of metabolism. Astonishingly, a reduction in gravitational stimuli will rapidly induce physiological and systemic de-conditioning. Over the course of the past 50 years, studies have demonstrated that the space environment and microgravity (μG) in particular, will cause physiological changes that may affect the performance and wellbeing of astronauts. These physiological changes are now better understood; prolonged exposure to a weightlessness environment (0G) can lead to significant loss of bone, muscle mass, strength, cardiovascular and sensory-motor de-conditioning, immune,

hormonal, and metabolic changes. The same paradigm holds true for other equally important environmental and physiological conditions such as physical inactivity, confinement, hyperbaric, and hypoxic stimuli.

The aim of this Research Topic, in cooperation with ISGP (International Society for Gravitational Physiology—www.isgp-space.org) was to collectively gather research, studies, novel thinking, and findings from the cornucopia of work being undertaken in this field of medicine.

GROUND MODELS OF WEIGHTLESSNESS

Dry immersion (DI), wet immersion, unilateral lower limb suspension, head down bed rest, and supine bed rest are ground based human models of microgravity. They induce and replicate, to various degrees, physical inactivity, and fluid transfer. As explored in their mini review (Pandianrajan and Hargens), these analogs to microgravity are complementary but should be employed cautiously and the experimental findings interrogated and interpreted objectively. Amirova et al. compared head down bed rest to dry immersion to induce cardiovascular deconditioning. Dry immersion reproduces most of the physiological effects of microgravity, importantly those such as centralization of body fluids, enhanced muscular inactivity, and support unloading. This modality of microgravity is well-understood as it was developed by Russian scientists in the early 1970s and has since been extensively employed in many studies (Navasiolava et al., 2011; Tomilovskaya et al., 2019). Support unloading is very specific to this model and induces important physiological adaptions and impairments, most notably for neuro-muscular function. Comparative studies of 21 days of head down bed rest with 3 days of dry immersion have demonstrated holistically comparable changes for the cardiovascular system. These adaptations however are more rapid and pronounced for the dry immersion model. Dry Immersion, originally developed as a model of microgravity, may also have potential therapeutic applications. For example, patients with Parkinson disease, may demonstrate and experience a beneficial effect with dry immersion. DI may not only beneficially impact and reduce muscular hypertonicity, but also potentially improves autonomic dysfunction (Megal et al.). This phenomenon is an exciting, novel, and important finding. Further translational studies utilizing and investigating the dry immersion model for therapeutic use should be actively encouraged!

CARDIOVASCULAR DECONDITIONING TO MICROGRAVITY

Actual and simulated weightlessness have well-described deleterious effects on the cardiovascular system. These multiple physiological adaptations and changes are termed cardiovascular de-conditioning. In their comprehensive review, Navasiolava et al. summarize the structural and functional (micro-) vascular changes induced by space flight and the various models of microgravity. Moreover, they also review the effects of prophylactic strategies and countermeasures to prevent cardiovascular de-conditioning. The endothelium, far from being an inert conduit for blood flow, is a dynamic adaptive mechanosensory tissue whose function is rapidly impaired by sedentariness and thus by weightlessness. Endothelial dysfunction may be an important arbiter of cardiovascular risk after long term exposure to microgravity.

Orthostatic intolerance is the principle acute symptom of cardiovascular deconditioning induced by weightlessness. Daily rise is a challenge for the cardiovascular system and this daily stimulation is necessary to keep the cardiovascular system reactive to gravity. Thoraco-cephalic fluid shift is a widely acknowledged consequence of weightlessness and may play a role in spaceflight associated neuro-ocular syndrome. However, our understanding of the mechanisms and physiological effects of this fluid shift is far from complete. Kirsch et al. (1984) followed and supported by Buckey et al. (1993) measured central venous pressure in astronauts and observed a decrease of central venous pressure as soon as the astronaut is exposed to 0G. Changes in the morphology of the thoracic cage, with its expansion in space environment, are very important considerations in our understanding of central venous pressure changes. Lee et al. employed a parabolic flight model to study fluid shift using ultrasound (internal jugular vein cross sectional area, inferior vena cava diameter and common carotid artery flow). Their data suggested that Gz levels >0.5 Gz are necessary to counteract, mitigate, and reduce the weightlessness induced fluid shift.

Impaired cerebral autoregulation is one of the postulated mechanisms underpinning orthostatic intolerance. However, the effects of microgravity on cerebral auto-regulation remain unclear. In their review, Kermorgant et al. considered different experimental approaches to evaluate cerebral autoregulation changes induced by spaceflight and ground-based analogs. Paradoxically, short terms studies have demonstrated a preserved or even an improved cerebral autoregulation, in contrast to long term studies, which have depicted impairment in cerebral autoregulation.

Autonomic nervous system dysfunction occurs after weightlessness exposure with an impairment of the sympathetic/para-sympathetic balance and a decrease in the cardiac baroreflex efficiency (Coupé et al., 2009). Heart rate and blood pressure variability analysis, ascertained by beat-to-beat recordings have been extensively performed both in the space environment and ground models to quantify and to explain this autonomic dysfunction. Heart rate and blood pressure changes are induced by closed loop regulation; thus, analysis of their spontaneous oscillations is particularly relevant. Borovik et al. used a phase synchronization index of beat-to-beat mean arterial pressure and heart rate to measure the baroreflex activity. The observed lack of increase of this index during head up tilt test post dry immersion corroborates a baroreflex disorder induced by weightlessness. Rusanov et al. observed changes in heart rate variability indicators after 5 days of dry immersion, indicating a shift in the autonomic balance toward a sympathetic activation. Jia et al. studied the relationship between blood perfusion in the lower extremities and hear rate variability at different positions and thus in relation with the gravity force.

COUNTERMEASURES TO FIGHT DECONDITIONING TO GRAVITY

As physical inactivity and weightlessness induced fluid shift is the main trigger of cardiovascular deconditioning, the more obvious countermeasures are based on physical exercise and interventions to limits this phenomenon. Countermeasures based on physical exercise are acknowledged to be the most effective strategy against deconditioning, considering its pleiotropic beneficial effect on human physiology. However, since physical exercise countermeasures are not sufficient, *per se*, to fully address cardiovascular deconditioning, it is evident complementary and adjuvant strategies should be explored.

Venoconstrictive thigh cuffs are currently employed by cosmonauts to limit symptoms associated with cephalic fluid shifts. This countermeasure was tested during a 5-day dry immersion study (Robin et al.). Although wearing thigh cuffs (10 h per day) in this ground model study slowed down and mitigated loss of body water and plasma loss induced by DI, their utilization unfortunately did not prevent or counteract orthostatic intolerance.

The "Cocktail Bedrest" investigation tested the effects of an antioxidant/anti-inflammatory cocktail (polyphenol, vitamin-E, selenium, and omega-3) over a 2-month head down bed rest study. Unfortunately, this supplementation was shown to be ineffective in preventing skeletal muscle deconditioning and moreover could impair the recovery process of the muscular function and rehabilitation. This study highlights the complexity of the redox balance in the body as well as the hormesis effect and functionality of pro-oxidant molecules during long term inactivity, playing a potentially important biological role in maintaining muscle health and function (Arc-Chagnaud et al.).

However, plant extracts and antioxidant factors still need to be considered and further investigated as adjuvant countermeasures. Hesperidin, a flavonoid antioxidant component, as well as its more soluble derivative, α-Glucosyl Hesperidin, limits ankle swelling caused by a prolonged sitting position (Nishimura et al.).

It is becoming evident that the optimal countermeasure strategy will employ a stratified and multi-combinatorial approach. The MNX (Medium duration Nutrition and Resistance-Vibration Exercise) 21-day bed rest tested the combination of a nutritional supplementation using Whey proteins together with vibration and resistive exercise. Unfortunately, those countermeasures even combined failed to prevent cardiovascular deconditioning. They did however mitigate the decrease of VO_2 max (Guinet et al.).

The "Cocktail Bedrest" and the "MNX" studies illustrate the difficulty and challenges in developing countermeasures to address the deconditioning induced by the suppression of gravity. This is due in no large part, to the fact that gravity is fundamental to health, wellbeing and normal physiological functionality of our integrated organ and tissue systems. Thus, the absence of gravity presents and remains a challenging environment to counteract and address. Extensive international studies are ongoing to test additional countermeasures (such as artificial gravity) and permutations and combinations thereof, to address the (patho-) physiological consequences to spaceflight deconditioning. Proposed long duration space flight, such as future Mars missions, will require the development of synergistic and optimal countermeasure protocols, failing which we will have no other choice but to replicate gravitational force itself using long arm rotating spaceships.

In addition to "prophylactic" strategies, "therapeutic" interventions have also been employed, since the first space flight, in the management of astronauts, cosmonauts, and taikonauts upon return to earth. Gradient compression garments (with a continuous gradient of compression from the feet until the abdomen) in the hours after long-duration spaceflight together with an end of mission fluid loading are efficient to prevent orthostatic intolerance after a 6-month space flight (Lee et al.).

DIVING EFFECTS ON THE CARDIOVASCULAR REGULATION

The cardiovascular system is challenged also by diving in several aspects. The first parameter is blood centralization and reduced interstitial extravasation of fluids due to both immersion and submersion. Several factors can explain this centralization, such as buoyancy, pressure gradient of hydrostatic pressure and pressure gradient between the lungs and the rest of the body. The authors (Weenink and Wingelaar) of a mini review paper argued that the compression effects on the body under immersion are not so important and could be compared to the pressure of a mild compression stocking. Although still debated (Regnard et al.—see commentary to Weenink's paper) this analysis could be of importance also for the model of dry immersion where the buoyancy effect directly counteracts gravity. Nevertheless, a direct consequence of this blood centralization is an increase in thoracic blood pressure which, in turn, leads to stimulation of the autonomous nervous system with a predominant parasympathetic activation (Schipke and Pelzer, 2001; Chouchou et al., 2009). As reported by Lundell et al. in this topic, cold exposure further increases parasympathetic activation. As highlighted by the authors, whether this potent parasympathetic activity due to the combined action of diving and cold could exert adverse effects in the case of long and cold dives merits further investigation.

A second concern, common to both diving and spaceflight, is the risk of decompression sickness (DCS) associated, respectively, to the ascent to the water surface and extravehicular activities. Currently, there is a body of literature showing that the risk of DCS after diving is decreased by nitric oxide administration whereas it is increased when NO synthesis is blocked (Wisløff et al., 2004; Dujić et al., 2006; Mazur et al., 2014). These data strongly suggest that the vascular endothelium plays a pivotal role in the development of DCS after diving, although this has never been scientifically demonstrated. The results of two studies published in this topic support this hypothesis by

showing, on the one hand, that bubble formation correlates with vascular compliance and NO bioavailability (Boussuges et al.) and, on the other hand, that experimentally induced DCS in rabbits can be treated by the administration of Ulinastatin, a drug which inhibits the release of inflammatory factors and alleviates endothelial injury/dysfunction (Meng et al.).

NECESSITY FOR ANIMAL AND CELLS MODELS

The use of animal as well as cell models is essential for studies into environmental physiology and physiopathology.

Pressure chambers to mimic hypo- and hyperbaric conditions in rats to simulate mountain ascent or deep-sea diving were used in three articles of this Research Topic. Flores et al. investigated cardioprotective effect of caloric restriction against right ventricular hypertrophy (RVH) induced by chronic hypoxia. After chronic (30 days) of hypobaric hypoxia at 428 Tor, equivalent to that at 4,600 m above sea level, a lower degree of RVH, higher AMPK activation, and no activation of mTOR were observed in a group of rats with restricted diet compared to *ad libitum* study group. This implicates body weight as a contributing factor to RVH at high altitudes.

Gaustad et al. continuously monitored hemodynamic parameters in an intact, spontaneously breathing rat during simulated diving tests in an air-filled hyperbaric chamber during all phases of a 600-kPa dry air dive: the diving conditions were well-tolerated by a healthy heart, whereas in a failing heart, acute cardiac decompensation was recorded. The dry diving model was also employed by Ardestani et al. to study endothelium function in different vessels of the cardiovascular compartment. A single simulated dive was specifically found to induce pulmonary artery endothelial dysfunction in ApoE knockout rats, and this was more profound in male than female rats. The authors concluded that the biological mechanisms contributing to these changes were different for males and females. Translation of these findings to humans may suggest caution for divers who are elderly or have reduced endothelial function.

Hindlimb unloading (HU) in rodents is a widely used model simulating the effects of exposure to microgravity. Tarasova et al. used this model to investigate the regional and tissue specific differences in the response of skeletal muscle and cutaneous arteries to gravitational unloading. HU induced contrasting structural and functional adaptations in forelimb and hindlimb skeletal muscle arteries. Additionally, HU had diverse effects in two hindlimb vascular regions. Importantly, HU impaired sympathetically induced arterial vasoconstriction was consistent with that observed, in humans following spaceflight.

Limitations of animal models in predicting human (patho-)physiological responses and in providing clinically relevant data, is a challenge in the translation of studies. The development and use of human dynamic cellular models or "organotypic systems," based on advanced technological platforms addresses this gap and deficit. The use of dynamic human primary cell systems coupled with emerging molecular, cellular, and (epi-)genetic technologies that allow precise control of the culture environment and analysis of meaningful endpoints paves the way for human organotypic systems as a major initiative in studying the effects of various environmental exposomes on physiological systems. Such a model was used by Liu et al. to investigate the contribution of ACE2 to mechano-transduction induced vascular remodeling under mechanical stretch and to investigate the possible underlying molecular mechanisms. Human aortic vascular smooth muscle cells (HaVSMCs) were stretched by special device *in vitro*. It was shown that mechanical stretch modulated the expression of the ACE2/Ang-(1–7) and ACE/AngII axis. ACE2 is mechano-sensitive and involved in stretch-induced dysfunction of HaVSMCs. Thus, ACE2 may contribute to the development of vascular remodeling under conditions of mechanical stretch. This observation may provide clinicians with opportunities to develop new therapeutic approaches for hypertension.

INTEGRATIVE PERSPECTIVES

Cross Acclimation Between Ambient Oxygen and Gravity

Counter-responses adjusting for hypoxia may conflict with orthostatic responses and induce an increase of orthostatic intolerance risk. The authors (Nourdine et al.) have shown that during hypoxic orthostatic challenge, a mobilization of the heart rate reserve and a delayed systemic vascular resistance index activation are key regulatory responses to preserve orthostatic tolerance. (Boussuges et al.) studied the potential interactions between hyperoxia and exercise. If hyperoxia decreased adenosine plasma levels and increased systemic vascular resistance at rest in healthy volunteers as expected, hyperoxia did not eliminate the increase in adenosine plasma levels and in systemic vascular resistance during low intensity exercise.

Perspectives With Proteomic Approach

As environmental conditions, especially gravity, have intrinsically complex interactions with our physiology, the use of integrative "omics" approaches in combination with data analysis is of particularly important relevance. Proteomic analysis performed on different body fluids refers to a systematic large-scale identification and quantification of proteins. Comparative analysis of different environmental exposomes can identify changes in differential protein expression and may identify novel mechanistic physiological pathways. The team of Prof. Larina, Moscow, successfully applied this method to understand mechanisms of cardiovascular changes induced by weightlessness in urine and blood samples (Pastushkova et al.; Rusanov et al.; Kashirina et al.; Kashirina et al.).

AUTHOR CONTRIBUTIONS

M-AC, OV, CG, MD, FG, and RM were co-editor of this Research Topic. All authors contributed to the preparation of this editorial and approved the submitted version.

ACKNOWLEDGMENTS

We sincerely thank all the authors, participants, and volunteers who have contributed to the success of this Research Topic.

REFERENCES

Buckey, J. C., Gaffney, F. A., Lane, L. D., Levine, B. D., Watenpaugh, D. E., and Blomqvist, C. G. (1993). Central venous pressure in space. *N. Engl. J. Med.* 328, 1853–1854. doi: 10.1056/NEJM199306243282516

Chouchou, F., Pichot, V., Garet, M., Barthélémy, J.-C., and Roche, F. (2009). Dominance in cardiac parasympathetic activity during real recreational SCUBA diving. *Eur. J. Appl. Physiol.* 106, 345–352. doi: 10.1007/s00421-009-1010-0

Coupé, M., Fortrat, J. O., Larina, I., Gauquelin-Koch, G., Gharib, C., and Custaud, M. A. (2009). Cardiovascular deconditioning: from autonomic nervous system to microvascular dysfunctions. *Respir. Physiol. Neurobiol.* 169(Suppl 1), S10–S12. doi: 10.1016/j.resp.2009.04.009

Dujić, Z., Palada, I., Valic, Z., Duplancić D., Obad, A., Wisløff, U., et al. (2006). Exogenous nitric oxide and bubble formation in divers. *Med. Sci. Sports Exerc.* 38, 1432–1435. doi: 10.1249/01.mss.0000228936.78916.23

Fregly, M. J. (1996). "Section 4, Chapter 1: Environmental Physiology," in *Handbook of Physiology*, eds M. J. Fregly and C. M. Blatteis (Oxford: Oxford University Press), 3–15.

Kirsch, K. A., Röcker, L., Gauer, O. H., Krause, R., Leach, C., Wicke, H. J., et al. (1984). Venous pressure in man during weightlessness. *Science*.225, 218–219. doi: 10.1126/science.6729478

Mazur, A., Buzzacott, P., Lambrechts, K., Wang, Q., Belhomme, M., Theron, M., et al. (2014). Different effect of l-NAME treatment on susceptibility to decompression sickness in male and female rats. *Appl. Physiol. Nutr. Metab.* 39, 1280–1285. doi: 10.1139/apnm-2014-0148

Navasiolava, N. M., Custaud, M. A., Tomilovskaya, E. S., Larina, I. M., Mano, T., Gauquelin- Koch, G., et al. (2011). Long-term dry immersion: review and prospects. *Eur. J. Appl. Physiol.* 111, 1235–1260. doi: 10.1007/s00421-010-1750-x

Schipke, J. D., and Pelzer, M. (2001). Effect of immersion, submersion, and scuba diving on heart rate variability. *Br. J. Sports Med.* 35, 174–180 doi: 10.1136/bjsm.35.3.174

Tomilovskaya, E., Shigueva, T., Sayenko, D., Rukavishnikov, I., and Kozlovskaya, I. (2019). Dry immersion as a ground-based model of microgravity physiological effects. *Front. Physiol.* 10:284. doi: 10.3389/fphys.2019.00284

Wisløff, U., Richardson, R. S., and Brubakk, A. O. (2004). Exercise and nitric oxide prevent bubble formation: a novel approach to the prevention of decompression sickness? *J. Physiol.* 555(Pt 3), 825–829. doi: 10.1113/jphysiol.2003.055467

Conflict of Interest: The authors declare that the research was conducted in the absence of any commercial or financial relationships that could be construed as a potential conflict of interest.

Publisher's Note: All claims expressed in this article are solely those of the authors and do not necessarily represent those of their affiliated organizations, or those of the publisher, the editors and the reviewers. Any product that may be evaluated in this article, or claim that may be made by its manufacturer, is not guaranteed or endorsed by the publisher.

frontiers in Physiology

MINI REVIEW
published: 23 June 2020
doi: 10.3389/fphys.2020.00716

Ground-Based Analogs for Human Spaceflight

Meenakshi Pandiarajan and Alan R. Hargens*

Department of Orthopaedic Surgery, Altman Clinical and Translational Research Institute, University of California, San Diego, San Diego, CA, United States

This mini-review provides an updated summary of various analogs for adaptations of humans to the microgravity of space. Microgravity analogs discussed in this paper include dry immersion, wet immersion, unilateral lower-extremity limb suspension, head down tilt (HDT), and supine bed rest. All Earth-based analogs are imperfect simulations of microgravity with their own advantages and disadvantages. This paper compares these five frequently used microgravity analogs to offer insights into their usefulness for various physiological systems. New developments for each human microgravity analog are explored and advantages of one analog are evaluated against other analogs. Furthermore, the newly observed risk of Spaceflight Associated Neuro-Ocular Syndrome (SANS) is included in this mini review with a discussion of the advantages and disadvantages of each method of simulation for the relatively new risk of SANS. Overall, the best and most integrated analog for Earth-based studies of the microgravity of space flight appears to be head-down tilt bed rest.

Keywords: bed rest, head down tilt, dry immersion, wet immersion, unilateral lower limb suspension

OPEN ACCESS

Edited by:
Marc-Antoine Custaud, Université d'Angers, France

Reviewed by:
Nandu Goswami, Medical University of Graz, Austria
Anne Pavy-Le Traon, Centre Hospitalier Universitaire de Toulouse, France

****Correspondence:***
Meenakshi Pandiarajan
mpandiarajan13@gmail.com

Specialty section:
This article was submitted to Environmental, Aviation and Space Physiology, a section of the journal Frontiers in Physiology

Received: *03 March 2020*
Accepted: *29 May 2020*
Published: *23 June 2020*

Citation:
Pandiarajan M and Hargens AR (2020) Ground-Based Analogs for Human Spaceflight. Front. Physiol. 11:716. doi: 10.3389/fphys.2020.00716

INTRODUCTION

This mini-review serves as an updated look upon the various analogs to microgravity. All established microgravity analogs discussed in this paper (dry immersion, wet immersion, unilateral lower-extremity limb suspension, head down tilt (HDT), and supine bed rest) are imperfect simulations of microgravity with their own merits and disadvantages. This paper serves to discuss new developments for each human microgravity analog as well as to compare these simulation methods to actual microgravity conditions of spaceflight. Furthermore, the newly observed risk of Spaceflight Associated Neuro-Ocular Syndrome (SANS) is included in this mini review with a discussion of the advantages/disadvantages of each method of simulation for space flight for the SANS risk. Due to format limitations, some aspects, such as metabolism and countermeasures, cannot be considered in this mini-review.

MICROGRAVITY ANALOGS

Five analogs are commonly used on Earth for simulating the microgravity of space (**Figure 1**). The well-established microgravity analogs discussed in this paper, dry immersion, wet immersion, unilateral lower-extremity limb suspension, HDT, and supine bed rest, have their own unique advantages and disadvantages in terms of applications to various physiological systems.

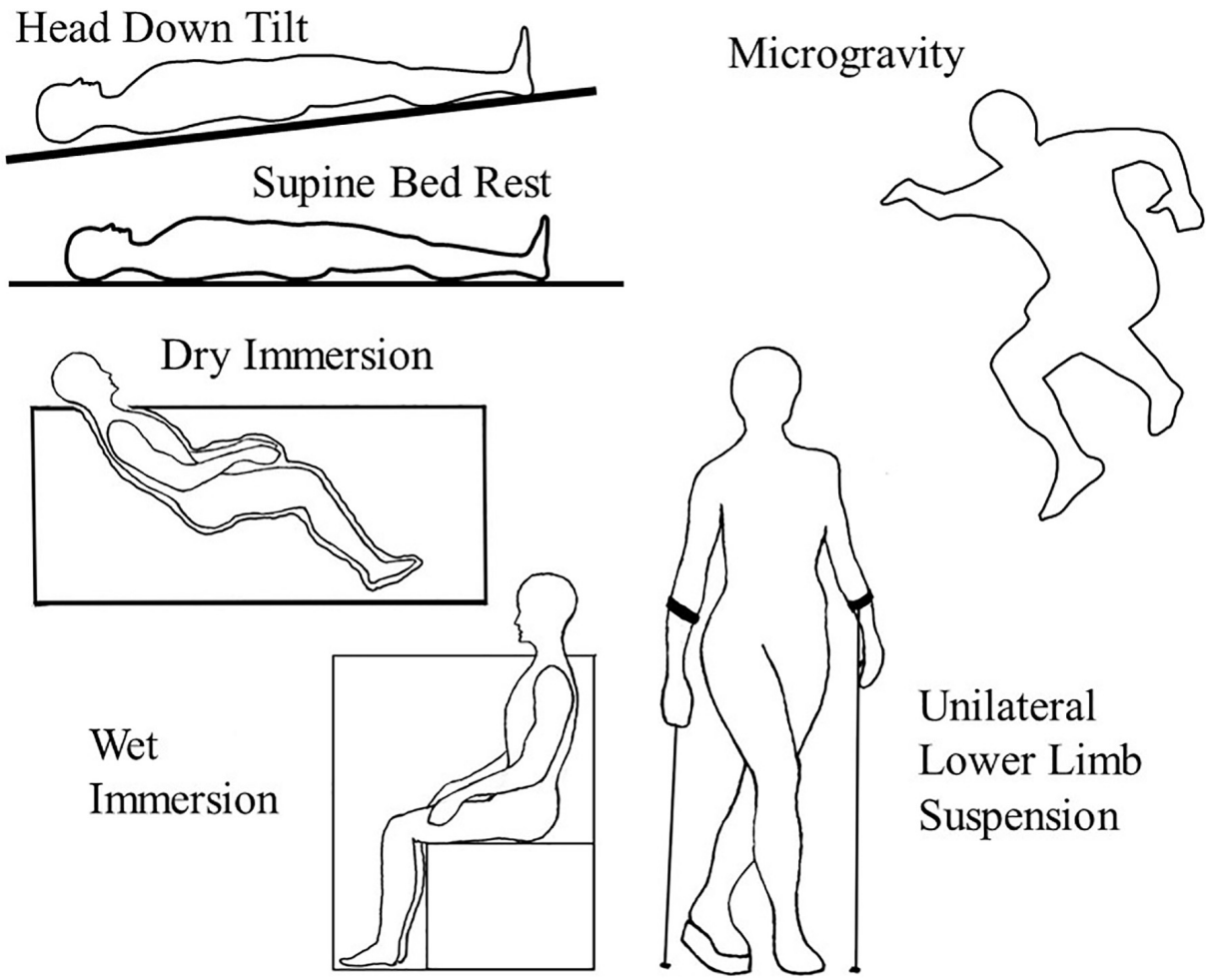

FIGURE 1 | Illustrates the positions and conditions of the various microgravity analogs in Earth's gravity as compared to actual microgravity (upper right) in which there is no weight bearing or vascular hydrostatic pressures.

DRY IMMERSION

Dry immersion is a microgravity simulation analog method developed in Russia in which the subject is encapsulated in a waterproof covering and submerged, from the neck down, in water. The water is held at a standard temperature of 32–34.5°C, which is thermoneutral, and the subjects are submerged just past their clavicles (Navasiolava et al., 2010). Subjects float, simulating the effects of microgravity. This method eliminates the risks associated with extensive and prolonged exposure in water (Watenpaugh, 2016). The near complete submersion in water allows for the simulation of cardiovascular and musculoskeletal effects of microgravity (Navasiolava et al., 2010). However, as this submersion is limited to the body below the neck, it is not a perfect analog for microgravity. The fluid shift in the head and neck occurs to lesser degree than strict HDT. It also requires that subjects leave the apparatus for hygienic purposes, impacting the study, and simulated effects (Abreu et al., 2017). Because the subject is not focused upon or supported by any structure, dry immersion allows for the observation of the effects of "supportlessness." Whereas methods such as HDT and supine bed rest redistribute stress to the posterior of the body, a lack of a support device means no loading effects are experienced the body. The effects of microgravity are demonstrated by dry immersion on a faster timeline than methods like HDT, presenting similar results to a 21-day HDT study in just 3 days (Tomilovskaya et al., 2019). 17% loss in plasma volume, comparable to loss experienced after spaceflight, is seen after 2 days of dry immersion (Treffel et al., 2017). Dry immersion also generates atrophy and loss of strength in the musculoskeletal system, with deteriorations in force and structure similar to those occurring in spaceflight during a comparable amount of time.

Dry immersion induces a head-ward fluid shift due to the hydrostatic compression of the subject. With increasing pressure with depth, lower limbs experience a higher level of head-ward fluid shift, (directing fluid to the upper body) similar to the shift seen in spaceflight. This fluid shift also decreases cardiovascular

stress and heart rate decreases within hours of dry immersion. Heart rate drops by 5 bpm and blood pressure decreases by 5 mmHg in the first 4 h (Navasiolava et al., 2010). However, unlike spaceflight, subjects experience an increase in central venous pressure though there are similar changes in heart size and stroke volume. Dry immersion also shows rapid muscle and bone loss, mainly attributed to the lack of gravitational stress placed on the body (Treffel et al., 2017). Within 7 days, bone density in the lower limbs drops 2% (Navasiolava et al., 2010). When upright on Earth without dry immersion, the postural muscles of the body need to support the weight of the body and counter the effects of gravity. However, when this stress is removed, through dry immersion, muscle loss occurs, especially for stabilizing muscles of the leg and spine. It is also noted that stabilizing muscles of the lower limbs have decreased strength and force production of 20% after 7 days of dry immersion (Navasiolava et al., 2010). The rate of muscular change is rapid with dry immersion, with maximum muscle stiffness achieved within 6 h of dry immersion as opposed to several days or weeks in HDT.

Because of the near-seated position of the subject, the gravitational forces upon the body vary. This is noted in the case of where torso movement is significantly more impaired than wrist movement, suggesting a difference in the reduction of gravitational forces across the body (Wang et al., 2015).

WET IMMERSION

Water immersion requires submersion in water from the neck down. However, extensive water immersion can induce subacute dermatitis in as little as 72 h, making this method unusable for long duration studies (Willis, 1973). The benefits of a water immersion study are similar to those of dry immersion but lack the longevity required for substantial human data and wide-spread implementation (Watenpaugh, 2016). Water Immersion utilizes the hydrostatic pressure of the water environment to counteract the intravascular hydrostatic pressure gradients. However, this pressure also causes an undue influence on breathing by exerting pressure on the chest, creating a negative pressure breathing effect (Norsk, 2014).

UNILATERAL LOWER LIMB SUSPENSION

Unilateral lower limb suspension is one of the most cost-effective methods to study the effects of microgravity and spaceflight on the human body (Hackney and Ploutz-Snyder, 2011). The method relies on the elevation of one leg, accomplished using a singular platform shoe and crutches. This unilateral suspension allows for the continued mobility of the subject as well as an inherent control limb in the study. Increased mobility is a crucial factor in determining cost effectivity and subject compliance as semi-normal mobility allows subjects to travel, work, and remain at home. This reduces costs incurred by methods that require hospital stays or constant monitoring. While reduced monitoring means that compliance is not completely verifiable, the decreased imposition on the subject's daily life allows for more volunteers and willing participants (Tesch et al., 2016).

This method has effects within 2–3 days of implementation, showing signs of muscle atrophy and deterioration. While this method cannot demonstrate global or cardiovascular changes from loss of hydrostatic pressures within the body, it is effective in demonstrating changes in the muscular and skeletal systems. The effects are localized to the lower leg, specifically affecting the postural muscles of the lower limb (Tesch et al., 2016). The use of lower limb suspension provides a unique benefit of coming with a built-in control. As only one leg is suspended, and thus unloaded, the other weight bearing leg and muscles can be used to evaluate the effects of the suspension. The core effect of this method, muscle atrophy, occurs at a relatively constant rate across time but does not occur uniformly across muscle fibers or individuals' muscles. These muscular changes are consistent with the changes that occur during spaceflight, happening in similar locations and rates (Adams et al., 2003). Changes in bone density are comparable to HDT, with a 0.70% loss in bone density being observed after 21 days, similar to a 0.73% loss observed in 28-day HDT (Rittweger et al., 2006).

There is little risk to the subject aside from increased risk of venous thromboembolism relative to bed rest and spaceflight, which can be mitigated with the use of compression socks (Bleeker et al., 2004). It is recommended that individuals with risk factors, such as women on contraceptives and those with an inherited risk of deep vein thrombosis, are excluded from ULLS studies (Bleeker et al., 2004). Head-ward fluid shifts and larger possible changes to the cardiovascular or musculoskeletal system are prevented in this method by localizing the unloading to one limb, thereby preventing long lasting effects and risk to the volunteer's health (Tesch et al., 2016). However, this localization prevents ULLS from being a valid method of study for global effects of spaceflight.

HEAD DOWN TILT

The focus of HDT bed rest is to induce head-ward fluid shifts. In microgravity, the body undergoes head-ward fluid shifts because hydrostatic pressures disappear, and arterial pressure is equalized throughout the body. Due to the presence of gravity on Earth, blood pressures are significantly higher in the lower limbs and feet than at the head. In order to reproduce this condition on Earth, subjects are placed in the supine position on a bed that is tilted 6 degrees to place the head closer to the ground and to elevate the feet (Hargens and Vico, 2016). Six-degrees HDT is the international standard for simulating weightlessness (Smith et al., 2011). As opposed to supine bed rest, HDT increases head-ward fluid shifts toward the head but alters the gravity vector over the entire body from anterior to posterior. This method requires sustained bed rest and a prolonged hospital stay, causing this analog to be expensive. For strict HDT, it is important that subjects do not leave this posture for short periods of time or use a pillow to prop up their heads.

The use of a pillow decreases ICP (supine 14 ± 2 mmHg vs. pillow, 10 ± 2 mmHg, $P = 0.05$), which may counteract visual symptoms that might occur (Lawley et al., 2017). Removing the visual impact is not conducive to studying SANS. Eating, showering, use of urinals and bed pans must be performed in HDT posture. However, unlike lower limb suspension, HDT allows for the observation of cardiovascular effects and head-ward fluid shifts for better studies of SANS and its mechanisms and responses (Hargens and Vico, 2016; Watenpaugh, 2016; Laurie et al., 2019).

Head down tilt redistributes pressure across the posterior of the body, rather than being focused in a head to feet direction. This posture does not completely remove the application of gravity and thus, does not completely simulate the effects of a microgravity environment. By inducing HDT, the cardiovascular system no longer has to work against the force of gravity, as when standing up, mimicking a lack of gravity (Watenpaugh, 2016). Head-ward fluid shifts and cardiovascular adaptations are akin to those found in spaceflight and microgravity (Hargens and Vico, 2016). Unlike microgravity, HDT does not create a loss in tissue weight but it does induce a greater amount of fluid toward the head. The skeletal system shows a decrease in bone density, when subjected to HDT without any countermeasures, especially in the lumbar spine, pelvis, and legs. Over HDT of 2–3 months, a decrease in bone density of 3.8% was seen in the hip and a 10% decrease at the heel (Hargens and Vico, 2016). As a result of HDT, these bones no longer bear weight, thus resulting in loss of bone quality density. This analog helps identify bone regions where subjects in a microgravity environment would experience the greatest loss of bone. Furthermore, loss in bone density in the lower, now non-weight bearing limbs, can be compared to that of the upper limbs, which are not weight bearing in any position, to isolate the changes due to HDT (Hargens and Vico, 2016). Proper experimental procedure for this method requires a separate control group to attempt to accurately gauge which effects can be attributed to the microgravity simulation method.

Spaceflight Associated Neuro-Ocular Syndrome is an outcome of long-term spaceflight. The exact cause of SANS and the factors that lead to it are still under extensive research (Mandsager et al., 2016; Laurie et al., 2019). One of the widely observed results of SANS is increased choroidal thickness and increased optic disk edema. Replicating these effects on Earth has yet to be done with any analog. However, similar results to SANS in space are achieved with HDT. An extended trial may be of value, as 70-day HDT was found to show greater retinal thickening (+18 μm [+5.3%] during 70-day vs. none in 14-day) and IOP increase (+1.79 mm Hg vs. +1.42 mm Hg) than 14-day HDT (Taibbi et al., 2016; Klassen et al., 2018). In addition, hypercapnia alongside HDT has shown an increase in IOP of 0.8 mmHg (95% CI, $P = 0.05$) when compared to normal HDT (Laurie et al., 2017). However, HDT also produces a higher level of retinal thickness than that experienced in spaceflight, with a mean difference of 37 μm (95% CI, 13–61 μm; $P = 0.005$) between grounded subjects and astronauts (Laurie et al., 2019).

SUPINE BED REST

Supine bed rest creates a uniform fluid distribution throughout the body (except for anterior to posterior fluid shifts and small hydrostatic pressure gradients) by having subjects lie in the supine position (Hargens and Vico, 2016). This method also results in the compression of posterior tissues unlike that of microgravity. In supine bed rest, the contact between the patient and the bed compresses tissues while microgravity has no such compression of tissues, e.g., during sleep. There has been little expansion in the use of this early analog for calcium balance studies. This method sometimes provides a control for HDT studies.

COMPARING METHODS

All current analogs to microgravity are imperfect analogs and need to be compared to evaluate their utility for a given project or space maladaptation (**Table 1**). Immersion generates an even distribution of gravitational forces (Norsk, 2014). While dry and wet immersions provide similar physiological reactions to HDT, responses to immersions are more rapid than HDT. Back pain with dry immersions seems more severe than that with wet immersion and HDT. It is important to recognize that immersion relies on the neutralization of internal pressures through the pressure of water and HDT provides a head-ward fluid shift due to jugular vein congestion and slightly higher venous and arterial pressures in the head and neck. Jugular vein flow is reduced in HDT in a manner similar to space flight. While unilateral

TABLE 1 | This table summarizes the observable effects.

	Dry immersion	Wet immersion	Unilateral lower limb suspension	Head down tilt	Supine bed rest
Mimics cardiovascular effects of space flight	***	**	*	***	**
Mimics musculoskeletal loss of space flight	**	*	***	***	***
Feasibility of maintaining position	**	*	*	***	***
Median duration	3–7 days	4 h	30 days	30 days	30 days
Maximum duration	56 days[13.14]	12 h[13.14]	42 days[13.6]	370 days[13.14]	

** is used to indicate weak comparability, ** is used to indicate moderate comparability, and *** indicates strong comparability. Feasibility of Maintaining Position includes the physical stress placed upon the subject as well as the costs and logistics involved. [13.6]is a reference to Hackney and Ploutz-Snyder (2011), [13.14]is a reference to Navasiolava et al. (2010).*

lower limb suspension is a cost-effective model for unloading of leg muscles and bones, it fails to account for the lack of gravitational stress and the head-ward fluid shifts seen in space (Tesch et al., 2016).

As it stands, no studies utilizing any method other than HDT and supine bed rest to study SANS have been published. One of the possible causes of SANS may be the increased differential between intercranial pressure and intraocular pressure that occurs in a microgravity environment (Laurie et al., 2017; Zhang and Hargens, 2018; Huang et al., 2019). Moreover, dry immersion, which may increase intracranial pressure mildly and chronically, may also be a viable method to study SANS (Arbeille et al., 2017) but the head and neck are still exposed to vascular hydrostatic pressure gradients due to gravity. Dry immersion has also been observed to increase optic nerve sheath diameter, which is linked to increased ICP (Kermorgant et al., 2017). While further studies need to be done, the best and most integrated analog for Earth-based studies of the microgravity of space flight appears to be HDT bed rest.

AUTHOR CONTRIBUTIONS

MP and AH contributed to the conception and creation of the manuscript. MP researched and wrote the initial draft of the manuscript. AH edited and advised on the manuscript. Both authors read and approved the submitted version of the manuscript.

FUNDING

This work was supported by the NASA grants NNX13AJ12G, NNX13AM89G, NNX14AP25G, NSSC19K030, and NSSC19K0409.

ACKNOWLEDGMENTS

We thank Prof. Laurence Vico and Philippe Arbeille for helpful discussions.

REFERENCES

Abreu, S. D., Amirova, L., Murphy, R., Wallace, R., Twomey, L., Gauquelin-Koch, G., et al. (2017). Multi-system deconditioning in 3-Day dry immersion without daily raise. *Front. Physiol.* 8:799. doi: 10.3389/fphys.2017.00799

Adams, G. R., Caiozzo, V. J., and Baldwin, K. M. (2003). Skeletal muscle unweighting: spaceflight and ground-based models. *J. Appl. Physiol.* 95, 2185–2201. doi: 10.1152/japplphysiol.00346.2003

Arbeille, P., Avan, P., Treffel, L., Zuj, K., Normand, H., and Denise, P. (2017). Jugular and portal vein volume, middle cerebral vein velocity, and intracranial pressure in dry immersion. *Aerosp. Med. Hum. Perform.* 88, 457–462. doi: 10.3357/amhp.4762.2017

Bleeker, M. W. P., Hopman, M. T. E., Rongen, G. A., and Smits, P. (2004). Unilateral lower limb suspension can cause deep venous thrombosis. *Ame. J. Physiol. Regul. Integrat. Comp. Physiol.* 286, R1176–R1177. doi: 10.1152/ajpregu.00718.2003

Hackney, K. J., and Ploutz-Snyder, L. L. (2011). Unilateral lower limb suspension: integrative physiological knowledge from the past 20 years (1991–2011). *Eur. J. Appl. Physiol.* 112, 9–22. doi: 10.1007/s00421-011-1971-7

Hargens, A. R., and Vico, L. (2016). Long-duration bed rest as an analog to microgravity. *J. Appl. Physiol.* 120, 891–903. doi: 10.1152/japplphysiol.00935.2015

Huang, A. S., Stenger, M. B., and Macias, B. R. (2019). Gravitational Influence on Intraocular Pressure. *J. Glaucoma* 28, 756–764. doi: 10.1097/ijg.0000000000001293

Kermorgant, M., Leca, F., Nasr, N., Custaud, M., Geeraerts, T., Czosnyka, M., et al. (2017). Impacts of simulated weightlessness by dry immersion on optic nerve sheath diameter and cerebral autoregulation. *Front. Physiol.* 8:780. doi: 10.3389/fphys.2017.00780

Klassen, S. A., Abreu, S. D., Greaves, D. K., Kimmerly, D. S., Arbeille, P., Denise, P., et al. (2018). Long-duration bed rest modifies sympathetic neural recruitment strategies in male and female participants. *J. Appl. Physiol.* 124, 769–779. doi: 10.1152/japplphysiol.00640.2017

Laurie, S. S., Lee, S. M. C., Macias, B. R., Patel, N., Stern, C., Young, M., et al. (2019). Optic disc edema and choroidal engorgement in astronauts during spaceflight and individuals exposed to bed rest. *JAMA Ophthalmol.* 138, 165–172. doi: 10.1001/jamaophthalmol.2019.5261

Laurie, S. S., Vizzeri, G., Taibbi, G., Ferguson, C. R., Hu, X., Lee, S. M. C., et al. (2017). Effects of short-term mild hypercapnia during head-down tilt on intracranial pressure and ocular structures in healthy human subjects. *Physiol. Rep.* 5:e13302. doi: 10.14814/phy2.13302

Lawley, J. S., Petersen, L. G., Howden, E. J., Sarma, S., Cornwell, W. K., Zhang, R., et al. (2017). Effect of gravity and microgravity on intracranial pressure. *J. Physiol.* 595, 2115–2127. doi: 10.1113/JP273557

Mandsager, K. T., Robertson, D., and Diedrich, A. (2016). The function of the autonomic nervous system during spaceflight. *Clin. Auton. Res.* 25, 141–151. doi: 10.1007/s10286-015-0285-y

Navasiolava, N. M., Custaud, M.-A., Tomilovskaya, E. S., Larina, I. M., Mano, T., Gauquelin-Koch, G., et al. (2010). Long-term dry immersion: review and prospects. *Eur. J. Appl. Physiol.* 111, 1235–1260. doi: 10.1007/s00421-010-1750-x

Norsk, P. (2014). Blood pressure regulation IV: adaptive responses to weightlessness. *Eur. J. Appl. Physiol.* 114, 481–497. doi: 10.1007/s00421-013-2797-2

Rittweger, J., Winwood, K., Seynnes, O., Boer, M. D., Wilks, D., Lea, R., et al. (2006). Bone loss from the human distal tibia epiphysis during 24 days of unilateral lower limb suspension. *J. Physiol.* 577, 331–337. doi: 10.1113/jphysiol.2006.115782

Smith, J. D., Cromwell, R. L., Kundrot, C. E., and Charles, J. B. (2011). *Six-Degree Head-Down tilt Bed Rest: Forty Years of Development as a Physiological Analog for Weightlessness*. Washington, DC: NASA.

Taibbi, G., Cromwell, R. L., Zanello, S. B., Yarbough, P. O., Ploutz-Snyder, R. J., Godley, B. F., et al. (2016). Ocular outcomes comparison between 14- and 70-day head-down-tilt bed rest. *Investigat. Opthalmol. Vis. Sci.* 57, 495–501. doi: 10.1167/iovs.15-18530

Tesch, P. A., Lundberg, T. R., and Fernandez-Gonzalo, R. (2016). Unilateral lower limb suspension: from subject selection to "omic" responses. *J. Appl. Physiol.* 120, 1207–1214. doi: 10.1152/japplphysiol.01052.2015

Tomilovskaya, E., Shigueva, T., Sayenko, D., Rukavishnikov, I., and Kozlovskaya, I. (2019). Dry immersion as a ground-based model of microgravity physiological effects. *Fronti. Physiol.* 10:284. doi: 10.3389/fphys.2019.00284

Treffel, L., Massabuau, N., Zuj, K., Custaud, M.-A., Gauquelin-Koch, G., Blanc, S., et al. (2017). Pain and vertebral dysfunction in dry immersion: a model of microgravity simulation different from bed rest studies. *Pain Res. Manag.* 2017, 1–10. doi: 10.1155/2017/9602131

Wang, P., Wang, Z., Wang, D., Tian, Y., Li, F., Zhang, S., et al. (2015). Altered gravity simulated by parabolic flight and water immersion leads to decreased trunk motion. *PLoS One* 10:e0133398. doi: 10.1371/journal.pone.0133398

Watenpaugh, D. E. (2016). Analogs of microgravity: head-down tilt and water immersion. *J. Appl. Physiol.* 120, 904–914. doi: 10.1152/japplphysiol.00986.2015

Willis, I. (1973). The effects of prolonged water exposure on human skin. *J. Investigat. Dermatol.* 60, 166–171. doi: 10.1111/1523-1747.ep12682082

Zhang, L.-F., and Hargens, A. R. (2018). Spaceflight-induced intracranial hypertension and visual impairment: pathophysiology and countermeasures. *Physiol. Rev.* 98, 59–87. doi: 10.1152/physrev.00017.2016

Conflict of Interest: The authors declare that the research was conducted in the absence of any commercial or financial relationships that could be construed as a potential conflict of interest.

frontiers in Physiology

REVIEW
published: 20 August 2020
doi: 10.3389/fphys.2020.00952

Vascular and Microvascular Dysfunction Induced by Microgravity and Its Analogs in Humans: Mechanisms and Countermeasures

Nastassia Navasiolava[1], Ming Yuan[2], Ronan Murphy[3], Adrien Robin[1,4], Mickael Coupé[4], Linjie Wang[2], Asmaa Alameddine[4], Guillemette Gauquelin-Koch[5], Claude Gharib[6], Yinghui Li[2] and Marc-Antoine Custaud[1,4]**

[1] Clinical Research Center, CHU d'Angers, Angers, France, [2] State Key Laboratory of Space Medicine Fundamentals and Application, China Astronaut Research and Training Center (ACC), Beijing, China, [3] School of Health and Human Performance, Faculty of Science & Health, Dublin City University, Dublin, Ireland, [4] Mitovasc, UMR INSERM 1083-CNRS 6015, Université d'Angers, Angers, France, [5] Centre National d'Études Spatiales (CNES), Paris, France, [6] Institut NeuroMyoGène, Faculté de Médecine Lyon-Est, Université de Lyon, Lyon, France

Weightlessness and physical inactivity have deleterious cardiovascular effects. The space environment and its ground-based models offer conditions to study the cardiovascular effects of physical inactivity in the absence of other vascular risk factors, particularly at the macro- and microcirculatory levels. However, the mechanisms involved in vascular dysfunction and remodeling are not sufficiently studied in the context of weightlessness and its analogs including models of physical inactivity. Here, we summarize vascular and microvascular changes induced by space flight and observed in models of microgravity and physical inactivity and review the effects of prophylactic strategies (i.e., countermeasures) on vascular and microvascular function. We discuss physical (e.g., exercise, vibration, lower body negative pressure, and artificial gravity) and nutritional/pharmacological (e.g., caloric restriction, resveratrol, and other vegetal extracts) countermeasures. Currently, exercise countermeasure appears to be the most effective to protect vascular function. Although pharmacological countermeasures are not currently considered to fight vascular changes due to microgravity, nutritional countermeasures are very promising. Dietary supplements/natural health products, especially plant extracts, should be extensively studied. The best prophylactic strategy is likely a combination of countermeasures that are effective not only at the cardiovascular level but also for the organism as a whole, but this strategy remains to be determined.

Keywords: vascular deconditioning, endothelium, vascular remodeling, vascular risk, prevention, shear stress

OPEN ACCESS

Edited by:
Alan R. Hargens, University of California, San Diego, United States

Reviewed by:
Philippe L. Arbeille, Centre Hospitalier Universitaire Trousseau de Tours, France
Michael D. Delp, Florida State University, United States
Martina Heer, International University of Applied Sciences Bad Honnef, Germany

***Correspondence:**
Yinghui Li
yinghuidd@vip.sina.com
Marc-Antoine Custaud
macustaud@chu-angers.fr

Specialty section:
This article was submitted to Environmental, Aviation and Space Physiology, a section of the journal Frontiers in Physiology

Received: *28 February 2020*
Accepted: *14 July 2020*
Published: *20 August 2020*

Citation:
Navasiolava N, Yuan M, Murphy R, Robin A, Coupé M, Wang L, Alameddine A, Gauquelin-Koch G, Gharib C, Li Y and Custaud M-A (2020) Vascular and Microvascular Dysfunction Induced by Microgravity and Its Analogs in Humans: Mechanisms and Countermeasures. Front. Physiol. 11:952. doi: 10.3389/fphys.2020.00952

INTRODUCTION

A host of physiological alterations occur in actual or simulated microgravity, including fluid changes, hormonal changes, muscle atrophy and force reduction, bone loss, autonomic dysregulation, cardiac atrophy, vascular impairment, and microcirculatory dysfunction (Coupé et al., 2009; Evans et al., 2018; Hughson et al., 2018). Surprisingly, the cardiovascular system of astronauts adapts well to microgravity. However, the price of this adaptation is rapid cardiovascular deconditioning – a syndrome combining orthostatic intolerance, increased heart rate, and decreased exercise capacity, accompanied by vascular disorders. Similar cardiovascular deconditioning is also observed on Earth and was first described in bedridden patients in 1945 (Keys, 1945). Physical inactivity is one of the key factors contributing to this cardiovascular deconditioning.

Sedentariness is among the most important behavioral risk factors for cardiovascular diseases (CVD). In terms of the cardiovascular system, the risk of being unfit exceeds the risks associated with smoking, elevated blood pressure, hypercholesterolemia, or obesity, whereas regular exercise is associated with a reduction in vascular events (Thijssen et al., 2010). Studying physical inactivity in healthy individuals in the absence of other vascular risk factors provides valuable information concerning vascular diseases. Because fighting gravity requires daily physical exercise, exposure to microgravity is associated with enhanced inactivity (Hughson, 2009; Hughson et al., 2018). Microgravity and its analogs – bed rest, head-down bed rest (HDBR) (Fortney et al., 1996; Pavy-Le Traon et al., 2007), and dry immersion (Navasiolava et al., 2011; Watenpaugh, 2016; Tomilovskaya et al., 2019) – offer unique models for studying the effects of global physical inactivity in healthy individuals (Widlansky, 2010). However, other models of pure physical inactivity are also valuable, such as remaining in a sitting position for a few hours (Restaino et al., 2015; Thosar et al., 2015; Morishima et al., 2016) or reducing walking to below 5,000 steps/day, which is easy to implement and is shown to impair vascular and metabolic functions (Boyle et al., 2013; Teixeira et al., 2017). Segmental inactivity models are also used, with unilateral lower limb suspension (Bleeker et al., 2005a,c) and limb casting (Green et al., 1997; Sugawara et al., 2004) being less extreme models. Although confinement has also been considered a model of spaceflight (Arbeille et al., 2014; Yuan et al., 2019), its associated inactivity is difficult to attest.

Several countermeasures to prevent microgravity- and inactivity-induced cardiovascular changes, including exercise, whole body vibration (WBV), lower body negative pressure (LBNP), centrifugation, caloric restriction, nutritional supplements, natural health products, and medications, have been evaluated. The protection of astronaut health is a critical issue in space medicine. However, knowledge acquired in this area could be extended to the general sedentary population.

Here, we will summarize the effects of microgravity and its analogs on macro- and microcirculation in humans. We will also review the effects of different countermeasures proposed in the context of microgravity and its analogs on vascular and microvascular functions.

VASCULAR AND MICROVASCULAR CHANGES INDUCED BY PHYSICAL INACTIVITY AND MICROGRAVITY

Conduit Artery Changes

Data on lower limb, brachial, and carotid arterial changes in modeled and actual microgravity are summarized in **Tables 1–4**.

Physical Inactivity Induces Structural Changes in Conduit Arteries

Physical inactivity has a marked effect on the structure of conduit arteries. For lower limb arteries, particularly unloaded in our models, physical inactivity is associated with inward remodeling and decreased lumen diameter to differing degrees (Sugawara et al., 2004; Bleeker et al., 2005a,b; de Groot et al., 2006; van Duijnhoven et al., 2010a; Palombo et al., 2015; Yuan et al., 2015) depending on intensity and duration of inactivity (Thijssen et al., 2010). Intima media thickness (IMT) at the femoral artery level remains unchanged after short-term inactivity, such as 7-day leg casting (Sugawara et al., 2004) and after 35-day HDBR (Palombo et al., 2015), but increases with longer inactivity, such as 60-day HDBR (van Duijnhoven et al., 2010a). At the carotid artery level, diameter remains unchanged (Arbeille et al., 1999; Bleeker et al., 2005b; van Duijnhoven et al., 2010a,b; Palombo et al., 2015; Yuan et al., 2015). For brachial artery, which is generally not unloaded in our models, diameter remains stable (Bonnin et al., 2001; de Groot et al., 2004; Hughson et al., 2007) or is very slightly decreased (Boyle et al., 2013; Bleeker et al., 2005b; Hamburg et al., 2007). IMT at the carotid level is unmodified (Palombo et al., 2015; Yuan et al., 2015) or increased (van Duijnhoven et al., 2010a) after long-term HDBR. Long-term confinement also increases carotid IMT as evidenced from Mars-520d (Arbeille et al., 2014) and CELSS-180d (Yuan et al., 2019) experiments. Concerning macrovascular elasticity at the femoral level, 35-day HDBR does not affect compliance (Palombo et al., 2015), whereas 7-day leg casting tends to decrease (Sugawara et al., 2004) and 60-day HDBR decreases compliance (Yuan et al., 2015). Carotid compliance is not modified by HDBR (Palombo et al., 2015; Yuan et al., 2015) or confinement (Yuan et al., 2019).

Regarding flight findings, a 6-month mission did not modify femoral or carotid diameter but rapidly and steadily increased carotid IMT up to 10–12% (Arbeille et al., 2016). Similarly, in the National Aeronautics and Space Administration twin study with one astronaut and one ground control, a 1-year mission increased carotid IMT by ∼20% (Garrett-Bakelman et al., 2019). However, Lee et al. (2020) did not observe changes in carotid IMT and stiffness at d15, d60, and d160 of long-term flight, while carotid diameter was increased (+5% during diastole). Lee et al. consider possibility that increase in IMT might be hidden by carotid distention. Findings from several inflight studies suggest that most astronauts represent increase in IMT. Presently no environmental (physical activity, nutrition, stress. . .) or genetic factor has been identified as a major factor related to this increase. Femoral IMT increases up to 10–15% (Arbeille et al., 2016; Hughson et al., 2018). Carotid (Hughson et al., 2016; Arbeille et al., 2017; Hughson et al., 2018) and femoral (Arbeille

TABLE 1 | Lower limb conduit arteries: effects of experimental models and countermeasures.

Variable	Inactivity model	Duration	Subjects Ctrl/CM	Vascular level	Estimated inactivity effect (without CM)	CM tested	Estimated CM effects	References
Diameter	Sitting	3 h	7M + 4F	Popliteal	No effect	Unilateral fidgeting bouts	No effect	Morishima et al. (2016)
	< 5,000 steps/d	5 d	11M	Popliteal	No effect	_	_	Boyle et al. (2013)
	< 5,000 steps/d	5 d	13M	Popliteal	↓2% (NS)	Unilateral foot heating bouts	Partly prevented (↓1% (NS))	Teixeira et al. (2017)
	Unilateral leg cast	7 d	8M	Femoral	↓5%	Contralateral leg	Completely prevented	Sugawara et al. (2004)
	Unilateral leg suspension	28 d	3M + 4F	Femoral	↓12%	Contralateral leg	Completely prevented	Bleeker et al. (2005a)
	Horizontal BR	25 d	8M/8M	Femoral	↓13%	RVE	Partially prevented (↓5%)	Bleeker et al. (2005b)
	HDBR	35 d	10M	Femoral	↓10%	_	_	Palombo et al. (2015)
	Horizontal BR	52 d	8M/8M	Femoral	↓17%	RVE	Partially prevented (↓6%)	Bleeker et al. (2005b)
	HDBR	56 d	7F/8F	Femoral	No effect	LBNP + aerobic + RE	No effect	Zuj et al. (2012b)
	HDBR	60 d	7M/7M	Femoral	↓33%	CHM	No effect	Yuan et al. (2015)
	HDBR	60 d	9M/9M	Femoral	↓24%	RE	No effect	van Duijnhoven et al. (2010a)
	HDBR	60 d	9M/9M	Femoral	↓24%	RVE	Partially prevented	van Duijnhoven et al. (2010a)
IMT	Unilateral leg cast	7 d	8M	Femoral	No effect	Contralateral leg	No effect	Sugawara et al. (2004)
	HDBR	35 d	10M	Femoral	No effect	_	_	Palombo et al. (2015)
	HDBR	60 d	9M/9M	Femoral	↑12%	RE	Prevented	van Duijnhoven et al. (2010a)
	HDBR	60 d	9M/9M	femoral	↑12%	RVE	Prevented	van Duijnhoven et al. (2010a)
Stiffness	Unilateral leg cast	7 d	8M	Femoral	↓ (NS)	Contralateral leg	Completely prevented	Sugawara et al. (2004)
	HDBR	35 d	10M	Femoral	no effect	_	_	Palombo et al. (2015)
	HDBR	60 d	7M/7M	Femoral	↑	CHM	No effect	Yuan et al. (2015)
Flow-mediated dilation	Sitting	3 h	12M crossover	Femoral	↓2-3%	Three bouts of 5-min walking	Completely prevented	Thosar et al. (2015)
	Sitting	3 h	7M+4F	popliteal	↓3%	Unilateral fidgeting bouts	↑3%	Morishima et al. (2016)
	Sitting	6 h	11M	Popliteal	↓4%	10-min walk post-sitting	Restored	Restaino et al. (2015)
	<5,000 steps/d	5 d	11M	Popliteal	↓3%	_	_	Boyle et al. (2013)
	< 5,000 steps/d	5 d	13M	Popliteal	↓4%	Unilateral foot heating bouts	Completely prevented	Teixeira et al. (2017)
	Unilateral leg suspension	28 d	3M + 4F	Femoral	↑3–4%	_	_	Bleeker et al. (2005a)
	Horizontal BR	25 d	8M/8M	Femoral	↑4%	RVE	Completely prevented	Bleeker et al. (2005b)

(Continued)

TABLE 1 | Continued

Variable	Inactivity model	Duration	Subjects Ctrl/CM	Vascular level	Estimated inactivity effect (without CM)	CM tested	Estimated CM effects	References
	HDBR	49 d	8M+5F	Tibial	↑5%	_	_	Platts et al. (2009)
	Horizontal BR	52 d	8M/8M	Femoral	↑4%	RVE	No effect	Bleeker et al. (2005b)
	HDBR	60 d	9M/9M	Femoral	↑7%	RE	Partially prevented (NS)	van Duijnhoven et al. (2010b)
	HDBR	60 d	9M/9M	Femoral	↑7%	RVE	Completely prevented	van Duijnhoven et al. (2010b)
Nitroglycerin-mediated dilation	Unilateral leg suspension	28 d	3M+4F	Femoral	↑4–5%	_	_	Bleeker et al. (2005a)
	Horizontal BR	25 d	8M/8M	Femoral	No effect	RVE	No effect	Bleeker et al. (2005b)
	HDBR	49 d	8M + 5F	Tibial	↑6–7% (NS)	_	_	Platts et al. (2009)
	Horizontal BR	52 d	8M/8M	Femoral	↑4%	RVE	No effect	Bleeker et al. (2005b)
	HDBR	56 d	7F/8F	Femoral	No effect	LBNP + aerobic + RE	No effect	Zuj et al. (2012b)

BR, bed rest; CHM, Chinese herbal medicine; CM, countermeasure; RE, resistive exercise; RVE, resistive vibration exercise; F, female; M, male; NS, not significant.

TABLE 2 | Common carotid artery: effects of experimental models and countermeasures.

Variable	Inactivity model	Duration	Subjects Ctrl/CM	Estimated inactivity effect (without CM)	CM tested	Estimated CM effects	References
Diameter	HDBR	7 d	8M crossover	↓5% (NS)	Thigh cuffs	No effect	Arbeille et al. (1999)
	HDBR	35 d	10M	No effect	_	_	Palombo et al. (2015)
	Horizontal BR	52 d	8M/8M	No effect	RVE	No effect	Bleeker et al. (2005b)
	HDBR	60 d	7M/7M	No effect	CHM	No effect	Yuan et al. (2015)
	HDBR	60 d	9M/9M	No effect	RE	No effect	van Duijnhoven et al. (2010a; 2010b)
	HDBR	60 d	9M/9M	No effect	RVE	No effect	van Duijnhoven et al. (2010a; 2010b)
IMT	Confinement	180 d	3M+1F	↑10–15%	_	_	Yuan et al. (2019)
	Confinement	520 d	6M	↑14–28%	_	_	Arbeille et al. (2014)
	HDBR	35 d	10M	No effect	_	_	Palombo et al. (2015)
	HDBR	60 d	7M/7M	No effect	CHM	No effect	Yuan et al. (2015)
	HDBR	60 d	9M/9M	↑17%	RE	Completely prevented	van Duijnhoven et al. (2010a)
	HDBR	60 d	9M/9M	↑17%	RVE	Completely prevented	van Duijnhoven et al. (2010a)
Stiffness	Confinement	180 d	3M+1F	No effect	_	_	Yuan et al. (2019)
	HDBR	35 d	10M	No effect	_	_	Palombo et al. (2015)
	HDBR	60 d	7M/7M	No effect	CHM	No effect	Yuan et al. (2015)

BR, bed rest; CHM, Chinese herbal medicine; CM, countermeasure; RE, resistive exercise; RVE, resistive vibration exercise; F, female; M, male; NS, not significant.

et al., 2017; Hughson et al., 2018) stiffness are also increased. Moreover, a 6-month flight reduced pulse transit time, suggesting stiffer central and peripheral arteries (Hughson et al., 2018). Limb conduit artery tone, as estimated by rheography, increased in a 6-month flight at the forearm but not at the calf level (Turchaninova et al., 2001).

Physical Inactivity and the Reactivity of Conduit Arteries

At the leg level, brief inactivity, such as that induced by a few hours of sitting, decreases endothelium-dependent vasodilation capacity as estimated by flow mediated dilation (FMD) (Restaino et al., 2015; Thosar et al., 2015; Morishima et al., 2016). Similarly, reducing daily physical activity by taking <5,000 steps/day decreases FMD response at the popliteal level, whereas basal popliteal diameter is unchanged (Boyle et al., 2013; Teixeira et al., 2017). In both cases, intermittent application of maneuvers increasing blood flow, such as fidgeting (Morishima et al., 2016) or foot heating to 42°C (Teixeira et al., 2017), preserves popliteal FMD. However, prolonged advanced inactivity does not change (de Groot et al., 2004) or even increases (Bleeker et al., 2005a,b; de Groot et al., 2006; Platts et al., 2009; van Duijnhoven et al., 2010b) FMD of leg arteries, which may be explained by inward remodeling of arterial vessels at the lower limb level. Smooth

TABLE 3 | Brachial artery: effects of experimental models and countermeasures.

Variable	Inactivity model	Duration	Subjects Ctrl/CM	Estimated inactivity effect (without CM)	CM tested	Estimated CM effects	References
Diameter	<5,000 steps/d	5 d	11M	↓5%	_	_	Boyle et al. (2013)
	Horizontal BR	5 d	14M+6F	↓2–3%	_	_	Hamburg et al. (2007)
	HDBR	7 d	8M/8M	No effect	Usual daily activity	No effect	Bonnin et al. (2001)
	Horizontal BR	52 d	8M/8M	↓6%	RVE	No effect	Bleeker et al. (2005b)
	HDBR	56 d	16F/8F	No effect	LBNP + aerobic + RE	No effect	Hughson et al. (2007)
IMT	HDBR	49 d	8M+5F	No effect	_	_	Platts et al. (2009)
Flow-mediated dilation	Sitting	6 h	11M	No effect	10-min walk post-sitting	No effect	Restaino et al. (2015)
	<5,000 steps/d	5 d	11M	no effect	_	_	Boyle et al. (2013)
	Horizontal BR	5 d	14M + 6F	No effect	_	_	Hamburg et al. (2007)
	HDBR	7 d	8M/8M	↑5%	Usual daily activity	Completely prevented	Bonnin et al. (2001)
Nitroglycerin-mediated dilation	Horizontal BR	5 d	14M+6F	No effect	_	_	Hamburg et al. (2007)
	HDBR	7 d	8M/8M	No effect	Usual daily activity	No effect	Bonnin et al. (2001)
	HDBR	49 d	8M+5F	No effect	_	_	Platts et al. (2009)

BR, bed rest; CM, countermeasure; RE, resistive exercise; RVE, resistive vibration exercise; F, female; M, male.

muscle vasodilator functions of large arteries are not impaired and may be enhanced after physical inactivity. At the brachial level, no significant changes in sensitivity to nitric oxide (NO) are observed after 5, 7, 49, or 56 days of bed rest (Bonnin et al., 2001; Hamburg et al., 2007; Platts et al., 2009). Changes at the lower limb level are less homogenous. Vasodilation in response to nitroglycerin is unmodified after 25 days of horizontal bed rest (Bleeker et al., 2005b) or 56 days of HDBR (Zuj et al., 2012b), tends to increase after 49 days of HDBR (Platts et al., 2009), and increases after 28 days of unilateral lower limb suspension (Bleeker et al., 2005a) or 52 days of horizontal bed rest (Bleeker et al., 2005b).

As for inflight reactivity of large arteries, endothelium-dependent and –independent vasodilation at brachial artery level is not substantially modified with long-term flight, while brachial diameter is unchanged (n = 13, measurements at d15, d60, d160; Lee et al., 2020).

Resistance Vessels and Microcirculation

Systemic Vascular Resistance

Total peripheral resistance characterizes in a integrative way the global resistance of all the systemic vasculature. In most HDBR and dry immersion studies, systemic vascular resistance is increased (Pavy-Le Traon et al., 2007; Navasiolava et al., 2011). By contrast, in inflight studies, systemic vascular resistance seems to be decreased as indirectly deduced from a measured decrease in blood pressure and increase in cardiac output, despite preserved or even increased sympathetic nervous activity (Norsk, 2019). Mechanisms for this unexpected systemic vasodilation remain to be identified. Proposed contributors are a headward fluid shift-induced decrease in lower body vessel stretch (with reduced myogenic tone), cardiac distention (with release of cardiac vasodilatory natriuretic peptides), and increased core body temperature (Norsk, 2019).

Regional and Organ Circulations

Data on changes at arteriolar and microcirculatory level in actual and modeled microgravity are summarized in **Tables 4**, **5**.

Lower- and upper limb vascular resistance

Limb vascular resistance can be measured directly at rest by Doppler ultrasound and estimated indirectly during inflation-deflation dynamic test by plethysmography. The assessment method for each result is indicated in **Tables 4**, **5**. At the lower limb level, most plethysmographic studies demonstrate a decrease in resting blood flow (Louisy et al., 1997; Christ et al., 2001; Bleeker et al., 2005a; Navasiolava et al., 2010) and increase in vascular resistance after inactivity (Kamiya et al., 2000; Pawelczyk et al., 2001), although some do not detect changes (Bonde-Petersen et al., 1994; Bleeker et al., 2005b). At the upper limb level, resting blood flow and resistance remain mostly unmodified by inactivity (Bonde-Petersen et al., 1994; Green et al., 1997; Pawelczyk et al., 2001; Bleeker et al., 2005b), although some studies report a decrease in resting flow (Crandall et al., 2003; Hesse et al., 2005). Furthermore, a lack of increase in lower limb vascular resistance (insufficient vasoconstriction) in response to LBNP was observed following 60-day HDBR in women, together with unmodified total sympathetic nerve activity as assessed by microneurography, suggesting that deconditioning concerned rather the distal vascular tree targets (vasomotor response) than autonomic regulation (Arbeille et al., 2008).

Regarding flight findings, calf resting flow decreased and vascular resistance increased early inflight (days 4–12), as estimated by plethysmography (Watenpaugh et al., 2001). On the other hand, direct measurement from femoral arterial flow revealed significant decrease of lower limb vascular resistance in 14-day and 6-month flight (Arbeille et al., 1995, 2001). A lack of increase in lower limb vascular resistance (vasoconstriction) in response to LBNP at 1st and 5th month of flight was documented,

TABLE 4 | Vascular changes induced by spaceflight.

Vascular level	Variable	Measurement timepoints	*n*	Flight effect	References
Central and peripheral vessels	Heart-finger pulse transit time	6 mo	8	↓5–6%	Hughson et al. (2016)
	Heart-ankle pulse transit time	6 mo	8	↓2–3%	Hughson et al. (2016)
Carotid	IMT	d15	10	↑10%	Arbeille et al. (2016)
	IMT	d115–165	10	↑12%	Arbeille et al. (2016)
	IMT	d15, d60, and d160	13	No effect	Lee et al. (2020)
	IMT	m1, m2, m6, m8, and m10	1	↑∼20%	Garrett-Bakelman et al. (2019)
	Diameter	d15 and d115–165	10	No effect	Arbeille et al. (2016)
	Diameter	m1, m2, m6, m8, and m10	1	↑∼7%	Garrett-Bakelman et al. (2019)
	Diameter	d15, d60, and d160	13	↑∼5%	Lee et al. (2020)
	Stiffness	pre/post 6-mo flight	8	↑17–30%	Hughson et al. (2016)
	Stiffness	Inflight 6-mo flight	10		Arbeille et al. (2017)
	Stiffness	d15, d60, and d160	13	No effect	Lee et al. (2020)
Upper limb	Brachial diameter	d15, d60, and d160	13	No effect	Lee et al. (2020)
	Brachial FMD	d15, d60, and d160	13	No effect	Lee et al. (2020)
	Brachial nitroglycerin-mediated dilation	d15, d60, and d160	13	No effect	Lee et al. (2020)
	Pulse blood filling	6 mo	11	↓12%	Turchaninova et al. (2001)
	Conduit arteries vascular tone (rheography)	6 mo	11	↑23%	Turchaninova et al. (2001)
	Pre-capillary vascular tone (rheography)	6 mo	11	↓60%	Turchaninova et al. (2001)
Lower limb	Femoral IMT	d15	10	↑10%	Arbeille et al. (2016)
	Femoral IMT	d115–165	10	↑15%	Arbeille et al. (2016)
	Femoral diameter	d15, d115–165	10	No effect	Arbeille et al. (2016)
	Femoral stiffness	d15, d115–165	10	↑20–30% (NS)	Arbeille et al. (2017)
	Resting vasular resistance (ultrasound)	1–6 mo	7	↓10%	Arbeille et al. (2001, 1995)
	Vasular resistance response to LBNP (ultrasound)	6 mo	7	↓(+40% pre vs +15% inflight)	Herault et al. (2000)
	Resting blood flow (ultrasound)	1–6mo	7	No effect	Arbeille et al. (2001)
	Resting blood flow (plethysmography)	d4–12	7	↓41%	Watenpaugh et al. (2001)
	Vascular resistance (plethysmography)	d4–12	7	↑93%	Watenpaugh et al. (2001)
	Pulse blood filling	6 mo	11	↓19%	Turchaninova et al. (2001)
	Conduit arteries vascular tone (rheography)	6 mo	11	No effect	Turchaninova et al. (2001)
	Pre-capillary vascular tone (rheography)	6 mo	11	No effect	Turchaninova et al. (2001)

as measured by Doppler ultrasound (Herault et al., 2000), similar to what observed in HDBR.

Rheography in a 6-month mission revealed pulse blood filling decrease at the forearm (−12%) and shin (−19%) levels. Also, pre-capillary vascular tone decreased at the forearm but not at the calf level (Turchaninova et al., 2001).

Cerebral circulation and question of spaceflight associated neuro-ocular syndrome (SANS)

Data concerning microgravity effect on cerebral autoregulation are controversial. Indeed, bed rest has been reported to impair (Zhang et al., 1997; Sun et al., 2005), or to maintain (Pavy-Le Traon et al., 2002), or to improve (Jeong et al., 2014; Kermorgant et al., 2019) cerebral autoregulation. Similarly, in astronauts cerebral autoregulation might be impaired (Zuj et al., 2012a), preserved (Herault et al., 2000; Arbeille et al., 2001; Iwasaki et al., 2007), or improved (Iwasaki et al., 2007). However, cerebral vascular resistance in flight remains globally stable (Arbeille et al., 1995, 2001).

Spaceflight associated neuro-ocular syndrome represents an issue for future long-term manned missions. SANS manifestations include fundus anomalies like optic disk edema, globe flattening, choroidal and retinal folds, nerve fiber layer infarcts (cotton wool spots), and hyperopic refractive error shifts (Lee et al., 2018). SANS can't be purely attributed to vascular problems. Current paradigm relates SANS rather to cephalad and

TABLE 5 | Regional limb circulation: effects of experimental models and countermeasures.

Vascular level	Variable	Inactivity model	Duration	Subjects Ctrl/CM	Estimated inactivity effect (without CM)	CM tested	Estimated CM effects	References
Lower limb	Resting blood flow (plethysmography)	Unilateral leg suspension	28 d	3M + 4F	↓24%	Contralateral leg	Completely prevented	Bleeker et al. (2005a)
	Resting blood flow (plethysmography)	HDBR	41 d	7M	↓49%	_	_	Louisy et al. (1997)
	Resting blood flow (ultrasound)	Horizontal BR	52 d	8M	No effect	RVE	no effect	Bleeker et al. (2005b)
	Resting blood flow (ultrasound)	HDBR	4, 7, and 42 d	8M	No effect	_	_	Arbeille et al. (2001)
	Resting blood flow (plethysmography)	HDBR	118 d	6M	↓43%	_	_	Christ et al. (2001)
	Vascular resistance (plethysmography)	HDBR	14 d	20M	↑50%	_	_	Kamiya et al. (2000)
	Vascular resistance (plethysmography)	HDBR	18 d	11M + 1F	↑35%	_	_	Pawelczyk et al. (2001)
	Vascular resistance (ultrasound)	HDBR	7 and 42 d	8M	↓10–20%	_	_	Arbeille et al. (2001)
	Vascular resistance (plethysmography)	Horizontal BR	20 d	6M+3F	No effect	_	_	Bonde-Petersen et al. (1994)
	Constriction to incremental L-NMMA (NO synthase inhibitor) (plethysmography)	Unilateral leg suspension	28 d	3M+4F	No effect	_	_	Bleeker et al. (2005c)
	Dilation post-occlusion (ultrasound)	Sitting	6 h	11M	↓43%	10-min walk post-sitting	restored	Restaino et al. (2015)
	Dilation post-occlusion (plethysmography)	Horizontal BR	5 d	10/9	↓22%	usual activity	completely prevented	Hamburg et al. (2007)
	Dilation to incremental SNP (plethysmography)	Unilateral leg suspension	28 d	3M + 4F	No effect	_	_	Bleeker et al. (2005c)
	Vasoconstriction to LBNP (ultrasound)	HDBR	28 d	6M/6M	Impaired vasoconstrictive response	Exercise + LBNP	Completely prevented	Arbeille et al. (1995)
	Vasoconstriction to LBNP (ultrasound)	HDBR	55 d	8F/8F	Impaired vasoconstrictive response	LBNP + aerobic + RE	Completely prevented	Arbeille et al. (2008)
Calf skin	Resting blood flow (laser Doppler)	Dry immersion	7 d	8M	↓30–40%	_	_	Navasiolava et al. (2010)
	Resting blood flow (laser Doppler)	HDBR	56 d	8F/8F	↓20% (NS)	LBNP + aerobic + RE	Completely prevented	Demiot et al. (2007)
	Resting blood flow (laser Doppler)	HDBR	60 d	7M/7M	↓30% (NS)	CHM	No effect	Yuan et al. (2015)
	Max dilation to heating (laser Doppler)	Dry immersion	7 d	8M	No effect	_	_	Navasiolava et al. (2010)
	Max dilation to heating (laser Doppler)	HDBR	56 d	8F/8F	No effect	LBNP + aerobic + RE	No effect	Demiot et al. (2007)
	Max dilation to heating (laser Doppler)	HDBR	60 d	7M/7M	No effect	CHM	No effect	Yuan et al. (2015)
	Dilation to ACh (laser Doppler)	Dry immersion	7 d	8M	↓17%	_	_	Navasiolava et al. (2010)
	Dilation to ACh (laser Doppler)	HDBR	56 d	8F/8F	↓11%	LBNP + aerobic + RE	Completely prevented	Demiot et al. (2007)
	Dilation to ACh (laser Doppler)	HDBR	60 d	7M/7M	↓15%	CHM	Completely prevented	Yuan et al. (2015)
	Dilation to SNP (laser Doppler)	Dry immersion	7 d	8M	No effect	_	_	Navasiolava et al. (2010)
	Dilation to SNP (laser Doppler)	HDBR	56 d	8F/8F	No effect	LBNP + aerobic + RE	No effect	Demiot et al. (2007)

(Continued)

TABLE 5 | Continued

Vascular level	Variable	Inactivity model	Duration	Subjects Ctrl/CM	Estimated inactivity effect (without CM)	CM tested	Estimated CM effects	References
	Dilation to SNP (laser Doppler)	HDBR	60 d	7M/7M	No effect	CHM	No effect	Yuan et al. (2015)
Upper limb	Resting blood flow (plethysmography)	HDBR	13 d	10M	↓19% (NS)	Low fat hypoenergetic diet (crossover)	No effect	Hesse et al. (2005)
	Resting blood flow (plethysmography)	HDBR	14 d	8/12	↓15%	Cycle ergometry	No effect	Crandall et al. (2003)
	Resting blood flow (plethysmography)	Forearm cast	42 d	6M/6M	No effect	Non-casted controls	No effect	Green et al. (1997)
	Resting blood flow (ultrasound)	Horizontal BR	52 d	8M/8M	No effect	RVE	No effect	Bleeker et al. (2005b)
	Resting resistance (plethysmography)	HDBR	18 d	11M + 1F	No effect	_	_	Pawelczyk et al. (2001)
	Resting resistance (plethysmography)	Horizontal BR	20 d	6M + 3F	No effect	_	_	Bonde-Petersen et al. (1994)
	Dilation to incremental ACh (plethysmography)	HDBR	13 d	10M	↓	Low fat hypoenergetic diet (crossover)	Completely prevented	Hesse et al. (2005)
	Constriction to L-NMMA (NO synthase inhibitor) (plethysmography)	Forearm cast	42 d	6M/6M	no effect	Non-casted controls	No effect	Green et al. (1997)
	Dilation post-occlusion (ultrasound)	Sitting	6 h	11M	↓31%	10-min walk post-sitting	No effect	Restaino et al. (2015)
	Dilation post-occlusion (ultrasound)	Horizontal BR	5 d	14M+6F/9	↓16%	Usual activity		Hamburg et al. (2007)
	Dilation post-occlusion (plethysmography)	HDBR	14 d	20M	↓30%	_	_	Shoemaker et al. (1998)
	Dilation to incremental SNP (plethysmography)	HDBR	13 d	10M	No effect	Low fat hypoenergetic diet (crossover)	No effect	Hesse et al. (2005)
	Dilation to heating (plethysmography)	HDBR	14 d	8/12	↓13%	Cycle ergometry	Completely prevented	Crandall et al. (2003)
Forearm skin	Dilation to ACh (laser Doppler)	Confinement	180 d	3M+1F	↓17%	_	_	Yuan et al. (2019)

BR, bed rest; CHM, Chinese herbal medicine; CM, countermeasure; RE, resistive exercise; RVE, resistive vibration exercise; F, female; M, male; NS, not significant.

orbital fluid transfer and chronic changes in intracranial pressure (Lee et al., 2018). The possible role of lymphatics and the venous system in SANS is under study. Indeed, microgravity-induced upward fluid redistribution induces jugular vein congestion (Herault et al., 2000; Arbeille et al., 2001).

Renal circulation

Similarly to brain, renal hemodynamics is characterized by high flow rate, is highly auto-regulated and not much affected by physical inactivity. Renal blood flow consists ∼20% of cardiac output at rest for kidneys mass of ∼0.4% body weight, to enable sufficient glomerular filtration rate of ∼180 L/day for precise regulation of fluid-volume homeostasis. In spaceflight renal plasma flow is stable, glomerular filtration rate is stable or increased, and filtration fraction tends to increase (Kramer et al., 2001). Thus we don't expect substantial microgravity-induced renal vascular dysfunction.

Endothelium-Dependent Vasodilation

Many physical inactivity studies show impaired endothelium-dependent vasodilation of microvessels, contrary to that observed for conduit arteries. Reduced reactive post-occlusion hyperemic responses are observed at the leg level after 6-h sitting (Restaino et al., 2015), at the forearm level after 14-day HDBR (Shoemaker et al., 1998), and at both leg and forearm levels after 5-day horizontal bed rest (Hamburg et al., 2007). Fourteen-day HDBR diminishes forearm skin vasodilation in response to heating (Crandall et al., 2003). Attenuation of endothelium-dependent vasodilation, measured using laser Doppler coupled with acetylcholine (ACh) iontophoresis, was observed in the calf skin after 2-month HDBR in men (Yuan et al., 2015) and women (Demiot et al., 2007) and after 7-day dry immersion (Navasiolava et al., 2010), as well as in forearm skin after 6-month confinement (Yuan et al., 2019). Similarly, Hesse et al. (2005) found reduced dilation in response to ACh

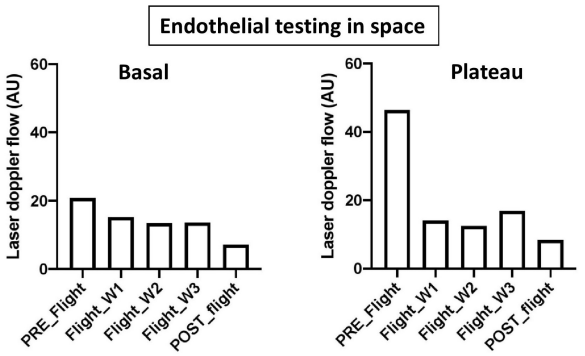

FIGURE 1 | ACh testing with iontophoresis at the forearm skin level in two astronauts during the Tiangong -2 3-week space flight (W1, W2, W3). Basal, skin blood flow before ACh stimulation; Plateau, plateau phase of endothelium-dependent vasodilation after ACh stimulation. Data are mean values.

assessed by plethysmography at the forearm level after 2-week HDBR.

Regarding flight findings, during the Tiangong-2 Chinese 3-week space mission, we assessed basal skin blood flow and endothelium-dependent vasodilation at the forearm level using laser Doppler flowmetry coupled with ACh iontophoresis (integrated in the Cardiospace system, CNES/ACC; for technical details, see Li et al., 2019). During and after flight, we observed a slight decrease in basal skin blood flow and an almost complete absence of ACh-induced vasodilation at the plateau phase, indicating endothelial impairment (**Figure 1**).

Endothelium-Independent Vasodilation

Microcirculatory smooth muscle vasodilator function appears to be preserved after physical inactivity. Endothelium-independent vasodilation in response to the NO donor sodium nitroprusside (SNP) remains unchanged at the arm resistance vessel level after 13 days of HDBR (Hesse et al., 2005) and at the skin microcirculatory level after 2 months of HDBR (Demiot et al., 2007) or 7 days of dry immersion (Navasiolava et al., 2010). Dilation in response to incremental SNP infusion at the leg resistance vessel level is not altered by 4-week leg suspension (Bleeker et al., 2005c). Also, NO contribution to baseline vascular tone as estimated by NO synthase blockage is not altered by 6-week forearm cast (Green et al., 1997) or 4-week leg suspension (Bleeker et al., 2005c).

These studies suggest that the global increase in vascular resistance induced by physical inactivity is not necessarily explained by an impairment of NO dilator pathways. Unlike conduit arteries, for which endothelium-dependent vasodilation predominantly occurs via the NO pathway, three vasodilative pathways (i.e., NO, prostaglandin, and EDHF) are important for resistive vessels. Thus, at the microcirculatory level prostaglandin or EDHF pathways should be taken into account also, as well as neurovascular interactions.

Circulating Markers of Endothelial State

Endothelial state markers are also impaired by physical inactivity. Data are summarized in **Table 6**. The number of circulating endothelial cells is increased after 2-month HDBR (Demiot et al., 2007). Circulating endothelial microparticles of an apoptotic phenotype increase after 5-day step limitation (Boyle et al., 2013), 7-day dry immersion (Navasiolava et al., 2010), and 60-day HDBR (Yuan et al., 2015). Some circulating angiogenic cell populations are reduced after 10-day limitation of high-intensity exercise in athletic individuals (Guhanarayan et al., 2014). Of note, endothelial glycocalyx, as assessed by blood levels of its components, is not altered after 5-day HDBR (Feuerecker et al., 2013). After 7-day dry immersion, the plasma level of VEGF decreases, whereas that of soluble E-selectin is unchanged, suggesting a decrease in antiapoptotic tone rather than inflammatory activation (Navasiolava et al., 2010). Soluble CD146, an endothelial molecule that appears to be involved in permeability and angiogenesis, is slightly decreased under 6-month confinement, 7-day dry immersion, and 4-day HDBR (Yuan et al., 2019) (**Figure 2**). These markers are likely mainly derived from the microvasculatory endothelium, considering that it is more extensive and more sensitive to physical inactivity than endothelium from large vessels.

Venous Circulation

Venous compartment has a capacitance reservoir function contributing to cardiac output control. Venous functions characteristics are complex, and include filling/emptying properties, muscular pump efficiency, microvascular filtration. Microgravity-induced venous alterations represent an important issue worth an extensive review paper. Here we discuss venous changes only briefly.

Jugular Veins

In 2019 the first episode of blood clotting in space has been reported (Marshall-Goebel et al., 2019). Venous thromboembolism in space is life threatening and potentially a mission critical risk. In a cohort of 11 ISS astronauts, a half had stagnant or retrograde flow in the internal jugular vein at d50, and 1 crew member developed an occlusive internal jugular vein thrombus. Thus, weightlessness is associated with abnormal and stagnant cerebral venous outflow, which may lead to thrombosis in otherwise healthy astronauts (Marshall-Goebel et al., 2019).

Lower Limb Veins

Venous diseases of the lower extremities are very common, affecting about 25% of adults in westernized societies, with the spectrum ranging from simple telangiectasias to venous ulcerations. In microgravity context, leg venous function is important, as increased venous compliance and altered filling/emptying contribute to post-flight orthostatic intolerance. Venous occlusion air plethysmography is the main functional tool to assess limb venous functions. Studies with this method have shown that filling function of veins is altered during simulated weightlessness and spaceflight (Louisy et al., 1997; Fortrat et al., 2017). Several factors may be involved: muscular atrophy, changes in body fluids, decrease in venous tone, increase

TABLE 6 | Circulating markers of endothelial state: effects of experimental models and countermeasures.

Variable	Inactivity model	Duration	Subjects Ctrl/CM	Estimated inactivity effect (without CM)	CM tested	Estimated CM effects	References
Circulating endothelial cells	HDBR	56 d	8F/8F	↑ (From 3.6/ml to 10.6/ml)	LBNP + aerobic + RE	Completely prevented	Demiot et al. (2007)
EMPs CD31+/CD42b- ("apoptotic")	<5,000 steps/d	5 d	11M	↑ (From 18/μL to 104/μL)	_	_	Boyle et al. (2013)
EMPs CD31 + CD41-("apoptotic")	Dry immersion	7 d	8M	↑ (From 42/μL to 65/μL)	_	_	Navasiolava et al. (2010)
EMPs CD31+/CD42b- ("apoptotic")	HDBR	60 d	7M/7M	↑ (From 46/μL to 97/μL)	CHM	Completely prevented	Yuan et al. (2015)
EMPs CD62E+("activated")	<5,000 steps/d	5 d	11M	No effect	_	_	Boyle et al. (2013)
Colony-forming unit-circulating angiogenic cells	Restraint from high-intensity exercise (athletes)	10 d	8M	↓36%	_	_	Guhanarayan et al. (2014)
CD34+ hemopoietic circulating angiogenic cells	Restraint from high-intensity exercise (athletes)	10 d	8M	No effect	_	_	Guhanarayan et al. (2014)
Components of endothelial glycocalyx	HDBR	5 d	12M crossover	No effect	Centrifugation	no effect	Feuerecker et al. (2013)
Soluble VEGF	Dry immersion	7 d	8M	↓27%	_	_	Navasiolava et al. (2010)
Soluble CD62E	Dry immersion	7 d	8M	No effect	_	_	Navasiolava et al. (2010)

CHM, Chinese herbal medicine; CM, countermeasure; RE, resistive exercise; EMPs, endothelial microparticles; F, female; M, male

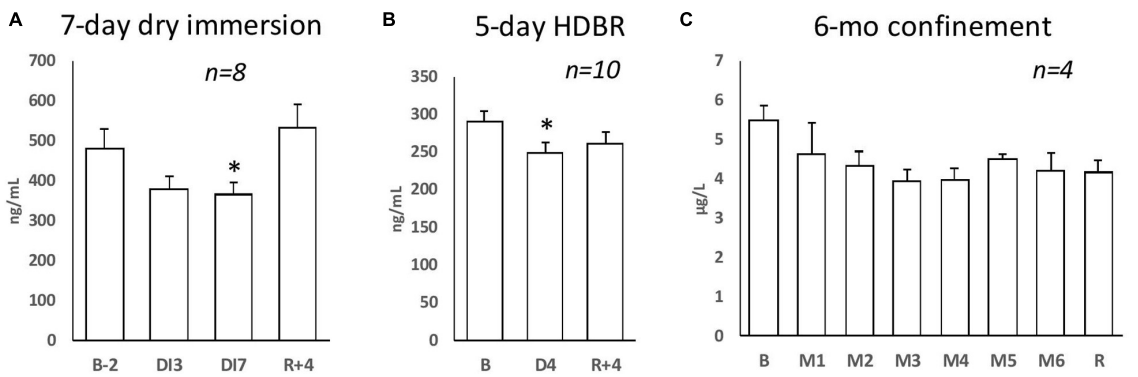

FIGURE 2 | Plasma level of sCD146 during **(A)** 7-day dry immersion and **(B)** 5-day HDBR. **(C)** Serum level of sCD146 during 6-month confinement. Data are mean ± SEM; *p < 0.05 vs B.

in venous compliance and changes at the microcirculatory level. Ultrasound measurement of venous cross-sectional area is a direct method to study main veins. Cross-sectional area increase in standing position after 90-day HDBR is greater in intolerant subjects (Belin de Chantemèle et al., 2004).

Splanchnic Level

Following 2-mo HDBR, baseline portal flow (proxy measured by portal vein cross-sectional area) diminishes by 19 ± 13%, related to decrease in blood volume. Splanchnic vasoconstrictive response to orthostatic stimulus (LBNP −45 mmHg), measured at portal vein level, is also decreased; moreover, insufficient flow reduction in splanchnic area is associated with orthostatic intolerance (Arbeille et al., 2008). These findings are in line with data of Behnke et al. (2013), showing impaired vasoconstriction of mesenteric veins in mice following 13–15-day flight.

MECHANISMS OF VASCULAR AND MICROVASCULAR CHANGES

Mechanical Factors as Mechanisms of Vascular and Microvascular Changes (Figure 3)

Shear Stress

Physical inactivity decreases tissue demands and is associated with a general decrease in blood flow and, hence, shear stress.

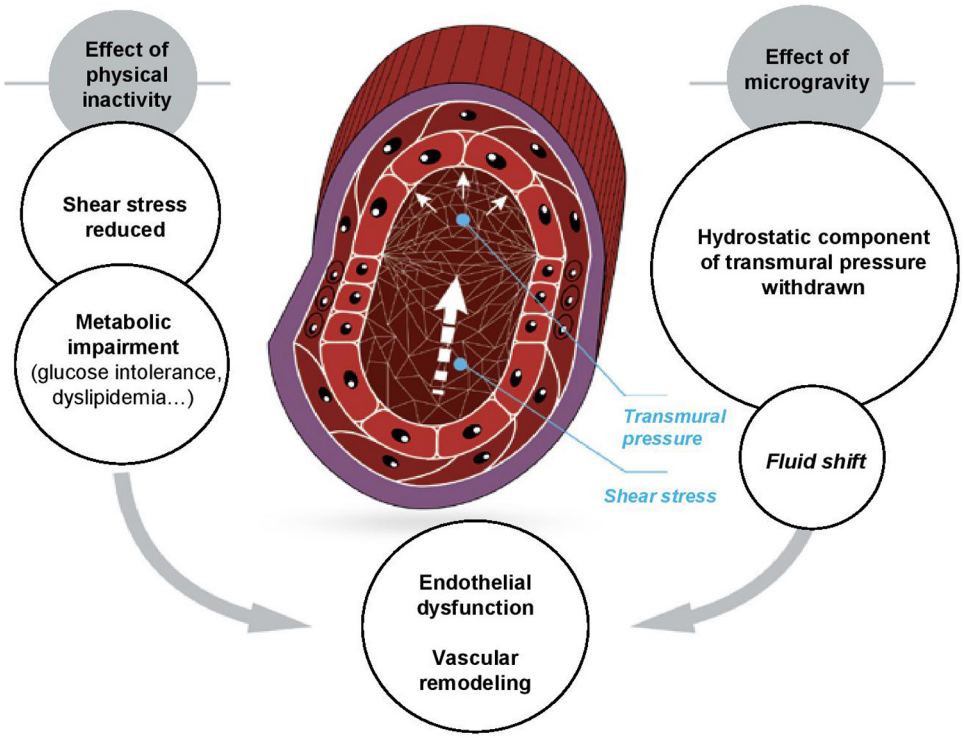

FIGURE 3 | Vessels and mechanical forces in microgravity.

This is particularly the case for lower limbs, which are extremely unloaded in our models compared with normal daily activity. Langille and O'Donnell (1986) were the first to show, using a rabbit model of unilateral external carotid artery ligation, that a decrease in blood flow for 2 weeks causes inward remodeling. This response is abolished when the endothelium is removed, indicating that chronic changes in shear stress mediate endothelium-dependent vascular remodeling. Despite comparatively low magnitude of shear stress (0.5–5 Pa vs. more than 1,000 Pa for circumferential stretch of vessel wall during cardiac cycle), this force governs vascular remodeling. Sensitivity of vessel to shear stress seemingly depends on abundance of VEGFR3 (Baeyens and Schwartz, 2016).

Inward remodeling of large vessels is believed to homeostatically regulate wall shear (Thijssen et al., 2010). A chronic shear stress diminution related to inactivity is particularly damaging to microcirculation (Boisseau, 2005). Differences in adaptation to an initial decrease in shear stress might underpin the differences in level of dysfunction for macro- and microcirculation. Whereas large vessel function is finally preserved, small vessels keep functional impairment.

Transmural Pressure

Vascular morphology and function, especially for smooth muscle cells, are sensitive to transmural pressure, which itself depends on blood and hydrostatic pressure. Systemic blood pressure is preserved or slightly decreased inflight (Norsk, 2019) and is not significantly modified by long-term bed rest (Fortney et al., 1996; van Duijnhoven et al., 2010a,b). However, hydrostatic pressure should be taken into account for vascular remodeling related to actual or simulated microgravity. Daily orthostatic stimulation induces large variations in hydrostatic pressure in the upper (up to −40 mmHg) and lower (up to +100 mmHg) parts of the body (Hargens and Watenpaugh, 1996). Hargens and Watenpaugh (1996) suggested that adaptation of vascular structure to microgravity is related to removal of the hydrostatic component (Zhang, 2001).

Metabolic Factors as Mechanisms of Vascular and Microvascular Changes

Several studies demonstrate that even short periods of physical inactivity (e.g., bed rest for 3-7 days, dry immersion for 5-7 days) increase fasting blood insulin (Blanc et al., 2000; Hamburg et al., 2007; Navasiolava et al., 2011; Coupe et al., 2013; De Abreu et al., 2017), impair glucose tolerance (Blanc et al., 2000; Smorawinski et al., 2000; Hamburg et al., 2007; De Abreu et al., 2017), and alter lipid profile (Hamburg et al., 2007; Navasiolava et al., 2011; Coupe et al., 2013; De Abreu et al., 2017). Similarly, a 6-month flight increased insulin resistance index and glycated albumin level, did not alter significantly lipid profile, and inconsistently affected markers of inflammatory and oxidative stress (Hughson et al., 2016).

These metabolic abnormalities are associated with endothelial dysfunction at the microvascular level, as shown after 5-day

bed rest (Hamburg et al., 2007), possibly by triggering several oxidative and pro-inflammatory pathways (e.g., increased reactive oxygen species production, activation of protein kinase C- and advanced glycation end product-induced pro-inflammatory signaling), leading to an unbalanced release of endothelial mediators. Of these mechanisms, increased oxidative stress seems to be the pivotal alteration (Potenza et al., 2009).

Inflammatory Factors and Oxidative Stress as Mechanisms of Vascular and Microvascular Changes

The question of whether physical inactivity itself induces inflammation and increases oxidative state remains unanswered. Although acute exercise can induce oxidative stress, it also appears necessary for upregulating endogenous antioxidant defenses (Bloomer, 2008). Physical inactivity might promote an inflammatory state indirectly via metabolic changes. For example, lipid modifications are associated with altered levels of circulating cytokines and adipocytokines (Petersen and Pedersen, 2005). However, in the context of acute physical inactivity, there is generally no change in circulating inflammatory markers, arguing against the presence of systemic inflammation in these models. Hamburg et al. (2007) noticed that after 5-day non-strict bed rest, metabolic changes (i.e., insulin resistance and dyslipidemia) are not accompanied by changes in systemic inflammatory markers (i.e., C-reactive protein, interleukin (IL)-6, and tumor necrosis factor receptor-II). Similarly, 5-day strict HDBR does not alter inflammatory parameters (i.e., white blood cell number and counts, proinflammatory cytokine IL-6 and IL-8 levels, innate and adaptive immune responses) (Feuerecker et al., 2013). Dry immersion for 5–7 days does not modify C-reactive protein level (Coupe et al., 2013; De Abreu et al., 2017) or white blood cell number (Kozinets et al., 1983; Navasiolava et al., 2010). However, long-duration spaceflight (>140 days) triggers a hyper-inflammatory and aging immune phenotype (i.e., "inflammaging") that appears to be related to inflight chronic stress, which may expose astronauts to risks for hypersensitivity diseases, such as allergies or autoimmune diseases (Buchheim et al., 2019). In 126–340-day spaceflight (n = 13) biomarkers of oxidative stress and inflammation increase inflight, but mostly restore within 1 week post-flight (Lee et al., 2020).

COUNTERMEASURES AND THEIR EFFECTS ON MACRO- AND MICROCIRCULATION

In this review we've chosen to discuss only countermeasures with potential cardiovascular effect, already tested using microgravity analogs (details on these countermeasures are summarized in **Supplementary Data 1**), or hypothetically applicable in microgravity context.

Physical Countermeasures

Exercise

Aerobic exercise

Several studies show that daily physical activity and arterial stiffness are inversely correlated (O'Donovan et al., 2014) and that aerobic exercise decreases arterial stiffness (Tanaka et al., 1998; Hayashi et al., 2005). Regular aerobic exercise improves endothelial vasodilatory capacity, which is impaired by aging, metabolic problems, and hypertension. For example, DeSouza et al. (2000) demonstrated that endurance-trained men show no age-related decline in endothelium-dependent vasodilation. Moreover, in middle-aged individuals, aerobic exercise (i.e., walking) for 3 months restores the vasodilatory function loss observed in sedentary counterparts (DeSouza et al., 2000). Similarly, daily 40-min aerobic exercise for 3 months via a home-based aerobic exercise-training program appears to improve endothelium-dependent vasodilation in overweight adults independently of changes in body mass or composition (Mestek et al., 2010). A regular aerobic exercise program for 3 months (5–7 times a week) is also effective in improving endothelium-dependent vasodilation in both normotensive and hypertensive individuals (Higashi et al., 1999). Cutaneous vasodilation during exercise, as measured by laser Doppler, is impaired after 13-day HDBR (Lee et al., 2002) or 115-day flight (Fortney et al., 1998). Cutaneous vasodilation in response to forearm heating as estimated by plethysmography is also impaired after 13 days of HDBR (Crandall et al., 2003), whereas aerobic exercise (daily supine cycling for 90 min) prevents this skin microcirculatory impairment (Crandall et al., 2003; Shibasaki et al., 2003).

Resistive exercise

Resistive exercise is another type of physical exercise that may be beneficial for patients with CVD (Braith and Beck, 2008). Compared with aerobic exercise, however, the effects of resistive exercise on vascular function are more controversial. Resistive training was initially contraindicated for patients with coronary artery disease but now appears to be safe for clinically stable patients. Resistive training prevents age-associated declines in skeletal muscle mass and function (Hurley and Roth, 2000), but the effect of resistive training on exercise capacity is more disputed. Some studies show an increase in VO_2 max after resistive training in patients with chronic heart failure, whereas others report no improvement. A study of patients with type 2 diabetes (Kadoglou et al., 2012) shows that resistive training does not affect VO_2 max, lipid profile, or body fat but improves glycemic control and basal insulin level. A meta-analysis of randomized controlled trials between 1980 and 2011 determined that high-intensity resistance training is associated with increased arterial stiffness in young individuals with low baseline stiffness, whereas no such association is observed for moderate-intensity resistance training (Miyachi, 2013). In 60-day HDBR, resistive exercise completely prevents increases in carotid and femoral IMT and partially preserves femoral FMD but does not prevent a decrease in femoral diameter (van Duijnhoven et al., 2010a,b).

High-intensity interval training

High-intensity interval training (HIIT) comprises short bouts of maximal-intensity exercise alternated with less intense recovery intervals. HIIT is now considered a potential inflight countermeasure (Hurst et al., 2019). A 2014 meta-analysis of randomized trials determined that HIIT is more effective in improving brachial artery vascular function than moderate-intensity continuous training, perhaps due to its tendency to positively influence cardiorespiratory fitness, traditional CVD risk factors, oxidative stress, inflammation, and insulin sensitivity (Ramos et al., 2015). Similarly, a recent study of healthy inactive adults shows that 12-week HIIT is more efficient in improving FMD and decreasing arterial stiffness than 12-week moderate continuous training (Ramírez-Vélez et al., 2019). In 60-day HDBR, high-intensity resistance training involving reactive jumps mitigates cardiovascular deconditioning (although arterial and microcirculatory state were not specifically assessed) (Maggioni et al., 2018). Resistive training impairs endothelial function as evidenced by decreased FMD, presumably due to a sustained elevation in blood pressure; however, high-intensity resistance exercise with low repetitions, which minimizes barostress on vasculature, maintains endothelial function (Morishima et al., 2018).

Combined resistive and aerobic exercise and endothelium

Combined resistive and aerobic exercise improves endothelium-dependent vasodilation (Maiorana et al., 2000). Demiot et al. (2007) showed that during 60-day HDBR, endothelium-dependent vasodilation and the number of circulating endothelial cells are preserved in individuals who engage in resistive exercise (i.e., flywheel) and aerobic exercise (i.e., treadmill) coupled with LBNP, indicating the protection of endothelial function.

Whole Body Vibration

Whole body vibration has been proposed as a therapeutic tool for many years. Numerous studies show WBV beneficial effects for bone mass (Gomez-Cabello et al., 2012), neuromuscular function (Bosco et al., 1999; Torvinen et al., 2002; Fontana et al., 2005), and the endocrine system (Di Loreto et al., 2004). Some studies suggest that WBV acutely decreases arterial stiffness. Specifically, Otsuki et al. (2008) showed that 10 sets of vibration (26 Hz) for 60 s in a static squat position decreases brachial-ankle pulse wave velocity, an index of arterial stiffness, immediately after the WBV trials, with a return to baseline within 60 min. In inactivity models, a combination of vibration and exercise has a beneficial vascular effect. In an experiment with 60-day HDBR (i.e., the second Berlin Bed Rest study), van Duijnhoven et al. (2010a; 2010b) compared resistive exercise alone and resistive exercise combined with WBV and found that combined countermeasures completely preserve superficial femoral artery FMD and partially preserve its diameter, whereas resistive exercise alone is not sufficient to counteract vascular changes. These results are in accordance with those of the first Berlin Bed Rest study, in which combined resistive exercise and WBV attenuated the decrease in femoral diameter induced by 52 days of horizontal bed rest and preserved femoral FMD after 24 days but not 52 days of bed rest (Bleeker et al., 2005b). The mechanisms involved in vascular protection by WBV remain unknown but could include immediate increases in femoral and popliteal artery blood flow and shear rate (Kerschan-Schindl et al., 2001).

LBNP

In HDBR studies, the effects of LBNP as a countermeasure were tested alone (Güell et al., 1991) and in association with exercise (Arbeille et al., 1995, 2008). LBNP countermeasure alone, with several sessions per day, mitigated orthostatic hypotension in response to tilt-test at the end of 30-day HDBR (Güell et al., 1991). A combination of LBNP with exercise preserved leg vasoconstrictive response to orthostatic stimulus following 1-month HDBR in men and 2-month HDBR in women, as measured by Doppler ultrasound, while in control subjects this vasoconstrictive response was decreased (Arbeille et al., 1995, 2008). Besides, this combined LBNP + exercise countermeasure prevented endothelial impairment induced by 2-month HDBR in women (Demiot et al., 2007). Today, LBNP can be used in combination with many countermeasures such as fluid loading (i.e., salt and water), nutrition supplementation, and exercise. With recent occurrence of thrombotic episode in flight, utility of LBNP countermeasure to counteract headward fluid shift and improve jugular blood flow patterns is discussed (Marshall-Goebel et al., 2019).

Artificial Gravity

Artificial gravity is a promising countermeasure that reproduces terrestrial conditions (Evans et al., 2018) and could be combined with exercise or vibration (Clement and Pavy-Le Traon, 2004). Even short intermittent 1-G exposure may suffice to prevent adverse effects of microgravity (Zhang, 2001). The effect of centrifugation on vascular function would also be interesting to study. We speculate that gravity reproduction could be beneficial for the cardiovascular system. However, gravity at the lower limb level is much greater in a short arm centrifuge, with potential negative effects to microcirculation. Studies specifically examining the vascular and microcirculatory consequences of artificial gravity are still lacking. However in a murine model, apoptosis of retinal vascular endothelial cells induced by 35-day spaceflight was mitigated by continuous 1-g artificial gravity (Mao et al., 2018).

Nutritional and Pharmacological Countermeasures

Caloric Restriction

Caloric restriction is a dietary intervention that maintains proper nutrition but reduces caloric intake. Caloric restriction might be beneficial for the cardiovascular system, even in healthy non-obese individuals. Lefevre et al. (2009) showed that 25% caloric restriction for 6 months (i.e., the CALERIE trial) decreased estimated 10-year CVD risk by 29%, although there was no effect on endothelial function as assessed by FMD at the brachial artery level. However, Hesse et al. (2005) demonstrated that 25% caloric restriction for 13 days, mainly achieved by reducing fat intake to a minimum recommended level of 60 g/day, improves the response of forearm resistance vessels to ACh.

Polyphenols and Other Natural Extracts

Polyphenols are organic, mainly natural substances characterized by the presence of several phenol structural units. They include simple phenols, flavonoids, and non-flavonoids such as stilbenes (e.g., resveratrol), saponin, curcumin, and tannins. Potential use of different polyphenols in prevention and treatment of CVD is reviewed in a recent paper of Giglio et al. (2018). Epidemiological studies show an inverse relationship between dietary polyphenol consumption and mortality from CVD (Middleton et al., 2000). Polyphenols exert numerous biological effects that might protect the cardiovascular system, including vasodilatory, antioxidant (Andriantsitohaina et al., 2012), anti-aggregatory, and cholesterol-lowering (Ngamukote et al., 2011) effects. Polyphenols may improve endothelial function. Polyphenol-rich products at relatively low doses, corresponding to two glasses of red wine or daily consumption of 46 g dark chocolate for 2 weeks, increase FMD in healthy individuals. Similarly, polyphenol-rich products as black tea, green tea, and red grape extracts improve FMD in individuals with coronary artery disease (Andriantsitohaina et al., 2012). Nutritional supplements rich in polyphenols such as chocolate (Garcia et al., 2018) and walnut extract (Papoutsi et al., 2008) could also have potential effects on blood vessels.

Resveratrol is a natural polyphenol synthesized by some plants. In particular it is contained in red wine. In human studies, acute resveratrol prescription improves FMD in overweight and mildly hypertensive individuals as soon as 1 h after consumption (Wong et al., 2011). Prescription of modified resveratrol for 3 months improves endothelial function in adults with metabolic syndrome (Fujitaka et al., 2011). In 60-day HDBR antioxidant/anti-inflammatory cocktail containing resveratrol and other polyphenols, vitamin E, selenium, and omega-3, was not efficient to prevent muscle mass and strength loss (Arc-Chagnaud et al., 2020). However, due to its pleiotropic effects, resveratrol may be a good candidate for correcting cardiovascular alterations.

Chinese herbal medicine is one of the most important modalities of traditional Chinese medical care. Chinese herbal medicine countermeasures against vascular deconditioning are attractive due to their pleiotropic effects that are not limited to a single mechanism or a single application point (Lu et al., 2004). In 60-day HDBR, TaikongYangxin ("outer space heart-nourishing"), a herbal formula created by the Chinese space agency to boost the physical conditions of astronauts and improve their adaptability in an extreme environment, contributes to the prevention of post-bedrest loss of vasoconstriction in leg and splanchnic areas (Yuan et al., 2012), improves microvascular endothelial function (decrease in plateau vasodilative response to ACh from 46 to 31% of maximal vasodilation to heating, induced by 60-day HDBR, was completely prevented) and preserves endothelial integrity (increase in "apoptotic" EMPs induced by 60-day HDBR was prevented) (Yuan et al., 2015). This herbal extract is composed of over 10 ingredients including Panax ginseng, Astragalus membranaceus, Ligusticum wallichii, Schisandra chinensis, Ophiopogon japonicas, Rehmania glutinosa, Drynaria fortunei, and Poria cocos. Several active components of this formula may be capable of ameliorating endothelium-dependent vasodilation with potential synergic interactions.

Medications

Unexpectedly, medications are almost not applied to protect vascular functions. Although midodrine (Platts et al., 2004) has been proposed to promote vasoconstriction after spaceflight and avoid orthostatic hypotension, its interactions with anti-emetics used in this context have interrupted the studies with this compound.

CONCLUSION AND PERSPECTIVES

Actual and simulated weightlessness causes both structural and functional vascular changes. Although a chronic decrease in shear stress due to physical inactivity appears to be the main contributing factor, metabolic and circulating factors should also be taken in account. Fluid shift-related changes in hydrostatic pressure seem to be less important on the arterial side.

Studies of vascular properties, although well developed (diameter, IMT, compliance and flow rate measurements for large vessels; vasodilation capacity assessment using ischemic stimulus, heating, ACh and NO-donors; some biological assays), explore the vessels only partially. There are many unresolved questions about vascular changes induced by physical inactivity. Vasodilation by prostaglandin pathways, microcirculatory neurovascular interactions, and endothelial changes at the organ level (e.g., muscles, bones, and brain) and their potential links to local oxidative stress are some areas that should be explored.

To date, countermeasures based on physical exercise remain most effective against vascular dysfunction induced by physical inactivity and space environment. Exercise modalities were recently extensively discussed in the *Frontiers* research topic "Optimization of exercise countermeasures for human space flight – lessons from terrestrial physiology and operational considerations" (Scott et al., 2020). Resistive exercise and vibration could provide additional benefits. Specialized diets and nutritional supplements are also very promising, particularly plant extracts and hypocaloric or lipid-depleted diets that could preserve endothelial function.

Furthermore, with deep space missions beyond Earth's protective magnetosphere, irradiation factors become other major contributors to cardiovascular (i.e., endothelial) impairment (Delp et al., 2016; Hughson et al., 2018), which implies the importance of antioxidants, nutraceuticals, and radiation shielding in a countermeasure program in addition to physical fitness.

AUTHOR CONTRIBUTIONS

All authors contributed in drafting and revising of this review manuscript.

FUNDING

The work was partially supported by CNES and Chinese Space Medical Experiment Project HYZHXM01001.

ACKNOWLEDGMENTS

The preliminary version of this review manuscript was a part of AA's Ph.D. thesis (Alameddine, 2015). This initial version has been extensively rewritten and upgraded for this manuscript submitted as an original publication. We are grateful to Sonia Morgan-Linnell for reviewing the syntax.

SUPPLEMENTARY MATERIAL

The Supplementary Material for this article can be found online at: https://www.frontiersin.org/articles/10.3389/fphys.2020.00952/full#supplementary-material

REFERENCES

Alameddine, A. (2015). *Vascular Dysfunction and Environmental Conditions in Humans and Animal Experimental Models (Dysfonction vasculaire et conditions environnementales dans des modèles expérimentaux chez l'homme et l'animal)*. Ph.D. thesis, University of Angers, Angers.

Andriantsitohaina, R., Auger, C., Chataigneau, T., Étienne-Selloum, N., Li, H., Martínez, M. C., et al. (2012). Molecular mechanisms of the cardiovascular protective effects of polyphenols. *Br. J. Nutr.* 108, 1532–1549. doi: 10.1017/s0007114512003406

Arbeille, P., Fomina, G., Roumy, J., Alferova, I., Tobal, N., and Herault, S. (2001). Adaptation of the left heart, cerebral and femoral arteries, and jugular and femoral veins during short- and long-term head-down tilt and spaceflights. *Eur. J. Appl. Physiol.* 86, 157–168. doi: 10.1007/s004210100473

Arbeille, P., Herault, S., Fomina, G., Roumy, J., Alferova, I., and Gharib, C. (1999). Influences of thigh cuffs on the cardiovascular system during 7-day head-down bed rest. *J. Appl. Physiol.* 87, 2168–2176. doi: 10.1152/jappl.1999.87.6.2168

Arbeille, P., Kerbeci, P., Mattar, L., Shoemaker, J. K., and Hughson, R. (2008). Insufficient flow reduction during LBNP in both splanchnic and lower limb areas is associated with orthostatic intolerance after bedrest. *Am. J. Physiol.* 295, H1846–H1854. doi: 10.1152/ajpheart.509.2008

Arbeille, P., Pavy-le Traon, A., Fomina, G., Vasseur, P., and Guell, A. (1995). Femoral flow response to lower body negative pressure: an orthostatic tolerance test. *Aviat. Space Environ. Med.* 66, 131–136.

Arbeille, P., Provost, R., Vincent, N., and Aubert, A. (2014). Adaptation of the main peripheral artery and vein to long term confinement (Mars 500). *PLoS One* 9:e83063. doi: 10.1371/journal.pone.0083063

Arbeille, P., Provost, R., and Zuj, K. (2016). Carotid and femoral artery intima-media thickness during 6 months of spaceflight. *Aerosp. Med. Hum. Perform.* 87, 449–453. doi: 10.3357/AMHP.4493.2016

Arbeille, P., Provost, R., and Zuj, K. (2017). Carotid and femoral arterial wall distensibility during long-duration spaceflight. *Aerosp. Med. Hum. Perform.* 88, 924–930. doi: 10.3357/AMHP.4884.2017

Arc-Chagnaud, C., Py, G., Fovet, T., Roumanille, R., Demangel, R., Pagano, A. F., et al. (2020). Evaluation of an antioxidant and anti-inflammatory cocktail against human hypoactivity-induced skeletal muscle deconditioning. *Front. Physiol.* 11:71. doi: 10.3389/fphys.2020.00071

Baeyens, N., and Schwartz, M. A. (2016). Biomechanics of vascular mechanosensation and remodeling. *Mol. Biol. Cell* 27, 7–11. doi: 10.1091/mbc.e14-11-1522

Behnke, B. J., Stabley, J. N., McCullough, D. J., Davis, R. T. III, Dominguez, J. M. II, Muller-Delp, J. M., et al. (2013). Effects of spaceflight and ground recovery on mesenteric artery and vein constrictor properties in mice. *FASEB J.* 27, 399–409. doi: 10.1096/fj.12-218503

Belin de Chantemèle, E., Pascaud, L., Custaud, M. A., Capri, A., Louisy, F., Ferretti, G., et al. (2004). Calf venous volume during stand-test after a 90-day bed-rest study with or without exercise countermeasure. *J. Physiol.* 561, 611–622. doi: 10.1113/jphysiol.2004.069468

Blanc, S., Normand, S., Pachiaudi, C., Fortrat, J. O., Laville, M., and Gharib, C. (2000). Fuel homeostasis during physical inactivity induced by bed rest. *J. Clin. Endocrinol. Metab.* 85, 2223–2233. doi: 10.1210/jc.85.6.2223

Bleeker, M. W., De Groot, P. C., Poelkens, F., Rongen, G. A., Smits, P., and Hopman, M. T. (2005a). Vascular adaptation to 4 wk of deconditioning by unilateral lower limb suspension. *Am. J. Physiol.* 288, H1747–H1755.

Bleeker, M. W., De Groot, P. C., Rongen, G. A., Rittweger, J., Felsenberg, D., Smits, P., et al. (2005b). Vascular adaptation to deconditioning and the effect of an exercise countermeasure: results of the Berlin Bed Rest study. *J. Appl. Physiol.* 99, 1293–1300. doi: 10.1152/japplphysiol.00118.2005

Bleeker, M. W., Kooijman, M., Rongen, G. A., Hopman, M. T., and Smits, P. (2005c). Preserved contribution of nitric oxide to baseline vascular tone in deconditioned human skeletal muscle. *J. Physiol.* 565, 685–694. doi: 10.1113/jphysiol.2005.085936

Bloomer, R. J. (2008). Effect of exercise on oxidative stress biomarkers. *Adv. Clin. Chem.* 46, 1–50. doi: 10.1016/s0065-2423(08)00401-0

Boisseau, M. R. (2005). Roles of mechanical blood forces in vascular diseases. A clinical overview. *Clin. Hemorheol. Microcirc.* 33, 201–207.

Bonde-Petersen, F., Suzuki, Y., Kawakubo, K., and Gunji, A. (1994). Effect of 20 days bed rest upon peripheral capillary filtration rate, venous compliance and blood flow in arms and legs. *Acta Physiol. Scand. Suppl.* 616, 65–69.

Bonnin, P., Ben Driss, A., Benessiano, J., Maillet, A., Pavy le Traon, A., and Levy, B. I. (2001). Enhanced flow-dependent vasodilatation after bed rest, a possible mechanism for orthostatic intolerance in humans. *Eur. J. Appl. Physiol.* 85, 420–426. doi: 10.1007/s004210100483

Bosco, C., Cardinale, M., and Tsarpela, O. (1999). Influence of vibration on mechanical power and electromyogram activity in human arm flexor muscles. *Eur. J. Appl. Physiol. Occup. Physiol.* 79, 306–311. doi: 10.1007/s004210050512

Boyle, L. J., Credeur, D. P., Jenkins, N. T., Padilla, J., Leidy, H. J., Thyfault, J. P., et al. (2013). Impact of reduced daily physical activity on conduit artery flow-mediated dilation and circulating endothelial microparticles. *J. Appl. Physiol.* 115, 1519–1525. doi: 10.1152/japplphysiol.00837.2013

Braith, R. W., and Beck, D. T. (2008). Resistance exercise: training adaptations and developing a safe exercise prescription. *Heart Fail. Rev.* 13, 69–79. doi: 10.1007/s10741-007-9055-9

Buchheim, J. I., Matzel, S., Rykova, M., Vassilieva, G., Ponomarev, S., Nichiporuk, I., et al. (2019). Stress related shift toward inflammaging in cosmonauts after long-duration space flight. *Front. Physiol.* 10:85. doi: 10.3389/fphys.2019.00085

Christ, F., Gamble, J., Baranov, V., Kotov, A., Chouker, A., Thiel, M., et al. (2001). Changes in microvascular fluid filtration capacity during 120 days of 6 degrees head-down tilt. *J. Appl. Physiol.* 91, 2517–2522. doi: 10.1152/jappl.2001.91.6.2517

Clement, G., and Pavy-Le Traon, A. (2004). Centrifugation as a countermeasure during actual and simulated microgravity: a review. *Eur. J. Appl. Physiol.* 92, 235–248.

Coupé, M., Fortrat, J. O., Larina, I., Gauquelin-Koch, G., Gharib, C., and Custaud, M. A. (2009). Cardiovascular deconditioning: from autonomic nervous system to microvascular dysfunctions. *Respir. Physiol. Neurobiol.* 169, S10–S12.

Coupe, M., Tomilovskaya, E., Larcher, F., Diquet, B., Pastushkova, L., Kozlovskaya, I., et al. (2013). Body fluid changes, cardiovascular deconditioning and metabolic impairment are reversed 24 hours after a 5-day dry immersion. *Open J. Nephrol.* 3, 13–24. doi: 10.4236/ojneph.2013.31004

Crandall, C. G., Shibasaki, M., Wilson, T. E., Cui, J., and Levine, B. D. (2003). Prolonged head-down tilt exposure reduces maximal cutaneous vasodilator and sweating capacity in humans. *J. Appl. Physiol.* 94, 2330–2336. doi: 10.1152/japplphysiol.00790.2002

De Abreu, S., Amirova, L., Murphy, R., Wallace, R., Twomey, L., Gauquelin-Koch, G., et al. (2017). Multi-system deconditioning in 3-day dry immersion without daily raise. *Front. Physiol.* 8:799. doi: 10.3389/fphys.2017.00799

de Groot, P. C., Bleeker, M. W., and Hopman, M. T. (2006). Magnitude and time course of arterial vascular adaptations to inactivity in humans. *Exerc. Sport Sci. Rev.* 34, 65–71. doi: 10.1249/00003677-200604000-00005

de Groot, P. C., Poelkens, F., Kooijman, M., and Hopman, M. T. (2004). Preserved flow-mediated dilation in the inactive legs of spinal cord-injured individuals. *Am. J. Physiol.* 287, H374–H380.

Delp, M. D., Charvat, J. M., Limoli, C. L., Globus, R. K., and Ghosh, P. (2016). Apollo lunar astronauts show higher cardiovascular disease mortality: possible deep space radiation effects on the vascular endothelium. *Sci. Rep.* 6:29901. doi: 10.1038/srep29901

Demiot, C., Dignat-George, F., Fortrat, J. O., Sabatier, F., Gharib, C., Larina, I., et al. (2007). WISE 2005: chronic bed rest impairs microcirculatory endothelium in women. *Am. J. Physiol.* 293, H3159–H3164.

DeSouza, C. A., Shapiro, L. F., Clevenger, C. M., Dinenno, F. A., Monahan, K. D., Tanaka, H., et al. (2000). Regular aerobic exercise prevents and restores age-related declines in endothelium-dependent vasodilation in healthy men. *Circulation* 102, 1351–1357. doi: 10.1161/01.cir.102.12.1351

Di Loreto, C., Ranchelli, A., Lucidi, P., Murdolo, G., Parlanti, N., De Cicco, A., et al. (2004). Effects of whole-body vibration exercise on the endocrine system of healthy men. *J. Endocrinol. Invest.* 27, 323–327. doi: 10.1007/bf03351056

Evans, J. M., Knapp, C. F., and Goswami, N. (2018). Artificial gravity as a countermeasure to the cardiovascular deconditioning of spaceflight: gender perspectives. *Front. Physiol.* 9:716. doi: 10.3389/fphys.2018.00716

Feuerecker, M., Feuerecker, B., Matzel, S., Long, M., Strewe, C., Kaufmann, I., et al. (2013). Five days of head-down-tilt bed rest induces noninflammatory shedding of L-selectin. *J. Appl. Physiol.* 115, 235–242. doi: 10.1152/japplphysiol.00381.2013

Fontana, T. L., Richardson, C. A., and Stanton, W. R. (2005). The effect of weight-bearing exercise with low frequency, whole body vibration on lumbosacral proprioception: a pilot study on normal subjects. *Aust. J. Physiother.* 51, 259–263. doi: 10.1016/s0004-9514(05)70007-6

Fortney, S. M., Mikhaylov, V., Lee, S. M., Kobzev, Y., Gonzalez, R. R., and Greenleaf, J. E. (1998). Body temperature and thermoregulation during submaximal exercise after 115-day spaceflight. *Aviat. Space Environ. Med.* 69, 137–141.

Fortney, S. M., Schneider, V. S., and Greenleaf, J. E. (1996). "The physiology of bed rest," in *Handbook of Physiology*, eds M. J. Fregly, and C. M. Blatteis, (New York, NY: Oxford University Press), 889–939.

Fortrat, J. O., de Holanda, A., Zuj, K., Gauquelin-Koch, G., and Gharib, C. (2017). Altered venous function during long-duration spaceflights. *Front. Physiol.* 8:694. doi: 10.3389/fphys.2017.00694

Fujitaka, K., Otani, H., Jo, F., Jo, H., Nomura, E., Iwasaki, M., et al. (2011). Modified resveratrol Longevinex improves endothelial function in adults with metabolic syndrome receiving standard treatment. *Nutr. Res.* 31, 842–847. doi: 10.1016/j.nutres.2011.09.028

Garcia, J. P., Santana, A., Baruqui, D. L., and Suraci, N. (2018). The Cardiovascular effects of chocolate. *Rev. Cardiovasc. Med.* 19, 123–127. doi: 10.31083/j.rcm.2018.04.3187

Garrett-Bakelman, F. E., Darshi, M., Green, S. J., Gur, R. C., Lin, L., Macias, B. R., et al. (2019). The NASA Twins Study: a multidimensional analysis of a year-long human spaceflight. *Science* 364:eaau8650. doi: 10.1126/science.aau8650

Giglio, R. V., Patti, A. M., Cicero, A., Lippi, G., Rizzo, M., Toth, P. P., et al. (2018). Polyphenols: potential use in the prevention and treatment of cardiovascular diseases. *Curr. Pharm. Des.* 24, 239–258. doi: 10.2174/1381612824666180130112652

Gomez-Cabello, A., Ara, I., Gonzalez-Aguero, A., Casajus, J. A., and Vicente-Rodriguez, G. (2012). Effects of training on bone mass in older adults: a systematic review. *Sports Med.* 42, 301–325. doi: 10.2165/11597670-000000000-00000

Green, D. J., O'Driscoll, J. G., Blanksby, B. A., and Taylor, R. R. (1997). Effect of casting on forearm resistance vessels in young men. *Med. Sci. Sports Exerc.* 29, 1325–1331. doi: 10.1097/00005768-199710000-00008

Güell, A., Braak, L., Le Traon, A., and Gharib, C. (1991). Cardiovascular adaptation during simulated microgravity: lower body negative pressure to counter orthostatic hypotension. *Aviat. Space Environ. Med.* 62, 331–335.

Guhanarayan, G., Jablonski, J., and Witkowski, S. (2014). Circulating angiogenic cell population responses to 10 days of reduced physical activity. *J. Appl. Physiol.* 117, 500–506. doi: 10.1152/japplphysiol.00087.2014

Hamburg, N. M., McMackin, C. J., Huang, A. L., Shenouda, S. M., Widlansky, M. E., Schulz, E., et al. (2007). Physical inactivity rapidly induces insulin resistance and microvascular dysfunction in healthy volunteers. *Arterioscler. Thromb. Vasc. Biol.* 27, 2650–2656. doi: 10.1161/atvbaha.107.153288

Hargens, A. R., and Watenpaugh, D. E. (1996). Cardiovascular adaptation to spaceflight. *Med. Sci. Sports Exerc.* 28, 977–982. doi: 10.1097/00005768-199608000-00007

Hayashi, K., Sugawara, J., Komine, H., Maeda, S., and Yokoi, T. (2005). Effects of aerobic exercise training on the stiffness of central and peripheral arteries in middle-aged sedentary men. *Jpn. J. Physiol.* 55, 235–239. doi: 10.2170/jjphysiol.s2116

Herault, S., Fomina, G., Alferova, I., Kotovskaya, A., Poliakov, V., and Arbeille, P. (2000). Cardiac, arterial and venous adaptation to weightlessness during 6-month MIR spaceflights with and without thigh cuffs (bracelets). *Eur. J. Appl. Physiol.* 81, 384–390. doi: 10.1007/s004210050058

Hesse, C., Siedler, H., Luntz, S. P., Arendt, B. M., Goerlich, R., Fricker, R., et al. (2005). Modulation of endothelial and smooth muscle function by bed rest and hypoenergetic, low-fat nutrition. *J. Appl. Physiol.* 99, 2196–2203. doi: 10.1152/japplphysiol.00888.2005

Higashi, Y., Sasaki, S., Kurisu, S., Yoshimizu, A., Sasaki, N., Matsuura, H., et al. (1999). Regular aerobic exercise augments endothelium-dependent vascular relaxation in normotensive as well as hypertensive subjects: role of endothelium-derived nitric oxide. *Circulation* 100, 1194–1202. doi: 10.1161/01.cir.100.11.1194

Hughson, R. L. (2009). Recent findings in cardiovascular physiology with space travel. *Respir. Physiol. Neurobiol.* 169, S38–S41.

Hughson, R. L., Helm, A., and Durante, M. (2018). Heart in space: effect of the extraterrestrial environment on the cardiovascular system. *Nat. Rev. Cardiol.* 15, 167–180. doi: 10.1038/nrcardio.2017.157

Hughson, R. L., Robertson, A. D., Arbeille, P., Shoemaker, J. K., Rush, J. W., Fraser, K. S., et al. (2016). Increased postflight carotid artery stiffness and inflight insulin resistance resulting from 6-mo spaceflight in male and female astronauts. *Am. J. Physiol.* 310, H628–H638. doi: 10.1152/ajpheart.00802.2015

Hughson, R. L., Shoemaker, J. K., Arbeille, P., Dyson, K. S., Edgell, H., Kerbeci, P., et al. (2007). WISE 2005: vascular responses to 60-day bed rest in women. *J. Gravit. Physiol.* 14, 53–54.

Hurley, B. F., and Roth, S. M. (2000). Strength training in the elderly: effects on risk factors for age-related diseases. *Sports Med.* 30, 249–268. doi: 10.2165/00007256-200030040-00002

Hurst, C., Scott, J. P. R., Weston, K. L., and Weston, M. (2019). High-intensity interval training: a potential exercise countermeasure during human spaceflight. *Front. Physiol.* 10:581. doi: 10.3389/fphys.2019.00581

Iwasaki, K., Levine, B. D., Zhang, R., Zuckerman, J. H., Pawelczyk, J. A., Diedrich, A., et al. (2007). Human cerebral autoregulation before, during and after spaceflight. *J. Physiol.* 579, 799–810. doi: 10.1113/jphysiol.2006.119636

Jeong, S. M., Hwang, G. S., Kim, S. O., Levine, B. D., and Zhang, R. (2014). Dynamic cerebral autoregulation after bed rest: effects of volume and exercise countermeasures. *J. Appl. Physiol.* 116, 24–31. doi: 10.1152/japplphysiol.00710.2013

Kadoglou, N. P., Fotiadis, G., Athanasiadou, Z., Vitta, I., Lampropoulos, S., and Vrabas, I. S. (2012). The effects of resistance training on ApoB/ApoA-I ratio, Lp(a) and inflammatory markers in patients with type 2 diabetes. *Endocrine* 42, 561–569. doi: 10.1007/s12020-012-9650-y

Kamiya, A., Iwase, S., Michikami, D., Fu, Q., Mano, T., Kitaichi, K., et al. (2000). Increased vasomotor sympathetic nerve activity and decreased plasma nitric oxide release after head-down bed rest in humans: disappearance of correlation between vasoconstrictor and vasodilator. *Neurosci. Lett.* 281, 21–24.

Kermorgant, M., Nasr, N., Custaud, M.-A., Navasiolava, N., Arbeille, P., Guinet, P., et al. (2019). Effects of resistance exercise and nutritional supplementation on dynamic cerebral autoregulation in head-down bed rest. *Front. Physiol.* 10:1114. doi: 10.3389/fphys.2019.01114

Kerschan-Schindl, K., Grampp, S., Henk, C., Resch, H., Preisinger, E., Fialka-Moser, V., et al. (2001). Whole-body vibration exercise leads to alterations in

muscle blood volume. *Clin. Physiol.* 21, 377–382. doi: 10.1046/j.1365-2281.2001.00335.x

Keys, A. (1945). Deconditioning and reconditioning in convalescence. *Surg. Clin. N. Am.* 25, 442–454.

Kozinets, G. I., Belakovskiĭ, M. S., Ushakov, A. S., Bykova, I. A., and Matveenko, V. P. (1983). Strukturnye i funktsional'nye izmeneniia éritrotsitov i leĭkotsitov cheloveka v usloviiakh 7-sutochnoĭ immersionnoĭ gipokinezii [Structural and functional changes in human erythrocytes and leukocytes during a 7-day immersion hypokinesia]. *Kosmicheskaia Biologiia i Aviakosmicheskaia Meditsina*, 17, 48–51.

Kramer, H. J., Heer, M., Cirillo, M., and De Santo, N. G. (2001). Renal hemodynamics in space. *Am. J. Kidney Dis.* 38, 675–678. doi: 10.1053/ajkd.2001.27754

Langille, B. L., and O'Donnell, F. (1986). Reductions in arterial diameter produced by chronic decreases in blood flow are endothelium-dependent. *Science* 231, 405–407. doi: 10.1126/science.3941904

Lee, A. G., Mader, T. H., Gibson, C. R., Brunstetter, T. J., and Tarver, W. J. (2018). Space flight-associated neuro-ocular syndrome (SANS). *Eye (Lond).* 32, 1164–1167. doi: 10.1038/s41433-018-0070-y

Lee, S. M., Williams, W. J., and Schneider, S. M. (2002). Role of skin blood flow and sweating rate in exercise thermoregulation after bed rest. *J. Appl. Physiol.* 92, 2026–2034. doi: 10.1152/japplphysiol.00105.2001

Lee, S. M. C., Ribeiro, L. C., Martin, D. S., Zwart, S. R., Feivezon, A. H., Laurie, S. S., et al. (2020). Arterial structure and function during and after long-duration spaceflight. *J. Appl. Physiol.* 129, 108–123. doi: 10.1152/japplphysiol.00550.2019

Lefevre, M., Redman, L. M., Heilbronn, L. K., Smith, J. V., Martin, C. K., Rood, J. C., et al. (2009). Caloric restriction alone and with exercise improves CVD risk in healthy non-obese individuals. *Atherosclerosis* 203, 206–213. doi: 10.1016/j.atherosclerosis.2008.05.036

Li, Y., Custaud, M. A., Yin, X., Lloret, J. C., Wang, J., Navasiolava, N., et al. (2019). Cardiovascular physiological research from ground simulation to spaceflight – application of new generation highly-integrated cardiospace system developed by Sino-French cooperation. *ICMASim Front. Event Abstr.* 114–120.

Louisy, F., Schroiff, P., and Guell, A. (1997). Changes in leg vein filling and emptying characteristics and leg volumes during long-term head-down bed rest. *J. Appl. Physiol.* 82, 1726–1733. doi: 10.1152/jappl.1997.82.6.1726

Lu, A. P., Jia, H. W., Xiao, C., and Lu, Q. P. (2004). Theory of traditional Chinese medicine and therapeutic method of diseases. *World J. Gastroenterol.* 10, 1854–1856.

Maggioni, M. A., Castiglioni, P., Merati, G., Brauns, K., Gunga, H. C., Mendt, S., et al. (2018). High-intensity exercise mitigates cardiovascular deconditioning during long-duration bed rest. *Front. Physiol.* 9:1553. doi: 10.3389/fphys.2018.01553

Maiorana, A., O'Driscoll, G., Cheetham, C., Collis, J., Goodman, C., Rankin, S., et al. (2000). Combined aerobic and resistance exercise training improves functional capacity and strength in CHF. *J. Appl. Physiol.* 88, 1565–1570. doi: 10.1152/jappl.2000.88.5.1565

Mao, X. W., Byrum, S., Nishiyama, N. C., Pecaut, M. J., Sridharan, V., Boerma, M., et al. (2018). Impact of spaceflight and artificial gravity on the mouse retina: biochemical and proteomic analysis. *Int. J. Mol. Sci.* 19:2546. doi: 10.3390/ijms19092546

Marshall-Goebel, K., Laurie, S. S., Alferova, I. V., Arbeille, P., Auñón-Chancellor, S. M., Ebert, D. J., et al. (2019). Assessment of jugular venous blood flow stasis and thrombosis during spaceflight. *JAMA Netw. Open* 2:e1915011. doi: 10.1001/jamanetworkopen.2019.15011

Mestek, M. L., Westby, C. M., Van Guilder, G. P., Greiner, J. J., Stauffer, B. L., and DeSouza, C. A. (2010). Regular aerobic exercise, without weight loss, improves endothelium-dependent vasodilation in overweight and obese adults. *Obesity* 18, 1667–1669. doi: 10.1038/oby.2009.467

Middleton, E. Jr., Kandaswami, C., and Theoharides, T. C. (2000). The effects of plant flavonoids on mammalian cells: implications for inflammation, heart disease, and cancer. *Pharmacol. Rev.* 52, 673–751.

Miyachi, M. (2013). Effects of resistance training on arterial stiffness: a meta-analysis. *Br. J. Sports Med.* 47, 393–396. doi: 10.1136/bjsports-2012-090488

Morishima, T., Restaino, R. M., Walsh, L. K., Kanaley, J. A., Fadel, P. J., and Padilla, J. (2016). Prolonged sitting-induced leg endothelial dysfunction is prevented by fidgeting. *Am. J. Physiol.* 311, H177–H182. doi: 10.1152/ajpheart.00297.2016

Morishima, T., Tsuchiya, Y., Iemitsu, M., and Ochi, E. (2018). High-intensity resistance exercise with low repetitions maintains endothelial function. *Am. J. Physiol.* 315, H681–H686. doi: 10.1152/ajpheart.00281.2018

Navasiolava, N. M., Custaud, M. A., Tomilovskaya, E. S., Larina, I. M., Mano, T., Gauquelin-Koch, G., et al. (2011). Long-term dry immersion: review and prospects. *Eur. J. Appl. Physiol.* 111, 1235–1260. doi: 10.1007/s00421-010-1750-x

Navasiolava, N. M., Dignat-George, F., Sabatier, F., Larina, I. M., Demiot, C., Fortrat, J. O., et al. (2010). Enforced physical inactivity increases endothelial microparticle levels in healthy volunteers. *Am. J. Physiol. Heart Circ. Physiol.* 299, 48–56.

Ngamukote, S., Mäkynen, K., Thilawech, T., and Adisakwattana, S. (2011). Cholesterol-lowering activity of the major polyphenols in grape seed. *Molecules* 16, 5054–5061. doi: 10.3390/molecules16065054

Norsk, P. (2019). Adaptation of the cardiovascular system to weightlessness: surprises, paradoxes and implications for deep space missions. *Acta Physiol.* 228:e13434. doi: 10.1111/apha.13434

O'Donovan, C., Lithander, F. E., Raftery, T., Gormley, J., Mahmud, A., and Hussey, J. (2014). Inverse relationship between physical activity and arterial stiffness in adults with hypertension. *J. Phys. Act. Health* 11, 272–277. doi: 10.1123/jpah.2012-0075

Otsuki, T., Takanami, Y., Aoi, W., Kawai, Y., Ichikawa, H., and Yoshikawa, T. (2008). Arterial stiffness acutely decreases after whole-body vibration in humans. *Acta Physiol.* 194, 189–194. doi: 10.1111/j.1748-1716.2008.01869.x

Palombo, C., Morizzo, C., Baluci, M., Lucini, D., Ricci, S., Biolo, G., et al. (2015). Large artery remodeling and dynamics following simulated microgravity by prolonged head-down tilt bed rest in humans. *Biomed Res. Int.* 2015:342565.

Papoutsi, Z., Kassi, E., Chinou, I., Halabalaki, M., Skaltsounis, L. A., and Moutsatsou, P. (2008). Walnut extract (*Juglans regia* L.) and its component ellagic acid exhibit anti-inflammatory activity in human aorta endothelial cells and osteoblastic activity in the cell line KS483. *Br. J. Nutr.* 99, 715–722. doi: 10.1017/s0007114507837421

Pavy-Le Traon, A., Costes-Salon, M. C., Vasseur-Clausen, P., Bareille, M.-P., Maillet, A., and Parant, M. (2002). Changes in kinetics of cerebral autoregulation with head-down bed rest. *Clin. Physiol. Funct. Imaging* 22, 108–114. doi: 10.1046/j.1365-2281.2002.00403.x

Pavy-Le Traon, A., Heer, M., Narici, M. V., Rittweger, J., and Vernikos, J. (2007). From space to Earth: advances in human physiology from 20 years of bed rest studies (1986-2006). *Eur. J. Appl. Physiol.* 101, 143–194. doi: 10.1007/s00421-007-0474-z

Pawelczyk, J. A., Zuckerman, J. H., Blomqvist, C. G., and Levine, B. D. (2001). Regulation of muscle sympathetic nerve activity after bed rest deconditioning. *Am. J. Physiol.* 280, H2230–H2239.

Petersen, A. M., and Pedersen, B. K. (2005). The anti-inflammatory effect of exercise. *J. Appl. Physiol.* 98, 1154–1162.

Platts, S. H., Martin, D. S., Stenger, M. B., Perez, S. A., Ribeiro, L. C., Summers, R., et al. (2009). Cardiovascular adaptations to long-duration head-down bed rest. *Aviat. Space Environ. Med.* 80(5 Suppl.), A29–A36.

Platts, S. H., Ziegler, M. G., Waters, W. W., Mitchell, B. M., and Meck, J. V. (2004). Midodrine prescribed to improve recurrent post-spaceflight orthostatic hypotension. *Aviat. Space Environ. Med.* 75, 554–556.

Potenza, M. A., Gagliardi, S., Nacci, C., Carratu', M. R., and Montagnani, M. (2009). Endothelial dysfunction in diabetes: from mechanisms to therapeutic targets. *Curr. Med. Chem.* 16, 94–112. doi: 10.2174/092986709787002853

Ramírez-Vélez, R., Hernández-Quiñones, P. A., Tordecilla-Sanders, A., Álvarez, C., Ramírez-Campillo, R., Izquierdo, M., et al. (2019). Effectiveness of HIIT compared to moderate continuous training in improving vascular parameters in inactive adults. *Lipids Health Dis.* 18:42. doi: 10.1186/s12944-019-0981-z

Ramos, J. S., Dalleck, L. C., Tjonna, A. E., Beetham, K. S., and Coombes, J. S. (2015). The impact of high-intensity interval training versus moderate-intensity continuous training on vascular function: a systematic review and meta-analysis. *Sports Med.* 45, 679–692. doi: 10.1007/s40279-015-0321-z

Restaino, R. M., Holwerda, S. W., Credeur, D. P., Fadel, P. J., and Padilla, J. (2015). Impact of prolonged sitting on lower and upper limb micro- and macrovascular dilator function. *Exp. Physiol.* 100, 829–838. doi: 10.1113/ep085238

Scott, J. P. R., Weber, T., and Green, D. A. (2020). Editorial: optimization of exercise countermeasures for human space flight—lessons from terrestrial physiology

and operational implementation. *Front. Physiol.* 10:1567. doi: 10.3389/fphys.2019.01567

Shibasaki, M., Wilson, T. E., Cui, J., Levine, B. D., and Crandall, C. G. (2003). Exercise throughout 6 degrees head-down tilt bed rest preserves thermoregulatory responses. *J. Appl. Physiol.* 95, 1817–1823. doi: 10.1152/japplphysiol.00188.2003

Shoemaker, J. K., Hogeman, C. S., Silber, D. H., Gray, K., Herr, M., and Sinoway, L. I. (1998). Head-down-tilt bed rest alters forearm vasodilator and vasoconstrictor responses. *J. Appl. Physiol.* 84, 1756–1762. doi: 10.1152/jappl.1998.84.5.1756

Smorawinski, J., Kaciuba-Uscilko, H., Nazar, K., Kubala, P., Kaminska, E., Ziemba, A. W., et al. (2000). Effects of three-day bed rest on metabolic, hormonal and circulatory responses to an oral glucose load in endurance or strength trained athletes and untrained subjects. *J. Physiol. Pharmacol.* 51, 279–289.

Sugawara, J., Hayashi, K., Kaneko, F., Yamada, H., Kizuka, T., and Tanaka, H. (2004). Reductions in basal limb blood flow and lumen diameter after short-term leg casting. *Med. Sci. Sports Exerc.* 36, 1689–1694. doi: 10.1249/01.mss.0000142410.45142.28

Sun, X. Q., Yao, Y. J., Yang, C. B., Jiang, S. Z., Jiang, C. L., and Liang, W. B. (2005). Effect of lower-body negative pressure on cerebral blood flow velocity during 21 days of head-down tilt bed rest. *Med. Sci. Monit.* 11, CR1–CR5.

Tanaka, H., DeSouza, C. A., and Seals, D. R. (1998). Absence of age-related increase in central arterial stiffness in physically active women. *Arterioscler. Thromb. Vasc. Biol.* 18, 127–132. doi: 10.1161/01.atv.18.1.127

Teixeira, A. L., Padilla, J., and Vianna, L. C. (2017). Impaired popliteal artery flow-mediated dilation caused by reduced daily physical activity is prevented by increased shear stress. *J. Appl. Physiol.* 123, 49–54. doi: 10.1152/japplphysiol.00001.2017

Thijssen, D. H., Maiorana, A. J., O'Driscoll, G., Cable, N. T., Hopman, M. T., and Green, D. J. (2010). Impact of inactivity and exercise on the vasculature in humans. *Eur. J. Appl. Physiol.* 108, 845–875. doi: 10.1007/s00421-009-1260-x

Thosar, S. S., Bielko, S. L., Mather, K. J., Johnston, J. D., and Wallace, J. P. (2015). Effect of prolonged sitting and breaks in sitting time on endothelial function. *Med. Sci. Sports Exerc.* 47, 843–849. doi: 10.1249/mss.0000000000000479

Tomilovskaya, E., Shigueva, T., Sayenko, D., Rukavishnikov, I., and Kozlovskaya, I. (2019). Dry immersion as a ground-based model of microgravity physiological effects. *Front. Physiol.* 10:284. doi: 10.3389/fphys.2019.00284

Torvinen, S., Kannu, P., Sievanen, H., Jarvinen, T. A., Pasanen, M., Kontulainen, S., et al. (2002). Effect of a vibration exposure on muscular performance and body balance. Randomized cross-over study. *Clin. Physiol. Funct. Imaging* 22, 145–152. doi: 10.1046/j.1365-2281.2002.00410.x

Turchaninova, V. F., Alferova, I. V., Golubchikova, Z. A., Lyamin, V. R., Krivolapov, V. V., and Khorosheva, E. G. (2001). "Functional state of cardiovascular system at rest," in *Orbital Station MIR*, eds A. I. Grigoriev et al. Vol. 1, (Moscow: SSC RF IMBP RAS), 267–276.

van Duijnhoven, N. T., Green, D. J., Felsenberg, D., Belavy, D. L., Hopman, M. T., and Thijssen, D. H. (2010a). Impact of bed rest on conduit artery remodeling: effect of exercise countermeasures. *Hypertension* 56, 240–246. doi: 10.1161/hypertensionaha.110.152868

van Duijnhoven, N. T., Thijssen, D. H., Green, D. J., Felsenberg, D., Belavy, D. L., and Hopman, M. T. (2010b). Resistive exercise versus resistive vibration exercise to counteract vascular adaptations to bed rest. *J. Appl. Physiol.* 108, 28–33. doi: 10.1152/japplphysiol.00760.2009

Watenpaugh, D. E. (2016). Analogs of microgravity: head-down tilt and water immersion. *J. Appl. Physiol.* 120, 904–914. doi: 10.1152/japplphysiol.00986.2015

Watenpaugh, D. E., Buckey, J. C., Lane, L. D., Gaffney, F. A., Levine, B. D., Moore, W. E., et al. (2001). Effects of spaceflight on human calf hemodynamics. *J. Appl. Physiol.* 90, 1552–1558. doi: 10.1152/jappl.2001.90.4.1552

Widlansky, M. E. (2010). The danger of sedenterism: endothelium at risk. *Am. J. Physiol.* 299, H243–H244.

Wong, R. H., Howe, P. R., Buckley, J. D., Coates, A. M., Kunz, I., and Berry, N. M. (2011). Acute resveratrol supplementation improves flow-mediated dilatation in overweight/obese individuals with mildly elevated blood pressure. *Nutr. Metab. Cardiovasc. Dis.* 21, 851–856. doi: 10.1016/j.numecd.2010.03.003

Yuan, M., Alameddine, A., Coupé, M., Navasiolava, N. M., Li, Y., Gauquelin-Koch, G., et al. (2015). Effect of Chinese herbal medicine on vascular functions during 60-day head-down bed rest. *Eur. J. Appl. Physiol.* 115, 1975–1983. doi: 10.1007/s00421-015-3176-y

Yuan, M., Coupé, M., Bai, Y., Gauquelin-Koch, G., Jiang, S., Aubry, P., et al. (2012). Peripheral arterial and venous response to tilt test after a 60-day bedrest with and without countermeasures (ES-IBREP). *PLoS One* 7:e32854. doi: 10.1371/journal.pone.0032854

Yuan, M., Custaud, M. A., Xu, Z., Wang, J., Yuan, M., Tafforin, C., et al. (2019). Multi-system adaptation to confinement during the 180-day controlled ecological life support system (CELSS) experiment. *Front. Physiol.* 10:575. doi: 10.3389/fphys.2019.00575

Zhang, L. F. (2001). Vascular adaptation to microgravity: what have we learned? *J. Appl. Physiol.* 91, 2415–2430. doi: 10.1152/jappl.2001.91.6.2415

Zhang, R., Zuckerman, J. H., Pawelczyk, J. A., and Levine, B. D. (1997). Effects of head-down tilt bed rest on cerebral hemodynamics during orthostatic stress. *J. Appl. Physiol.* 83, 2139–2145. doi: 10.1152/jappl.1997.83.6.2139

Zuj, K. A., Arbeille, P., Shoemaker, J. K., Blaber, A. P., Greaves, D. K., Xu, D., et al. (2012a). Impaired cerebrovascular autoregulation and reduced co(2) reactivity after long duration spaceflight. *Am. J. Physiol. Heart Circ. Physiol.* 302, 2592–2598. doi: 10.1152/ajpheart.00029.2012

Zuj, K. A., Edgell, H., Shoemaker, J. K., Custaud, M. A., Arbeille, P., and Hughson, R. L. (2012b). WISE 2005: responses of women to sublingual nitroglycerin before and after 56 days of 6° head-down bed rest. *J. Appl. Physiol.* 113, 434–441. doi: 10.1152/japplphysiol.00445.2012

Conflict of Interest: The authors declare that the research was conducted in the absence of any commercial or financial relationships that could be construed as a potential conflict of interest.

frontiers in Physiology

ORIGINAL RESEARCH
published: 19 May 2020
doi: 10.3389/fphys.2020.00395

Cardiovascular System Under Simulated Weightlessness: Head-Down Bed Rest vs. Dry Immersion

Liubov Amirova[1,2], Nastassia Navasiolava[2], Ilya Rukavishvikov[1], Guillemette Gauquelin-Koch[3], Claude Gharib[4], Inessa Kozlovskaya[1], Marc-Antoine Custaud[2,5] and Elena Tomilovskaya[1]**

[1] Laboratory of Gravitational Physiology of the Sensorimotor System, Institute of Biomedical Problems, Russian Academy of Sciences, Moscow, Russia, [2] Laboratoire MITOVASC, UMR Institut National de la Santé et de la Recherche Médicale 1083, Centre National de la Recherche Scientifique 6015, Université d'Angers, Angers, France, [3] Centre National d'Etudes Spatiales, Paris, France, [4] Institut NeuroMyogène, Université Claude Bernard Lyon 1, Lyon, France, [5] Centre de Recherche Clinique, Centre Hospitalier Universitaire d'Angers, Angers, France

OPEN ACCESS

Edited by:
Airong Qian, Northwestern Polytechnical University, China

Reviewed by:
Jochen Zange, Helmholtz Association of German Research Centers (HZ), Germany
Ana Diaz Artiles, Texas A& M University, United States
Danilo Cialoni, Dan Europe Foundation, Italy

***Correspondence:**
Liubov Amirova
lyubove.dmitrieva@gmail.com
Elena Tomilovskaya
finegold@yandex.ru

Specialty section:
This article was submitted to Environmental, Aviation and Space Physiology, a section of the journal Frontiers in Physiology

Received: *28 October 2019*
Accepted: *02 April 2020*
Published: *19 May 2020*

Citation:
Amirova L, Navasiolava N, Rukavishvikov I, Gauquelin-Koch G, Gharib C, Kozlovskaya I, Custaud M-A and Tomilovskaya E (2020) Cardiovascular System Under Simulated Weightlessness: Head-Down Bed Rest vs. Dry Immersion. Front. Physiol. 11:395. doi: 10.3389/fphys.2020.00395

Background: The most applicable human models of weightlessness are −6° head-down bed rest (HDBR) and head-out dry immersion (DI). A detailed experimental comparison of cardiovascular responses in both models has not yet been carried out, in spite of numerous studies having been performed in each of the models separately.

Objectives: We compared changes in central hemodynamics, autonomic regulation, plasma volume, and water balance induced by −6° HDBR and DI.

Methods: Eleven subjects participated in a 21-day HDBR and 12 subjects in a 3-day DI. During exposure, measurements of the water balance, blood pressure, and heart rate were performed daily. Plasma volume evolution was assessed by the Dill–Costill method. In order to assess orthostatic tolerance time (OTT), central hemodynamic responses to orthostatic stimuli, and autonomous regulation, the 80° lower body negative pressure–tilt test was conducted before and right after both exposures.

Results: For most of the studied parameters, the changes were co-directional, although they differed in their extent. The changes in systolic blood pressure and total peripheral resistance after HDBR were more pronounced than those after DI. The OTT was decreased in both groups: to 14.2 ± 3.1 min (vs. 27.9 ± 2.5 min before exposure) in the group of 21-day HDBR and to 8.7 ± 2.1 min (vs. 27.7 ± 1.2 min before exposure) in the group of 3-day DI.

Conclusions: In general, cardiovascular changes during the 21-day HDBR and 3-day DI were co-directional. In some cases, changes in the parameters after 3-day DI exceeded changes after the 21-day HDBR, while in other cases the opposite was true. Significantly stronger effects of DI on cardiovascular function may be due to hypovolemia and support unloading (supportlessness).

Keywords: support unloading, lower body negative pressure, water balance, orthostatic tolerance, autonomous regulation, microgravity models

INTRODUCTION

Piloted space flights have been carried out for more than 50 years, yet the problem of cardiovascular deconditioning following microgravity exposure still exists and the problem of orthostatic stability disorders remains relevant. On the other hand, the study of the orthostatic instability mechanisms in astronauts may be complicated due to the small "*n*" and biased due to the obligatory use of onboard countermeasures. An alternative approach is the application of ground models to reproduce the major effects of microgravity in the human body, with the possibility of applying complex techniques at any time of exposure. The most applicable human models are head-down bed rest (HDBR) and dry immersion (DI; Shulzhenko and Vill-Villiams, 1976; At'kov and Bednenko, 1987; Grigor'ev et al., 2004; Pavy-Le Traon et al., 2007; Navasiolava et al., 2011a; Tomilovskaya et al., 2019). Being similar in their effects on the human body, these models, however, differ in their specifics and acting factors. The HDBR, as the name implies, implicates a long (from several weeks to a year) stay in the supine position. In our study, the position was anti-orthostatic (the head was tilted down by −6° to the horizontal). Thus, body liquids and the supporting surface are redistributed. The immersion is called "dry" because a waterproof film separates the subject from the water (unlike "wet" immersion, where the skin of a human or animal is in direct contact with the water). Due to the almost absolutely uniform weight distribution, the subject is affected by full support unloading. However, there are very few works comparing these models and their effects on the human body (Navasiolava et al., 2011a; Watenpaugh, 2016; Tomilovskaya et al., 2019). At the same time, a large number of original articles are devoted to the study of various systems in HDBR and DI. Thus, it makes sense to compare the effects of −6° HDBR and DI on human physiological systems, in particular the cardiovascular system.

In space, weightlessness immediately induces an upward fluid shift with the puffy face/chicken leg syndrome (Thornton and Hoffler, 1977). The onboard infrared photographs of the Skylab 4 crew members showed relatively empty lower limb veins, while the head veins were always fully filled and expanded (Gibson, 1977). The fluid shift leads to an increased venous return to the right heart. Receptors located in this zone give the signals about hypervolemia and initiate a decrease in the circulating plasma volume, mainly due to a decrease in fluid intake. As a consequence, the body fluid balance may be negative on the first day of exposure, after which a new equilibrium is established. Moreover, an increase in transcapillary filtration to the interstitial space contributes to a reduction in plasma volume (Watenpaugh et al., 2001).

In microgravity, the upward fluid shift initiates all subsequent changes in the cardiovascular system, including changes in the arterial and venous hemodynamics as well as in the vascular tone (Pestov and Gerathewohl, 1975; Gazenko, 1984; Kotovskaya and Fomina, 2013; Norsk et al., 2015). First of all, there is an increase in the stroke volume (SV; Buckey et al., 1996; Videbaek and Norsk, 1997), which leads to an increase in cardiac output by 18–26% because the heart rate is unchanged or decreased (Prisk et al., 1993; Fritsch-Yelle et al., 1996; Shykoff et al., 1996; Norsk et al., 2006, 2015).

While the central blood volume increases in weightlessness, the blood pressure either does not change or slightly decreases (Fritsch-Yelle et al., 1996; Shykoff et al., 1996; Norsk et al., 2006). During short-term space missions, a decrease in diastolic arterial pressure by 5 mmHg within the initial 2 weeks of spaceflight was reported, although there were no changes in systolic or mean arterial pressure. Therefore, because the cardiac output increased, the mean arterial pressure remained unchanged by the dilation of the arterial resistance vessels, inducing a decrease in systemic vascular resistance (Fritsch-Yelle et al., 1996; Shykoff et al., 1996; Norsk et al., 2006, 2015).

These changes are adaptive and normal for microgravity, but, upon returning to Earth, cardiovascular deconditioning can threaten the health of astronauts. Upon landing, a reverse fluid shift to the lower body occurs. Together with a reduced blood volume, this may compromise the adequate brain perfusion. The loss of muscle and vascular tone contributes to blood sequestration in the lower body. The prolonged absence of orthostatic stimuli during the spaceflight also leads to autonomic dysfunction and the inability to adequately respond to gravitational stimulus. Thus, without proper countermeasures, the astronaut may experience pre-syncope or syncope when upright (Martin and Meck, 2004).

Cardiovascular deconditioning is also characteristic of HDBR and DI, differing, however, in details. Head-down bed rest is the most popular model of microgravity since it provides a fairly accurate reproduction of most of the physiological effects of weightlessness due to immobilization, inactivity, and limitation of gravitational stimuli, such as posture and direction change (Fortney et al., 1996; Hargens and Vico, 2016; Watenpaugh, 2016; Klassen et al., 2018; Mulavara et al., 2018). Various angles of head-down tilt (usually −6°) can be used, contributing to a headward fluid shift (Greenleaf, 1984; At'kov and Bednenko, 1987; Grigor'ev et al., 2004). This thoraco-cephalic fluid shift and an increased venous blood flow to the right atrium together lead to changes in the secretion of vasopressin and aldosterone (Knight et al., 2009a,b). This results in a decrease in water reabsorption, an increase in sodium excretion by the kidneys, an increase in diuresis, and a decrease in plasma volume. It has been found that even an 8-h HDBR already causes an increase in blood supply to the head and chest by 6–9% compared with the initial horizontal position (Osadchii et al., 1997). In an experiment with exposure to a 7-day HDBR, the blood supply to the upper torso on the second and the seventh day has been shown to increase by 11 and 23%, respectively (Lobachik et al., 1991). A longer stay in HDBR is accompanied by the development of compensatory-adaptive reactions. Changes in plasma volume occur rather quickly and, after 6.5 h, reach a level of −9.2%. Despite the differences in the methods used, in general, the authors indicate a decrease in plasma volume

Abbreviations: ANOVA, analysis of variance; B-, days before exposure; DBP, diastolic blood pressure; DI, dry immersion; ECG, electrocardiogram; HDBR, head down bed rest; HR, heart rate; LBNP, lower body negative pressure; OTT, orthostatic tolerance time; PV, plasma volume; R0, end-exposure day; R+, days of recovery period; SBP, systolic blood pressure; SEM, standard error of the mean; SV, stroke volume; TPR, total peripheral resistance.

by 6–15% with an HDBR duration from several days to a month and a half (Maillet et al., 1994; Sigaudo et al., 1996; Johansen et al., 1997; Blanc et al., 1998; Custaud et al., 2002). As in spaceflight, cardiovascular deconditioning characterized by orthostatic intolerance and reduced exercise capacity is observed at the end of bed rest (Pavy-Le Traon et al., 2007; Barbic et al., 2019).

The advantage of DI compared to the more widely known HDBR is support unloading ("supportlessness"), a state similar to weightlessness, with water hydrostatic pressure distributed equally over the body surface. The absence of support gradient provides conditions similar to a complete lack of support (Grigor'ev et al., 2004; Navasiolava et al., 2011a). Dry immersion promotes rapid gravitational deconditioning, which, for some systems (e.g., for the neuromuscular system), exceeds the deconditioning induced by spaceflight itself (Navasiolava et al., 2011a; Tomilovskaya et al., 2019). There is also evidence that DI has a more powerful effect on the cardiovascular system than does −8° HDBR (Krupina et al., 1982). Dry immersion, as well as HDBR, is accompanied by central hypervolemia, inducing an increase in cardiac dimension with heart stretching. For this reason, plasma volume decreases by approximately 15% within the first day of DI (Leach Huntoon et al., 1998) and remains stable thereafter (Gogolev et al., 1980; Larina et al., 2008; Nesterovskaia et al., 2008; Pakharukova et al., 2009; Navasiolava et al., 2011b). Decreased plasma volume is associated with diuresis and natriuresis (Epstein, 1992). The absence of changes in the levels of renin or aldosterone on days 3 and 7 is the evidence that the major redistribution of fluids is completed by that time and the water–electrolyte balance is stabilized.

Changes in blood supply to the vessels are followed by changes in central hemodynamics. The immediate effects of immersion in the first hours are an increase in SV and cardiac output, as well as a decrease in heart rate, blood pressure, and total peripheral vascular resistance (Modak and Banerjee, 2004; Bart et al., 2007; Ayme et al., 2014). An increase in cardiac output in the first hours of immersion is assumed to be associated with the redistribution of blood to the upper half of the body, while its decrease after 1 day is due to a decrease in the central blood volume as a result of the initiation of Parin and Henry–Gower reflexes. The parameters of blood pressure do not undergo significant changes. There is only a slight decrease in systolic blood pressure by 5–10 mmHg under immersion.

The idea of comparing the two models is not new. However, a detailed experimental comparison of the cardiovascular responses in both models has not yet been carried out, in spite of numerous studies having been performed using each of the models separately. Our analysis of the literature data allows us to suggest that the effect of DI may be stronger than that of HDBR. Therefore, we decided to test the hypothesis that the effects of 21-day −6° HDBR and 3-day DI for the cardiovascular system are comparable and to evaluate the optimal protocol (i.e., the optimal duration), which may be important for future studies. The aim of this work was to compare changes in the central hemodynamics, autonomic regulation, plasma volume, and water balance induced by the exposure to either −6° HDBR or DI.

MATERIALS AND METHODS

Study Population

We analyzed raw data from two different experiments with participation of healthy European male volunteers: 21-day −6° HDBR (n = 11) and 3-day DI (n = 12). A comparison of these experiments was not part of the original study design. However, since the experimental protocols were identical, conducted and processed by the same team of authors, and both exposures are the model of microgravity physiological effects, we considered that comparing these data is reasonable. Both studies were performed at the MEDES Space Clinic (Toulouse, France) and conformed to the standards set by the Declaration of Helsinki. All subjects were informed about the experimental procedures and gave their written consent.

The first experiment analyzed in our paper was taken from the Medium duration Nutrition and vibration eXercise (MNX) Bed-Rest Study conducted from November 6, 2012 to December 20, 2013. This study was organized as three 21-day HDBR sessions ("Pure exposure," "Exercise & vibration," or "Exercise & vibration plus nutrition," in a random order) separated by a 3-month washout. Moreover, all three sessions before HDBR did not significantly differ by hemodynamic parameters during the 80° tilt test from each other. The same volunteers participated in all three sessions. In this paper, we present data only from the "Pure exposure" session, referred to in the text as "HDBR exposure." Twelve volunteers were recruited, but one dropped out of the experiment; thus, the data were obtained from 11 subjects. The MNX Bed-Rest Study was approved by the local Ethics Committee (CPP Sud-Ouest Outre-Mer I) and the French Health Authorities (no. ID RCB: 2012-A00337-36).

The second experiment was a 3-day head-out DI study conducted from January 13, 2015 to February 19, 2015. This study was organized as a single session. Twelve volunteers were recruited; all of them completed the session. The study was approved by the local Ethics Committee (CPP Sud-Ouest Outre-Mer I, France) and the French Health Authorities (no. ID RCB: 2014-A 00904-43).

Different volunteers participated in the 21-day −6° HDBR or the 3-day DI. Anthropometric data for the two groups were not significantly different (unpaired t-test with Welch's correction, $p < 0.05$; **Table 1**).

Study Protocol

In this study, the standard HDBR protocol was used. According to the experimental conditions, the subjects were lying for 21 days on the bed with a −6° inclination in the head direction. During the bed rest, the subjects continuously maintained a head-down position with their back or one shoulder and buttocks in contact with the bed. During HDBR, the subjects were not allowed to sit or to stand up. Moreover, they were allowed to use a pillow. All measurements and hygiene procedures were carried out in a horizontal position. The room temperature was set at 23–25°C.

Head-out DI lasted 3 days. Throughout the exposure, the subjects were in a bath filled with tap water and a waterproof film separated them from the water. The large surface area of the film

TABLE 1 | Comparative data of two groups.

Experimental groups	−6° head-down bed rest	Dry immersion	Significant differences (unpaired *t* test with Welch's correction)
Duration (days)	21	3	–
Number of subjects, *n*	11	12	–
Age (years)	34 ± 2	32 ± 1	ns ($p = 0.24$, $t = 1.23$, $df = 16.0$)
Height (cm)	176 ± 2	178 ± 2	ns ($p = 0.55$, $t = 0.61$, $df = 21.0$)
Weight (kg)	70 ± 2	75 ± 2	ns ($p = 0.17$, $t = 1.42$, $df = 19.8$)
BMI (kg/m^2)	22.4 ± 0.5	23.6 ± 0.4	ns ($p = 0.13$, $t = 1.58$, $df = 20.1$)

Data are the mean ± SEM.

allows the subject to easily be in the depth of the water and does not constrain his limbs. The size of the bath is designed in such a way that the subject does not touch its walls when immersed. The subjects were allowed to be immersed up to the armpits. The water temperature for DI was continuously maintained at 32.5–33.5°C (thermoneutral). During the immersion, the subjects remained continuously immersed, except for short out-of-bath periods for hygiene, weighing, and some specific measurements, when the subjects were maintained in the −6° head-down position. The total out-of-bath supine time within the 72 h of immersion was 4.7 ± 0.16 h (mean ± SEM).

During both types of exposure, the subjects were under 24-h video monitoring. The beginning and end of both simulations occurred at 09:00 h. The light-off period was set at 23:00–07:00 h. Before, during, and after exposures, water intake was *ad libitum*. The diet was the same for all participants; it was standardized according to body weight in energy and nutrients based on WHO recommendations. The experimental protocols lasted 60 days (36 days in the facility) for the 21-day HDBR and 8 days for the 3-day DI. Comparative data on exposure times are presented in **Figure 1**.

Measurements

Diuresis, Water Intake, and Partial Water Balance

Water intake and diuresis were measured daily beginning 7 days before HDBR and ending 6 days after it, as well as beginning 3 days before DI and ending 1 day after it. Water balance was calculated as the difference between the consumed water and urine volume. Water in exhaled air and sweating were not registered.

Plasma Volume Evolution

Blood sampling for hemoglobin (Hb) and hematocrit (Hct) was performed in the morning before breakfast at before exposure, as well as on the 13th day of HDBR and after 3 days of DI. The percent change in plasma volume vs. before exposure was calculated using the Dill and Costill formula (Dill and Costill, 1974): DPV(%) = 100 × [HbB (1 − 0.01 Hcti)]/[Hbi (1 − 0.01 HctB)] − 100, where HbB and HctB are the initial values and Hbi and Hcti are those during exposure.

Daily Blood Pressure and Heart Rate Measurement

Brachial blood pressure and heart rate were measured twice a day (at 7 a.m. and 7 p.m.) throughout the stay at the MEDES facility.

Lower Body Negative Pressure–Tilt Test

The tilt test combined with lower body negative pressure (LBNP) was performed at before exposures and at R0 immediately following simulation (first rising after HDBR and DI). Finger blood pressure (Nexfin, Bmeye, United States) and ECG (Biopac, MP150, United States) were continuously recorded in the supine position for 5 min, then in the 80° tilt position for 15 min, and then during LBNP steps of −10 mmHg every 3 min. The test was considered to be accomplished at −80-mmHg LBNP step for HDBR and at −60-mmHg step for DI. Orthostatic tolerance time (OTT) was measured as the entire verticalization period in accordance with the standard procedure described by Protheroe et al. (2013). The test was stopped earlier upon appearance of pre-syncopal signs, request to stop, systolic blood pressure ≤80 mmHg, and heart rate (HR) <50 bpm or >170 bpm.

To assess hemodynamic and autonomic responses to the tilt test, we selected the last 3 min of baseline stable supine recordings. In the tilt period, the last 3 min of stable records (excluding pre-syncope symptoms) were assessed. Heart rate, blood pressure (systolic, diastolic), SV, and total peripheral resistance (TPR) were determined. Autonomic cardiac modulation was assessed *via* heart rate variability (HRV) markers—normalized low- (LF) and high-frequency (HF) spectrum power, sympathetic index (LF/HF), and spontaneous baroreflex sensitivity (SBRS)—as detailed in De Abreu et al. (2017).

Statistical Analysis

The results are presented as the mean ± SEM. All statistical analyses were performed using the GraphPad Prism program (8.3.0). Firstly, we assessed the normal distribution of anthropometric parameters by the Anderson–Darling test in groups ($p > 0.05$; the distribution is normal). We compared them using the unpaired *t*-test with Welch's correction to ensure the groups were not significantly different (**Table 1**). Then, since the groups appeared comparable by anthropometric parameters, we compared the groups by other parameters. Three factors were used in the study: time (before and after exposure), models (HDBR and DI), and tilt (supine and 80° tilt). For comparison of the partial water balance in −6° HDBR and DI, we used two-way repeated measures ANOVA (time × models). Plasma volume evolution was analyzed by ordinary two-way ANOVA (time × models). Daily blood pressure and heart rate measurements were not compared between models because of the different durations of exposures.

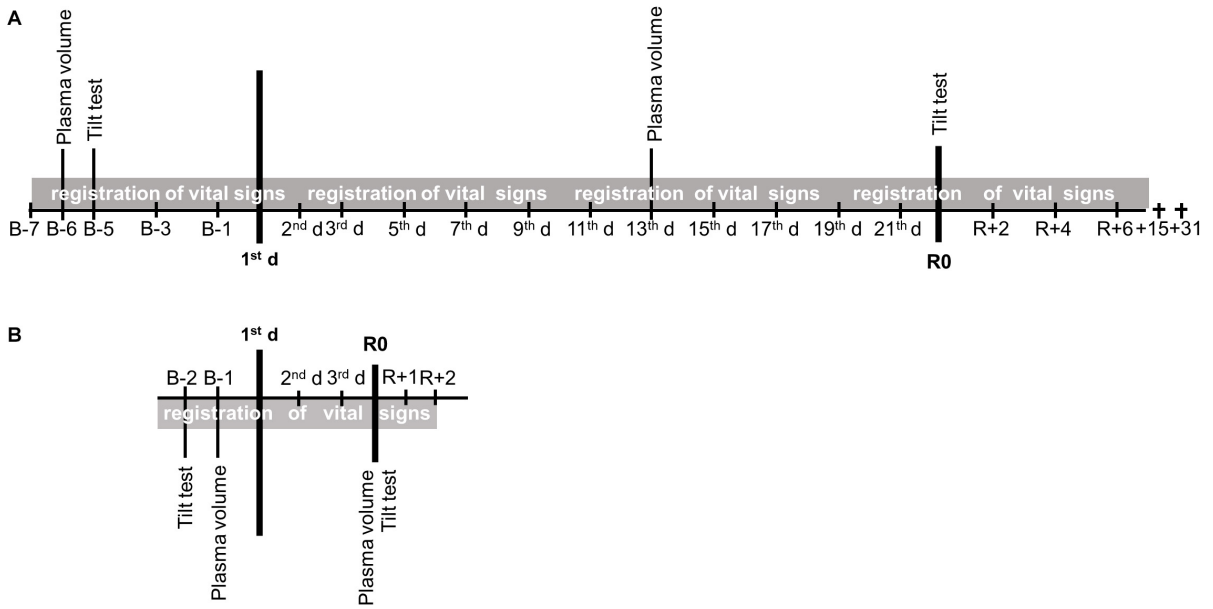

FIGURE 1 | The protocols. **(A)** 21-day head-down bed rest (HDBR). **(B)** 3-day dry immersion (DI).

When comparing within each model, one-way repeated measures ANOVA was applied. Orthostatic tolerance time was tested by ordinary two-way ANOVA (tilt × models). Three-way ANOVA (time × models × tilt) was used for the hemodynamic parameters and HRV tilt test data. Bonferroni *post hoc* test was applied for all comparisons, the values of which are given in the text when the differences are significant. The significance level was set at $\alpha = 0.05$.

RESULTS

Diuresis, Water Intake, and Partial Water Balance

Pre-bed rest water intake was 3.0–3.6 kg/day and diuresis was 2.3–2.7 kg/day; thus, water balance was positive and consisted of 0.6–1.3 kg/day (**Figure 2A**). Pre-immersion water intake was 3.0 kg/day, diuresis was 2.3–2.4 kg/day, and water balance consisted of 0.5–0.6 kg/day (**Figure 2B**).

On the first day of HDBR, there were a decrease in water intake and an increase in diuresis, which led to a nearly zero water balance ($p < 0.001$). However, on the second day of HDBR, water balance was positive and stabilized on a new level. On the first day of exposure to DI, a negative water balance was recorded ($p < 0.001$), the values of which exceeded those in the HDBR (**Figure 2C**). On the second and third days of immersion, water balance was stabilized on a positive level by reducing the water intake and diuresis (**Figure 2B**).

After the completion of either HDBR or DI, an increase in water balance was recorded ($p < 0.001$), which was due to an increase in the water intake and a decrease in diuresis. Starting from R + 1 day, water balance was not significantly different from the before exposure level. During the recovery period after DI, the water balance tended to restore; however, it did not reach the before exposure level.

We also compared the water balance at several time points: on the first, 13th, and 21st days for HDBR and on the first, second, and third days for DI (**Figure 2C**, upper and lower scales, respectively). As can be seen from the figure, the changes in water balance have a practically identical shape in both models. Although global two-way ANOVA was not significantly different in both time ($p < 0.001$) and model ($p = 0.003$) factors, the Bonferroni multiple comparisons *post hoc* test did not reveal differences in the latter.

It is worth noting that the total body mass of subjects progressively decreased during the experiments. The body mass loss was −3.4 kg ($p < 0.001$) on the 21st day of the −6° HDBR and was −1.4 kg ($p < 0.001$) on the third day of DI. Detailed data on the change in the body mass of subjects and the ratio of the partial water balance to it are given in the **Supplementary Material**.

Plasma Volume Evolution

Plasma volume significantly decreased during both exposures ($p < 0.001$; **Figure 3**). At the end of the 3-day DI, the decrease in plasma volume was significantly greater ($p = 0.003$) than that on the 13th day of HDBR (14 ± 2% after DI vs. 10 ± 6% during HDBR).

Daily Blood Pressure and Heart Rate Measurements

The data on blood pressure and heart rate changes during the experiments are presented in **Tables 2** and **3**. During HDBR, blood pressure did not significantly change; the heart rate became

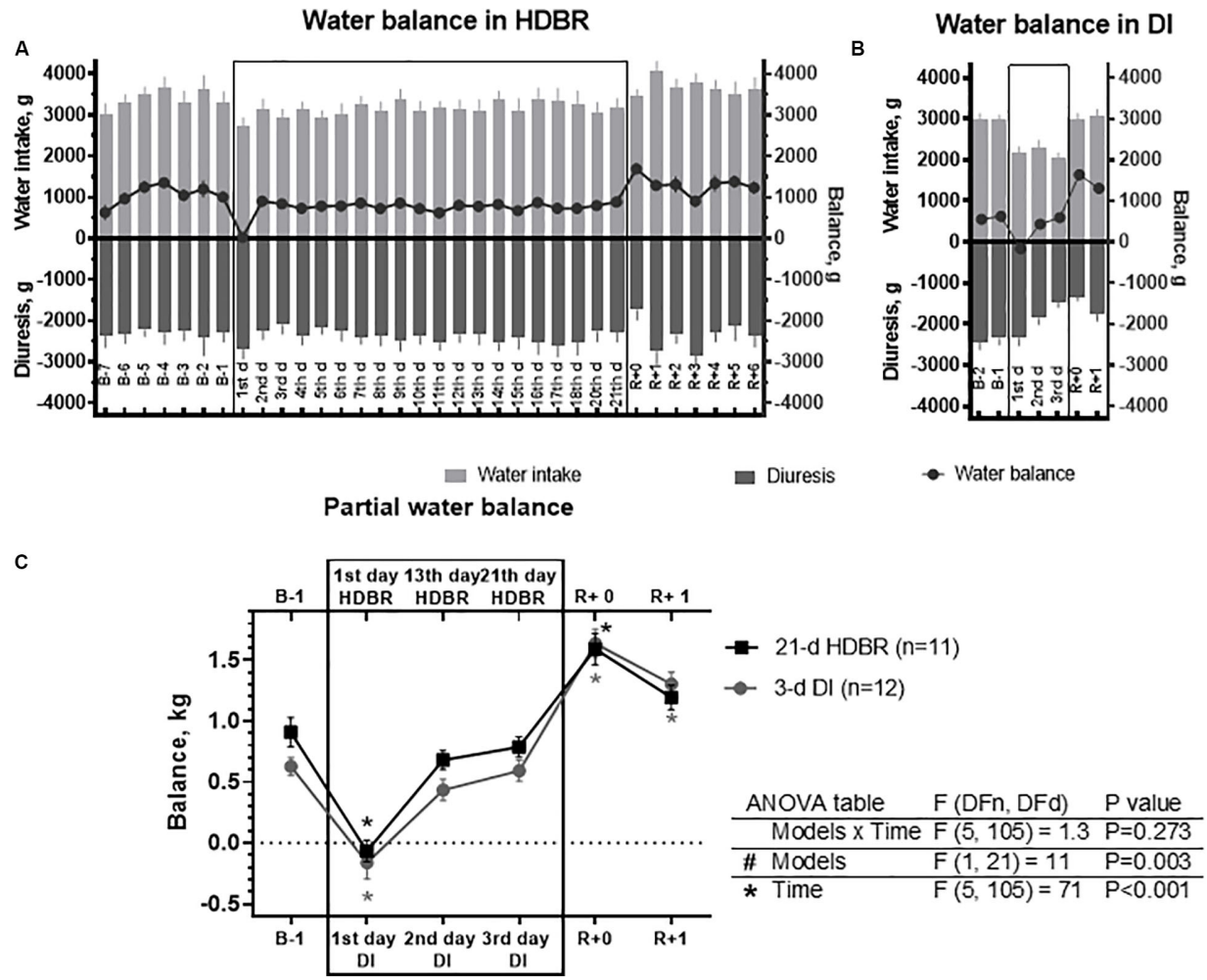

FIGURE 2 | Changes in partial water balance in the 21-day head-down bed rest (HDBR) **(A)**, 3-day dry immersion (DI) **(B)**, and their comparison between both groups **(C)**. Data are the mean ± SEM. *$p < 0.05$ vs. before exposure.

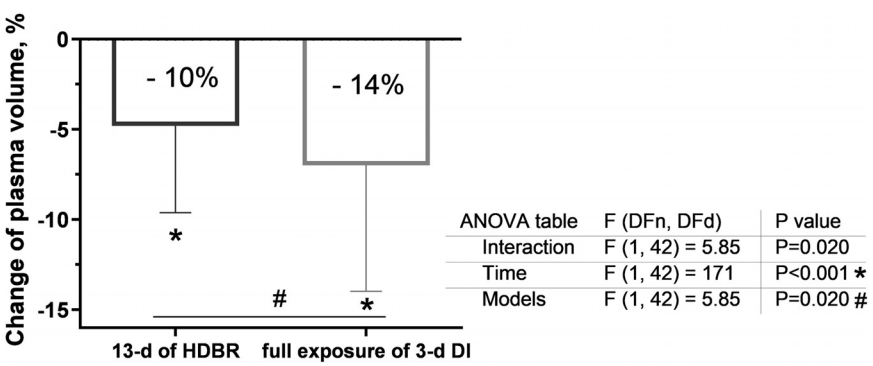

FIGURE 3 | Changes in plasma volume on the 13th day of head-down bed rest (HDBR) and at the end of the 3-day dry immersion (DI). Data are the mean ± SEM. *$p < 0.05$ vs. before exposure; #$p < 0.05$ between groups.

slightly decreased. On the first ($p < 0.01$), second ($p < 0.01$), third ($p < 0.01$), sixth ($p = 0.01$), seventh ($p < 0.01$), eighth ($p = 0.03$), and 13th ($p = 0.01$) days of HDBR, the heart rate was significantly decreased, and on the first ($p = 0.01$) and second ($p < 0.01$) days of recovery it was significantly increased compared to the before exposure level (average of 7 days before HDBR).

TABLE 2 | Blood pressure and heart rate before, during, and after the 21-day −6° head-down bed rest (HDBR) at 7 pm.

		Average	B-7	B-6	B-5	B-4	B-3	B-2	B-1	1st day	2nd day	3rd day	4th day	5th day	6th day	7th day	8th day	9th ayd	10th day
SBP (mmHg)	Mean	116.4	117.5	118.9	114.5	113.5	114.9	118.9	116.9	113.6	113.9	113.5	117.5	114.0	113.7	116.5	114.6	114.6	114.3
	SEM	2.4	3.6	3.4	4.0	2.5	3.5	2.3	3.4	2.6	3.0	3.4	3.8	3.8	3.8	2.8	2.5	3.8	3.1
DBP (mmHg)	Mean	65.3	66.5	65.0	65.9	61.7	64.6	67.0	66.5	64.5	65.0	62.8	65.2	64.8	63.9	66.5	66.0	66.5	64.8
	SEM	1.2	1.6	2.1	1.7	2.4	1.8	1.6	1.5	2.2	0.89	2.7	1.8	1.3	2.2	2.2	1.4	1.4	1.5
HR (bpm)	Mean	59.8	51.6	59.4	71.4	57.5	65.4	58.7	54.4	**50.5***	**50.4***	**49.6***	51.6	50.5	**50.9***	**50.4***	**52.4***	53.4	53.0
	SEM	3.4	3.4	3.9	4.8	3.5	4.7	3.6	3.6	**2.3**	**2.4**	**2.4**	2.2	2.5	**2.6**	**2.3**	**2.9**	2.7	1.8
		11th day	**12th day**	**13th day**	**14th day**	**15th day**	**16th day**	**17th day**	**18th day**	**19th day**	**20th day**	**21st day**	**R0**	**R + 1**	**R + 2**	**R + 3**	**R + 4**	**R + 5**	**R + 6**
SBP (mmHg)	Mean	116.2	115.1	113.1	114.3	114.8	113.8	113.1	115.8	113.7	116.3	114.2	119.2	116.7	114.2	119.2	114.5	114.5	115.2
	SEM	4.1	2.2	1.2	4.6	3.9	3.4	2.2	3.5	3.1	2.5	3.0	2.8	4.0	2.8	2.8	3.5	2.7	3.3
DBP (mmHg)	Mean	67.3	66.3	62.9	66.7	65.5	63.6	65.0	66.0	63.1	66.7	66.4	70.2	69.2	65.5	71.0	65.9	65.8	65.8
	SEM	1.5	2.0	2.4	1.5	1.9	1.9	2.2	2.0	2.4	1.7	2.9	2.8	2.2	1.5	1.6	2.8	1.4	1.8
HR (bpm)	Mean	52.2	52.6	**51.7***	51.5	55.5	51.8	54.1	55.4	60.3	56.9	57.1	**69.2***	**77.0***	60.9	66.7	67.9	62.6	61.7
	SEM	1.5	2.7	**2.4**	2.0	3.3	1.8	2.8	2.4	3.9	2.3	2.2	**4.1**	**3.4**	3.7	3.4	4.1	3.7	3.0

*Data are the mean ± SEM. B-, days before exposure; R+, days of recovery period. *p < 0.05 vs. average for 7 days before HDBR are indicated in bold.*

TABLE 3 | Blood pressure and heart rate before, during, and after the 3-day dry immersion (DI) at 7 pm.

		Average	B-3	B-2	B-1	DI 1	DI 2	DI 3	R0	R + 1
SBP (mmHg)	Mean	125.1	128.7	123.9	122.7	**115.8***	121.5	125.9	130.5	128.7
	SEM	2.6	2.5	3.7	2.4	**3.5**	2.9	3.0	2.9	2.4
DBP (mmHg)	Mean	68.3	68.2	66.8	69.8	**62.3***	65.1	69.8	**74.2***	74.0
	SEM	1.7	1.7	1.8	2.3	**1.9**	2.2	1.3	**1.9**	2.3
HR (bpm)	Mean	56.4	56.9	58.4	53.9	59.0	53.9	58.0	**69.4***	58.3
	SEM	1.9	2.1	2.3	1.6	3.47	1.9	2.8	**2.6**	2.1

*Values are the mean ± SEM. B-, days before exposure; R +, days of recovery period. *p < 0.05 vs. average for 3 days before DI are indicated in bold.*

During DI, the first day was marked by decreases in systolic blood pressure (SBP; $p = 0.027$) and diastolic blood pressure (DBP; $p < 0.01$), whereas heart rate did not change. On the first day of recovery, diastolic blood pressure ($p = 0.048$) and heart rate ($p < 0.01$) significantly increased compared to the average of 3 days before DI.

Hemodynamic and Autonomic Responses to the Tilt Test

Before either HDBR or DI exposure, SBP during the tilt test increased in both groups vs. the supine position ($p = 0.02$ for DI; **Figure 4A**). After the 21-day HDBR and 3-day DI, the changes in SBP had the opposite characteristic: SBP dropped by ∼17 mmHg after HDBR ($p = 0.002$) and by ∼10 mmHg after DI exposures.

Diastolic blood pressure during the tilt test increased significantly vs. the supine position compared to that before HDBR and DI ($p < 0.001$; **Figure 4B**). After either the 21-day HDBR or 3-day DI, a DBP increase during table rotation was less pronounced than that before exposures, especially for HDBR. Diastolic blood pressure in the supine position was higher after DI compared to that before exposure ($p = 0.046$).

Before either HDBR or DI exposure, heart rate during the tilt test increased in both groups by ∼12 bpm vs. the supine position ($p < 0.001$; **Figure 4C**). After exposures, HR was higher by 11–13 bpm even at rest ($p = 0.047$ for DI). During the tilt test, HR significantly increased by 65–70% vs. the supine position ($p < 0.001$) and by 47–50% vs. before exposure ($p < 0.001$) in both groups.

Before both exposures, the TPR during the tilt test increased ($p = 0.029$ for HDBR; **Figure 5A**). After exposures, during the tilt test, the TPR had a slight tendency to increase in the DI group and to decrease in the HDBR group compared to those before exposures ($p < 0.001$).

Before either HDBR or DI exposure, SV during the tilt test decreased ($p < 0.001$; **Figure 5B**). After exposures, the SV decrease during the tilt test was more pronounced. However, after DI, these changes achieved significance compared to those before exposure ($p < 0.001$).

Spontaneous baroreflex sensitivity during the tilt test significantly dropped compared to that before exposures ($p = 0.002$ for HDBR and $p < 0.001$ for DI; **Figure 6A**). After HDBR and DI, supine SBRS was lower than the initial level ($p = 0.026$ for HDBR and $p = 0.004$ for DI), decreasing further in response to tilt ($p = 0.047$ for HDBR and $p < 0.001$ for DI). The changes in both groups were similar.

Before either HDBR or DI exposure, an increase in sympathetic index (SI) reflecting cardiac sympathetic activation was observed in response to orthostasis ($p = 0.030$ for DI). After the 21-day HDBR and 3-day DI, SI was slightly increased even at rest (**Figure 6B**) and had a tendency to increase during the tilt test.

Orthostatic Tolerance

The OTT is an integrative measure of the success of the strategy to provide the upright position of the body. Before both exposures, OTT consisted of 27–28 min, corresponding to ∼50 mmHg (**Figure 7**, right scale) of LBNP. After exposures, the OTT decreased in both groups ($p < 0.001$): to 14.2 ± 3.1 min after the 21-day HDBR and to 8.7 ± 2.1 min after the 3-day DI.

DISCUSSION

Main Findings

The main finding is that cardiovascular changes induced by the 21-day −6° HDBR and 3-day DI are comparable, despite the sevenfold difference in the duration of exposures.

Both models reproduce the absence of physical loads. Thus, deep hypokinesia is reproduced in both models. The strict horizontal position (without daily raise) during the protocols of HDBR and DI has a detraining effect on the cardiovascular and other systems. However, the degree of reproduction of such an important factor as support unloading differs: in HDBR, support loads are redistributed from the soles to the surface of the back, buttocks, and the back surfaces of the legs; in DI, there is virtually no support due to buoyancy. We believe that support unloading is an important factor in the development of microgravitational deconditioning and that its increase leads to stronger effects in a short time.

Fluid Shift Influence

The parameter that differs between the −6° HDBR and DI models is the mechanism that provides the fluid shift. In HDBR, it is achieved by an anti-orthostatic position, which promotes fluid transition to the upper parts of the body. A number of authors have shown that the fluid shift processes during HDBR occur quite quickly. Water intake, diuresis, and plasma volume stabilized on a new level by the third to fourth day or earlier (Greenleaf, 1983; Meck et al., 2009; Navasiolava et al., 2011a). In our case, the water balance was established on the second day

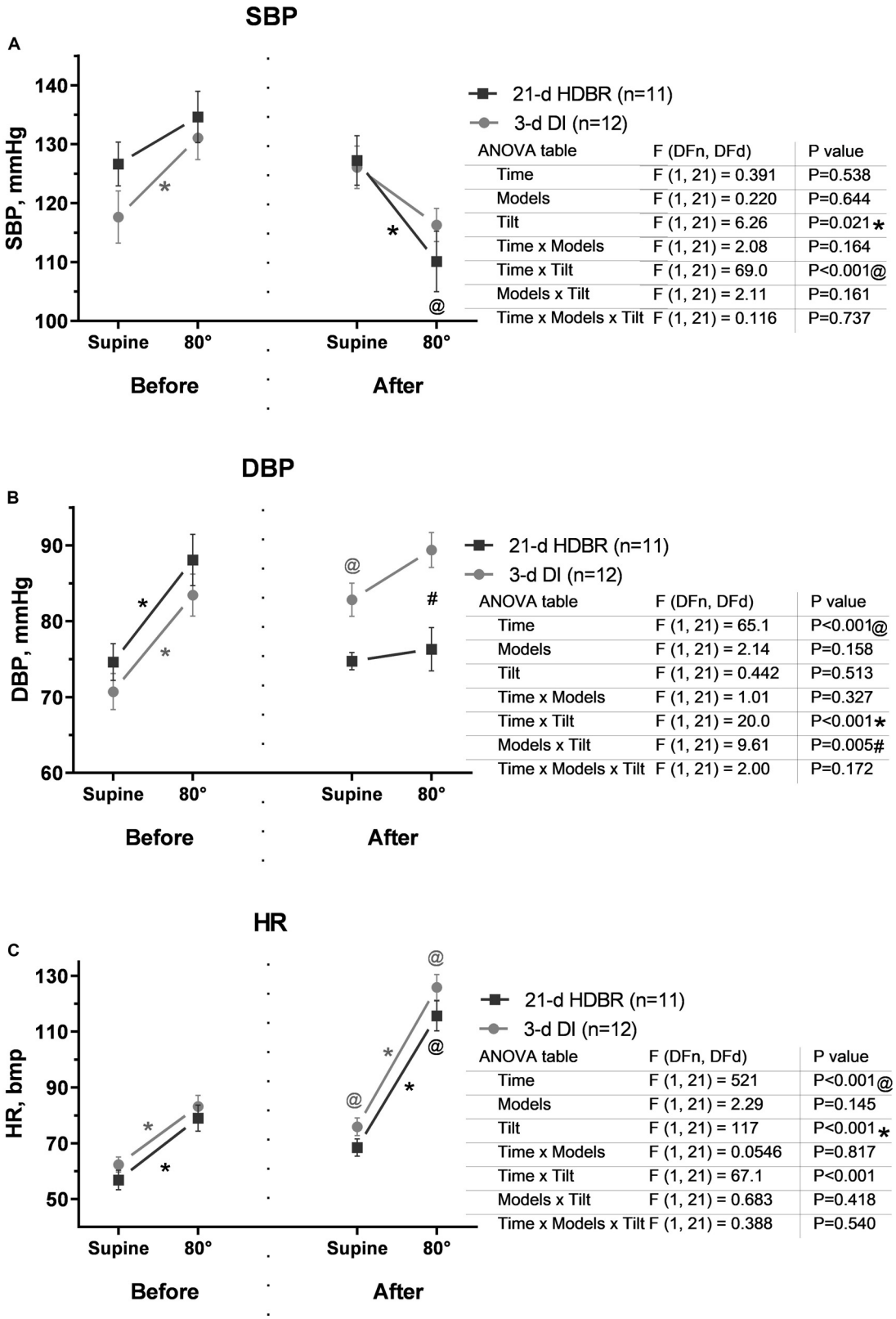

FIGURE 4 | Changes in systolic blood pressure **(A)**, diastolic blood pressure **(B)**, and heart rate **(C)** in response to the 80° tilt test before and after the 21-day head-down bed rest (HDBR) and 3-day dry immersion (DI). Data are the mean ± SEM. $^{\#}p < 0.05$ between groups; $^{*}p < 0.05$, 80° vs. the supine position; $^{@}p < 0.05$, before vs. after exposure.

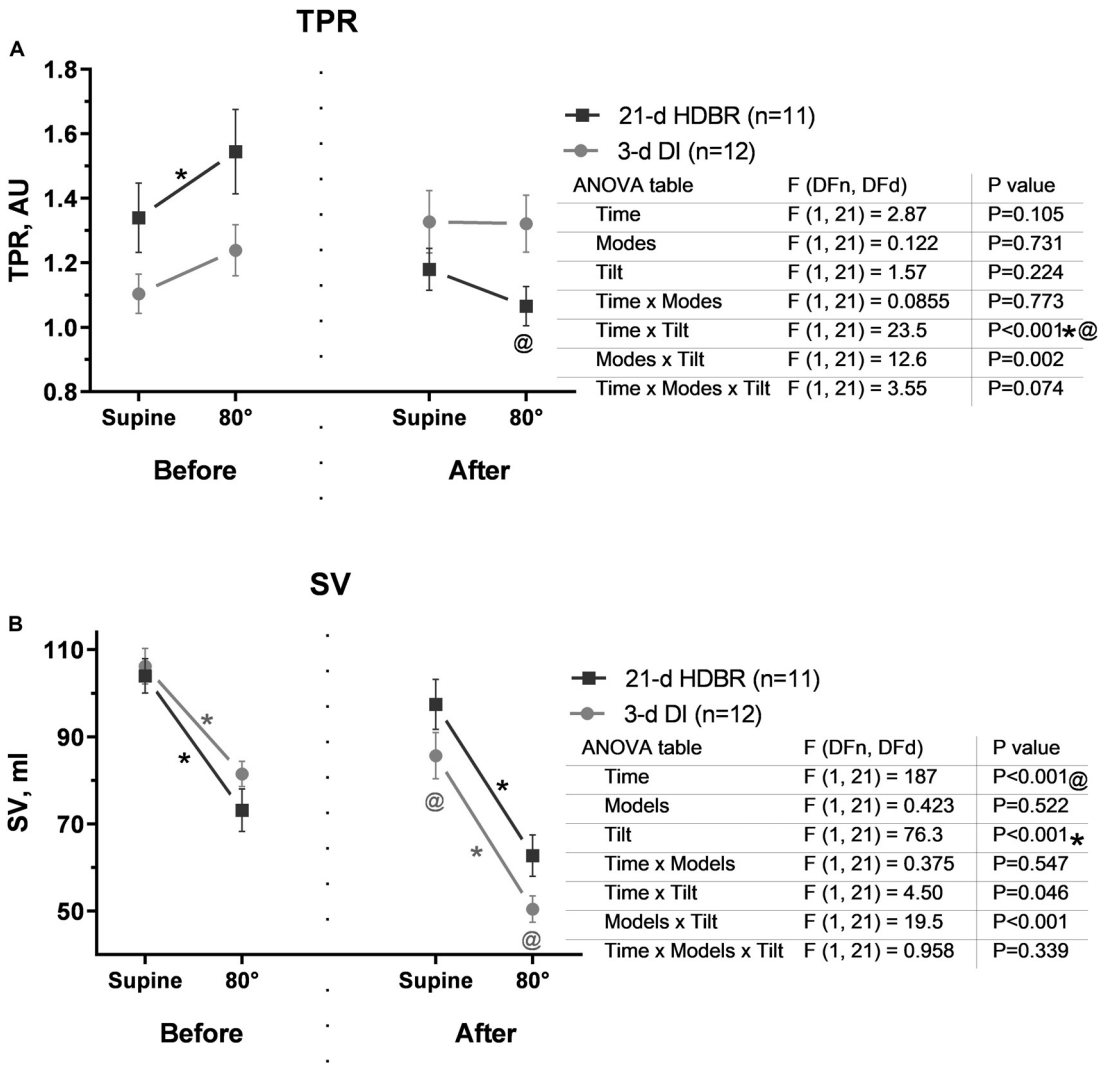

FIGURE 5 | Changes in total peripheral resistance **(A)** and stroke volume **(B)** in response to the 80° tilt test before and after the 21-day head-down bed rest (HDBR) and 3-day dry immersion (DI). Data are the mean ± SEM. $^{\#}p < 0.05$ between groups; $^{*}p < 0.05$, 80° vs. the supine position; $^{@}p < 0.05$, before vs. after exposure.

of HDBR. In the immersion, in contrast to HDBR, hydrostatic compression induces fluid centralization. According to a review article by E. Tomilovskaya et al., fluid shift occurs in DI faster than in HDBR (during the first day) (Tomilovskaya et al., 2019). Interestingly, in our study, the effect of the 3-day DI on water intake and diuresis was more pronounced (but not significantly) than in the 21-day −6° HDBR. In both cases, the fluid shift occurs, simulating the conditions of spaceflight.

In our study, there was a significant progressive decrease in the subject's body mass. However, surprisingly, fluid loss did not play a dominant role in this. Before the exposures, all subjects lived in a hospital (for 7 days before HDBR and 3 days before DI) and received a standard regulated diet. We assume that the transition to a more proper and balanced nutrition could contribute to a weight loss in our study. Also, we suggest that body mass decrease in the last stages of HDBR could be associated with muscle loss, which is observed in other bed rest studies (Shenkman et al., 1997; Stuempfle and Drury, 2007; Dirks et al., 2016; Kramer et al., 2017; Shenkman and Kozlovskaya, 2019).

Central Hemodynamic Parameters

Despite the similarity of the cardiovascular changes, we observed a number of differences in the effects of the two models. After the completion of the 21-day HDBR and 3-day DI, resting tachycardia and orthostatic intolerance were detected, accompanied by a relative decrease in upright SBP, DBP, SV, and TPR and an increase in HR in response to tilt. Our results are in agreement with literature data (Buckey et al., 1996; Knight et al., 2009a) and indicate a significant cardiovascular deconditioning after both simulations. Interestingly, supine TPR and DBP had a tendency to increase following DI, but not HDBR. These parameters may suggest an increase in initial vascular tone, the important role of which was indicated by several

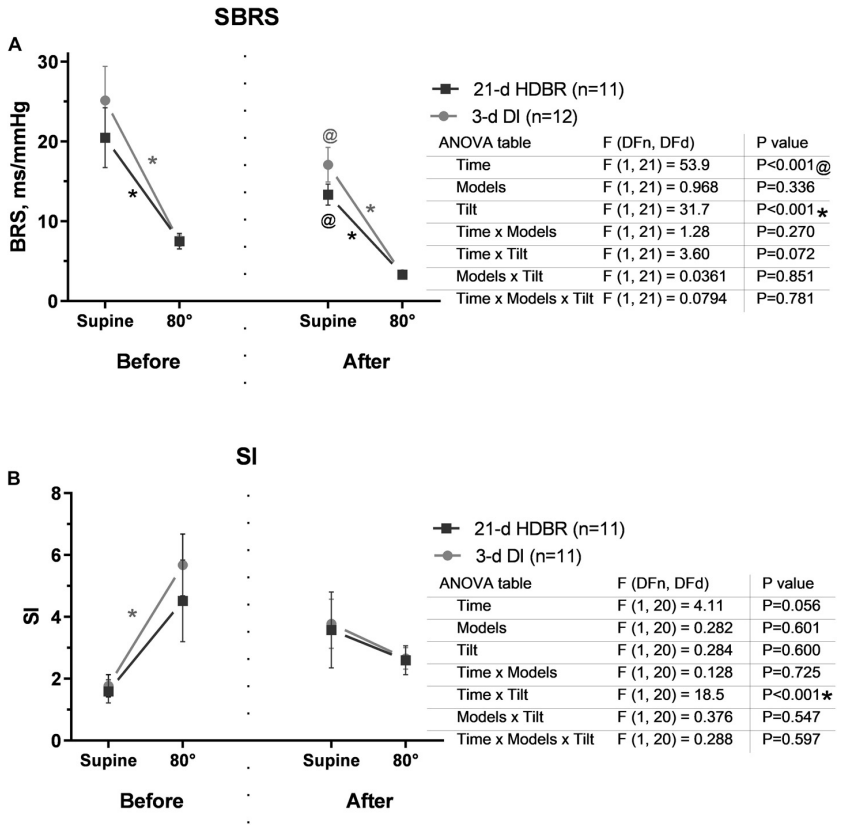

FIGURE 6 | Changes in spontaneous baroreflex **(A)** and sympathetic index **(B)** in response to the 80° tilt test before and after the 21-day head-down bed rest (HDBR) and 3-day dry immersion (DI). Data are the mean ± SEM. $^{\#}p < 0.05$ between groups; $^{*}p < 0.05$, 80° vs. the supine position; $^{@}p < 0.05$, before vs. after exposure.

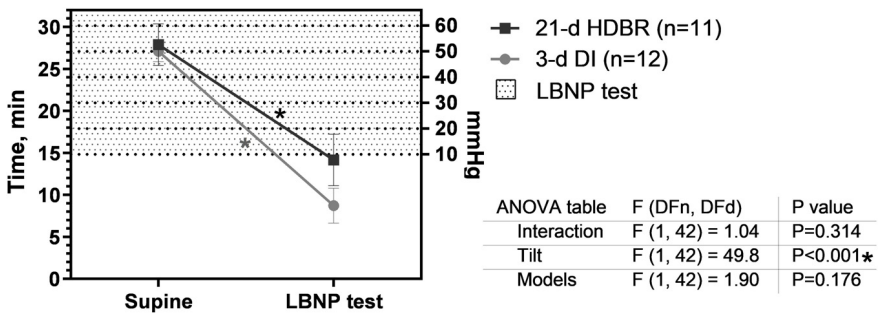

FIGURE 7 | Orthostatic tolerance time before and after the 21-day head-down bed rest (HDBR) and 3-day dry immersion (DI). Data are the mean ± SEM. $^{*}p < 0.05$ vs. before exposure.

authors (Convertino et al., 1999; Vinogradova et al., 2002). According to the Convertino hypothesis (Convertino et al., 1999), the diminished vasoconstrictive reserve may be the main mechanism of vasoconstrictor insufficiency in case of orthostatic intolerance. The maximal capacity of vasoconstriction is not altered under microgravity (Convertino et al., 1999), but hypovolemia may induce an increase in initial vasoconstriction and, thus, decrease the vasoconstrictive reserve (Convertino et al., 1999).

Autonomic Regulation of Cardiovascular Functions

Autonomic regulation is extremely important in maintaining blood pressure homeostasis during verticalization (Mano, 2005). In our studies, baroreflex sensitivity was reduced both at rest and during the tilt test after exposure, suggesting a reduced capacity of the baroreflex loop to regulate blood pressure (Tank et al., 1995). Both after the 21-day HDBR and 3-day DI, the SI failed to increase in the upright position, which is one of the signs of autonomic insufficiency.

Orthostatic Intolerance

The time of orthostatic stability, an integrative parameter of the cardiovascular state, demonstrates the efficacy of the strategy of vertical stance maintenance. In our study, the OTT after both exposures decreased without a significant difference between groups. However, the signs of orthostatic insufficiency observed after the 3-day DI tended to be more pronounced (8.7 min in DI vs. 14.2 min in HDBR), probably due to a more pronounced post-exposure hypovolemia and diminished vasoconstrictive reserve.

Evaluation of the Optimal Protocol

DI was seven times shorter than HDBR, yet we detected similar changes in the studied parameters, which suggest an accelerated cardiovascular impairment in DI compared to HDBR. However, the cardiovascular deconditioning appears rather quickly and then remains at a rather stable level; probably, comparing experiments of the same duration would show the same degree of cardiovascular deconditioning, which undoubtedly requires verification. Seventy-five percent of the 3-day DI subjects and 55% of the 21-day HDBR subjects were not able to complete the tilt test. This complies with literature data on HDBR of various durations: 5 out of 11 (45%), after 4 days ($p = 0.15$); four out of six (67%), after 14 days ($p = 0.7$); five out of nine (56%), after 28 or 30 days ($p = 0.35$); and four out of seven (57%), after 42 days of HDBR ($p = 0.4$) (Pavy-Le Traon et al., 2007).

It is interesting to note that, when applying two- or three-way ANOVA to analyze central hemodynamic parameters, HRV, and plasma volume, the interaction of such factors as time and tilt was identified, which may indicate that they are co-directional. The interaction of the model and tilt factors was found in DBP, TPR, and SV. However, possible interpretations should be made with caution.

Study Limitation

The protocols of the 21-day HDBR and 3-day DI were followed independently of each other; therefore, their durations differed by seven times. However, despite the fact that the use of the same research methods in both models made it possible to compare the obtained data, it is worth reminding that it was not planned for as the original protocols, and this may introduce certain limitations. Still, it is of interest to make consistent experimental comparisons of protocols of the same duration [both short (3–5 days) and longer (several weeks)].

Increasing the sample size would also have a positive effect on the reliability of the results. However, a sample of 10–12 subjects is quite common in space biology studies.

CONCLUSION

In general, cardiovascular changes during the 21-day −6° HDBR and head-out 3-day DI were co-directional. Frequently, changes after 3-day DI were equal to or exceeded changes after 21-day HDBR. Significantly stronger effects of DI on cardiovascular function can be caused not only by a more pronounced hypovolemia but also by support unloading (supportlessness). The support deafferentation plays a trigger role in the development of hypogravitational disorders. This was shown for the sensorimotor system (Grigor'ev et al., 2004; Kozlovskaya et al., 2007); however, for other systems, the role of support afferentation is under question. A decrease in postural muscle tone in response to a decrease in support afferentation may be responsible for the orthostatic impairment *via* a decrease in the efficiency of the muscle pump promoting venous return.

DATA AVAILABILITY STATEMENT

The datasets generated for this study are available on request to the corresponding author.

ETHICS STATEMENT

MNX Bed-Rest study was approved by the local Ethic Committee (CPP Sud-Ouest Outre-Mer I) and French Health Authorities (NO ID RCB: 2012-A00337-36). Dry Immersion study was approved by the local Ethic Committee (CPP Sud-Ouest Outre-Mer I, France) and French Health Authorities (NO ID RCB: 2014-A 00904-43). The patients/participants provided their written informed consent to participate in this study.

AUTHOR CONTRIBUTIONS

LA conducted measurements, processing results and writing the manuscript. NN participated in critically revision of the manuscript. IR, GG-K and CG helped to organize the DI procedure in MEDES and participated in discussion of the results. IK, M-AC and ET participated in concepting of the idea and critical revision of the manuscript.

FUNDING

The study was supported by grants from MEDES (organization of the study), from Russian Scientific Foundation (processing of the results, grant No. 19-15-00435), and from CNES and IBMP (support of young scientists).

ACKNOWLEDGMENTS

The team of authors sincerely thanks Valentina M. Romantchikova for editing and for valuable advice on the manuscript.

SUPPLEMENTARY MATERIAL

The Supplementary Material for this article can be found online at: https://www.frontiersin.org/articles/10.3389/fphys.2020.00395/full#supplementary-material

REFERENCES

At'kov, O. Y., and Bednenko, B. C. (1987). *Hypokinesia, Weightlessness: Clinical and Physiological Aspects*. Moscow: Nauka.

Ayme, K., Gavarry, O., Rossi, P., Desruelle, A. V., Regnard, J., Boussuges, A., et al. (2014). Effect of head-out water immersion on vascular function in healthy subjects. *Appl. Physiol. Nutr. Metab.* 39, 425–431. doi: 10.1139/apnm-2013-0153

Barbic, F., Heusser, K., Minonzio, M., Shiffer, D., Cairo, B., Tank, J., et al. (2019). Effects of prolonged head-down bed rest on cardiac and vascular baroreceptor modulation and orthostatic tolerance in healthy individuals. *Front. Physiol.* 10:1061. doi: 10.3389/fphys.2019.01061

Bart, V., Beckers, F., Couckuyt, K., and Liu, J. (2007). "Dynamic cardiovascular control during one hour of thermoneutral head-out of water immersion," in *Proceedings of the 16 IAA Humans in Space Symposium*, Beijing, 223.

Blanc, S., Normand, S., Ritz, P., Pachiaudi, C., Vico, L., Gharib, C., et al. (1998). Energy and water metabolism, body composition and hormonal changes induced by 42 days of enforced inactivity and simulated weightlessness. *J. Clin. Endocrinol. Metab.* 83, 4289–4297. doi: 10.1210/jcem.83.12.5340

Buckey, J. C., Lane, L. D., Levine, B. D., Watenpaugh, D. E., Wright, S. J., Moore, W. E., et al. (1996). Orthostatic intolerance after spaceflight. *J. Appl. Physiol.* 81:7.

Convertino, V. A., Koenig, S. C., Fanton, J. W., Reister, C. A., Gaffney, F. A., Ludwig, D. A., et al. (1999). Alterations in the volume stimulus-renal response relationship during exposure to simulated microgravity. *J. Gravit. Physiol.* 6, 1–9.

Custaud, M. A., de Souza Neto, E. P., Abry, P., Flandrin, P., Millet, C., Duvareille, M., et al. (2002). Orthostatic tolerance and spontaneous baroreflex sensitivity in men versus women after 7 days of head-down bed rest. *Auton. Neurosci.* 100, 66–76. doi: 10.1016/s1566-0702(02)00132-7

De Abreu, S., Amirova, L., Murphy, R., Wallace, R., Twomey, L., Gauquelin-Koch, G., et al. (2017). Multi-system deconditioning in 3-day dry immersion without daily raise. *Front. Physiol.* 8:799. doi: 10.3389/fphys.2017.00799

Dill, D. B., and Costill, D. L. (1974). Calculation of percentage changes in volumes of blood, plasma, and red cells in dehydration. *J. Appl. Physiol.* 37, 247–248. doi: 10.1152/jappl.1974.37.2.247

Dirks, M. L., Wall, B. T., van de Valk, B., Holloway, T. M., Holloway, G. P., Chabowski, A., et al. (2016). One Week of bed rest leads to substantial muscle atrophy and induces whole-body insulin resistance in the absence of skeletal muscle lipid accumulation diabetes. *Diabetes* 65, 2862–2875. doi: 10.2337/db15-1661

Epstein, M. (1992). Renal effects of head-out water immersion in humans: a 15-year update. *Physiol. Rev.* 72, 563–621. doi: 10.1152/physrev.1992.72.3.563

Fortney, S. M., Schneider, V. S., and Greenleaf, J. E. (1996). "The physiology of bed rest," in *Handbook of Physiology Section 4: Environmental Physiology*, eds M. J. Fregly, and C. M. Blatteis, (New York, NY: Oxford University Press), 889–939.

Fritsch-Yelle, J. M., Charles, J. B., Jones, M. M., and Wood, M. L. (1996). Microgravity decreases heart rate and arterial pressure in humans. *J. Appl. Physiol.* 80, 910–914. doi: 10.1152/jappl.1996.80.3.910

Gazenko, O. G. (1984). Results and prospects of physiological studies in spaceflights. *Vestn. Akad. Med. Nauk SSSR.* 4:7.

Gibson, E. G. (1977). *Skylab-4 Grew Observations//Biomedical Results From Skylab*. Washington, DC: US Gov. Print. Off. (NASA; SP-377), 22–26.

Gogolev, K. I., Aleksandrova, E. A., and Shul'zhenko, E. B. (1980). Comparative assessment of changes during antiorthostatic hypokinesia and immersion in man. *Hum. Physiol.* 6, 392–396.

Greenleaf, J. E. (1983). *Bed-rest studies - Fluid, and Electrolyte Responses*. Washington, DC: NASA.

Greenleaf, J. E. (1984). Physiology of fluid and electrolyte responses during inactivity: water immersion and bed rest. *Med. Sci. Sports Exerc.* 16, 20–25.

Grigor'ev, A. I., Kozlovskaya, I. B., and Shenkman, B. S. (2004). Role of support afferentation in organizing the tonic muscular system. *Russ. Physiol.* 5, 508–521.

Hargens, A. R., and Vico, L. (2016). Long-duration bed rest as an analog to microgravity. *J. Appl. Physiol.* 120, 891–903. doi: 10.1152/japplphysiol.00935.2015

Johansen, L. B., Gharib, C., Allevard, A. M., Sigaudo, D., Christensen, N. J., Drummer, C., et al. (1997). Haematocrit, plasma volume and noradrenaline in humans during simulated weightlessness for 42 days. *Clin. Physiol.* 17, 203–210. doi: 10.1046/j.1365-2281.1997.02626.x

Klassen, S. A., De Abreu, S., Greaves, D. K., Kimmerly, D. S., Arbeille, P., Denise, P., et al. (2018). Long-duration bed rest modifies sympathetic neural recruitment strategies in male and female participants. *J. Appl. Physiol.* 124, 769–779. doi: 10.1152/japplphysiol.00640.2017

Knight, J., Nigam, Y., and Jones, A. (2009a). Effects of bedrest 1: cardiovascular, respiratory and haematological systems. *Nurs. Times* 105, 16–20.

Knight, J., Nigam, Y., and Jones, A. (2009b). Effects of bedrest 2: gastrointestinal, endocrine, renal, reproductive and nervous systems. *Nurs. Times* 105, 24–27.

Kotovskaya, A. R., and Fomina, G. A. (2013). Prediction of human orthostatic tolerance by changes in arterial and venous hemodynamics in the microgravity environment. *Hum. Physiol.* 39, 25–33.

Kramer, A., Gollhofer, A., Armbrecht, G., Felsenberg, D., and Gruber, M. (2017). How to prevent the detrimental effects of two months of bed-rest on muscle, bone and cardiovascular system: an RCT. *Sci. Rep* 7:13177. doi: 10.1038/s41598-017-13659-8

Krupina, T. N., Yarulin, K. H. K. H., and Kotovskaya, A. R. (1982). Features of the reaction of the cardiovascular system and metabolism in older people during hypokinesia and immersion. *Kosm. Biol. Aviakosm Med.* 1, 51–51.

Larina, I. M., Custaud, M. A., and Pastushkova, L. K. H. (2008). Water-electrolyte metabolism, renal function and cutaneous microcirculation in human subjects during 7-day dry immersion. *Aviakosm. Ekolog. Med.* 42, 29–34.

Leach Huntoon, C. S., Grigoriev, A. I., and Natochin, Y. V. (1998). Fluid and electrolyte regulation in spaceflight. *Sci. Technol. Ser.* 94:238.

Lobachik, V. I., Abrosimov, S. V., Zhidkov, V. V., and Endeka, D. K. (1991). Hemodynamic effects of microgravity and their groundbased simulations. 8th IAA Man in space symposium. *Acta Astronaut.* 23, 35–40.

Maillet, A., Pavy-Le Traon, A., Allevard, A. M., Sigaudo, D., Hughson, R. L., Gharib, C., et al. (1994). Hormone changes induced by 37.5-h head-down tilt (-6). *J. Appl. Physiol.* 68, 497–503. doi: 10.1007/bf00599519

Mano, T. (2005). Autonomic neural functions in space. *Curr. Pharm. Biotechnol.* 6, 319–324.

Martin, D. S., and Meck, J. V. (2004). Presyncopal/non-presyncopal outcomes of post spaceflight stand tests are consistent from flight to flight. *Aviat. Space Environ. Med.* 75, 65–67.

Meck, J., Dreyer, S. A., and Warren, L. E. (2009). Long-duration head-down bed rest: project overview, vital signs, and fluid balance. *Aviat. Space Environ. Med.* 80(5 Suppl), A1–A8. doi: 10.3357/asem.br01.2009

Modak, S., and Banerjee, P. K. (2004). Studies of left ventricular functions by systolic time intervals on exposure to dry immersion Indian. *J. Aerospace Med.* 48:48.

Mulavara, A. P., Peters, B. T., Miller, C. A., Kofman, I. S., Reschke, M. F., Taylor, L. C., et al. (2018). Physiological and functional alterations after spaceflight and bed rest. *Med. Sci. Sports Exerc.* 50, 1961–1980. doi: 10.1249/MSS.0000000000001615

Kozlovskaya, I. B., Sayenko, I. V., and Sayenko, D. G. (2007). Role of support afferentation in control of the tonic muscle activity. *Acta Astronaut.* 60, 285–294. doi: 10.1016/j.actaastro.2006.08.010

Navasiolava, N. M., Custaud, M. A., Tomilovskaya, E. S., Larina, I. M., Mano, T., Gauquelin-Koch, G., et al. (2011a). Long-term dry immersion: review and prospects. *Eur. J. Appl. Physiol.* 111, 1235–1260. doi: 10.1007/s00421-010-1750-x

Navasiolava, N. M., de Germain, V., Levrard, T., Larina, I. M., Kozlovskaya, I. B., Diquet, B., et al. (2011b). Skin vascular resistance in the standing position increases significantly after 7 days of dry immersion. *Auton. Neurosci.* 160, 64–68. doi: 10.1016/j.autneu.2010.10.003

Nesterovskaia, A. I. U., Morukov, B. V., Vorontsov, A. L., Markin, A. A., Zhuravleva, O. A., Zabolotskaia, I. V., et al. (2008). Evaluation of the 7-day immersion effect on the renal excretory function. *Aviakosm. Ekolog. Med.* 42, 52–56.

Norsk, P., Asmar, A., Damgaard, M., and Christensen, N. J. (2015). Fluid shifts, vasodilatation and ambulatory blood pressure reduction during long duration spaceflight. *J. Physiol.* 593, 573–584. doi: 10.1113/jphysiol.2014.284869

Norsk, P., Damgaard, M., Petersen, L., Gybel, M., Pump, B., Gabrielsen, A., et al. (2006). Vasorelaxation in space. *Hypertens* 47, 69–73.

Osadchii, L. I., Balueva, T. V., and Sergeev, I. V. (1997). Hemodynamic structure of antiorthostatic reactions: relationship of mechanical activity of the heart and arterial pressure. *Aviakosm. Ekolog. Med.* 31, 19–23.

Pakharukova, N. A., Pastushkova, L. H., and Larina, I. M. (2009). "Changes of healthy human serum proteome profile during 7-day dry immersion," in *Proceedings of the Summary Book of 30th Annual International Gravitational Physiology Meeting*, Xi'an, 56.

Pavy-Le Traon, A., Heer, M., Narici, M. V., Rittweger, J., and Vernikos, J. (2007). From space to Earth: advances in human physiology from 20 years of bed rest studies (1986-2006). *Eur. J. Appl. Physiol.* 101, 143–194. doi: 10.1007/s00421-007-0474-z

Pestov, I. D., and Gerathewohl, S. J. (1975). "Weightlessness," in *Foundations of Space Biology and Medicine*, Vol. 2, eds M. Calvin, and O. G. Gazenko, (Washington, DC: NASA), 324.

Prisk, G. K., Guy, H. J., Elliott, A. R., Deutschman, R. A., and West, J. B. (1993). Pulmonary diffusing capacity, capillary blood volume and cardiac output during sustained microgravity. *J. Appl. Physiol.* 75, 15–26. doi: 10.1152/jappl.1993.75.1.15

Protheroe, C. L., Ravensbergen, H. R., Inskip, J. A., and Claydon, V. E. (2013). Tilt testing with combined lower body negative pressure: a "gold standard" for measuring orthostatic tolerance. *J. Vis. Exp.* 73:e4315. doi: 10.3791/4315

Shenkman, B. S., and Kozlovskaya, I. B. (2019). Cellular responses of human postural muscle to dry immersion. *Front. Physiol.* 10:187. doi: 10.3389/fphys.2019.00187

Shenkman, B. S., Kozlovskaya, I. B., Nemirovskaya, T. L., and Tcheglova, I. A. (1997). Human muscle atrophy in supportlessness: effects of short-term exposure to dry immersion. *J. Gravit. Physiol.* 4, 137–138.

Shulzhenko, E. B., and Vill-Villiams, I. F. (1976). The opportunity to conduct long-term water immersion method Dry Immersion. *Russ. Biol. Aerospace Med.* 9, 82–84.

Shykoff, B. E., Fahri, L. E., Olszowka, A. J., Pendergast, D. R., Rokitka, M. A., Eisenhardt, C. G., et al. (1996). Cardiovascular response to submaximal exercise in sustained microgravity. *J. Appl. Physiol.* 81, 26–32. doi: 10.1152/jappl.1996.81.1.26

Sigaudo, D., Fortrat, J. O., Maillet, A., Allevard, A. M., Pavy-Le Traon, A., Hughson, R. L., et al. (1996). Comparison of a 4-day confinement and head-down tilt on endocrine response and cardiovascular variability in humans. *Eur. J. Appl. Physiol. Occup. Physiol.* 73, 28–37. doi: 10.1007/bf00262806

Stuempfle, K., and Drury, D. (2007). The physiological consequences of bed rest. *J. Exerc. Physiol.* 10, 32–41. doi: 10.1016/s1073-4449(99)70030-0

Tank, J., Baevsky, R. M., and Weck, M. (1995). Hemodynamic regulation during postural tilt assessed by heart rate- and blood-pressure variability combined with impedance cardiography. *Wien. Med. Wochenschr.* 145, 616–625.

Thornton, W. E., and Hoffler, G. W. (1977). "Hemodynamic studies of the legs under weightlessness," in *Biomedical Results from Skylab. NASA SP-377*, eds L. F. Dietlein, and R. S. Johnston, (Washington, DC: NASA), 324–329.

Tomilovskaya, E., Shigueva, T., Sayenko, D., Rukavishnikov, I., and Kozlovskaya, I. (2019). Dry immersion as a ground-based model of microgravity physiological effects. *Front. Physiol.* 10:284. doi: 10.3389/fphys.2019.00284

Videbaek, R., and Norsk, P. (1997). Atrial distension in humans during microgravity induced by parabolic flights. *J. Appl. Physiol.* 83, 1862–1866. doi: 10.1152/jappl.1997.83.6.1862

Vinogradova, O. L., Popov, D. V., Saenko, I. V., and Kozlovskaya, I. B. (2002). Muscle transverse stiffness and venous compliance under conditions of simulated supportlessness. *J. Gravit. Physiol.* 9, 327–329.

Watenpaugh, D. E. (2016). Analogs of microgravity: head-down tilt and water immersion. *J. Appl. Physiol.* 120, 904–914. doi: 10.1152/japplphysiol.00986.2015

Watenpaugh, D. E., Buckey, J. C., Lane, L. D., Gaffney, F. A., Levine, B. D., Moore, W. E., et al. (2001). Effects of spaceflight on human calf hemodynamics. *J. Appl. Physiol.* 90, 1552–1558. doi: 10.1152/jappl.2001.90.4.1552

Conflict of Interest: The authors declare that the research was conducted in the absence of any commercial or financial relationships that could be construed as a potential conflict of interest.

frontiers in Physiology

REVIEW
published: 03 July 2020
doi: 10.3389/fphys.2020.00778

Impacts of Microgravity Analogs to Spaceflight on Cerebral Autoregulation

Marc Kermorgant[1], Nathalie Nasr[1,2], Marek Czosnyka[3,4], Dina N. Arvanitis[1], Ophélie Hélissen[1], Jean-Michel Senard[1,5] and Anne Pavy-Le Traon[1,2]*

[1] INSERM UMR 1048, Institute of Cardiovascular and Metabolic Diseases (I2MC), Toulouse, France, [2] Department of Neurology, Institute for Neurosciences, Toulouse University Hospital, Toulouse, France, [3] Brain Physics Laboratory, Division of Neurosurgery, Department of Clinical Neurosciences, Cambridge University Hospital, Cambridge, United Kingdom, [4] Institute of Electronic Systems, Warsaw University of Technology, Warsaw, Poland, [5] Department of Clinical Pharmacology, Toulouse University Hospital, Toulouse, France

It is well known that exposure to microgravity in astronauts leads to a plethora physiological responses such as headward fluid shift, body unloading, and cardiovascular deconditioning. When astronauts return to Earth, some encounter problems related to orthostatic intolerance. An impaired cerebral autoregulation (CA), which could be compromised by the effects of microgravity, has been proposed as one of the mechanisms responsible for orthostatic intolerance. CA is a homeostatic mechanism that maintains cerebral blood flow for any variations in cerebral perfusion pressure by adapting the vascular tone and cerebral vessel diameter. The ground-based models of microgravity are useful tools for determining the gravitational impact of spaceflight on human body. The head-down tilt bed rest (HDTBR), where the subject remains in supine position at −6 degrees for periods ranging from few days to several weeks is the most commonly used ground-based model of microgravity for cardiovascular deconditioning. head-down bed rest (HDBR) is able to replicate cephalic fluid shift, immobilization, confinement, and inactivity. Dry immersion (DI) model is another approach where the subject remains immersed in thermoneutral water covered with an elastic waterproof fabric separating the subject from the water. Regarding DI, this analog imitates absence of any supporting structure for the body, centralization of body fluids, immobilization and hypokinesia observed during spaceflight. However, little is known about the impact of microgravity on CA. Here, we review the fundamental principles and the different mechanisms involved in CA. We also consider the different approaches in order to assess CA. Finally, we focus on the effects of short- and long-term spaceflight on CA and compare these findings with two specific analogs to microgravity: HDBR and DI.

Keywords: cerebral autoregulation, head-down bed rest, dry immersion, spaceflight analog, microgravity

OPEN ACCESS

Edited by:
Richard D. Boyle, National Aeronautics and Space Administration (NASA), United States

Reviewed by:
Ana Diaz Artiles, Texas A&M University, United States
Allison Paige Anderson, University of Colorado Boulder, United States

****Correspondence:***
Marc Kermorgant
marc.kermorgant@gmail.com

Specialty section:
This article was submitted to Environmental, Aviation and Space Physiology, a section of the journal Frontiers in Physiology

Received: *31 January 2020*
Accepted: *15 June 2020*
Published: *03 July 2020*

Citation:
Kermorgant M, Nasr N, Czosnyka M, Arvanitis DN, Hélissen O, Senard J-M and Pavy-Le Traon A (2020) Impacts of Microgravity Analogs to Spaceflight on Cerebral Autoregulation. Front. Physiol. 11:778. doi: 10.3389/fphys.2020.00778

INTRODUCTION

Analogs to microgravity for cardiovascular deconditioning such as head-down bed rest (HDBR) and dry immersion (DI) are essentials models for determining the effects of spaceflight on astronauts' body. Due to the cost and the limited number of space missions, these analogs are good alternatives for gravitational research (Herranz et al., 2013; Hargens and Vico, 2016). HDBR is

the most commonly used ground-based model of microgravity for cardiovascular deconditioning and the subject remains in supine position at −6 degrees head-down tilt bed rest (HDTBR) for either short periods (from 1 week to 1 month), or sometimes longer periods (>1 month). HDBR mimics cephalic fluid shift, immobilization, confinement, and inactivity. It would appear that vestibular function and gravitational stimuli are also affected, however to a lesser extent compared to those observed during spaceflight (Pavy-Le Traon et al., 2007). DI model is another approach where the subject remains immersed in thermoneutral water covered with an elastic waterproof fabric separating the subject from the water. Thus, the subject is freely suspended while remaining dry. One of the main features of DI is that imitates absence of any supporting structure for the body, centralization of body fluids, immobilization and hypokinesia observed during spaceflight (Navasiolava et al., 2011a). DI impacts a wide range of physiological mechanisms such as a diminution in neuromuscular system (Grigorieva and Kozlovskaya, 1983; Kozlovskaya et al., 1984), an alteration in cardiovascular system associated with sympathoexcitation (Iwase et al., 2000), a possible impact on intracranial pressure (ICP) (Avan et al., 2013; Rukavishnikov et al., 2013; Kermorgant et al., 2017). Tomilovskaya et al. (2019) emphasized the effectiveness of DI and its ability to induce rapid physiological changes more than others ground-based models of microgravity. During human spaceflight, the absence of gravity induces headward fluid shift and leads to cardiovascular deconditioning notably characterized by orthostatic intolerance when astronauts come back on Earth (Fritsch-Yelle et al., 1994, 1996a; Buckey et al., 1996; Meck et al., 2001; Levine et al., 2002; Blaber et al., 2011; Platts et al., 2014; Lee et al., 2015; Fu et al., 2019). Several mechanisms for post-flight orthostatic intolerance were suggested. Fritsch et al. (1992) proved that after 4- to 5-day space shuttle mission, a diminution in vagal control of the sinus node was observed in 12 astronauts. These findings suggest that an impaired vagal response may be involved in post-flight orthostatic intolerance. Buckey et al. (1996) showed that after 9–14 days of spaceflight, approximately two-thirds of the astronauts presented signs of orthostatic intolerance and those with severe signs of post-flight orthostatic intolerance had disturbed total peripheral resistances. Fritsch-Yelle et al. (1996b) corroborated these previous findings. Indeed after 8–16 days of spaceflight, approximately one-third of astronauts suffered from orthostatic intolerance had lower standing peripheral vascular resistance associated with smaller increases of plasma noradrenaline and greater decreases in systolic and diastolic pressures suggesting a hypoadrenergic responsiveness. Perhonen et al. (2001) demonstrated the reduction in left ventricular cardiac mass after a spaceflight of 10 days in four astronauts that suggesting that cardiac atrophy, by altering diastolic filling, may be involved in orthostatic intolerance. Some studies proposed that hypovolemia induces orthostatic intolerance (Waters et al., 2002; Shi et al., 2004). However, Shi et al. (2004) treated seven astronauts by restoring fluid volume with fludrocortisone (a synthetic mineralocorticoid) but this treatment failed to prevent the onset of orthostatic intolerance. The signals from vestibular system, and more specifically otolith organs, contributes to the arterial pressure control at the onset of standing (Yates and Kerman, 1998; Tanaka et al., 2009, 2012, 2014, 2017; Hallgren et al., 2015, 2016; Morita et al., 2016). Some studies also proposed that impairment of cerebral autoregulation (CA) may contribute to reduced orthostatic tolerance after spaceflight or ground-based of model microgravity (Zhang et al., 1997; Novak et al., 1998; Iwasaki et al., 2007). CA is a specific homeostatic mechanism that regulates and maintains CBF constant against any changes in fluctuation in arterial blood pressure (ABP) or ICP in order to preserve cerebral function (Lassen, 1959, 1964; Johnson, 1986; van Beek et al., 2008; Armstead, 2016; Claassen et al., 2016). Lassen (1959) described the autoregulation curve with three specific phases showing a CBF plateau distinguishing the lower limit from the upper limit of autoregulation. Above these limits, CA may be lost and CBF can no longer remain steady. **Figure 1** represents the theoretical autoregulation curve. In normal adults, an average CBF is 50 mL/min/100 g of brain tissue (Lassen et al., 1960; Lassen, 1985). In normotensive and healthy adults, the CBF is well maintained with cerebral perfusion pressure (CPP) between 50 and 150 mm Hg or mean arterial pressure between 60 and 160 mm Hg (Rosner and Becker, 1984; Paulson et al., 1990; Peterson et al., 2011; Armstead, 2016). However, normal value for ICP is difficult to define. Indeed in healthy conditions, this depends on age and posture (Czosnyka and Pickard, 2004). However, a normal range was defined for ICP values: 5–15 mm Hg (7.5–20 cm H_2O) in horizontal position (Rangel-Castillo et al., 2008) and around −10 mm Hg in vertical position (Chapman et al., 1990). CPP depends on two-factors, ABP and ICP and their relationship can be established as follows: CPP = ABP−ICP. Thus, an increased ICP would lead to a diminution in CPP which may induce a cerebral vasodilatation eliciting a reduction in CBF (Rangel-Castillo et al., 2008). The response of CA occurs in a few seconds after CPP changes in order to maintain CBF in a normal range of pressure (Paulson et al., 1990; Franco Folino, 2007; Zhang and Hargens, 2018).

In this review, we first recall the mechanisms involved in CA and the different approaches allowing to assess this homeostatic mechanism. Finally, we will seek to bring together information about the impacts of spaceflight and the most commonly used microgravity analogs on CA.

MECHANISMS INVOLVED IN CEREBRAL BLOOD FLOW REGULATION

For decades, at least four theories are evoked to determine the mechanisms responsible for regulation of CBF: myogenic, neurogenic, metabolic and endothelial theories (Strandgaard and Paulson, 1984; Paulson et al., 1990; Peterson et al., 2011; Armstead, 2016; Rivera-Lara et al., 2017):

- The myogenic mechanism refers to the adaptation of the vascular smooth muscle to changes in transmural pressure with the corresponding vasoconstriction and vasodilatation in response to increased and reduced pressure (Ibrahim et al., 2006). Non-selective cation channels were found in vascular smooth muscle and they

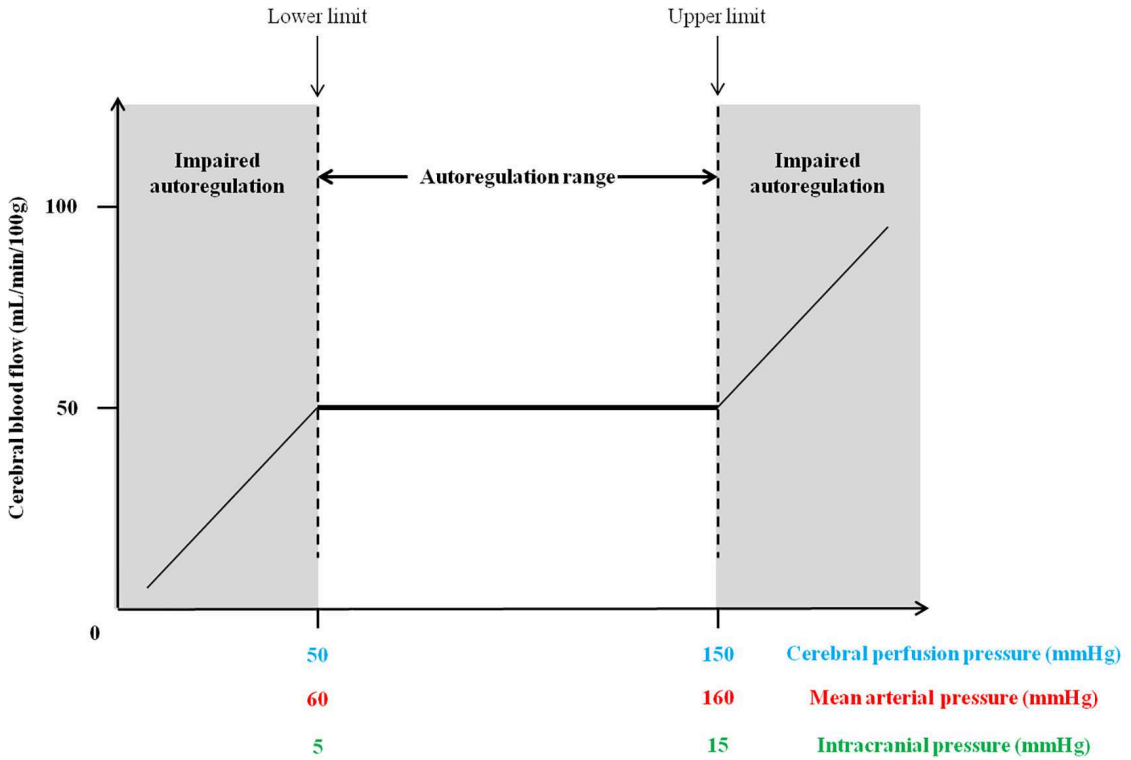

FIGURE 1 | Theoretical cerebral autoregulation curve with the autoregulation plateau where cerebral blood flow remains constant with the upper and lower limits of the autoregulatory range.

are strongly involved in myogenic mechanism. Indeed, a depolarization phenomenon will induce an influx of Ca^{2+} leading to vasoconstriction (Davis and Hill, 1999). The myogenic mechanism accounts for 31% of the pressure-flow relationship (Hamner and Tan, 2014).

- The neurogenic mechanism involves the innervation of the cerebral circulation with a broad panel of neurotransmitters with vasodilator and vasoconstrictor properties. Evidence shows the implication of sympathetic nervous system. Its activation shifts the upper limit of CA curve toward higher pressures in order to protect the brain against ABP increase. In parallel, it is believed that parasympathetic nervous system plays a minor role in CA. The latter, once activated, has cerebral vasodilatory effects (Hamel, 2006). Sympathetic and parasympathetic mechanisms account respectively for 20 and 11% of the pressure-flow relationship (Hamner and Tan, 2014). Perivascular nerves and astrocytes would have the ability to sense changes in CPP and adjust accordingly the sympathetic activity (Hamel, 2006; Marina et al., 2020). The astrocytes, due to their intrinsic function, may be considered as intracranial baroreceptors and play a major role in CA (Marina et al., 2020).
- The metabolic mechanism contributes to control CBF with the help of a plethora of vasoactive mediators (ions, metabolite byproducts, neurotransmitters, etc.). The vasoactive ions (K^+, H^+, Ca^{2+}) have mainly vasodilatory properties and an elevated concentrations of these ions may lead to vasodilatation (Faraci and Sobey, 1998; Nguyen et al., 2000). The metabolic factors (lactate, CO_2, adenosine) possess potent vasodilatory properties (Ko et al., 1990; Li and Iadecola, 1994; Attwell and Iadecola, 2002). The vasoactive neurotransmitters (dopamine, acetylcholine, gamma-amino butyric acid, vasoactive intestinal peptide) would also contribute to cerebral vasodilation (Girouard and Iadecola, 2006; Bor-Seng-Shu et al., 2012; Fantini et al., 2016).
- The endothelial mechanism, involving vasodilators (nitric oxide, carbon monoxide, prostacyclin) and vasoconstrictors (endothelin-1, thromboxane A2, angiotensin II) secreted by the endothelium in a paracrine fashion, may also play a key role in CA (Golding et al., 2002; Rivera-Lara et al., 2017; Silverman and Petersen, 2020).

DETERMINATION OF CEREBRAL AUTOREGULATION: STATIC AND DYNAMIC METHODS

Two methods can be applied in order to assess CA: static and dynamic methods. The static method assesses the global efficiency of the CA but not takes into account the latency, while dynamic method assesses latency and then efficiency of the CA (Tiecks et al., 1995).

The static approach consists to determine CBF changes in response to a steady-state change in ABP and necessitates the administration of vasoactive drugs (Tiecks et al., 1995). An autoregulatory index can be established as the percent change in cerebrovascular resistance related to the percent change in ABP (Tiecks et al., 1995) or percent change in CPP (Priesman et al., 2005). An autoregulatory index of 100% corresponds to perfect CA and 0% corresponds to absent CA. Microvascular CBF measurement in small cerebral arterioles can provide information about the state of CA. Continuous-wave near infrared spectroscopy and diffuse correlation spectroscopy are considered as robust quantitative method in the assessment of CA (Kim et al., 2010, 2018; Caicedo et al., 2012; Durduran and Yodh, 2014; Kainerstorfer et al., 2015; Armstead, 2016). As these methods assess CA from stabilized CBF over several minutes, these methods can be encompassed in the static approach of CA.

The dynamic approach relies on the rapid changes in ABP, the CBF response to these changes, and, in particular the time to return to its baseline values (Tiecks et al., 1995; Armstead, 2016). Several methods can be applied to determine dynamic CA. The first corresponds to the slope of cerebrovascular resistance recovery determined by the CPP to CBF ratio. An abrupt slope means an enhanced CA, while a gradual moderate slope indicates an impaired CA (Tiecks et al., 1995). A rise in CPP leads to a cerebral vasoconstriction, whereas a decline in CPP leads to cerebral vasodilation (Silverman and Petersen, 2020). CA can also be assessed by transfer function analysis between mean ABP and mean CBFV signals. A cross-spectral analysis is then applied to obtain three specific frequency-dependent parameters: transfer function coherence, gain and phase. The coherence measures the degree of linearity of the relationship between mean ABP and mean CBFV. The coherence value close to 1 indicates a strong linear relationship between mean ABP and mean CBFV with high signal-to-noise ratio, while the coherence approximating with value near zero may suggest a non-linear relationship, a presence of extraneous noise or other influencing variables (Marmarelis, 1988; Giller, 1990; Liu et al., 2015). Furthermore, a threshold of coherence over 0.5 depicts that transfer function gain and phase are valid (Diehl et al., 1995; Zhang et al., 1998). The gain reflects to what extent the transmission from the ABP signal variation impacts on the CBFV signal. The phase describes the delay between sinusoidal components of ABP signal and CBFV signal and was considered as temporal relation between these signals (Zhang et al., 1998; Liu et al., 2015). The mechanism of CA has the characteristics of a high-pass filter that dampens slow fluctuations of blood pressure (Zhang et al., 1998). The most commonly ranges used to calculate the mean values of the transfer function (coherence, phase and gain) are: very low frequency (VLF: 0.02–0.07 Hz), low frequency (LF: 0.07–0.20 Hz) and high frequency (HF: 0.20–0.35 Hz) (Zhang et al., 1998, 2009). It is now accepted that elevated coherence and gain with a reduced phase shift reflect an impaired CA (Giller, 1990; Immink et al., 2004; van Beek et al., 2008; Hamner et al., 2010; Donnelly et al., 2016). Several indices of dynamic CA have also been established and derived from transcranial Doppler and correspond to correlation coefficient of blood flow velocity with CPP (Mx) or ABP (Mxa), or slow waves in ICP with ABP (PRx). An unaltered CA is determined for $Mx < 0$, $Mxa < 0.3$, or $PRx < 0$, while CA is considered impaired for $Mx > 0$, $Mxa > 0.3$, or $PRx > 0$ (Czosnyka et al., 2001; Steiner et al., 2003; Sorrentino et al., 2011).

In addition, Nasr et al. (2014) found an inverse and strong correlation between baroreflex sensitivity and CA in healthy controls. This suggests that baroreflex modulation of the autonomic drive may play an important role on CA.

IMPACTS OF SPACEFLIGHT ON CEREBRAL AUTOREGULATION

Despite the numerous studies on spaceflight cardiovascular adaptation, the impact of microgravity on CA in astronauts remains unclear. **Table 1** summarizes methods used to assess CA in spaceflight.

Gazenko et al. (1981) reported that after spending several months in space, cosmonauts experienced a dramatic fall in pulse blood filling of cerebral vessels (similar to CBF pulsatility) corresponding to an improved cerebral vasoconstriction. Alternatively, during 6-months MIR spaceflights, the cerebral vascular resistance measured by resistance index was preserved in six cosmonauts (Herault et al., 2000). However, Arbeille et al. (2001) did not observe any significant changes in cerebral perfusion after short or long duration spaceflight despite a reduction in middle cerebral artery resistance index and middle cerebral artery mean flow velocity, as

TABLE 1 | List of authors and the methods used to assess cerebral autoregulation in spaceflight.

References	Methods	Subjects	Time duration
Gazenko et al., 1981	CBF	6 crewmembers	185 days
Bagian and Hackett, 1991	MCA blood flow velocity	4 crewmembers	N/A
Herault et al., 2000	CFR, Q_{CA}, R_{CA}	6 cosmonauts	6 months
Arbeille et al., 2001	Q_{CA}, R_{CA}	1–9 men + 1 woman	2 days to 6 months
Iwasaki et al., 2007	MCA blood flow velocity, CBFV, TFA (VLF, LF, HF)	6 men	1–2 weeks
Kotovskaia and Fomina, 2010	CBF	26 cosmonauts	8–438 days
Blaber et al., 2011	MCAv, CR, TFA (VLF, LF)	20 men + 7 women	8–16 days
Zuj et al., 2012	CBFV, CR, PI	6 men + 1 woman	58–199 days
Marshall-Goebel et al., 2019	JVBF	9 men + 2 women	210 ± 76 days

CBFV, cerebral blood flow velocity; CFR, cerebral to femoral flow ratio; CR, cerebrovascular resistance; HF, high frequency; JVBF, jugular venous blood flow; LF, low frequency; MCAv, middle cerebral artery velocity; PI, Gosling pulsatility index; Q_{CA}, middle cerebral artery mean flow velocity; R_{CA}, cerebral artery resistance index; TFA, transfer function analysis; VLF, very low frequency.

well as a diminution in cardiac volume, lower limb arterial resistance and an enlargement of jugular and femoral veins in cosmonauts. Bagian and Hackett (1991) did not see any significant modifications in CBFV directly measured by transcranial Doppler in crewmembers after 10 h in-flight. Iwasaki et al. (2007) also reported in six male crewmembers after a 1 and 2-week spaceflight, a reduction in gain function in the low frequency range (0.07–0.20 Hz) with no change in CBFV. These findings indicate a preserved or even better dynamic CA on landing day. Furthermore, a large hemodynamic dataset collected over 20 years in 26 cosmonauts aboard orbital stations Salyut 7 and Mir, show maintained cerebral circulation with a stabilized CBF even after long duration exposure to microgravity (Kotovskaia and Fomina, 2010). Several assumptions can be established to explain this enhancement in CA. First of all, Iwasaki et al. (2007) hypothesized that CA improvement would be due to the impact of microgravity which raises the responsiveness of cerebral vascular smooth muscle to changes of transmural pressure. Noteworthy is the cardiovascular autonomic nervous system which is known to be altered both in short- and long-duration space flight (Ertl et al., 2000; Sigaudo-Roussel et al., 2002; Eckberg et al., 2010) interacts with CA. Moreso, the baroreflex sensitivity which plays a key role in short-term blood pressure variations has been shown to be inversely correlated to CA in healthy individuals and the supposed mechanism for inverse correlation between baroreflex sensitivity and CA is an increased sympathetic tone associated with lower baroreflex sensitivity (Nasr et al., 2014). This suggests that baroreflex modulation of the autonomic drive may play a role on CA. These may indeed be one of the underlying physiological mechanisms explaining that CA was often preserved or even enhanced in spaceflight, and, could be related to changes in baroreflex sensitivity. However inter-individual variability of baroreflex sensitivity is known to be important and due to small numbers of individuals in space studies, this key interaction between impaired baroreflex sensitivity and preserved or even enhanced CA to date may have eluded identification. Pertaining to this mechanism of interaction between autonomic nervous system and CA, prior data have shown enhanced sympathetic nervous activity during prolonged exposure to microgravity (Ertl et al., 2002). This could explain preserved or better CA in most of the studies in space flight as CA is dependent on cerebral vasomotor tone which increases with afferent sympathetic drive.

A study performed in 27 astronauts, who took part in different shuttle missions lasting few days, described an impairment in CA reflected by an increase in the gain function between CBF and blood pressure (Blaber et al., 2011). This study showed that astronauts who were orthostatically tolerant presented no signs of an impaired CA, those who were orthostatically intolerant had a severe impairment in CA on landing day. These results suggest that one of the reasons leading to presyncope in astronauts is that there is a mismatch of blood pressure and CBF. Another study demonstrated in seven astronauts, which spent several days on the International Space Station, a decrease in cerebrovascular dynamic autoregulation and CO_2 reactivity, thus characterizing an altered CA (Zuj et al., 2012). A recent work revealed that among 11 healthy crewmembers who spent a mean of 210 days in spaceflight, 6 crewmembers presented stagnant or reverse flow in the internal jugular vein (Marshall-Goebel et al., 2019), which could jeopardize cerebral circulation (Zhou et al., 2018). They suggested that cerebrovascular alterations could be due to chronic elevation in cerebral blood pressure and chronic exposure to elevated atmospheric P_{CO2} as seen in long-duration spaceflight. Studies performed in animal models may provide an answer, though a partial one. In contrast to the hindlimb unloading in rodent, few of them were conducted during spaceflight. However, Taylor et al. (2013) demonstrated in female C57BL/6 mice that a 13-day spaceflight induced a diminished myogenic vasoconstriction and stiffness of posterior communicating arteries and an increased maximal diameter of basilar artery suggesting that cerebral perfusion could be altered. Another study showed that spaceflight induced an altered cerebral artery vasomotor in mice. Indeed, Sofronova et al. (2015) depicted in male C57BL/6N that a 30-day spaceflight attenuated vasoconstrictor and vasodilator properties in basilar artery thus likely impairing cerebral perfusion.

IMPACTS OF SPACEFLIGHT ANALOGS ON CEREBRAL AUTOREGULATION

Data on CA are controversial during ground-based model of microgravity. **Table 2** summarizes methods used to assess CA in analogs to spaceflight.

Guell et al. (1979) observed in four healthy subjects who underwent 4° HDT for 7 days, a rapid decrease *in loco*-regional CBF after 2 h followed by an increase after 48 h. In a similar study, these same authors only found in six healthy subjects an elevation *in loco*-regional CBF (Guell et al., 1982). These differences may be explained by the techniques used to measure loco-regional CBF which were different between these studies (respectively measured by transcranial Doppler and Xenon-133 techniques). Furthermore, another study also showed an increase in CBFV in six volunteers who underwent exposure to a 5-min 6° HDT (Kawai et al., 1992). These same authors described an increase in CBFV during HDT and a significant decrease in CBFV after 24 h of 6° HDT in eight healthy male subjects suggesting that CBFV may have a key role in syncope in astronauts when they come back on Earth (Kawai et al., 1993). Although Frey et al. (1993) found a diminution in blood flow velocity in the middle cerebral artery in nine men after 2 days of 10° HDT, but was inversely correlated with percent changes in retinal vascular diameters, suggested that CBF was not diminished. Satake et al. (1994), with the help of image analysis using single photon emission computer tomography, demonstrated that a significant increase in CBF in men was occurred in the basal ganglia and the cerebellum at 5 min after the onset of HDT, but not in the cerebral hemisphere. Pavy-Le Traon et al. (1995) showed in 12 healthy volunteers who underwent 28 days of HDBR, no changes in middle cerebral artery velocities recorded indirectly by transcranial Doppler indicating a preserved cerebral circulation. However, subjects

TABLE 2 | List of authors and the methods used to assess cerebral autoregulation in analogs to spaceflight.

References	Methods	Subjects	Time duration	Analogs
Guell et al., 1979	rCBF	4 men	7 days	4° HDT
Guell et al., 1982	rCBF	6 men	7 days	4° HDT
Kawai et al., 1992	CBFV	6 subjects	5 min	6° HDT
Frey et al., 1993	MCA blood flow velocity	9 men	2 days	10° HDT
Kawai et al., 1993	CBFV	8 men	1 day	6° HDT
Satake et al., 1994	CBF	Men	N/A	6° HDT
Pavy-Le Traon et al., 1995	MCAv, CR	12 men	28 days	6° HDT
Savin et al., 1995	MCAv	10 subjects	10 min	10° HDT
Zhang et al., 1997	CBFV	11 men + 1 woman	14 days	6° HDT
Arbeille et al., 1998	MCAv, CFR	8 men	4 days	6° HDT
Heckmann et al., 1999	CBFV, PI	11 men + 2 women	1 min	80° HDT
Arbeille et al., 2001	Q_{CA}, R_{CA}	6 to 19 men	1 h to 42 days	6° HDT
Sun et al., 2001	CBF, CR	12 men	21 days	6° HDT
Yao et al., 2001	ACAv, MCAv, PCAv, PI, RI	6 men	21 days	6° HDT
Pavy-Le Traon et al., 2002	MCAv, CR	8 women	7 days	6° HDT
Sun et al., 2002	MCAv	8 men	4 days	6° HDT
Yasumasa et al., 2002	CBFV	8 men	1 day	6° HDT
Sun et al., 2005	CBFV	12 men	21 days	6° HDT
Greaves et al., 2007	MCAv, CR, ARMA	24 women	60 days	6° HDT
Yang et al., 2011	CBFV, S/D, PI, RI	12 men	4 days	6° HDT
Geinas et al., 2012	MCAv, PCAv, CR, TFA (VLF, LF)	17 men + 4 women	>7–8 min	90°HDT
Jeong et al., 2014	TFA (VLF, LF, HF)	18 men + 3 women	18 days	6° HDT
Yang et al., 2015	CBFV	10 men and women	15 s	10°, 25°, and 55° HDT
Marshall-Goebel et al., 2016	Blood flow velocity	9 men	4.5 h	6°, 12°, and 18° HDT
Kermorgant et al., 2017	TFA (VLF, LF, HF), Mxa	12 men	3 days	DI
Ogoh et al., 2017	CBF	12 men	3 days	DI
Kermorgant et al., 2019	MCAv, TFA (VLF, LF), Mxa	12 men	21 days	6° HDT

ACAv, anterior cerebral artery velocity; ARMA, autoregressive moving average; CBFV, cerebral blood flow velocity; CFR, cerebral to femoral flow ratio; CR, cerebrovascular resistance; DI, dry immersion; HDT, head-down tilt; HF, high frequency; LF, low frequency; MCAv, middle cerebral artery velocity; Mxa, autoregulatory index; PCAv, posterior cerebral artery velocity; PI, Gosling pulsatility index; Q_{CA}, middle cerebral artery mean flow velocity; R_{CA}, cerebral artery resistance index; rCBF, loco-regional cerebral blood flow; RI, Pourcelot resistance index; S/D, CBFV systolic/CBFV diastolic; TFA, transfer function analysis; VLF, very low frequency.

presenting presyncopal symptoms had a drop in middle cerebral artery velocities indicating an impaired CA. An increase in middle cerebral artery velocity has also been observed in 10 subjects at during 10° HDT, which was restored at the end of the experiment (Savin et al., 1995). Heckmann et al. (1999) did not find any significant changes in CBFV measured by transcranial Doppler sonography but an increase pulsatility index after 1-min 80° HDT in 13 healthy volunteers. In a 4-day of HDBR study, no major changes were observed in dynamic CA in eight healthy volunteers during head-up tilt (Arbeille et al., 1998). The same authors did not find any significant changes in cerebral perfusion in men in a 42-day HDT despite an increase in cerebral artery resistance index and a decrease in middle cerebral artery mean flow velocity during the early phase of HDT (4–5 days) (Arbeille et al., 2001). Another study performed in eight healthy women showed that cerebrovascular resistance was preserved during and after a 7-day HDBR suggesting an unaltered CA. In this study, five of eight women who presented orthostatic intolerance had a time to maximum decrease in cerebrovascular resistance larger than the three women who did not, suggesting that some differences in CA may be related to orthostatic intolerance (Pavy-Le Traon et al., 2002). Consistently, Yasumasa et al. (2002) found an elevated CBFV in eight men, measured by transcranial Doppler, during the early phase (first 6 h) of 6° HDT. Moreover, a 60-day HDTBR study demonstrated that among 24 healthy women, those who exhibited few changes in orthostatic tolerance presented a preserved dynamic CA, determined by autoregressive moving average (Greaves et al., 2007). Also, Geinas et al. (2012) did not observe any significant changes in CBFV in 21 healthy young adults, even after severe changes in posture (90° HDT), although ABP was elevated compared to supine position. Similarly, a 18-day HDBR study performed in 14 healthy adults depicted a decrease in transfer function gain. These findings stated an improved dynamic CA (Jeong et al., 2014). Yang et al. (2015) found in 10 subjects an elevation in CBFV after acute consecutive exposure to randomized 10°, 25°, and 55° HDT; however, an autoregulatory correction index was applied in this study and revealed a modified but an unimpaired cerebrovascular autoregulation. Moreover, a recent work in 12 healthy male subjects who underwent 21 days of HDBR showed that autoregulatory index Mxa was reduced reflecting an enhanced dynamic CA (Kermorgant et al., 2019). Following an extensive literature search, we found only few studies that measured CA after DI. Kermorgant et al. (2017) demonstrated that the effects of

3-day DI would improve CA. Indeed, a decrease in autoregulatory index Mxa associated with an increase in the cross-spectral phase shift were observed in 12 healthy male subjects. Ogoh et al. (2017) showed in the same study that DI affected both anterior and posterior cerebral vasculature, but did not provoke a heterogeneous CBF response in each cerebral artery (internal carotid, external carotid, common carotid, and vertebral arteries) measured by Doppler ultrasonography. As previously suggested for spaceflight, one suggestion for CA improvement is that microgravity could increase the responsiveness of cerebral vascular smooth muscle to changes of transmural pressure (Iwasaki et al., 2007). However, plasma volume may also play a key role in this enhancement. Indeed, previous authors found that a diminution in plasma volume provoked a reduction in transfer function gain (corresponding to an enhanced CA), while when plasma volume was restored by volume loading, transfer function gain was increased (corresponding to an impaired CA) (Ogawa et al., 2007, 2009; Jeong et al., 2014). Consistently, several studies showed a reduction in plasma volume both in HDBR (Convertino et al., 1990; Iwasaki et al., 2000; Belin de Chantemèle et al., 2004) and in DI (Navasiolava et al., 2011b; de Abreu et al., 2017).

However, although Zhang et al. (1997) did not observe any significant modifications in CBFV in 12 subjects. The authors documented an impaired CA reflected by a greater decline in CBF during lower body negative pressure after 2 weeks of HDBR. They also speculated that impairment of CA may be involved in orthostatic intolerance after bed rest. Sun et al. (2001) performed a 21-day HDT study with or without the effects of lower body negative pressure in 12 healthy male subjects in order to investigate potential changes of CBF. Six of twelve subjects were allocated in control group (without lower body negative pressure) and they exhibited an increase in cerebral vascular resistance and a decrease in CBF measured by rheoencephalogram. They further showed, a diminution in CBFV measured by transcranial Doppler sonography, on the last day of a 4-day HDT study conducted in eight healthy male volunteers. The same authors further identified a reduction in CBFV determined by transcranial Doppler technique in 12 healthy male volunteers during a 21-day 6° HDTBR study (Sun et al., 2005). Yao et al. (2001) confirmed these previous reports with a 21-day HDT study performed in six healthy male. Indeed, they described in these subjects a reduced systolic blood velocity of both side middle cerebral artery and mean blood velocity of right middle cerebral artery. Moreover, Yang et al. (2011) found changes in cerebrovascular functions in six healthy male subjects after a 4-day HDT with reductions in CBFV, pulsatility index, resistance index, and S/D (corresponding to CBFV systolic/CBFV diastolic). All these parameters returned to basal values after HDBR. Similar findings were observed with a reduction in CBFV, measured with phase-contrast magnetic resonance imaging, in nine healthy male subjects after short-term exposure (∼4.5 h) to randomized 6°, 12°, and 18° HDT angles (Marshall-Goebel et al., 2016). The mechanisms involved in this impairment remain unclear. However, alterations in CA may be explained by a potential rise in ICP. Indeed, Kermorgant et al. (2017) found that ICP (indirectly measured by optic nerve sheath diameter) was negatively correlated with the autoregulatory index (Mxa) and coherence after 3-day DI in healthy volunteers. Despite an overall improvement in CA, subjects with low values of optic nerve sheath diameter (corresponding to low values of ICP) presented a better CA than subjects with high values of optic nerve sheath diameter (corresponding to high values of ICP). Moreover, it has been shown that patients with head-injury with the presence of an elevated ICP presented an impaired CA (Czosnyka et al., 2001). However, many studies showed that pronounced HDT led to a rise in ICP. Chin et al. (2015) showed that 3 min Trendelenburg position (corresponding to ∼30° HDT) were sufficient to induce an elevation in optic nerve sheath diameter compared to supine position in anesthetized patients. Another study performed in healthy subjects showed an elevation in optic nerve sheath diameter after 5 h in 18° HDT position (Marshall-Goebel et al., 2017). Petersen et al. (2016) also demonstrated in ambulatory neurosurgical patients that ICP (measured directly by tip-transducer) was significantly increased with HDT (10°: 14.3 mm Hg and 20°: 19.0 mm Hg) compared to supine position (0°: 9.4 mm Hg). Animal models may provide further explanations. Indeed, tail-suspended rat model is an efficiency method to reproduce major physiological changes observed in space flight, just as long-term bed rest (Morey-Holton and Globus, 2002; Morey-Holton et al., 2005; Carpenter et al., 2010; Chowdury et al., 2013). Studies performed in hindlimb suspension in rat showed that this alteration can originate from several factors including, an elevation in cerebrovascular resistance accompanied by a reduction in blood flow, hypertrophy phenomenon, a rise in myogenic tone. and vasoreactivity in cerebral arteries (Geary et al., 1998; Wilkerson et al., 1999; Morey-Holton and Globus, 2002; Morey-Holton et al., 2005; Lin et al., 2009).

CONCLUSION

Either in spaceflight or in ground-based model of microgravity, most of short-term studies show a preserved or even an improved CA. However, long-term studies depict an impairment in CA. One of the main reasons for the discrepancy may depend on baseline orthostatic tolerance. Indeed, it would seem that subjects who are orthostatically tolerant have a preserved or even an enhanced CA. In contrast, subjects who are orthostatically intolerant would present an impaired CA (Blaber et al., 2011). These differences can also be attributed to the methods used to assess CA and the interpretation of each measure should be made cautiously (Tzeng et al., 2012). Furthermore, as highlighted by Armstead (2016) and Zhang and Hargens (2018), none efficient methods exist to accurately measure CBFV. The assessment of CA should be compared by gender. In fact, several studies showed gender differences in CBFV (Ackerstaff et al., 1990; Marinoni et al., 1998), cerebral vasomotor (Karnik et al., 1996) and cerebrovascular reactivities (Kastrup et al., 1997), CA both in young and old adults (Wang et al., 2005; Deegan et al., 2009). Moreover, regional differences were observed between

anterior and posterior cerebral circulation and this should have been taken into account during the assessment of CA (Roth et al., 2017). Petersen and Ogoh (2019) also suggested that dynamic CA could be over- or underestimated due to the fact that gravitational stress may alter regional arterial pressure and ICP/CPP differently. Additional studies are needed in order to determine more accurately the impact of microgravity on CA. Finally, although residual effects of gravity remain, HDBR and DI could be considered as robust ground-based analogs to spaceflight for studying CA in humans during microgravity.

AUTHOR CONTRIBUTIONS

MK, NN, MC, DA, OH, J-MS, and AP-L wrote and edited the manuscript. All authors contributed to the article and approved the submitted version.

ACKNOWLEDGMENTS

OH was supported by Centre National d'Etudes Spatiales (CNES).

REFERENCES

Ackerstaff, R. G., Keunen, R. W., van Pelt, W., Montauban van Swijndregt, A. D., and Stijnen, T. (1990). Influence of biological factors on changes in mean cerebral blood flow velocity in normal ageing: a transcranial doppler study. *Neurol. Res.* 12, 187–191. doi: 10.1080/01616412.1990.11739941

Arbeille, P., Fomina, G., Roumy, J., Alferova, I., Tobal, N., and Herault, S. (2001). Adaptation of the left heart, cerebral and femoral arteries, and jugular veins during short- and long-term head-down tilt and spaceflights. *Eur. J. Appl.Physiol.* 86, 157–168. doi: 10.1007/s004210100473

Arbeille, P., Sigaudo, D., Pavy-Le Traon, A., Herault, S., Porcher, M., and Gharib, C. (1998). Femoral to cerebral arterial blood flow redistribution and femoral vein distension during orthostatic tests after 4 days in the head-down tilt position or confinement. *Eur. J. Appl. Physiol. Occup. Physiol.* 78, 208–218. doi: 10.1007/s004210050409

Armstead, W. M. (2016). Cerebral blood flow autoregulation and dysautoregulation. *Anesthesiol. Clin.* 34, 465–477. doi: 10.1016/j.anclin.2016.04.002

Attwell, D., and Iadecola, C. (2002). The neural basis of functional brain imaging signals. *Trends Neurosci.* 25, 621–625. doi: 10.1016/s0166-2236(02)02264-6

Avan, P., Rukavishnikov, I., Madero, B., Tomilovskaya, E., Normand, H., Kozlovskaya, I., et al. (2013). "Assessment of intracranial pressure changes with otoacoustic emission under conditions of simulated microgravity," in *Proceedings of 19th IAA Humans in Space Symposium*, Cologne.

Bagian, J. P., and Hackett, P. (1991). Cerebral blood flow: comparison of ground-based and spaceflight data and correlation with space adaptation syndrome. *J. Clin. Pharmacol.* 31, 1036–1040. doi: 10.1002/j.1552-4604.1991.tb03668.x

Belin de Chantemèle, E., Blanc, S., Pellet, N., Duvareille, M., Ferretti, G., Gauquelin-Koch, G., et al. (2004). Does resistance exercise prevent body fluid changes after a 90-day bed rest? *Eur. J. Appl. Physiol.* 92, 555–564. doi: 10.1007/s00421-004-1121-6

Blaber, A. P., Goswami, N., Bondar, R. L., and Kassam, M. S. (2011). Impairment of cerebral blood flow regulation in astronauts with orthostatic intolerance after flight. *Stroke* 42, 1844–1850. doi: 10.1161/STROKEAHA.110.610576

Bor-Seng-Shu, E., Kita, W. S., Figueiredo, E. G., Paiva, W. S., Fonoff, E. T., Teixeira, M. J., et al. (2012). Cerebral hemodynamics: concepts of clinical importance. *Arq. Neuropsiquiatr.* 70, 352–356. doi: 10.1590/s0004-282x2012000500010

Buckey, J. C. Jr., Lane, L. D., Levine, B. D., Watenpaugh, D. E., Wright, S. J., Moore, W. E., et al. (1996). Orthostatic intolerance after spaceflight. *J. Appl. Physiol. (1985)* 81, 7–18. doi: 10.1152/jappl.1996.81.1.7

Caicedo, A., Naulaers, G., Lemmers, P., van Bel, F., Wolf, M., and Van Huffel, S. (2012). Detection of cerebral autoregulation by near-infrared spectroscopy in neonates: performance analysis of measurement methods. *J. Biomed. Opt.* 17:117003. doi: 10.1117/1.JBO.17.11.117003

Carpenter, R. D., Lang, T. F., Bloomfield, S. A., Bloomberg, J. J., Judex, S., Keyak, J. H., et al. (2010). Effects of long-duration spaceflight, microgravity, and radiation on the neuromuscular, sensorimotor, and skeletal systems. *J. Cosmol.* 12, 3778–3780.

Chapman, P. H., Cosman, E. R., and Arnold, M. A. (1990). The relationship between ventricular fluid pressure and body position in normal subjects and subjects with shunts: a telemetric study. *Neurosurgery* 26, 181–189. doi: 10.1097/00006123-199002000-00001

Chin, J.-H., Seo, H., Lee, E. H., Lee, J., Hyuk, J., Hwang, J. H., et al. (2015). Sonographic optic nerve sheath diameter as a surrogate measure for intracranial pressure in anesthetized patients in the Trendelenburg position. *BMC Anesthesiol.* 15:43. doi: 10.1186/s12871-015-0025-9

Chowdury, P., Long, A., Harris, G., Soulsby, M. E., and Dobretsov, M. (2013). Animal models of simulated microgravity: a comparative study of hindlimb unloading via tail versus pelvic suspension. *Physiol. Rev.* 1:e00012. doi: 10.1002/phy2.12

Claassen, J. A., Meel-van den Abeelen, A. S., Simpson, D. M., Panerai, R. B., and international Cerebral Autoregulation Research Network (CARNet), (2016). Transfer function analysis of dynamic cerebral autoregulation: a white paper from the international cerebral autoregulation research network. *J. Cereb. Blood Flow Metab.* 36, 665–680. doi: 10.1177/0271678X15626425

Convertino, V. A., Doerr, D. F., Eckberg, D. L., Fritsch, J. M., and Vernikos-Danellis, J. (1990). Head-down bed rest impairs vagal baroreflex responses and provokes orthostatic hypotension. *J. Appl. Physiol.* 68, 1458–1464. doi: 10.1152/jappl.1990.68.4.1458

Czosnyka, M., and Pickard, J. D. (2004). Monitoring and interpretation of intracranial pressure. *J. Neurol. Neurosurg. Psychiatry* 75, 813–821. doi: 10.1136/jnnp.2003.033126

Czosnyka, M., Smielewski, P., Piechnik, S., Steiner, L. A., and Pickard, J. D. (2001). Cerebral autoregulation following head injury. *J. Neurosurg.* 2001, 756–763. doi: 10.3171/jns.2001.95.5.0756

Davis, M. J., and Hill, M. A. (1999). Signaling mechanisms underlying the vascular myogenic response. *Physiol. Rev.* 79, 387–423. doi: 10.1152/physrev.1999.79.2.387

de Abreu, S., Amirova, L., Murphy, R., Wallace, R., Twomey, L., Gauquelin-Koch, G., et al. (2017). Multi-system deconditioning in 3-day dry immersion without daily rise. *Front. Physiol.* 8:799. doi: 10.3389/fphys.2017.00799

Deegan, B. M., Sorond, F. A., Lipsitz, L. A., Olaighin, G., and Serrador, J. M. (2009). Gender related differences in cerebral autoregulation in older healthy subjects. *Conf. Proc. IEEE Eng. Med. Biol. Soc.* 2009, 2859–2862. doi: 10.1109/IEMBS.2009.5333604

Diehl, R. R., Linden, D., Lücke, D., and Berlit, P. (1995). Phase relationship between cerebral blood flow velocity and blood pressure. A clinical test of autoregulation. *Stroke.* 26, 1801–1804. doi: 10.1161/01.str.26.10.1801

Donnelly, J., Budohoski, K. P., Smielewski, P., and Czosnyka, M. (2016). Regulation of the cerebral circulation: bedside assessment and clinical implications. *Crit. Care.* 20:129. doi: 10.1186/s13054-016-1293-6

Durduran, T., and Yodh, A. G. (2014). Diffuse correlation spectroscopy for non invasive, microvascular cerebral blood flow measurement. *NeuroImage* 85, 51–63. doi: 10.1016/j.neuroimage.2013.06.017

Eckberg, D. L., Halliwill, J. R., Beightol, L. A., Brown, T. E., Taylor, J. A., and Goble, R. (2010). Human vagal baroreflex mechanisms in space. *J. Physiol.* 588, 1129–1138. doi: 10.1113/jphysiol.2009.186650

Ertl, A. C., Diedrich, A., and Biaggioni, I. (2000). Baroreflex dysfunction induced by microgravity: potential relevance to postflight orthostatic intolerance. *Clin. Auton. Res.* 10, 269–277. doi: 10.1007/bf02281109

Ertl, A. C., Diedrich, A., Biaggioni, I., Levine, B. D., Robertson, R. M., Cox, J. F., et al. (2002). Human muscle sympathetic nerve activity and plasma noradrenaline kinetics in space. *J. Physiol.* 538, 321–329. doi: 10.1113/jphysiol.2001.012576

Fantini, S., Sassaroli, A., Tgavalekos, K. T., and Kornbluth, J. (2016). Cerebral blood flow and autoregulation: current measurement techniques and prospects for noninvasive optical methods. *Neurophotonics* 3:031411. doi: 10.1117/1.NPh.3.3.031411

Faraci, F. M., and Sobey, C. G. (1998). Role of potassium channels in regulation of cerebral vascular tone. *J. Cereb. Blood Flow Metab.* 18, 1047–1063. doi: 10.1097/00004647-199810000-00001

Franco Folino, A. (2007). Cerebral autoregulation and syncope. *Prog. Cardiovasc. Dis.* 50, 49–80. doi: 10.1016/j.pcad.2007.01.001

Frey, M. A. B., Mader, T. H., Bagian, J. P., Charles, J. B., and Meehan, R. T. (1993). Cerebral blood velocity and other cardiovascular-responses to 2 days of head-down tilt. *J. Appl. Physiol.* 74, 319–325. doi: 10.1152/jappl.1993.74.1.319

Fritsch, J. M., Charles, J. B., Bennett, B. S., Jones, M. M., and Eckberg, D. L. (1992). Short-duration spaceflight impairs human carotid baroreceptor-cardiac reflex responses. *J. Appl. Physiol. (1985)* 73, 664–671. doi: 10.1152/jappl.1992.73.2.664

Fritsch-Yelle, J. M., Charles, J. B., Jones, M. M., Beightol, L. A., and Eckberg, D. L. (1994). Spaceflight alters autonomic regulation of arterial pressure in humans. *J. Appl. Physiol. (1985)* 77, 1776–1783. doi: 10.1152/jappl.1994.77.4.1776

Fritsch-Yelle, J. M., Charles, J. B., Jones, M. M., and Wood, M. L. (1996a). Microgravity decreases heart rate and arterial pressure in humans. *J. Appl. Physiol. (1985)* 80, 910–914. doi: 10.1152/jappl.1996.80.3.910

Fritsch-Yelle, J. M., Whitson, P. A., Bondar, R. L., and Brown, T. E. (1996b). Subnormal norepinephrine release relates to presyncope in astronauts after spaceflight. *J. Appl. Physiol. (1985)* 81, 2134–2141. doi: 10.1152/jappl.1996.81.5.2134

Fu, Q., Shibata, S., Hastings, J. L., Platts, S. H., Hamilton, D. M., Bungo, M. W., et al. (2019). Impacts of prolonged spaceflight on orthostatic tolerance during ambulation and blood pressure profiles in astronauts. *Circulation* 140, 729–738. doi: 10.1161/CIRCULATIONAHA.119.041050

Gazenko, O. G., Genin, A. M., and Egorov, A. D. (1981). Summary of medical investigations in the U.S.S.R. manned space missions. *Acta Astronaut.* 8, 907–917. doi: 10.1016/0094-5765(81)90061-8

Geary, G. G., Krause, D. N., Purdy, R. E., and Duckles, S. P. (1998). Simulated microgravity increases myogenic tone in rat cerebral arteries. *J. Appl. Physiol. (1985)* 85, 1615–1621. doi: 10.1152/jappl.1998.85.5.1615

Geinas, J. C., Marsden, K. R., Tzeng, Y. C., Smirl, J. D., Smith, K. J., Willie, C. K., et al. (2012). Influence of posture on the regulation of cerebral perfusion. *Aviat. Space Environ. Med.* 83, 751–757. doi: 10.3357/asem.3269.2012

Giller, C. A. (1990). The frequency-dependent behavior of cerebral autoregulation. *Neurosurgery* 27, 362–368. doi: 10.1227/00006123-199009000-00004

Girouard, H., and Iadecola, C. (2006). Neurovascular coupling in the normal brain and in hypertension, stroke, and Alzheimer disease. *J. Appl. Physiol. (1985)* 100, 328–335. doi: 10.1152/japplphysiol.00966.2005

Golding, E. M., Marrelli, S. P., You, J., and Bryan, R. M. Jr. (2002). Endothelium-derived hyperpolarizing factor in the brain: a new regulator of cerebral blood flow? *Stroke* 33, 661–663. doi: 10.1161/str.33.3.661

Greaves, D. K., Arbeille, P., and Hughson, R. L. (2007). WISE 2005: altered cerebrovascular autoregulation after 60 day head-down bed rest. *J. Gravit. Physiol.* 14, 61–62.

Grigorieva, H. P., and Kozlovskaya, I. B. (1983). Influence 7-day immersion unloading on speed-strength properties of skeletal muscle. *Space Biol. Aerospace Med.* 4, 21–25.

Guell, A., Bes, A., Braak, L., and Barrère, M. (1979). Effects of a weightlessness simulation on the velocity curves measured by Doppler sonography at the level of the carotid system. *Physiologist* 22, 25–26.

Guell, A., Dupui, P., Barrère, M., Fanjaud, A., Bes, A., and Kotowskaia, A. (1982). Changes in the loco-regional cerebral blood flow (r.C.B.F.) during a simulation of weightlessness. *Acta Astronaut.* 9, 689–690. doi: 10.1016/0094-5765(82)90049-2

Hallgren, E., Kornilova, L., Fransen, E., Glukhikh, D., Moore, S. T., Clément, G., et al. (2016). Decreased otolith-mediated vestibular response in 25 astronauts induced by long-duration spaceflight. *J. Neurophysiol.* 115, 3045–3051. doi: 10.1152/jn.00065.2016

Hallgren, E., Migeotte, P. F., Kornilova, L., Delière, Q., Fransen, E., Glukhikh, D., et al. (2015). Dysfunctional vestibular system causes a blood pressure drop in astronauts returning from space. *Sci. Rep.* 5:17627. doi: 10.1038/srep17627

Hamel, E. (2006). Perivascular nerves and the regulation of cerebrovascular tone. *J. Appl. Physiol. (1985)* 100, 1059–1064. doi: 10.1152/japplphysiol.00954.2005

Hamner, J. W., and Tan, C. O. (2014). Relative contributions of sympathetic, cholinergic, and myogenic mechanisms to cerebral autoregulation. *Stroke* 45, 1771–1777. doi: 10.1161/STROKEAHA.114.005293

Hamner, J. W., Tan, C. O., Lee, K., Cohen, M. A., and Taylor, J. A. (2010). Sympathetic control of the cerebral vasculature in humans. *Stroke* 41, 102–109. doi: 10.1161/STROKEAHA.109.557132

Hargens, A. R., and Vico, L. (2016). Long-duration bed rest as an analog to microgravity. *J. Appl. Physiol.* 120, 891–903. doi: 10.1152/japplphysiol.00935.2015

Heckmann, J. G., Hilz, M. J., Hagler, H., Mück-Weymann, M., and Neundijrfer, B. (1999). Transcranial Doppler sonography during acute 80° head-down tilt (HDT) for the assessment of cerebral autoregulation in humans. *Neurol. Res.* 21, 457–462. doi: 10.1080/01616412.1999.11740959

Herault, S., Fomina, G., Alferova, I., Kotovskaya, A., and Arbeille, P. (2000). Cardiac, arterial and venous adaptation to weightlessness during 6-month MIR spaceflights with and without thigh cuffs (bracelets). *Eur. J. Appl. Physiol.* 81, 384–390. doi: 10.1007/s004210050058

Herranz, R., Anken, R., Boonstra, J., Braun, M., Christiansen, P. C., de Geest, M., et al. (2013). Ground-based facilities for simulation of microgravity: organism-specifications for their use, and recommended terminology. *Astrobiology* 13, 1–17. doi: 10.1089/ast.2012.0876

Ibrahim, J., McGee, A., Graham, D., McGrath, J. C., and Dominiczak, A. F. (2006). Sex-specific differences in cerebral arterial myogenic tone in hypertensive and normotensive rats. *Am. J. Physiol. Heart Circ. Physiol.* 290, 1081–1089. doi: 10.1152/ajpheart.00752.2005

Immink, R. V., van den Born, B. J., van Montfrans, G. A., Koopmans, R. P., Karemaker, J. M., and van Lieshout, J. J. (2004). Impaired cerebral autoregulation in patients with malignant hypertension. *Circulation* 110, 2241–2245. doi: 10.1161/01.CIR.0000144472.08647.40

Iwasaki, K., Levine, B. D., Zhang, R., Zuckerman, J. H., Pawelczyk, J. A., Diedrich, A., et al. (2007). Human cerebral autoregulation before, during and after spaceflight. *J. Physiol.* 579, 799–810. doi: 10.1113/jphysiol.2006.119636

Iwasaki, K., Zhang, R., Zuckerman, J. H., Pawelczyk, J. A., and Levine, B. D. (2000). Effect of head-down-tilt bed rest and hypovolemia on dynamic regulation of heart rate and blood pressure. *Am. J. Physiol. Regul. Integr. Comp. Physiol.* 279, 189–199. doi: 10.1152/ajpregu.2000.279.6.R2189

Iwase, S., Sugiyama, Y., Miwa, C., Kamiya, A., Mano, T., Ohira, Y., et al. (2000). Effects of three days of dry immersion on muscle sympathetic nerve activity and arterial blood pressure in humans. *J. Auton. Nerv. Syst.* 79, 156–164. doi: 10.1016/S0165-1838(99)00076-4

Jeong, S. M., Hwang, G. S., Kim, S. O., Levine, B. D., and Zhang, R. (2014). Dynamic cerebral autoregulation after bed rest: effects of volume and exercise countermeasures. *J. Appl. Physiol.* 116, 24–31. doi: 10.1152/japplphysiol.00710.2013

Johnson, P. C. (1986). Autoregulation of blood flow. *Circ. Res.* 59, 483–495. doi: 10.1161/01.res.59.5.483

Kainerstorfer, J. M., Sassaroli, A., Tgavalekos, K. T., and Fantini, S. (2015). Cerebral autoregulation in the microvasculature measured with near-infrared spectroscopy. *J. Cereb. Blood Flow Metab.* 35, 959–966. doi: 10.1038/jcbfm.2015.5

Karnik, R., Valentin, A., Winkler, W. B., Khaffaf, N., Donath, P., and Slany, J. (1996). Sex-related differences in acetazolamide-induced cerebral vasomotor reactivity. *Stroke* 27, 56–58. doi: 10.1161/01.str.27.1.56

Kastrup, A., Thomas, C., Hartmann, C., and Schabet, M. (1997). Sex dependency of cerebrovascular CO2 reactivity in normal subjects. *Stroke* 28, 2353–2356. doi: 10.1161/01.str.28.12.2353

Kawai, Y., Murthy, G., Watenpaugh, D. E., and Hargens, A. R. (1992). Cerebral blood flow velocity increases with acute head-down tilt of humans. *Physiologist* 35, 186–187.

Kawai, Y., Murthy, G., Watenpaugh, D. E., Breit, G. A., Deroshia, C. W., and Hargens, A. R. (1993). Cerebral blood flow velocity in humans exposed to 24h head-down tilt. *J. Appl. Physiol. (1985)* 74, 3046–3051. doi: 10.1152/jappl.1993.74.6.3046

Kermorgant, M., Leca, F., Nasr, N., Custaud, M.-A., Geeraerts, T., Czosnyka, M., et al. (2017). Impacts of simulated weightlessness by dry immersion on optic

nerve sheath diameter and cerebral autoregulation. *Front. Physiol.* 8:780. doi: 10.3389/fphys.2017.00780

Kermorgant, M., Nasr, N., Custaud, M.-A., Navasiolava, N., Arbeille, P., Guinet, P., et al. (2019). Effects of resistance exercise and nutritional supplementation on dynamic cerebral autoregulation in head-down bed rest. *Front. Physiol.* 10:1114. doi: 10.3389/fphys.2019.01114

Kim, J. M., Choi, J. K., Choi, M., Ji, M., Hwang, G., Ko, S. B., et al. (2018). Assessment of cerebral autoregulation using continuous-wave near-infrared spectroscopy during squat-stand maneuvers in subjects with symptoms of orthostatic intolerance. *Sci. Rep.* 8:13257. doi: 10.1038/s41598-018-31685-y

Kim, M. N., Durduran, T., Frangos, S., Edlow, B. L., Buckely, E. M., Moss, H. E., et al. (2010). Noninvasive measurement of cerebral blood flow and blood oxygenation using near infrared and diffuse correlation spectroscopies in critically brain injured adults. *Neurocrit. Care* 12, 173–180. doi: 10.1007/s12028-009-9305-x

Ko, R. K., Ngai, A. C., and Winn, H. R. (1990). Role of adenosine in regulation of regional cerebral blood flow in sensory cortex. *Am. J. Physiol.* 259, 1703–1708. doi: 10.1152/ajpheart.1990.259.6.H1703

Kotovskaia, A. R., and Fomina, G. A. (2010). [The features of adaptation and disadaptation of the human cardiovascular system in the space flight conditions]. *Fiziol. Cheloveka.* 36, 78–86.

Kozlovskaya, I. B., Grigoriev, H. P., and Gevlich, A. I. (1984). Comparative analysis of the influences of weightlessness and its models on speed-strength properties and skeletal muscle tone. *Russ. Biol. Aerospace Med.* 6, 22–25.

Lassen, N. A. (1959). Cerebral blood flow and oxygen consumption in man. *Physiol. Rev.* 39, 183–238. doi: 10.1152/physrev.1959.39.2.183

Lassen, N. A. (1964). Autoregulation of cerebral blood flow. *Circ. Res.* 15, 201–204.

Lassen, N. A. (1985). Normal average value of cerebral blood flow in younger adults is 50 ml/100 g/min. *J. Cereb. Blood Flow Metab.* 5, 347–349. doi: 10.1038/jcbfm.1985.48

Lassen, N. A., Feinberg, I., and Lane, M. H. (1960). Bilateral studies of cerebral oxygen uptake in young and aged normal subjects and in patients with organic dementia. *J. Clin. Invest.* 39, 491–500. doi: 10.1172/JCI104063

Lee, S. M. C., Feiveson, A. H., Stein, S., Stenger, M. B., and Platts, S. H. (2015). Orthostatic intolerance after ISS and space shuttle missions. *Aerosp. Med. Hum. Perform.* 86, 54–67. doi: 10.3357/AMHP.EC08.2015

Levine, B. D., Pawelczyk, J. A., Ertl, A. C., Cox, J. F., Zuckerman, J. H., Diedrich, A., et al. (2002). Human muscle sympathetic neural and haemodynamic responses to tilt following spaceflight. *J. Physiol.* 538, 331–340. doi: 10.1113/jphysiol.2001.012575

Li, J., and Iadecola, C. (1994). Nitric oxide and adenosine mediate vasodilation during functional activation in cerebellar cortex. *Neuropharmacology* 33, 1453–1461. doi: 10.1016/0028-3908(94)90049-3

Lin, L. J., Gao, F., Bai, Y. G., Bao, J. X., Huang, X. F., Ma, J., et al. (2009). Contrasting effects of simulated microgravity with and without daily -Gx gravitation on structure and function of cerebral and mesenteric small arteries in rats. *J. Appl. Physiol. (1985)* 107, 1710–1721. doi: 10.1152/japplphysiol.00493.2009

Liu, X., Czosnyka, M., Donnelly, J., Budohoski, K. P., Varsos, G. V., Nasr, N., et al. (2015). Comparison of frequency and time domain methods of assessment of cerebral autoregulation in traumatic brain injury. *J. Cereb. Blood Flow Metab.* 35, 248–256. doi: 10.1038/jcbfm.2014.192

Marina, N., Christie, I. N., Korsak, A., Doronin, M., Brazhe, A., Hosford, P. S., et al. (2020). Astrocytes monitor cerebral perfusion and control systemic circulation to maintain brain blood flow. *Nat. Commun.* 11:131. doi: 10.1038/s41467-019-13956-y

Marinoni, M., Ginanneschi, A., Inzitari, D., Mugnai, S., and Amaducci, L. (1998). Sex-related differences in human cerebral hemodynamics. *Acta Neurol. Scand.* 97, 324–327. doi: 10.1111/j.1600-0404.1998.tb05961.x

Marmarelis, V. Z. (1988). Coherence and apparent transfer function measurements for nonlinear physiological systems. *Ann. Biomed. Eng.* 16, 143–157. doi: 10.1007/bf02367386

Marshall-Goebel, K., Ambarki, K., Eklund, A., Malm, J., Mulder, E., Gerlach, D., et al. (2016). Effects of short-term exposure to head-down tilt on cerebral hemodynamics: a prospective evaluation of a spaceflight analog using phase-contrast MRI. *J. Appl. Physiol. (1985)* 120, 1466–1473. doi: 10.1152/japplphysiol.00841.2015

Marshall-Goebel, K., Laurie, S. S., Alferova, I. V., Arbeille, P., Auñón-Chancellor, S. M., Ebert, D. J., et al. (2019). Assessment of jugular venous blood flow stasis and thrombosis during spaceflight. *JAMA Netw. Open.* 2:e1915011. doi: 10.1001/jamanetworkopen.2019.15011

Marshall-Goebel, K., Mulder, E., Donoviel, D., Strangman, G., Suarez, J. I., Venkatasubba Rao, C., et al. (2017). An international collaboration studying the physiological and anatomical cerebral effects of carbon dioxide during head-down tilt bed rest: the SPACECOT study. *J. Appl. Physiol. (1985)* 122, 1398–1405. doi: 10.1152/japplphysiol.00885.2016

Meck, J. V., Reyes, C. J., Perez, S. A., Goldberger, A. L., and Ziegler, M. G. (2001). Marked exacerbation of orthostatic intolerance after long- vs. short-duration spaceflight in veteran astronauts. *Psychosom. Med.* 63, 865–873. doi: 10.1097/00006842-200111000-00003

Morey-Holton, E., and Globus, R. K. (2002). Hindlimb unloading rodent model: technical aspects. *J. Appl. Physiol. (1985)* 92, 1367–1377. doi: 10.1152/japplphysiol.00969.2001

Morey-Holton, E., Globus, R. K., Kaplansky, A., and Durnova, G. (2005). The hindlimb unloading rat model: literature overview, technique update and comparison with space flight data. *Adv. Space Biol. Med.* 10, 7–40. doi: 10.1016/s1569-2574(05)10002-1

Morita, H., Abe, C., and Tanaka, K. (2016). Long-term exposure to microgravity impairs vestibulo-cardiovascular reflex. *Sci. Rep.* 6:33405. doi: 10.1038/srep33405

Nasr, N., Czosnyka, M., Pavy-Le Traon, A., Custaud, M.-A., Liu, X., Varsos, G. V., et al. (2014). Baroreflex and cerebral autoregulation are inversely correlated. *Circ. J.* 78, 2460–2467. doi: 10.1253/circj.cj-14-0445

Navasiolava, N. M., Custaud, M. A., Tomilovskaya, E. S., Larina, I. M., Mano, T., Gauquelin-Koch, G., et al. (2011a). Long-term dry immersion: review and prospects. *Eur. J. Appl. Physiol.* 111, 1235–1260. doi: 10.1007/s00421-010-1750-x

Navasiolava, N. M., Pajot, A., Gallois, Y., Pastushkova, L., Kulchitsky, V. A., Gauquelin-Koch, G., et al. (2011b). NT-ProBNP levels, water and sodium homeostasis in healthy men: effects of 7 days of dry immersion. *Eur. J. Appl. Physiol.* 111, 2229–2237. doi: 10.1007/s00421-011-1858-7

Nguyen, T. S., Winn, H. R., and Janigro, D. (2000). ATP-sensitive potassium channels may participate in the coupling of neuronal activity and cerebrovascular tone. *Am. J. Physiol. Heart Circ. Physiol.* 278, 878–885. doi: 10.1152/ajpheart.2000.278.3.H878

Novak, V., Novak, P., Spies, J. M., and Low, P. A. (1998). Autoregulation of cerebral blood flow in orthostatic hypotension. *Stroke* 29, 104–111. doi: 10.1161/01.str.29.1.104

Ogawa, Y., Iwasaki, K., Aoki, K., Saitoh, T., Kato, J., and Ogawa, S. (2009). Dynamic cerebral autoregulation after mild dehydration to simulate microgravity effects. *Aviat. Space Environ. Med.* 80, 443–447. doi: 10.3357/asem.2449.2009

Ogawa, Y., Iwasaki, K., Aoki, K., Shibata, S., Kato, J., and Ogawa, S. (2007). Central hypervolemia with hemodilution impairs dynamic cerebral autoregulation. *Anesth. Analg.* 105, 1389–1396. doi: 10.1213/01.ane.0000281910.95740.e4

Ogoh, S., Hirasawa, A., de Abreu, S., Denise, P., and Normand, H. (2017). Internal carotid, external carotid and vertebral artery blood flow responses to 3 days of head-out dry immersion. *Exp. Physiol.* 102, 1278–1287. doi: 10.1113/EP086507

Paulson, O. B., Strandgaard, S., and Edvinsson, L. (1990). Cerebral autoregulation. *Cerebrovasc. Brain Metab. Rev.* 2, 161–192.

Pavy-Le Traon, A., Costes-Salon, M. C., Vasseur-Clausen, P., Bareille, M.-P., Maillet, A., and Parant, M. (2002). Changes in kinetics of cerebral autoregulation with head-down bed rest. *Clin. Physiol. Func. Imaging* 22, 108–114. doi: 10.1046/j.1365-2281.2002.00403.x

Pavy-Le Traon, A., Heer, M., Narici, M. V., Rittweger, J., and Vernikos, J. (2007). From space to Earth: advances in human physiology from 20 years of bed rest studies (1986-2006). *Eur. J. Appl. Physiol.* 101, 143–194. doi: 10.1007/s00421-007-0474-z

Pavy-Le Traon, A., Vasseur, P., Arbeille, P., Güell, A., Bes, A., and Gharib, C. (1995). Effects of 28-day head-down tilt with and without countermeasures on lower body negative pressure responses. *Aviat. Space Environ. Med.* 66, 982–991.

Perhonen, M. A., Franco, F., Lane, L. D., Buckey, J. C., Blomqvist, C. G., Zerwekh, J. E., et al. (2001). Cardiac atrophy after bed rest and spaceflight. *J. Appl. Physiol. (1985)* 91, 645–653. doi: 10.1152/jappl.2001.91.2.645

Petersen, L. G., and Ogoh, S. (2019). Gravity, intracranial pressure, and cerebral autoregulation. *Physiol. Rep.* 7:e14039. doi: 10.14814/phy2.14039

Petersen, L. G., Petersen, J. C., Andresen, M., Secher, N. H., and Juhler, M. (2016). Postural influence on intracranial and cerebral perfusion pressure in ambulatory neurosurgical patients. *Am. J. Physiol. Regul. Integr. Comp. Physiol.* 310, 100–104. doi: 10.1152/ajpregu.00302.2015

Peterson, E. C., Wang, Z., and Britz, G. (2011). Regulation of cerebral blood flow. *Int. J. Vasc. Med.* 2011:823525. doi: 10.1155/2011/823525

Platts, S. H., Bairey Merz, C. N., Barr, Y., Fu, Q., Gulati, M., Hughson, R., et al. (2014). Effects of sex and gender on adaptation to space: cardiovascular alterations. *J. Womens Health (Larchmt)* 23, 950–955. doi: 10.1089/jwh.2014.4912

Priesman, S., Marks, R., Nahtomi-Shick, O., and Sidi, A. (2005). Preservation of static and dynamic cerebral autoregulation after mild hypothermic cardiopulmonary bypass. *Br. J. Anaesth.* 95, 207–211. doi: 10.1093/bja/aei147

Rangel-Castillo, L., Gopinath, S., and Robertson, C. S. (2008). Management of intracranial hypertension. *Neurol. Clin.* 26, 521–541. doi: 10.1016/j.ncl.2008.02.003

Rivera-Lara, L., Zorrilla-Vaca, A., Geocadin, R. G., Healy, R. J., Ziai, W., and Mirski, M. A. (2017). Cerebral autoregulation-oriented therapy at the bedside: a comprehensive review. *Anesthesiology* 126, 1187–1199. doi: 10.1097/ALN.0000000000001625

Rosner, M. J., and Becker, D. P. (1984). Origin and evolution of plateau waves. Experimental observations and a theoretical model. *J. Neurosurg.* 60, 312–324. doi: 10.3171/jns.1984.60.2.0312

Roth, W., Morgello, S., Goldman, J., Mohr, J. P., Elkind, M. S., Marshall, R. S., et al. (2017). Histopathological differences between the anterior and posterior brain arteries as a function of aging. *Stroke* 48, 638–644. doi: 10.1161/STROKEAHA.116.015630

Rukavishnikov, I. V., Tomilovskaya, E. S., Matsnev, E. I., Denise, P., and Avan, P. (2013). Otoacoustic emission as a mediate method of intracranial pressure assesement under conditions of simulation of microgravity physiological effects. *Aviakosm Ekolog. Med.* 47:130.

Satake, H., Konishi, T., Kawashima, T., Matsunami, K., Uno, T., and Imai, S., et al. (1994). Intracranial blood flow measured with single photon emission computer tomography (SPECT) during transient -6 degrees head-down tilt. *Aviat. Space. Environ. Med.* 65, 117–122.

Savin, E., Bailliart, O., Checoury, A., Bonnin, P., Grossin, C., and Martineaud, J. P. (1995). Influence of posture on middle cerebral artery mean flow velocity in humans. *Eur. J. Appl. Physiol. Occup. Physiol.* 71, 161–165. doi: 10.1007/bf00854974

Shi, S. J., South, D. A., and Meck, J. V. (2004). Fludrocortisone does not prevent orthostatic hypotension in astronauts after spaceflight. *Aviat. Space Environ. Med.* 75, 235–239.

Sigaudo-Roussel, D., Custaud, M.-A., Maillet, A., Guell, A., Kaspranski, R., Hughson, R. L., et al. (2002). Heart rate variability after prolonged spaceflights. *Eur. J. Appl. Physiol.* 86, 258–265. doi: 10.1007/s00421-001-0551-7

Silverman, A., and Petersen, N. H. (2020). *Physiology, Cerebral Autoregulation*. Treasure Island, FL: StatPearls Publishing.

Sofronova, S. I., Tarasova, O. S., Gaynullina, D., Borzykh, A. A., Behnke, B. J., Stabley, J. N., et al. (2015). Spaceflight on the Bion-M1 biosatellite alters cerebral artery vasomotor and mechanical properties in mice. *J. Appl. Physiol. (1985)* 118, 830–838. doi: 10.1152/japplphysiol.00976.2014

Sorrentino, E., Budohoski, K. P., Kasprowicz, M., Smielewski, P., Matta, B., Pickard, J. D., et al. (2011). Critical thresholds for transcranial Doppler indices of cerebral autoregulation in traumatic brain injury. *Neurocrit. Care* 14, 188–193. doi: 10.1007/s12028-010-9492-5

Steiner, L. A., Coles, J. P., Czosnyka, M., Minhas, P. S., Fryer, T. D., Aigbirhio, F. I., et al. (2003). Cerebrovascular pressure reactivity is related to global cerebral oxygen metabolism after head injury. *J. Neurol. Neurosurg. Psychiatry* 74, 765–770. doi: 10.1136/jnnp.74.6.765

Strandgaard, S., and Paulson, O. B. (1984). Cerebral autoregulation. *Stroke* 15, 413–416. doi: 10.1161/01.str.15.3.413

Sun, X. Q., Pavy-Le Traon, A., and Gharib, C. (2002). Change of cerebral blood flow velocity during 4 d head-down tilt bed rest. *Space Med. Med. Eng. (Beijing)* 15, 163–166.

Sun, X. Q., Yao, Y. J., Wu, X. Y., Hao, W. Y., Jiang, S. Z., and Qiao, Z. L. (2001). Changes of cerebral blood flow during 21 d head-down tilt bed rest and the effect of lower body negative pressure during the last week. *Space Med. Med. Eng. (Beijing)* 14, 92–96.

Sun, X. Q., Yao, Y. J., Yang, C. B., Jiang, S. Z., Jiang, C. L., and Liang, W. B. (2005). Effect of lower-body negative pressure on cerebral blood flow velocity during 21 days head-down tilt bed rest. *Med. Sci. Monit.* 11, CR1–CR5.

Tanaka, K., Abe, C., Awazu, C., and Morita, H. (2009). Vestibular system plays a significant role in arterial pressure control during head-up tilt in young subjects. *Auton. Neurosci.* 148, 90–96. doi: 10.1016/j.autneu.2009.03.007

Tanaka, K., Abe, C., Sakaida, Y., Aoki, M., Iwata, C., and Morita, H. (2012). Subsensory galvanic vestibular stimulation augments arterial pressure control upon head-up tilt in human subjects. *Auton. Neurosci.* 166, 66–71. doi: 10.1016/j.autneu.2011.10.003

Tanaka, K., Ito, Y., Ikeda, M., and Katafuchi, T. (2014). RR interval variability during galvanic vestibular stimulation correlates with arterial pressure upon head-up tilt. *Auton. Neurosci.* 18, 100–106. doi: 10.1016/j.autneu.2014.04.001

Tanaka, K., Nishimura, N., and Kawai, Y. (2017). Adaptation to microgravity, deconditioning, and countermeasures. *J. Physiol. Sci.* 67, 271–281. doi: 10.1007/s12576-016-0514-8

Taylor, C. R., Hanna, M., Behnke, B. J., Stabley, J. N., McCullough, D. J., Davis, R. T. III, et al. (2013). Spaceflight-induced alterations in cerebral artery vasoconstrictor, mechanical, and structural properties: implications for elevated cerebral perfusion and intracranial pressure. *FASEB J.* 27, 2282–2292. doi: 10.1096/fj.12-222687

Tiecks, F. P., Lam, A. M., Aaslid, R., and Newell, D. W. (1995). Comparison of static and dynamic cerebral autoregulation measurements. *Stroke* 26, 1014–1019. doi: 10.1161/01.str.26.6.1014

Tomilovskaya, E., Shigueva, T., Sayenko, D., Rukavishnikov, I., and Kozlovskaya, I. (2019). Dry immersion as a ground-based model of microgravity physiological effects. *Front. Physiol.* 10:284. doi: 10.3389/fphys.2019.00284

Tzeng, Y. C., Ainslie, P. N., Cooke, W. H., Peebles, K. C., Willie, C. K., MacRae, B. A., et al. (2012). Assessment of cerebral autoregulation: the quandary of quantification. *Am. J. Physiol. Heart Circ. Physiol.* 303, 658–671. doi: 10.1152/ajpheart.00328.2012

van Beek, A. H., Claassen, J. A., Rikkert, M. G., and Jansen, R. W. (2008). Cerebral autoregulation: an overview of current concepts and methodology with special focus on the elderly. *J. Cereb. Blood Flow Metab.* 28, 1071–1085. doi: 10.1038/jcbfm.2008.13

Wang, X., Krishnamurthy, S., Evans, J., Bhakta, D., Justice, L., Bruce, E., et al. (2005). Transfer function analysis of gender-related differences in cerebral autoregulation. *Biomed. Sci. Instrum.* 41, 48–53.

Waters, W. W., Ziegler, M. G., and Meck, J. V. (2002). Postspaceflight orthostatic hypotension occurs mostly in women and is predicted by low vascular resistance. *J. Appl. Physiol. (1985)* 92, 586–594. doi: 10.1152/japplphysiol.00544.2001

Wilkerson, M. K., Muller-Derp, J., Colleran, P. N., and Delp, M. D. (1999). Effects of hindlimb unloading on rat cerebral, splenic, and mesenteric resistance artery morphology. *J. Appl. Physiol. (1985)* 87, 2115–2121. doi: 10.1152/jappl.1999.87.6.2115

Yang, C., Gao, Y., Greaves, D. K., Villar, R., Beltrame, T., Fraser, K. S., et al. (2015). Prior head-down tilt does not impair the cerebrovascular response to head-up tilt. *J. Appl. Physiol. (1985)* 118, 1356–1363. doi: 10.1152/japplphysiol.00871.2014

Yang, C. B., Wang, Y. C., Gao, Y., Geng, J., Wu, Y. H., Zhang, Y., et al. (2011). Artificial gravity with ergometric exercise preserves the cardiac, but not cerebrovascular, functions during 4 days of head-down bed rest. *Cytokine* 56, 648–655. doi: 10.1016/j.cyto.2011.09.004

Yao, Y. J., Wu, X. Y., Sun, X. Q., Wang, Z. B., Jiang, C. L., and Jiang, S. Z. (2001). Changes of human cerebral bottom arterial hemodynamics during 21 d head-down tilt (-6 degrees) bed-rest. *Space Med. Med. Eng. (Beijing)* 14, 11–16.

Yasumasa, A., Inoue, S., Tatebayashi, K., Shiraishi, Y., and Kawai, Y. (2002). Effects of head-down tilt on cerebral blood flow in humans and rabbits. *J. Gravit. Physiol.* 9, 89–90.

Yates, B. J., and Kerman, I. A. (1998). Post-spaceflight orthostatic intolerance: possible relationship to microgravity-induced plasticity in the vestibular system. *Brain Res. Brain Res. Rev.* 28, 73–82. doi: 10.1016/s0165-0173(98)00028-9

Zhang, L. F., and Hargens, A. R. (2018). Spaceflight-induced intracranial hypertension and visual impairment: pathophysiology and countermeasures. *Physiol. Rev.* 98, 59–87. doi: 10.1152/physrev.00017.2016

Zhang, R., Behbehani, K., and Levine, B. D. (2009). Dynamic pressure–flow relationship of the cerebral circulation during acute increase in arterial pressure. *J. Physiol.* 587, 2567–2577. doi: 10.1113/jphysiol.2008.168302

Zhang, R., Zuckerman, J. H., Giller, C. A., and Levine, B. D. (1998). Transfer function analysis of dynamic cerebral autoregulation in humans. *Am. J. Physiol.* 274, 233–241.

Zhang, R., Zuckerman, J. H., Pawelczyk, J. A., and Levine, B. D. (1997). Effects of head-down-tilt bed rest on cerebral hemodynamics during orthostatic stress. *J. Appl. Physiol. (1985)* 83, 2139–2145. doi: 10.1152/jappl.1997.83.6.2139

Zhou, D., Ding, J.-Y., Ya, J.-Y., Pan, L.-Q., Yan, F., Yang, Q., et al. (2018). Understanding jugular venous outflow disturbance. *CNS Neurosci. Ther.* 24, 473–482. doi: 10.1111/cns.12859

Zuj, K. A., Arbeille, P., Shoemaker, J. K., Blaber, A. P., Greaves, D. K., Xu, D., et al. (2012). Impaired cerebrovascular autoregulation and reduced co(2)reactivity after long duration spaceflight. *Am. J. Physiol. Heart Circ. Physiol.* 302, 2592–2598. doi: 10.1152/ajpheart.00029.2012

Conflict of Interest: The authors declare that the research was conducted in the absence of any commercial or financial relationships that could be construed as a potential conflict of interest.

frontiers in Physiology

ORIGINAL RESEARCH
published: 17 July 2020
doi: 10.3389/fphys.2020.00784

Efficacy of Gradient Compression Garments in the Hours After Long-Duration Spaceflight

Stuart M. C. Lee[1], L. Christine Ribeiro[1], Steven S. Laurie[1], Alan H. Feiveson[2], Vladimir V. Kitov[3], Igor S. Kofman[1], Brandon R. Macias[1], Marissa Rosenberg[1], Ilya V. Rukavishnikov[3], Elena S. Tomilovskaya[3], Jacob J. Bloomberg[2], Inessa B. Kozlovskaya[3†], Millard F. Reschke[2] and Michael B. Stenger[2]*

[1]KBR, Houston, TX, United States, [2]Lyndon B. Johnson Space Center, National Aeronautics and Space Administration, Houston, TX, United States, [3]Department of Sensory-Motor Physiology and Countermeasures, Institute of Biomedical Problems of the Russian Academy of Sciences, Moscow, Russia

OPEN ACCESS

Edited by:
Ronan Padraic Murphy, Dublin City University, Ireland

Reviewed by:
Ke Lv, China Astronaut Research and Training Center, China
Ana Diaz Artiles, Texas A&M University, United States

***Correspondence:**
Stuart M. C. Lee
stuart.lee-1@nasa.gov

†Deceased

Specialty section:
This article was submitted to Environmental, Aviation and Space Physiology, a section of the journal Frontiers in Physiology

Received: *09 March 2020*
Accepted: *15 June 2020*
Published: *17 July 2020*

Citation:
Lee SMC, Ribeiro LC, Laurie SS, Feiveson AH, Kitov VV, Kofman IS, Macias BR, Rosenberg M, Rukavishnikov IV, Tomilovskaya ES, Bloomberg JJ, Kozlovskaya IB, Reschke MF and Stenger MB (2020) Efficacy of Gradient Compression Garments in the Hours After Long-Duration Spaceflight. Front. Physiol. 11:784. doi: 10.3389/fphys.2020.00784

The incidence of presyncopal events is high soon after a long-duration spaceflight; >60% of returning astronauts could not complete a 10-min 80° head-up tilt test on landing day (R+0) after ~6 months of spaceflight. The objective of this study was to demonstrate the ability of a lower body gradient compression garment (GCG) to protect against an excessive increase in heart rate and a decrease in blood pressure during standing after long-duration spaceflight.

Methods: Eleven astronauts (9 M, 2 F) volunteered to participate. The stand test protocol consisted of 2 min of prone rest followed by 3.5 min of standing. Subjects completed one familiarization session, two preflight data collection sessions in standard clothing, and three tests on landing day while wearing GCG. Postflight tests were conducted 1–4 h (R+0A), ~12 h (R+0B), and ~28 h after landing (R+0C).

Results: All astronauts completed the stand test preflight. Three astronauts were unable to attempt the stand test at R+0A, and one of these was unable to start the test at R+0B. One astronaut was unable to complete 3.5 min of standing at R+0B (test ended at 3.3 min). Review of the individual's blood pressure data revealed no hypotension but the astronaut reported significant motion sickness. Of the astronauts who participated in testing on landing day, the heart rate and mean arterial pressure responses to standing (stand-prone) were not different than preflight at any of the postflight sessions.

Conclusion: Wearing the GCG after spaceflight prevented the tachycardia that normally occurs while standing after spaceflight without compression garments and protected against a decrease in blood pressure during a short stand test.

Keywords: stand test, orthostatic tolerance, lower body compression, heart rate, blood pressure, International Space Station

INTRODUCTION

We have previously reported that 60–80% of astronauts experienced orthostatic intolerance during 10 min of 80° head-up tilt conducted in the controlled conditions of the laboratory 4–6 h after landing from long-duration spaceflight (Meck et al., 2001; Lee et al., 2015). Currently, astronauts returning from the International Space Station (ISS) under normal circumstances receive assistance from ground support personnel to exit the Soyuz vehicle and are attended to by medical personnel immediately after landing (Baker et al., 2019), thus controlling the risk of orthostatic intolerance. However, in off-nominal conditions, such as a ballistic re-entry when the Soyuz capsule lands miles from support personnel (Carreau, 2008; Pettit, 2010), the crew must function autonomously, and thus the consequences of the astronauts experiencing orthostatic intolerance may be more substantial. Therefore, instituting countermeasures that reduce the likelihood of orthostatic intolerance to preserve capabilities in the minutes and hours after landing can be critical for astronaut health and safety.

We have studied cardiovascular responses to standing and during the performance of functional tasks following Space Shuttle (Arzeno et al., 2013; Stenger et al., 2013) and earlier ISS missions (Mulavara et al., 2018) without lower body compression garments, but postflight testing of ISS astronauts was not possible in the previous study until ~24 h after landing. However, recovery of the orthostatic responses to upright posture is profound within the first 24 h of landing. There are anecdotal reports of signs and symptoms of orthostatic intolerance at the landing site (Pettit, 2010), but the incidence of presyncope during tilt tests is substantially reduced the day after landing (Lee et al., 2015). Thus, the objective of this study was to quantify the effectiveness of the gradient compression garment (GCG) immediately post-landing and during the first day of recovery. We have previously demonstrated the efficacy of a next-generation lower body GCG after 2 weeks of bed rest as a spaceflight analog (Stenger et al., 2014) and during the first few hours after Space Shuttle missions (Stenger et al., 2013), but it was unclear as to whether these garments would provide sufficient protection from orthostatic intolerance immediately after landing from longer missions. Heart rate and blood pressure measurements during preflight stand tests without the GCG were compared to those obtained when astronauts completed the same testing protocol three times in the first 24 h after landing while wearing the GCG.

MATERIALS AND METHODS

This was a joint study conducted by the Cardiovascular and Vision Laboratory and the Neurosciences Laboratory at National Aeronautics and Space Administration (NASA) Johnson Space Center in collaboration with the Institute of Biomedical Problems of the Russian Academy of Sciences. Eleven astronauts from NASA, the European Space Agency, and the Japan Aerospace Exploration Agency (9 M, 2 F; 50 ± 6 year; 77.8 ± 8.7 kg; 173.0 ± 5.9 cm; 26.0 ± 3.3 $kg{\cdot}m^{-2}$; mean ± SD), who completed ISS missions (194 ± 65 day) consented to participate in this investigation. Study protocols and procedures were reviewed and approved by the NASA Johnson Space Center Institutional Review Board, Institute of Biomedical Problems Bioethics Committee, and the ISS Human Research Multilateral Review Board.

Data Collection Timeline

Astronauts completed preflight testing in normal clothing in the laboratory. Astronauts participated in a familiarization session scheduled ~180 days before launch and two preflight data collections at ~90 (L-90) and ~60 days (L-60) days before launch. All astronauts landed in the Russian Soyuz spacecraft, and therefore all were required to wear the Russian lower body compression garment (Kentavr) during re-entry and landing (Vil-Viliams et al., 1998; Platts et al., 2009). After extraction from the capsule at the landing zone, astronauts were carried to the medical tent for a brief physical examination by their flight surgeon. Thereafter, with the assistance of trained operators and the crew surgeon, astronauts doffed their Kentavr and donned the GCG. Testing occurred as soon as possible after landing (R+0A), either in the tent at the Soyuz landing site or after transport by helicopter to Karaganda or Dzhezkazgan Airports in Kazakhstan. No intravenous fluids (IV) were administered prior to testing at the landing site, but often astronauts received at least 1 L of IV fluids during transport by helicopter to the airport (Mulavara et al., 2018). The number of astronauts participating at each of the postflight test sessions varied. At R+0A, six of the seven astronauts participated in testing in the tent (1.9 ± 0.7 h after landing; range: 1.2–2.6 h), and one completed testing at the airport (4.3 h after landing). Subsequent testing (R+0B) occurred 12.2 ± 1.0 h after landing (range: 10.7–13.9 h) either in Germany (n = 1), Norway (n = 4), or Scotland (n = 4) at the refueling stop during travel back to Houston and again at Johnson Space Center (R+0C) 27.7 ± 1.8 h after the landing (range: 25.6–30.7 h, n = 11). Flight surgeons were requested to maintain a log of fluids and food consumed as well as medication and IV administered from the time of landing until R+0C. Subjects were not required to wear the GCG between test sessions.

Stand Test

Subjects were instrumented with a Holter monitor (Mortara H12+, Mortara Instruments, Milwaukee, WI) for continuous recording of ECG (1 kHz) and calculation of heart rate, a Portapres® ambulatory blood pressure monitor (Finapres Medical Systems B.V., The Netherlands) for the continuous recording of arterial blood pressure (100 Hz) with height correction, and a calibrated blood pressure sphygmomanometer and brachial cuff (Welch Allyn, Skaneateles Falls, NY).

The stand test began with the astronaut prone on a mat. A manual blood pressure measurement was obtained by ~1 min and 45 s of rest, and then the astronaut stood as quickly as possible when a command to stand was issued at 2 min.

Astronauts were instructed to not press down on the finger cuff while standing up from prone so as not to disturb the blood pressure signal. Astronauts stood with their gaze facing forward for 3.5 min. At the completion of the stand test, the test operator asked the astronaut to report their perception of motion sickness, ranging from 1 (no symptoms) to 20 (nausea to the point of vomiting).

For preflight testing in particular, astronauts were asked to maintain normal behavior patterns for intake of alcohol or caffeine prior to testing, maintain normal medications, avoid exposure to unusual motion conditions such as NASA's Neutral Buoyancy Laboratory training or virtual reality training for at least 24 h, and avoid maximal exercise in the 24 h before testing. For all tests, astronauts were requested to avoid alcohol consumption, exercise, and heavy meals within 4 h before the session (light snack within 2 h prior to testing was acceptable).

Gradient Compression Garment

In collaboration with the manufacturer of JOBST medical compression garments (Essity, Stockholm, Sweden), we developed an elastic three-piece GCG consisting of two thigh-high stockings and shorts that extend to the bottom of the rib cage that provides a continuous gradient of compression from the feet to the top of the garment. Compression is 55 mmHg at the ankle and gradually decreases along the leg to 35 mmHg at the knee and 18 mmHg at the top of the thigh, and further reduces to ~16 mmHg compression over the abdomen.

The GCGs were constructed for each subject based on detailed abdominal and lower body circumferences measured approximately 120 days before launch (L-120). Leg circumference was measured every 3.8 cm (1.5 inch) from the base of the toes to the top of the thigh. Additional measurements were obtained along the torso ending just below the breast-line. The desired tension was verified by the manufacturer when the garments were stretched to dimensions similar to that expected when the subjects donned the GCG using a Hosiery and Allied Trades Research Association (HATRA) test instrument that is identified in the British Standard for testing compression in elastic stockings. Validation of this line of garments was reviewed and approved by the FDA. Subjects donned the garments at L-90 to verify proper sizing and comfort. Due to time constraints on landing day, we were unable to measure the level of compression during postflight testing.

End-of-Mission Fluid Loading

Astronauts are advised by Russian medical specialists to consume 18–20 ml/kg body weight of sodium chloride-water solution or equivalent dry salt with water with 3–4 meals in the last 12–20 h before landing (Kozlovskaya et al., 1995). Kozlovskaya and Grigoriev (2004) report that cosmonauts who participate in this form of end-of-mission fluid loading better tolerate the final phase of the spaceflight mission and the postflight reconditioning program.

Data Reduction

Ectopic beats and artifacts were removed from the R-wave to R-wave (R-R) tracing derived from the Holter monitor and from the continuous blood pressure tracing before analysis through visual inspection (Arzeno et al., 2013). R-R and blood pressure data during the transition from prone to standing were not included in the analyses; blood pressure and electrocardiogram data from the time that the subject was fully upright until the time that the data were stable were discarded. Data were considered stable following the brief decrease in blood pressure with the transition to standing that sometimes was difficult to interpret due to artifact from the astronauts pressing on the finger cuff when pushing off the floor. The transition time from prone to standing was not consistent across test days, likely related to postflight sensorimotor disturbances, instability, and decreased muscle strength (L-90: 4.8 ± 1.7 s, range 2.7–9.4 s, n = 11; L-60: 4.8 ± 2.4 s, range 2.6–11.5 s, n = 11; R+0A: 14.8 ± 3.5 s, range 11.1–20.0 s, n = 7; R+0B: 10.8 ± 4.7 s, range 6.7–20.3, n = 9; R+0C: 8.2 ± 2.3 s, range 4.4–13.0 s, n = 11), as has been previously observed (Miller et al., 2018; Mulavara et al., 2018). Mean heart rate and mean arterial pressure were calculated for the 2 min of prone rest and ~3 min of standing. The manual blood pressure obtained during the prone period was used to calibrate the Portapres blood pressure signal to the manual blood pressure.

Statistical Analyses

Data from all the astronauts were available from the preflight testing, but results from the familiarization session on L-180 were not used in these analyses. Data collection in the field environment precluded acquisition of all data in the postflight period such that calibrated blood pressure data were not available for two subjects and during standing for one subject at R+0B. Thus, these data were not considered in our analyses. Data from the one astronaut who stood for all but the last 12 s of the standing on R+0B were included in these analyses.

Taking into account the longitudinal design and missing data, mixed linear regression models with random intercepts at the subject level and fixed session effects were used to estimate mean heart rate, mean arterial pressure, and the response to standing (stand-prone) for heart rate (ΔHR) and mean arterial pressure (ΔMAP) for preflight and each of three postflight test sessions as well as the change from preflight for each postflight session. ΔHR and ΔMAP were analyzed separately for each combination of posture (prone and standing). In all analyses, standard errors were estimated by clustered bootstrapping to account for non-normality of residuals. After fitting the ΔHR regression models, point estimates and 95% confidence intervals for the mean preflight to postflight change in heart rate, mean arterial pressure, ΔHR, and ΔMAP were calculated to provide a quantitative assessment of how well compression garments can control the amount of these changes during recovery from spaceflight, taking uncertainty into account. Following the approach of Fraser (2019), we also report p-value function plots that express the relative support of the data for

preflight to postflight changes in ΔHR mean exceeding or changes in ΔMAP mean lower than hypothetical values within a range of interest.

Given that there was no control group of ISS astronauts for this study, we compared preflight to postflight changes in ΔHR from a similar study without compression garments (Mulavara et al., 2018) to those observed in the current study using a mixed regression model accommodating study-specific between-subject variances on combined data on both studies. In the comparison subjects, ISS astronauts (11 M, 2 F) participated in inflight exercise countermeasures as prescribed by specialists from their respective space agency using a combination of resistive and cardiovascular exercise (Loehr et al., 2015), completed 159 ± 17 day of spaceflight, and were tested ~1 day after landing, similar to R+0C. Bed rest subjects (9 M) participated in an exercise countermeasure protocol similar to that used by ISS astronauts, did not participate in an end-of-bed rest fluid loading protocol, and were tested within an hour of rising from 70 days of 6° head-down tilt bed rest, similar to R+0A. Formal statistical inference on the effectiveness of the compression garments was based on this comparison for the outcome ΔHR at R+0A and at R+0C with significance defined as $p < 0.025$, controlling the family-wise Type I error to 0.05 or less (Bonferroni adjustment). No data corresponding to R+0B were available.

RESULTS

All astronauts were able to complete all the tests before flight, and all participated in at least one test on landing day. Data from one subject at R+0A and R+0B were not analyzed because the astronaut was provided the wrong size GCG for those tests, but this individual did wear the correct GCG at R+0C so those data are included in the analyses. Of the remaining 10 astronauts, three were unable to participate in the stand test at R+0A, and one of these also was unable to participate in the stand test at R+0B. Of the astronauts who participated in the stand test on landing day, the mean motion sickness score was 10 (range: 3–18), 6 (range: 2–14), and 5 (range: 1–13) at R+0A, R+0B, and R+0C, respectively.

Estimated means and 95% confidence intervals for heart rate and mean arterial pressure for prone rest, standing, and the change from prone to standing are shown in **Table 1** for preflight and each postflight session. These results are consistent with the hypothesis that when wearing the GCG there would be no meaningful preflight to postflight mean change in either the ΔHR or ΔMAP from prone to standing. The mean (±SE) ΔHR before flight without the GCG was 10 ± 1 bpm (**Figure 1**), and the estimated mean differences from preflight ΔHR (95% CI) were +3 bpm (−2, 8) at R+0A, +4 bpm (−1, 9) at R+0B, and −3 bpm (−8, 1) at R+0C when wearing the GCG. Relative degree of data support ($\log_{10}$ p) for the preflight to postflight mean change of ΔHR exceeding hypothetical values ranging from −5 to +15 bpm is shown in **Figure 2** for each postflight session. Compared with corresponding estimates of mean pre- to post-best or mean preflight to postflight change in ΔHR from Mulavara et al. (2018), the mean preflight to postflight change in ΔHR in astronauts wearing the GCG at R+0A was 15 bpm less than bed rest subjects not wearing the GCG [$t(18) = -4.0$, $p = 0.0009$] and 13 bpm less than ISS astronauts not wearing the GCG at R+0C [$t(26) = -4.2$, $p = 0.0003$].

In our ISS astronauts, the mean (±SE) ΔMAP from prone to standing before flight was 5 ± 1 mmHg when not wearing the GCG, and the estimated changes from preflight ΔMAP (95% CI) were −1 mmHg (−8, 5) at R+0A, −3 mmHg (−8, 3) at R+0B, and −1 mmHg (−6, 4) at R+0C when wearing the GCG. Relative degree of data support ($\log_{10}$ p) for mean change of ΔMAP being lower than hypothetical values ranging from −20 to +10 mmHg is shown in **Figure 2** for each postflight session.

One subject was able to complete only 3.3 of the 3.5 min of standing at R+0B, requesting test termination due to apparent symptoms of motion sickness. At the end of the stand test, this astronaut reported a motion sickness score of 14 out of 20, the highest score reported for any subject participating in the stand test at R+0B. Retrospective review of the beat-to-beat blood pressure tracing revealed no indications of hypotension (**Figure 3**).

Of the 10 astronauts for whom IV and oral fluid data were recorded, nine reported oral ingestion of additional fluids in the 24 h before landing. Specifically, seven astronauts reported that they completed the protocol for end-of-mission fluid loading as prescribed by the Russian medical personnel, two reported ingesting 650–3,000 ml of fluid of unknown composition in addition to their normal consumption, and one did not report ingesting any additional fluid. Crew surgeon notes indicated that most astronauts received some IV fluids and all drank water or other beverages during the return to Houston. Of the data recorded by the crew surgeons, total IV fluid administration ranged from 300 to 4,000 ml, and oral fluid consumption ranged from 500 to 4,500 ml (**Table 2**). In these astronauts, many received anti-emetics before landing, and several received the same or similar medications during the first 25–30 h after landing (**Table 3**).

TABLE 1 | Estimated mean and 95% confidence intervals for heart rate and mean arterial pressure during prone rest (prone) and standing (stand) and the response to standing (Δ, stand-prone) before flight (preflight: mean of the two preflight tests, L-90 and L-60) and at R+0A (1.2–4.4 h after landing), R+0B (10.7–13.9 h after landing), and R+0C (25.6–30.7 h after landing). All means and confidence intervals were calculated with mixed-model linear regression analysis.

		Prone		Stand		Δ (Stand-prone)	
	n	**Mean**	**95% CI**	**Mean**	**95% CI**	**Mean**	**95% CI**
				Heart Rate (bpm)			
Preflight	11	61	59, 64	71	68, 75	10	8, 13
R+0A	7	65	61, 68	78	71, 84	13	9, 17
R+0B	9	66	62, 69	80	74, 85	14	10, 18
R+0C	11	70	67, 72	76	71, 81	7	3, 10
				Mean Arterial Pressure (mmHg)			
Preflight	11	91	88, 95	96	93, 100	5	3, 7
R+0A	7	102	94, 109	105	99, 112	3	-2, 9
R+0B	7	97	91, 103	97	88, 106	2	-3, 7
R+0C	11	97	92, 101	101	94, 107	4	-1, 8

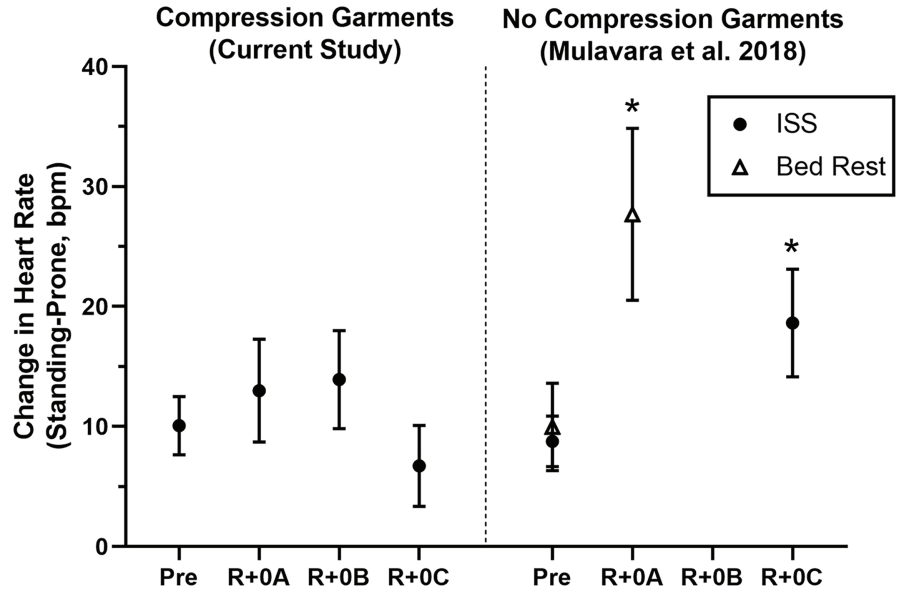

FIGURE 1 | Mean change (±95% CI) in heart rate (Standing-Prone, bpm) in ISS astronauts (closed circles) participating in the current study who wore the GCG only during postflight tests (R+0A: 1.2–4.4 h; R+0B: 10.7–13.9 h; and R+0C: 25.6–30.7 h after landing) and in ISS astronauts (11 M, 2 F) and bed rest subjects (open triangles; 9 M) who participated in the same stand test protocol but did not wear compression garments (Mulavara et al., 2018). Results from these comparison groups of ISS astronauts and bed rest subjects are shown at time points comparable to the current study, and results were calculated in the same manner as in this study. *Significantly greater preflight to postflight change in the heart rate response to standing than when wearing the GCG.

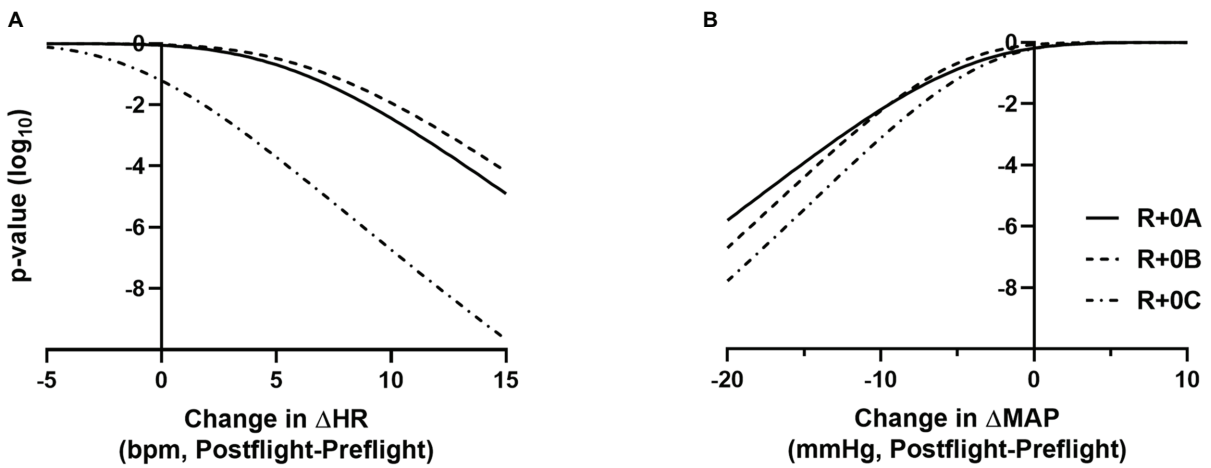

FIGURE 2 | *p*-value functions (log_{10} metric) showing how well the data supports the mean preflight to postflight change in ΔHR exceeding N bpm, for $-5 < N < 15$ **(A)** and the mean preflight to postflight change in ΔMAP being lower than N mmHg, for $-20 < N < +10$ **(B)**. Plots are shown for R+0A, R+0B, and R+0C. For example, an actual mean preflight to postflight change in ΔHR exceeding 10 bpm at R+0A is not supported by the data ($p < 10^{-3}$), and there is very little data support for a mean preflight to postflight change in ΔMAP being less than −15 mmHg at R+0A ($p < 10^{-4}$).

DISCUSSION

Here we report for the first time that use of GCGs throughout the first 24 h after returning from long-duration spaceflight provides effective protection from the development of orthostatic intolerance during a brief stand test, extending our findings after short-duration spaceflight (Stenger et al., 2013). Given that the incidence of orthostatic intolerance is markedly increased after long-duration flight (Meck et al., 2001; Lee et al., 2015), and two astronauts in this study participated in missions greater than 270 days, these results suggest that use of the GCG can mitigate the risk of orthostatic intolerance after long-duration missions. However, astronauts demonstrating the most severe symptoms, such as nausea and/or dizziness, did not attempt to complete these tests, highlighting that integrated physiological responses are needed during re-acclimation to a gravitational environment.

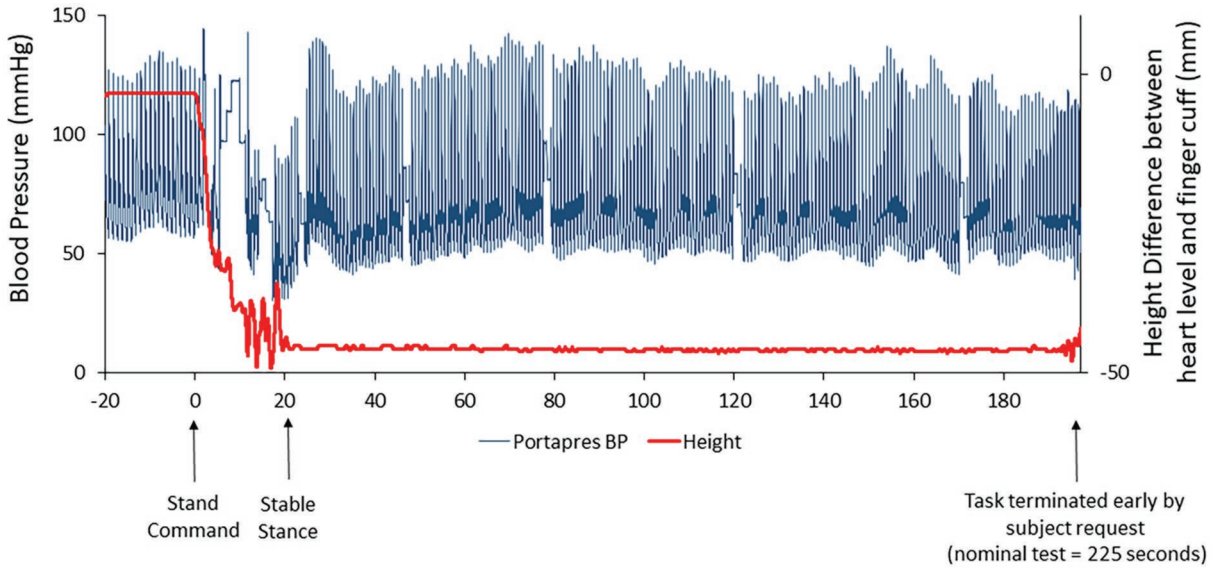

FIGURE 3 | Beat-to-beat blood pressure tracing (raw data; blue line) in one subject who was unable to complete the stand test on R+0B. The red line represents the height correction sensor for the ambulatory blood pressure device (Portapres®) that was placed at heart level on the subject's arm. The height correction is near "0" when the subject is prone but decreases when the subject is standing. Retrospective review of these data suggested that the subject was not hypotensive.

TABLE 2 | Intravenous fluids administered by the flight surgeon and oral fluids ingested by the astronauts in the first 25–30 h after landing as recorded in the flight surgeon log. Prescribed: did the astronaut perform the end-of-mission fluid loading protocol as prescribed by the Russian medical personnel. NA, records not available; NR, none recorded.

	Fluid load		Kazakhstan		Midway		JSC	
	Prescribed	Amount (ml)	IV (ml)	Oral (ml)	IV (ml)	Oral (ml)	IV (ml)	Oral (ml)
1	Yes	NR	1000	400	1000	444	2000	2000
2	NA	NA	NA	NA	NA	NA	NA	NA
3	No	3000	1000	NR	1000	860	NR	500
4	NR	NR	NR	300	800	1500	NR	1850
5	Yes	NR	NR	500	1000	NR	NR	NR
6	Yes	NR	500	3500	NR	250	NR	750
7	Yes	900	2000	355	NR	355	NR	500
8	Yes	2600	1000	1000	NR	1000	NR	1000
9	Yes	NR	NR	473	NR	500	NR	937
10	Yes	NR	1000	NR	NR	944	NR	794
11	NR	650	300	NR	NR	NR	NR	NR

Even with the current suite of countermeasures in use (Kozlovskaya and Grigoriev, 2004; Lee et al., 2015; Loehr et al., 2015), not all astronauts will be tolerant of the upright posture during the period immediately following landing.

Although astronauts who did not wear the GCG were not tested as controls in this study, comparisons to similar data that have been previously published support the efficacy of the GCG as a countermeasure to orthostatic stress. In ISS astronauts who participated in early ISS missions (Expedition 1–17) and were tilted to 80° head-up without compression garments within 4 h of landing (n = 5), the average increase in heart rate from supine to 3 min of head-up tilt was ~25 bpm, resulting in a ~15 bpm higher standing heart rate than that measured during the same test before flight (Lee et al., 2015). These early ISS astronauts were prescribed exercise countermeasures using a similar philosophy by employing a combination of resistive and cardiovascular exercise (Lee et al., 2019), although the countermeasure hardware available during the early ISS missions was less robust than currently available (Korth, 2015; Loehr et al., 2015). Also, in bed rest subjects who performed an exercise countermeasures protocol similar to that used by ISS astronauts, the ΔHR from prone to standing in the same stand test protocol as used in this study increased from 7 bpm before bed rest to 25 bpm after bed rest (**Figure 1**; Mulavara et al., 2018). In contrast, in the current study of astronauts who completed the stand test in a similar timeframe, the mean change in heart rate from prone to standing at R+0A was only 13 bpm, which was only 3 bpm greater than preflight. From the p-value plots that we present here (**Figure 2**), the data did not support that when wearing the GCG after spaceflight the ΔHR from prone to standing will increase by more than 10 bpm during the stand test at R+0A. These findings are particularly important in our subjects given that six of the subjects tested at R+0A had not received IV fluids prior to testing at the landing zone in Kazakhstan, and therefore we expect that they would have been plasma volume depleted compared to their preflight condition (Meck et al., 2001). Our current findings were unchanged without the inclusion of the one astronaut who was tested at R+0A after receiving IV fluids.

There are no corresponding data against which to compare our R+0B data, but there are a few reports of orthostatic responses 1 day after landing (R+1), which is similar to the collection

TABLE 3 | Antiemetic medications received by the astronauts before landing (>6 h before R+0A), before R+0A (<6 h), and in the first 25–30 h after landing.

Subject	Before landing	Before R+0A	Kazakhstan to refueling	Refueling to JSC
1	Meclizine	Ondansetron, Promethazine	Meclizine	Promethazine
2	Not available	Not available	Not available	Not available
3	None reported	Promethazine	None reported	None reported
4	Ondansetron	None reported	Promethazine	None reported
5	None reported	Ondansetron, Promethazine, Meclizine	Promethazine	None reported
6	Scopalmine	None reported	Scopalamine	Scopalamine
7	Meclizine	Ondansetron	None reported	Meclizine
8	Meclizine	Meclizine, Ondansetron	None reported	None reported
9	Meclizine	Meclizine	None reported	None reported
10	Meclizine	Meclizine	None reported	None reported
11	None reported	None reported	None reported	None reported

time of R+0C. In the astronauts participating in early ISS missions mentioned previously, the elevated ΔHR in response to tilt and elevated heart rate when tilted still were evident at R+1 (Lee et al., 2015). More recently, we reported that the ΔHR to the same stand test protocol as in the current study was 10 bpm greater on R+1 compared to preflight in ISS astronauts without the GCG, despite no difference in plasma volume between preflight and R+1 (Mulavara et al., 2018). In contrast, in the current study the ΔHR from prone to standing at R+0C was not different than preflight. However, Wood et al. (2019a,b) recently reported that the mean change in heart rate during a supine-sit-stand test, in which the stand portion was 3 min, did not change from preflight to postflight (preflight: 19; R+1: 21 bpm) in nine ISS astronauts, although the standing heart rate in those astronauts was significantly greater on R+1 (preflight: 75, R+1: 85 bpm). Together, results from the current study suggest that the GCG is an effective countermeasure to orthostatic stress on R+0.

There are potential limitations of comparisons of the current stand test results to other spaceflight studies, including that the duration of the stand portion of our protocol was shorter than some previous investigations during which presyncope was reported (Meck et al., 2001; Lee et al., 2015) and that the tilt test is considered to be more provocative. This stand duration was chosen such that failure to complete the stand test would not encourage the astronauts or flight surgeons to waive the remaining sensorimotor tests that were conducted in conjunction with this data collection (Mulavara et al., 2018). That mean arterial pressure was maintained in our subjects during standing when wearing the GCG is encouraging but results from our previous tilt test studies (Meck et al., 2001; Lee et al., 2015) suggest that this may have been an inadequate duration to observed decreases in blood pressure if the GCG was not effective.

An overall limitation of postflight studies of astronauts is that each crewmember is handled differently based upon their individual symptoms, the clinical judgment of the crew surgeon, and the conditions at the landing site. For example, in this study in some cases test sessions were waived or the protocol truncated due to the condition of the astronaut or the poor weather conditions at the landing zone (i.e., R+0A testing conducted at their airport in Kazakhstan instead of at the landing zone), and astronauts received different amounts of IV fluids or different medications. While these situations do not result in an ideal experimental design, they represent the actual conditions in which the data were collected and the range of conditions of ISS astronauts in the immediate post-landing period. Different number of subjects participated in postflight tests at R+0A and R+0B, which combined with our relatively small sample size, likely contributed to the width of the confidence intervals. Thus, we have attempted to document the conditions of each astronaut during testing to aid in the interpretation of these results.

Symptoms of motion sickness are common among astronauts after spaceflight (Jennings 1998) and influence tolerance to standing on landing day. In astronauts who are unable even to begin an orthostatic test, as we observed in this and our previous study (Lee et al., 2015), it is difficult to clearly ascribe a cause since there were no sensorimotor or cardiovascular data collected. Further complicating this matter is an interrelationship between the sensorimotor and cardiovascular dysfunction and the similarity of the symptoms, which might result in misclassification of the condition (Lackner, 2014). Appropriate monitoring of cardiovascular responses during sensorimotor challenges is required to differentiate the source of the symptoms. Astronauts often receive medication for motion sickness (Jennings, 1998; Shi et al., 2011), and in the 10 of 11 astronauts for whom we have at least partial reports from the flight surgeons, seven received at least one dosage of medication prophylactically before landing, six received medications soon before R+0A, five received medication in transit from Kazakhstan to the refueling stop, and three received medications between the refueling stop and arrival at JSC.

In particular, we were interested in examining information regarding astronauts who were unable to start the stand test at R+0A and R+0B as well as the one astronaut who started but was unable to complete the stand test at R+0B. Two of the three astronauts who were unable to begin the stand test at R+0A received at least one dose of Promethazine, either intramuscularly or intravenously, before testing was planned to begin. Although these two individuals likely were suffering from more significant sensorimotor disturbances, even if they had started the test they may not have been able to complete it. Promethazine is a H1-receptor antagonist that induces presyncope during orthostasis, primarily through an inhibition of sympathetic responses to protect blood pressure with no effect on heart rate (Shi et al., 2011). However, the one astronaut who was unable to start testing at R+0A and R+0B received only Meclizine and Zofran prior to R+0A, and no antiemetic medications were recorded before R+0B. Based upon notes received from the crew surgeon, the astronaut who started the stand test at R+0B but was unable to stand for the whole time, apparently suffered from symptoms of motion sickness throughout the 24-h period after landing. Symptoms included

nausea and vomiting, and the individual received multiple dosages of Meclizine (25 mg, prophylactically), Zofran (4 mg SL), and Promethazine (12.5 mg IV) as well as normal saline IV (4 × 1 L).

Medications administered for motion sickness might have influenced our results at other times as well. For example, five of the seven astronauts had standing heart rates that were similar to or lower than the preflight value but two had standing heart rates that were more than 15 bpm higher at R+0A than preflight. Interestingly, mean arterial pressure was higher at R+0A than preflight in these two subjects, but these two individuals reported the highest motion sickness scores of the astronauts who completed testing at this time point. These two subjects also were the only ones who received Meclizine, another H1-receptor antagonist, ~30 min before testing, one of the potential side effects being sinus tachycardia.

Given that women have a higher incidence of postflight orthostatic intolerance than men (Fritsch-Yelle et al., 1996; Waters et al., 2002), it is important to assess whether the garments are effective for both sexes. While the number and proportion of women with spaceflight exposures were relatively low during the Space Shuttle (Harm et al., 2001) and early ISS programs, the number of women selected as astronauts and who have flown to space has steadily increased. Differences between sexes with regard to postflight orthostatic intolerance have been proposed to result from larger spaceflight-induced reductions in plasma volume in women coupled with a greater dependence on volume status (Waters et al., 2002) and heart rate responses (Gotshall et al., 1991; Frey et al., 1994), lower vascular resistance (Waters et al., 2002), and a smaller, less compliant left ventricle (Fu et al., 2004). Unfortunately, no women wore lower body compression garments in our previous study of Shuttle astronauts after short-duration spaceflight (Stenger et al., 2010, 2013), but four of the 16 subjects studied in a 14-day bed rest study were women, and no subjects became presyncopal when wearing the GCG during a 15-min 80° head-up tilt test on the last day of bed rest (Stenger et al., 2014). In the current study, two of 11 ISS astronauts were women, the ΔHR from prone to standing after spaceflight was similar or lower than preflight, and neither experienced hypotensive responses during the stand test while wearing the GCG.

We have previously reported that the incidence of presyncope during orthostatic tests dramatically decreases in the days after landing (Meck et al., 2001; Lee et al., 2015; Mulavara et al., 2018), yet some crewmembers are still intolerant of the upright posture or become hypotensive while standing during the days after return to Earth. Thus, wearing compression garments for several days after landing is warranted in some individuals. For example, we (Lee et al., 2015) previously reported that one ISS astronaut was unable even to start the tilt test on R+1, and two astronauts failed to complete the entire 10 min of tilt on R+3. Further, Wood et al. (2019a) reported that two astronauts (of 9 M astronauts) became hypotensive during a 3-min stand test conducted 18–36 h after landing. However, Fu et al. (2019) observed no hypotensive events using ambulatory blood pressure recordings acquired in 12 ISS astronauts, including four women, when participating in activities of daily living in the first 24 h after landing. Interpretation of ambulatory data is complicated because the authors had insufficient information to determine when the astronauts were wearing the Russian Kentavr or were supine during the postflight period. The plane transporting the astronauts back from Kazakhstan is equipped with a bed for each astronaut, which would be well-utilized if the individual suffered from sensorimotor disturbances, and many astronauts continue to wear the Kentavr or other compression garments.

Our data highlight the efficacy of the GCG during standing in the postflight period but the GCG has not been tested or relied upon during re-entry and landing. In the Soyuz and the currently planned configuration for the Orion capsule, the vast majority of the acceleration is directed anterior-posterior (G_x) such that the head-to-foot (G_z) stress is minimized and the likelihood of acceleration-related hypotension is minimized. The benefits of astronauts wearing compression garments during re-entry and landing would be more pronounced in vehicles that return from space with the subjects in position such that the acceleration vector is directed from the head to the foot, as was the situation during Space Shuttle landings. Though lower body compression garments were shown to be efficacious during re-entry of the Space Shuttle (Perez et al., 2003), NASA and the Russian Space Agency have no immediate plans for future space vehicles traveling to and from ISS in which the acceleration would be experienced by astronauts in G_z. However, NASA plans to return to the moon by 2024 in a space vehicle that may include G_z accelerations with the astronauts standing, as they did during the Apollo missions. Not providing a seat for lunar descent and ascent reduces mass and volume requirements for the space capsule. There were no reports of hypotension during lunar descent and ascent, but the Apollo astronauts all were men and at least partially selected based upon their ability to tolerate sustained G-forces. Plasma volume (Leach et al., 1996) and the ability to tolerate orthostatic stress rapidly declines (Nixon et al., 1979; Bungo and Johnson, 1983) in the first few days of spaceflight, and thus some individuals might not be able to tolerate the G_z accelerations during descent to and ascent from the lunar surface. For example, women are more likely to experience orthostatic intolerance during re-exposure to gravity (Fritsch-Yelle et al., 1996; Waters et al., 2002), even at levels less than 1-G_z. Grenon et al. (2006) reported 50% of women could not complete a 10-min 30° head-up tilt test after 2 weeks of bed rest. This tilt angle approximates the orthostatic stress equivalent to 0.5-G_z, which is in the range of G_z experienced by Apollo astronauts during lunar descent and ascent. It is likely that a lower body compression garment like the GCG would be helpful in this situation.

CONCLUSION

Wearing a garment that provides a gradient compression from the feet to over the abdomen after long-duration spaceflight prevented the tachycardia that normally occurs while standing after spaceflight without compression garments and protected against a decrease in blood pressure during a short stand test. A GCG would be an efficacious countermeasure to orthostatic intolerance during re-entry and landing and would provide orthostatic support during the reconditioning period.

DATA AVAILABILITY STATEMENT

Given the unique nature and size of our subject population, it is not possible to make these data publicly-available without compromising subject confidentiality and privacy. Requests to access the datasets should be directed to NASA's Life Sciences Data Archive (https://lsda.jsc.nasa.gov/).

ETHICS STATEMENT

The studies involving human participants were reviewed and approved by NASA Johnson Space Center Institutional Review Board, Institute of Biomedical Problems Bioethics Committee, and the ISS Human Research Multilateral Review Board. The participants provided their written informed consent to participate in this study.

AUTHOR CONTRIBUTIONS

SML contributed to the study design, implementation, interpretation of results, drafting and revision of the manuscript, and approval of final draft. LR contributed to the study implementation, editing of the manuscript, and approval of final draft. SSL contributed to the interpretation of results, editing of the manuscript, and approval of final draft. AF contributed to the statistical analyses, drafting and editing of the manuscript, and approval of final draft. VK contributed to the study implementation and approval of final draft. IK contributed to the study implementation, editing of the manuscript, and approval of final draft. BM contributed to the interpretation of results, editing of the manuscript, and approval of final draft. MR contributed to the study implementation, editing of the manuscript, and approval of final draft. IR contributed to the study implementation and approval of final draft. ET contributed to the study design, implementation, editing of the manuscript, and approval of final manuscript. JB contributed to the study design, implementation, interpretation of results, editing of the manuscript, and approval of final draft. IK contributed to the study design, implementation, editing of the manuscript, approval of final draft, and secured funding. MFR contributed to the study design, implementation, interpretation of results, editing of the manuscript, approval of final draft, and secured funding. MS contributed to the study design, implementation, interpretation of results, editing of the manuscript, approval of final draft, and secured funding. All authors contributed to the article and approved the submitted version.

FUNDING

This research was funded by NASA's Human Research Program and the Russian Academy of Sciences (63.1).

ACKNOWLEDGMENTS

The authors thank the astronauts who participated in this study; Kevin Tucker and Mary Ann Hettich of Essity with whom we collaborated in the design and who constructed the GCG for this and our previous studies; personnel from the Johnson Space Center Cardiovascular and Vision Laboratory, the Johnson Space Center Neurosciences Laboratory, the Gagarin Cosmonaut Training Center, and the Institute of Biomedical Problems who collected and compiled the data, including Nichole Beltran, Dr. Alexey Grishin, Natalya Lysova, Nikolay Osetskiy, Sondra Perez, Elena Fomina, and Michael Willig; NASA and Russian Space Agency nurses, flight surgeons, astronauts, and management personnel who assisted with donning the GCG and experiment hardware, spotting subjects, and recording data during the postflight phase; and the ISS Medical Project for overall coordination of scheduling of data collection sessions. This study was one arm of a larger project titled, "Recovery of Functional Performance following Long Duration Space Flight" (co-principal investigators, Drs. Millard Reschke and Inessa Kozlovskaya).

REFERENCES

Arzeno, N. M., Stenger, M. B., Bloomberg, J. J., and Platts, S. H. (2013). Spaceflight-induced cardiovascular changes and recovery during NASA's functional task test. *Acta Astronaut.* 92, 10–14. doi: 10.1016/j.actaastro.2012.05.023

Baker, E., Barratt, M. R., Sams, C. F., and Wear, M. K. (2019). "Human response to space flight" in *Principles of clinical medicine for space flight*. eds. M. R. Barratt, E. S. Baker and S. L. Pool. *2nd Edn.* (New York, NY: Springer), 367–411.

Bungo, M. W., and Johnson, P. C. (1983). Cardiovascular examinations and observations of deconditioning during the space shuttle orbital flight test program. *Aviat. Space Environ. Med.* 54, 1001–1004.

Carreau, M. (2008). U.S. astronaut recalls terrifying Soyuz descent. In: *Houst. Chron.* Available at: http://www.chron.com/news/nation-world/article/U-S-astronaut-recalls-terrifying-Soyuz-descent-1759455.php (Accessed Auguest 20, 2017).

Fraser, D. A. S. (2019). The *p*-value function and statistical inference. *Am. Stat.* 73, 135–147. doi: 10.1080/00031305.2018.1556735

Frey, M. A., Tomaselli, C. M., and Hoffler, W. G. (1994). Cardiovascular responses to postural changes: differences with age for women and men. *J. Clin. Pharmacol.* 34, 394–402. doi: 10.1002/j.1552-4604.1994.tb04979.x

Fritsch-Yelle, J. M., Whitson, P. A., Bondar, R. L., and Brown, T. E. (1996). Subnormal norepinephrine release relates to presyncope in astronauts after spaceflight. *J. Appl. Physiol.* 81, 2134–2141. doi: 10.1152/jappl.1996.81.5.2134

Fu, Q., Arbab-Zadeh, A., Perhonen, M. A., Zhang, R., Zuckerman, J. H., and Levine, B. D. (2004). Hemodynamics of orthostatic intolerance: implications for gender differences. *Am. J. Physiol. Heart Circ. Physiol.* 286, H449–H457. doi: 10.1152/ajpheart.00735.2002

Fu, Q., Shibata, S., Hastings, J. L., Platts, S. H., Hamilton, D. M., Bungo, M. W., et al. (2019). Impact of prolonged spaceflight on orthostatic tolerance during ambulation, and blood pressure profiles in astronauts. *Circulation* 140, 729–738. doi: 10.1161/CIRCULATIONAHA.119.041050

Gotshall, R. W., Tsai, P. F., and Frey, M. A. (1991). Gender-based differences in the cardiovascular response to standing. *Aviat. Space Environ. Med.* 62, 855–859.

Grenon, S. M., Xiao, X., Hurwitz, S., Sheynberg, N., Kim, C., Seely, E. W., et al. (2006). Why is orthostatic tolerance lower in women than in men? Renal and cardiovascular responses to simulated microgravity and the role of midodrine. *J. Investig. Med.* 54, 180–190. doi: 10.2310/6650.2006.05064

Harm, D. L., Jennings, R. T., Meck, J. V., Powell, M. R., Putcha, L., Sams, C. P., et al. (2001). Invited review: gender issues related to spaceflight: a NASA perspective. *J. Appl. Physiol.* 91, 2374–2383. doi: 10.1152/jappl.2001.91.5.2374

Jennings, R. T. (1998). Managing space motion sickness. *J. Vestib. Res.* 8, 67–70.

Korth, D. W. (2015). Exercise countermeasure hardware evolution on ISS: the first decade. *Aerosp. Med. Hum. Perform.* 86, A7–A13. doi: 10.3357/amhp.ec02.2015

Kozlovskaya, I. B., and Grigoriev, A. I. (2004). Russian system of countermeasures on board of the International Space Station (ISS): the first results. *Acta Astronaut.* 55, 233–237. doi: 10.1016/j.actaastro.2004.05.049

Kozlovskaya, I. B., Grigoriev, A. I., and Stepantzov, V. I. (1995). Countermeasure of the negative effects of weightlessness on physical systems in long-term space flights. *Acta Astronaut.* 36, 661–668. doi: 10.1016/0094-5765(95)00156-5

Lackner, J. R. (2014). Motion sickness: more than nausea and vomiting. *Exp. Brain Res.* 232, 2493–2510. doi: 10.1007/s00221-014-4008-8

Leach, C. S., Alfrey, C. P., Suki, W. N., Leonard, J. I., Rambaut, P. C., Inners, L. D., et al. (1996). Regulation of body fluid compartments during short-term spaceflight. *J. Appl. Physiol.* 81, 105–116. doi: 10.1152/jappl.1996.81.1.105

Lee, S. M. C., Feiveson, A. H., Stein, S. P., Stenger, M. B., and Platts, S. H. (2015). Orthostatic intolerance after International Space Station and Space Shuttle Missions. *Aerosp. Med. Hum. Perform.* 86, A54–A67. doi: 10.3357/AMHP.EC08.2015

Lee, S. M. C., Scheuring, R. A., Guilliams, M. E., and Kerstman, E. L. (2019). "Physical performance, countermeasures, and postflight reconditioning" in *Principles of clinical medicine for space flight*. eds. M. R. Barratt, E. S. Baker and S. L. Pool. *2nd Edn.* (New York, NY: Springer Science+Business Media LLC), 609–658.

Loehr, J. A., Guilliams, M. E., Petersen, N., Goldberger, A. L., and Ziegler, M. G. (2015). Physical training for long-duration spaceflight. *Aerosp. Med. Hum. Perform.* 86, A14–A23. doi: 10.3357/AMHP.EC03.2015

Meck, J. V., Reyes, C. J., Perez, S. A., Goldberger, A. L., and Ziegler, M. G. (2001). Marked exacerbation of orthostatic intolerance after long- vs. short-duration spaceflight in veteran astronauts. *Psychosom. Med.* 63, 865–873. doi: 10.1097/00006842-200111000-00003

Miller, C. A., Kofman, I. S., Brady, R. R., May-Phillips, T. R., Batson, C. D., Lawrence, E. L., et al. (2018). Functional task and balance performance in bed rest subjects and astronauts. *Aerosp. Med. Hum. Perform.* 89, 805–815. doi: 10.3357/AMHP.5039.2018

Mulavara, A. P., Peters, B. T., Miller, C. A., Kofman, I. S., Reschke, M. F., Taylor, L. C., et al. (2018). Physiological and functional alterations after spaceflight and bed rest. *Med. Sci. Sports Exerc.* 50, 1961–1980. doi: 10.1249/MSS.0000000000001615

Nixon, J. V., Murray, R. G., Bryant, C., Johnson, R. L., Mitchell, J. H., Holland, O. B., et al. (1979). Early cardiovascular adaptation to simulated zero gravity. *J. Appl. Physiol.* 46, 541–548. doi: 10.1152/jappl.1979.46.3.541

Perez, S. A., Charles, J. B., Fortner, G. W., Hurst, V., and Meck, J. V. (2003). Cardiovascular effects of anti-G suit and cooling garment during space shuttle re-entry and landing. *Aviat. Space Environ. Med.* 74, 753–757.

Pettit, D. (2010). Mars landing on earth: an Astronaut's perspective. *J. Cosmol.* 12, 3529–3536.

Platts, S. H., Tuxhorn, J. A., Ribeiro, L. C., Stenger, M. B., Lee, S. M. C., and Meck, J. V. (2009). Compression garments as countermeasures to orthostatic intolerance. *Aviat. Space Environ. Med.* 80, 437–442. doi: 10.3357/ASEM.2473.2009

Shi, S. -J., Platts, S. H., Ziegler, M. G., and Meck, J. V. (2011). Effects of promethazine and midodrine on orthostatic tolerance. *Aviat. Space Environ. Med.* 82, 9–12. doi: 10.3357/ASEM.2888.2011

Stenger, M. B., Brown, A. K., Lee, S. M. C., Locke, J. P., and Platts, S. H. (2010). Gradient compression garments as a countermeasure to post-spaceflight orthostatic intolerance. *Aviat. Space Environ. Med.* 81, 883–887. doi: 10.3357/ASEM.2781.2010

Stenger, M. B., Lee, S. M. C., Ribeiro, L. C., Phillips, T. R., Ploutz-Snyder, R. J., Willig, M. C., et al. (2014). Gradient compression garments protect against orthostatic intolerance during recovery from bed rest. *Eur. J. Appl. Physiol.* 114, 597–608. doi: 10.1007/s00421-013-2787-4

Stenger, M. B., Lee, S. M. C., Westby, C. M., Ribeiro, L. C., Phillips, T. R., Martin, D. S., et al. (2013). Abdomen-high elastic gradient compression garments during post-spaceflight stand tests. *Aviat. Space Environ. Med.* 84, 459–466. doi: 10.3357/asem.3528.2013

Vil-Viliams, I. F., Kotovskaya, A. R., Gavrilova, L. N., VYu, L., and Yarov, A. S. (1998). Human +Gx tolerance with the use of anti-G suits during descent from orbit of the Soyuz space vehicles. *J. Gravit. Physiol.* 5, P129–P130.

Waters, W. W., Ziegler, M. G., and Meck, J. V. (2002). Postspaceflight orthostatic hypotension occurs mostly in women and is predicted by low vascular resistance. *J. Appl. Physiol.* 92, 586–594. doi: 10.1152/japplphysiol.00544.2001

Wood, K. N., Greaves, D. K., and Hughson, R. L. (2019a). Inter-relationships between pulse arrival time and arterial blood pressure during postural transitions before and after spaceflight. *J. Appl. Physiol.* 127, 1050–1057. doi: 10.1152/japplphysiol.00317.2019

Wood, K. N., Murray, K. R., Greaves, D. K., and Hughson, R. L. (2019b). Inflight leg cuff test does not identify the risk for orthostatic hypotension after long-duration spaceflight. *NPJ Microgravity* 5, 1–8. doi: 10.1038/s41526-019-0082-3

Conflict of Interest: SML, LR, SSL, IK, BM, and MR were employed by KBR, under the Human Health and Performance Contract to NASA, during the performance of this study.

The remaining authors declare that the research was conducted in the absence of any commercial or financial relationships that could be construed as a potential conflict of interest.

frontiers in Physiology

ORIGINAL RESEARCH
published: 17 November 2021
doi: 10.3389/fphys.2021.760875

Blood Plasma Proteins Associated With Heart Rate Variability in Cosmonauts Who Have Completed Long-Duration Space Missions

Ludmila Kh. Pastushkova[1‡], Vasily B. Rusanov[1‡], Anna G. Goncharova[1], Andrei M. Nosovskiy[1], Elena S. Luchitskaya[1], Daria N. Kashirina[1], Alexey S. Kononikhin[2,3], Anna R. Kussmaul[1], Yusef D. Yakhya[1], Irina M. Larina[1†] and Evgeny N. Nikolaev[2*†]*

[1]Institute of Biomedical Problems of the Russian Academy of Sciences, Moscow, Russia, [2]Skolkovo Institute of Science and Technology, Skolkovo, Russia, [3]V.L. Talrose Institute for Energy Problems of Chemical Physics, N.N. Semenov Federal Center of Chemical Physics, Russian Academy of Sciences, Moscow, Russia

The study presents the results of evaluating the changes in the concentrations of blood plasma proteins associated with heart rate variability (HRV) in cosmonauts who have completed space missions lasting about 6 months. The concentrations of 125 proteins were quantified in biological samples of the cosmonauts' blood plasma. The subgroups of proteins associated with the physiological processes of the HRV autonomic regulation were identified using bioinformatic resources (Immunoglobulin heavy constant mu, Complement C1q subcomponent subunit C, Plasma serine protease inhibitor, Protein-72 kDa type IV collagenase, Fibulin-1, Immunoglobulin lambda constant 3). The concentration of these proteins in the blood plasma before the flight, and the dynamics of concentration changes on the 1st and 7th days of the post-flight rehabilitation period differed in the groups of cosmonauts with a predominance of sympathetic or parasympathetic modulating autonomous influences. The dynamics of changes in the concentrations of the identified set of proteins reveal that in cosmonauts with a predominance of sympathetic modulating influences, the mechanisms of autonomic regulation are exposed to significant stress in the recovery period immediately after the completion of the space mission, compared with the cosmonauts with a predominance of parasympathetic modulating influences.

Keywords: cosmonauts, long-duration space missions, blood proteome, heart rate variability, sympathetic and parasympathetic regulation

OPEN ACCESS

Edited by:
Marc-Antoine Custaud, Université d'Angers, France

Reviewed by:
Amber M. Paul, National Aeronautics and Space Administration (NASA), United States
Carlo Capelli, University of Verona, Italy

***Correspondence:**
Anna R. Kussmaul
annakussmaul@gmail.com
Evgeny N. Nikolaev
e.nikolaev@skoltech.ru

†These authors have contributed equally to this work

‡These authors share first authorship

Specialty section:
This article was submitted to Environmental, Aviation and Space Physiology, a section of the journal Frontiers in Physiology

Received: *19 August 2021*
Accepted: *21 October 2021*
Published: *17 November 2021*

Citation:
Pastushkova LK, Rusanov VB, Goncharova AG, Nosovskiy AM, Luchitskaya ES, Kashirina DN, Kononikhin AS, Kussmaul AR, Yakhya YD, Larina IM and Nikolaev EN (2021) Blood Plasma Proteins Associated With Heart Rate Variability in Cosmonauts Who Have Completed Long-Duration Space Missions. Front. Physiol. 12:760875. doi: 10.3389/fphys.2021.760875

INTRODUCTION

One of the urgent tasks of space medicine, in our opinion, is the search for biomarkers of cardiac activity before preparation for space flight and at the stage of post-flight rehabilitation. Nowadays the age of cosmonauts is increases, as well as the risk of serious life-threatening cardiovascular events does. The identification of personalized metabolic markers will allow the identification of not present at risk of cardiovascular risks cosmonauts. This is relevant not

only for space medicine but also for public health since the number of people, who can move from a group with a low risk of cardiovascular diseases to a group with a high one, when exogenous factors change is quite large. In addition, early diagnostics of the appearance of violations of the mechanisms of regulation of cardiac activity will prevent possible negative effects of lunar soon planned exploration missions and flights beyond the low earth orbit. Thus, need to identify preclinical biomarkers, which characterize the functional state and adaptive capabilities of the body and predict the personalized state of health.

To assess cardiovascular risks in cosmonauts, the Russian space cardiology uses an approach that is primarily based on the study of regulation mechanisms of the circulatory system (Baevsky and Chernikova, 2016).

The analysis of heart rate variability (HRV) is one of the commonly recognized methodological approaches for studying the adaptation to extreme conditions since it allows to assess of the state of systems involved in the regulation of blood circulation (Baevsky and Chernikova, 2017).

The duration of a cardiac cycle can be measured by the RR interval from the electrocardiogram (ECG) because the R peaks are the easiest to detect in the ECG signal. The control of the heart rate is modulated by both sympathetic nervous system (SNS) and parasympathetic nervous system (PNS) branches of autonomic nervous system (ANS). The PNS regulates the hearts' functions rapidly. In contrast, the SNS regulates the heart functions slower. The ANS is therefore responsible for changing the duration of RR interval from one beat to another (Acharya et al., 2007). This phenomenon is called HRV (Ernst, 2017; Holzman and Bridgett, 2017; Massaro and Pecchia, 2019; Karemaker, 2020).

Despite the available data from the studies of autonomic regulation mechanisms in the cardiovascular system (CVS) conducted on board of the International Space Station (ISS), as well as after space missions (SM; Baevsky et al., 2011, 2013; Hughson, 2012; Vandeput et al., 2013; Xu et al., 2013; Otsuka et al., 2018), the criteria for the probability of adverse cardiovascular events using the assessment of the functional state of cosmonauts according to the HRV analysis and taking into account the identified type of autonomic regulation in space flight conditions have not been defined sufficiently due to the individual typological features of autonomic regulation (Baevsky and Chernikova, 2016).

Proteomic approaches are unequivocally powerful tools that may provide a deeper understanding of the molecular mechanisms associated with cardiovascular events. Cardiovascular proteomics is an emerging field and significant progress has been made during the past few years with the aim of defining novel candidate biomarkers and obtaining insight into molecular physiology and pathophysiology of the cardiovascular system (Mokou et al., 2017).

In our opinion, cardiovascular proteomics reflects the processes of protein interactions in the regulation of the cardiovascular system, and, possibly, the dynamics of adaptation to complex extreme influences, as well as the possibility of returning to the original patterns of the genetically determined regulation of the cardiovascular system. The use of proteomics methods will make it possible to define the participation of the metabolic network in the blood circulation regulation, and, possibly, to identify the metabolic markers involved in maintaining the autonomic homeostasis.

The purpose of the study is to evaluate the changes in the concentrations of blood plasma proteins associated with HRV in cosmonauts who performed long-duration space missions.

MATERIALS AND METHODS

The study involved 7 Russian cosmonauts (males, average age 44 ± 6 years, body mass index 26.5 ± 2) who performed long-duration space missions on the ISS lasting 169–199 days. The investigations were performed on pre-launch days 30–45 (Pre) and on the background of acute readaptation or recovery after landing days 1 (R + 1) and 7 (R + 1).

All cosmonauts provided written informed consent to participate in the investigations approved by the Biomedicine Ethics Committee of the Institute of Biomedical Problems of the Russian Academy of Sciences at Physiology Section of the Russian Bioethics Committee of Russian Federation National Commission for UNESCO and Human Research Multilateral Review Board, NASA, Houston, TX, United States.

The blood was taken from a vein in the elbow pit 30 days prior to the launch and a day after the landing (after 25.2 ± 0.1 h) into the SARSTEDT-Monovette® tubes containing EDTA. The plasma was separated by centrifugation and frozen at a temperature of −80°C. No protease inhibitors or antimicrobial agents were added.

The target quantitative analysis was performed using liquid chromatography and tandem mass spectrometry with multiple reactions monitoring (LC/MRM-MS). The LC/MRM-MS analysis was performed on UPLC 1290 Infinity chromatograph system (Agilent Technologies) using a Zorbax Eclipse Plus RP-UHPLC chromatographic column coupled to triple quadrupole mass spectrometer Agilent 6,490 as previously discussed (Larina et al., 2017). MassHunter quantitative analysis software (version B. 07.00, Agilent) was used to analyze LC/MRM data. For target quantitative analysis, BAK 125 kit (MRM Proteomics Inc., Canada) containing both stable-isotope labeled internal standard (SIS) and natural (NAT) synthetic proteotypic peptides was used for concentration measurements of the corresponding 125 proteins in plasma. 13C/15N-labeled peptide analogues were used as internal standards for the quantitative determination of plasma proteins. They were synthesized and purified using reversed-phase high-performance liquid chromatography (RP-HPLC), followed by evaluation on MALDI-TOF-MS. The purity of SIS peptides averaged 94.2% (Kuzyk et al., 2013).

The HRV analysis was carried out in 5-min ECG samples at rest in the supine position. The raw data used for the analysis are presented in the attached file. Cardiovascular regulatory mechanisms condition was assessed according to the recommendations developed by the European cardiological and North American electrophysiological Societies (Camm et al., 1996; Standards of measurement, physiological interpretation,

and clinical use, 1996). The HRV analysis was performed at the same time as the collection of samples of biological material.

Depending on the type of autonomic regulation in cosmonauts before the flight, the associative relationships between some proteome proteins and HRV characteristics were analyzed. To determine the molecular functions, biological processes and signaling pathways carried out with the participation of certain proteins, the DAVID online resource[1] and the PubMed search engine[2] were used. Additional information about the properties and molecular weight of proteins was obtained using the Uniprot database[3] and the STRING online software.[4]

The analysis of experimental data was performed using the Factorial ANOVA statistical module of the Statistica v. 7 software package.

Ward's method of cluster analysis was used for statistical analysis (Hartigan, 1975). The statistical hypothesis that the examined sample was taken from the normal distribution was tested. The statistical Shapiro–Wilk test was used for this purpose. This test is one of the most effective tests of normality, and p value was <0.325, i.e., the null hypothesis of belonging to the normal distribution was not rejected. The differences between the experimental samples were found using the Tukey's honestly significant difference test.

RESULTS

We have used Wards' cluster analysis method, which made it possible, taking into account the individual variance of the initial background indicators, to form stable groups. We classified cosmonauts according to the predominant type of autonomic regulation (sympathetic or parasympathetic) using data of HRV analysis, which allowed, by assessing RR variability, to evaluate the modulating effect of the corresponding section of the ANS on the mechanisms of cardiovascular homeostasis regulation (**Figure 1**):

Group 1($n=4$) – cosmonauts with a predominance of sympathetic modulating influences (sympathetic).

Group 2($n=3$) – cosmonauts with a predominance of parasympathetic modulating influences (parasympathetic).

To obtain the most informative indicators characterizing to the predominant type of autonomic regulation, we used the methods of cluster and discriminant analysis. As a result, the classification functions were determined, which included the following indicators, the most informative for this group of cosmonauts, reflecting autonomic homeostasis: SDNN (ms), pNN50 (%), HF (ms^2).

SDNN (ms) is the standard deviation obtained for the total dataset of interbeat intervals and reflects the integral effect of regulatory systems.

pNN50 (%) - is the number of pairs of adjacent intervals differing by more than 50 ms, in % of the total number of RR intervals in the array, an indicator of the parasympathetic regulatory branch prevalence over the sympathetic.

Power HF (mc^2) - is the raw power of HRV high-frequency component related to the total power of fluctuations and reflects the relative activity of the parasympathetic regulatory component.

Before the mission, these indicators showed significant differences between the groups, which confirmed the dominance of the corresponding types of autonomic regulation (**Figure 2**).

The influence of factors characteristic for coming back to Earth after a space mission forces the body to re-adapt to earthly conditions providing the necessary cardiovascular homeostasis. At this point, regardless of the regulation type, the maintenance of the adaptive reserves involves the expenditure of a significant amount of energy resources. This is reflected in a decrease in the overall HRV and the effectiveness of regulatory systems (SDNN), as well as a decrease in parasympathetic influences (pNN50 and HF).

Our study is a continuation of previously published data (Larina et al., 2017), which quantified a set of proteins that perform their function in the extracellular fluid and are used clinically to diagnose non-communicable diseases. In conducting our investigation, we focused on those that could be associated with the mechanisms of autonomic regulation of heart rhythm.

The concentrations of 125 proteins have been quantified in the biological samples of the cosmonauts' blood plasma. After dividing the astronauts into groups depending on the type of autonomic regulation, we determined the statistical differences in the protein concentration before the flight and identified the proteins associated with this physiological process.

Among the 125 proteins, differences in plasma concentration of 6 proteins were noted in the groups of cosmonauts with a predominance of sympathetic or parasympathetic modulating influences before the mission: Immunoglobulin heavy constant mu (gene IGHM); Complement C1q subcomponent subunit C (gene C1QC); Plasma serine protease inhibitor (Gene SERPINA5); Protein-72 kDa type IV collagenase (Gene MMP2); Protein-Fibulin-1 (Gene FBLN1); Protein-Immunoglobulin lambda constant 3 (Gene IGLC3).

However, while significant differences in the concentrations of proteins associated with the processes of heart rhythm autonomic regulation were detected before the mission, these features did not occur in the post-mission period (**Table 1**). Nevertheless, the participation of these proteins in cardiovascular processes may reflect the molecular mechanisms of adaptation in weightlessness depend on different types of autonomic regulation.

There were no significant changes in the level of IGHM after the space mission in the group of cosmonauts with a predominance of sympathetic modulating influences. The group of cosmonauts with a predominance of parasympathetic modulating influences demonstrated a moderate increase in the content of this protein that persisted to the 7th day after landing. Thus, the discovered baseline differences in individuals with a predominance of sympathetic or parasympathetic regulatory influences became less noticeable in the post-mission period. At the same time, the dynamic of IGHM concentration in the group with a predominance of parasympathetic modulating

[1]https://www.david.ncifcrf.gov
[2]https://www.ncbi.nlm.nih.gov/pubmed
[3]https://www.uniprot.org
[4]https://www.string-db.org

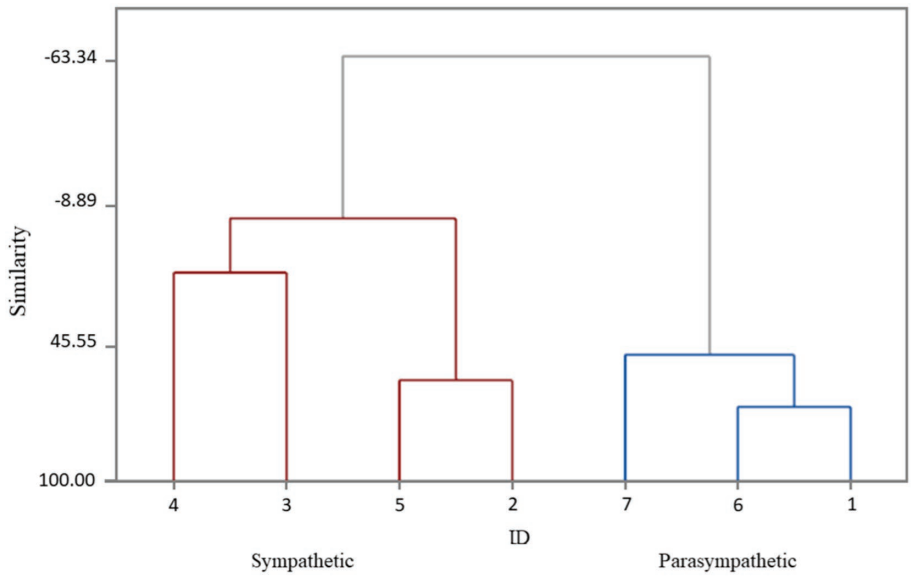

FIGURE 1 | The division of cosmonauts into groups depending on the predominant type of autonomic regulation (Dendrogram Ward Linkage; Euclidean Distance). ID 4; 3; 5; 2 (red line) – cosmonauts with a predominance of sympathetic modulating influences (sympathetic). ID 7; 6; 1 (blue line) – cosmonauts with a predominance of parasympathetic modulating influences (parasympathetic).

influences may indicate that the cardiovascular system of the cosmonauts with this type of autonomic influences is more exposed to space flight factors (**Figure 3**).

The data presented in **Figure 4** show that before the mission the concentration of C1QC significantly differs in cosmonauts with a predominance of sympathetic or parasympathetic influences. However, on the first day after landing and seven days after the end of the mission, the groups do not differ. The group with a predominance of sympathetic modulating influences revealed an increase in the level the protein on the first day with a tendency to return to the baseline values on the seventh day after landing. On the contrary, there was a tendency to decrease on the first day after the flight with the return to baseline values on the seventh day in the group with a predominance of parasympathetic modulating influences. These multidirectional trends lead to smoothing out the differences noted in the baseline period.

Similar to the previous protein markers, the level of SERPINA5 significantly differed in the identified groups before the mission. The effect of space flight on its concentration in the blood was different in the two selected groups (**Figure 5**). In addition, in the group with a predominance of sympathetic modulating influences, there was a tendency to increase the level of plasma serine protease inhibitor on the seventh day after landing. In the second group, on the contrary, there was a tendency to decrease on the first day after the flight with a relative increase to the level of baseline values on the seventh day. Thus, the space flight conditions have opposite effects on the level of plasma serine protease inhibitor in the groups of cosmonauts with different dominant autonomic influences.

As can be seen from **Figure 6**, the group of cosmonauts with a predominance of sympathetic modulating influences showed no changes in the level 72 kDa type IV collagenase on the first day after the mission, but an increase in the level of this protein was noted on the seventh day of the recovery period. On the contrary, the group of cosmonauts with a predominance of parasympathetic modulating influences demonstrated a tendency to decrease the level of this protein on the first day and the seventh day after the mission.

The group of cosmonauts with a predominance of sympathetic modulating influences demonstrated a pronounced increase in the level of FBLN1on the first day with a continued increase by the seventh day of the recovery period (**Figure 7**). Cosmonauts with a predominance of parasympathetic modulating influences, on the contrary, showed a tendency to a sharp decrease in its level on the first day and a relative increase, almost to baseline values on the seventh day after the mission.

In the group of cosmonauts with a predominance of sympathetic modulating influences, there were no changes in the level of IGLC3 after the mission. The group of cosmonauts with a predominance of parasympathetic modulating influences indicated a tendency to increase on the first day and a relative decrease on the seventh day after the mission. In addition, the concentration of this protein was significantly higher in cosmonauts with a predominance of sympathetic modulating influences (**Figure 8**).

DISCUSSION

The significant intergroup differences discovered during the statistical analysis were expressed before the space mission. Therefore, the cosmonauts with a predominance of sympathetic and parasympathetic types of autonomic regulation were

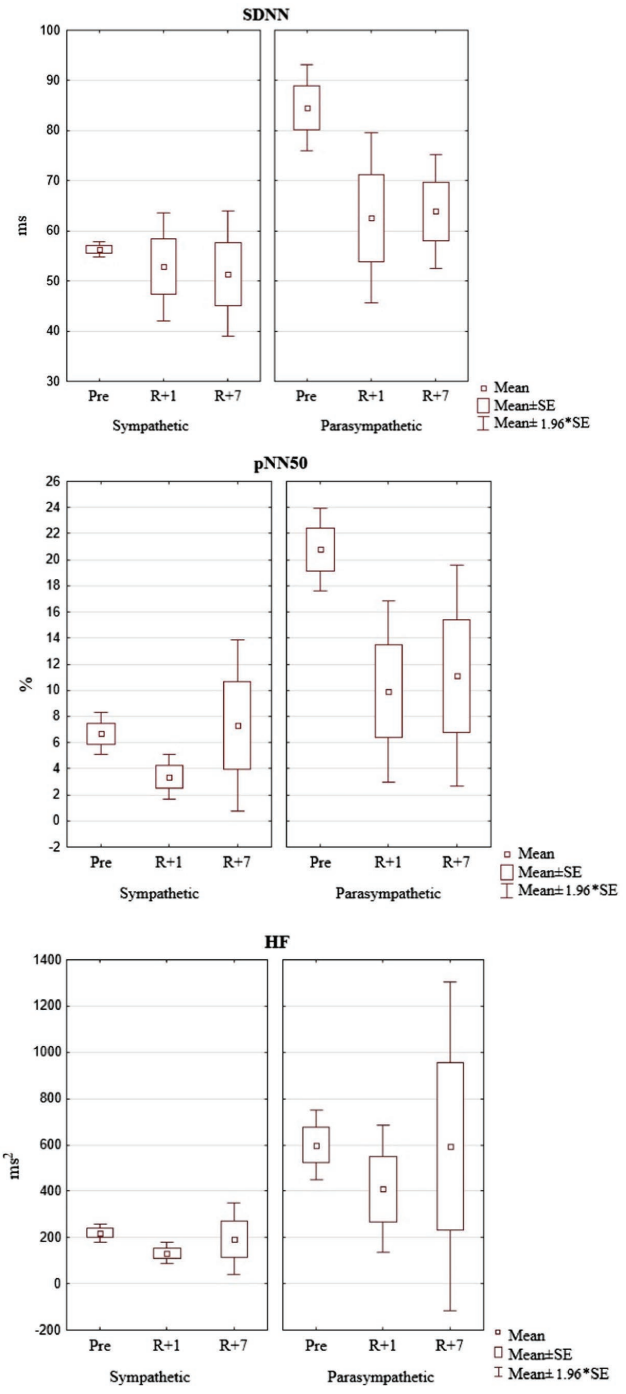

FIGURE 2 | The dynamics of the HRV parameters pre-mission (Pre), on the 1st day (R + 1) and on the 7th day (R + 7) after landing (the cosmonauts are grouped into clusters depending on the time of research).

unequally exposed to space flight factors. However, after the mission the differences in the levels of the identified proteins between the groups were leveled, there were no significant differences between the group's average indicators either on the 1st or 7th day after landing.

On one hand the data obtained can obviously indicate that the extreme factors identical in duration and direction of exposure have such an intense effect on the body that the final molecular parameters become unified in the processes ensuring an adequate level of cardiovascular system functioning under the changed conditions, regardless of the differences in HRV regulation.

On the other hand, the intra-group dynamics of changes in the concentrations of the discussed set of proteins compared to the preflight values shows that the mechanisms of autonomic regulation in cosmonauts with a predominance of sympathetic modulating influences are significantly more exposed to stress under the influence of space flight factors (and its final stage) than in cosmonauts with a predominance of parasympathetic modulating influences. In the first group, among the proteins associated with HRV regulation, the majority of proteins increased their levels by the 1st and/or 7th days after the mission. On the contrary, the concentration of most of these proteins in the second group decreased. It is obvious that the limiting factor of our research is the insignificant number of cosmonauts who took part in it, and our assumptions, undoubtedly, should be confirmed or refuted on more representative cosmonaut groups.

Using bioinformatic resources, we focused on the biological functions of the identified proteins and protein interactions that may be reflected in the mechanisms of the heart rate autonomic regulation.

Immunoglobulin Heavy Constant Mu (gene IGHM)

It is known that the IgM level correlates with higher systolic blood pressure and may indirectly reflect the phenomena of subclinical peripheral atherosclerosis (Swärd et al., 2020). On the other hand, the effect of space flight on the dynamics of the range of antibodies in a healthy person has not been sufficiently studied. When studying the IgM of five cosmonauts 25 days prior to the launch, then after 64 ± 11 and 129 ± 20 days spent on the ISS, and then 1, 7 and 30 days after the landing, it was found that the IgM representation in the cosmonauts differs from the control samples ($n = 4$) before the launch, and that the samples of two of the five analysed cosmonauts showed significant changes in the IgM spectrum during the mission. These modifications were noticeable for a period of up to 30 days after the landing. These changes affected the specificity of IgM binding sites, and coincided with a higher response to stress, which is confirmed by the data we obtained on the relationship of IgM changes and the implementation of an individual response to stress (Buchheim et al., 2020; Bajwa and Mohammed, 2021).

Complement C1q Subcomponent Subunit C (gene C1qc)

C1q is a target recognition protein of the classical complement pathway. It is believed that the components of the C1qc complement are responsible for "aging," myocardial fibrosis (Bartling et al., 2019). Considering the connection of C1q with an individual

TABLE 1 | The reliability of differences in the level of proteins between the groups in the baseline period, on the 1st and the 7th days after the mission.

Protein	Value of *P* preflight group 1/ preflight group 2	Value of *P* R+1 group 1/ R+1 group 2	Value of *P* R+7 group 1/ R+7 group 2
Immunoglobulin heavy constant mu	0.016267	0.255209	0.141407
Complement C1q subcomponent subunit C	0.022965	0.687916	0.439854
Plasma serine protease inhibitor	0.009249	0.507887	0.471242
Protein-72 kDa type IV collagenase	0.041004	0.134357	0.302210
Fibulin-1	0.000652	0.488081	0.837809
Immunoglobulin lambda constant 3	0.010391	0.689207	0.663312

response to stress, it is necessary to note the proven connection between a number of protein components, including Hspd1, Actb, Mgst1, THBS4, Syp, C1q, Serpine, Plat and Ngf, which are associated with cellular stress, neural plasticity reactions and hippocampal responses to trauma and damage (Hao and Wang, 2017).

Plasma Serine Protease Inhibitor (Gene SERPINA5)

In regard to our study, the role of SERPINA5—an inhibitor of plasma serine protease—is expressed in its participation in the regulation of intravascular and extravascular proteolytic activity that ensures coagulation (thrombosis and thrombolysis), neurotrophic effects, hormone transportation, the activation of the complement system, pro-inflammatory activity and angiogenesis (Meijers et al., 2002). It is noted that SERPINA5 indirectly regulates blood pressure, HRV and numerous other physiological processes (Koukos et al., 2011; Zheng et al., 2013). This protein is an inhibitor of plasma serine protease and a powerful inhibitor of activated protein C (APC), which plays an important role in the pathway of anticoagulant protein C and at tissue damage sites in tissue regeneration processes (Hughson, 2012).

Protein-72 kDa Type IV Collagenase (Gene MMP2)

From the point of view of the main processes that distinguish the groups of cosmonauts with different types of heart rhythm autonomic regulation, MMP2-72 kDa type IV collagenase provides the destruction of extracellular matrix proteins and impacts several non-matrix proteins that stimulate vasoconstriction (Chan et al., 2019). It also participates in the formation of fibrovascular tissues in association with MMP-14, as well as the in vascular network remodelling, angiogenesis, tissue repair, inflammation and rupture of atherosclerotic plaques (Batista et al., 2019).

The myocardial expression of MMP-2 has been noted to increase with heart failure and pressure overload (Barhoumi et al., 2017). By affecting the formation of endothelin-1, MMP-2 causes vasoconstriction thus regulating vascular tone and reactivity.

There is evidence that chronic psychological stress is associated with increased expression and activity of mRNA matrix metalloproteinases MMP-2 and MMP-9, as well as the destruction of elastin in damaged carotid arteries (Meng et al., 2020).

Protein-Fibulin-1 (Gene FBLN1)

FBLN1 is a member of the extracellular matrix glycoprotein family, involved in such cellular functions as adhesion, migration and differentiation and fibrosis. Fibulin can also play a role in hemostasis and thrombosis due to its ability to bind fibrinogen and to be included in the blood clot (Sang et al., 2021).

FBLN1 together with MMP2 are involved in the organization of the extracellular matrix and the change of its properties.

The analysis of hereditary disorders associated with altered collagen structure or leading to its excessive degradation allows to make a conclusion on the functional significance of collagen as an ECM element for assessing the state of the vascular wall, that is reflected in the autonomic regulation of heart rhythm (Arseni et al., 2018).

Protein- Immunoglobulin Lambda Constant 3 (Gene IGLC3)

The secreted immunoglobulins mediate the effector phase of humoral immunity, which results in the elimination of bound antigens (Schroeder and Cavacini, 2010; McHeyzer-Williams et al., 2012). The role of immunoglobulin (Protein - Immunoglobulin lambda constant 3) in the aspect of its effect on HRV has not been sufficiently covered in the available literature. It is possible that its participation in the cardiovascular system functions is not direct but mediated by other physiological processes that respond to space flight effectors. In our study, it was noted as a protein with significantly different concentrations between groups of cosmonauts with a predominance of sympathetic or parasympathetic modulating influences.

In previous studies of the cosmonauts' urine proteome, we identified various groups of proteins associated with heart rhythm regulation (Pastushkova et al., 2019, 2020). It was shown that the urine proteome in individuals with the predominance of sympathetic and parasympathetic regulation differed in three proteins: cadherin-13, mucin-1, alpha-1 of collagen subunit type VI, which does not contradict, but complements the results of the blood proteome described above. It should be noted that in this work, the list of quantifiable proteins was narrower, since it was studied on a targeted basis, and was based on the results of previous studies that allowed us to narrow the search patterns.

Using the STRING software, we identified the processes that connect the abovementioned proteins of the blood proteome and the previously studied urine proteins. It is noteworthy that both these blood proteins and urine proteins are involved in the implementation of the same biological processes (**Table 2**).

CONCLUSION

Undoubtedly, the controlling mechanisms of the ANS reflected in the HRV are genetically determined, but they undergo

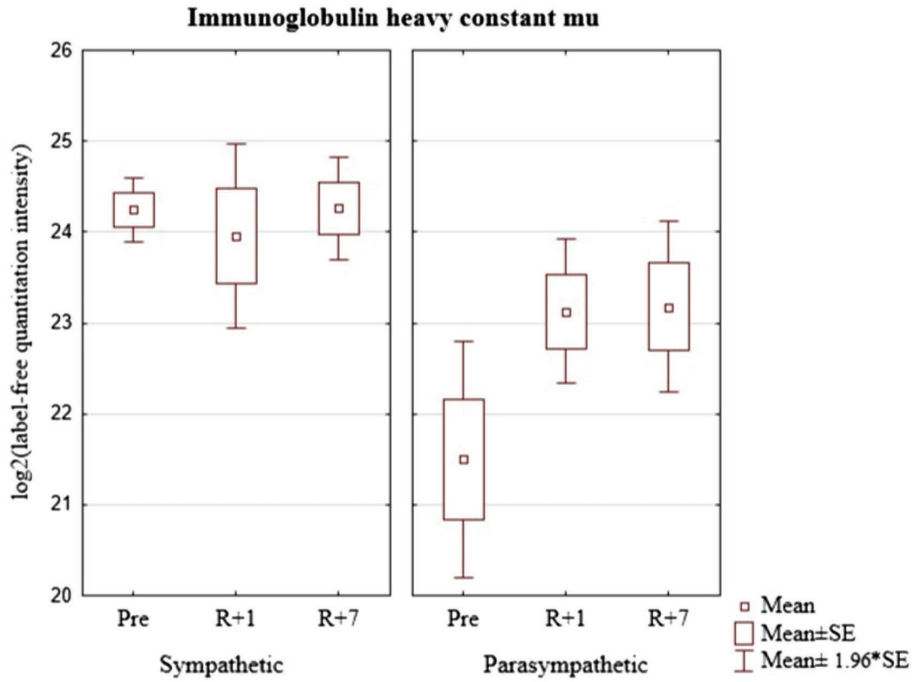

FIGURE 3 | Immunoglobulin heavy constant mu (gene IGHM) in cosmonaut groups pre-mission (Pre), on the 1st day (R + 1) and on the 7th day (R + 7) after landing.

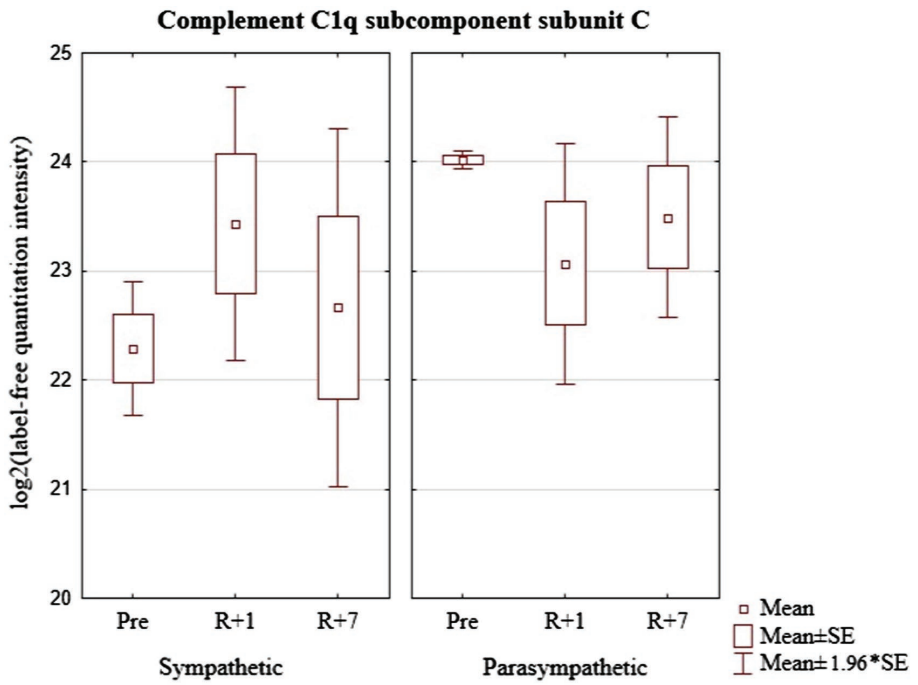

FIGURE 4 | Complement C1q subcomponent subunit C (geneC1q) in cosmonaut groups pre-mission (Pre), on the 1st day (R + 1) and on the 7th day (R + 7) after landing.

changes in healthy individuals with age, as well as under the influence of extreme environmental factors.

In weightlessness, the new hemodynamic situation causes changes in the functioning of the mechanisms of blood circulation autonomic regulation. At the same time, the blood proteome dynamically reacts to a set of external and internal space flight factors, ensuring the adaptation of the cosmonauts' bodies.

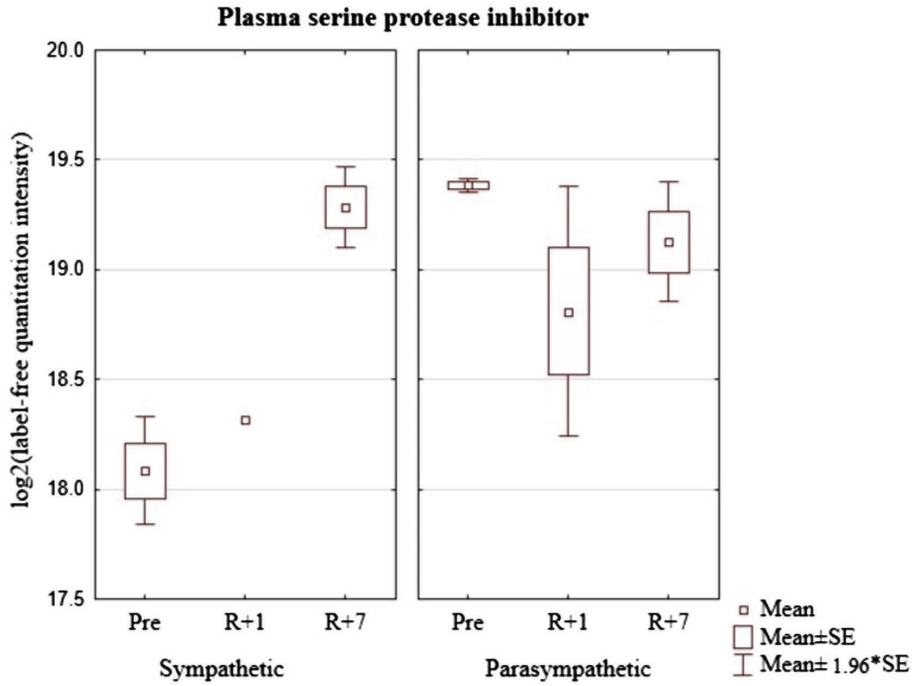

FIGURE 5 | Plasma serine protease inhibitor (Gene-SERPINA5) in cosmonaut groups pre-mission (Pre), on the 1st day (R + 1) and on the 7th day (R + 7) after landing.

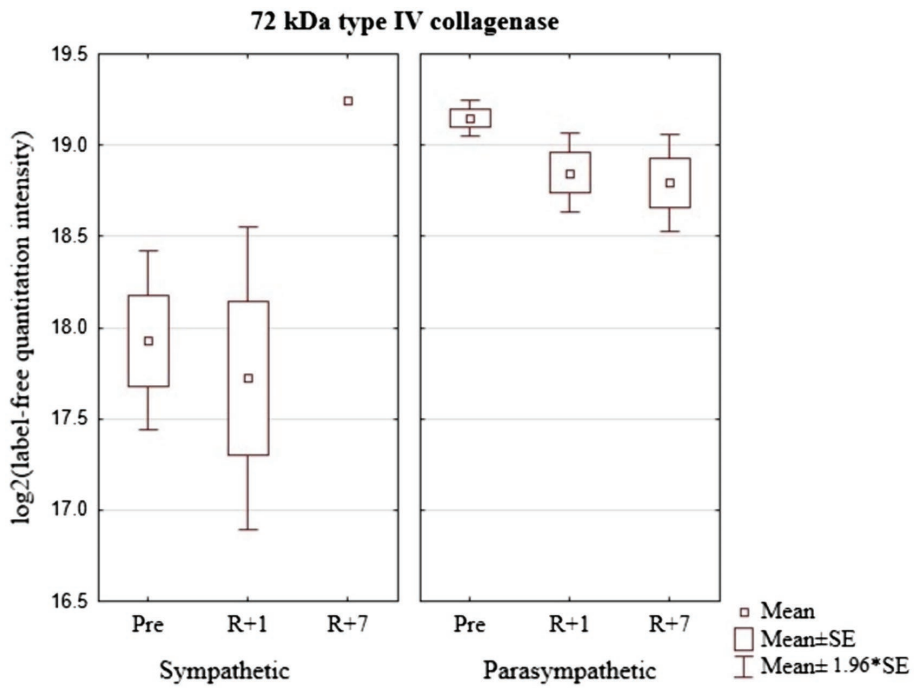

FIGURE 6 | Protein-72 kDa type IV collagenase (Gene MMP2) in cosmonaut groups pre-mission (Pre), on the 1st day (R + 1) and on the 7th day (R + 7) after landing.

The changes in modulating regulatory influences reflected in the HRV are aimed at maintaining the autonomic homeostasis. In our study, this is confirmed by the fact that before the space mission, specific features of both HRV and the concentration of certain proteins of the blood proteome were noted in cosmonauts with a predominance

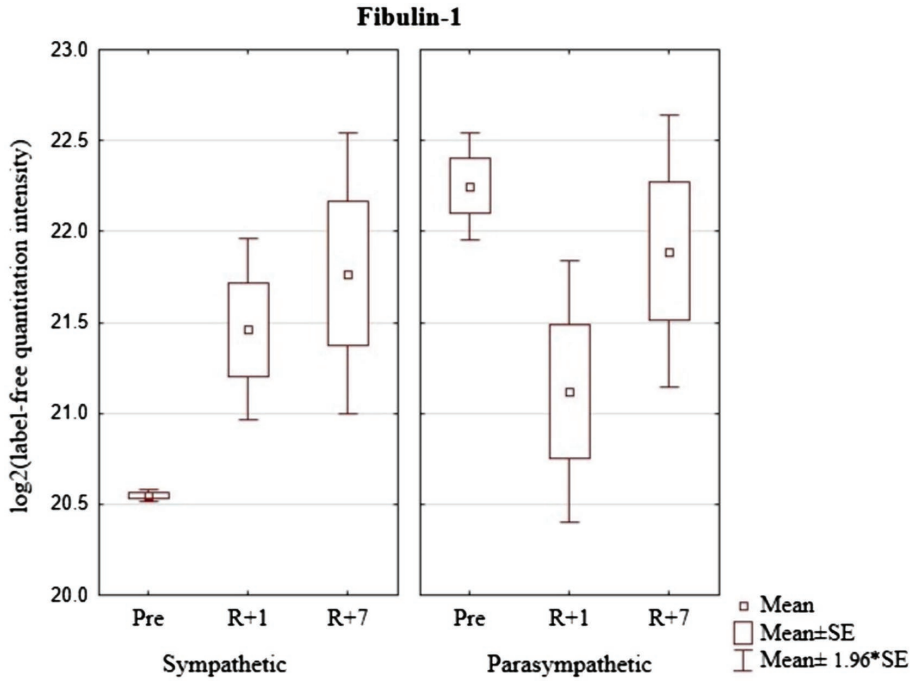

FIGURE 7 | Protein-Fibulin-1 (Gene FBLN1) in cosmonaut groups pre-mission (Pre), on the 1st day (R+1) and on the 7th day (R+7) after landing.

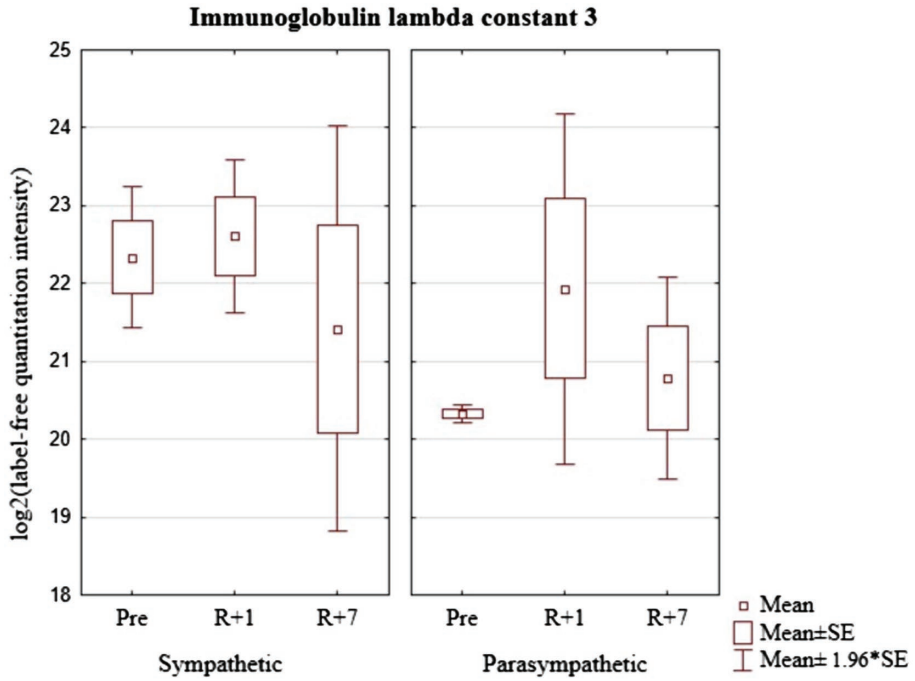

FIGURE 8 | Immunoglobulin lambda constant 3 (Gene IGLC3) levels in cosmonaut groups pre-mission (Pre), on the 1st day (R+1) and on the 7th day (R+7) after landing.

of sympathetic or parasympathetic influences. Staying in the conditions of a long-duration space flight levels the types of regulation and changes the proteomic composition. On the first day after landing, a new HRV-associated proteomic composition is formed that probably ensures the success of the acute period of readaptation after landing, while

TABLE 2 | Characteristics of the main processes regulating HRV common to the blood and urine proteome in the baseline period.

Search ID	Process	Number of participating proteins	Names of participating proteins
GO:0007162	negative regulation of cell adhesion	3	CDH13,FBLN1,MUC1
GO:0032101	regulation of response to external stimulus	4	MMP2,CDH13,C1QC,MUC1
GO:0048661	positive regulation of smooth muscle cell proliferation	2	MMP2,CDH13
GO:0072376	protein activation cascade	2	FBLN1,C1QC
CL:731	Collagen formation, and Molecules associated with elastic fibers	3	MMP2,COL6A5,FBLN1
CL:732	Collagen biosynthesis and modifying enzymes, and Elastic fiber formation	2	COL6A5,FBLN1
hsa04610	Complement and coagulation cascades	2	SERPINA5,C1QC

dynamically changing by the seventh day. The intra-group dynamics of the changes in the concentrations of the discussed set of proteins show that the mechanisms of HRV regulation in cosmonauts with a predominance of sympathetic modulating influences are more exposed to stress than same in astronauts with a predomination of parasympathetic modulating influences in the readaptation period after the space mission in comparison with the average group concentrations before the mission.

DATA AVAILABILITY STATEMENT

The raw data supporting the conclusions of this article will be made available by the authors, without undue reservation.

ETHICS STATEMENT

The studies involving human participants were reviewed and approved by Biomedicine Ethics Committee of the Institute of Biomedical Problems of the Russian Academy of Sciences at Physiology Section of the Russian Bioethics Committee of Russian Federation National Commission for UNESCO and Human Research Multilateral Review Board, NASA, Houston, TX, United States. The patients/participants provided their written informed consent to participate in this study.

AUTHOR CONTRIBUTIONS

IL, VR, EN, and EL conceived and designed the experiments. LP, VBR, DK, and EL performed the experiments. AK, AG, AN, and YY analyzed the data. VR, LP, AG, and AK wrote the paper. All authors read and approved the final manuscript.

FUNDING

The study was supported by Russian Science Foundation, grant #19-14-00306 (in part of quantitative blood proteomic study by mass spectrometry). The work was carried out within the framework of the basic Russian Academy of Sciences themes 64.1 and 65.3 for 2013–2023 years.

ACKNOWLEDGMENTS

Authors would like to thank all the cosmonauts who took part in this research.

REFERENCES

Acharya, U. R., Suri, J. S., Spaan, J. A. E., and Krishnan, S. M. (2007). *Advances in CardiacSignal Processing*, Berlin, Heidelberg: Springer.

Arseni, L., Lombardi, A., and Orioli, D. (2018). From structure to phenotype: impact of collagen alterations on human health. *Int. J. Mol. Sci.* 19:1407. doi: 10.3390/ijms19051407

Baevsky, R. M., and Chernikova, A. G. (2016). Assessment of adaptation risk in an individual Prenosological monitoring system. *Neurosci. Behav. Physiol.* 46, 437–445. doi: 10.1007/s11055-016-0255-4

Baevsky, R. M., and Chernikova, A. G. (2017). Heart rate variability analysis: physiological foundations and main methods. *Cardiometry* 10, 66–76. doi: 10.12710/cardiometry.2017.10.6676

Baevsky, R. M., Chernikova, A. G., Funtova, I. I., and Tank, J. (2011). Assessment of individual adaptation to microgravity during long term space flight based on stepwise discriminant analysis of heart rate variability parameters. *Acta Astronaut.* 69, 1148–1152. doi: 10.1016/j.actaastro.2011.07.011

Baevsky, R. M., Luchitskaya, E. S., Funtova, I. I., and Chernikova, A. G. (2013). Study of the autonomic regulation of blood circulation during a long-term space flight. *Hum. Physiol.* 39, 486–495. doi: 10.1134/S0362119713050046

Bajwa, S. F., and Mohammed, R. H. A. (2021). *Type II Hypersensitivity Reaction*. Treasure Island (FL): StatPearls Publishing.

Barhoumi, T., Fraulob-Aquino, J. C., Mian, M. O. R., Ouerd, S., Idris-Khodja, N., Huo, K., et al. (2017). Matrix metalloproteinase-2 knockout prevents angiotensin II-induced vascular injury. *Cardiovasc. Res.* 113, 1753–1762. doi: 10.1093/cvr/cvx115

Bartling, B., Niemann, K., Pliquett, R. U., Treede, H., and Simm, A. (2019). Altered gene expression pattern indicates the differential regulation of the immune response system as an important factor in cardiac aging. *Exp. Gerontol.* 117, 13–20. doi: 10.1016/j.exger.2018.05.001

Batista, F. P., de Aguiar, R. B., Sumikawa, J. T., Lobo, Y. A., Bonturi, C. R., Ferreira, R. D. S., et al. (2019). Crataeva tapia bark lectin (CrataBL) is a chemoattractant for endothelial cells that targets heparan sulfate and promotes in vitro angiogenesis. *Biochimie* 166, 173–183. doi: 10.1016/j.biochi.2019.04.011

Buchheim, J. I., Ghislin, S., Ouzren, N., Albuisson, E., Vanet, A., Matzel, S., et al. (2020). Plasticity of the human IgM repertoire in response to long-term spaceflight. *FASEB J.* 34, 16144–16162. doi: 10.1096/fj.202001403RR

Camm, A. J., Malik, M., Bigger, J. T., Breithardt, G., Cerutti, S., Cohen, R. J., et al. (1996). Heart rate variability. Standards of measurement, physiological interpretation, and clinical use. Task force of the european society of cardiology and the north american society of pacing and electrophysiology (membership of the task force listed in the appendix). *Eur. Heart J.* 17, 354–381. doi: 10.1093/oxfordjournals.eurheartj.a014868

Chan, B. Y. H., Roczkowsky, A., Cho, W. J., Poirier, M., Lee, T. Y. T., Mahmud, Z., et al. (2019). Junctophilin-2 is a target of matrix metalloproteinase-2 in

myocardial ischemia-reperfusion injury. *Basic Res. Cardiol.* 114:42. doi: 10.1007/s00395-019-0749-7

Ernst, G. (2017). Hidden signals-The history and methods of heart rate variability. *Front. Public Health* 5:265. doi: 10.3389/fpubh.2017.00265

Hao, H., and Wang, S. (2017). Hypothermia induced by anesthesia regulates various signals expressions in the hippocampus of animals. *Biomed. Pharmacother.* 95, 1321–1330. doi: 10.1016/j.biopha.2017.09.046

Hartigan, J. A. (1975). *Clustering Algorithms* New York, NY United States: John Wiley & Sons.

Holzman, J. B., and Bridgett, D. J. (2017). Heart rate variability indices as bio-markers of top-down self-regulatory mechanisms: A meta-analytic review. *Neurosci. Biobehav. Rev.* 74, 233–255. doi: 10.1016/j.neubiorev.2016.12.032

Hughson, R. L., Shoemaker, J. K., Blaber, A. P., Arbeille, P., Greaves, D. K., Pereira-Junior, P. P., et al. (2012). Cardiovascular regulation during long-duration spaceflights to the international Space Station. *J. Appl. Physiol.* 112, 719–727. doi: 10.1152/japplphysiol.01196.2011

Karemaker, J. M. (2020). Interpretation of heart rate variability: The art of looking Through a keyhole. *Front. Neurosci.* 14:609570. doi: 10.3389/fnins.2020.609570

Koukos, G., Sevigny, L., Zhang, P., Covic, L., and Kuliopulos, A. (2011). Serine and metalloprotease signaling through PAR1 in arterial thrombosis and vascular injury. *IUBMB Life* 63, 412–418. doi: 10.1002/iub.465

Kuzyk, M. A., Parker, C. E., Domanski, D., and Borchers, C. H. (2013). Development of MRM-based assays for the absolute quantitation of plasma proteins. *Methods Mol. Biol.* 1023, 53–82. doi: 10.1007/978-1-4614-7209-4_4

Larina, I. M., Percy, A. J., Yang, J., Borchers, C. H., Nosovsky, A. M., Grigoriev, A. I., et al. (2017). Protein expression changes caused by spaceflight as measured for 18 Russian cosmonauts. *Sci. Rep.* 7:8142. doi: 10.1038/s41598-017-08432-w

Massaro, S., and Pecchia, L. (2019). Heart rate variability (HRV) analysis: A methodology for organizational neuroscience. *Organ. Res. Methods* 22, 354–393. doi: 10.1177/1094428116681072

McHeyzer-Williams, M., Okitsu, S., Wang, N., and McHeyzer-Williams, L. (2012). Molecular programming of B cell memory. *Nat. Rev. Immunol.* 12, 24–34. doi: 10.1038/nri3128

Meijers, J. C., Marquart, J. A., Bertina, R. M., Bouma, B. N., and Rosendaal, F. R. (2002). Protein C inhibitor (plasminogen activator inhibitor-3) and the risk of venous thrombosis. *Br. J. Haematol.* 118, 604–609. doi: 10.1046/j.1365-2141.2002.03652.x

Meng, X., Piao, L., Wang, H., Inoue, A., Huang, Z., Jiang, H., et al. (2020). Deficiency of cysteinyl cathepsin K suppresses the development of experimental intimal hyperplasia in response to chronic stress. *J. Hypertens.* 38, 1514–1524. doi: 10.1097/HJH.0000000000002424

Mokou, M., Lygirou, V., Vlahou, A., and Mischak, H. (2017). Proteomics in cardiovascular disease: recent progress and clinical implication and implementation. *Exp. Rev. Proteom.* 14, 117–136. doi: 10.1080/14789450.2017.1274653

Otsuka, K., Cornelissen, G., Kubo, Y., Shibata, K., Hayashi, M., Mizuno, K., et al. (2018). Circadian challenge of astronauts' unconscious mind adapting to microgravity in space, estimated by heart rate variability. *Sci. Rep.* 8:10381. doi: 10.1038/s41598-018-28740-z

Pastushkova, L. H., Rusanov, V. B., Goncharova, A. G., Brzhozovsky, A. G., Kononikhin, A. S., Chernikova, A. G., et al. (2019). Urine proteome changes associated with autonomic regulation of heart rate in cosmonauts. *BMC Syst. Biol.* 13:17. doi: 10.1186/s12918-019-0688-9

Pastushkova, L. H., Rusanov, V. B., Orlov, O. I., Goncharova, A. G., Chernikova, A. G., Kashirina, D. N., et al. (2020). The variability of urine proteome and coupled biochemical blood indicators in cosmonauts with different preflight autonomic status. *Acta Astronaut.* 168, 204–210. doi: 10.1016/j.actaastro.2019.12.015

Sang, Y., Mao, K. M., Huang, Y., Wu, X. F., Wang, X. F., Ruan, L., et al. (2021). Relationship between the plasma Fibulin-1 levels, pulse wave velocity, and vascular age in asymptomatic hyperuricemia. *Curr. Med. Sci.* 41, 94–99. doi: 10.1007/s11596-021-2324-3

Schroeder, H. W. Jr., and Cavacini, L. (2010). Structure and function of immunoglobulins. *J. Allergy Clin. Immunol.* 125, 41–52. doi: 10.1016/j.jaci.2009.09.046

Swärd, P., Tofik, R., Bakoush, O., Torffvit, O., Nilsson, P. M., and Christensson, A. (2020). Patterns of urinary albumin and IgM associate with markers of vascular ageing in young to middle-aged individuals in the Malmö offspring study. *BMC Cardiovasc. Disord.* 20:358. doi: 10.1186/s12872-020-01638-3

Vandeput, S., Widjaja, D., Aubert, A. E., and van Huffel, S. (2013). Adaptation of autonomic heart rate regulation in astronauts after spaceflight. *Med. Sci. Monit.* 19, 9–17. doi: 10.12659/msm.883724

Xu, D., Shoemaker, J. K., Blaber, A. P., Arbeille, P., Fraser, K., and Hughson, R. L. (2013). Reduced heart rate variability during sleep in long-duration spaceflight. *Am. J. Physiol. Regul. Integr. Comp. Physiol.* 305, 164–170. doi: 10.1152/ajpregu.00423.2012

Zheng, D., Chen, H., Davids, J., Bryant, M., and Lucas, A. (2013). Serpins for diagnosis and therapy in cancer. *Cardiovasc. Hematol. Disord. Drug Targets* 13, 123–132. doi: 10.2174/1871529X11313020005

Conflict of Interest: The authors declare that the research was conducted in the absence of any commercial or financial relationships that could be construed as a potential conflict of interest.

Publisher's Note: All claims expressed in this article are solely those of the authors and do not necessarily represent those of their affiliated organizations, or those of the publisher, the editors and the reviewers. Any product that may be evaluated in this article, or claim that may be made by its manufacturer, is not guaranteed or endorsed by the publisher.

frontiers in Physiology

ORIGINAL RESEARCH
published: 28 July 2020
doi: 10.3389/fphys.2020.00863

Venous and Arterial Responses to Partial Gravity

Stuart M. C. Lee[1], David S. Martin[1], Christopher A. Miller[1], Jessica M. Scott[2], Steven S. Laurie[1], Brandon R. Macias[1], Nathaniel D. Mercaldo[1], Lori Ploutz-Snyder[3] and Michael B. Stenger[4]*

[1]KBR, Houston, TX, United States, [2]Memorial Sloan Kettering Cancer Center, New York, NY, United States, [3]School of Kinesiology, University of Michigan, Ann Arbor, MI, United States, [4]Lyndon B. Johnson Space Center, National Aeronautics and Space Administration, Houston, TX, United States

Introduction: Chronic exposure to the weightlessness-induced cephalad fluid shift is hypothesized to be a primary contributor to the development of spaceflight-associated neuro-ocular syndrome (SANS) and may be associated with an increased risk of venous thrombosis in the jugular vein. This study characterized the relationship between gravitational level (G_z-level) and acute vascular changes.

Methods: Internal jugular vein (IJV) cross-sectional area, inferior vena cava (IVC) diameter, and common carotid artery (CCA) flow were measured using ultrasound in nine subjects (5F, 4M) while seated when exposed to 1.00-G_z, 0.75-G_z, 0.50-G_z, and 0.25-G_z during parabolic flight and while supine before flight (0-G analog). Additionally, IJV flow patterns were characterized.

Results: IJV cross-sectional area progressively increased from 12 (95% CI: 9–16) mm^2 during 1.00-G_z seated to 24 (13–35), 34 (21–46), 68 (40–97), and 103 (75–131) mm^2 during 0.75-G_z, 0.50-G_z, and 0.25-G_z seated and 1.00-G_z supine, respectively. Also, IJV flow pattern shifted from the continuous forward flow observed during 1.00-G_z and 0.75-G_z seated to pulsatile flow during 0.50-G_z seated, 0.25-G_z seated, and 1.00-G_z supine. In contrast, we were unable to detect differences in IVC diameter measured during 1.00-G seated and any level of partial gravity or during 1.00-G_z supine. CCA blood flow during 1.00-G seated was significantly less than 0.75-G_z and 1.00-G_z supine but differences were not detected at partial gravity levels 0.50-G_z and 0.25-G_z.

Conclusions: Acute exposure to decreasing G_z-levels is associated with an expansion of the IJV and flow patterns that become similar to those observed in supine subjects and in astronauts during spaceflight. These data suggest that G_z-levels greater than 0.50-G_z may be required to reduce the weightlessness-induced headward fluid shift that may contribute to the risks of SANS and venous thrombosis during spaceflight.

Keywords: internal jugular vein, parabolic flight, spaceflight-associated neuro-ocular syndrome, venous thrombosis, artificial gravity, gravity levels

OPEN ACCESS

Edited by:
Marc-Antoine Custaud, Université d'Angers, France

Reviewed by:
Danilo Cialoni, Dan Europe Foundation, Italy
Ulrich Limper, Klinikum der Universität Witten/Herdecke, Germany

****Correspondence:***
Stuart M. C. Lee
stuart.lee-1@nasa.gov

Specialty section:
This article was submitted to Environmental, Aviation and Space Physiology, a section of the journal Frontiers in Physiology

Received: *20 March 2020*
Accepted: *26 June 2020*
Published: *28 July 2020*

Citation:
Lee SMC, Martin DS, Miller CA, Scott JM, Laurie SS, Macias BR, Mercaldo ND, Ploutz-Snyder L and Stenger MB (2020) Venous and Arterial Responses to Partial Gravity. Front. Physiol. 11:863. doi: 10.3389/fphys.2020.00863

INTRODUCTION

When a person stands upright on Earth, gravity pulls body fluids (e.g., blood, lymph, and cerebrospinal fluid) toward their feet, resulting in approximately 70% of body fluids residing below heart level (Rowell, 1993). During spaceflight, the absence of a head-to-foot hydrostatic pressure gradient causes these fluids to redistribute, resulting in a fluid shift toward the head (Thornton et al., 1987). These fluid shifts toward the head during weightlessness initially cause rapid alterations in the cardiovascular system, particularly in the venous circulation (Martin et al., 2016) as well as the cerebrospinal fluid (Lawley et al., 2017). Chronic exposure to weightlessness without countermeasures results in cardiovascular deconditioning (Hargens and Watenpaugh, 1996) and regional adaptations in the blood vessels (Zhang, 2001).

Long-duration stays in weightlessness also have resulted in changes in the function and structure of the eye in some astronauts that has been described as spaceflight-associated neuro-ocular syndrome (SANS; Lee et al., 2016; Macias et al., 2020). The leading hypothesis is that ocular changes result from chronic exposure to the weightlessness-induced fluid shift (Stenger et al., 2017). A consequence of the headward fluid shift appears to be congestion of the veins that drain the head (Arbeille et al., 2015; Marshall-Goebel et al., 2019). This, in turn, may impair cerebrospinal and lymphatic fluid drainage from the skull (Macintyre, 2013), which may underlie some of the changes in the eye. Previous work demonstrated that jugular vein cross-sectional area (Arbeille et al., 2015) and pressure (Marshall-Goebel et al., 2019) are increased in weightlessness (0-G) relative to the upright posture in normal gravity (1.00-G_z). Further, we have recently documented IJV flow pattern changes that might contribute to an increased risk of venous thrombosis (Marshall-Goebel et al., 2019).

Reversing the headward fluid shift has been proposed as a method to relieve venous congestion associated with weightlessness to mitigate the risk of SANS and venous thrombosis. One approach for achieving this effect is to create artificial gravity by centrifugation (Clément et al., 2015). However, how much gravity is required to sufficiently shift fluids footward is unresolved. Parabolic flight provides a unique opportunity to evaluate the acute changes associated with varying levels of gravity (G_z-levels) and to describe how vascular parameters change at levels less than 1.00-G_z. Characterizing these physiological changes in response to varying G_z-levels is an important step in determining what G_z-level may be required to reverse weightlessness-induced fluid shifts to serve as a viable countermeasure during long-duration spaceflight. Further, this information might provide the basis for a prediction of whether G_z-levels experienced on the Moon and Mars will be sufficient to prevent SANS development during exploration missions.

MATERIALS AND METHODS

Overall Protocol

This study characterized a set of vascular parameters at different G_z-levels and hydrostatic gradients, including preflight supine (1.00-G_z supine), 0.25-, 0.50-, and 0.75-G_z while seated during parabolic flight, and 1.00-G_z seated during level flight between parabolas. Weightless parabolas (0-G) were not included in this parabolic flight campaign. Vascular measurements included internal jugular vein (IJV) cross-sectional area, flow characterization, and pressure; common carotid artery (CCA) cross-sectional area and flow; and inferior vena cava (IVC) diameter using ultrasound. Beat-to-beat finger blood pressure and heart rate from a three-lead ECG configuration (Finapres Medical Systems, Amsterdam-Zuidoost, Netherlands) also were acquired. Study protocols were reviewed and approved by the French National Comité de Protection des Personnes and the NASA Johnson Space Center Institutional Review Board. This study was one of 11 experiments included in the parabolic flight campaign managed by Novespace, Inc. (Bordeaux-Mérignac, France) as part of the first International Space Life Sciences Working Group Campaign in June 2018.

Each flight included 31 parabolas (**Figure 1**), with the first parabola serving as a "practice" parabola to verify equipment operation. Then six sets of five parabolas were performed, each set at one of three different G_z-levels (0.25-G, 0.50-G, and 0.75-G_z; **Table 1**). The order of the G_z-levels was not randomly assigned within or across days of flight but differed across days. Each parabola started with a pull-up and ended with a "pull-out" maneuver (hypergravity phase to enter and exit the parabolic flight profile) at 1.8-G, both lasting about 20 s. Accelerometer data measured in the cockpit of the plane by Novespace and collected by our group independently in the experiment area (APDM, Inc.; Portland, OR) were used to identify the respective partial gravity epochs within which data were analyzed. The air pressure in the cabin was maintained at approximately 600 mmHg (800 mbars) during the parabolas, which corresponded to an altitude of about 2,000 m. The temperature was controlled to be between 20 and 25°C.

Subjects

Potential test subjects were identified by Novespace based upon selection criteria provided by the investigators. Subjects had to be between 25 and 55 years old to be similar in age to the astronaut corps (Harm et al., 2001), but there was no preferential recruitment by sex. Subjects had to be between 157 and 183 cm tall (61 and 72 in) to be secured safely in the seat. Preference was given for subjects with previous parabolic flight experience to increase the likelihood that the variable G-levels would be tolerated. Subjects were required to be French citizens to qualify for medical and life insurance in the event of an emergency but also needed to have sufficient command of English, so that the test operators could communicate with them.

In the week before the flights, subjects were screened by one of the investigators (DSM) to ensure adequate visualization of the relevant anatomy with ultrasound within the time constraints of each parabolic maneuver. Nine subjects (5F, 4M) were identified, with three subjects participating in testing on each of 3 flight days. Subjects were 39 ± 6 years old (mean ± SD; range: 34–50 years), 171 ± 11 cm tall (157–187 cm), and weighed 65 ± 10 kg (50–85 kg). All subjects were received verbal instruction and written documentation regarding study protocols and encouraged to ask

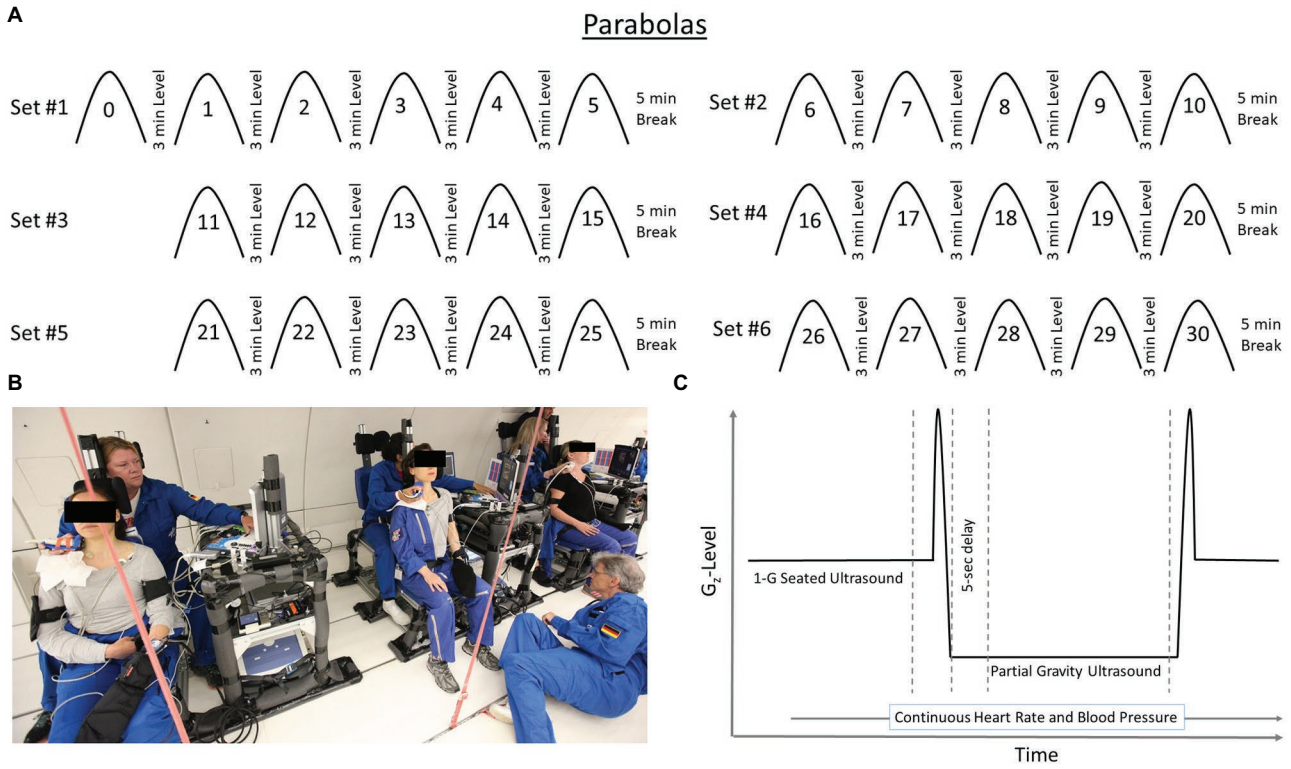

FIGURE 1 | Each flight day consistent of 31 parabolas **(Panel A)** producing partial gravity levels of 0.25-, 050-, and 0.75-G_z. Data were not analyzed for the first parabola (parabola 0) as it was considered a practice parabola for operators and subjects. Specially-designed chairs **(Panel B)** were constructed to accommodate the sonographer positioned directly behind the test subjects during the flights. Such an alignment was necessary to acquire high-quality ultrasound images. Subjects and operators wore lap belts to prevent excessive upward movement in partial gravity, and subjects rested against a back pad that extended above the level of their head. Additionally, a pad on the left side of the head allowed the subjects to relax their neck muscles. Hardware racks were positioned next to each subject such that the ultrasound machine was readily available to the sonographer, and other hardware for the measurement and recording of heart rate and blood pressure located such that the study's engineer could monitor them. Within a parabola **(Panel C)**, data were collected and analyzed during level flight before the hypergravity phase of the parabola and after 5 s of partial gravity. Depiction of time on *x*-axis and G_z-level on the *y*-axis are not to scale.

questions before providing written informed consent. Written informed consent also was obtained from all participants for the publication of any potentially identifiable images.

All but one subject was administered an antiemetic (subcutaneous scopolamine, 0.25 mg/ml saline) under the supervision of the flight medical doctor before boarding the airplane. Dosages administered ranged from 0.2 ml (0.05 mg) to 0.7 ml (0.175 mg), with the majority of the subjects receiving 0.5–0.7 ml (0.125–0.175 mg). Although oral scopolamine is associated with orthostatic hypotension in some individuals (Nuotto, 1983), no symptoms were reported during this study. Further, subjects did not report any motion sickness symptoms during the flights that would have precluded participation in the experiment.

Ultrasound Measures

Within 3 h before the flight, baseline measurements were acquired while the subjects were supine. A sonographer acquired ultrasound images (Vivid q, GE Healthcare, Chicago, IL) of the right IJV for off-line analysis of cross-sectional area, Doppler flow characterization (Marshall-Goebel et al., 2019), and estimates of IJV pressure (Martin et al., 2015, 2016); right CCA for the calculation of cross-sectional area and flow; and the IVC for the measurement of diameter. IJV images were acquired just proximal to the confluence of either the facial or superior thyroid veins, IVC images were acquired 1–2 cm from the right atrium, and CCA images were acquired ~2 cm below the carotid bulb. Venous measurements were obtained at the end of a tidal expiration. The sonographer ensured that the vessel walls could be clearly visualized and marked the skin at the probe locations where these images were obtained during the preflight baseline, so that images were acquired from the same location during parabolic flight. IJV and CCA imaging and Doppler were acquired with 12–5 MHz linear array probe (12L-RS, GE Healthcare, Chicago, IL), and IVC imaging was acquired with a 4 MHz phased array probe (M4S-RS, GE Healthcare, Chicago, IL). IJV pressure was acquired with the same 12–5 MHz linear array probe attached to a VeinPress (Meridian GMBH, Bern, Switzerland) using methods previously described (Martin et al., 2015, 2016).

During the flight, subjects were seated upright to experience the stressors associated with different G_z-levels, and the sonographers were seated directly behind them, reaching around the subject to acquire IJV, IVC, and carotid images.

TABLE 1 | The order of G_z-levels within and across days was not randomized, but the order of G_z-levels varied across days.

	Parabolas	G_z-Level	Ultrasound measures
Day 1	0–5	0.25	IJV pressure and area
	6–10	0.50	IJV pressure and area
	11–15	0.75	IJV pressure and area
	16–20	0.25	IJV flow, CCA flow and diameter, IVC diameter
	21–15	0.50	IJV flow, CCA flow and diameter, IVC diameter
	26–30	0.75	IJV flow, CCA flow and diameter, IVC diameter
Day 2	0–5	0.50	IJV pressure and area
	6–10	0.75	IJV pressure and area
	11–15	0.25	IJV pressure and area
	16–20	0.50	IJV flow, CCA flow and diameter, IVC diameter
	21–15	0.75	IJV flow, CCA flow and diameter, IVC diameter
	26–30	0.25	IJV flow, CCA flow and diameter, IVC diameter
Day 3	0–5	0.75	IJV pressure and area
	6–10	0.25	IJV pressure and area
	11–15	0.50	IJV pressure and area
	16–20	0.75	IJV flow, CCA flow and diameter, IVC diameter
	21–15	0.25	IJV flow, CCA flow and diameter, IVC diameter
	26–30	0.50	IJV flow, CCA flow and diameter, IVC diameter

Both the sonographer and the subject wore a lap belt to prevent excessive upward movements when in partial gravity. Subjects rested against a pad that extended above the level of their head, and the head was supported on the left side with an additional pad that allowed the subjects to relax their neck muscles. The same sequence of ultrasound images was acquired during each of the partial gravity conditions and during level flight, with the sonographer focusing on the acquisition of 1 parameter in each parabola. Sonographers acquired 1.00-G seated ultrasound images during level flight in the minute before the 1.8-G_z pull-up and acquired the partial gravity images from 5 s after the start of the partial gravity period until the end of the parabola. Heart rate and blood pressure were recorded continuously.

Data Reduction

Average values for heart rate and blood pressure were calculated for periods during level flight from 40 to 10 s prior to the hypergravity phase (1.80-G_z pull-up) and for periods of partial gravity from 5 s after achieving partial gravity until the pull-out. Mean arterial pressure was calculated as the average of the whole blood pressure waveform. Three separate ultrasound images were acquired for each target in each condition and stored for offline analysis. Two sonographers independently analyzed each image in a blinded fashion, and their results (cross-sectional area, diameter, and velocity time integral) were compared. When the inter-observer difference exceeded 10% for an IJV cross-sectional area measurement or a carotid measurement or if it exceeded 20% for an IVC diameter measurement, a third sonographer analyzed the image; the average of the two closest values were used for statistical analyses.

We characterized the venous blood flow within the IJV using a 1–4 grading system that incorporated direction and pattern of the Doppler signal (Marshall-Goebel et al., 2019). Continuous forward IJV flow (head to heart direction) was scored as grade 1, pulsatile forward flow was scored as grade 2, stagnant flow was scored as grade 3, and reverse flow (toward the head) was scored as grade 4. Two trained sonographers independently scored the IJV waveforms for which there was only one discrepancy between the two raters (n = 45; 0.75-G_z rater 1 = 2 and rater 2 = 1). The Cohen's kappa associated these ratings was 0.95 (95% CI 0.84–1.00). Due to the near perfect agreement, the discrepant value from rater 1 (senior level sonographer), along with all other identical ratings, was used for this analysis.

Data were not available for all conditions for some subjects due to technical or logistical difficulties. Beat-to-beat finger blood pressure data were not available for two subjects on day 1 and one subject on day 2. IJV cross-sectional area for one subject at all G_z-levels and IJV pressure for all subjects while seated at 0.75- and 1.00-G_z were not of adequate quality for analysis. IJV pressure measurements are particularly difficult in the seated posture in 1.00-G_z, given that the IJV is largely collapsed in this condition. A subset of the IJV pressure data was determined to be acceptable by one of the investigators (DSM) for five subjects during 1.00-G_z supine and while seated at 0.25- and 0.50-G_z. No acceleration data were recorded by the experiment's accelerometer on day 2, so accelerometer data from Novespace were analyzed for that day only.

Statistical Approach

Descriptive and graphical summaries [mean ± SD, range (minimum, maximum), and box/line plots] were computed to summarize parabolic flight by G_z-level. Separate linear regression models were constructed to quantify the association between each outcome (heart rate, mean arterial pressure, IJV cross-sectional area, IVC diameter, CCA flow, and cross-sectional area) and G-level (1.00-G_z seated, 0.75-G_z, 0.50-G_z, 0.25-G_z, and 1.00-G_z supine). G_z-level was modeled as a series of indicator variables, where 1.00-G_z (seated) was defined as the referent value. Model parameters were estimated using generalized estimating equations using an independence correlation structure (GEE-Ind) to account for repeated measurements within subject. Linear combinations of parameters were computed to estimate both main effects (e.g., expected IJV cross-sectional area at 1.00-G_z seated) and differences (e.g., difference in the expected IJV cross-sectional area at 0.75-G_z vs. 1.00-G_z seated) along with 95% confidence intervals and p-values (*via* Wald tests for difference comparisons only). A logistic regression model was constructed to quantify the relationship between IJV flow ratings (1 = pulsatile forward, 0 = continuous forward) and G-level. Odds ratios (OR), 95% confidence intervals, and p-values were computed using GEE-Ind to summarize the comparison when comparing each partial gravity level to 1.00-G_z seated. IJV pressures were compared among subjects with both

0.50-G_z seated and 1.00-G_z supine conditions using a paired *t*-test. All analyses were performed using R 3.6.2 (R Core Team, 2019).

RESULTS

Parabolic Flight

The duration of the reduced gravity periods depended on the gravity level, with mean parabola durations of 22.1 ± 2.3, 32.1 ± 1.8, and 45.2 ± 4.1 s for 0.25-, 0.50-, and 0.75-G_z, respectively. The mean G_z-levels measured across the 3 flight days were 0.25 ± 0.02, 0.50 ± 0.02, and 0.75 ± 0.02 G_z. The G_z-level during straight-and-level flight preceding each parabola was 1.00 ± 0.05 G_z (**Figure 2**).

Blood Pressure and Heart Rate

Mean arterial blood pressure and heart rate by G_z-level are presented in **Table 2**. Mean arterial pressure during 1.00-G_z seated was significantly greater than mean arterial pressure during 0.75-G_z, 0.50-G_z, and 0.25-G_z. Similarly, heart rate during 1.00-G_z seated rest was greater than heart rate during 0.50-G_z and 0.25-G_z. We were unable to detect differences in heart rate when comparing 1.00-G_z seated to 0.75-G_z.

Vascular Responses

Vascular dimensions and flow by G_z-level are presented in **Table 3**. IJV cross-sectional area during 1.00-G_z seated was significantly smaller than at all evaluated partial gravity levels (**Figure 3**). In contrast, we were unable to detect differences in IVC diameter between measurements acquired during 1.00-G_z seated and any level of partial gravity or during 1.00-G_z supine. CCA blood flow during 1.00-G seated was significantly less than 0.75-G_z and 1.00-G_z supine, but differences were not detected at partial gravity levels 0.50-G_z and 0.25-G_z. Differences in the average CCA cross-sectional area were not detected between any of the evaluated conditions.

During 1.00-G_z seated and 0.75-G_z seated, the IJV waveform was characterized as continuous forward flow (score = 1) in all but one subject in each condition (**Figure 4**). At lower G_z-levels, pulsatile forward flow (score = 2) became more apparent. Waveforms in four of nine, five of eight, and seven of eight subjects were scored as two at 0.50-G_z seated, 0.25-G_z seated, and 1.00-G_z supine, respectively. IJV flow scores were not different than 1.00-G_z seated at 0.75-G_z [*OR* = 1.0 (95% CI: 0–24), p = 1.00] and at 0.50-G_z [*OR* = 5.6 (95% CI: 1–38), p = 0.08], but IJV flow scores were significantly different than 1.00-G_z seated when compared to 0.25-G_z

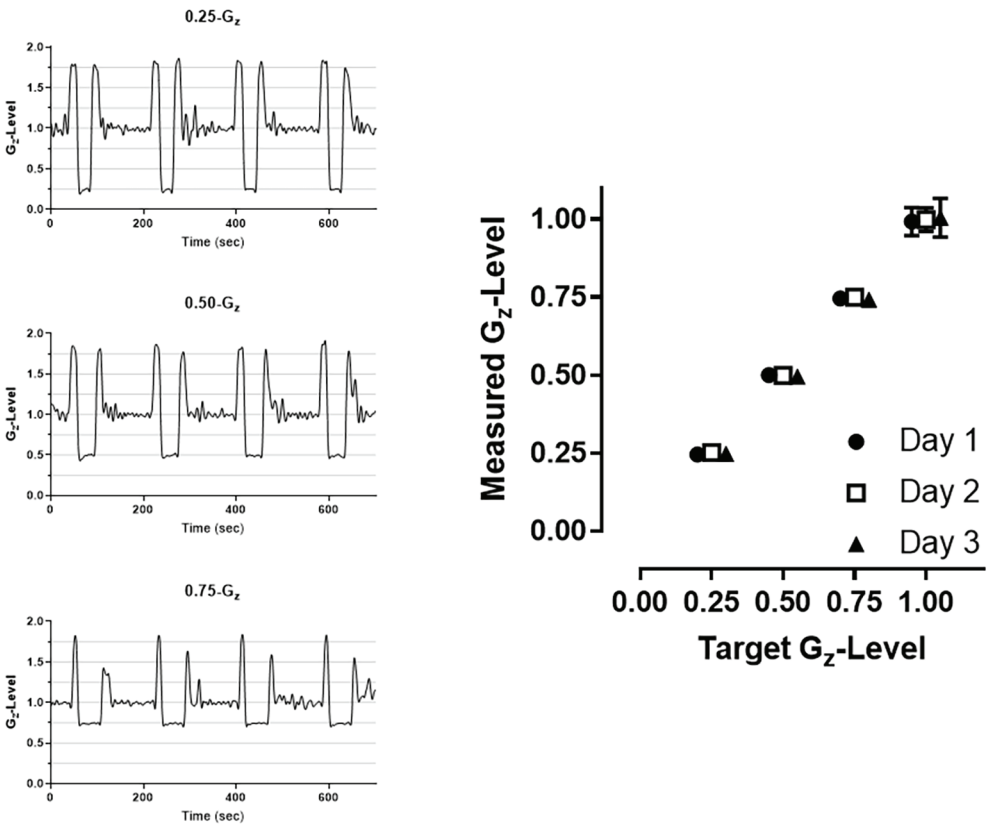

FIGURE 2 | Examples of raw accelerometer data collected at each of the three G-levels **(left panels)** and mean (±SD) G-level attained across all parabolas within a given day **(right panel)**. 1.00-G corresponds to level flight periods between parabolas. Error bars displaying SD may not be visible due to the low degree of variability across parabolas. Data are offset to demonstrate consistency across the 3 days (Circle: day 1; Square: day 2; Triangle: day 3).

TABLE 2 | Mean heart rate and blood pressure while seated in 1.00-G_z and during partial gravity.

	Mean	95% CI	Difference from 1-G_z	95% CI	*p*
Heart rate (bpm)					
1-G_z Seated	60	(51, 68)	–	–	–
0.75-G_z	58	(51, 66)	−2	(−5, 1)	0.256
0.50-G_z	56	(49, 63)	−4	(−7, −1)	0.015
0.25-G_z	56	(49, 62)	−4	(−7, −1)	0.006
Mean arterial pressure (mmHg)					
1-G_z Seated	95	(79, 111)	–	–	–
0.75-G_z	89	(74, 103)	−7	(−9, −4)	<0.001
0.50-G_z	85	(66, 103)	−10	(−16, −5)	<0.001
0.25-G_z	80	(66, 94)	−15	(−17, −13)	<0.001

TABLE 3 | Mean vascular dimensions and flow while seated in 1.00-G_z and partial gravity and while supine in 1.00-G_z (0-G_z analog).

	Mean	95% CI	Difference from 1-G_z	95% CI	*p*
IJV area (mm^2)					
1-G_z Seated	12	(9, 16)	–	–	–
0.75-G_z	24	(13, 35)	12	(1, 23)	0.032
0.50-G_z	34	(21, 46)	21	(8, 35)	0.002
0.25-G_z	68	(40, 97)	56	(27, 85)	<0.001
1-G_z Supine	108	(74, 131)	91	(64, 118)	<0.001
IVC diameter (cm)					
1-G_z Seated	1.68	(1.45, 1.92)	–	–	–
0.75-G_z	1.66	(1.44, 1.88)	−0.02	(−0.20, 0.15)	0.783
0.50-G_z	1.81	(1.61, 2.02)	0.13	(−0.01, 0.27)	0.071
0.25-G_z	1.69	(1.46, 1.91)	0.01	(−0.02, 0.22)	0.955
1-G_z Supine	1.81	(1.57, 2.05)	0.12	(−0.10, 0.35)	0.280
CCA flow (ml/min)					
1-G_z Seated	786	(635, 837)	–	–	–
0.75-G_z	895	(686, 1,103)	159	(24, 294)	0.021
0.50-G_z	845	(650, 1,039)	109	(−82, 300)	0.265
0.25-G_z	826	(688, 963)	90	(−4, 184)	0.060
1-G_z Supine	836	(783, 891)	101	(21, 181)	0.013
CCA cross-sectional area (cm)					
1-G_z Seated	0.33	(0.31, 0.35)	–	–	–
0.75-G_z	0.33	(0.31, 0.35)	0.01	(−0.01, 0.02)	0.350
0.50-G_z	0.33	(0.30, 0.36)	0.00	(−0.01, 0.01)	0.466
0.25-G_z	0.34	(0.31, 0.36)	0.01	(0.00, 0.02)	0.118
1-G_z Supine	0.32	(0.29, 0.34)	−0.01	(−0.02, 0.00)	0.147

[*OR* = 12 (95% CI: 1–102), $p = 0.026$] and 1.00-G_z supine [*OR* = 56 (95% CI: 4–862), $p = 0.004$]. Waveforms corresponding to grades 3 and 4 were not observed in our subjects during parabolic flight.

One of the investigators (DSM) visually inspected all IJV pressure measurements to ensure the technical quality of the imaging before analyses were performed. This approach determined that data collected while subjects were seated at 0.75- and 1.00-G_z were not technically adequate, but data were available for six subjects during three conditions: preflight supine in 1.00-G_z and while seated at 0.25- and 0.50-G_z. Individual data represented in **Figure 5** are the mean of at least three IJV pressure measurements. In the three subjects with technically-adequate images in all three conditions, there appeared to be minimal difference in IJV pressure from 1.00-G_z supine to 0.25-G_z seated for two subjects and an increased IJV pressure in one subject. However, IJV pressure at 0.50-G_z seated (9.5 ± 3.4 mmHg) was lower than 1.00-G_z supine (19.1 ± 7.6 mmHg) for all five subjects [difference: 9.6 (95% CI: 5.0–14.1), $p = 0.003$].

DISCUSSION

The principal finding from this study was that compared to measurements acquired in the seated posture in 1.00-G_z, IJV cross-sectional area increases and IJV flow pattern becomes pulsatile as the G-level decreases during brief periods of partial gravity produced by parabolic flight. There are two important perspectives that can be derived from these results. First, our data suggest that the minimum G_z-level required to preserve hydrostatic conditions in the venous system of the upper body close to the upright 1.00-G_z posture, preventing IJV engorgement and changes in IJV flow patterns associated with the headward fluid shift in weightlessness, is greater than 0.50-G_z. Second, our data suggest that G_z-levels on the Moon (0.16-G_z) and Mars (0.38-G_z) would not be sufficient to prevent the headward distribution of venous blood that distends and changes the basic flow characteristics of the IJV. Future work will be required to verify that these observations during acute partial gravity are representative of the effects of chronic exposures (Shelhamer, 2016) and to determine whether partial gravity exposures during long-duration stays on the Moon and Mars will be protective against the risks of SANS and IJV thrombosis relative to weightlessness.

Systemic Hemodynamics

We report here for the first time the heart rate and blood pressure responses across the range from 1.00- to 0.25-G_z, although measures have been obtained during parabolic flight simulating lunar and Martian gravity (Widjaja et al., 2015; Beck et al., 2018). Lower mean arterial pressure has been reported previously while seated in 0-G produced by parabolic flight, likely resulting from increase in central blood volume (Lathers et al., 1989; Mukai et al., 1991), reduced sympathetic activity, and peripheral vasodilation (Iwase et al., 1999; Ogoh et al., 2015), but no similar data are available across this range of partial gravity levels. In apparent agreement with studies in weightlessness, mean arterial pressure appeared to decrease as G_z-level decreased in this study presumably as the headward in fluid shift increased. We also observed that heart rate was lower during the two lowest partial gravity levels. Reduced heart rate during 0-G has not been consistently observed in previous parabolic studies (Lathers et al., 1989; Mukai et al., 1991), perhaps, because of differences in body postures or the duration of parabolas. In general, these responses are consistent with a centralization of blood volume.

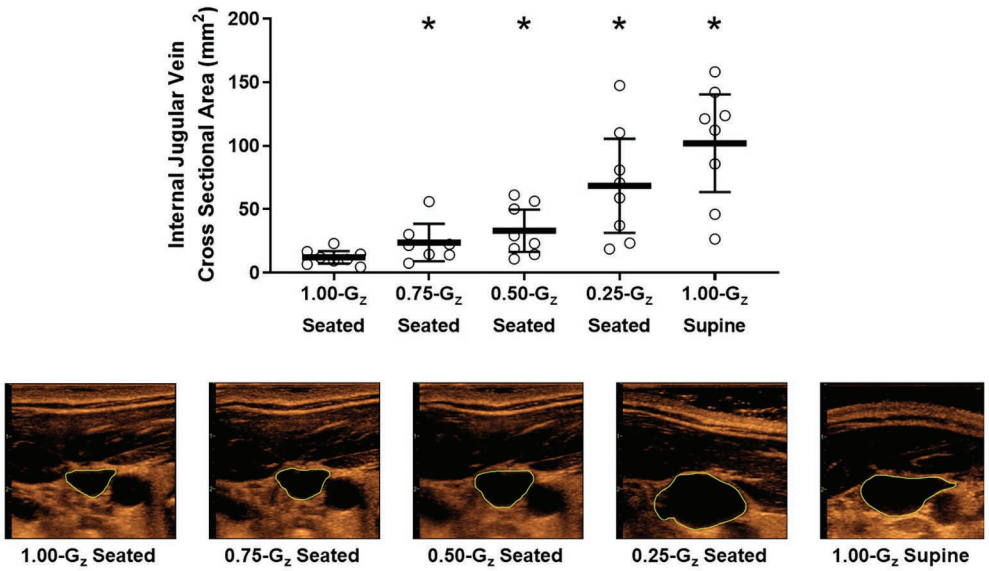

FIGURE 3 | Internal jugular vein (IJV) cross-sectional area **(upper panel)** and representative images from 1 subject **(lower panel)** acquired by ultrasound during seated rest across different G_z-levels and during 1.00-G supine rest. Open circles represent individual data. Black bar represents mean and 95% confidence interval. *Significantly different than seated 1.00-G ($p < 0.05$).

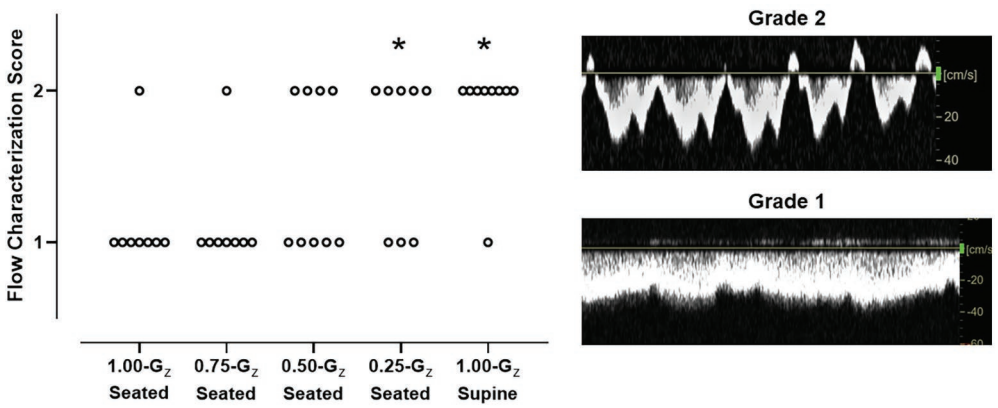

FIGURE 4 | IJV flow characterization scores during 1.00-G_z supine rest (0-G surrogate) and during seated rest across G_z-levels. Scores for each individual subject are represented. IJV flow was categorized by two expert sonographers using a 4-point scale, from continuous forward flow to stasis (Marshall-Goebel et al., 2019), but IJV flow in these subjects scored only to be either 1 (continuous forward flow) or 2 (pulsatile forward flow). Scoring differed between the two sonographers for only one subject at 1 G-level. Scores only from one rater (senior level sonographer) are shown. $n = 9$ for 0.50-G_z and 1.00-G_z supine; and $n = 8$ for 1.00-G_z seated, 0.75-G_z seated, and 0.25-G_z seated. *Distribution of IJV flow scores significantly different ($p < 0.05$) than 1.00-G_z seated.

Arterial Flow to the Head

When considering the effects of partial gravity levels on cranial venous parameters, one must also consider the effects of cranial arterial flow. In this study, we did not observe an effect of G_z-level on CCA diameter; although CCA flow was higher during 1-G_z supine than during 1-G_z seated, similar to previous observations (Sato et al., 2012; van Campen et al., 2018), the effects during partial gravity levels were not consistent. While an increase in CCA flow might be suggestive of elevated cerebral blood, middle cerebral artery flow velocity does not increase during weightlessness produced by parabolic flight due to systemic vasodilation (Ogoh et al., 2015), even though central blood volume and cardiac output may be higher (Ogoh et al., 2005). Although not examined in this study, we have no reason to suspect that the cerebral autoregulation was altered during these partial gravity levels.

Venous Drainage From the Head

Previous observations during spaceflight (Arbeille et al., 2015; Marshall-Goebel et al., 2019) and weightlessness during parabolic flight (Martin et al., 2016) are consistent with venous congestion,

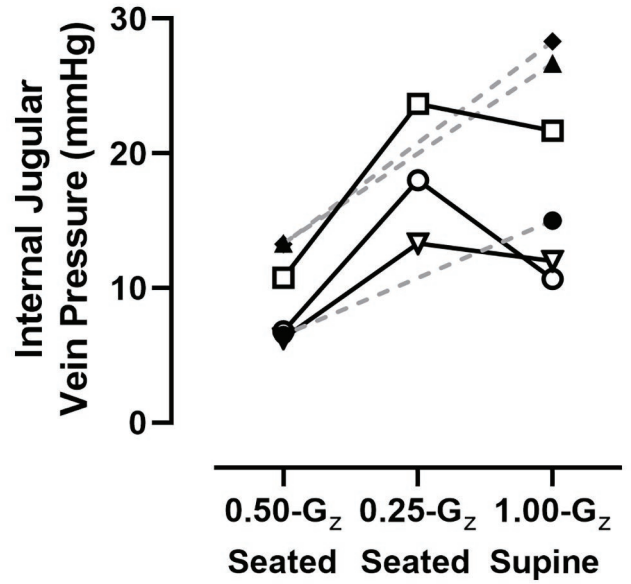

FIGURE 5 | IJV pressure measured in six subjects using compression sonography. Individual results represented here are the mean of at least three measurements for each condition. Dashed lines are provided for subjects with data only from 1.00-G_z supine and 0.50-G_z seated to illustrate trends within those individual subjects and not meant to suggest predicted values at 0.25-G_z.

and in this study, as the G_z-level deceased during parabolic flight, a graded expansion of the IJV was observed. The blood volume located above the heart level (Lawley et al., 2017) likely increased as G_z-level decreased due to a reduced hydrostatic pressure gradient between the head and the heart. Caudal fluid shifts during parabolic flight when transitioning from 1.00-G_z to 0-G_z are evident from measures of lower limb circumference (Bailliart et al., 1998) and thoracic impedance (Mukai et al., 1991), but no similar data have been acquired during these novel partial gravity conditions to explain our IJV cross-sectional area findings. However, manipulation of the hydrostatic gradient in a ground-based study using graded head-up tilt angles (Valdueza et al., 2000) produced a similar effect on IJV cross-sectional area as during this partial gravity parabolic flight experiment. In this study, mean IJV cross-sectional area increased almost 10-fold from 1.00-G_z seated to 1.00-G_z supine, but individual variation between subjects was clear, as is variation in the magnitude of the response between studies (Valdueza et al., 2000; Lawley et al., 2017; Marshall-Goebel et al., 2019). Location of the measurement along the IJV is one source of variation (Magnano et al., 2016; Marshall-Goebel et al., 2018), but images were obtained in similar sites. Individual variability in the response of the IJV cross-sectional area to posture changes likely reflect individual differences in anatomical structures, IJV valve patency, and vessel function, including between-subject differences in upper body venous compliance.

Though in this experiment we sought to describe the response of IJV cross-sectional area across the range of G_z-levels, this parabolic flight campaign did not include 0-G parabolas. Reduced weighting of tissue overlying the IJV might contribute to IJV expansion during partial gravity by increasing transmural pressure compared to 1.00-G_z supine, similar to the explanation postulated for the decrease in central venous pressure during weightlessness (Buckey et al., 1993, 1996; Foldager et al., 1996; Videbaek and Norsk, 1997), and thus, using measures acquired during 1.00-G_z supine as our 0-G analog may have underestimated the effects. The IJV is a low pressure vessel with high compliance such that even small changes in pressure would result in large changes in IJV dimensions (Magnano et al., 2016). Others (Arbeille et al., 2015; Lawley et al., 2017) reported that the IJV is enlarged during weightlessness beyond that measured during supine rest in 1.00-G_z. In contrast, we recently reported (Marshall-Goebel et al., 2019) that IJV cross-sectional area measurements during spaceflight were not different than those measured while supine before spaceflight.

While IJV cross-sectional area during full and partial gravity appears to represent a continuum across 1.00-G seated and partial G_z levels, the flow with the IJV may not follow this same pattern. We observed normal, continuous, or pulsatile forward IJV flow in all the subjects during seated and supine 1.00-G_z, but during parabolic flight we observed a G_z-level dependent transition from forward flow in the 1.00-G_z seated posture to pulsatile flow in partial gravity. Mean IJV cross-sectional area increased ~100% from 1.00-G_z seated to 0.75-G_z seated with no corresponding change in IJV flow character, and the transition from continuous forward to pulsatile flow did not occur in more than half of the subjects until 0.50-G_z seated when mean IJV cross-sectional area had almost tripled. The G_z-level at which the transition occurred was not the same across subjects, but in general was consistent once the flow pattern became pulsatile as the G_z-level decreased. Transition of the flow pattern likely results from filling of the vessel and stretching of the vein wall to an individual's threshold such that the energy transmitted from cardiac contractions and respiration are more easily transmitted across the continuous fluid column (Anliker et al., 1969) and reflected in the character of IJV flow.

In the three gravity conditions in which technically sound measures of IJV pressure were acquired, it was apparent that IJV pressure decreases as G_z-level increases. In the 1.00-G seated condition, the IJV is not engorged (Valdueza et al., 2000; Cirovic et al., 2003), as reflected in our IJVA measures, and thus, even small amounts of externally-applied pressure will compress the vessel making the measurement difficult. In our experience in the laboratory under more controlled conditions, IJV pressure measured with compression sonography when seated in normal gravity is between 0 and 10 mmHg (Marshall-Goebel et al., 2019). IJV pressure at 0.75-G_z appears to be similarly difficult but the measurement was easier to acquire when the vessel became engorged and easier to visualize at lower G-levels and while supine. Our measurements in 1.00-G_z supine are between that which we previously reported during supine in 1.00-G_z (9.9 ± 5.1 mmHg) and while seated in 0-G_z (23.9 ± 5.6 mmHg; Martin et al., 2016). The difference between our current results and those we previously published likely reflects the smaller amount of data available in these subjects in combination with the individual variability that we previously observed with this measurement technique (Martin et al., 2015).

Because the methodology requires compression of the overlying tissues to compress the vein, between-subject differences could arise because of differences in tissue stiffness, thickness in subcutaneous tissues, or the location chosen along the IJV to conduct compression measures. However, given the consistency of the response between 1.00-G_z supine and 0.50-G_z seated, we are confident that the pattern of IJV pressures presented here reflects actual pressure changes within the IJV during partial gravity conditions. We observed a similar trend in non-invasive IJV pressure measurements during our previous parabolic flight campaign in two subjects (Martin et al., 2016); IJV pressure was highest during 0-G_z, decreased somewhat at 0.16-G_z (lunar gravity), but decreased by ~50% at 0.38-G_z (Martian gravity).

Importantly, these data were collected during acute exposures, and thus, it is not clear what effects will be observed during chronic stays in weightlessness or partial gravity when IJV dimensions, pressures, and flow patterns would be chronically altered compared to the normal exposures in Earth gravity. For example, the IJV flow pattern was normal in 11 astronauts before spaceflight, transitioning from continuous forward flow when seated to pulsatile flow when supine, but the sustained headward fluid shift might promote progression to more abnormal flow patterns in some individuals. After ~50 and ~150 days of spaceflight, while most observations of IJV flow were pulsatile (11 of 21 observations), some were stagnant (7 of 21 observations) or reversed direction (2 of 21 observations; Marshall-Goebel et al., 2019). Given that venous stasis is a risk factor for thrombus formation (Previtali et al., 2011) and that an occlusive thrombus has been observed in one astronaut and suspected in a second (Marshall-Goebel et al., 2019), maintenance of normal IJV hemodynamics during sustained exposures to weightlessness or partial gravity are likely important to crew health and performance.

A potential confounding factor to consider when interpreting IJV cross-sectional area, flow characteristics, and pressure during parabolic flight is the potential change in the vessels carrying cranial venous outflow in different G_z-levels (Valdueza et al., 2000; Zivadinov and Chung, 2013). For example, in an upright posture in 1.00-G_z when venous outflow is assisted by gravity, drainage of the head occurs primarily through the vertebral veins, and the IJV is largely collapsed; vertebral vein flow is three times greater than that in the IJV, and IJV cross-sectional area is 10–15% of that which was measured while supine (Valdueza et al., 2000; Cirovic et al., 2003). As subjects are tilted toward supine, vertebral venous flow progressively decreases while IJV cross-sectional area and flow increases, such that venous outflow occurs predominantly through the IJV. To our knowledge, no similar data exist with which to compare flows and diameters across different veins during weightlessness and partial gravity.

Previously we suggested that changes in the IJV hemodynamics might be influenced directly by venous return from the lower body (Martin et al., 2016); increased venous return from the lower body with little change or decreased flow through the superior vena cava could contribute to increased right atrial filling and IJV distension during parabolic flight. In this study, we measured IVC diameter which has been used clinically as an index of fluid status and venous return. IVC diameter is decreased in individuals with low blood volume (Mandelbaum and Ritz, 1996) and decreased further upon standing in subjects who suffer from orthostatic intolerance (Ishizaki et al., 2004). We observed that IVC diameter generally was unchanged across G-levels, and subjects did not report any symptoms of motions sickness or orthostatic hypotension during the parabolic maneuvers. While these results suggest that IJV hemodynamics is not directly influenced, measurement of flow from the IVC is required to confirm this.

Countermeasures

Given that the weightlessness-induced headward fluid shift and associated IJV congestion are hypothesized to be contributing factors to the risk of SANS (Stenger et al., 2017) and IJV thrombosis (Marshall-Goebel et al., 2019), countermeasures that reverse the headward fluid shift may be protective of astronaut health during long-duration spaceflight. In addition to artificial gravity through short-arm centrifugation (Clément et al., 2015), countermeasures that have been proposed for the purpose of redistributing fluids to the lower body and relieving venous congestion during spaceflight include lower body negative pressure (Watkins et al., 2017; Marshall-Goebel et al., 2019), occlusive thigh cuffs (Balasubramanian et al., 2018), and exercise (Scott et al., 2019). An impedance threshold breathing device, which increases the resistance to inspiration and thus creates more negative pressure in the chest, also might assist with reducing IJV congestion (Convertino et al., 2005).

This study provides evidence that countermeasures targeting the prevention of the weightlessness-induced headward fluid shift will need to produce hemodynamic effects in excess of that created by 0.50-G_z to meaningfully reduce venous congestion. Compared to 1.00-G_z supine, our 0-G analog, exposure to 0.25-G_z produced a 30% reduction in IJV cross-sectional area and a mild reduction in IJV pressure; yet, the majority of subjects still exhibited a pulsatile IJV flow pattern. At 0.50-G_z, IJV cross-sectional area was further reduced and IJV pressure approached that measured during 1.00-G_z seated, but still IJV flow was pulsatile in four of nine subjects. However, at 0.75-G_z, IJV flow was continuous in seven of eight subjects, and IJV cross-sectional area was reduced from 0-G by 80%. It is important to note, however, that our data result from an acute exposure and that we did not observe any IJV waveforms representative of stagnant (grade 3) or reverse flow (grade 4) at lower G-levels. Thus, from these data, it is not possible to ascertain whether partial gravity exposures would restore normal, forward, or pulsatile IJV flow once stagnant or reverse flow patterns have developed during prolonged weightlessness. In fact, in only three of the seven cases, in which stagnant or reverse flow was observed after ~50 and ~150 days of spaceflight was lower body negative pressure at 25 mmHg of decompression, a level of lower body negative pressure does not approximate 1.00-G_z levels of orthostatic stress (Wolthuis et al., 1974), effective in restoring forward or pulsatile IJV flow (Marshall-Goebel et al., 2019). Thus, astronauts spending extended periods of time in lunar (0.16-G_z) and Martian (0.38-G_z) may not be at a reduced risk of SANS and IJV thrombosis when in these partial gravity environments. Recently, Baranov et al. (2016) reported,

there was insufficient evidence to conclude that IJV diameter measured in six subjects after a simulated 3-week lunar mission [consisting 1 week of continuous 6° head-down tilt bed rest followed by 2 weeks of bed rest in which the subjects were horizontal (0° of tilt) for 8 h during sleep and at 9.6° of head-up tilt for 16 h during the day] differed from the IJV diameter of five subjects who underwent 3 weeks of simulated weightlessness (continuous 6° head-down tilt bed rest). Thus, countermeasures that would be employed by astronauts while weightless during transit to and from their destination also may be required during stays on these extraterrestrial surfaces.

Limitations

Several limitations of this study should be acknowledged. First, IJV measures were acquired on the right side only, and we did not determine left or right side IJV dominance in these subjects. Thus, we cannot comment as to the hemodynamics on the left IJV, which generally has a smaller diameter than the right side and may have lower distensibility (Magnano et al., 2016) or the combined effects on venous flow from both vessels. Second, it is important to note that data acquisition during parabolic flight occurred while the subjects were in the upright, seated posture, so that the hydrostatic column in the G_z axis would be influenced by the different G_z-levels in the same way that they would be during an artificial gravity countermeasure in weightlessness and during habitation of low gravity environments. This posture, however, has the potential to exaggerate fluid shifts during parabolic flight, in comparison to the fluid shifts associated with steady-state condition during longer partial gravity exposures (Norsk et al., 1987; Pantalos et al., 1999; Petersen et al., 2011). Abdominal organs and the volume of blood trapped in the abdomen when seated during hypergravity would be expected to move rapidly headward during the transition to reduced gravity, but these effects have not been measured in partial gravity conditions like those in this campaign. Third, we did not specifically control or measure fluid intake or hydration of our subjects, which may have contributed to the between-subject variability of the response to partial gravity. Hydration had a graded effect on right and left atrial pressures and volumes during weightlessness in instrumented non-human primates in parabolic flight (Latham et al., 1994), particularly right atrial pressure in the upright posture when the animals were volume depleted. Finally, these analyses do not control for the seated height of our test subjects, which could contribute to differences in hydrostatic pressure gradients across individuals, although in our statistical design subjects served as their own controls.

CONCLUSIONS

We report for the first time that IJV cross-sectional area increases and the IJV flow pattern becomes more pulsatile as the G_z-level decreases during partial gravity parabolic flight. While there is no clear answer yet as to the amount of caudal fluid shift required to mitigate the risk of SANS and IJV thrombosis during long-duration spaceflight, these results suggest that G_z-levels greater than 0.50-G_z will be necessary to be protective and that there may be a risk of SANS and IJV thrombosis in the lunar and Mars environments. Validation of a countermeasure prescription (magnitude of fluid shift reversal, frequency, and duration) during long-duration spaceflight and assessment of the cumulative response to prolonged habitation in a partial gravity environment are required to substantiate these assertions. Inflight monitoring of the caudal fluid shifts and the effectiveness of countermeasures will be helpful in optimizing the countermeasure prescription and efficacy.

DATA AVAILABILITY STATEMENT

Requests to access the datasets should be directed to NASA's Life Sciences Data Archive (https://lsda.jsc.nasa.gov/).

ETHICS STATEMENT

The studies involving human participants were reviewed and approved by French National Comité de Protection des Personnes and the NASA Johnson Space Center Institutional Review Board. The participants provided their written informed consent to participate in this study. Written informed consent also was obtained from all participants for the publication of any potentially identifiable images.

AUTHOR CONTRIBUTIONS

SMCL contributed to the study design and implementation, interpretation of results, drafting and revision of the manuscript, and approval of final draft. DM contributed to the study design and implementation (including oversight of ultrasound procedures, data collection, and analyses), editing of the manuscript, and approval of final draft. CM contributed to the study implementation (including engineering support and data collection), editing of the manuscript, and approval of final draft. JS contributed to the study design, editing of the manuscript, and approval of final draft. SSL contributed to the interpretation of results, editing of the manuscript, and approval of final draft. BM contributed to the interpretation of results, editing of the manuscript, approval of final draft, and secured funding. NM contributed to the statistical analyses, interpretation of the results, drafting and revision of the manuscript, and approval of final draft. LP-S and MS contributed to the study design, editing of the manuscript, approval of final draft, and secured funding. All authors contributed to the article and approved the submitted version.

FUNDING

This research was funded by NASA's Human Research Program and by NASA NNX16AO73G (LP-S).

ACKNOWLEDGMENTS

The authors thank the following individuals for their valuable contributions to this study: the subjects for their participation; sonographers Monica Randall, Alma Montez, and Kathleen Garcia for their efforts to capture ultrasound images and venous pressure data; Rebecca Cox and Monica Randall for ultrasound analyses; Frederic Gai of Novespace who served as our experiment coordinator; Pierre Denise, MD, of Centre Hospitalier Universitaire de Caen who served as the official representative to the French National Comité de Protection des Personnes; Dr. Alan Feiveson for his assistance in study design and consultation on statistical methods; and Dr. Gilles Clement for overall guidance in the execution of an international parabolic flight campaign.

REFERENCES

Anliker, M., Wells, M. K., and Ogden, E. (1969). The transmission characteristics of large and small pressure waves in the abdominal vena cava. *IEEE Trans. Biomed. Eng.* 16, 262–273. doi: 10.1109/tbme.1969.4502658

Arbeille, P., Provost, R., Zuj, K., and Vincent, N. (2015). Measurements of jugular, portal, femoral, and calf vein cross-sectional area for the assessment of venous blood redistribution with long duration spaceflight (vessel imaging experiment). *Eur. J. Appl. Physiol.* 115, 2099–2106. doi: 10.1007/s00421-015-3189-6

Bailliart, O., Capderou, A., Cholley, B. P., Kays, C., Rivière, D., Téchoueyres, P., et al. (1998). Changes in lower limb volume in humans during parabolic flight. *J. Appl. Physiol.* 85, 2100–2105. doi: 10.1152/jappl.1998.85.6.2100

Balasubramanian, S., Tepelus, T., Stenger, M. B., Lee, S. M. C., Laurie, S. S., Liu, J. H. K., et al. (2018). Thigh cuffs as a countermeasure for ocular changes in simulated weightlessness. *Ophthalmology* 125, 459–460. doi: 10.1016/j.ophtha.2017.10.023

Baranov, M. V., Katuntsev, V. P., Shpakov, A. V., and Baranov, V. M. (2016). A method of ground simulation of physiological effects of hypogravity on humans. *Bull. Exp. Biol. Med.* 160, 401–405. doi: 10.1007/s10517-016-3181-0

Beck, P., Tank, J., Gauger, P., Beck, L. E. J., Zirngibl, H., Jordan, J., et al. (2018). Modeling human orthostatic responses on the moon and on Mars. *Clin. Auton. Res.* 28, 325–332. doi: 10.1007/s10286-018-0527-x

Buckey, J. C., Gaffney, F. A., Lane, L. D., Levine, B. D., Watenpaugh, D. E., and Blomqvist, C. G. (1993). Central venous pressure in space. *N. Engl. J. Med.* 328, 1853–1854. doi: 10.1056/NEJM199306243282516

Buckey, J. C. Jr., Gaffney, F. A., Lane, L. D., Levine, B. D., Watenpaugh, D. E., Wright, S. J., et al. (1996). Central venous pressure in space. *J. Appl. Physiol.* 81, 19–25. doi: 10.1152/jappl.1996.81.1.19

Cirovic, S., Walsh, C., Fraser, W. D., and Gulino, A. (2003). The effect of posture and positive pressure breathing on the hemodynamics of the internal jugular vein. *Aviat. Space Environ. Med.* 74, 125–131.

Clément, G. R., Bukley, A. P., and Paloski, W. H. (2015). Artificial gravity as a countermeasure for mitigating physiological deconditioning during long-duration space missions. *Front. Syst. Neurosci.* 9:92. doi: 10.3389/fnsys.2015.00092

Convertino, V. A., Cooke, W. H., and Lurie, K. G. (2005). Inspiratory resistance as a potential treatment for orthostatic intolerance and hemorrhagic shock. *Aviat. Space Environ. Med.* 76, 319–325.

Foldager, N., Andersen, T. A., Jessen, F. B., Ellegaard, P., Stadeager, C., Videbaek, R., et al. (1996). Central venous pressure in humans during microgravity. *J. Appl. Physiol.* 81, 408–412. doi: 10.1152/jappl.1996.81.1.408

Hargens, A. R., and Watenpaugh, D. E. (1996). Cardiovascular adaptation to spaceflight. *Med. Sci. Sports Exerc.* 28, 977–982. doi: 10.1097/00005768-199608000-00007

Harm, D. L., Jennings, R. T., Meck, J. V., Powell, M. R., Putcha, L., Sams, C. P., et al. (2001). Invited review: gender issues related to spaceflight: a NASA perspective. *J. Appl. Physiol.* 91, 2374–2383. doi: 10.1152/jappl.2001.91.5.2374

Ishizaki, Y., Fukuoka, H., Ishizaki, T., Kino, M., Higashino, H., Ueda, N., et al. (2004). Measurement of inferior vena cava diameter for evaluation of venous return in subjects on day 10 of a bed-rest experiment. *J. Appl. Physiol.* 96, 2179–2186. doi: 10.1152/japplphysiol.01097.2003

Iwase, S., Mano, T., Cui, J., Kitazawa, H., Kamiya, A., Miyazaki, S., et al. (1999). Sympathetic outflow to muscle in humans during short periods of microgravity produced by parabolic flight. *Am. J. Phys.* 277, R419–R426. doi: 10.1152/ajpregu.1999.277.2.R419

Latham, R. D., Fanton, J. W., Vernalis, M. N., Gaffney, F. A., and Crisman, R. P. (1994). Central hemodynamics in a baboon model during microgravity induced by parabolic flight. *Adv. Space Res.* 14, 349–358. doi: 10.1016/0273-1177(94)90422-7

Lathers, C. M., Charles, J. B., Elton, K. F., Holt, T. A., Mukai, C., Bennett, B. S., et al. (1989). Acute hemodynamic responses to weightlessness in humans. *J. Clin. Pharmacol.* 29, 615–627. doi: 10.1002/j.1552-4604.1989.tb03390.x

Lawley, J. S., Petersen, L. G., Howden, E. J., Sarma, S., Cornwell, W. K., Zhang, R., et al. (2017). Effect of gravity and microgravity on intracranial pressure. *J. Physiol.* 595, 2115–2127. doi: 10.1113/JP273557

Lee, A. G., Tarver, W. J., Mader, T. H., Gibson, C. R., Hart, S. F., and Otto, C. A. (2016). Neuro-ophthalmology of space flight. *J. Neuroophthalmol.* 36, 85–91. doi: 10.1097/WNO.0000000000000334

Macias, B. R., Patel, N. B., Gibson, C. R., Samuels, B. C., Laurie, S. S., Otto, C., et al. (2020). Association of long-duration spaceflight with anterior and posterior ocular structure changes in astronauts and their recovery. *JAMA Ophthalmol.* 138, 1–7. doi: 10.1001/jamaophthalmol.2020.0673

Macintyre, I. (2013). A hotbed of medical innovation: george Kellie (1770-1829), his colleagues at Leith and the Monro-Kellie doctrine. *J. Med. Biogr.* 22, 93–100. doi: 10.1177/0967772013479271

Magnano, C., Belov, P., Krawiecki, J., Hagemeier, J., Beggs, C., and Zivadinov, R. (2016). Internal jugular vein cross-sectional area enlargement is associated with aging in healthy individuals. *PLoS One* 11:e0149532. doi: 10.1371/journal.pone.0149532

Mandelbaum, A., and Ritz, E. (1996). Vena cava diameter measurement for estimation of dry weight in haemodialysis patients. *Nephrol. Dial. Transplant.* 11(Suppl. 2), 24–27. doi: 10.1093/ndt/11.supp2.24

Marshall-Goebel, K., Laurie, S. S., Alferova, I. V., Arbeille, P., Auñón-Chancellor, S. M., Ebert, D. J., et al. (2019). Assessment of jugular venous blood flow stasis and thrombosis during spaceflight. *JAMA Netw. Open* 2:e1915011. doi: 10.1001/jamanetworkopen.2019.15011

Marshall-Goebel, K., Stevens, B., Rao, C. V., Suarez, J. I., Calvillo, E., Arbeille, P., et al. (2018). Internal jugular vein volume during head-down tilt and carbon dioxide exposure in the SPACECOT study. *Aerosp. Med. Hum. Perform.* 89, 351–356. doi: 10.3357/AMHP.4934.2018

Martin, D. S., Lee, S. M. C., Matz, T. P., Westby, C. M., Scott, J. M., Stenger, M. B., et al. (2016). Internal jugular pressure increases during parabolic flight. *Phys. Rep.* 4:e13068. doi: 10.14814/phy2.13068

Martin, D. S., Lee, S. M. C., Stein, S. P., Stenger, M. B., Feiveson, A. H., Matz, T. P., et al. (2015). Report No.: NASA/TM-2015-218572. Pilot study to evaluate a novel non-invasive technology to measure peripheral venous pressure. Houston, TX: NASA Johnson Space Center.

Mukai, C. N., Lathers, C. M., Charles, J. B., Bennett, B. S., Igarashi, M., and Patel, S. (1991). Acute hemodynamic responses to weightlessness during parabolic flight. *J. Clin. Pharmacol.* 31, 993–1000. doi: 10.1002/j.1552-4604.1991.tb03662.x

Norsk, P., Foldager, N., Bonde-Petersen, F., Elmann-Larsen, B., and Johansen, T. S. (1987). Central venous pressure in humans during short periods of weightlessness. *J. Appl. Physiol.* 63, 2433–2437. doi: 10.1152/jappl.1987.63.6.2433

Nuotto, E. (1983). Psychomotor, physiological and cognitive effects of scopolamine and ephedrine in healthy man. *Eur. J. Clin. Pharmacol.* 24, 603–609. doi: 10.1007/BF00542208

Ogoh, S., Brothers, R. M., Barnes, Q., Eubank, W. L., Hawkins, M. N., Purkayastha, S., et al. (2005). The effect of changes in cardiac output on middle cerebral artery mean blood velocity at rest and during exercise. *J. Physiol.* 569, 697–704. doi: 10.1113/jphysiol.2005.095836

Ogoh, S., Hirasawa, A., Raven, P. B., Rebuffat, T., Denise, P., Lericollais, R., et al. (2015). Effect of an acute increase in central blood volume on cerebral hemodynamics. *Am. J. Phys. Regul. Integr. Comp. Phys.* 309, R902–R911. doi: 10.1152/ajpregu.00137.2015

Pantalos, G., Hart, S., Matias, J., Sharp, M. K., Watenpaugh, D. E., Buckey, J. C., et al. (1999). Venous and esophageal pressure in humans during parabolic flight. *FASEB J.* 13:A108.

Petersen, L. G., Damgaard, M., Petersen, J. C. G., and Norsk, P. (2011). Mechanisms of increase in cardiac output during acute weightlessness in humans. *J. Appl. Physiol.* 111, 407–411. doi: 10.1152/japplphysiol.01188.2010

Previtali, E., Bucciarelli, P., Passamonti, S. M., and Martinelli, I. (2011). Risk factors for venous and arterial thrombosis. *Blood Transfus.* 9, 120–138. doi: 10.2450/2010.0066-10

R Core Team. (2019). *R: A language and environment for statistical computing*. R Foundation for Statistical Computing: Vienna, Austria. Available from: https://www.R-project.org/

Rowell, L. B. (1993). *Human cardiovascular control*. New York, NY: Oxford University Press.

Sato, K., Fisher, J. P., Seifert, T., Overgaard, M., Secher, N. H., and Ogoh, S. (2012). Blood flow in internal carotid and vertebral arteries during orthostatic stress. *Exp. Physiol.* 97, 1272–1280. doi: 10.1113/expphysiol.2012.064774

Scott, J. M., Tucker, W. J., Martin, D., Crowell, J. B., Goetchius, E., Ozgur, O., et al. (2019). Association of exercise and swimming goggles with modulation of cerebro-ocular hemodynamics and pressures in a model of spaceflight-associated neuro-ocular syndrome. *JAMA Ophthalmol.* 137, 652–659. doi: 10.1001/jamaophthalmol.2019.0459

Shelhamer, M. (2016). Parabolic flight as a spaceflight analog. *J. Appl. Physiol.* 120, 1442–1448. doi: 10.1152/japplphysiol.01046.2015

Stenger, M. B., Tarver, W. J., Brunstetter, T., Gibson, C. R., Laurie, S. S., Lee, S. M. C., et al. (2017). Risk of spaceflight associated neuro-ocular syndrome (SANS). Houston, TX: National Aeronautics and Space Administration. Available at: https://humanresearchroadmap.nasa.gov/evidence/reports/SANS.pdf

Thornton, W. E., Moore, T. P., and Pool, S. L. (1987). Fluid shifts in weightlessness. *Aviat. Space Environ. Med.* 58, A86–A90.

Valdueza, J. M., von Münster, T., Hoffman, O., Schreiber, S., and Einhäupl, K. M. (2000). Postural dependency of the cerebral venous outflow. *Lancet* 355, 200–201. doi: 10.1016/S0140-6736(99)04804-7

van Campen, C. M. C., Verheugt, F. W. A., and Visser, F. C. (2018). Cerebral blood flow changes during tilt table testing in healthy volunteers, as assessed by Doppler imaging of the carotid and vertebral arteries. *Clin. Neurophysiol. Pract.* 3, 91–95. doi: 10.1016/j.cnp.2018.02.004

Videbaek, R., and Norsk, P. (1997). Atrial distension in humans during microgravity induced by parabolic flights. *J. Appl. Physiol.* 83, 1862–1866. doi: 10.1152/jappl.1997.83.6.1862

Watkins, W., Hargens, A. R., Seidl, S., Clary, E. M., and Macias, B. R. (2017). Lower-body negative pressure decreases noninvasively measured intracranial pressure and internal jugular vein cross-sectional area during head-down tilt. *J. Appl. Physiol.* 123, 260–266. doi: 10.1152/japplphysiol.00091.2017

Widjaja, D., Vandeput, S., Van Huffel, S., and Aubert, A. E. (2015). Cardiovascular autonomic adaptation in lunar and martian gravity during parabolic flight. *Eur. J. Appl. Physiol.* 115, 1205–1218. doi: 10.1007/s00421-015-3118-8

Wolthuis, R. A., Bergman, S. A., and Nicogossian, A. E. (1974). Physiological effects of locally applied reduced pressure in man. *Physiol. Rev.* 54, 566–595. doi: 10.1152/physrev.1974.54.3.566

Zhang, L. F. (2001). Vascular adaptation to microgravity: what have we learned? *J. Appl. Physiol.* 91, 2415–2430. doi: 10.1152/jappl.2001.91.6.2415

Zivadinov, R., and Chung, C. -P. (2013). Potential involvement of the extracranial venous system in central nervous system disorders and aging. *BMC Med.* 11:260. doi: 10.1186/1741-7015-11-260

Conflict of Interest: SMCL, DM, CM, SSL, BM, and NM were employed by KBR, under the Human Health and Performance Contract to NASA, during the performance of this study.

The remaining authors declare that the research was conducted in the absence of any commercial or financial relationships that could be construed as a potential conflict of interest.

frontiers in Physiology

ORIGINAL RESEARCH
published: 05 May 2020
doi: 10.3389/fphys.2020.00383

DI-5-CUFFS: Venoconstrictive Thigh Cuffs Limit Body Fluid Changes but Not Orthostatic Intolerance Induced by a 5-Day Dry Immersion

*Adrien Robin[1,2], Aline Auvinet[1], Bernard Degryse[3], Ronan Murphy[3], Marie-Pierre Bareille[4], Arnaud Beck[4], Claude Gharib[5], Guillemette Gauquelin-Koch[6], Aude Daviet[7], Françoise Larcher[7], Marc-Antoine Custaud[1,2] and Nastassia Navasiolava[1,2]**

[1] Centre de Recherche Clinique, CHU d'Angers, Angers, France, [2] Mitovasc UMR INSERM 1083-CNRS 6015, Université d'Angers, Angers, France, [3] School of Health and Human Performance, Dublin City University, Dublin, Ireland, [4] MEDES, Toulouse, France, [5] Faculté de Médecine Lyon-Est, Institut NeuroMyoGène, Université de Lyon, Lyon, France, [6] Centre National d'Etudes Spatiales, Paris, France, [7] Laboratoire de Biochimie, CHU d'Angers, Angers, France

OPEN ACCESS

Edited by:
Dieter Blottner,
Charité – Universitätsmedizin Berlin, Germany

Reviewed by:
Nandu Goswami,
Medical University of Graz, Austria
Satoshi Iwase,
Aichi Medical University, Japan

***Correspondence:**
Nastassia Navasiolava
nastassia.navasiolava@chu-angers.fr

Specialty section:
This article was submitted to Environmental, Aviation and Space Physiology, a section of the journal Frontiers in Physiology

Received: 17 January 2020
Accepted: 30 March 2020
Published: 05 May 2020

Citation:
Robin A, Auvinet A, Degryse B, Murphy R, Bareille M-P, Beck A, Gharib C, Gauquelin-Koch G, Daviet A, Larcher F, Custaud M-A and Navasiolava N (2020) DI-5-CUFFS: Venoconstrictive Thigh Cuffs Limit Body Fluid Changes but Not Orthostatic Intolerance Induced by a 5-Day Dry Immersion. Front. Physiol. 11:383. doi: 10.3389/fphys.2020.00383

Venoconstrictive thigh cuffs are used by cosmonauts to ameliorate symptoms associated with cephalad fluid shift. A ground simulation of microgravity, using the dry immersion (DI) model, was performed to assess the effects of thigh cuffs on body fluid changes and dynamics, as well as on cardiovascular deconditioning. Eighteen healthy men (25–43 years), randomly divided into two groups, (1) control group or (2) group with thigh cuffs worn 10 h/day, underwent 5-day DI. Cardiovascular responses to orthostatic challenge were evaluated using the lower body negative pressure (LBNP) test; body fluid changes were assessed by bio-impedance and hormonal assay; plasma volume evolution was estimated using hemoglobin-hematocrit; subjective tolerance was assessed by questionnaires. DI induced a decrease in plasma volume of 15–20%. Reduction in total body water of 3–6% stabilized toward the third day of DI. This reduction was derived mostly from the extracellular compartment. During the acute phase of DI, thigh cuffs limited the decrease in renin and the increase in N-terminal prohormone of brain natriuretic peptide (NT-proBNP), the loss in total body water, and tended to limit the loss in calf volume, extracellular volume and plasma volume. At the later stable phase of DI, a moderate protective effect of thigh cuffs remained evident on the body fluids. Orthostatic tolerance time dropped after DI without significant difference between groups. Thigh cuff countermeasure slowed down and limited the loss of body water and tended to limit plasma loss induced by DI. These observed physiological responses persisted during periods when thigh cuffs were removed. However, thigh cuffs did not counteract decreased tolerance to orthostatic challenge.

Keywords: simulated microgravity, thigh cuffs, countermeasure, fluid shift, volemia, bio-impedance, orthostatic tolerance, LBNP

Abbreviations: BP, blood pressure; DI, dry immersion; DPV, percent change in plasma volume; ECF, extracellular fluid; HDBR, head-down bed rest; HR, heart rate; hs-CRP, high-sensitivity C-reactive protein; IBI, inter-beat interval; ICF, intracellular fluid; LBNP, lower body negative pressure; SBRS, spontaneous baroreflex sensitivity; SV, stroke volume; TBW, total body water; VO_2peak, peak oxygen uptake.

INTRODUCTION

Dry immersion involves immersing the subject in thermoneutral water covered with an elastic waterproof fabric. Subject is freely suspended in the water mass but remains dry (**Figure 1**). Together with HDBR, DI has been widely reported to be an effective ground-based model to reproduce and study most of the effects of microgravity, including physical inactivity and fluid centralization (Navasiolava et al., 2011; Tomilovskaya et al., 2019). Effects on fluid transfer and fluid compartments are pronounced and rapid with DI (Leach Huntoon et al., 1998; Navasiolava et al., 2011; Coupe et al., 2013). Orthostatic tolerance substantially decreases (Navasiolava et al., 2011; De Abreu et al., 2017). Hypovolemia reaches 15–17%, similar to that observed under actual microgravity (Leach Huntoon et al., 1998; Navasiolava et al., 2011; Coupe et al., 2013; De Abreu et al., 2017), but higher than that observed under HDBR.

Visual impairment and particular neuro-ocular findings, known as spaceflight associated neuro-ocular syndrome (SANS), represent an issue for future long-term manned missions. Current paradigm relates them with cephalad and orbital fluid transfer and chronic changes in intracranial pressure (Taibbi et al., 2016; Balasubramanian et al., 2018; Lee et al., 2018; Goswami et al., 2019). It has been shown that changes in optic nerve sheath diameter (ONSD), a surrogate marker of intracranial pressure, are pronounced under DI (Kermorgant et al., 2017), with increase in ONSD about 30% throughout 3-day DI.

Testing countermeasures against fluid transfer is a priority in preparation of deep space missions, to fight not only cardiovascular deconditioning, but also SANS. DI model is particularly well adapted for a rapid evaluation of countermeasures against fluid transfer and its consequences.

Venoconstrictive thigh cuffs ("Bracelets") are empirical countermeasure used by Russian cosmonauts to sequester fluids in the lower limbs and mitigate the subjective sensation of head congestion during spaceflight. They represent strips containing elastic and non-elastic segments to conform to the shape of the upper thigh, placed tightly around thighs (**Figure 2**). They are recommended for onboard application up to 10 h per day without interruption (removed for sleep and exercise), or, if uncomfortable for legs, by periods of 2–3 h wearing/20–30 min rest. Thigh cuffs are effective in alleviating the symptoms associated with cephalad fluid shift in the early hours and days in space (Arbeille et al., 1999; Fomina et al., 2004). They were first used in 1984 during the 232-day flight and have been implemented and employed as a standard countermeasure since 1990 (Arbeille et al., 1999). During short-term flights, thigh cuffs improved cervico-cephalic hemodynamics with an observed reduction of venous stasis (Fomina et al., 2004). Some effects of thigh cuffs have already been studied during a 7-day HDBR protocol (Custaud et al., 2000; Millet et al., 2000; Pavy-Le Traon et al., 2001). Their use for 10 h per day limited plasma volume loss and baroreflex impairment, but was not sufficient to prevent orthostatic intolerance as evaluated by a 10-minute stand test.

Thus, for the present experiment we have chosen the model of DI because of its strong and rapid effects on fluid transfer, in order to further study and evaluate the efficacy of thigh cuffs in terms of body fluid compartments and cardiovascular impairment.

We aimed to test the hypothesis that intermittent application of thigh cuffs during DI, by counteracting fluid transfer, would

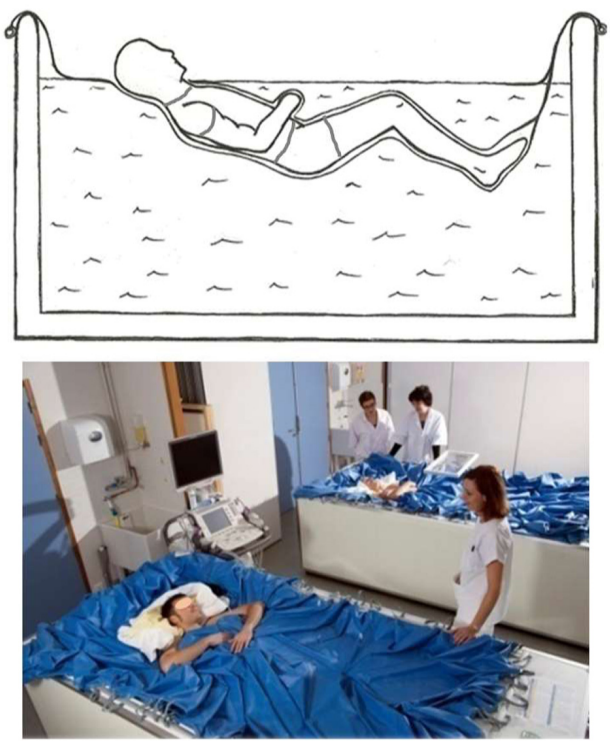

FIGURE 1 | Dry immersion method: the subject is immersed in thermoneutral water covered with an elastic waterproof fabric (Photo MEDES).

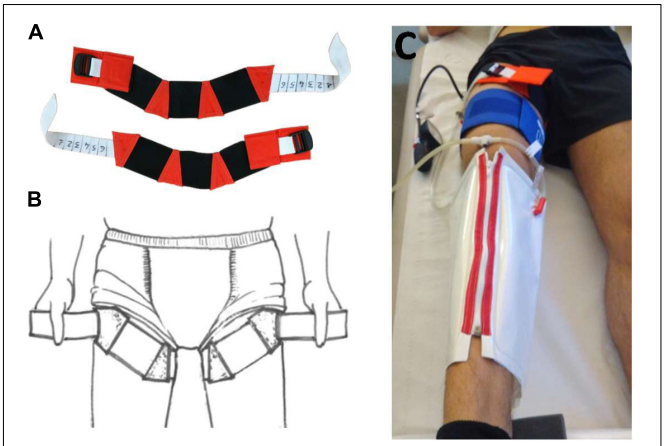

FIGURE 2 | Thigh cuffs countermeasure. **(A)** Venoconstrictive thigh cuffs ("Bracelets"), strips containing elastic and non-elastic segments to conform to the shape of the upper thigh. **(B)** schema of thigh cuffs wearing. **(C)** individual adjustment of thigh cuffs with plethysmography performed at B-2 (Photo MEDES).

limit body fluid changes, orthostatic intolerance and general cardiovascular deconditioning, induced by a 5-day DI.

MATERIALS AND METHODS

Subjects

Twenty healthy men were recruited. Two subjects withdrew before B-5 for reasons unrelated to the protocol. A total of eighteen subjects were included in the study and randomly divided at B-2 into Control or Cuffs group (9/9 split). All subjects were informed about the experimental procedures and gave their written consent. The experimental protocol conformed to the standards set by the Declaration of Helsinki and was approved by the local Ethic Committee (CPP Est III: October 2, 2018, n° ID RCB 2018-A01470-55) and French Health Authorities (ANSM: August 13, 2018). ClinicalTrials.gov Identifier: NCT03915457.

Baseline characteristics are detailed in **Table 1**. There was no significant difference between groups at baseline.

General Protocol, Dry Immersion Organization, Thigh Cuff Countermeasure

The study was conducted at the MEDES space clinic, Toulouse, France from 19/11/2018 to 23/03/2019. Ten scientific teams took part to this experiment to study the main physiological functions. The data collected by our team and presented in this paper focus on body fluids and cardiovascular deconditioning.

Subjects arrived in the evening of B-5 and left in the morning of R + 2. The experimental protocol included 4 days of ambulatory baseline measurements before immersion (B-4 to B-1), 5 days (120 h) of dry immersion (DI-1 to DI-5) and 2 days of ambulatory recovery (R0, R + 1).

Of note, DI experiments are performed since 1975, and until 2015 they included a short daily raise for personal hygiene procedures and weighing (Navasiolava et al., 2011). Importantly, short daily orthostatic stimulation could act as countermeasure for cardiovascular deconditioning. In order to eliminate this unwanted effect, "strict" DI protocol does not permit subjects to rise at all, and a 6° head-down position is maintained when the subjects are out of water, as is observed in strict bedrest protocols. We've chosen to perform strict DI which seems closer to actual flight in terms of cardiovascular deconditioning (more pronounced orthostatic intolerance), and similar to non-strict DI and flight in terms of hypovolemia.

Subjects randomized to Cuffs group wore the thigh cuffs during the 5 days of DI, from 10:00 to 18:00 at DI-1 and from 08:00 to 18:00 at DI-2 - DI-5. At DI-1, thigh cuffs were put on immediately prior to the onset of immersion at 10:00. Thigh cuffs were adapted to each subject to have the same effects on lower-limb distensibility as at counter pressure of about 30 mmHg. Individual adjustment was determined with calf plethysmography performed in the supine position at B-2 (**Figure 2**). 30 mmHg was selected, which is also the initial thigh cuff pressure used by cosmonauts and the pressure tested and evaluated during a 7-day HDBR held at MEDES in 1997–1998 (Arbeille et al., 1999; Custaud et al., 2000; Millet et al., 2000; Pavy-Le Traon et al., 2001).

General protocol of strict DI was conducted according to methodology detailed in De Abreu et al. (2017). Two subjects, one Control and one Cuffs, underwent DI simultaneously in the same room, in two separate baths (except for two subjects, one Control and one Cuffs, who had no test partner). Thermoneutral water temperature was continuously maintained. Light-off period was set at 23:00–07:00. Daily hygiene, weighing and some specific measurements required extraction from the bath. During these out-of-bath periods, subjects maintained the 6° head-down position. Total out-of-bath supine time for the 120 h of immersion was 9.7 ± 1.3 h. On DI-1–DI-4 out-of-bath time was 1.1 ± 0.6 h/day. On DI-5 out-of-bath time was 5.3 ± 1.1 h, because of muscle biopsy and MRI procedures. Otherwise, during DI, subjects remained immersed in a supine position for all activities and were continuously observed by video monitoring. Body weight, BP, HR and tympanic body temperature were measured daily. The frames of adequate water intake were fixed at 35–60 ml/kg/day; within these frames water intake throughout the protocol was *ad libitum*. The meals of each experiment day were identical for all participants and dietary intake was individually tailored and controlled during the study. A timeline schematic of different aspects of our study is presented in **Figure 3**.

Daily Questionnaires

Estimation was performed each morning and evening from B-1 to R0. Visual analog scale 0-to-10 was used to assess General discomfort, Back pain, Quality of night sleeping and Discomfort at thigh level. Scoring scheme of 0-to-5 was used for "Fluid shift" complaints -face swelling sensation, nasal congestion, impaired vision.

Blood Studies

Antecubital venous blood samples were collected before (B-1, DI-1-morning) and during immersion (DI-1-evening, DI-3, DI-5). Morning blood sampling was performed before breakfast. Plasma and serum samples were analyzed for electrolytes (Na^+, K^+, Cl^-), glucose, proteins, creatinine, osmolality, high-sensitivity CRP, renin, NT-proBNP, triglycerides, and cholesterol. Hemoglobin (Hb) and hematocrit (Hct) were assessed on DI-1-morning, DI-1-evening, DI-3-morning, DI-5-morning, DI-5-evening, R0-morning (in the evening - with cuffs still in place for Cuffs group).

As the minimal detectable level for NT-proBNP was 35 ng/L and for hs-CRP was 0.2 mg/L, results less than minimal detectable level were taken for half minimal value.

Plasma Volume Evolution

Percent change in plasma volume on DI-1-evening, DI-3-morning, DI-5-morning, DI-5-evening, R0-morning vs. baseline (DI-1-morning before the onset of immersion) was estimated using Hb and Hct count (Dill and Costill formula):

$$\mathrm{DPV}(\%) = 100 \times [\mathrm{HbB}(1 - 0.01\mathrm{Hcti})]/ [\mathrm{Hbi}(1 - 0.01\mathrm{HctB})] - 100$$

TABLE 1 | Baseline group characteristics at B-2.

	Age (y)	Height (cm)	Weight (kg)	BMI (kg/m^2)	VO_2peak (ml/min/kg)	Morning HR (bpm)	Morning SBP (mmHg)	Morning DBP (mmHg)
Control (n = 9)	33.9 ± 7.1	176 ± 6	73.9 ± 7.5	23.9 ± 1.7	46.5 ± 8.1	57 ± 6	115 ± 11	68 ± 5
Cuffs (n = 9)	34.1 ± 3.7	180 ± 4	74.3 ± 8.8	22.7 ± 1.8	46.9 ± 5.8	58 ± 8	117 ± 10	68 ± 9

Values are mean ± SD. Unpaired T-test did not reveal significant differences between groups.

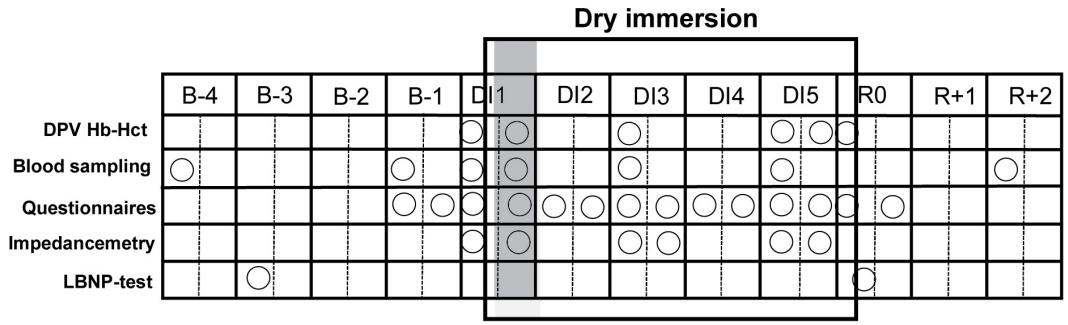

FIGURE 3 | Schematic outlining of dry immersion method and the experimental protocol. B-4 - B-1, baseline days prior to immersion; DI-1–DI-5, days of dry immersion; R0–R + 2, recovery days; circles, data collection points; DPV, percent change in plasma volume; shadowed, first day of immersion.

Additionally DPV vs. B-1 baseline was calculated for DI-1-evening, DI-3 and DI-5 using plasma protein count (Coupe et al., 2013):

$$\mathrm{DPV}(\%) = 100 \times [\mathrm{ProtB}/\mathrm{Proti}] - 100$$

Urine Sampling

Urine pools were collected throughout the protocol according to 16 h:8 h light on/off periods (07:00–23:00 pool for "day" and 23:00–07:00 pool for "night"), and urine volume was measured. Urine samples were analyzed for osmolality. Free water and osmolal clearances were calculated for days B-2, DI-2, DI-4, using the data on 24-hour urine excretion (combined day- and night-pools) from these days and the morning blood samples from the next days (i.e., B-1, DI-3, DI-5). For DI-1, free water- and osmolal clearances were calculated using urine sample from "day" urine pool of DI-1 and blood sample of the evening of DI-1.

VO_2peak Test

Peak oxygen uptake bicycle ergometer test was performed in the evening of B-2 and R0. Peak oxygen uptake, peak power and peak HR were recorded.

Lower Body Negative Pressure Test

The LBNP test (as an orthostatic-like stimulation for cardiovascular system) had been chosen to assess cardiovascular deconditioning and tolerance to orthostatic challenge before and after immersion. Although not exactly an orthostatic challenge, LBNP induces fluid shifts and related hemodynamic responses similar to head-up tilt due to fluid translocation to the lower part of the body. LBNP has the advantage that, unlike actual orthostasis, it does not induce otolith Gz stimulation and thus allows for the study of the isolated contribution of central hypovolemia induced by orthostatic challenges (Goswami et al., 2019).

This test was conducted in the morning in a temperature-controlled room (range 22–26°C) on B-3 and immediately following DI on R0 (first orthostatic challenge after DI). The subject remained supine for 20 min, then supine baseline data were recorded for 5 min. After that, LBNP was applied with steps of −10 mmHg every 3 min. The test was considered finished upon accomplishing a LBNP step of −60 mmHg. Test was stopped earlier upon appearance of pre-syncopal signs, request to stop, systolic BP $\leq$ 80 mmHg, HR $<$ 50 bpm or $>$ 170 bpm.

During the LBNP test, finger blood pressure (Nexfin, BMeye, United States) and standard ECG (Biopac, ECG 100C, United States) were recorded continuously. Orthostatic tolerance time was measured. HR, systolic and diastolic BP, SV, SBRS were estimated as detailed in De Abreu et al. (2017). To estimate hemodynamic and baroreflex responses we've taken 3 min of stable baseline recording and the totality of each 3-minute LBNP step.

In addition, HR and BP were monitored independently of data collection with an ECG monitor and an automated sphygmomanometer.

Bio-Impedancemetry

Bio-impedance measurements by Bodystat QuadScan 4000 (Bodystat Ltd., Isle of Man, United Kingdom) were performed supine out-of-bath in the morning before application of cuffs and in the evening with cuffs still in place (Cuffs group) at DI-1, DI-3, and DI-5. Baseline measurement was DI-1-morning before the onset of immersion. Subjects were weighed prior to each measurement. Measurements were repeated twice, with mean values being calculated. To assure the same electrodes placement

for subsequent measurements, their positions at wrist, ankle and knee were marked on the skin.

Fluid Compartments

Whole body wrist-ankle measurement was used to estimate TBW, ECF, and ICF.

Calf Volume Evolution

Segmental bio-impedancemetry was used to estimate the change in lower leg total water approximating change in calf volume. Current source electrodes were placed above patella and at metatarsus. Voltage detection electrodes were placed immediately below patella and at the ankle. Resistance at frequency of 50 kHz was measured. Change in total water was calculated as a relative change of impedance index L^2/R, where L is lower leg length (constant during protocol) and R is resistance (Organ et al., 1994).

Statistical Analysis

Data are presented as mean ± SD. The overall effect of immersion and the effect of the countermeasure were tested with two-way repeated-measures ANOVA, with day of measurement as the within-subject factor and group as the between-subject factor. Statistically significant differences were further analyzed by pairwise comparisons with Sidak correction for multiple comparisons. Multiplicity adjusted P value ≤ 0.05 was considered significant. Analyses were performed using Prism GraphPad 8.1.2.

RESULTS

General Data, Body Weight

HR, BP and body temperature remained within normal limits throughout the protocol.

In the evening of DI-1 (8 h after the onset of DI) recorded weight loss was 0.8 ± 0.9 kg for Controls and 0.4 ± 0.2 kg for Cuffs, and in the morning of DI-2 recorded weight loss was 1.3 ± 0.4 kg for Controls and 1.4 ± 0.3kg for Cuffs, without significant difference between groups. At the end of DI (morning of R0) body weight decreased by approximately 2 kg (2.5 ± 0.3% in control group and 2.6 ± 0.6% in cuffs group) vs. morning of DI-1, without significant difference between groups.

Daily Questionnaires

Reported data for the daily questionnaires are presented in **Figure 4**. We observed important inter-subject variance in auto-reported questionnaires. Globally, sleep quality dropped about 4 points at the first night under DI (from 7–8 to 3–4 out of 10), then partially restored up to 6 points beginning with the 3rd night. Similarly, general discomfort and back pain increased about 3 points for the first 2 days. Subjects did not report substantial discomfort at thigh level. Thigh cuffs did not affect or modify sleep quality, general discomfort, back pain and discomfort at thigh level.

Fluid Shift Complaints

Face swelling sensation during DI with intensity of 1–2 out of 5 was reported by 4 Control subjects and 1 Cuffs subject, impaired vision with intensity of 1–2 out of 5 - by 3 Control subjects and 1 Cuffs subject. Nasal congestion score (0-to-5) was 0.4 ± 0.4 in Cuffs and 0.7 ± 0.8 in Controls at baseline, and 0.4 ± 0.5 in Cuffs and 0.6 ± 0.8 in Controls under DI, unmodified by immersion. During the first 12 h of DI only one Control subject reported slight face puffiness (already documented at the morning of B-1), impaired vision was not observed, and nasal congestion was the same as in the morning just prior to DI.

Cardiovascular Deconditioning

Tolerance to LBNP Challenge

We observed pronounced decrease in tolerance to LBNP after DI, with tolerance time drop from 17.4 ± 1.4 min at B-3 to 13.8 ± 4.1 min at R0 for Controls, and from 17.3 ± 1.2 min to 14.3 ± 2.6 min for Cuffs, without significant difference between groups (**Figure 5A**).

Tolerance for different LBNP steps is shown in **Figure 5B**. Before DI all subjects finished 40mmHg LBNP step; 7 Controls and 6 Cuffs accomplished the totality of 6 steps. Immediately after DI, 3 Controls and 2 Cuffs were intolerant to 40 mmHg step; only 2 subjects (Controls) finished the totality of 6 steps.

Resting HR and BP

Resting supine HR and BP (both systolic and diastolic) after DI were significantly increased ∼11 bpm and ∼8 mmHg, respectively (R0 vs. B-3), without significant difference between groups.

HR and BP in Response to LBNP

At R0 HR to−10 mmHg step increased ∼15 bpm, and HR to the last LBNP step tolerated both before and after immersion increased ∼40 bpm vs. B-3, similarly in both groups. DBP, but not SBP, was slightly increased during the last tolerated step.

IBI, SV, SBRS Response to LBNP

Variability in number of non-finishers at different LBNP steps limits the utility of statistics, so we've chosen to show just individual data (**Figure 6**). LBNP steps led to the expected decreases in IBI, SV, and SBRS, more pronounced after immersion and without marked differences between groups.

VO_2peak Test

Peak oxygen uptake decreased approximately 3 ml/min/kg (by 6 ± 11% in Controls and by 7 ± 8% in Cuffs) at the evening of R0 vs. evening of B-2. Peak power was about 10% reduced following DI. Peak HR was not significantly modified by DI. There was no significant difference between groups in VO_2peak, peak power and peak HR before or after DI.

Plasma Volume Evolution

Data are shown in **Figure 7**. Within the first 8h of immersion, DPV determined by Hb and Hct count decreased by approximately 9% in Controls and approximately 7% in Cuffs. Globally, immersion induced decrease in plasma volume

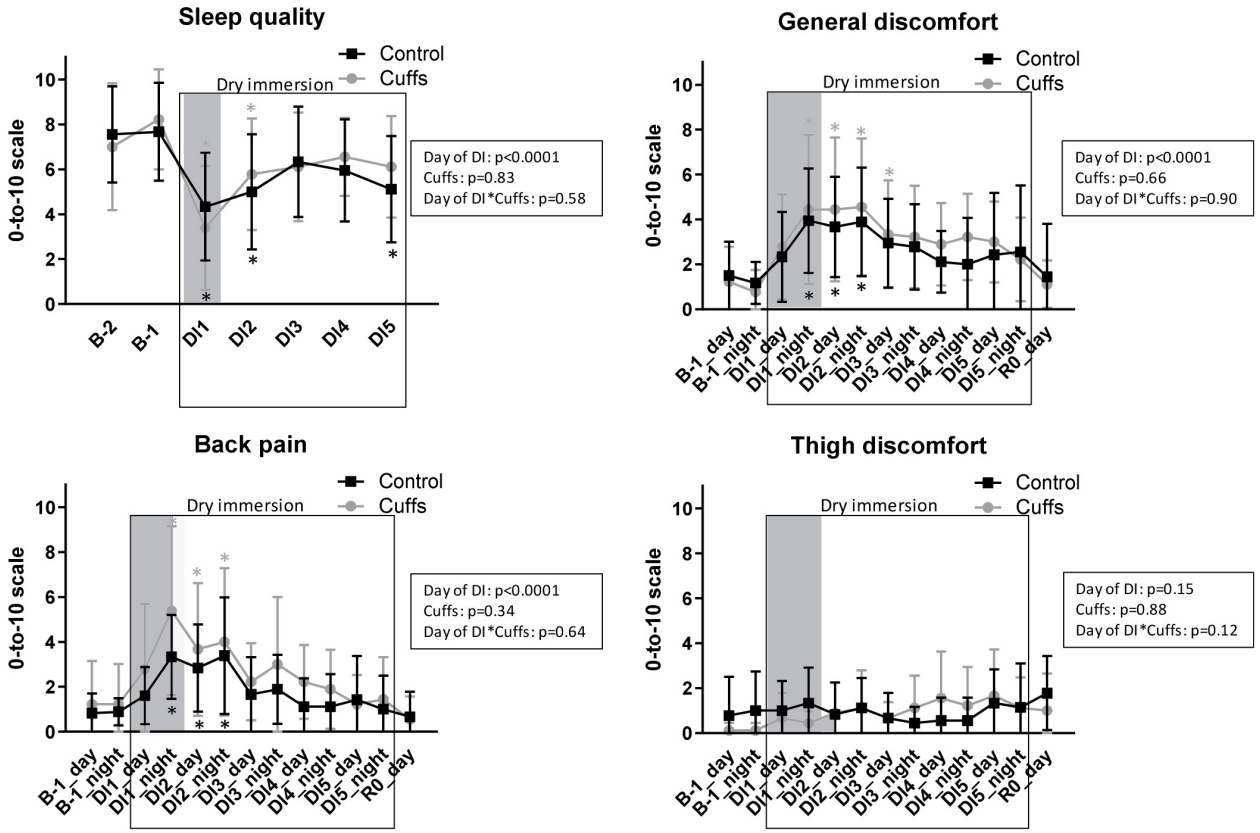

FIGURE 4 | Night sleep quality, general discomfort, back pain and discomfort at the thigh level as reported by subjects. Mean ± SD. *$p < 0.05$ vs. B-1. Shadowed, first 24 h of immersion.

of 15–20% ($p < 0.0001$), while thigh cuffs tended to limit this plasma volume loss by 1/4–1/3 ($p = 0.09$). Some restoration was observed at the evening of DI-5 (DPV −12 ± 6% for Controls and −7 ± 5% for Cuffs), probably related to prolonged stay out-of-bath on this day.

Plasma Volume Estimation Using Protein Count

Plasma protein count revealed no change in plasma volume within the first 8 h of immersion, with subsequent reduction in Controls (8 ± 5% at the morning of DI-3 and 4 ± 6% at the morning of DI-5), but not in Cuffs (**Figure 8**). Plasma volume modifications estimated via Hb-Hct and protein count showed correlation with Pearson $r = 0.55$ ($p < 0.0001$).

Fluid Compartments

Data are shown in **Figure 9**. At the first evening of immersion TBW and ECF significantly decreased about 2–5% in Controls, and slightly non-significantly decreased in Cuffs (TBW loss in Controls 1.3 ± 0.7 L, in Cuffs 0.5 ± 0.7 L; ECF loss in Controls 0.6 ± 0.3 L, in Cuffs 0.3 ± 0.3 L). ICF was not significantly modified initially. Reduction in TBW and ECF was stabilized in Controls toward the third day of DI at 3–6% level (TBW loss 1.5–2L, ECF loss 0.7–0.8 L). Thigh cuffs statistically significantly limited losses in TBW by ∼1L (0.5–1.1 L loss) and ECF by ∼ 0.5L (0.2–0.5 L loss).

Calf Volume Evolution

Calf volume evolution is shown in **Figure 10**. At the first evening of immersion Controls had a 5 ± 2% decrease, and Cuffs a 2 ± 4% decrease vs. baseline (morning of DI-1). Later on, both groups showed 3–5% decrease in calf volume under immersion. Substantial difference between groups was observed at the evening of DI-5.

Day- and Night-Time Diuresis and Urinary Osmolality

Under DI, daytime diuresis in Cuffs was slightly less and urine slightly more concentrated than in Controls. In contrast, night-time diuresis in Cuffs was slightly more than in Controls and urine slightly less concentrated (**Figure 11**). However these differences between groups did not reach statistical significance.

Free Water- and Osmolal Clearances

At first day of immersion free water clearance became positive and increased only in Controls, whereas osmolal clearance was 2-times increased in both groups (**Figure 12**). Later on, free water

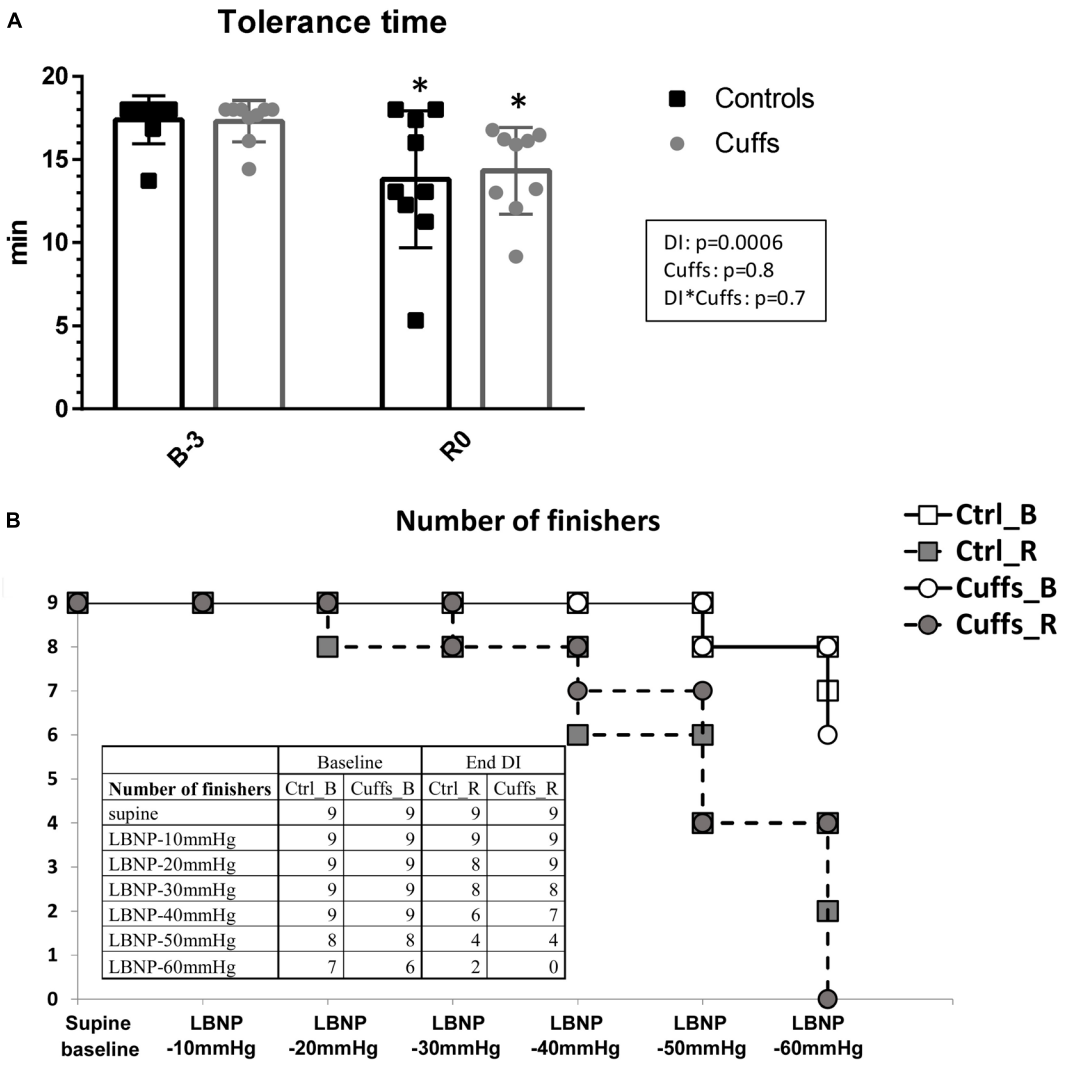

	Baseline		End DI	
Number of finishers	Ctrl_B	Cuffs_B	Ctrl_R	Cuffs_R
supine	9	9	9	9
LBNP-10mmHg	9	9	9	9
LBNP-20mmHg	9	9	8	9
LBNP-30mmHg	9	9	8	8
LBNP-40mmHg	9	9	6	7
LBNP-50mmHg	8	8	4	4
LBNP-60mmHg	7	6	2	0

FIGURE 5 | Tolerance time to LBNP challenge **(A)** and number of finishers for different LBNP steps **(B)** before and immediately after 5-day DI. Mean ± SD. *$p < 0.05$ vs. B-3.

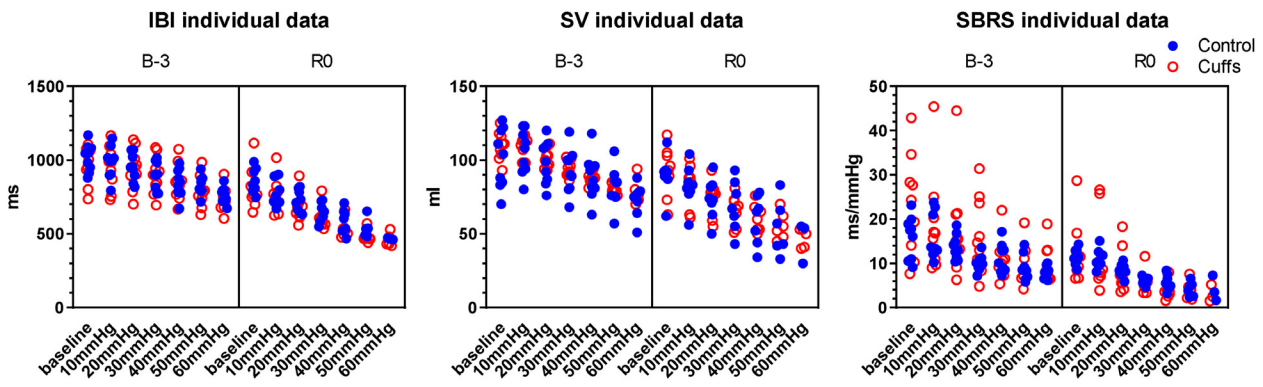

FIGURE 6 | Responses to LBNP-test before and after immersion: inter-beat interval (IBI), stroke volume (SV), spontaneous baroreflex sensitivity (SBRS). Individual data.

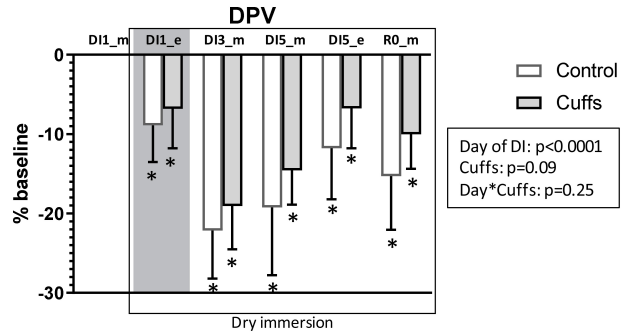

FIGURE 7 | Variations in plasma volume in percentage of baseline, calculated by hemoglobin and hematocrit count. Mean ± SD. *$p < 0.05$ vs. baseline. Shadowed, 8 h after the onset of immersion.

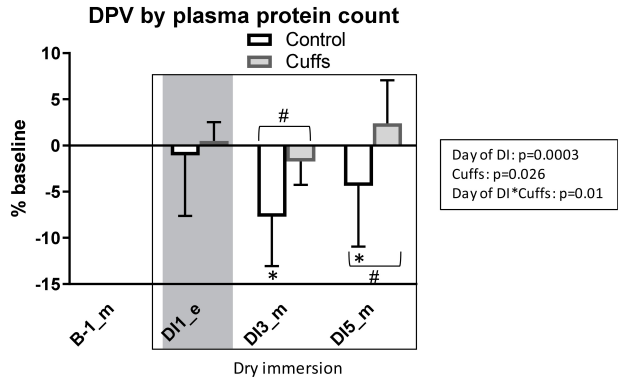

FIGURE 8 | Variations in plasma volume in percentage of baseline, estimated by plasma proteins count. Mean ± SD. *$p < 0.05$ vs. baseline; #$p < 0.05$ vs. Control. Shadowed, 8 h after the onset of immersion.

clearance did not differ from baseline, and osmolal clearance was slightly increased (significantly at DI-4).

Cardiovascular Hormones Regulating Volemia

After the first 8 h of DI, at the evening of DI-1, NT-proBNP was significantly increased and renin was significantly decreased in Controls but not in Cuffs (**Figure 13**). At the morning timepoints of DI-3 and DI-5 (14 h without cuffs) groups did not differ.

Blood Studies

Blood Biochemistry

Blood biochemistry remained within normal values at all measurements; hs-CRP showed a stable low level. Blood osmolality remained unmodified. DI was accompanied by a significant increase in blood proteins in Controls but not in Cuffs beginning with DI-3. Total cholesterol and LDL cholesterol expectedly increased slightly under immersion (**Table 2**). DI is systematically accompanied by such changes in lipid profile (Navasiolava et al., 2011; De Abreu et al., 2017; Tomilovskaya et al., 2019), seemingly due to inactivity-related metabolic impairment (De Abreu et al., 2017).

DISCUSSION

Thigh cuff countermeasure slowed down and lightened thoracic fluid shift and the effects of DI on body fluids. During the acute phase of DI, thigh cuffs limited the decrease in renin and the increase in NT-proBNP, the loss in TBW, and tended to limit the loss in calf volume, extracellular volume and plasma volume. At the later stable phase of DI, a moderate effect of thigh cuffs remained evident on the body fluids, with limitation of TBW loss and tendency to limit plasma volume loss. However orthostatic tolerance time dropped after DI without significant difference between groups.

Global Tolerance

This 5-day immersion was relatively well tolerated, as it is usually described for DI studies (Navasiolava et al., 2011; Tomilovskaya et al., 2019). All 18 subjects accomplished the protocol. Most of subjects expectedly experienced backache, general discomfort and sleep decline at the beginning of DI. First night was the most difficult, but by the third day symptoms were alleviated. Cuffs wearing did not cause notable discomfort at the thigh level and did not modify general state.

Body Fluids Changes During DI and Thigh Cuffs Effects

Our DI induced acute expansion of central volume within the first hours, followed by a steady hypovolemic state.

First 8–12 h of DI were accompanied by acute increase in NT-proBNP together with renin suppression, increase in free water and osmolal clearances, 9% decrease in plasma volume, 1.3 L loss in TBW, 0.6 L loss in ECF, and an about 5% decrease in calf volume. Such alterations are expected at the beginning of immersion, when, with hydrostatic compression and increased water and sodium excretion, body fluids decrease, especially in the plasma and extracellular compartments (Leach Huntoon et al., 1998; Navasiolava et al., 2011; Coupe et al., 2013). Thigh cuffs lightened these initial alterations by sequestrating fluids in lower limbs (Arbeille et al., 1999). Alleviation of central hypervolemia was seen as diminution in acute hormonal responses in Cuffs group, as well as non-increase in free water clearance (only Control group excreted diluted urine at the first day of DI).

At the third day of immersion a novel steady state of body fluids is established with lowered fluid content, as it is typically observed under DI (Leach Huntoon et al., 1998; Navasiolava et al., 2011; Coupe et al., 2013). In the group with cuffs a decrease in plasma volume, in TBW and in extracellular water tends to be smaller than in the control group. Cuffs effects remained visible in periods when cuffs were removed, as evidenced by persistent difference in TBW and ECF between Controls and Cuffs both in the morning of DI-3 (overnight without cuffs) and in the evening of DI-3 (10 h with cuffs).

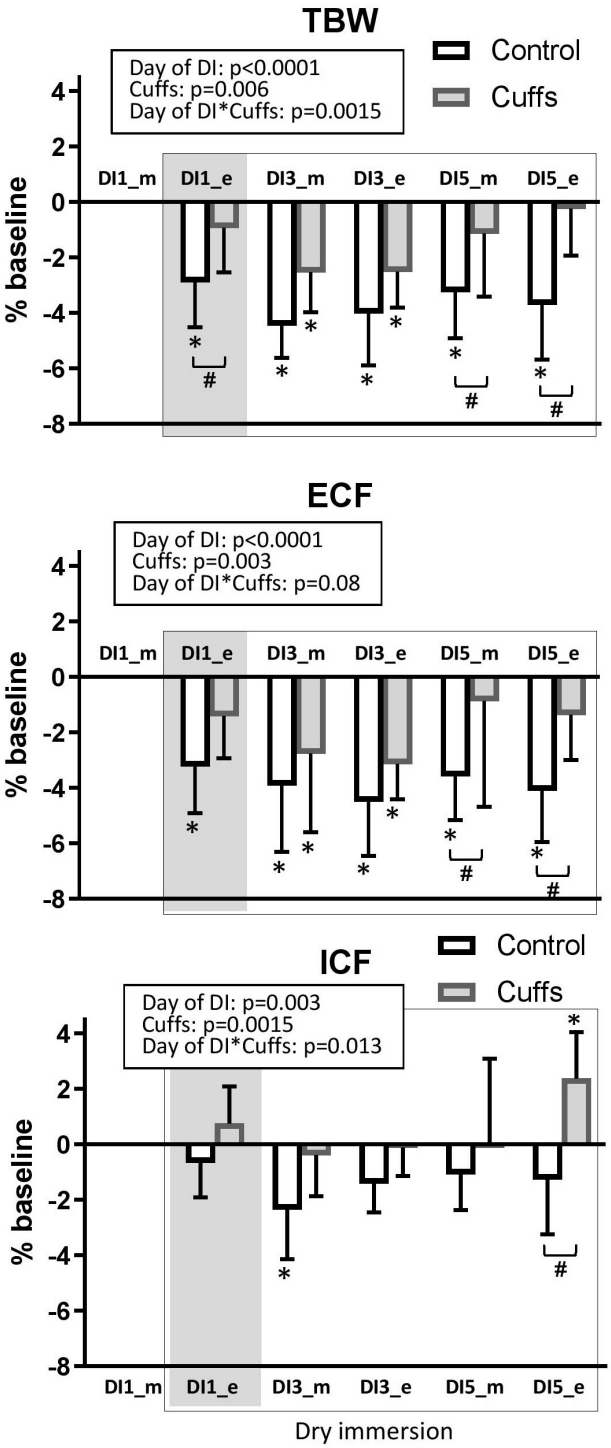

FIGURE 9 | Variations of fluid compartments. Mean ± SD. *$p < 0.05$ vs. baseline, #$p < 0.05$ vs. Control. Shadowed, 8 h after the onset of immersion.

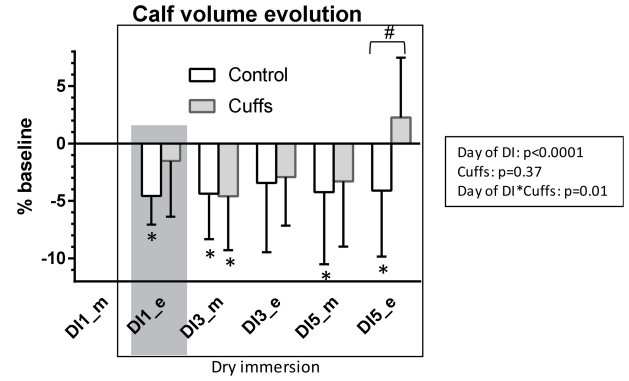

FIGURE 10 | Variations in calf volume. Mean ± SD. *$p < 0.05$ vs. baseline; #$p < 0.05$ vs. Control. Shadowed, 8 h after the onset of immersion.

However, cuffs effects are obviously more pronounced during the day (with cuffs) and partially suppressed during the night, as evidenced by higher diuresis levels each day of DI in the control group whereas it was higher in the group with cuffs in the night.

Globally, sequestrating effect of cuffs alleviated but not completely prevented body fluid changes induced by DI. Counter pressure of 30 mmHg seems not sufficient to completely re-create the effect of periodic "cardiovascular" gravity under immersion. Centralizing effect of continuous hydrostatic compression induced by DI is very strong, as evidenced by the absence of significant differences in calf volume between groups at the evening of DI-3, after 10 h with cuffs.

Interestingly, estimation of plasma volume loss by proteinemia exhibited a much smaller hypovolemia in contrast to Hb-Hct, apparently due to the partial protein transfer to the interstitial space. This transfer might increase the oncotic pressure of interstitial fluid and thus limit its loss (Chaika and Balakhovskii, 1982; Coupe et al., 2013). This transfer is significantly more important in the group with cuffs. Wearing cuffs may facilitate this transfer of proteins to the interstitial sector at the lower limb level. Surprisingly, at the evening of DI-5, calf volume increases in the group with cuffs in contrast to DI-3 evening. Our hypothesis is that during DI- 5 the time out of bath (5.3 ± 1.1 h) was significantly more important that the other days of DI because of other protocols implemented that day, especially the MRI procedure. During that day the cuffs effect, less counteracted by squeezing force, became unmasked and more evident.

Fluid Shift Complaints Are Very Moderate; Thigh Cuffs Lessen Fluid Shift Complaints

Literature mentions that fluid shift complaints occur under DI (Navasiolava et al., 2011; Tomilovskaya et al., 2019). However, systematic data on their occurrence and intensity are lacking. In our study we've undertaken a systematic report. Surprisingly, "cephalad" fluid shift complaints were very mild under our DI. Less than half of Controls noted puffy

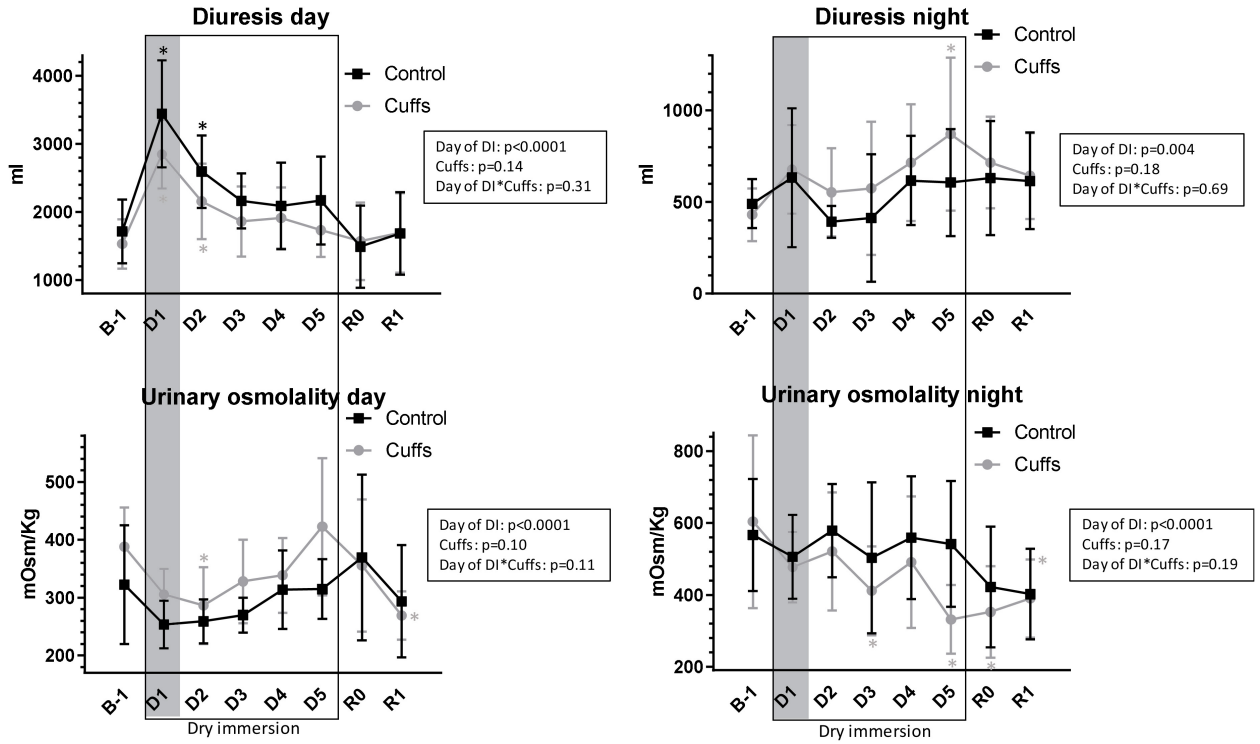

FIGURE 11 | Daytime and night-time diuresis and urinary osmolality. Mean ± SD. *$p < 0.05$ vs. B-1. Shadowed, first 24 h of immersion.

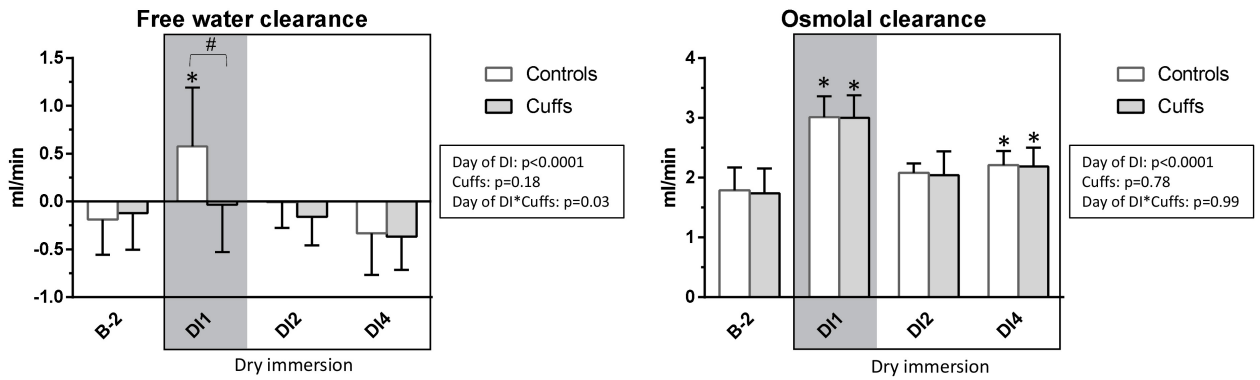

FIGURE 12 | Free water- and osmolal clearances. Mean ± SD. *$p < 0.05$ vs. baseline; #$p < 0.05$ vs. Control. Shadowed, first ~12 h of immersion.

face sensation; nasal congestion score was not substantially modified under DI. For comparison, 7-day HDBR without countermeasure was accompanied by fluid shift complaints in 5 out of 8 subjects (Pavy-Le Traon et al., 2001). A possible mechanistic reason being that DI centralizes fluids rather than pooling them to the head as with HDBR [though jugular veins congestion is present at the beginning of DI (Arbeille et al., 2017)]. Another possibility is that fluid loss is very sharp in DI compared to HDBR, with a rapid transition to new homeostatic steady state within 24–48 h (Leach Huntoon et al., 1998; Navasiolava et al., 2011; Coupe et al., 2013). Only one Cuffs (vs. 4 Controls) noted puffy face, suggesting efficiency of thigh cuffs in preventing subjective discomfort.

Cardiovascular Deconditioning and Orthostatic Tolerance; No Effect of Thigh Cuffs

Dry immersion induced expected marked cardiovascular deconditioning observed as decrease in time of tolerance to orthostatic stimulus, increased tachycardia, together with reduction in SV and SBRS both at supine rest and in response to LBNP steps, and diminished exercise capacity (VO_2peak and peak power). DI (Iarullin et al., 1987;

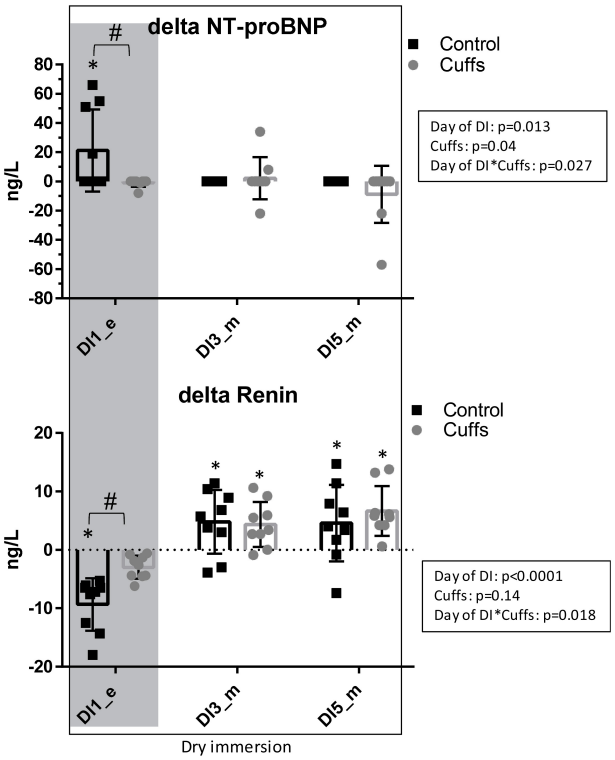

FIGURE 13 | Variations in blood NT-proBNP and Renin, the difference between values under immersion and B-1 baseline. Mean ± SD. *$p < 0.05$ vs. baseline; #$p < 0.05$ vs. Control. Shadowed, 8 h after the onset of immersion.

Miwa et al., 1997; Iwase et al., 2000; Navasiolava et al., 2011; Coupe et al., 2013) and especially strict DI (De Abreu et al., 2017) are acknowledged as effective experimental modalities for enhanced cardiovascular deconditioning. Thigh cuffs countermeasure did not substantially modify this deconditioning and particularly was unable to improve cardiovascular responses to the LBNP test after immersion.

Interestingly, Fomina et al. (2004) found that thigh cuffs use for 8–9 h daily in short-term missions up to 1 month notably improved cardiovascular adaptation to microgravity with decrease in initial subjective discomfort and cervico-cephalic venous stasis estimated by echography. However, cuffs had no effect on post-flight orthostatic tolerance evaluated by active and passive testing (n = 6 cosmonauts with cuffs and 7 without cuffs). Furthermore, thigh cuffs use in 7-day HDBR for 10 h daily did not improve orthostatic tolerance (Custaud et al., 2000). However the 10-minute stand test applied in that study could lack the sensitivity to detect the potential modest thigh cuffs effect on orthostatic tolerance. Thus it was evident that a more effective method was required to elucidate the effect. The accepted gold standard for measuring orthostatic tolerance is tilt testing with combined LBNP (Protheroe et al., 2013). However, there was a risk that this method would not be sufficiently discriminative in case of a strict DI protocol. Most of subjects could appear intolerant to tilt prior to the implementation of the LBNP steps. Indeed, in a recent study with 3-day strict DI (De Abreu et al., 2017) it has been demonstrated that there is a drastic loss of tolerance in response to 15-minute tilt followed by -10 mmHg LBNP steps: after DI, 9 out of 12 subjects tolerated less than 8 min of tilt, 4 out of 12 – less than 5 min of tilt, and only 2 of the 12 subjects finished the first LBNP step. In order to overcome this limitation an LBNP test alone was selected, which allows testing cardiovascular responses much more progressively. Nonetheless, no observable effect of thigh cuffs on orthostatic intolerance was detected.

Factors Which May Limit Thigh Cuffs Efficacy

Three factors may underpin the observed limited efficacy of thigh cuffs in our 5-day strict DI study. First, the discontinuity

TABLE 2 | Blood assessment (chemistry, cardiovascular hormones, metabolic parameters).

	Control				Cuffs			
Variable	**B-1_m**	**DI-1_e**	**DI-3_m**	**DI-5_m**	**B-1_m**	**DI-1_e**	**DI-3_m**	**DI-5_m**
Sodium, mmol/L	141 ± 2	140 ± 2	139 ± 2	139 ± 2	141 ± 2	139 ± 3	138 ± 4*	138 ± 5*
Chlorine, mmol/L	106 ± 2	105 ± 2	103 ± 3*	103 ± 3*	106 ± 1	105 ± 2	104 ± 3*	103 ± 3*
Potassium, mmol/L	3.8 ± 0.2	4.0 ± 0.3*	3.9 ± 0.2	3.9 ± 0.2	3.9 ± 0.2	4.0 ± 0.2	4.0 ± 0.2	4.0 ± 0.2
Proteins, g/L	67 ± 4	68 ± 2	73 ± 3*	71 ± 4*	67 ± 3	66 ± 3	68 ± 4#	65 ± 4#
Creatinine, μmol/L	75 ± 8	74 ± 8	78 ± 7	76 ± 11	73 ± 6	69 ± 9	72 ± 9	70 ± 7
Glucose, mmol/L	4.3 ± 0.3	4.5 ± 0.6	4.3 ± 0.4	4.2 ± 0.4	4.5 ± 0.5	4.9 ± 0.6	4.4 ± 0.3	4.3 ± 0.4
Cholesterol, mmol/L	4.9 ± 1.0	4.9 ± 0.8	5.3 ± 0.8*	4.9 ± 0.7	4.2 ± 0.7	4.1 ± 0.6	4.4 ± 0.7#	4.0 ± 0.7
HDL, mmol/L	1.3 ± 0.3	1.3 ± 0.3	1.4 ± 0.3	1.2 ± 0.2	1.4 ± 0.3	1.4 ± 0.2	1.4 ± 0.2	1.3 ± 0.2*
LDL, mmol/L	3.1 ± 0.7	3.0 ± 0.6	3.5 ± 0.6*	3.3 ± 0.5	2.4 ± 0.6	2.1 ± 0.7*#	2.6 ± 0.6#	2.4 ± 0.5#
Triglycerides, mmol/L	1.0 ± 0.4	1.1 ± 0.2	1.1 ± 0.4	1.0 ± 0.4	0.8 ± 0.2	1.0 ± 0.3	0.8 ± 0.2	0.8 ± 0.3
hs-CRP, mg/L	0.4 ± 0.2	0.3 ± 0.1	0.5 ± 0.3	0.5 ± 0.3	1.2 ± 1.7	0.8 ± 1.1	0.9 ± 1	0.8 ± 0.7
Osmolality, mOsmol/kg	292 ± 5	294 ± 3	293 ± 4	293 ± 5	293 ± 4	294 ± 7	293 ± 5	292 ± 6

*Values are mean ± SD; *$p \leq 0.05$ vs. baseline; #$p < 0.05$ vs. Control; m, morning; e, evening; shadowed, 8 h after the onset of immersion.*

in cuffs application, with a daily break for 14 h leads to at least partial reversal during the night of what was gained during the day. Second, continuous squeezing force created by immersion and acting on the whole body and on the deeper immersed lower limbs in particular, actively counteracts the sequestrating effect of the cuffs. Third, the increase in lower limb venous compliance induced by cuffs themselves might contribute to orthostatic intolerance and counterbalance the positive effects of thigh cuffs on partial preservation of volemia and body fluids.

Study Limitations

Thigh cuffs were applied only intermittently. We did not test 24-hour application to avoid deleterious venous effects with a potential risk of venous thrombosis, and to reproduce inflight usage.

Lower body negative pressure-test was limited to 6 steps and finished upon accomplishing −60 mmHg step, so at baseline we did not reach intolerance in most subjects. This might contribute to diminution of test sensitivity. Using supine LBNP in individuals with high LBNP tolerance may necessitate the use of very high LBNP suction levels, which may result in misleading physiological responses due to discomfort (Goswami et al., 2019). Besides we wanted to avoid negative effects at lower limb microcirculatory level, such as petechiae.

Periodic disruption of DI due to hygiene and protocols needs, and in particular long out-of-bath period at DI-5 for experimental procedures, could influence results. Out-of-bath time was measured and limited as much as possible.

CONCLUSION

Thigh cuff countermeasure slowed down and limited loss of body water and tended to limit plasma loss, with persistence of the effect in periods when thigh cuffs were removed. However, it did not counteract decreased tolerance to orthostatic challenge. Therefore, intermittent application of thigh cuffs is an effective, easy-to-use, low-cost passive inflight countermeasure to improve general state during initial adaptation to microgravity, limit cephalad fluid shift and its potential sequelae. However, it is not to be considered as a countermeasure for post-flight orthostatic intolerance.

DATA AVAILABILITY STATEMENT

The datasets generated for this study are available on request to the corresponding author.

ETHICS STATEMENT

The study was reviewed and approved by CPP Est III, CHRU de Nancy, 54511 Vandoeuvre-les-Nancy cedex 9. The participants provided their written informed consent to participate in this study.

AUTHOR CONTRIBUTIONS

RM, M-PB, AB, CG, GG-K, M-AC, and NN conceived and designed the study. AR, AA, BD, AB, AD, FL, M-AC, and NN acquired the data and analyzed the sample. All authors Analysis and interpretation of results, drafting and revising the manuscript.

FUNDING

This dry immersion protocol was supported by CNES (DAR CNES N° 2018 – 4800000970).

ACKNOWLEDGMENTS

We thank the volunteers and the stuff of MEDES for participation in this protocol at the MEDES space clinic in 2018–2019.

REFERENCES

Arbeille, P., Avan, P., Treffel, L., Zuj, K., Normand, H., and Denise, P. (2017). Jugular and portal vein volume, middle cerebral vein velocity, and intracranial pressure in dry immersion. *Aerosp. Med. Hum. Perform.* 88, 457–462. doi: 10.3357/AMHP.4762.2017

Arbeille, P., Herault, S., Fomina, G., Roumy, J., Alferova, I., and Gharib, C. (1999). Influences of thigh cuffs on the cardiovascular system during 7-day head-down bed rest. *J. Appl. Physiol.* 87, 2168–2176. doi: 10.1152/jappl.1999.87.6.2168

Balasubramanian, S., Tepelus, T., Stenger, M. B., Lee, S. M. C., Laurie, S. S., Liu, J. H. K., et al. (2018). Thigh cuffs as a countermeasure for ocular changes in simulated weightlessness. *Ophthalmology* 125, 459–460. doi: 10.1016/j.ophtha.2017.10.023

Chaika, A. M., and Balakhovskii, I. S. (1982). Changes in plasma and extracellular fluid volumes and plasma protein mass under conditions of head-down tilt hypokinesia and immersion. *Kosm. Biol. Aviakosm. Med.* 16, 22–28.

Coupe, M., Tomilovskaya, E., Larcher, F., Diquet, B., Pastushkova, L., Kozlovskaya, I., et al. (2013). Body fluid changes, cardiovascular deconditioning and metabolic impairment are reversed 24 hours after a 5-day dry immersion. *Open J. Nephrol.* 3, 13–24. doi: 10.4236/ojneph.2013.31004

Custaud, M. A., Millet, C., Frutoso, J., Maillet, A., Gauquelin, G., Gharib, C., et al. (2000). No effect of venoconstrictive thigh cuffs on orthostatic hypotension induced by head-down bed rest. *Acta Physiol. Scand.* 170, 77–85. doi: 10.1046/j.1365-201x.2000.00763.x

De Abreu, S., Amirova, L., Murphy, R., Wallace, R., Twomey, L., Gauquelin-Koch, G., et al. (2017). Multi-system deconditioning in 3-day dry immersion without daily raise. *Front. Physiol.* 8:799. doi: 10.3389/fphys.2017.00799

Fomina, G., Kotovskaya, A., Arbeille, F., Pochuev, V., Zhernavkov, A., and Ivanovskaya, T. (2004). Changes in hemodynamic and post-flights orthostatic tolerance of cosmonauts under application of the preventive device–thigh cuffs bracelets in short-term flights. *J. Gravit. Physiol.* 11, 229–230.

Goswami, N., Blaber, A. P., Hinghofer-Szalkay, H., and Convertino, V. A. (2019). Lower body negative pressure: physiological effects, applications, and implementation. *Physiol. Rev.* 99, 807–851. doi: 10.1152/physrev.00006.2018

Iarullin, K. H., Simonov, L. G., and Vtoryi, S. A. (1987). Changes in regional and central hemodynamics during a 7-day immersion in water [in Russian, English summary]. *Kosm. Biol. Aviakosm. Med.* 21, 45–50.

Iwase, S., Sugiyama, Y., Miwa, C., Kamiya, A., Mano, T., Ohira, Y., et al. (2000). Effects of three days of dry immersion on muscle sympathetic nerve activity and arterial blood pressure in humans. *J. Auton. Nerv. Syst.* 79, 156–164. doi: 10.1016/s0165-1838(99)00076-4

Kermorgant, M., Leca, F., Nasr, N., Custaud, M. A., Geeraerts, T., Czosnyka, M., et al. (2017). Impacts of simulated weightlessness by dry immersion on optic nerve sheath diameter and cerebral autoregulation. *Front. Physiol.* 8:780. doi: 10.3389/fphys.2017.00780

Leach Huntoon, C.S., Grigoriev, A.I., and Natochin, Y.V.(eds) (1998). Fluid and electrolyte regulation in spaceflight. San Diego, CA: American Astronautical Society, vol 94.

Lee, A. G., Mader, T. H., Gibson, C. R., Brunstetter, T. J., and Tarver, W. J. (2018). Space flight-associated neuro-ocular syndrome (SANS). *Eye* 32, 1164–1167. doi: 10.1038/s41433-018-0070-y

Millet, C., Custaud, M. A., Allevard, A. M., Gharib, C., Gauquelin-Koch, G., and Fortrat, J. O. (2000). Adaptations to a 7-day head-down bed rest with thigh cuffs. *Med. Sci. Sports. Exerc.* 32, 1748–1756. doi: 10.1097/00005768-200010000-00014

Miwa, C., Sugiyama, Y., Iwase, S., Mano, T., Ohira, Y., Grigoriev, A., et al. (1997). Effects of three days of dry immersion on heart rate and blood pressure variabilities during head-up tilting in humans. *Environ. Med.* 41, 135–137.

Navasiolava, N. M., Custaud, M. A., Tomilovskaya, E. S., Larina, I. M., Mano, T., Gauquelin-Koch, G., et al. (2011). Long-term dry immersion: review and prospects. *Eur. J. Appl. Physiol.* 111, 1235–1260. doi: 10.1007/s00421-010-1750-x

Organ, L. W., Bradham, G. B., Gore, D. T., and Lozier, S. L. (1994). Segmental bioelectrical impedance analysis: theory and application of a new technique. *J. Appl. Physiol.* 77, 98–112. doi: 10.1152/jappl.1994.77.1.98

Pavy-Le Traon, A., Maillet, A., Vasseur Clausen, P., Custaud, M. A., Alferova, I., Gharib, C., et al. (2001). Clinical effects of thigh cuffs during a 7-day 6 degrees head-down bed rest. *Acta Astronaut.* 49, 145–151. doi: 10.1016/s0094-5765(01)00092-3

Protheroe, C. L., Ravensbergen, H. R., Inskip, J. A., and Claydon, V. E. (2013). Tilt testing with combined lower body negative pressure: a "gold standard" for measuring orthostatic tolerance. *J. Vis. Exp.* 73:e4315. doi: 10.3791/4315

Taibbi, G., Cromwell, R. L., Zanello, S. B., Yarbough, P. O., Ploutz-Snyder, R. J., Godley, B. F., et al. (2016). Ocular outcomes comparison between 14- and 70-day head-down-tilt bed rest. *Invest. Ophthalmol. Vis. Sci.* 57, 495–501. doi: 10.1167/iovs.15-18530

Tomilovskaya, E., Shigueva, T., Sayenko, D., Rukavishnikov, I., and Kozlovskaya, I. (2019). Dry immersion as a ground-based model of microgravity physiological effects. *Front. Physiol.* 10:284. doi: 10.3389/fphys.2019.00284

Conflict of Interest: The authors declare that the research was conducted in the absence of any commercial or financial relationships that could be construed as a potential conflict of interest.

frontiers in Physiology

ORIGINAL RESEARCH
published: 21 May 2020
doi: 10.3389/fphys.2020.00455

Phase Coupling Between Baroreflex Oscillations of Blood Pressure and Heart Rate Changes in 21-Day Dry Immersion

Anatoly S. Borovik[1], Evgeniya A. Orlova[1], Elena S. Tomilovskaya[1], Olga S. Tarasova[1,2] and Olga L. Vinogradova[1,3]*

[1] State Research Center of the Russian Federation, Institute of Biomedical Problems, Russian Academy of Sciences, Moscow, Russia, [2] Faculty of Biology, M.V. Lomonosov Moscow State University, Moscow, Russia, [3] Faculty of Basic Medicine, M.V. Lomonosov Moscow State University, Moscow, Russia

Introduction: Dry immersion (DI) is a ground-based experimental model which reproduces the effects of microgravity on the cardiovascular system and, therefore, can be used to study the mechanisms of post-flight orthostatic intolerance in cosmonauts. However, the effects of long-duration DI on cardiovascular system have not been studied yet. The aim of this work was to study the effects of 21-day DI on systemic hemodynamics and its baroreflex control at rest and during head-up tilt test (HUTT).

Methods: Ten healthy young men were exposed to DI for 21 days. The day before, on the 7th, 14th, and 19th day of DI, as well as on the 1st and 5th days of recovery they were subjected to HUTT: 15 min in supine position and then 15 min of orthostasis (60°). ECG, arterial pressure, stroke volume and respiration rate were continuously recorded during the test. Phase synchronization index (PSI) of beat-to-beat mean arterial pressure (MAP) and heart rate (HR) in the frequency band of baroreflex waves (~0.1 Hz) was used as a quantitative measure of baroreflex activity.

Results: During DI, strong tachycardia and the reduction of stroke volume were observed both in supine position and during HUTT, these indicators did not recover on post-immersion day 5. In contrast, systolic arterial pressure and MAP decreased during HUTT on 14th day of DI, but then restored to pre-immersion values. Before DI and on day 5 of recovery, a transition from supine position to orthostasis was accompanied by an increase in PSI at the baroreflex frequency. However, PSI did not change in HUTT performed during DI and on post-immersion day 1. The amplitude of MAP oscillations at this frequency were increased by HUTT at all time points, while an increase of respective HR oscillations was absent during DI.

Conclusion: 21-day DI drastically changed the hemodynamic response to HUTT, while its effect on blood pressure was reduced between days 14 and 19, which speaks in favor of the adaptation to the conditions of DI. The lack of increase in phase synchronization of baroreflex MAP and HR oscillations during HUTT indicates disorders of baroreflex cardiac control during DI.

Keywords: dry immersion, cardiovascular system, head-up tilt, baroreflex, heart rate, blood pressure, phase synchronization

OPEN ACCESS

Edited by:
Costantino Balestra, Haute École Bruxelles-Brabant (HE2B), Belgium

Reviewed by:
Alessandro Marroni, DAN Europe Foundation, Malta
Pierre Lafere, Université de Bretagne Occidentale, France

****Correspondence:***
Anatoly S. Borovik
asbor@mail.ru

Specialty section:
This article was submitted to Environmental, Aviation and Space Physiology, a section of the journal Frontiers in Physiology

Received: *31 January 2020*
Accepted: *09 April 2020*
Published: *21 May 2020*

Citation:
Borovik AS, Orlova EA, Tomilovskaya ES, Tarasova OS and Vinogradova OL (2020) Phase Coupling Between Baroreflex Oscillations of Blood Pressure and Heart Rate Changes in 21-Day Dry Immersion. Front. Physiol. 11:455. doi: 10.3389/fphys.2020.00455

INTRODUCTION

Long-duration exposure to microgravity is accompanied by profound changes in most of the physiological systems (Demontis et al., 2017), including disturbances in the sensorimotor, skeletal, and muscular systems, as well as changes in the regulation of cardiovascular system (LeBlanc et al., 2000; Eckberg, 2003). Obviously, such changes significantly limit the ability of cosmonauts to perform tasks after returning to the gravitational environment, which can significantly complicate their professional activity after landing not only on Earth, but also on the Moon (Rudas et al., 1999; Hughson et al., 2012).

Among the mechanisms for maintaining cardiovascular homeostasis after a long space flight, the leading role belongs to the reflexes from baroreceptors of the aortic arch and carotid sinuses (Benarroch, 2009). In addition, the reflexes from cardiopulmonary receptors play an important role in maintaining orthostatic tolerance (Convertino, 2014). Due to the activity of these reflexes, transition of human body from supine position to orthostasis is accompanied by regulatory changes in the cardiovascular system, which prevent blood pressure decrease, despite redistribution of blood in the body (Thrasher, 1994; Stewart, 2012). Under conditions of a long space flight, the baroreflex is impaired, which is one of the reasons for orthostatic intolerance after returning to Earth (Buckey et al., 1996; Waters et al., 2002).

To study the effects of microgravity on cardiovascular system, head-down bed rest (Kamiya et al., 2000; Grigoriev and Kozlovskaya, 2018) and dry immersion (Shul'zhenko and Will-Williams, 1976; Shulzhenko et al., 1976) are commonly used as ground-based models. Of note, the second model, in comparison with the first, better reproduces the effects of real space flight on most body systems (Tomilovskaya et al., 2019). Cardiovascular effects of dry immersion that last no more than 7 days are relatively well described (Iwase et al., 2000; Vinogradova et al., 2002; Navasiolava et al., 2011; de Abreu et al., 2017). In general, post-immersion changes in the cardiovascular system are similar to those observed after space flight. After 3 days of dry immersion, an increase in supine muscle sympathetic nerve activity (MSNA) was described along with unaltered HR and blood pressure (Iwase et al., 2000). In a later study, 3-day immersion without daily raise was followed by slight increases in supine heart rate (HR) and diastolic arterial pressure and a decrease in stroke volume (SV) (de Abreu et al., 2017). Importantly, the exposure to dry immersion environment dramatically changes all cardiovascular responses to orthostatic challenge: SV, blood pressure and HR shifts become significantly increased compared to their baseline values (Iwase et al., 2000; de Abreu et al., 2017), while no change in MSNA response to orthostasis is shown (Iwase et al., 2000). However, the effects of long-duration dry immersion on cardiovascular system and its regulation have not been studied yet.

The analysis of HR variability showed that autonomic cardiac control is readjusted during dry immersion toward predominance of the sympathetic mechanisms (Eshmanova et al., 2008). The sensitivity of the cardiac baroreflex estimated by the analysis of spontaneous HR and blood pressure fluctuations at the frequency of about 0.1 Hz (baroreflex waves; Julien, 2006; Stauss, 2007) was shown to decrease after dry immersion at supine position and an even more pronounced decrease is observed during head-up tilt test (de Abreu et al., 2017). It should be noted that when studying spontaneous oscillations of HR and blood pressure coordinated by the baroreflex, their amplitude characteristics are traditionally analyzed (Cooke et al., 1999; Akimoto et al., 2011; de Abreu et al., 2017). Noteworthy, the complex dynamics of physiological signals is also determined by their phase relationships. In this study, we introduce a novel approach to the assessment of baroreflex activity, based on the calculation of the phase relations of blood pressure and HR oscillations at the frequency of baroreflex waves using the phase synchronization index (PSI) (Borovik et al., 2014, 2019; Negulyaev et al., 2019). This method of analysis has several important advantages, since it provides more stable results than traditional methods (such as cross-spectral analysis) and does not require long continuous recording (Negulyaev et al., 2019). According to our previous data, PSI of blood pressure and HR in baroreflex frequency range increased significantly during orthostatic challenge in volunteers (Borovik et al., 2014) as well as during central hypovolemia induced by hemorrhage in laboratory rats (Negulyaev et al., 2019).

Orthostatic intolerance after dry immersion is associated with a decrease in MSNA, HR, and blood pressure (Iwase et al., 2000), as in vasovagal syncope which is clearly linked to the impaired baroreflex regulation of hemodynamics (Ogoh et al., 2004; Guasti et al., 2010; Schwartz et al., 2013b). Phase synchronization of baroreflex blood pressure and MSNA oscillations disappears in patients with vasovagal syncope during head-up tilt test a few minutes before the drop in blood pressure (Schwartz et al., 2013a). Regarding the phase synchronization of blood pressure and HR during syncope, we showed, for the first time, that the absence of PSI increase at an early stage of the head-up tilt test is associated with subsequent decompensation of hemodynamics and orthostatic intolerance (Borovik et al., 2019). These results suggest PSI of blood pressure and HR to be an informative measure of baroreflex activity in humans exposed to conditions of simulated or real microgravity.

Therefore, the aim of this work was to study the effects of long-duration (21-day) exposure to dry immersion on systemic hemodynamics and on the activity of a baroreflex (using PSI) during an orthostatic challenge (head-up tilt test).

METHODS

The study was conducted at dry immersion facilities of the Institute of Biomedical Problems, Russian Academy of Sciences (Tomilovskaya et al., 2019). The protocol of the study conforms to the Declaration of Helsinki and was approved by the Biomedical Ethics Committee of the Institute of Biomedical Problems, Russian Academy of Sciences (protocol N483 from 03.08.2018).

Design of the Experiment

Ten healthy men (mean age 29.3 ± 3.8 years; height 176.4 ± 3.8 cm; weight 71 ± 10.6 kg; body mass index 22.7 ± 2.7) participated in the experiments. All subjects were familiarized with the protocol and informed of the risks associated with the experiment and gave their written consent to participate in the study. They were controlled by a medical team on duty during dry immersion exposure (21 days) as well as for 2 days before exposure and 2 days after its accomplishment. The beginning and the end of immersion both were at 8:45.

The experiment consisted of five stages. At each stage, two subjects were water immersed in two separate immersion baths. Water temperature in the bath was kept at 33 ± 1°C. Every evening (between 21:00 and 22:00), the subjects were lifted out of the bath for about 20 min for hygienic procedures. Our cardiovascular measurements (3 times during the immersion period – see Head-Up Tilt Test) were performed between 12:00 and 13:00 (before the lunch). For some studies, outside the scope of our experiment, the subjects were removed from the bath for a short time, during the measurements the subjects were in a supine position. In regular days (without orthostatic test) the time spent by the subjects outside the bath in the supine position was 15 ± 3 min, and in the sitting or standing position – 8 ± 2 min. In days with orthostatic tests these time intervals were extended to 57 ± 16 min and 22 ± 5 min respectively.

In the time free from procedures and measurements, the subjects could read, use the notebook or cellphone, watch TV, etc. Sleep time (light-off period) was 23:00–07:00. The total time spent by the subjects in the bath was 492 ± 2 h.

Head-Up Tilt Test

Before the tilt test, the subject maintained supine position for 15 min. Then he was tilted to the 60° angle and the measurements were continued for another 16 min. In the head-up position the subject sat on the saddle, his legs hanging freely and not touching the support. At the request of the subject or with signs of the presyncope state, he was immediately returned to the supine position. Respiration frequency was constant during the test and controlled by the voice commands from the computer. Within the group of subjects, the respiratory rate ranged from 12 to 14 cycles per min. It was selected individually for each subject to be the most different from the frequency of baroreflex waves (∼0.1 Hz) but to remain comfortable for the subject.

During the experiment, ECG (PneumoCard, Medical computer systems, Russia), blood pressure and stroke volume (SV) (Finometer, Finapres Medical Systems, the Netherlands) and respiration frequency (nasal thermistor sensor) were continuously recorded. All signals were digitized at 1 kHz using E14-140 ADC (L-Card, Russia) and PowerGraph software (DISoft, Russia).

For each subjects, the measurements were performed six times: a day before the start of dry immersion (background measurement, B-1), on the 7th, 14th, and 19th days of the immersion (measurements DI7, DI14, and DI19, respectively) and also on days 1 and 5 after the end of immersion (during recovery period, measurements R1 and R5); R1 measurement was performed 28 h after the subject was lifted out of the bath. Such a schedule of measurements allowed us to study the time-course of cardiovascular changes during exposure to dry immersion and the recovery after cessation of the exposure.

Data Processing

Data processing was performed *off-line* using home-made programs working under MATLAB (MathWorks Inc., United States). First, systolic, diastolic, pulse and mean arterial pressure (MAP) values as well as HR and SV values were determined for every cardiac cycle. Further calculations were performed in two 15 min intervals, the first of which preceded the head-up tilt (supine position), and the second began 1 min after changing the position of the body (orthostasis).

Calculation of Phase Synchronization Index

Baroreflex functioning was estimated by phase coupling of spontaneous MAP and HR oscillations in the frequency range of baroreflex waves (∼0.1 Hz), i.e., by the constancy of the difference in their phases. For this purpose, PSI of MAP and HR was calculated. The algorithm of PSI calculation was described in detail in our previous works (Borovik et al., 2014; Negulyaev et al., 2019). In brief, MAP and HR were resampled at 5 Hz using linear interpolation, then narrow-band signals were extracted by digital filtering from the obtained time series. Thereafter, the narrow-band MAP and HR signals were presented in the form of an analytic signal, that allowed us to determine their phases φ. For each frequency, normalized phase difference between HR and MAP was then calculated:

$$\Delta\varphi = (\varphi_{HR} - \varphi_{MAP})/2\pi \; mod1 \quad (1)$$

To quantitate the degree of phase synchronization at the certain frequency, PSI was obtained based on the calculation of Shannon entropy of $\Delta\varphi$ distribution (Tass et al., 1998). Determined in this way, PSI is equal to 1 for "ideal" synchronization and is equal to zero for its complete absence. Using this algorithm, PSI values were obtained in the range from 0.02 to 0.5 Hz. Mean PSI in the band of interest (0.07–0.13 Hz) was calculated by averaging the respective values.

Spectral Analysis

Time series of MAP and HR were resampled at 5 Hz using linear interpolation. 102.4 s segments of equidistant time series (512 samples, half-overlapping from segment to segment) were then subjected to discrete fast Fourier transform to yield power spectra. Mean values of power spectral density (PSD) of MAP and HR in the baroreflex frequency band (from 0.07 to 0.13 Hz) were then calculated.

Statistical Analysis

Statistical data analysis was performed in GraphPad Prism 7.0 (GraphPad Software, La Jolla, CA, United States). The values are given as mean and SEM, besides anthropometric data and time intervals which are given as mean and SD. To estimate statistically significant differences Wilcoxon test was used. Statistical significance was reached at $p < 0.05$.

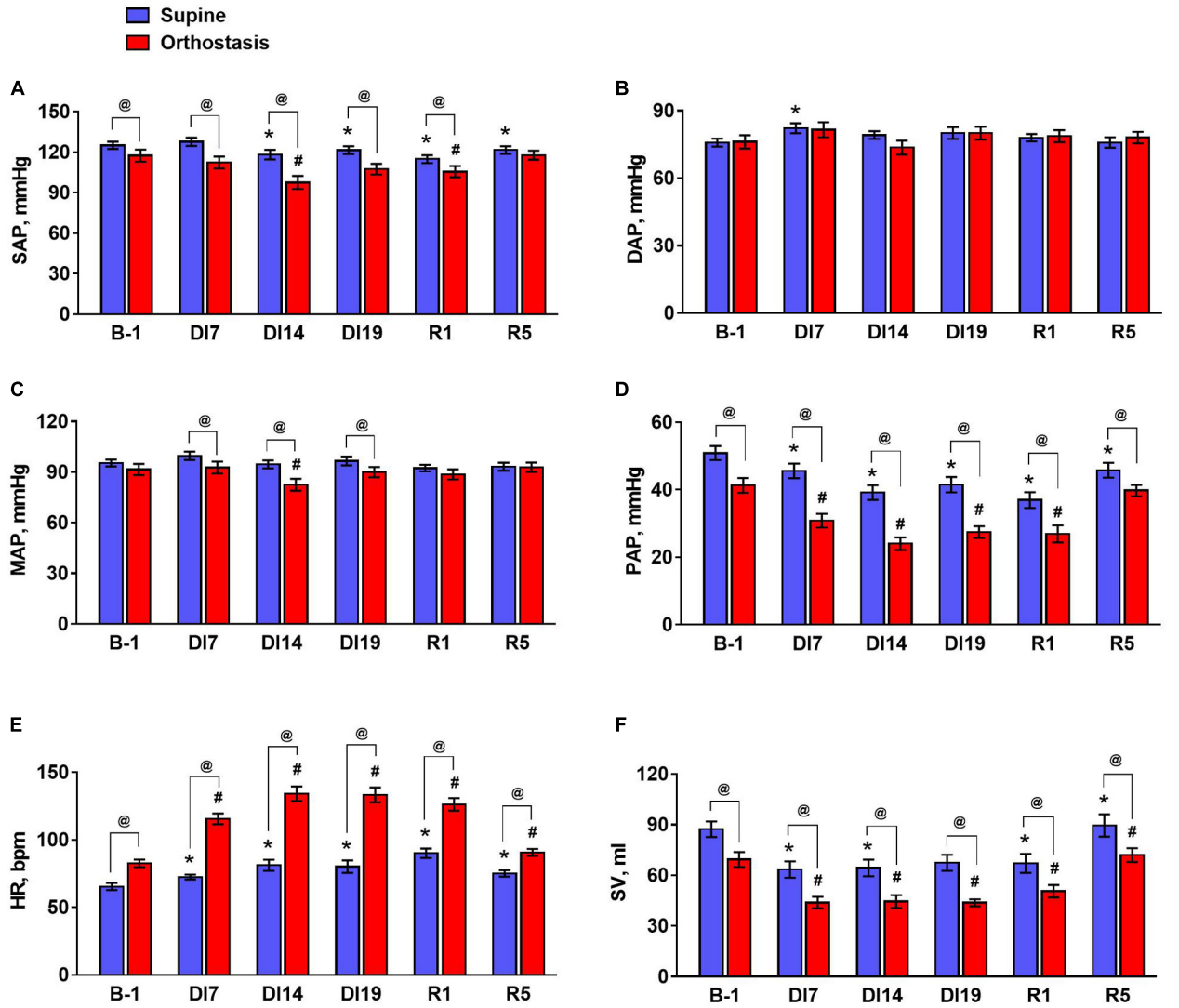

FIGURE 1 | The values of hemodynamic parameters during tilt test 1 day before dry immersion (B-1), during dry immersion (DI7, DI14, and DI19) and during the recovery period (R1 and R5). **(A)** Systolic arterial pressure, SAP; **(B)** diastolic arterial pressure, DAP; **(C)** mean arterial pressure, MAP; **(D)** pulse arterial pressure, PAP; **(E)** heart rate, HR; **(F)** stroke volume, SV. Data are given for a group of 10 subjects (Mean ± SEM). $^{*}p < 0.05$ compared with the value in supine position before immersion; $^{\#}p < 0.05$ compared with the value in head-up position before immersion; $^{@}p < 0.05$ compared with the corresponding value in the supine position.

RESULTS

The Effect of Dry Immersion on Hemodynamic Parameters During Orthostatic Challenge

An exposure to dry immersion environment for 21 days led to significant changes in regulation of cardiovascular system, which were reflected in the values of hemodynamic parameters as well as in their responses to orthostatic challenge. In each subject, the mean values of hemodynamic parameters were calculated for a supine position and for orthostasis (**Figure 1**). In addition, the changes of the parameters on transition from the supine to the head-up position (as a percentage of background values) were calculated (**Figure 2**).

During the exposure to dry immersion, a slight decrease in systolic arterial pressure in the supine position was seen (**Figure 1A**). Diastolic pressure in the supine position was increased by 7 days of dry immersion and then did not differ from the baseline value (**Figure 1B**). Supine MAP did not change during the experiment (**Figure 1C**). In orthostasis, decreases in systolic (**Figure 1A**) and MAP (**Figure 1C**) were observed on day 14 of dry immersion. Accordingly, more pronounced responses of these indicators during orthostatic challenge were demonstrated on day 14 while on day 19 their responses did not change compared to pre-immersion values (**Figures 2A,C**). Pulse arterial pressure was the most affected by dry immersion: supine and orthostatic values of this indicator decreased (**Figure 1D**) and its response to orthostatic challenge increased (**Figure 2D**) starting from day 7 of the exposure. During the recovery, the

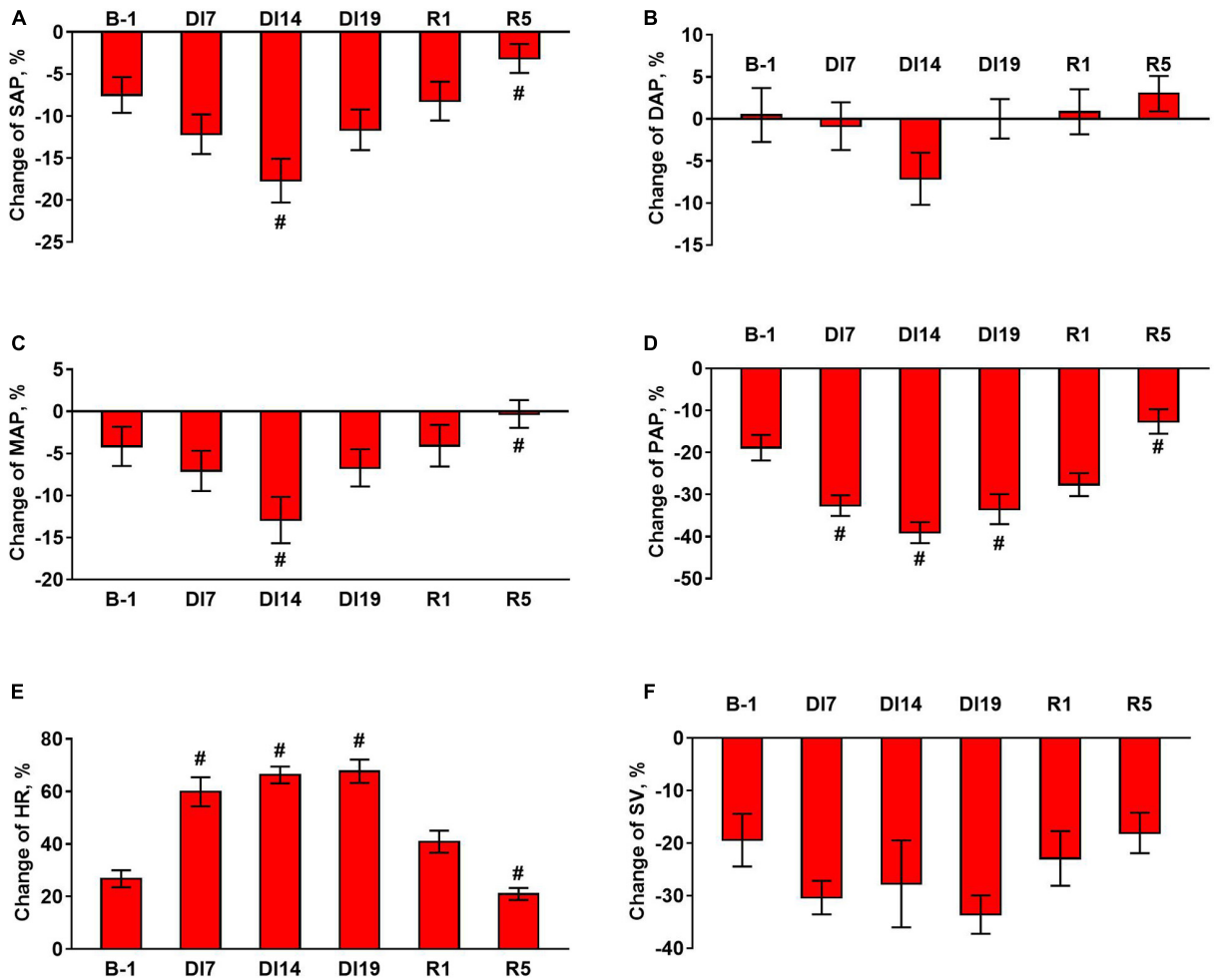

FIGURE 2 | Changes in hemodynamic parameters during tilt test 1 day before dry immersion (B-1), during dry immersion (DI7, DI14, and DI19) and during the recovery period (R1 and R5). **(A)** Systolic arterial pressure, SAP; **(B)** diastolic arterial pressure, DAP; **(C)** mean arterial pressure, MAP; **(D)** pulse arterial pressure, PAP; **(E)** heart rate, HR; **(F)** stroke volume, SV. Data are given for a group of 10 subjects (Mean ± SEM). $^{\#}p < 0.05$ compared with the value before immersion.

systolic and pulse pressures in the supine position remained lower than before the immersion.

HR significantly increased during dry immersion in the supine position and especially at orthostasis (**Figure 1E**); the response of HR to the change of body position also increased significantly (**Figure 2E**). On the contrary, SV in supine position as well as at orthostasis decreased during dry immersion compared with the pre-immersion values (**Figure 1F**), although the percent reduction of SV in response to orthostatic challenge did not change (**Figure 2F**). The effects of dry immersion on HR and SV were prominently developed on the 7th day and were clearly seen even on the 5th day of recovery.

The Effect of Dry Immersion on Phase Synchronization of MAP and HR During Orthostatic Challenge

PSI spectra showed two distinct peaks in the frequency range studied (**Figure 3**). The high-frequency peak reflected the phase synchronization of MAP and HR at the respiration frequency. The amplitude of this peak did not depend on the body position during the tilt test and did not change during dry immersion and the recovery period. The frequency of this peak also did not change during the experiment, since the respiration rate was fixed (see Methods).

The position of the low-frequency peak corresponded to the frequency of baroreflex waves (about 0.1 Hz). Before the dry immersion, the change in body position from supine to orthostasis was followed by a significant increase of the low-frequency peak amplitude on PSI spectrum, which reflects an increase in the phase coupling of MAP and HR oscillations. However, during the exposure to dry immersion (on days 7, 14, and 19), the amplitude of the low-frequency peak on PSI spectrum did not change during head-up tilt test, which indicates a violation of the baroreflex control of HR. On the 5th day of recovery the spectra of PSI were very similar to respective spectra obtained before the dry immersion.

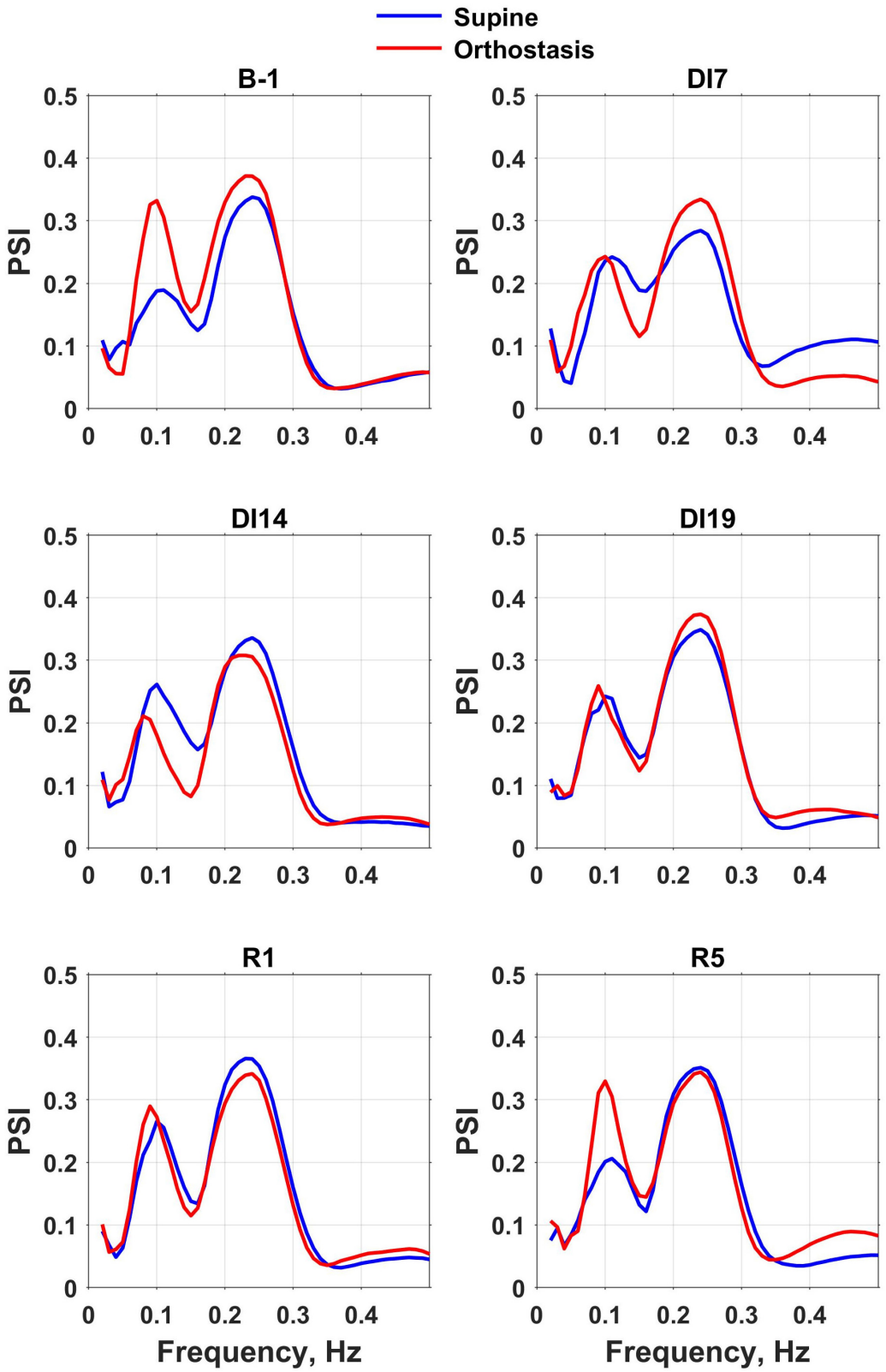

FIGURE 3 | Phase synchronization index (PSI) spectra of mean blood pressure and heart rate calculated for the intervals corresponding to the supine and head-up position in a tilt test performed the day before dry immersion (B-1) during dry immersion (DI7, DI14, and DI19) and in the recovery period (R1 and R5). PSI spectra averaged over the group of 10 subjects are presented.

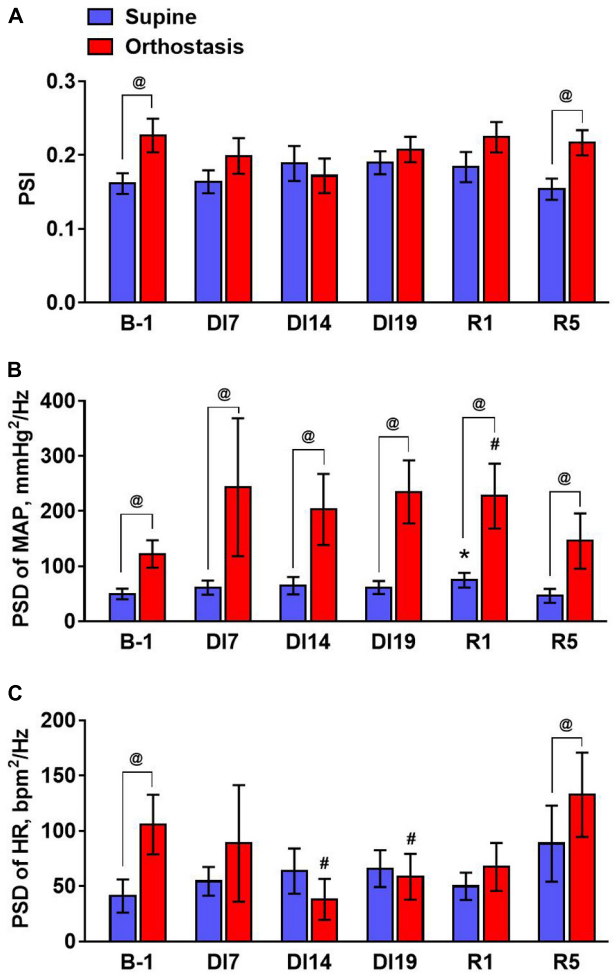

FIGURE 4 | The values of the phase synchronization index of MAP and heart rate **(A)**, mean spectral density of MAP **(B)**, and heart rate oscillations **(C)** averaged in the baroreflex frequency range (from 0.07 to 0.13 Hz) during tilt test performed 1 day before dry immersion (B-1), during dry immersion (DI7, DI14, and DI19) and in the recovery period (R1 and R5). Data are given for a group of 10 subjects (Mean ± SEM). $^{\#}p < 0.05$ compared with the value in orthostasis before immersion; $^{@}p < 0.05$ compared with the corresponding value in the supine position.

To quantify the effects of dry immersion on phase synchrony of MAP and HR, the average values of PSI were calculated in the frequency band from 0.07 to 0.13 Hz (**Figure 4A**). An increase in PSI in this frequency range during orthostasis was observed only in the tests performed before DI and on the 5th day of recovery. Importantly, oscillations of MAP in the frequency band from 0.07 to 0.13 Hz increased during the tilt test at all stages of the experiment – before and during dry immersion as well as during the recovery period (**Figure 4B**). However, oscillations of HR in this frequency band increased only in the tilt test performed before dry immersion and on the 5th day of recovery (**Figure 4C**). Moreover, on days 14 and 19 of the immersion, the power of HR fluctuations during orthostasis was reduced compared to the value before dry immersion.

DISCUSSION

Dry immersion is perhaps the most severe ground-based model of gravitational unloading. Up to now, reported studies focused on cardiovascular changes that occurred under the conditions of short-term (from 3 to 7 days) dry immersion (Navasiolava et al., 2011). Our work is the first comprehensive study of changes in cardiovascular system during a much longer (21 days) exposure to dry immersion. When planning the experiment, we were concerned that the subjects' orthostatic tolerance would be severely deteriorated after such a long DI exposure. However, these concerns did not materialize. Tilt tests performed on days 7 and 14 of dry immersion were the most difficult for subjects according to their subjective assessment. On day 7 one of the subjects had signs of a pre-syncope condition during orthostasis and on day 14 of the immersion two cases of a pre-syncope condition were recorded (the measurements were canceled ahead of schedule). However, on day 19 head-up tilt test was better tolerated according to both subjective sensations, which correlated with the reduced effects of dry immersion on some cardiovascular indicators between day 14 and day 19. This observation can reflect the adaptation of cardiovascular system and the body as a whole to the conditions of dry immersion.

We conducted detailed studies of hemodynamic changes caused by prolonged exposure to DI, both at rest (in a supine position) and during orthostatic challenge (passive head-up tilt test). It was shown that the levels of systolic and MAP decreased during orthostasis on day 14 of dry immersion, but did not change on day 19. Along with that, HR during dry immersion was increased even at rest and increased sharply in response to the transition of body to head-up position. This effect was observed already on the 7th day and practically did not change with further increase of dry immersion duration. Therefore, the data obtained indicate that the pattern of hemodynamic changes associated with a prolonged exposure to dry immersion is similar to that observed with shorter exposure (Navasiolava et al., 2011). However, we showed for the first time that major changes in hemodynamic parameters develop by 7–14 days of immersion and then stabilize. Importantly, the dynamics of cardiovascular system shifts during dry immersion is similar to that in space flight: severe alterations at the beginning of the flight subside or stabilize at later stages (Hughson et al., 2012; Eckberg et al., 2016). It can also be noted that even after prolonged DI, hemodynamic parameters almost return to their initial values as soon as on the 5th day of recovery.

To evaluate the changes in the cardiac baroreflex during simulated gravitational unloading, we used a novel approach based on estimation of the phase relations of BP and HR fluctuations in the frequency range of baroreflex waves (Borovik et al., 2014, 2019; Negulyaev et al., 2019). Importantly, the observed changes in cardiac baroreflex sensitivity during orthostasis depend on the method of assessing baroreflex activity. Using the neck suction technique, an increase in baroreflex sensitivity during transition to head-up position (tilt test) has been shown (Ogoh et al., 2003; Akimoto et al., 2011). However, using the sequence method, a decrease in the sensitivity of the baroreflex was shown (Akimoto et al., 2011; Silvani et al., 2017).

A similar decrease in the sensitivity of cardiac baroreflex during tilt test was revealed using cross-spectral analysis: a decrease in the amplitude of the transfer function between blood pressure and heart rate in the range of baroreflex waves (Cooke et al., 1999; Akimoto et al., 2011). Of note, the methods which are commonly used for assessing baroreflex activity in physiological experiments and in medical practice are based on recording changes in HR with changes in BP. In our method, as well as in cross-spectral analysis, spontaneous fluctuations of BP and HR are studied, but PSI is used as a quantitative measure of the phase coupling of these fluctuations (Tass et al., 1998) showing the degree of their synchronization in a certain frequency range. We have shown that the value of the PSI of BP and BP oscillations at the frequency of baroreflex waves correlated well with the coherence calculated by the cross-spectral method (Negulyaev et al., 2019).

It should be noted that, in addition to baroreflex activity, diverse factors related to the vital activity of the body and external influences affect vascular tone and heart function. Such influences induce non-periodic changes in hemodynamic parameters and can mask the relatively regular respiratory and baroreflex waves of blood pressure and heart rate. We showed that PSI is less affected by random fluctuations in hemodynamic parameters than coherence and gain of spontaneous cardiac baroreflex (Negulyaev et al., 2019) and, therefore, can be used to characterize the activity of cardiac baroreflex when analyzing the relatively "noisy" time series. In contrast to the decrease in the amplitude of the transfer function between blood pressure and heart rate in the frequency band of baroreflex waves (Cooke et al., 1999; Akimoto et al., 2011), the phase coupling of BP and HR oscillations at the baroreflex frequency was augmented in our study during orthostasis. Using cross-correlation analysis, Silvani et al. (2017) also showed an increase in the coupling of blood pressure and heart rate fluctuations when the body position was changed from horizontal to vertical. Based on the analysis of changes in heart rate variability indicators concomitant with orthostasis, the authors made a bold conclusion that changes in baroreflex sensitivity are associated with a decrease in vagal effects on the heart, and increased coupling of blood pressure and heart rate fluctuations, at least in part, is associated with increased fluctuations in vascular resistance in a head-up position (Silvani et al., 2017).

Starting from Ekberg's classical studies, it is known that the baroreflex sensitivity in space flight and in the ground-based simulations of gravitational unloading decreases or remains unchanged (Fritsch et al., 1992; Eckberg, 2003; Ferretti et al., 2009; Hughson et al., 2012; de Abreu et al., 2017). Our data on the ceased effect of orthostasis on PSI of blood pressure and HR during the whole 21-day exposure to dry immersion are in accordance with these earlier reports. On the 5th day of the recovery period, the baroreflex control of HR was restored: the similar changes in PSI spectrum were observed during tilt test, as before the start of dry immersion. Our data suggest that impaired phase coupling of blood pressure and heart rate during simulated microgravity was not associated with reduced amplitude of oscillations in vascular resistance in a head-up position, which is supported by the data on preserved control of MSNA in dry immersion environment (Iwase et al., 2000). However, the transition of blood pressure oscillations into HR oscillations was greatly disturbed by dry immersion. Therefore, our studies have shown that long-duration exposure to dry immersion results in prominent changes of heart rate baroreflex control.

Along with reporting novel observations our study has several limitations. First, the dynamics of PSI of blood pressure and HR during post-immersion period should have been studied in more detail, which would indicate the day on which the restoration of baroreflex control after long-duration dry immersion occurs. The second limitation is the relatively small number of the dry immersion experiment participants, in future the observed data need to be confirmed on a larger number of subjects. The next one is lumbar pain which occurs during exposure to dry immersion (de Abreu et al., 2017) and therefore could influence the results of our orthostatic tests. To control this factor, the participants were asked daily to evaluate lumbar pain using a subjective 10-level score. Importantly, lumbar pain was reported by the participants during days 3–5 of immersion, but not on day 6 and later. Therefore, lumbar pain could not affect the results of orthostatic tests, which were performed starting from immersion day 7.

CONCLUSION

In this work, for the first time, the changes in hemodynamic parameters were studied during a prolonged (21 days) exposure to dry immersion environment, ground-based model of the effects of microgravity. It was shown that changes in hemodynamic parameters in response to orthostatic challenge are most pronounced on days 7–14 of dry immersion. Violation of baroreflex control was detected already on the 7th day of exposure to dry immersion, persisted during the entire period of exposure and in the early recovery period (1st day). It should be noted that the absence of changes in the PSI in the baroreflex frequency range with a change in body position in the tilt test is typical for patients with fainting of a vasovagal nature (Borovik et al., 2019). Thus, our novel method can be used for assessing orthostasis-induced changes in baroreflex activity in the conditions of microgravity and in the development of countermeasures aimed at preventing orthostatic intolerance that occurs in cosmonauts/astronauts when they return to Earth's gravity.

DATA AVAILABILITY STATEMENT

The datasets generated for this study are available on request to the corresponding author.

ETHICS STATEMENT

All the procedures were conducted in accordance with the Declaration of Helsinki and were approved by the Biomedical Ethics Committee of the Institute of Biomedical Problems, Russian Academy of Sciences (protocol N483 from 03.08.2018). All potential risks were explained to the participants, and they gave written informed consent to participate in the experiment.

The participants were controlled by a medical team on 24 h duty during dry immersion exposure, 2 days before the dry immersion and 2 post-immersion days. The participants were provided by accident insurance during the experiment.

AUTHOR CONTRIBUTIONS

AB, EO, ET, and OV conceived and designed the study. AB and EO were involved in the acquisition of the data. AB, EO, and OT analyzed cardiovascular data and performed the statistical analysis. AB, EO, and OT drafted the manuscript. AB, ET, and OV revised the manuscript critically. All authors given final approval of the version to be submitted.

FUNDING

Cardiovascular studies were performed according to the Plan for Fundamental Research of State Research Center of the Russian Federation – Institute of Biomedical Problems, Russian Academy of Sciences. The organization of 21-day dry immersion experiment was supported by the Russian Science Foundation (Grant N19-15-00435).

ACKNOWLEDGMENTS

We thank Acad. O. I. Orlov for the opportunity to participate in the 3-week immersion experiment and Prof. I. B. Kozlovskaya for fruitful discussions of the results.

REFERENCES

Akimoto, T., Sugawara, J., Ichikawa, D., Terada, N., Fadel, P. J., and Ogoh, S. (2011). Enhanced open-loop but not closed-loop cardiac baroreflex sensitivity during orthostatic stress in humans. *Am. J. Physiol. Integr. Comp. Physiol.* 301, R1591–R1598. doi: 10.1152/ajpregu.00347.2011

Benarroch, E. E. (2009). Implications of the arterial baroreflex functional organization and involvement in neurologic disease. *Neurology* 71, 1733–1738. doi: 10.1212/01.wnl.0000335246.93495.92

Borovik, A. S., Kuznetsov, S. Y., and Vinogradova, O. L. (2014). "Phase synchronization of arterial pressure and heart rate as a measure of baroreflex activity," in *Proceedings of the 2014 8th Conference of the European Study Group on Cardiovascular Oscillations (ESGCO)*. Piscataway, NJ: IEEE, 217–218.

Borovik, A. S., Negulyaev, V. O., Tarasova, O. S., Kheymets, G. I., Pevzner, A. V., Ermishkin, V. V., et al. (2019). Disorders of synchronization of blood pressure and heart rate precede the development of vasovagal syncope during orthostasis. *Hum. Physiol.* 45, 405–411. doi: 10.1134/s0362119719040029

Buckey, J. C., Lane, L. D., Levine, B. D., Watenpaugh, D. E., Wright, S. J., Moore, W. E., et al. (1996). Orthostatic intolerance after spaceflight. *J. Appl. Physiol.* 81, 7–18. doi: 10.1152/jappl.1996.81.1.7

Convertino, V. A. (2014). Neurohumoral mechanisms associated with orthostasis: reaffirmation of the significant contribution of the heart rate response. *Front. Physiol.* 5:236. doi: 10.3389/fphys.2014.00236

Cooke, W. H., Hoag, J. B., Crossman, A. A., Kuusela, T. A., Tahvanainen, K. U., and Eckberg, D. L. (1999). Human responses to upright tilt: a window on central autonomic integration. *J. Physiol.* 517(Pt 2), 617–628. doi: 10.1111/j.1469-7793.1999.0617t.x

de Abreu, S., Amirova, L., Murphy, R., Wallace, R., Twomey, L., Gauquelin-Koch, G., et al. (2017). Multi-system deconditioning in 3-day dry immersion without daily raise. *Front. Physiol.* 8:799. doi: 10.3389/fphys.2017.00799

Demontis, G. C., Germani, M. M., Caiani, E. G., Barravecchia, I., Passino, C., and Angeloni, D. (2017). Human pathophysiological adaptations to the space environment. *Front. Physiol.* 8:547. doi: 10.3389/fphys.2017.00547

Eckberg, D. L. (2003). Bursting into space: Alterations of sympathetic control by space travel. *Acta Physiol. Scand.* 177, 299–311. doi: 10.1046/j.1365-201X.2003.01073.x

Eckberg, D. L., Diedrich, A., Cooke, W. H., Biaggioni, I., Buckey, J. C., Pawelczyk, J. A., et al. (2016). Respiratory modulation of human autonomic function: long-term neuroplasticity in space. *J. Physiol.* 594, 5629–5646. doi: 10.1113/JP271656

Eshmanova, A. K., Luchitskaya, E. S., and Baevsky, R. M. (2008). Investigation into vegetative regulation of blood circulation during 7-day dry immersion. *Aviakosmicheskaya i Ekol. Med.* 42, 45–51.

Ferretti, G., Iellamo, F., Pizzinelli, P., Kenfack, M. A., Lador, F., Lucini, D., et al. (2009). Prolonged head down bed rest-induced inactivity impairs tonic autonomic regulation while sparing oscillatory cardiovascular rhythms in healthy humans. *J. Hypertens.* 27, 551–561. doi: 10.1097/HJH.0b013e328322ca2f

Fritsch, J. M., Charles, J. B., Bennett, B. S., Jones, M. M., and Eckberg, D. L. (1992). Short-duration spaceflight impairs human carotid baroreceptor-cardiac reflex responses. *J. Appl. Physiol.* 73, 664–671. doi: 10.1152/jappl.1992.73.2.664

Grigoriev, A. I., and Kozlovskaya, I. B. (eds) (2018). *One-Year Anti-Orthostatic Hypokinesia (ANOG) - a Physiological Model of Interplanetary Space Flight*. Moscow: Russian Academy of Sciences.

Guasti, L., Mainardi, L. T., Baselli, G., Simoni, C., Cimpanelli, M., Braga, S. S., et al. (2010). Components of arterial systolic pressure and RR-interval oscillation spectra in a case of baroreflex failure, a human open-loop model of vascular control. *J. Hum. Hypertens.* 24, 417–426. doi: 10.1038/jhh.2009.79

Hughson, R. L., Shoemaker, J. K., Blaber, A. P., Arbeille, P., Greaves, D. K., Pereira-Junior, P. P., et al. (2012). Cardiovascular regulation during long-duration spaceflights to the International Space Station. *J. Appl. Physiol.* 112, 719–727. doi: 10.1152/japplphysiol.01196.2011

Iwase, S., Sugiyama, Y., Miwa, C., Kamiya, A., Mano, T., Ohira, Y., et al. (2000). Effects of three days of dry immersion on muscle sympathetic nerve activity and arterial blood pressure in humans. *J. Auton. Nerv. Syst.* 79, 156–164. doi: 10.1016/S0165-1838(99)00076-74

Julien, C. (2006). The enigma of Mayer waves: Facts and models. *Cardiovasc. Res.* 70, 12–21. doi: 10.1016/j.cardiores.2005.11.008

Kamiya, A., Iwase, S., Kitazawa, H., Mano, T., Vinogradova, O. L., and Kharchenko, I. B. (2000). Baroreflex control of muscle sympathetic nerve activity after 120 days of 6 degrees head-down bed rest. *Am. J. Physiol. Regul. Integr. Comp. Physiol.* 278, R445–R452.

LeBlanc, A., Schneider, V., Shackelford, L., West, S., Oganov, V., Bakulin, A., et al. (2000). Bone mineral and lean tissue loss after long duration space flight. *J. Musculoskelet. Neuronal Interact.* 1, 157–160.

Navasiolava, N. M., Custaud, M. A., Tomilovskaya, E. S., Larina, I. M., Mano, T., Gauquelin-Koch, G., et al. (2011). Long-term dry immersion: Review and prospects. *Eur. J. Appl. Physiol.* 111, 1235–1260. doi: 10.1007/s00421-010-1750-x

Negulyaev, V. O., Tarasova, O. S., Tarasova, N. V., Lukoshkova, E. V., Vinogradova, O. L., and Borovik, A. S. (2019). Phase synchronization of baroreflex oscillations of blood pressure and pulse interval in rats: the effects of cardiac autonomic blockade and gradual blood loss. *Physiol. Meas.* 40:054003. doi: 10.1088/1361-6579/ab10d6

Ogoh, S., Volianitis, S., Nissen, P., Wray, D. W., Secher, N. H., and Raven, P. B. (2003). Carotid baroreflex responsiveness to head-up tilt-induced central hypovolaemia: effect of aerobic fitness. *J. Physiol.* 551, 601–608. doi: 10.1113/jphysiol.2003.046029

Ogoh, S., Volianitis, S., Raven, P. B., and Secher, N. H. (2004). Carotid baroreflex function ceases during vasovagal syncope. *Clin. Auton. Res.* 14, 30–33. doi: 10.1007/s10286-004-0156-4

Rudas, L., Crossman, A. A., Morillo, C. A., Halliwill, J. R., Tahvanainen, K. U. O., Kuusela, T. A., et al. (1999). Human sympathetic and vagal baroreflex responses to sequential nitroprusside and phenylephrine. *J. Physiol.* 276, H1691–H1698. doi: 10.1152/ajpheart.1999.276.5.h1691

Schwartz, C. E., Lambert, E., Medow, M. S., and Stewart, J. M. (2013a). Disruption of phase synchronization between blood pressure and muscle sympathetic nerve activity in postural vasovagal syncope. *Am. J. Physiol. Circ. Physiol.* 305, H1238–H1245. doi: 10.1152/ajpheart.00415.2013

Schwartz, C. E., Medow, M. S., Messer, Z., and Stewart, J. M. (2013b). Spontaneous fluctuation indices of the cardiovagal baroreflex accurately measure the baroreflex sensitivity at the operating point during upright tilt. *Am. J. Physiol. Integr. Comp. Physiol.* 304, R1107–R1113. doi: 10.1152/ajpregu.00559.2012

Shulzhenko, E., Vil-Vilyams, I., Khudyakova, M., and Grigoryev, A. (1976). Deconditioning during prolonged immersion and possible countermeasures. *Life Sci. Sp. Res.* 14, 289–294.

Shul'zhenko, E., and Will-Williams, I. (1976). Possibility of carrying out prolonged water immersion by the method of "dry" submersion. *Kosm. Biol. Aviakosm. Med.* 10, 82–84.

Silvani, A., Calandra-Buonaura, G., Johnson, B. D., van Helmond, N., Barletta, G., Cecere, A. G., et al. (2017). Physiological mechanisms mediating the coupling between heart period and arterial pressure in response to postural changes in humans. *Front. Physiol.* 8:163. doi: 10.3389/fphys.2017.00163

Stauss, H. M. (2007). Identification of blood pressure control mechanisms by power spectral analysis. *Clin. Exp. Pharmacol. Physiol.* 34, 362–368. doi: 10.1111/j.1440-1681.2007.04588.x

Stewart, J. M. (2012). Mechanisms of sympathetic regulation in orthostatic intolerance. *J. Appl. Physiol.* 113, 1659–1668. doi: 10.1152/japplphysiol.00266.2012

Tass, P., Rosenblum, M. G., Weule, J., Kurths, J., Pikovsky, A., Volkmann, J., et al. (1998). Detection of n:m phase locking from noisy data: application to magnetoencephalography. *Phys. Rev. Lett.* 81, 3291–3294. doi: 10.1103/PhysRevLett.81.3291

Thrasher, T. N. (1994). Baroreceptor regulation of vasopressin and renin secretion: Low-pressure versus high-pressure receptors. *Front. Neuroendocrinol.* 15:1007. doi: 10.1006/frne.1994.1007

Tomilovskaya, E., Shigueva, T., Sayenko, D., Rukavishnikov, I., and Kozlovskaya, I. (2019). Dry immersion as a ground-based model of microgravity physiological effects. *Front. Physiol.* 10:284. doi: 10.3389/fphys.2019.00284

Vinogradova, O. L., Popov, D. V., Saenko, I. V., and Kozlovskaya, I. B. (2002). *Muscle Transverse Stiffness and Venous Compliance Under Conditions of Simulated Supportlessness*. Paris: European Space Agency, 65–67.

Waters, W. W., Ziegler, M. G., and Meck, J. V. (2002). Postspaceflight orthostatic hypotension occurs mostly in women and is predicted by low vascular resistance. *J. Appl. Physiol.* 92, 586–594. doi: 10.1152/japplphysiol.00544.2001

Conflict of Interest: The authors declare that the research was conducted in the absence of any commercial or financial relationships that could be construed as a potential conflict of interest.

frontiers in Physiology

ORIGINAL RESEARCH
published: 10 July 2020
doi: 10.3389/fphys.2020.00692

The Effect of Five-Day Dry Immersion on the Nervous and Metabolic Mechanisms of the Circulatory System

Vasily B. Rusanov[1], Ludmila Kh. Pastushkova[1], Irina M. Larina[1], Anna G. Chernikova[1], Anna G. Goncharova[1], Andrei M. Nosovsky[1], Daria N. Kashirina[1], Alexander G. Brzhozovsky[1,2], Nastassia Navasiolava[3], Alexey S. Kononikhin[2,4], Anna R. Kussmaul[1], Marc-Antoine Custaud[3] and Evgeny N. Nikolaev[2]**

[1] Institute of Biomedical Problems of the Russian Academy of Sciences, Moscow, Russia, [2] Skolkovo Institute of Science and Technology, Skolkovo, Russia, [3] University of Angers, Angers, France, [4] V.L. Talrose Institute for Energy Problems of Chemical Physics, N.N. Semenov Federal Center of Chemical Physics, Russian Academy of Sciences, Moscow, Russia

OPEN ACCESS

Edited by:
François Guerrero,
Université de Bretagne Occidentale, France

Reviewed by:
Jacques Regnard,
University of Franche-Comté, France
Gerardo Bosco,
University of Padua, Italy

***Correspondence:**
Anna R. Kussmaul
annakussmaul@gmail.com
Evgeny N. Nikolaev
e.nikolaev@skoltech.ru

Specialty section:
This article was submitted to Environmental, Aviation and Space Physiology, a section of the journal Frontiers in Physiology

Received: 06 February 2020
Accepted: 27 May 2020
Published: 10 July 2020

Citation:
Rusanov VB, Pastushkova LK, Larina IM, Chernikova AG, Goncharova AG, Nosovsky AM, Kashirina DN, Brzhozovsky AG, Navasiolava N, Kononikhin AS, Kussmaul AR, Custaud M-A and Nikolaev EN (2020) The Effect of Five-Day Dry Immersion on the Nervous and Metabolic Mechanisms of the Circulatory System. Front. Physiol. 11:692. doi: 10.3389/fphys.2020.00692

The purpose of the study was to investigate the regulatory and metabolic changes in the circulatory system when simulating microgravity conditions in a five-day dry immersion. These changes reflect the adaptation processes characteristic for the initial stages of a space flight or a short-duration space flight. Studies were conducted with 13 healthy male volunteers aged 21 to 29 years. The assessment of regulatory and metabolic processes in the circulatory system was based on the heart rate variability (HRV) and urine proteomic profile analysis. It was found that the restructuring of hemodynamics during 5 days hypogravity begins with the inclusion of the nervous circuit of regulation, and for manifestations at the body fluids protein composition level and activation of the metabolic regulation, these periods are apparently insufficient. Perhaps this is due to the fact that the metabolic regulation, being evolutionarily ancient and genetically determined, is more stable and requires more time for its pronounced activation when stimulated by extreme life conditions.

Keywords: circulatory system, regulatory mechanisms, proteomics, dry immersion, effects of microgravity

INTRODUCTION

It is well-known that during space flight, the effect of microgravity has a direct influence on the cardiovascular system, including bioelectric changes in the myocardium and its remodeling, autonomic reflexes and associated physiological processes (Lees, 2005; Shen and Frishman, 2019). Moreover, a normal level of functioning is maintained due to changes in regulatory adaptive mechanisms (Otsuka et al., 2018). The heart rate (HR) reflects cardiovascular homeostasis and is associated with various regulatory influences. During space flight, the resting HR varies slightly compared to terrestrial conditions, and the main changes are manifested in autonomic balance shifts (Baevsky, 1997). From this point of view, we consider the stable level of functioning (resting HR, for instance) as a homeostatic level of regulation, and observed changes in the HR autonomic regulation are considered as adaptive.

For developing the preventive measures aimed at eliminating the negative effects of microgravity and maintaining the cosmonauts operability, studies in model experiments are used, the relevance of the tasks in which increases owing to the planned Moon and Mars expeditions outside the low Earth.

"Dry" immersion (DI; reproduction of the supportlessness conditions) is a model used in gravitational physiology to simulate the effects of microgravity on body systems. DI reproduces cardiovascular, motor and other changes similar to those observed in space flights. Moreover, the severity and directionality of adaptation processes under immersion exposure are with those observed in space flights of various durations (Tomilovskaya et al., 2019).

The purpose of the study was to investigate the regulatory and metabolic changes in the circulatory system when simulating microgravity conditions in a five-day DI as a reflection of the adaptation processes in this system characteristic for the initial stages of space flight or for space flight of short duration.

MATERIALS AND METHODS

The studies were conducted at the "dry immersion" stand of the Institute of Biomedical Problems of the Russian Academy of Sciences (IBMP RAS), with the participation of 13 healthy male volunteers aged 21 to 29 years. All volunteers were allowed to participate in the study by a medical expert commission. The research procedures and methods were reviewed and approved by the IBMP RAS Commission on Biomedical Ethics (protocol No. 273 dated June 23, 2010), and the written voluntary Informed consent was obtained from the participating in the study testers. To simulate the physiological effects of microgravity, the subjects were immersed in water in lying down to the level of the shoulder upper third (water t = 33–34°C) without contact with it, since they were separated from the water by a waterproof, freely fixed to the sides fabric, being freely "hung out" in an immersion environment (Tomilovskaya et al., 2019). During DI, the volunteers were not subjected to either pharmacological or any other additional influences aimed at preventing developing adaptive shifts in physiological systems.

Regulatory and metabolic processes in the circulatory system were evaluated on the basis of heart rate variability (HRV) and urine proteomic profile analysis, since HRV indicators reflect the general state of regulatory mechanisms, and the molecular level of heart rate physiological regulation is reflected in the extracellular fluid protein composition studied by proteomics based on mass spectrometry (Pastushkova et al., 2019).

We estimated the total, for 5 days, impact of immersion effects on these processes. Therefore, the data obtained only before and after DI (at 2 days before the start of the experiment and at + 1 day after the end of the exposure) have been analyzed.

The HRV analysis was carried out in 5-min ECG samples at rest in supine position. The cardiovascular regulatory mechanisms condition was assessed according to the recommendations developed by the European cardiological and North American electrophysiological Societies (No Author List, 1996). The following indicators were analyzed:

Heart rate (bpm) – heart rate, reflects the current level of functioning of the circulatory system.

pNN50 (%) – is the numbe of pairs of adjacent intervals differing by more than 50 ms, in% of the total number of cardiointervals in the array, an indicator of the parasympathetic regulatory branch prevalence over the sympathetic.

Stress index (conventional units) – stress index, index of regulatory systems stress, characterizes the degree to which the activity of sympathetic regulation mechanisms prevails over parasympathetic ones. The SI is used in occupational and environmental studies to quantify the physical and mental stress of work processes (Quendler et al., 2017), to assess the HRV seasonal features (Markov et al., 2016), to evaluate the activation of the adaptive capabilities of the organism, expressed through an imbalance of the autonomic nervous system due to sympathetic predominance (Konstantinova et al., 2017). The SI is included in calculated HRV parameters in the Kubios HRV software[1].

The stress-index (SI) is calculated by geometric methods for assessing the RR intervals distribution over the period of investigation. For the purpose, variation curve (histogram of RR intervals distribution) is built and main characteristics are determined including Mo (mode), AMo (mode amplitude), and MxDMn (variation range).

Mode is the most common interval value in a dynamic series. In case of normal distribution and high process stationarity, Mo differs little from mathematical expectation (M).

AMo (mode amplitude) is a number of intervals corresponding to mode value in% to sample size.

Variation range MxDMn shows the degree of interval variativity in a current dynamic series. It is calculated from the difference of maximum (Mx) and minimum (Mn) intervals and, therefore, can be distorted by arrhythmias or artifacts.

The variation pulsometry data is used to calculate the stress-index.

SI = AMo/(2Mo × MxDMn). The SI characterizes the activity of sympathetic regulation. Activation of the sympathetic regulation during mental or physical stresses manifests itself by rhythm stabilization, decrease of the range of interval duration, and increase of the number of intervals with similar duration (AMo growth). Normal SI fluctuates within 80–150 conventional units. It is very sensitive to the sympathetic tone rise.

The SI is known in Russia since 1970-th and it is almost similar to triangular index, total number of all NN intervals divided by the height of the histogram of all NN intervals measured on a discrete scale with bins of 7·8125 ms (1/128 s).

Power HF (mc^2) – is the raw power of HRV high-frequency component from the total power (sum of HF, LF, and VLF spectral components), the relative level of parasympathetic activity.

Power LF (mc^2) – is the raw power of HRV low-frequency component from the total power (sum of HF, LF, and VLF spectral components), the relative activity of the subcortical sympathetic vasomotor center in the medulla oblongata.

[1]https://www.kubios.com/about-hrv/

LF and HF may also be measured in normalized units (n.u.) which represent the relative value of each power component in proportion to the total power minus the VLF component.

LF/HF (conventional units) is the ratio of the high-frequency and low-frequency components spectral power, an indicator characterizing the balance of sympathetic and parasympathetic influences and the relative activity of the subcortical sympathetic center.

Changes in the extracellular fluid protein composition were evaluated in the study of urine proteome. Urine collection was carried out in the daytime, in the form of a freely separated 2-nd morning fraction, which was subsequently prepared for mass spectrometric analysis, according to the standard protocol (Nkuipou-Kenfack et al., 2014). Urine samples were subjected to preparation, consisting of stages: recovery, alkylation, protein deposition, and proteolysis using trypsin.

The shotgun proteomics methodology was used for semi-quantitative analysis of the obtained polypeptide mixture. The mixture was separated by liquid chromatography (Agilent 1100, Agilent Technologies Inc., Santa Clara, United States) in three repetitions and analyzed by 7T LTQ-FT Ultra hybrid mass spectrometer (Thermo, Bremen, Germany) of ion cyclotron resonance combined with a linear quadrupole ion trap. A column with reversed phase ReproSil-Pur C18 (particle diameter 3 μm, pore diameter 100 Å, Dr. Maisch GmbH, Ammerbuch-Entringen, Germany) manufactured using a capillary emitter (Pico-tip, New Objective Inc., United States), has been used for chromatography.

The peptides mixture was analyzed using the Xcalibur software (Thermo, Bremen, Germany) in data dependent aqusition (DDA) mode. Proteins were identified with the help of MaxQuant software, using the SwissProt database. Only proteins that were identified by at least 2 peptides with one which is unique to the protein were subjected to further analysis.

Two hundred fifty six different proteins were identified after chromatography-mass spectrometric analysis of all urine samples by UniProtKB nomenclature.

The method of principal components was used for statistical analysis (Nosovsky et al., 2018), and the Perseus software package was used to determine molecular functions and biological processes with the participation of identified proteins.

RESULTS

When assessing the dynamics of the mean group values of HRV indicators characterizing the modulating effect of the ANS sympathetic (SI) and ANS parasympathetic (pNN50) branch after DI exposure, a shift in the autonomic balance toward sympathetic activation was revealed. However, other indicators characterizing the certain aspects of the regulatory mechanism have not changed. High-frequency oscillations (HF) and low-frequency oscillations (LF), also had unreliable changes after immersion (**Table 1**).

The activation of sympathetic nerve regulatory mechanisms occurred as a result of the interaction of homeostatic and adaptive mechanisms in order to maintain cardiovascular homeostasis and increase adaptive capabilities and mobilize functional reserves. Apparently, after 5-day immersion, the mechanisms of the nervous regulation of the heart rhythm are turned on primarily. At the same time, systemic homeostasis does not change, as evidenced by the stability of heart rate parameter, an integral physiological indicator of most stress-limiting body systems, including the cardiovascular system.

TABLE 1 | Heart rate variability indices before and after 5-days dry immersion.

Indicator	Before immersion (M)	After immersion (M)
pNN50 (%)	23,97	15,19*
SI (c.u.)	117,03	183,07*
TP(mc^2)	4623,83	3430,76*
HF(mc^2)	1611,53	1123,84
LF(mc2)	2912,3	2306,92
HF(n.u.)	36,2	32,1
LF(n.u.)	63,4	67,9
LF/HF(c.u.)	3,60	3,92
HR(bpm)	76,30	84,92

Significant changes after immersion (the Wilcoxon signed-rank test $p < 0.05$).

One of the regulation systems is the humoral-metabolic system, which exerts an effect through the activity of biologically active substances circulating in body fluids and tissues, including of protein nature (proteins). From the general list of 256 proteins, detected prior to the immersion exposure in the urine proteomic profile, we identified 6 proteins that reflect regulatory processes in the circulatory system: CADM4, Immunoglobulin heavy alpha-1 (IGHA1), TF, AXL, Gal-3BP, and MXRA8.

The physiological (and regulatory) role of the mentioned proteins was clarified by manual annotation using open databases.

However, statistical analysis showed the absence of significant changes in the concentrations of these proteins in the urine proteome after 5-day immersion (**Figure 1**). Perhaps this is due to the fact that the metabolic contour of regulation, is more stable and requires more time for its pronounced activation when stimulated by extreme life conditions. In this regard, it seems logical that the 5-day duration of immersion does not change the metabolic mechanisms of regulation, which are reflected in the urine proteomic profile.

DISCUSSION

Our analysis before exposure to a five-day DI revealed the presence of proteins associated with the regulation of cardiovascular system. In our opinion, this combination provides a balance of cardiovascular homeostasis, and is associated with complex interacting processes of atherogenesis, neoangiogenesis, calcium channels activation, changes in cell adhesion, and transmembrane properties, and extracellular matrix metabolism. At the tissue level, signaling proteins are involved in changing the vascular wall stiffness and the endothelium properties, affecting the peripheral vascular resistance.

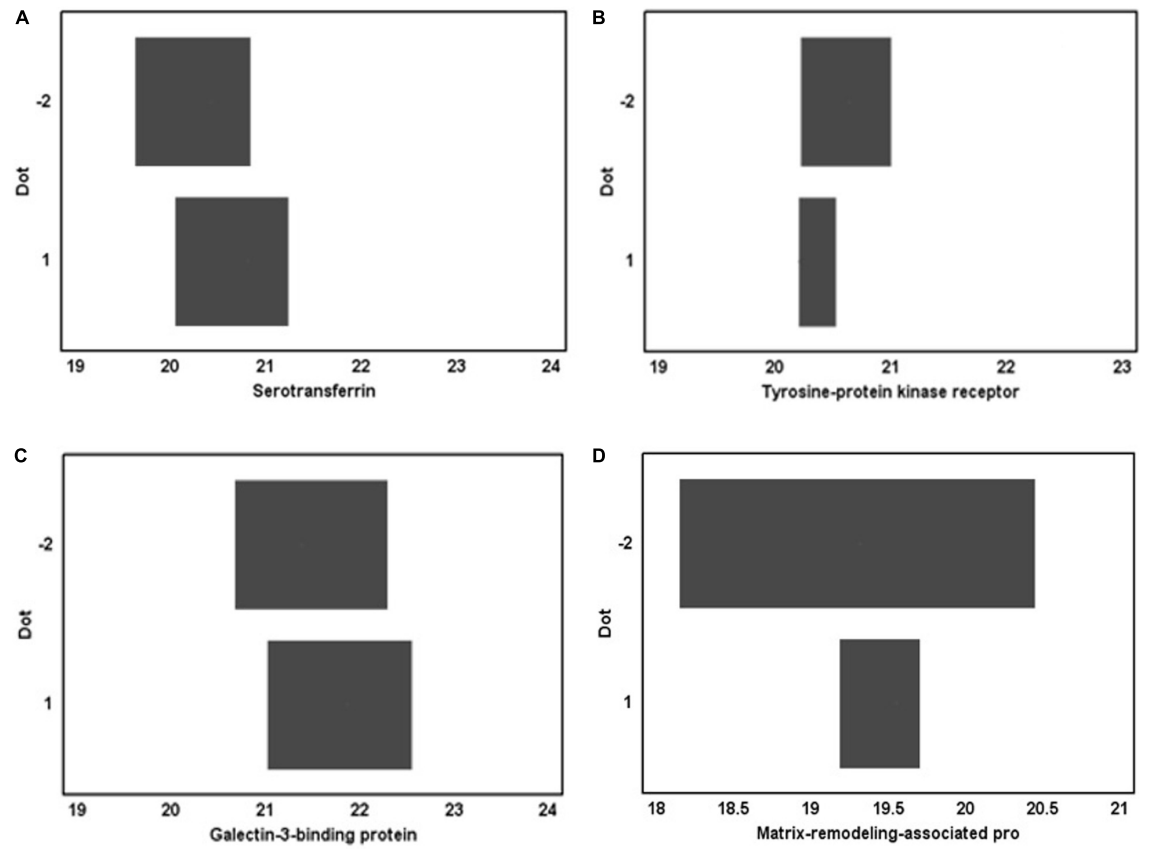

FIGURE 1 | Proteins identified in the urine proteomic profile before DI and their concentration after immersion exposure. **(A)** serotransferrin, **(B)** tyrosine-protein kinase receptor, **(C)** galectin-3-binding protein, and **(D)** matrix-remodeling-associated protein.

Together with HRV indices, proteome signaling molecules reflect the nervous and metabolic control mechanisms condition and realize a homeostatic role, and the orientation and intensity of changes in both patterns determine the adaptation strategy of the circulatory system in the acute period of body adaptation when simulating the conditions and physiological effects of microgravity.

CADM4-membrane protein is involved in the transmission of a nerve impulse as a stimulus of cardiac contraction (Zeng and Yelon, 2014). Nectins and nectin-like molecules (Necls)/Cadms are Ca2 + -dependent adhesion molecules of the immunoglobulin superfamily expressed in cell of most types. Nectins mediate not only homotypic, but also heterotypic cell adhesion, in contrast to classical cadherins, which are involved only in homophilic adhesion. The participation of nectins and Necls in the organogenesis of sensory organs – the eyes, inner ear, and cerebral cortex, and in various developmental processes, including the formation of synapses, axons, and myelination, helps to understand the connecting role of cell adhesion molecules in the implementation of nerve impulse transmission and the features of its effect (Lambert et al., 2016).

Immunoglobulin heavy alpha-1 is a membrane-bound or secreted glycoprotein produced by b-lymphocytes. Apparently, it is the main regulatory protein that affects the arteries, veins and cardiac muscle stiffness and elasticity, mediating the features of cardiac contraction in accordance with the rigidity of the vascular wall. The IGHA1 associations with the influence of main factors determining the vascular wall stiffness and elasticity and with chronic vascular diseases has been proved. The proteins associated with atherosclerosis are: IGHA1, serum amyloid A1 (SAA), and four complement cascade proteins: complement factor B (CFAB), complement C2 (CO2), complement C3 (CO3), and complement C1s (C1S) – a subcomponent that is proposed to be considered as biomarkers of the cardiovascular risk (Gordon et al., 2018). Cavassan et al. (2019) identified immunoglobulin heavy constant alpha 1 and seven more proteins that assotiate with the presence of congestive heart failure, hypertension, and the patient's age.

TF is a plasma glycoprotein that is synthesized in the liver. It is believed that the study of serotransferrin metabolism is important in the study of the vascular diseases pathogenesis (Golizeh et al., 2017). An association of endothelial damage with a violation of the rheological properties of blood and serotransferrin was noticed (Orlov et al., 2012).

AXL is expressed mainly in the vascular endothelium, and is involved in the regulation of proliferation, migration, invasion, and the formation of endothelial cells (Li et al., 2017). It was shown that Gas6/UFO signaling plays an important role

in the survival of endothelial cells during the development of acidosis (Gustafsson et al., 2009). AXL is involved in the angiogenesis regulation. It was found that patients with heart failure and severe left ventricular remodeling processes have a higher level of sAXL, which indicates the potential role of the GAS6-AXL system in the pathophysiology of these processes (Caldentey et al., 2019). Increased AXL expression in arteries was revealed in patients after coronary artery bypass grafting. AXL stimulates STAT1 signaling (a member of the transcription factors of signal converters and transcription activators family) by inhibiting SOCS1 (cytokine signaling suppressors) in activated smooth muscle cells during venous transplant remodeling (Batchu et al., 2015).

Gal-3BP – stimulates intercellular adhesion and regulates intercellular transmission of pro-inflammatory signals, including in macrophages originating from human monocytes (DeRoo et al., 2015; Gleissner et al., 2017; Sun et al., 2017). Gal-3BP levels are independently associated with markers of metabolic and inflammatory response. Subcellular microvesicles containing galectin-3-binding protein are involved in the transmission of information from cell to cell and regulate immunity, hemostasis, transferring at the cell membrane allotted areas (size from 200 to 1000 nm), usually called microparticles (MP). The number and, in particular, the MP composition seem to reflect the state of their parent cells. Therefore, the components of the MPs protein composition may have great potential as clinical biomarkers studied by proteomics. The overexpression of galectin-3-binding protein was observed in patients with venous thromboembolism and systemic autoimmune diseases. Thus, this protein can act as a marker of "pathogenic" subcellular microvesicles (Nielsen et al., 2017). It is associated with the process of atherosclerosis and its level increasing is prognostically unfavorable for patients with coronary artery disease, since this protein is highly expressed in atherosclerotic plaques and its content correlates with the clinical manifestations of ischemia. It is supposed that quantitative characteristics of this protein level help to monitor the processes of atherosclerotic plaques destabilization (Hao et al., 2019).

MXRA8 through intermediaries is associated with cell adhesion proteins, participating in the processes of normal permeability at the tissue level (Yonezawa et al., 2003; Zhang et al., 2018), and probably, through this, taking part in the regulatory processes of the circulatory system.

CONCLUSION

Under the conditions of "dry immersion" there is a change in the autonomic regulatory mechanisms of the circulatory system. This is due to hypogravity conditions and is primarily associated with elimination of the support reaction, redistribution of body fluid volumes and loss of water by the body. This changes cause energy-metabolic shifts that require activation of the corresponding regulatory mechanisms (Larina et al., 2011). This is similar to the physiological effects observed in space flights. Most of these changes are characterized by both very rapid progression and recovery upon returning to normal conditions – as a result it is believed that microgravity causes functional changes in the cardiovascular system that are adaptive in their nature (Aubert et al., 2016; Garrett-Bakelman et al., 2019). In addition, Sun et al. (2015) revealed phase changes in HRV in three-day and five-day immersion dynamics, manifested in the ANS sympathetic branch modulating effects decrease in the first two days of DI.

The hemodynamics restructuring during 5-days hypogravity begins by the involvement of the "nervous contour of regulation," and for manifestations at the level of body fluids protein composition, activation of the "metabolic contour of regulation," this DI duration is, obviously, insufficient. The obtained data require further studies in the direction of clarifying the time at which the "metabolic regulatory contour" become active. In the framework of a unified concept about a hierarchy of control levels in biological systems, it is important to evaluate the dynamics of the human body biological fluids proteome, in particular urine, as the most accessible of them for research in relation to the control mechanisms of regulation.

DATA AVAILABILITY STATEMENT

The datasets generated for this study are available on request to the corresponding author.

ETHICS STATEMENT

The studies involving human participants were reviewed and approved by Institute of Biomedical Problems of the Russian Academy of Sciences Commission on Biomedical Ethics. The patients/participants provided their written informed consent to participate in this study.

AUTHOR CONTRIBUTIONS

IL, VR, EN, and M-AC conceived and designed the experiments. LP, VR, DK, and NN performed the experiments. AC, AB, ASK, AG, NN, and AN analyzed the data. VR, LP, AC, AG, and ARK wrote the manuscript. All authors read and approved the final manuscript.

FUNDING

Research related to the high-resolution mass spectrometry study of urine proteome was supported by the Russian Science Foundation Grant No. 19-14-00306.

ACKNOWLEDGMENTS

The work was carried out within the framework of the basic Russian Academy of Sciences themes 63.1, 64.1, and 65.3 for 2013–2020 years. The authors of the manuscript are sincerely grateful to the team of Dry Immersion. Organizers – Department of Dr. E. Tomilovskaya, IBMP RAS.

REFERENCES

Aubert, A. E., Larina, I., Momken, I., Blanc, S., White, O., Kim Prisk, G., et al. (2016). Towards human exploration of space: the THESEUS review series on cardiovascular, respiratory, and renal research priorities. *NPJ Microgr.* 1:16031. doi: 10.1038/npjmgrav.2016.31

Baevsky, R. M. (1997). Noninvasive methods in space cardiology. *J. Cardiovasc. Diagn. Proced. Fall* 14, 161–171.

Batchu, S. N., Xia, J., Ko, K. A., Doyley, M. M., Abe, J.-I., Morrell, C. N., et al. (2015). Axl modulates immune activation of smooth muscle cells in vein graft remodeling. *Am. J. Physiol. Heart Circ. Physiol.* 309, H1048–H1058. doi: 10.1152/ajpheart.00495.2015

Caldentey, G., García De Frutos, P., Cristóbal, H., Garabito, M., Berruezo, A., Bosch, X., et al. (2019). Serum levels of Growth Arrest-Specific 6 protein and soluble AXL in patients with ST-segment elevation myocardial infarction. *Eur. Heart J. Acute Cardiovasc. Care* 8, 708–716. doi: 10.1177/2048872617740833

Cavassan, N. R. V., Camargo, C. C., de Pontes, L. G., Barraviera, B., Ferreira, R. S., Miot, H. A., et al. (2019). Correlation between chronic venous ulcer exudate proteins and clinical profile: a cross-sectional study. *J. Proteomics* 192, 280–290. doi: 10.1016/j.jprot.2018.09.009

DeRoo, E. P., Wrobleski, S. K., Shea, E. M., Al-Khalil, R. K., Hawley, A. E., Henke, P. K., et al. (2015). The role of galectin-3 and galectin-3–binding protein in venous thrombosis. *Blood* 125, 1813–1821. doi: 10.1182/blood-2014-04-569939

Garrett-Bakelman, F. E., Darshi, M., Green, S. J., Gur, R. C., Lin, L., Macias, B. R., et al. (2019). The NASA Twins Study: a multidimensional analysis of a year-long human spaceflight. *Science* 364:eaau8650. doi: 10.1126/science.aau8650

Gleissner, C. A., Erbel, C., Linden, F., Domschke, G., Akhavanpoor, M., Helmes, C. M., et al. (2017). Galectin-3 binding protein, coronary artery disease and cardiovascular mortality: insights from the LURIC study. *Atherosclerosis* 260, 121–129. doi: 10.1016/j.atherosclerosis.2017.03.031

Golizeh, M., Lee, K., Ilchenko, S., Ösme, A., Bena, J., Sadygov, R. G., et al. (2017). Increased serotransferrin and ceruloplasmin turnover in diet-controlled patients with type 2 diabetes. *Free Radic. Biol. Med.* 113, 461–469. doi: 10.1016/j.freeradbiomed.2017.10.373

Gordon, S. M., Chung, J. H., Playford, M. P., Dey, A. K., Sviridov, D., Seifuddin, F., et al. (2018). High density lipoprotein proteome is associated with cardiovascular risk factors and atherosclerosis burden as evaluated by coronary CT angiography. *Atherosclerosis* 278, 278–285. doi: 10.1016/j.atherosclerosis.2018.09.032

Gustafsson, A., Matuszewska, D., Johansson, M., Ekman, C., Hafizi, S., Ljungberg, B., et al. (2009). Differential expression of Axl and Gas6 in renal cell carcinoma reflecting tumor advancement and survival. *Clin. Cancer Res.* 15, 4742–4749. doi: 10.1158/1078-0432.CCR-08-2514

Hao, X., Liming, C., Hang, L., Cui, Y., Cui, L., Zhang, P., et al. (2019). Expression of Mac-2 binding protein in human carotid atheroma is associated with plaque instability and clinical manifestations. *Biomed. Pharmacother.* 110, 465–472. doi: 10.1016/j.biopha.2018.12.015

Konstantinova, E., Maslakova, T., Zhivoderov, A., Shalaumova, Y., and Varaksin, A. (2017). Imbalances of the autonomic nervous system in people living in radioactive contaminated territories: radioactivity and vegetative imbalance. *Int. J. Radiat. Res.* 15, 317–320.

Lambert, N. G., ElShelmani, H., Singh, M. K., Mansergh, F. C., Wride, M. A., Padilla, M., et al. (2016). Risk factors and biomarkers of age-related macular degeneration. *Prog. Retin. Eye Res.* 54, 64–102. doi: 10.1016/j.preteyeres.2016.04.003

Larina, I. M., Baevsky, R. M., Pastushkova, L. K., Navasiolava, N. M., Custaud, M.-A., Eshmanova, A. K., et al. (2011). Seven-day dry immersion: interrelationship between the changes in the water-electrolyte balance and cardiovascular responses. *Hum. Physiol.* 37, 602–609. doi: 10.1134/S0362119711050124

Lees, P. J. (2005). Cardiology in space. *Hellenic J. Cardiol.* 46, 320–323.

Li, X., Chen, M., Lei, X., Huang, M., Ye, W., Zhang, R., et al. (2017). Luteolin inhibits angiogenesis by blocking Gas6/Axl signaling pathway. *Int. J. Oncol.* 51, 677–685. doi: 10.3892/ijo.2017.4041

Markov, A., Solonin, I., and Bojko, E. (2016). Heart rate variability in workers of various professions in contrasting seasons of the year. *Int. J. Occup. Med. Environ. Health* 29, 793–800. doi: 10.13075/ijomeh.1896.00276

Nielsen, C. T., Østergaard, O., Rasmussen, N. S., Jacobsen, S., and Heegaard, N. H. H. (2017). A review of studies of the proteomes of circulating microparticles: key roles for galectin-3-binding protein-expressing microparticles in vascular diseases and systemic lupus erythematosus. *Clin. Proteomics* 14:11. doi: 10.1186/s12014-017-9146-0

Nkuipou-Kenfack, E., Koeck, T., Mischak, H., Pich, A., Schanstra, J. P., Zürbig, P., et al. (2014). Proteome analysis in the assessment of ageing. *Ageing Res. Rev.* 18, 74–85. doi: 10.1016/j.arr.2014.09.002

No Author List (1996). Heart rate variability. Standards of measurement, physiological interpretation, and clinical use. Task force of the european society of cardiology and the north american society of pacing and electrophysiology (membership of the task force listed in the appendix). *Eur. Heart J.* 17, 354–381.

Nosovsky, A., Vassilieva, G., and Kaminskaya, E. (2018). Application of multidimensional projections in the practice of medical and biological research. *Norwegian J. Dev. Int. Sci.* 15, 9–13.

Orlov, V. N., Lukach, V. N., Dolgich, V. T., Soboleva, E. L., and Ivanova, A. M. (2012). The contribution of the impaired iron metabolism in the development of microcirculation disorders in reperfusion (experimental study). *Sibirskiy Med. J.* 112, 71–74.

Otsuka, K., Cornelissen, G., Kubo, Y., Shibata, K., Hayashi, M., Mizuno, K., et al. (2018). Circadian challenge of astronauts' unconscious mind adapting to microgravity in space, estimated by heart rate variability. *Sci. Rep.* 8:10381. doi: 10.1038/s41598-018-28740-z

Pastushkova, L. H., Rusanov, V. B., Goncharova, A. G., Brzhozovsky, A. G., Kononikhin, A. S., Chernikova, A. G., et al. (2019). Urine proteome changes associated with autonomic regulation of heart rate in cosmonauts. *BMC Syst. Biol.* 13(Suppl. 1):17. doi: 10.1186/s12918-019-0688-9

Quendler, E., Trieb, K., and Nimmerichter, A. (2017). Validation of automated detection of physical and mental stress during work in a Hühnermobil 225. *Ann. Agric. Environ. Med.* 24, 329–331. doi: 10.5604/12321966.1235183

Shen, M., and Frishman, W. H. (2019). Effects of spaceflight on cardiovascular physiology and health. *Cardiol. Rev.* 27, 122–126. doi: 10.1097/CRD.0000000000000236

Sun, I., Voronkov, Y. I., Ardashev, V. N., and Glychova, S. I. (2015). Heart rhythm variability analysis and assessment of the spinal pain syndrome during dry immersion. *Aviakosm Ekolog. Med.* 49, 33–37.

Sun, Y. X., Gao, C. Y., Wang, X. Q., Yuan, Y. Q., Liu, Y. H., and Jia, J. G. (2017). Serum quantitative proteomic analysis of patients with keshan disease based on iTRAQ labeling technique: a first term study. *J. Trace Elem. Med. Biol.* 44, 331–338. doi: 10.1016/j.jtemb.2017.09.012

Tomilovskaya, E., Shigueva, T., Sayenko, D., Rukavishnikov, I., and Kozlovskaya, I. (2019). Dry immersion as a ground-based model of microgravity physiological effects. *Front. Physiol.* 10:284. doi: 10.3389/fphys.2019.00284

Yonezawa, T., Ohtsuka, A., Yoshitaka, T., Hirano, S., Nomoto, H., Yamamoto, K., et al. (2003). Limitrin, a novel immunoglobulin superfamily protein localized to glia limitans formed by astrocyte endfeet. *Glia* 44, 190–204. doi: 10.1002/glia.10279

Zeng, X. X., and Yelon, D. (2014). Cadm4 restricts the production of cardiac outflow tract progenitor cells. *Cell. Rep.* 7, 951–960. doi: 10.1016/j.celrep.2014.04.013

Zhang, R., Kim, A. S., Fox, J. M., Nair, S., Basore, K., Klimstra, W. B., et al. (2018). Mxra8 is a receptor for multiple arthritogenicalphaviruses. *Nature* 557, 570–574. doi: 10.1038/s41586-018-0121-3

Conflict of Interest: The authors declare that the research was conducted in the absence of any commercial or financial relationships that could be construed as a potential conflict of interest.

The handling editor is currently organizing a Research Topic with one of the authors M-AC.

frontiers in Physiology

DATA REPORT
published: 11 January 2022
doi: 10.3389/fphys.2021.753291

Proteomic Characterization of Dry Blood Spots of Healthy Women During Simulation the Microgravity Effects Using Dry Immersion

Daria N. Kashirina[1], Alexander G. Brzhozovskiy[1,2], Wen Sun[1], Ludmila Kh. Pastushkova[1], Olga V. Popova[1], Vasiliy B. Rusanov[1], Evgeny N. Nikolaev[2], Irina M. Larina[1] and Alexey S. Kononikhin[1,2]**

[1] Institute of Biomedical Problems – Russian Federation State Scientific Research Center, Russian Academy of Sciences, Moscow, Russia, [2] CDISE, Skolkovo Institute of Science and Technology, Moscow, Russia

Keywords: proteomics, dried blood spots, dry immersion, timsTOF pro mass spectrometry, red blood cells

OPEN ACCESS

Edited by:
Marc-Antoine Custaud, Université d'Angers, France

Reviewed by:
Mauricio Zamorano, University of La Frontera, Chile
Jochen Zange, German Aerospace Center (DLR), Germany

****Correspondence:***
Daria N. Kashirina
daryakudryavtseva@mail.ru
Alexey S. Kononikhin
alex.kononikhin@gmail.com

Specialty section:
This article was submitted to Environmental, Aviation and Space Physiology, a section of the journal Frontiers in Physiology

Received: *04 August 2021*
Accepted: *22 September 2021*
Published: *11 January 2022*

Citation:
Kashirina DN, Brzhozovskiy AG, Sun W, Pastushkova LK, Popova OV, Rusanov VB, Nikolaev EN, Larina IM and Kononikhin AS (2022) Proteomic Characterization of Dry Blood Spots of Healthy Women During Simulation the Microgravity Effects Using Dry Immersion. Front. Physiol. 12:753291. doi: 10.3389/fphys.2021.753291

INTRODUCTION

Dry immersion (DI) is one of the most widely used terrestrial microgravity models. Dry immersion accurately and quickly reproduces most of the physiological effects of the early period of space flights (Tomilovskaya et al., 2019). The model simulates such factors of space flight as lack of support, mechanical and axial unloading, lack of physical activity. Almost complete immersion in water makes it possible to simulate cardiovascular, musculoskeletal, and other effects of microgravity (Navasiolava et al., 2010). There is a 17% loss of plasma volume observed after 2 days of DI and which is comparable to post-flight observation (Treffel et al., 2017). Dry immersion experiment used as microgravity model leads to the body fluid media displacement as in space flight, which is associated with a uniform compression of the subject's body. Body fluid media displacement leads to a decrease in heart rate within a few hours after immersion in water. At the same time, the heart rate is reduced by five beats per minute, and the blood pressure is reduced by 5 mm Hg in the first 4 h (Navasiolava et al., 2010). Similar changes in heart size and stroke volume are observed both in DI and in space flight. Dry immersion also causes muscle wasting and changes in the structure of the musculoskeletal system similar in nature and timing of development to those changes that occur in space flight. This is mainly due to the absence of gravitational stress exerted on the object of study (Treffel et al., 2017). Although the physiological response of the organism to DI conditions is similar to that during the space flight there are some differences that need to be studied on molecular level.

Regulatory and metabolic changes occurring in DI are reflected in the protein composition of body fluids. In the blood, these changes were previously fragmentarily studied. Thus, in an experiment with 5-day DI with 20 young healthy men, an increase in the level of unconjugated bilirubin and myoglobin in serum was revealed, which confirmed that DI could promote hemolysis and myolysis. Increases in hepcidin, ferritin, and haptoglobin have also been shown, which may be associated with increased serum iron levels (Nay et al., 2020). Previously, a 7-day experiment simulating unsupported conditions was conducted with participation of five healthy male volunteers who were not exposed to any additional influences. The results obtained by the method of two-dimensional electrophoresis showed a change in the concentration of proteins of the hemostasis and complement systems: a decrease in the concentration of α-, β-fibrinogen, factor C4B complement, and serum amyloid P (Trifonova et al., 2010). On the last day of 7-day DI a significant decrease in fragments of fibrinopeptide A and peptide activator of coagulation factor XIII was found both in the control group and in the group with prophylaxis. A lower concentration

of these proteins could indicate a decrease in the fibrinolytic activity of the blood and shifts in the hemostatic system during immersion (Pakharukova et al., 2011). At the same time, on the 7th day after the end of the experiment, a significant increase in the blood level of apolipoproteins A–I, A–IV, and also E after DI was observed which may indicate a changes in the functioning of lipid transport during the adaptation period (Trifonova et al., 2010). In the course of 5-day DI with 14 men participants, an increase in the peaks of proteins C3 and C4 of the complement system, high molecular weight kininogen and fibrinogen was found which also may confirm the involvement of the hemostasis and the complement systems in the body's response to conditions of DI (Pastushkova et al., 2012). Comparative analysis of changes in the protein composition of blood after a real space flight and model experiments (21 days of head-down bed rest and 21 days of DI) revealed nine common proteins (A1BG, A2M, SERPINA1, SERPINA3, SERPING1, SERPINC1, HP, CFB, TF) which change the level after landing and in the ground experiments. These proteins made it possible to identify processes influenced by microgravity, including hemostasis, platelet degranulation, and protein metabolism (Brzhozovskiy et al., 2019).

Proteomics methods have not yet become widespread in the study of the effects of extreme conditions on the human body. Analysis of human blood and urine proteome is challenging because almost all proteins synthesized in the human body get into the plasma and the dynamic range of proteins concentrations is quite large. The next challenge is data analysis and interpretation since most of proteins are multifunctional and participate in many biological pathways forming a complex network of molecular interactions. Nevertheless, proteomic methods have made it possible to determine proteins that respond to a complex set of DI conditions. System analysis of the proteomic data and biological pathways made it possible to clarify the molecular mechanisms of changes caused by DI in various physiological systems, including the cardiovascular system. Proteome changes in biological fluids may indicate the processes of atherogenesis, neoangiogenesis, changes in cell adhesion, metabolism of the extracellular matrix, which ultimately may affect the function of the heart and blood vessels (Rusanov et al., 2020). In addition to confirming the already known effects of microgravity, proteomic analysis is able to reveal new effects that appear at the molecular level but have not yet been considered.

Proteomics methods are becoming more powerful and sensitive tools for studying the protein composition in different biological samples. Dried blood spot (DBS) micro-sampling technique has already been found to be useful for both population-wide screening and in research studies. Detecting up to 700 proteins in DBS sample has become quite possible which expand the availability for detecting and quantifying proteins (Eshghi et al., 2020). A deep blood proteome analysis can facilitate the discovery of new data and mechanisms of human adaptive response to DI conditions.

Thus, the aim of the study was to apply blood proteome analysis with DBS micro-sampling technique to study on the molecular level the physiological response to the DI conditions and provide new information about previously unknown mechanisms of the adaptive processes. In this work an untargeted proteomic analysis of DBS samples collected from six healthy young women during 3 days DI experiment was performed. As far as we know this is the first proteomic study of the female reaction to simulated weightlessness. The adaptive reactions of the body were monitored on a daily basis during DI experiment.

MATERIALS AND METHODS

Dry Immersion Experiment Design

Six healthy young women (age 30.17 ± 5.5 years) participated in the experiment with 3-day DI. The study involving women was carried out for the first time. The experiment was organized by the State Research Center of the Russian Federation—IBMP RAS, Moscow, and carried out at the "dry immersion" stand on the territory of the IBMP RAS. The stand is a part of the unique scientific installation "Medical and technical complex for the development of innovative technologies of space biomedicine in the interests of ensuring orbital and interplanetary flights, as well as the development of practical health care." The bath was modified, which made it possible to automate many technical systems while strictly preserving all its functional qualities.

All the volunteers were found healthy by the medical expert commission and admitted to conduct the tests. Previously, the research procedures and methods were reviewed and approved by the Commission on Biomedical Ethics at the IBMP RAS. All subjects signed written informed consent. To simulate the physiological effects of microgravity, the subjects were immersed in water in a prone position to the level of the upper third of the shoulder (water $t = 33$–34°C), but did not come into contact with it, being separated from the water by a waterproof fabric, which was fixed to the sides in such a way that it remained free, not taut. During the DI, volunteers were not exposed to any additional influences aimed at preventing the development of adaptive shifts in physiological systems. Every evening the subject was raised from the bath for an average of 15–20 min for hygiene procedures, most of which were carried out in the subject's lying position. The diet was balanced. Water consumption was free. In order to avoid various influences on the studied parameters of the hormonal background of the normal menstrual cycle, the participants were synchronized by the phase of the cycle for the period of the beginning of the study (proliferative phase).

Capillary Blood Sampling

Capillary blood was obtained by puncturing the phalanx of the fourth finger with an automatic scarifier. Using an automatic pipette, 40 μl of blood was taken and placed on filter paper for drying. After collection, the blood stains were dried on filters at ambient temperature (19–26°C) for 2–3 h with minimal exposure to sunlight, and then placed in a zip-lock bag. The filters were stored at a temperature of −20°C before further sample preparation for LC-MS/MS analysis.

Sample Preparation

The DBS was excised and placed in a 1.5 ml polypropylene Eppendorf tube. Proteins were extracted in 1 ml of a solution of 25 mM ammonium bicarbonate, 1% sodium deoxycholate, and

5 mM TCEP (tris (2-carboxyethyl) phosphine hydrochloride) (Thermo Scientific) at 60°C with vortexing at 1,000 rpm (Thermomixer, Eppendorf) for 1 h.

The sample preparation method included reduction with 0.1 M dithiothreitol in 0.1 M Tris buffer (pH 8.5) containing 8 M urea for 30 min at 47°C, as well as alkylation with 0.05 M iodoacetate and incubation for 30 min in the dark at room temperature. Then precipitation was carried out with five volumes of acetone in the presence of 0.1% TFA at −20°C overnight.

The sample preparation procedure was completed by trypsinolysis in 0.05 M ammonium bicarbonate buffer. To the precipitated mixture of proteins were added 100 μl of the buffer and 2 μl of trypsin solution at a concentration of 1 μg/μl in 50 mM acetic acid. Incubation was carried out overnight in a thermomixer at 37°C with shaking at 750 rpm. Then, 1 μl of a 10% aqueous formic acid solution was added to inactivate trypsin and precipitate DOC. The sample was centrifuged at 21,000 g for 10 min, and 20 μl of the supernatant was transferred to a new tube. At this stage, the sample was ready for mass spectrometric analysis.

LC–MS/MS Proteomic Analysis

The resulted tryptic peptide mixture was analyzed using liquid chromatography–mass spectrometry method based on a nano-HPLC Dionex Ultimate3000 system (Thermo Fisher Scientific, USA) and a timsTOF Pro (Bruker Daltonics, USA) mass spectrometer. A packed emitter column (C18, 25 cm × 75 μm × 1.6 μm) (Ion Optics, Parkville, Australia) was used to separate peptides at a flow rate of 400 nl/min by gradient elution from 4 to 90% of phase B during 40 min. Mobile phase A consisted of 0.1% formic acid in water and mobile phase B consisted of 0.1% formic acid in acetonitrile.

Mass spectrometric analysis was performed using the parallel accumulation serial fragmentation (PASEF) acquisition method (Meier et al., 2018). An electrospray ionization (ESI) source was operated at 1,500 V capillary voltage, 500 V end plate offset, and 3.0 L/min of dry gas at temperature of 180°C. The measurements were carried out in the m/z range from 100 to 1,700 Th. The ion mobility was in the range from 0.60 to 1.60 V s/cm^2. The total cycle time was 1.88 s and the number of PASEF MS/MS scans was set to 10.

Data Analysis

The LC-MS/MS data obtained were analyzed using PEAKS Studio 8.5. The database search for protein/peptides identification was performed against the SwissProt database with the following parameters: parent mass error tolerance–20 ppm; fragment mass error tolerance −0.03 Da; enzyme—trypsin; missed cleavages–3; fixed modifications—Carbamidomethyl (C); variable modifications—Oxidation (M), Acetylation (N-term). False discovery rate (FDR) threshold was set to 0.01. All the LC-MS/MS and proteomics results have been deposited to the ProteomeXchange Consortium via the PRIDE (Vizcaino et al., 2016) partner repository with the dataset identifier PXD027654 and 10.6019/PXD027654. Proteins quantification was carried out using label-free method using normalized intensities of corresponding tryptic peptides across all samples and represented by a normalized intensity profile (sample area units from PEAKS) that was extracted from LC-MS/MS data.

Statistical Methods

To identify significant differences in the concentration of proteins between the points of the experiment, analysis of variance (ANOVA, p-value < 0.05) was used in the Statistica 12 program.

Bioinformatic Tools

Functional protein annotation was carried out using the String web resource (https://string-db.org).

Dynamics of Proteomic Changes via Dry Blood Spots

All dry blood spots (DBS) were analyzed with one of the top proteomics methods based on the PASEF acquisition approach implemented on the timsTOF Pro instruments. The approach allowed us to perform deep DBS proteome analysis and to identify ∼500–700 proteins in each sample with relative concentrations of each protein. A total of 1,256 proteins were identified and the relative concentrations were determined at least at one of the five experimental points during DI experiment.

Comparison of the relative concentrations of proteins made it possible to reveal the dynamics of changes in the content of proteins in the DBS samples. As a result of ANOVA 24 proteins were identified as significantly different (p-value < 0.05) between the time points during DI experiment (**Table 1**). A *post-hoc* analysis by the Tukey method showed that statistically significant differences in protein concentrations mainly occurs on 2nd and 3rd days of DI relative to the background (2 days before DI). At the same time the proteins with the most significantly changed level at the end of DI experiment and relative to the background were identified. The summary information regarding significantly changed proteins is presented in **Table 1** and shows the day of the experiment on which the protein concentration significantly differed from the background values. It is interesting to note that on first day of DI only one protein differed from the background while on the second day 12 proteins differed. However, on the third day some adaptation to the experimental conditions was observed—eight proteins differed. After leaving the experiment on the second day 5 proteins still did not come to background levels. Among these proteins is the proteasome subunit alpha type-2 (PSMA2) which is involved in the proteolytic degradation of most intracellular proteins. It should be noted that proteasomal protein degradation is enhanced including the response to oxidative stress (Kaya and Radhakrishnan, 2020). Concentrations of immunoglobulin heavy constant alpha 1 (IGHA1), profilin-1 (PFN1) which at low concentrations enhances polymerization of actin, lumican (LUM) that is extracellular matrix protein, remained below the background level.

The set of significantly changed proteins was divided into up-regulated and down-regulated proteins and analyzed using the String internet resource (**Figure 1**). According to the GO database, the following biological processes are

TABLE 1 | DBS proteins with significantly different (p-value < 0.05) relative concentrations** between the three time points during 3 days dry immersion (DI) and background (2 days before DI).

Protein	Gene	p-Values	Background (Mean ± SD)	First day of DI (Mean ± SD)	Second day of DI (Mean ± SD)	Third day of DI (Mean ± SD)	Two days after DI (Mean ± SD)
Serum albumin	ALB	0.019	4,534,033 ± 555,854	3,938,016 ± 764,137	3,960,933 ± 659,299	3,186,150 ± 402,832*	3,966,716 ± 651,992
Apolipoprotein A4	APOA4	0.027	126,956 ± 71,690	67,194 ± 41,250	54,624 ± 30,611*	42,357 ± 31,252*	89,280 ± 37,731
Angiotensinogen	AGT	0.046	72,563 ± 18,358	51,576 ± 8,891*	56,961 ± 30,298	38,088 ± 16,585*	67,992 ± 19,284
Hemopexin	HPX	0.025	184,660 ± 54,157	132,260 ± 56,296	110,542 ± 41,070*	89,996 ± 38,298*	137,266 ± 44,999
Bisphosphoglycerate mutase	BPGM	0.021	68,275 ± 60,399	58,244 ± 31,321	41,146 ± 10,969	129,953 ± 71,012	52,283 ± 25,731
Immunoglobulin heavy constant alpha 1	IGHA1	0.021	194,255 ± 42,435	151,775 ± 52,739	123,237 ± 43,118*	109,179 ± 48,846*	124,086 ± 30,872*
Proteasome subunit alpha type-2	PSMA2	0.030	9,528 ± 2,142	11,238 ± 2,685	15,998 ± 6,500*	9,925 ± 3,357	14,012 ± 2,639*
Transketolase	TKT	0.037	15,578 ± 7,274	24,559 ± 13,108	18,371 ± 7,727	30,221 ± 9,080*	16,935 ± 2,844
Phosphoglucomutase-2	PGM2	0.020	3,996 ± 2,215	6,258 ± 1,979	6,521 ± 1,588*	3,858 ± 1,513	7,120 ± 2,414*
Importin-9	IPO9	0.026	1,194 ± 220	1,316 ± 380	2,348 ± 839*	1,147 ± 767	1,224 ± 476
Lumican	LUM	0.011	12,078 ± 4,667	10,564 ± 2,619	6,078 ± 3,544*	5,317 ± 3,669*	6,838 ± 2,869*
Nucleosome assembly protein 1-like 4	NAP1L4	0.028	2,829 ± 1,767	2,065 ± 709	2,023 ± 917	1,264 ± 466	3,636 ± 1,162
Translin	TSN	0.017	564 ± 307	894 ± 580	1,652 ± 673*	442 ± 255	855 ± 563
Profilin-1	PFN1	0.030	2,904 ± 361	1,633 ± 776	420 ± 0*		878 ± 473*
NIF3-like protein 1	NIF3L1	0.039	1,168 ± 397	519 ± 203	1,890 ± 739	694 ± 17	1,221 ± 232
Exportin-2	CSE1L	0.032	630 ± 450	255 ± 158	188 ± 37	405 ± 148	1,815 ± 1,043
Carbonyl reductase (NADPH) 1	CBR1	0.043	920 ± 207	1,272 ± 707	1,789 ± 587*	708 ± 248	867 ± 425
Ras-related protein Rap-1b	RAP1B	0.039	6,920 ± 3,406	3,812 ± 2,846	9,128 ± 3,673	4,029 ± 2,010	7,560 ± 3,022
Myosin light chain 4	MYL4	0.011	906 ± 352	1,601 ± 902	1,386 ± 745	2,820 ± 1,050*	952 ± 262
Carboxymethylenebutenolidase homolog	CMBL	0.018	1,359 ± 565	842 ± 213	1,498 ± 374	606 ± 58	392 ± 113
NEDD8-activating enzyme E1 catalytic subunit	UBA3	0.008	527 ± 386	464 ± 47	1,799 ± 478	1,056 ± 100	800 ± 307
Thyroxine-binding globulin	SERPINA7	0.017	3,665 ± 618	3,076 ± 794	648 ± 218*	2,049 ± 1,157	4,010 ± 925
Zyxin	ZYX	0.043	804 ± 811	787 ± 699	1,462 ± 381	1,750 ± 236	532 ± 269
Aquaporin-1	AQP1	0.001	425 ± 285	734 ± 267	3,213 ± 0*	440 ± 29	355 ± 151

** *Normalized intensity profile (sample area units).*

* *Proteins with concentration significantly differed from the background values (2 days before DI) according to the results of post-hoc analysis.*

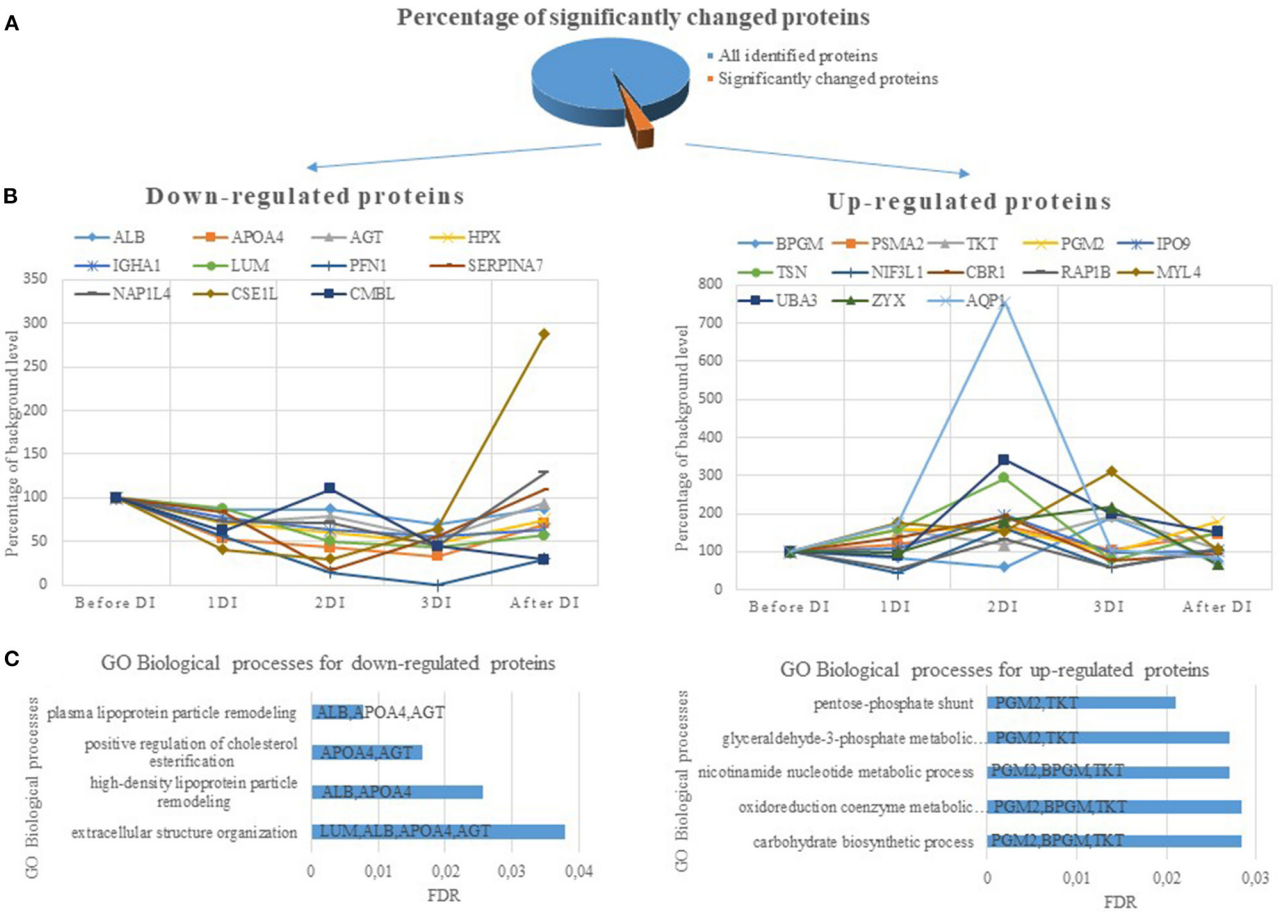

FIGURE 1 | (A) The percentage of significantly changed proteins during 3 days dry immersion (DI). **(B)** The dynamics for up- and down-regulated proteins. The dynamics of changes in the protein content is indicated as a percentage of the background level (2 days before DI, the level at this experimental point is taken as 100%). **(C)** Biological processes involving DBS proteins with significantly different concentrations during 3 days DI. The value of the column means FDR (the smaller the FDR, the more reliable the process). The columns indicate the genes of proteins involved in this biological process.

distinguished for down-regulated proteins: processes associated with remodeling of plasma lipoproteins and organization of extracellular structures. For up-regulated proteins, biological processes associated with the pentose phosphate shunt have been identified. This reveals a cluster of proteins (PGM2, TKT, BPGM) (**Figure 1**) involved in different metabolic processes—carbohydrate biosynthetic process, nicotinamide nucleotide metabolic process, oxidoreduction coenzyme metabolic process. These proteins significantly increased on the second or third day of DI. Phosphoglucomutase-2 (PGM2) catalyzes the conversion of the nucleoside breakdown products ribose-1-phosphate and deoxyribose-1-phosphate to the corresponding 5-phosphopentoses. It also catalyzes the interconversion of glucose-1-phosphate and glucose-6-phosphate. Transketolase (TKT) like the PGM2 is also involved in glyceraldehyde-3-phosphate biosynthetic process. Bisphosphoglycerate mutase (BPGM) plays a key role in regulating hemoglobin oxygen affinity by controlling the levels of its allosteric effector 2,3-bisphosphoglycerate. These proteins are cytosolic proteins and they got into the analysis as a result of lysis of blood cells that were in a DBS samples. The most likely the main contribution to the change in the concentration of these proteins was made by erythrocytes, since there are the most active reactions of the pentose phosphate pathway along with the cytosol of liver cells, adipose tissue, and adrenal cortex. The pentose phosphate pathway of glucose oxidation is not associated with the formation of energy but provides anabolism of cells. In erythrocytes only NADPH is formed as a product of the pentose phosphate pathway. In this case pentose is not the final product as it is converted into phosphohexose which close the cycle or go into glycolysis completing the shunt. NADPH is an important component of antioxidant defense and it is necessary for the regeneration of glutathione which together with glutathione peroxidase destroys reactive oxygen species (ROS). Since NADPH is formed in erythrocytes only in pentose-phosphate shunt reactions an increase in the concentration of proteins of the pentose-phosphate shunt may be a response to oxidative stress.

Indeed physical inactivity was shown to enhance muscle ROS production (Lawler et al., 2003; Agostini et al., 2010) and to affect activity of antioxidant systems (Banerjee et al., 2003; Agostini et al., 2010). Experimental bed rest has been shown to be associated with oxidative stress and activation of the glutathione system (Dalla Libera et al., 2009; Agostini et al., 2010). Glutathione is one of the major antioxidant systems stimulated both at muscular and systemic level by activation of oxidative processes (Dobrowolny et al., 2008). Its action is principally mediated by a reaction catalyzed by glutathione peroxidase leading to oxidized glutathione disulfides (Lu, 2000). Glutathione concentration is particularly abundant in the liver and erythrocytes where it acts as local and systemic antioxidant agent (Qi et al., 2013). It's worth noting that countering oxidative stress can reduce muscle loss. Thus, antioxidant supplementation prevented disuse atrophy in animal models (Betters et al., 2004; Momken et al., 2011). There is a need to develop means to prevent oxidative stress during low physical activity. This is important because physical inactivity was shown to increase vascular superoxide production and impair endothelium-dependent vasorelaxation, which may contribute to endothelial dysfunction and atherosclerosis.

In general only blood cell cytosol proteins concentration increased while extracellular proteins (ALBU, APOA4, AGT, LUM, HPX, SERPINA7) decreased (**Table 1**; **Figure 1**) during DI and more strongly with each day of immersion. Such dynamics of proteins is possibly associated with a decrease in the synthesizing function of the liver. The data on the main site of synthesis of the aforementioned proteins lead to this conclusion. However, the influence of other factors on the change in the concentration of these proteins is not excluded. Thus a decrease in APOA4 may be associated with a decrease in high density lipoproteins which was detected after short (Leach, 1992) and long-term (Markin et al., 1998) space flights. Angiotensinogen reacted to the experimental conditions earlier than other proteins and a significant decrease in its concentration was observed on the first day. Angiotensinogen is a precursor of angiotensin and plays an important role in the renin-angiotensin system which is known to be involved in the adaptation of the body's water-electrolyte metabolism to the conditions of simulated microgravity (Gharib and Hughson, 1992). Therefore, a change in the concentration of angiotensinogen under DI conditions is natural and connected with redistribution of body fluids and changes in the volume of circulating blood. In addition a change in the concentration of aquaporin could be due to a decrease in the volume of circulating plasma. Aquaporin forms a water-specific channels in plasma membranes of red cells and thereby allowing water to move in the direction of an osmotic gradient. Indeed, numerous studies have shown that simulated microgravity affects aquaporins (Bu et al., 2012; Tamma et al., 2014).

The study of the physiological functions via DBS proteome analysis thus confirm the already established ideas about the physiological response to the DI conditions and provide new information about previously unknown mechanisms of the adaptive processes. Revealing of a new blood proteome specific changes due to extreme conditions including physical inactivity can identify potential targets for intervention and prevention of negative consequences.

As far as we know this is the first proteomics study concerning female response to simulated microgravity during 3-days DI. The DBS with capillary blood sampling was selected as a perspective sample collection technique which is less invasive and allows sampling with a greater frequency both in the ground based experiments and space flight conditions.

DATA AVAILABILITY STATEMENT

The datasets presented in this study can be found in online repositories. The names of the repository/repositories and accession number(s) can be found below: http://www.proteomexchange.org/, PXD027654.

ETHICS STATEMENT

The studies involving human participants were reviewed and approved by Commission on Biomedical Ethics at the IBMP RAS. The patients/participants provided their written informed consent to participate in this study.

AUTHOR CONTRIBUTIONS

IL, VR, AK, and EN conceived and designed the experiments. OP and WS collected samples of dry blood spots. DK and WS performed sample preparation to mass-spectrometry. AK and AB conducted mass-spectrometric analysis. DK, AK, and LP wrote the article. All authors contributed to the article and approved the submitted version.

FUNDING

This work was supported by the by Russian Science Foundation, grant # 21-74-20173.

ACKNOWLEDGMENTS

The team of authors expresses gratitude to Dr. Elena Tomilovskaya for the opportunity to participate in the Dry Immersion experiment.

REFERENCES

Agostini, F., Dalla Libera, L., Rittweger, J., Mazzucco, S., Jurdana, M., Mekjavic, I. B., et al. (2010). Effects of inactivity on human muscle glutathione synthesis by a double-tracer and single-biopsy approach. *J. Physiol.* 588(Pt 24), 5089–5104. doi: 10.1113/jphysiol.2010.198283

Banerjee, A. K., Mandal, A., Chanda, D., and Chakraborti, S. (2003). Oxidant, antioxidant and physical exercise. *Mol.*

Cell. Biochem. 253, 307–312. doi: 10.1023/a:1026032404105

Betters, J. L., Criswell, D. S., Shanely, R. A., Van Gammeren, D., Falk, D., Deruisseau, K. C., et al. (2004). Trolox attenuates mechanical ventilation-induced diaphragmatic dysfunction and proteolysis. *Am. J. Respir. Crit. Care Med.* 170, 1179–1184. doi: 10.1164/rccm.200407-939OC

Brzhozovskiy, A. G., Kononikhin, A. S., Pastushkova, L. C., Kashirina, D. N., Indeykina, M. I., Popov, I. A., et al. (2019). The effects of spaceflight factors on the human plasma proteome, including both real space missions and ground-based experiments. *Int. J. Mol. Sci.* 20, 3194. doi: 10.3390/ijms20133194

Bu, G., Shuang, F., Wu, Y., Ren, D., and Hou, S. (2012). AQP9: a novel target for bone loss induced by microgravity. *Biochem. Biophys. Res. Commun.* 419, 774–778. doi: 10.1016/j.bbrc.2012.02.100

Dalla Libera, L., Ravara, B., Gobbo, V., Tarricone, E., Vitadello, M., Biolo, G., et al. (2009). A transient antioxidant stress response accompanies the onset of disuse atrophy in human skeletal muscle. *J. Appl. Physiol. (1985)* 107, 549–557. doi: 10.1152/japplphysiol.00280.2009

Dobrowolny, G., Aucello, M., Rizzuto, E., Beccafico, S., Mammucari, C., Bonconpagni, S., et al. (2008). Skeletal muscle is a primary target of SOD1G93A-mediated toxicity. *Cell Metab.* 8, 425–436. doi: 10.1016/j.cmet.2008.09.002

Eshghi, A., Pistawka, A. J., Liu, J., Chen, M., Sinclair, N. J. T., Hardie, D. B., et al. (2020). Concentration determination of >200 proteins in dried blood spots for biomarker discovery and validation. *Mol. Cell. Proteomics* 19, 540–553. doi: 10.1074/mcp.TIR119.001820

Gharib, C., and Hughson, R. L. (1992). Fluid and electrolyte regulation in space. *Adv. Space Biol. Med.* 2, 113–130. doi: 10.1016/s1569-2574(08)60019-2

Kaya, H. E. K., and Radhakrishnan, S. K. (2020). Trash Talk: mammalian proteasome regulation at the transcriptional level. *Trends Genet.* 37, 160–173. doi: 10.1016/j.tig.2020.09.005

Lawler, J. M., Song, W., and Demaree, S. R. (2003). Hindlimb unloading increases oxidative stress and disrupts antioxidant capacity in skeletal muscle. *Free Radic. Biol. Med.* 35, 9–16. doi: 10.1016/s0891-5849(03)00186-2

Leach, C. S. (1992). Biochemical and hematologic changes after short-term space flight. *Microgravity Q.* 2, 69–75.

Lu, S. C. (2000). Regulation of glutathione synthesis. *Curr. Top Cell Regul.* 36, 95–116. doi: 10.1016/s0070-2137(01)80004-2

Markin, A., Strogonova, L., Balashov, O., Polyakov, V., and Tigner, T. (1998). The dynamics of blood biochemical parameters in cosmonauts during long-term space flights. *Acta Astronaut.* 42, 247–253. doi: 10.1016/s0094-5765(98)00121-0

Meier, F., Brunner, A. D., Koch, S., Koch, H., Lubeck, M., Krause, M., et al. (2018). Online parallel accumulation–serial fragmentation (PASEF) with a novel trapped ion mobility mass spectrometer. *Mol. Cell. Proteomics* 17, 2534–2545. doi: 10.1074/mcp.TIR118.000900

Momken, I., Stevens, L., Bergouignan, A., Desplanches, D., Rudwill, F., Chery, I., et al. (2011). Resveratrol prevents the wasting disorders of mechanical unloading by acting as a physical exercise mimetic in the rat. *FASEB J.* 25, 3646–3660. doi: 10.1096/fj.10-177295

Navasiolava, N. M., Custaud, M.-A., Tomilovskaya, E. S., Larina, I. M., Mano, T., Gauquelin-Koch, G., et al. (2010). Long-term dry immersion: review and prospects. *Eur. J. Appl. Physiol.* 111, 1235–1260. doi: 10.1007/s00421-010-1750-x

Nay, K., Koechlin-Ramonatxo, C., Rochdi, S., Island, M. L., Orfila, L., Treffel, L., et al. (2020). Simulated microgravity disturbs iron metabolism and distribution in humans: lessons from dry immersion, an innovative ground-based human model. *FASEB J.* 34, 14920–14929. doi: 10.1096/fj.202001199RR

Pakharukova, N., Larina, I., Pastushkova, L., and Grigoriev, A. (2011). Changes of human serum proteome profile during 7-day "dry" immersion. *Acta Astronaut.* 68, 1523–1528. doi: 10.1016/j.actaastro.2009.10.014

Pastushkova, L. K., Pakharukova, N. A., Novoselova, N. M., Dobrokhotov, I. V., Valeeva, O. A., Custaud, M. -A., et al. (2012). Direct proteomic profiling of human urine and blood serum in an experiment with 5-day dry immersion. *Aviakosm. Ekolog. Med.* 46, 31–37.

Qi, L., Qi, Q., Prudente, S., Mendonca, C., Andreozzi, F., di Pietro, N., et al. (2013). Association between a genetic variant related to glutamic acid metabolism and coronary heart disease in individuals with type 2 diabetes. *J. Am. Med. Assoc.* 310, 821–828. doi: 10.1001/jama.2013.276305

Rusanov, V. B., Pastushkova, L. K., Larina, I. M., Chernikova, A. G., Goncharova, A. G., Nosovsky, A. M., et al. (2020). The effect of five-day dry immersion on the nervous and metabolic mechanisms of the circulatory system. *Front. Physiol.* 11, 692. doi: 10.3389/fphys.2020.00692

Tamma, G., Di Mise, A., Ranieri, M., Svelto, M., Pisot, R., Bilancio, G., et al. (2014). A decrease in aquaporin 2 excretion is associated with bed rest induced high calciuria. *J. Transl. Med.* 12, 133. doi: 10.1186/1479-5876-12-133

Tomilovskaya, E., Shigueva, T., Sayenko, D., Rukavishnikov, I., and Kozlovskaya, I. (2019). Dry immersion as a ground-based model of microgravity physiological effects. *Front. Physiol.* 10, 284. doi: 10.3389/fphys.2019.00284

Treffel, L., Massabuau, N., Zuj, K., Custaud, M.-A., Gauquelin-Koch, G., Blanc, S., et al. (2017). Pain and vertebral dysfunction in dry immersion: a model of microgravity simulation different from bed rest studies. *Pain Res. Manag.* 2017, 1–10. doi: 10.1155/2017/9602131

Trifonova, O. P., Pastushkova, L. H., Samenkova, N. F., and Pyatnitskii, M. A. (2010). Change in the protein composition of blood plasma in an experiment with a 7-day dry immersion. *Aviakosm. Ekolog. Med.* 44, 24–28.

Vizcaino, J. A., Csordas, A., del-Toro, N., Dianes, J. A., Griss, J., Lavidas, I., et al. (2016). Update of the PRIDE database and its related tools. *Nucleic Acids Res.* 44, 447–456. doi: 10.1093/nar/gkv1145

Conflict of Interest: The authors declare that the research was conducted in the absence of any commercial or financial relationships that could be construed as a potential conflict of interest.

frontiers in Physiology

ORIGINAL RESEARCH
published: 06 October 2021
doi: 10.3389/fphys.2021.712365

Autonomic Function in Parkinson's Disease Subjects Across Repeated Short-Term Dry Immersion: Evidence From Linear and Non-linear HRV Parameters

Liudmila Gerasimova-Meigal[1*†], *Alexander Meigal*[1†], *Nadezhda Sireneva*[1] *and Irina Saenko*[2]

[1] *Department of Physiology and Pathophysiology, Petrozavodsk State University, Petrozavodsk, Russia,* [2] *Institute of Biomedical Problems, Russian Academy of Sciences (RAS), Moscow, Russia*

OPEN ACCESS

Edited by:
Ronan Padraic Murphy, Dublin City University, Ireland

Reviewed by:
Jesús Álvarez-Herms, Ministerio de Educación Cultura y Deporte, Spain
Marc-Antoine Custaud, Université d'Angers, France

***Correspondence:**
Liudmila Gerasimova-Meigal
gerasimova@petrsu.ru

[†] *These authors have contributed equally to this work*

Specialty section:
This article was submitted to Environmental, Aviation and Space Physiology, a section of the journal Frontiers in Physiology

Received: *20 May 2021*
Accepted: *06 September 2021*
Published: *06 October 2021*

Citation:
Gerasimova-Meigal L, Meigal A, Sireneva N and Saenko I (2021) Autonomic Function in Parkinson's Disease Subjects Across Repeated Short-Term Dry Immersion: Evidence From Linear and Non-linear HRV Parameters. Front. Physiol. 12:712365. doi: 10.3389/fphys.2021.712365

Several studies have shown that "dry" immersion appears as a promising method of rehabilitation for Parkinson's disease. Still, little is known about the cardiovascular reaction in "dry" immersion (DI), especially in Parkinson's disease (PD). Therefore, this study was aimed to evaluate the effect of repeated 45-min DI sessions on autonomic function in subjects with PD. The study group consisted of 20 subjects with PD [13 men, seven women, aged 51–66 years old, Hoehn & Yahr (H&Y) staged 1–3] were enrolled in the study according to inclusion and non-inclusion criteria. The DI program was comprised of seven 45-min DI sessions, applied within 25–30 days. Blood pressure (BP), heart rate (HR), and electrocardiogram (ECG) in the standard lead II were recorded at 1st, 4th, and 7th DI, before, on the 15, 30, and 40th min of DI session. Autonomic function was assessed with analysis of heart rate variability (HRV) using Kubios Standard version 2 software. Linear (time- and frequency-domain) and non-linear (correlation dimension, entropies, DFA1 and DFA2, percent of determinism, and recurrence) were computed. At baseline condition, time- and frequency-domain HRV parameters showed low variability of HR, which indicates reduced autonomic neurogenic control of HR. Throughout the DI session, systolic and diastolic BP has decreased by 5–7 mm Hg ($p < 0.001$), and time- and frequency-domain parameters of HRV have significantly increased, what can be regarded as compensatory mechanisms of hemodynamics during DI. The structure of the regulatory input to the heart seen by HRV was characterized by low complexity and reduced autonomic neurogenic control of HR. Across the program of DI sessions, the hypotensive effect was documented, but no notable modification of the HRV-parameters was found. The absence of long-term modification of the studied parameters can be attributed both to deconditioning environmental effect of DI and limited adaptation of the organism due to neurodegeneration in PD. That should be taken into consideration when planning rehabilitation measures in subjects of older age and chronic somatic diseases with modeled microgravity.

Keywords: dry immersion (DI), Parkinson's disease (PD), heart rate variabiity (HRV), blood pressure (BP), heart rate (HR)

INTRODUCTION

"Dry" immersion, along with antiorthostatic hypokinesia and parabolic flights, refers to methods of Earth-based modeling of microgravity (Pandiarajan and Hargens, 2020). Under modeled microgravity, the body of the subject experiences the main effects of space flight, such as redistribution of the extracellular fluid of the body, hypokinesia, and lack of support (Tomilovskaya et al., 2019; Pandiarajan and Hargens, 2020). Compared with other methods, "dry" immersion (DI) is considered the most sparing method of modeling microgravity in Earth conditions, since the redistribution of blood to the upper body and head that occurs during DI session is not so pronounced as with other methods, e.g., antiorthostatic hypokinesia (Watenpaugh, 2016; Tomilovskaya et al., 2019; Amirova et al., 2020).

Besides space physiology, DI has begun to be used in rehabilitation to normalize increased muscle tone and blood pressure (BP) in patients with chronic diseases of the nervous, circulatory, and musculoskeletal systems (Tomilovskaya et al., 2019).

Earlier we have shown that ground-based microgravity modeled with a short-term session of DI diminished tremor and muscle rigidity in Parkinson's disease (PD; Meigal et al., 2018, 2021a; Miroshnichenko et al., 2018), which can be attributed to the well-established atonia-inducing effect of DI on the skeletal muscle of healthy subjects (Navasiolava et al., 2011; Amirova et al., 2020). Additionally, the performance of the visual-motor reaction time tasks with higher cognition demand has improved after a program of DI sessions (Meigal et al., 2021b). However, these positive effects do not translate to quality of life and activity of daily living, or body balance (Meigal et al., 2018, 2021a).

Parkinson's disease is known as neurodegenerative disease, characterized by lowered dopamine production in the central nervous system (CNS) what leads to several cardinal motor symptoms, such as rest tremor, elevated muscle tone or rigidity, brady- or akinesia, and impairment of postural reactivity and gait (Rodriguez-Oroz et al., 2009; Reich and Savitt, 2019). Besides motor and cognition deficits, dysfunction of the autonomic nervous system, or dysautonomia, is a common feature of PD (Metzger and Emborg, 2019), which often precedes the motor symptoms (Chen et al., 2020). Dysautonomia in PD is represented by cardiovascular, gastrointestinal, and urinary disorders, hyperhidrosis, sexual dysfunction, thermoregulatory aberrance, and pupillo-motor abnormalities (Postuma et al., 2013; Metzger and Emborg, 2019; Chen et al., 2020). Autonomic dysregulation in PD is determined by neurodegeneration associated with alpha-synuclein deposition in neurons of the central and peripheral autonomic nervous system (Chen et al., 2020), including the enteral nervous system (Jain, 2011). There are studies that allowed hypothesizing that the "gut-brain axis" also contributes to PD pathogenesis (Schaeffer et al., 2020; Lee et al., 2021). Cardiac and extra-cardiac sympathetic denervation, provoked by alpha-synuclein deposition in autonomic nerves, along with arterial baroreflex failure is regarded as major mechanisms for orthostatic hypotension, BP lability, and supine hypertension (Jain and Goldstein, 2012). Signs of orthostatic hypotension are seen in 40% of subjects with advanced PD (Jain and Goldstein, 2012).

Heart rate variability in PD is vastly investigated with traditional linear parameters, which indicate diminished sympathetic and parasympathetic autonomic activity (Jain, 2011; Jain and Goldstein, 2012; Soares et al., 2013; Maetzler et al., 2015; Gibbons et al., 2017; Palma and Kaufmann, 2018; Akbilgic et al., 2020; Li et al., 2020). Only a few studies on non-linear parameters of heart rate variability (HRV) in PD are available in pre-existing literature (Kallio et al., 2002; Pursiainen et al., 2002; Palma and Kaufmann, 2018), though non-linear parameters of HRV are widely used to study other kinds of pathologies (Voss et al., 2009; Shaffer and Ginsberg, 2017). Non-linear parameters inform the temporal structure and complex patterns of a signal, and they often outmatch the linear ones by sensitivity to specific features of biosignals. For example, entropy, correlation dimension, and rate of recurrence of surface electromyogram presented better sensitivity to clinical motor symptoms in subjects with PD (Meigal et al., 2013).

In our earlier study in subjects with PD, we found that BP has modestly decreased after a single 45-min session of DI (Meigal et al., 2018). Also, the autonomic dysfunction, evaluated with a rating scale, has decreased by 50% after a program of seven sessions of DI (Meigal et al., 2017, 2020). Similarly, the modest decrease of BP and heart rate (HR), as well as the increased variability of HR, which evidenced on compensatory mechanisms, was detected during 45-min DI sessions in healthy young subjects (Gerasimova-Meigal and Meigal, 2019; Meigal et al., 2020). These data are in line with the dynamics of BP and HR in healthy young subjects during short-term DI (3–5 days; Tomilovskaya et al., 2019; Amirova et al., 2020). Nonetheless, many humoral factors, which are important for systemic vascular resistance and microcirculation, for example, markers of endothelial state and inflammation, are perceived unchanged by 7 days of DI (Tomilovskaya et al., 2019; Amirova et al., 2020). The microbiome, as one of the important components of human metabolic homeostasis and immunity (Turroni et al., 2020), proved rather stable at the early stages of under analog microgravity experiments (Jin et al., 2019). Therefore, one cannot expect a substantial contribution of the gut-brain axis in subjects with PD specifically under short-term DI sessions.

Several similar to DI water-related rehabilitation approaches are currently used either for PD or arterial hypertension, for example, the so-called "passive heat therapy" which stands for warm water immersion (Brunt et al., 2016; Masiero et al., 2019; Sugawara and Tomoto, 2020), and "aquatic therapy" that is exercising in thermoneutral water (Carroll et al., 2017; Kim et al., 2018; Sato et al., 2019). Most of these studies reported the beneficial effect of water immersion on BP and HR. The study of Parker et al. (2018) reported on the modest increase of the variability of heart rate in healthy subjects under immersion in warm water (at 36°C), although this study has not specified the parameters of HRV.

Therefore, given that (1) either warm water immersion or aquatic therapy exerts beneficial effects on hemodynamics and HRV in healthy subjects and on hemodynamics in subjects with

TABLE 1 | The anthropologic and clinical data of the subjects with PD.

	Men ($n = 13$)	Women ($n = 7$)
Age, years	58 ± 8	64 ± 4
Height, m	1.79 ± 0.06	1.58 ± 0.05
Weight, kg	77.1 ± 10.3	76.6 ± 10.1
Stage by Hoehn & Yahr	1–3	
Disease duration, years	3–6	
LED*, mg/day	344–763	

**LED (levodopa equivalent dose) was calculated with the formula of Nutt et al. (2003).*

PD, (2) single one short-term DI session exerts an effect on blood pressure in PD, and (3) DI strongly affects hemodynamics and HRV in healthy subjects, we hypothesized that HRV and hemodynamics in subjects with PD would have also been modulated under conditions of DI. Additionally, as non-linear parameters are highly sensitive to the temporal structure of a signal, we also aimed at evaluating the effect of DI on autonomic regulation in PD with both linear and non-linear parameters of HRV.

MATERIALS AND METHODS

Participants

The study enrolled 20 subjects with PD, 13 men and seven women. These subjects have participated in our previously published studies (Meigal et al., 2018, 2021a,b; Miroshnichenko et al., 2018), where one can find their individual clinical and anthropological characteristics and medication. General characteristic of the subjects is presented in **Table 1**. Individual data is presented in **Supplementary Table 1**. One man subject participated five times and another man subject participated three times within the years 2016–2019. A total of 26 DI courses were conducted.

The general inclusion criterion was the verified diagnosis of PD. The non-inclusion criteria for the DI group included a variety of pathologies that potentially could have worsened under DI, e.g., epilepsy, administration of muscle relaxants, hypovolemia, atrial fibrillation, hemorrhage of various etiology, lung diseases in the acute stage, myocardial infarction, oncologic problems, and blood clotting disorders such as phlebothrombosis or thrombophlebitis (Tomilovskaya et al., 2019). None of the subjects had brain trauma in anamnesis, including those associated with such sports as boxing and football. The study involved only patients who did not require drugs with a notable effect on autonomic regulation and/or cardiac function, for example, β-adrenoblockers. The non-inclusion criterion for HRV measurements was cardiac arrhythmias. After a comprehensive verbal explanation, all participants signed an informed consent form to participate. The study protocol was approved by the joint Ethics committee of the Ministry of Health care of the Republic of Karelia and Petrozavodsk State University (Statement of approval No. 31, 18.12.2014). Before the program of DI sessions, all PD subjects were examined with an active orthostatic test for orthostatic tolerance. In none of the subjects, orthostatic hypotension was found (Gerasimova-Meigal et al., 2021).

The DI Intervention

The condition of DI was induced by means of the "Medical Facility of Artificial Weightlessness" (MEDSIM, Center for Aerospace Medicine and Technologies, State Scientific Center of Russian Federation "Institute of Biomedical Problems," Moscow, Russia) housed in Petrozavodsk State University (Petrozavodsk, Russia). A detailed description of the procedure of DI applied to the group of PD subjects is available in our earlier papers (Meigal et al., 2018, 2021a,b; Miroshnichenko et al., 2018). The short-term DI session lasted 45-min. The DI session was carried out "on-medication," starting at 9:30 AM. To synchronize the effects of anti-PD therapy with that of DI, subjects took their medicines 2 h before the study, at 7: 30 AM. During DI, subjects were lying in a head-out-of-water supine position in a bathtub with water individually adjusted for thermal comfort (32–34°C). One day prior to the study, the subjects underwent trial 15-min DI to identify hemodynamic changes during immersion and to get familiarized with the procedure. The program of DI comprised seven short-term DI sessions, conducted twice a week (total DI dose was 5.25 h), within 25–30 days (every 3–4 days).

Outcome Measures

Within one DI session, data were collected before (baseline test), on the 15, 30, and 40 min of DI session. Across the program of DI, data were collected at the 1st, 4th, and 7th DI sessions.

Systolic and diastolic BP and HR were measured with UA-705 digital tonometer (A&D Company Ltd., Japan). ECG was recorded in the standard lead II for 5 min with the "VNS-Spectr" device (Neurosoft Ltd., Ivanovo, Russia). All ECG records were visually inspected for stationarity, and all artifacts were manually corrected. Only ECG records without arrhythmias on ECG (5-min long) were considered for HRV analysis. Further, HRV analysis was performed in accordance with international standards of measurement, physiological interpretation, and clinical use (Heart rate variability, 1996; Shaffer and Ginsberg, 2017). Linear (time- and frequency-domain) and non-linear (correlation dimension, entropies, DFA1 and DFA2, and percent of determinism and recurrence) were computed with Kubios Standard version 2 software (University of Eastern Finland, Kuopio, Finland; Tarvainen et al., 2014).

Time-domain HRV parameters included the HR, MeanRR, standard deviation (SDNN), root mean squared difference (RMSSD), the proportion of successive intervals >50 ms (pNN 50%) of normal RRi (NN), and triangular interpolation of the RR histogram index (TINN).

Frequency-domain HRV parameters included the total power (TP) spectrum of RRi, power spectrum at very low (VLF; <0.04 Hz), low (LF;0.04–0.15 Hz), and high-frequency bands (HF;0.15–0.40 Hz), the LF/HF ratio, and spectrum structure (% VLF, % LF, % HF, LF n.u, HF n.u.).

The analysis of non-linear HRV parameters included estimation of the indices of the Poincaré ellipse (SD1 and SD2) and recurrence plot (Mean line length—Lmean, Max

line length—Lmax, recurrence rate—REC, determinism—DET, Shannon entropy—ShanEn), and others parameters approximated (ApEn) and sample (SampEn) entropy, parameters of detrended fluctuation analysis (DFA) with self-similarity indices for short (α1) and longtime intervals (α2), and correlation dimension (D2) (Voss et al., 2009; Tarvainen et al., 2014; Shaffer and Ginsberg, 2017).

Statistical Analysis

Data were analyzed using IBM SPSS Statistics 21 software (SPSS, IBM Company, Chicago, IL, USA). Within one DI session, the SPSS Friedman test with further *post-hoc* comparisons (the Newman-Keuls test) was applied to find the differences between hemodynamic and HRV parameters at study points. Across the program of DI, the difference between studied parameters was estimated with ANOVA and non-parametric correlation (Spearmen test). The interaction between the parameters of hemodynamics and autonomic regulation within one DI session was assessed using the non-parametric correlation analysis (Spearmen test) and regression analysis. The results were considered significant at $p < 0.05$.

RESULTS

Within one DI session, the values of BP and HR tended to decrease (**Figure 1**). Thus, at baseline condition, systolic and diastolic BP was 117 ± 11 and 73 ± 7 mm Hg on average, respectively, while HR was 70 ± 9 min^{-1}. Under one DI session, both systolic and diastolic BP has decreased by 5–7 mm Hg, and HR has decreased by 6–8 min^{-1} ($p < 0.001$). No difference between men and women subjects was found, which allowed forming one unified study group.

Across the program of DI sessions, the modest hypotensive effect was also the characteristic. Before the 1st DI, systolic BP was, on average, 118 ± 13 mm Hg, and diastolic BP – 72 ± 8 mm Hg. Before the 7th DI session, systolic BP was 111 ± 14 mm Hg ($p < 0.001$), and diastolic BP was 68 ± 8 mm Hg ($p < 0.001$).

Table 2 summarizes the results of HRV analysis within the DI session presented as Me (25%; 75%). At baseline condition, time-domain HRV parameters (SDNN, RMSSD, and pNN50) corresponded to low variability of HR, which, in turn, indicated reduced parasympathetic control of the heart rhythm (Heart rate variability, 1996; Shaffer and Ginsberg, 2017). The frequency-domain HRV parameters (TP and its LF and HF components) were decreased, which reflects the general deficit of the autonomic neurogenic control of HR. The ratio of main frequency domains was 56–27–17% (VLF > LF > HF), which indicated the predominance of humoral metabolic factors in the regulation of HR.

Within one DI session, the marked increase of both time- (SDNN, RMSSD, and pNN50) and frequency-domain (TP and its VLF, LF, and HF components) HRV parameters was found on the 15, 30, and 40th min of DI (see **Table 2**). This indicated the autonomic neurogenic parasympathetic and sympathetic response to DI. Nonetheless, the structure of the HRV spectrum did not significantly change except for a slight decrease in the VLF percentage. Similarly, no changes in entropy (ShanEn, ApEn, and SampEn) and DFA indices were found within one DI session. This evidenced that the time structure of the regulatory influence on the heart rate stood unchanged. The dynamics of HRV parameters were highly reproducible, i.e., it was almost identical among all sessions of DI.

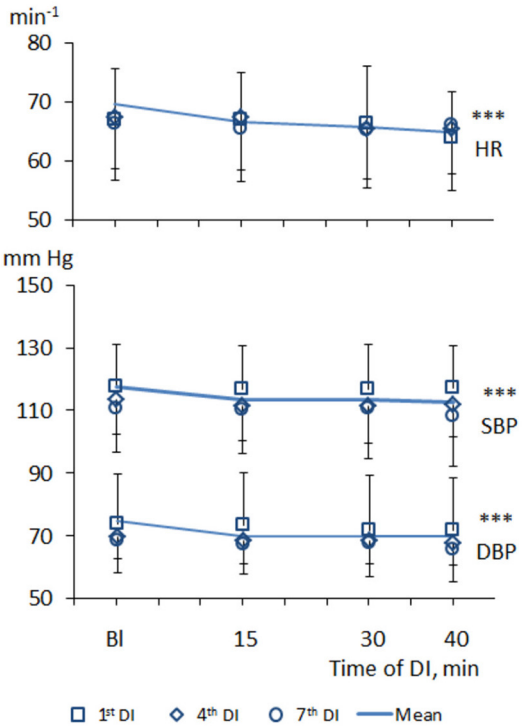

FIGURE 1 | Dynamics of heart rate and blood pressure in PD patients during repeated "dry" immersion sessions. HR, heart rate; SBP, systolic blood pressure; DBP, diastolic blood pressure. The blue line represents the mean of tree studied DI sessions. The difference from the baseline condition ***$p <$ 0.001 (Friedman test).

Across the program of DI sessions, no significant change of HRV parameters was found. The dynamics of time-domain HRV parameters (SDNN and pNN50) are presented in **Figure 2**, the HRV spectrum is shown in **Figure 3**, and D2 is shown in **Figure 4**. The main effect and interaction by short-term DI sessions and a course of DI on hemodynamics and HRV parameters (general linear model) are presented in **Supplementary Table 2**.

The interaction between hemodynamics and autonomic regulation was assessed using correlation and regression analysis. At baseline condition, few correlations were found between HRV and HR, but not BP (**Figure 5**). Namely, there was a negative correlation between the HR and HRV indices of the parasympathetic activity. At the 40th min of DI, more correlations were found between the parameters of HRV and HR and BP (see **Figure 5**). The results of regression analysis were in line with that of correlation analysis, indicating the same associations between parameters (**Supplementary Table 3**). This

TABLE 2 | Heart rate variability parameters in PD subjects under short-term DI sessions (average of all studied DI sessions).

Parameter	Baseline	DI:15	DI:30	DI:40	Significance[a]
Time-domain HRV parameters					
MeanRR, ms	885.4 (794.3; 960.1)	931.7 (851.1; 999.3)***	939.5 (885.9; 996.9)***	952.1 (893.2; 1011.3)***	<0.001
SDNN, ms	24.7 (19.0; 32.1)	28.9 (21.1; 41.2)**	35.3 (26.0; 48.0)***	37.4 (23.6; 45.9)***	<0.001
RMSSD, ms	16.6 (10.5; 20.0)	19.4 (13.2; 25.9)	23.5 (14.4; 34.4)	24.3 (15.0; 30.4)	
pNN50, %	0.6 (0.0; 1.8)	1.3 (0.0; 4.6)	2.9 (0.3; 8.0)***	3.2 (0.4; 7.4)***	<0.001
TINN, ms	110.0 (75.0; 145.0)	110.0 (77.5; 145.0)	122.5 (83.8; 181.3)*	115.0 (77.5; 162.5)	<0.05
Frequency-domain HRV parameters					
TP, ms^2	406 (208; 705)	786 (330; 1596)***	1133 (479; 1959)***	1076 (418; 2133)***	<0.001
VLF, ms^2	223 (129; 389)	324 (164; 849)	507 (249; 1013)***	594 (230; 890)***	<0.001
LF, ms^2	100 (44; 211)	198 (80; 413)***	238 (106; 594)***	259 (109; 729)***	<0.001
HF, ms^2	58 (30; 128)	118 (55; 244)***	156 (80; 259)***	189 (79; 275)***	<0.001
LF/HF	1.562 (1.001; 2.463)	1.659 (1.101; 2.874)	1.94 (0.98; 2.91)	1.837 (1.049; 3.223)	
VLF, %	57.3 (45.7; 70.3)	52.5 (35.5; 68.5)	53.5 (33.6; 68.2)	52.2 (40.4; 60.4) *	<0.05
LF, %	23.2 (17.5; 30.5)	26.6 (19.0; 40.6)	27.0 (19.6; 39.4)	30.9 (19.8; 38.7)	
HF, %	15.0 (10.2; 20.3)	15.3 (9.1; 27.0)	14.2 (9.3; 26.8)	16.9 (11.1; 25.6)	
LF, n.u.	61.8 (50.3; 71.2)	62.4 (52.4; 74.2)	36.5 (25.6; 50.4)	64.8 (51.2; 76.3)	
HF, n.u.	38.2 (28.8; 49.7)	37.6 (25.8; 47.7)	53.5 (33.6; 68.2)	36.1 (23.7; 48.8)	
Non-linear HRV parameters					
SD1, ms	11.9 (7.5; 14.4)	13.7 (9.4; 18.3)***	16.4 (9.8; 24.4)***	16.9 (10.6; 21.3)***	<0.001
SD2, ms	33.7 (23.8; 43.6)	37.0 (28.7; 54.6)	46.1 (33.7; 62.8)	51.1 (30.1; 63.4)	
Lmean, beats	14.15 (10.90; 17.71)	12.95 (9.60; 16.33)*	13.23 (10.77; 18.13)	11.90 (9.55; 15.45)**	<0.001
Lmax, beats	269 (190; 324)	206 (128; 286)*	222 (133; 296)	201 (128; 274)***	<0.001
REC, %	41.06 (35.32; 46.79)	39.99 (29.43; 45.18)	40.32 (32.35; 46.55)	37.00 (31.15; 43.27)	
DET, %	98.97 (98.13; 99.42)	98.69 (97.56; 99.43)	99.04 (98.42; 99.48)	98.74 (97.73; 99.34)	
ShanEn	3.409 (3.181; 3.645)	3.333 (3.032; 3.575)	3.336 (3.144; 3.607)	3.279 (3.024; 3.535)	
ApEn	1.119 (1.046; 1.160)	1.085 (1.017; 1.146)	1.095 (1.026; 1.137)	1.102 (1.039; 1.129)	
SampEn	1.482 (1.274; 1.700)	1.477 (1.225; 1.642)	1.421 (1.224; 1.590)	1.508 (1.298; 1.652)	
DFA:α1	1.162 (0.976; 1.313)	1.163 (0.944; 1.359)	1.185 (0.943; 1.357)	1.161 (1.051; 1.312)	
DFA:α2	1.007 (0.872; 1.100)	0.986 (0.765; 1.104)	0.977 (0.805; 1.097)	1.014 (0.863; 1.082)	
D2	0.341 (0.121; 0.700)	0.624 (0.237; 1.230)***	0.800 (0.480; 1.950)***	0.968 (0.361; 2.492)***	<0.001

[a] *The significance is based on Friedman test with further post-hoc comparisons (the Newman-Keuls test); the difference from the baseline condition: *p < 0.05, **p < 0.01, ***p < 0.001.*

indicated the emergence of systemic compensatory mechanisms which help to maintain BP in PD subjects under DI.

DISCUSSION

According to the working hypothesis of this study, in subjects with PD under conditions of DI one could expect the decrease of BP and modifications of autonomic regulation seen with HRV parameters. In line with this hypothesis, we found that both systolic and diastolic BP, indeed decreased within one DI session, by some 5–7 mm Hg, and HR, by 6–8 min^{-1}. In the program of DI sessions, both diastolic and systolic BP has significantly decreased by 8–10 mm Hg on the fourth DI session. Most of HRV time-domain parameters (SDNN and pNN50) and the power of all bands of the frequency spectrum (TP, VLF, LF, and HF) have significantly increased within a single DI. Also, there was a notable tendency of VLF to decrease by the 40th min of a single DI session. As for the non-linear parameters of HRV, only correlation dimension (D2) and SD1 have significantly increased along with the DI session. By contrast, all kinds of entropy and DFA indices, and recurrent rates did not respond to the conditions of DI. Across the DI program, none of the HRV parameters has been significantly modified. Altogether, these data suggested that in subjects with PD the autonomic cardiac regulation and hemodynamics are strongly and beneficially modified within a 45-min DI session, but these parameters remained largely unchanged across the program of seven DI sessions. Several factors may have contributed to such outcome, among which are (1) ambient temperature, (2) conditions of immersion *per se*, (3) baroreceptor reflex sensitivity (BRS), and (4) PD-specific impairment of the autonomic nervous system.

Hemodynamics

The "Warm Water" Immersion Effect

The conditions of DI comprised of two major physical factors, namely, immersion and temperature. These factors probably differentially contributed to the result. Some studies report that even a short-term immersion in water with a temperature

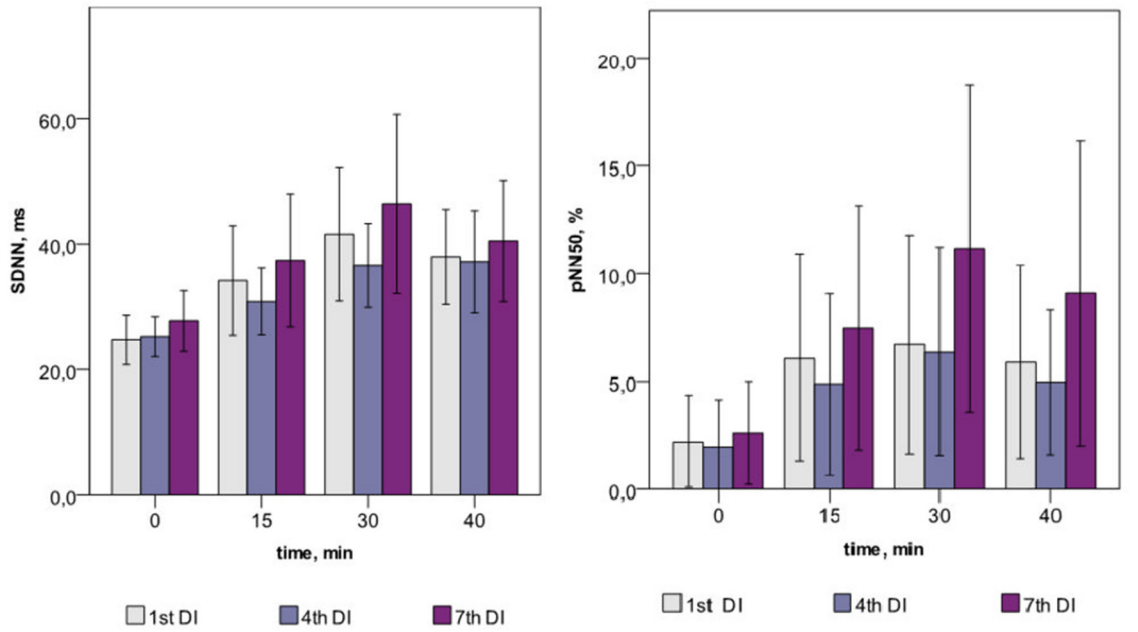

FIGURE 2 | Time-domain HRV parameters in PD patients during repeated "dry" immersion sessions.

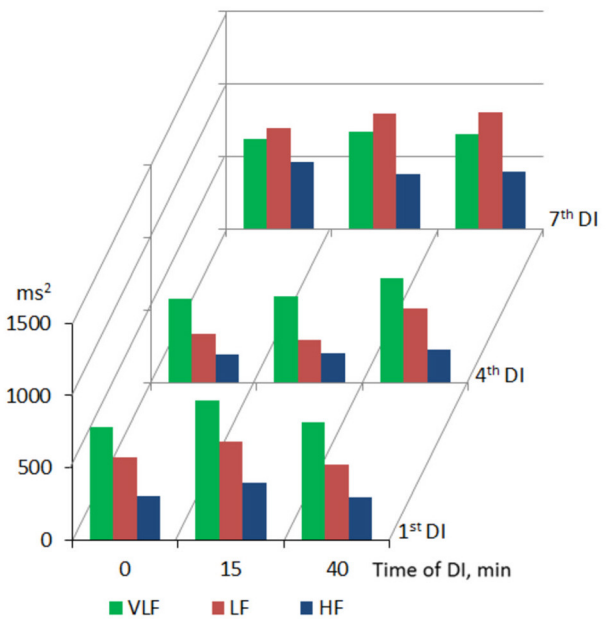

FIGURE 3 | Frequency-domain HRV parameters in PD patients during repeated ""dry" immersion sessions.

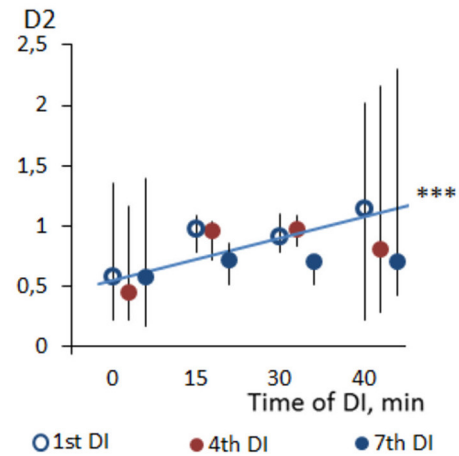

FIGURE 4 | Dynamics of correlation dimension (D2) of HRV in PD patients during repeated "dry" immersion sessions. The blue line represents the regression line of D2 within the DI session (average of three studied DI sessions). ***$p < 0.001$ (Friedman test).

up to 40°C can provoke the so-called "warm water" effect in a form of mental and muscular relaxation in PD (Masiero et al., 2019). Even 5-min warm water immersion significantly improved arterial wall stiffness what lasts for at least 15 min after the session of warm water immersion (Sugawara and Tomoto, 2020). In the study of Brunt et al. (2016), the program of five 1-h warm water immersion at 40.5°C within 8 weeks ("passive heat therapy") significantly increased flow-mediated arterial dilatation, reduced arterial stiffness mean arterial and diastolic BP, and carotid intima-media thickness in young healthy subjects. In the present study, the water temperature at DI was 32°C, which can generally be considered as thermoneutral.

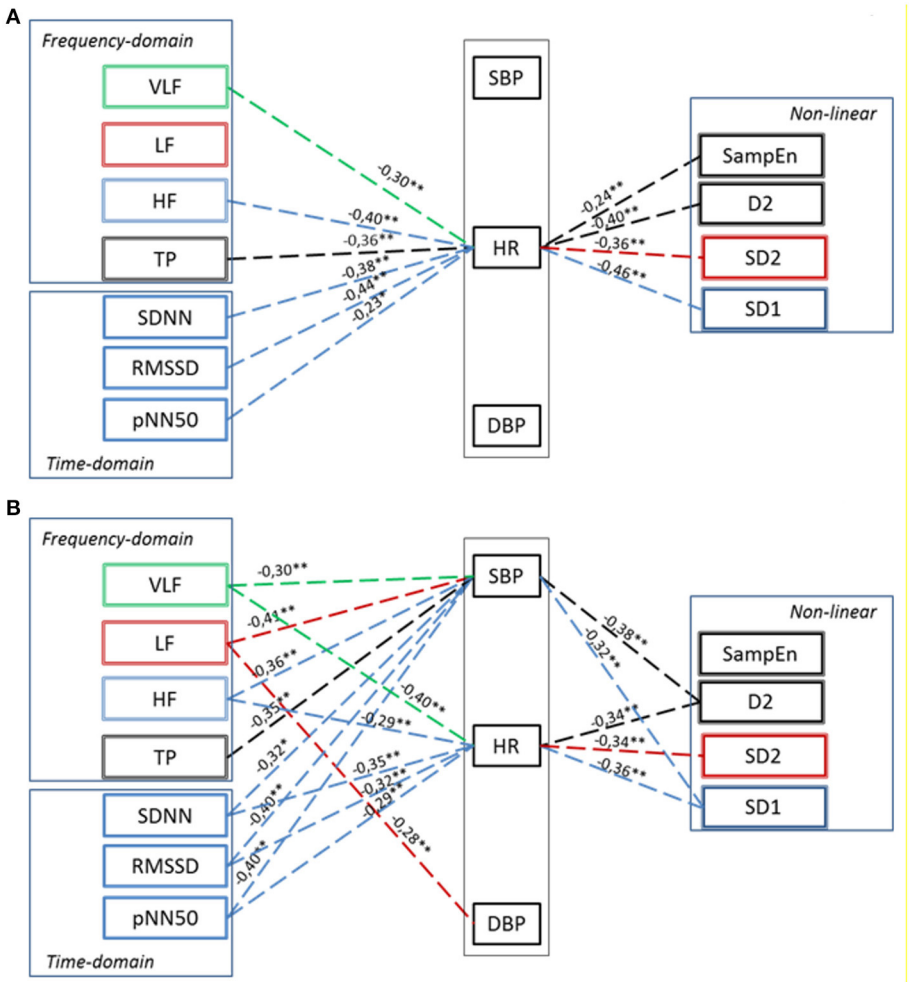

FIGURE 5 | Correlation between Hemodynamics and HRV parameters in PD patients in baseline conditions **(A)** and at 40th minute of "dry" immersion session **(B)**. HR, heart rate; SBP, systolic blood pressure; DBP, diastolic blood pressure. Dashed line—the negative correlation. Significance of Spearman correlation coefficient: $^{*}p < 0.05$, $^{**}p < 0.01$.

Therefore, it is not likely that temperature was the leading factor in BP modification. However, the separate effect of DI, "no-dry" water immersion, and water temperature is still to be evaluated (Sugawara and Tomoto, 2020).

Water Immersion Effect

Conditions, which are similar to the program of DI or sessions of warm water immersion, are represented by varied protocols of so-called "aquatic therapy," which appear as physical exercising in a water pool at thermoneutral water temperature. In most studies with these protocols, both systolic and diastolic BP has decreased by 10 mm Hg just some minutes after immersion in water (Ward et al., 2005; Júnior et al., 2020). Aquatic therapy is widely used to treat mental and motor disorders in PD (Carroll et al., 2017; Kim et al., 2018; Sato et al., 2019). Surprisingly, hemodynamics and HRV in subjects with PD under aquatic therapy appear largely uninvestigated.

Dry Immersion Effect

There is a lack of studies on cardiovascular responses in humans to a very short (within 1 h) DI session. Still, it is known that in healthy subjects, during the 1st h of DI, total peripheral resistance has decreased by 7%, which led to diastolic BP decreased by 5 mm Hg, and HR by 5 min^{-1} (Ogoh et al., 2017; Navasiolava et al., 2020). Similar results were reported in the study by Meigal et al. (2020). We regarded that decrease of the total peripheral vascular resistance has contributed to the decrease of BP in subjects with PD. Altogether, we regarded that the effect of DI on subjects with PD can be attributed to the condition of immersion to water.

HRV Parameters

Baroreceptor Reflex Sensitivity

Baroreceptor-heart rate reflex sensitivity (BRS) appears as an important determinant of the short-term regulation of BP (Nasr et al., 2005). In healthy subjects, conditions of DI provoked attenuation of BRS what was seen as increased

orthostatic hypotension and, hence, decreased orthostatic tolerance (Tomilovskaya et al., 2019; Borovik et al., 2020). However, this result was obtained after much longer DI sessions (3–21 days). In subjects with PD, BRS is substantially decreased, which is associated with orthostatic hypotension (Blaho et al., 2017; Gerasimova-Meigal et al., 2021), arterial stiffness, presence of central α-synuclein aggregation, cardiac sympathetic denervation, attenuated muscle sympathetic nerve activity (Sabino-Carvalho et al., 2021). In our study, none of the subjects with PD had signs of orthostatic hypotension what was earlier reported in the study by Gerasimova-Meigal et al. (2021). Nonetheless, attenuation of BRS may still have contributed to the decrease of BP in subjects with PD under DI sessions.

Baseline HRV Data in PD

Before the program of DI sessions, HRV was clearly reduced in subjects with PD, according to decreased values of time- and frequency-domain parameters. This indicated the decrease of *both* sympathetic and parasympathetic autonomic activity, which is consistent with earlier numerous studies (Jain, 2011; Jain and Goldstein, 2012; Soares et al., 2013; Maetzler et al., 2015; Gibbons et al., 2017; Akbilgic et al., 2020; Li et al., 2020). The low value of the parasympathetic-linked HRV parameters might evidence attenuated cardiorespiratory coupling (Heart rate variability, 1996; Shaffer and Ginsberg, 2017). As for non-linear parameters of HRV, indices, which characterized parasympathetic and sympathetic nervous activity (SD1 and SD2, correspondingly), were reduced in PD in comparison with older non-PD subjects (Kallio et al., 2002; Voss et al., 2009). Correlation dimension (D2), which characterized self-similarity of a signal, or the number of regulation inputs (differential equations) was markedly decreased in PD subjects in comparison with that of non-PD subjects (Acharya et al., 2014). Surprisingly, entropy and DFA indices, and recurrence rate of PD subjects generally fitted values regarded as normal for healthy older people (Voss et al., 2009; Acharya et al., 2014). Altogether, HRV signal in PD subjects can be regarded as less complex in comparison to age-matched healthy controls, which accords with evidence of decreased autonomic control at PD, presented by traditional HRV parameters.

HRV During a Single One DI Session

Within one DI session, almost all time- and frequency-domain HRV parameters have significantly increased. For example, the value of pNN50 has increased by three times by the end of the DI session. Such a result represents the growing variability of HR under the conditions of DI in PD subjects. As for non-linear parameters, SD1, which informs on the parasympathetic control of the heart, has significantly increased from 7–14 to 10–21, which is close to the values of healthy older subjects (Voss et al., 2009). The correlation dimension of HRV has also increased by three times, which indicates on growing complexity of the signal and, hence, emerging regulating inputs. We assume that such inputs could be associated with BRS and, emerging cardiorespiratory coupling, therefore, increased parasympathetic and sympathetic nervous control of HRV. A similar phenomenon of stronger cardiorespiratory coupling we reported in our earlier study with a deep breathing test (Gerasimova-Meigal et al., 2021). Altogether, the HRV of PD subjects after a 45-min DI session has clearly shifted in the direction of "normal" age-matched values. Such modification was possibly provoked by the "centralization" of circulation due to the compression effect of DI on peripheral tissue (Navasiolava et al., 2011; Tomilovskaya et al., 2019; Pandiarajan and Hargens, 2020).

HRV During the Program of DI Sessions

Compared with one DI session (acute effect), the effect of the program of DI sessions on HRV parameters was strikingly weak. This evidences the limited capability of the autonomic nervous system in PD to restore its functioning, presumably due to profound neurodegeneration. In turn, it indicates reduced mechanisms of neuroplasticity in PD. Similarly, in our earlier study, we have demonstrated no HRV dynamics seen with cardiovascular tests during the program of DI (Gerasimova-Meigal et al., 2021). Such results accord with the study of Rocha et al. (2018) in which a program of game-based rehabilitation in PD presented no modification of HRV. Traces of adaptation are usually seen after repetitive exposures (pre-conditioning), which are usually associated with intensive metabolic response to the intervention, e.g., cold, hypoxia, or physical exercise. Unlike pre-conditioning, DI appears as a rather deconditioning factor (Acket et al., 2018). We presume that the absence of long-term modification of the studied parameters can be attributed to the different environmental effects of DI. Additionally, limited modification of the studied parameters to the program of DI sessions could be linked to the limited adaptation capacity of the organism of a PD subject.

Correlation Between BP, HR, and HRV

The phenomenon of cardiovascular coupling is well-known and documented. For example, both feedback (from BP on HR, *via* the mechanism of BRS), and feedforward (from HR on BP) influences are known to take place (Schulz et al., 2013). However, in patients with PD, we did not find a correlation between BP and HR at baseline conditions, which might inform on cardiovascular uncoupling in PD. This could well-originate from reduced BRS, which is the characteristic of PD. Still, there was a correlation between HR and almost all HRV parameters. That is not surprising because HR appeared as a kind of "parent" signal for all HRV parameters. Also, the correlation between HR and HRV indices of parasympathetic activity (SDNN, RMSSD, pNN50, TP, HF, and SD1) was negative, which is consistent with consensus on autonomic control of the cardiovascular system (Heart rate variability, 1996; Shaffer and Ginsberg, 2017). The negative correlation between hemodynamic parameters and HRV indices of sympathetic activity (LF and SD2) did not fit this consensus, probably due to impaired sympathetic control and baroreflex sensitivity, which is often observed in PD patients (Blaho et al., 2017; Gerasimova-Meigal et al., 2021).

By contrast, under the conditions of DI significant correlations appeared between HRV parameters and systolic BP, which evidenced the temporal emergence of causal coupling between BP and HR. That is in line with the data on modification of values of HRV parameters during the DI session. In a way, during DI

the cardiovascular system of PD subjects looks more susceptive to regulation.

CONCLUSION

At baseline condition, time- and frequency-domain HRV parameters in subjects with PD showed low variability of HR, which indicates its reduced autonomic neurogenic control. The temporal structure of the regulatory input to the heart seen with non-linear parameters of HRV was characterized by low complexity. Within one DI session, systolic and diastolic BP has modestly decreased, and time- and frequency-domain parameters of HRV have significantly increased, what altogether evidenced by compensatory hemodynamics mechanisms during DI. Across the program of DI sessions, the hypotensive effect was also present, but no notable modification of the HRV-parameters was found. The absence of long-term modification of the studied parameters can be attributed both to deconditioning effect of the DI, and limited adaptation to DI in subjects with PD due to neurodegeneration. That should be taken into consideration when planning either rehabilitation measures in subjects of older age with modeled microgravity or space flights in older candidates.

LIMITATIONS

There were several limitations to our study. First, an adequate age-matched control group would hardly be formed, because all potential older subjects are characterized by multimorbidity. Therefore, our study was designed only as a self-control one. Second, we experienced some difficulties with recruiting subjects to the study, as many of the candidate subjects did not meet strict inclusion criteria due to health status, especially cardiac arrhythmias, which did not allow using HRV analysis for assessment of autonomic regulation.

PROSPECTIVE

For a better insight into the mechanisms of the autonomic nervous regulation in PD subjects under DI, one should consider investigating (1) cardiorespiratory coupling of HRV during DI session and (2) to evaluate HRV, BP, and HR in healthy controls during a short-term DI session to make comparison with the group of PD subjects. In addition to the main purpose of this study, we are convinced that it can also contribute to the field of space physiology since all the subjects in our study were elderly people who are expected to take on a significant proportion of commercial space travel in the future. Space tourism will evolve toward suborbital space flights, which are expected to last for shorter periods of time. For example, Amazon CEO Jeff Besos recently announced that an 82-year-old woman will join him on a space trip (Wattles, 2021b), and Richard Bronson has already performed such a trip (Wattles, 2021a). Thus, this study closed an important gap in ground-based space experiments, since most of them last for longer periods (several hours, days, weeks) and attract mostly younger healthy subjects. For this reason, this study is one of the few exploratory ones in a row with our previous studies (Meigal et al., 2018, 2020, 2021a,b) in space neuroscience and space suborbital tourism.

DATA AVAILABILITY STATEMENT

The raw data supporting the conclusions of this article will be made available by the authors, without undue reservation.

ETHICS STATEMENT

The studies involving human participants were reviewed and study protocol was approved by joint Ethic Committee of the Ministry of Health care of the Republic of Karelia and Petrozavodsk State University (Statement of approval No. 31, 18.12.2014). The patients/participants provided their written informed consent to participate in this study.

AUTHOR CONTRIBUTIONS

LG-M contributed to the basic concept of the study, study design and implementation (supervising the DI procedure, monitoring the ECG, blood pressure, and clinical condition of the subjects during DI), the statistical analysis, the interpretation of results, writing the manuscript, and approval of the final draft. AM contributed to the basic concept of the study, study design, statistical analysis, interpretation of results, writing the manuscript, and approval of the final draft. NS contributed to the study design and implementation (supervising the DI procedure, monitoring the ECG, blood pressure of the subjects during DI, and data analyses), the interpretation of results, and approval of the final draft. IS contributed to the basic concept of the study, study design, the interpretation of results, and approval of the final draft. All authors contributed to the article and approved the submitted version.

FUNDING

This research was financially supported by the Ministry of Science and Higher Education of the Russian Federation (Theme No. 0752-2020-0007).

ACKNOWLEDGMENTS

The authors thank the subjects for their participation; engineer Kirill Prochorov for keeping the MEDSIM equipment in order.

SUPPLEMENTARY MATERIAL

The Supplementary Material for this article can be found online at: https://www.frontiersin.org/articles/10.3389/fphys.2021.712365/full#supplementary-material

REFERENCES

Acharya, U. R., Faust, O., Sree, V., Swapna, G., Martis, R. J., Kadri, N. A., et al. (2014). Linear and non-linear analysis of normal and CAD-affected heart rate signals. *Comput. Methods Progr. Biomed.* 113, 55–68. doi: 10.1016/j.cmpb.2013.08.017

Acket, B., Amirova, L., Gerdelat, A., Cintas, P., Custaud, M. A., and Pavy-LeTraon, A. (2018). Dry immersion as a model of deafferentation: a neurophysiology study using somatosensory evoked potentials. *PLoS ONE* 13:e0201704. doi: 10.1371/journal.pone.0201704

Akbilgic, O., Kamaleswaran, R., Mohammed, A., Ross, G. W., Masaki, K., Petrovitch, H., et al. (2020). Electrocardiographic changes predate Parkinson's disease onset. *Sci. Rep.* 10:11319. doi: 10.1038/s41598-020-68241-6

Amirova, L., Navasiolava, N., Rukavishvikov, I., Gauquelin-Koch, G., Gharib, C., Kozlovskaya, I., et al. (2020). Cardiovascular system under simulated weightlessness: head-down bed rest vs. dry immersion. *Front. Physiol.* 11:395. doi: 10.3389/fphys.2020.00395

Blaho, A., Šutovský, S., Valkovič, P., Šiarnik, P., Sýkora, M., and Turčáni, P. (2017). Decreased baroreflex sensitivity in Parkinson's disease is associated with orthostatic hypotension. *J. Neurol. Sci.* 377, 207–211. doi: 10.1016/j.jns.2017.03.044

Borovik, A. S., Orlova, E. A., Tomilovskaya, E. S., Tarasova, O. S., and Vinogradova, O. L. (2020). Phase coupling between baroreflex oscillations of blood pressure and heart rate changes in 21-day dry immersion. *Front. Physiol* 11:455. doi: 10.3389/fphys.2020.00455

Brunt, V. E., Howard, M. J., Francisco, M. A., Ely, B. R., and Minson, C. T. (2016). Passive heat therapy improves endothelial function, arterial stiffness and blood pressure in sedentary humans. *J. Physiol.* 594, 5329–5342. doi: 10.1113/JP272453

Carroll, L. M., Volpe, D., Morris, M. E., Saunders, J., and Clifford, A. M. (2017). Aquatic exercise therapy for people with Parkinson disease: a randomized controlled trial. *Arch. Phys. Med. Rehabil.* 98, 631–638. doi: 10.1016/j.apmr.2016.12.006

Chen, Z., Li, G., and Liu, J. (2020). Autonomic dysfunction in Parkinson's disease: implications for pathophysiology, diagnosis, and treatment. *Neurobiol. Dis.* 134:104700. doi: 10.1016/j.nbd.2019.104700

Gerasimova-Meigal, L., and Meigal, A. (2019). Time- and frequency-domain parameters of heart rate variability and blood pressure in Parkinson's disease patients under dry immersion. *Front. Physiol.* 26:11. doi: 10.3389/conf.fphys.2018.26.00011

Gerasimova-Meigal, L. I., Sireneva, N. V., and Meigal, A.,Yu. (2021). Estimation of the effect of the course of short-term sessions "dry" immersion on autonomic regulation in patients with parkinsonism. *Hum. Physiol.* 47, 51–57. doi: 10.1134/S0362119721040046

Gibbons, C. H., Simon, D. K., Huang, M., Tilley, B., Aminoff, M. J., Bainbridge, J. L., et al. (2017). Autonomic and electrocardiographic findings in Parkinson's disease. *Auton. Neurosci.* 205, 93–98. doi: 10.1016/j.autneu.2017.04.002

Heart rate variability (1996). Standards of measurement, physiological interpretation, and clinical use. Task Force of the European Society of Cardiology and the North American Society of Pacing and Electrophysiology. *Eur. Heart J.* 17, 354–381.

Jain, S. (2011). Multi-organ autonomic dysfunction in Parkinson disease. *Parkinsonism Relat. Disord.* 17, 77–83. doi: 10.1016/j.parkreldis.2010.08.022

Jain, S., and Goldstein, D. S. (2012). Cardiovascular dysautonomia in Parkinson disease: from pathophysiology to pathogenesis. *Neurobiol. Dis.* 46, 572–580. doi: 10.1016/j.nbd.2011.10.025

Jin, M., Wang, J., Zhang, H., Zhou, H., and Zhao, K. (2019). Simulated wightlessness perturbs the intestinal metabolomic profile of rats. *Front. Physiol.* 10:1279. doi: 10.3389/fphys.2019.01279

Júnior, F. A., Gomes, S. G., da Silva, F. F., Souza, P. M., Oliveira, E. C., Coelho, D. B., et al. (2020). The effects of aquatic and land exercise on resting blood pressure and post-exercise hypotension response in elderly hypertensives. *Cardiovasc. J. Afr.* 31, 116–122. doi: 10.5830/CVJA-2019-051

Kallio, M., Suominen, K., Bianchi, A. M., Mäkikallio, T., Haapaniemi, T., Astafiev, S., et al. (2002). Comparison of heart rate variability analysis methods in patients with Parkinson's disease. *Med. Biol. Eng. Comput.* 40, 408–414. doi: 10.1007/BF02345073

Kim, J. H., Jung, Y. S., Kim, J. W., Ha, M. S., Ha, S. M., and Kim, D. Y. (2018). Effects of aquatic and land-based exercises on amyloid beta, heat shock protein 27, and pulse wave velocity in elderly women. *Exp. Gerontol.* 108, 62–68. doi: 10.1016/j.exger.2018.03.024

Lee, H. S., Lobbestael, E., Vermeire, S., Sabino, J., and Cleynen, I. (2021). Inflammatory bowel disease and Parkinson's disease: common pathophysiological links. *Gut* 70, 408–417. doi: 10.1136/gutjnl-2020-322429

Li, Y., Wang, J., Li, X., Jing, W., Omorodion, I., and Liu, L. (2020). Association between heart rate variability and Parkinson's disease: a meta-analysis. *Curr. Pharm. Des.* 27, 2056–2067. doi: 10.2174/1871527319666200905122222

Maetzler, W., Karam, M., Berger, M. F., Heger, T., Maetzler, C., Ruediger, H., et al. (2015). Time- and frequency-domain parameters of heart rate variability and sympathetic skin response in Parkinson's disease. *J. Neural Transm.* 122, 419–425. doi: 10.1007/s00702-014-1276-1

Masiero, S., Maghini, I., Mantovani, M. E., Bakdounes, L., Koutsikos, K., Del Felice, A., et al. (2019). Is the aquatic thermal environment a suitable place for providing rehabilitative treatment for person with Parkinson's disease? A retrospective study. *Int. J. Biometeorol.* 63, 13–18. doi: 10.1007/s00484-018-1632-1

Meigal, A., Gerasimova-Meigal, L., Saenko, I., and Subbotina, N. (2018). Dry immersion as a novel physical therapeutic intervention for rehabilitation of Parkinson's disease patients: a feasibility study. *Phys. Med. Rehab. Kuror.* 28, 275–281. doi: 10.1055/a-0577-5139

Meigal, A., Tretjakova, O. G., Gerasimova-Meigal, L., and Saenko, I. (2021a). Vertical spatial orientation in patients with parkinsonism under the state of a single "dry" immersion and a course of immersions. *Hum. Physiol.* 47, 183–192. doi: 10.1134/S0362119721020079

Meigal, A., Yu., Gerasimova-Meigal, L. I., Saenko, I. V., Subbotina, N. S., Tret'yakova, O. G., et al. (2017). The effect of "dry" immersion as microgravity analogue on neurological symptoms in parkinsonism. *Aviakosm. Ekol. Med.* 51, 53–59. doi: 10.21687/0233-528X-2017-51-7-53-59

Meigal, A. Y., Gerasimova-Meigal, L. I., and Saenko, I. V. (2020). Physiological reactions of patients with parkinsonism to simulated microgravity using "dry" immersion: a pilot study. *Hum. Physiol.* 46, 579–586. doi: 10.1134/S0362119720050096

Meigal, A. Y., Rissanen, S. M., Tarvainen, M. P., Airaksinen, O., Kankaanpää, M., and Karjalainen, P. A. (2013). Non-linear EMG parameters for differential and early diagnostics of Parkinson's disease. *Front. Neurol.* 4:135. doi: 10.3389/fneur.2013.00135

Meigal, A. Y., Tretjakova, O. G., Gerasimova-Meigal, L. I., and Sayenko, I. V. (2021b). Program of seven 45-min dry immersion sessions improves choice reaction time in Parkinson's disease. *Front. Physiol.* 11:621198. doi: 10.3389/fphys.2020.621198

Metzger, J. M., and Emborg, M. E. (2019). Autonomic dysfunction in Parkinson disease and animal models. *Clin. Auton. Res.*29, 397–414. doi: 10.1007/s10286-018-00584-7

Miroshnichenko, G. G., Meigal, A. Y., Saenko, I. V., Gerasimova-Meigal, L. I., Chernikova, L. A., Subbotina, N. S., et al. (2018). Parameters of surface electromyogram suggest that dry immersion relieves motor symptoms in patients with parkinsonism. *Front. Neurosci.* 12:667. doi: 10.3389/fnins.2018.00667

Nasr, N., Pavy-Le Traon, A., and Larrue, V. (2005). Baroreflex sensitivity is impaired in bilateral carotid atherosclerosis. *Stroke* 36, 1891–1895. doi: 10.1161/01.STR.0000177890.30065.cb

Navasiolava, N., Yuan, M., Murphy, R., Robin, A., Coupé, M., Wang, L., et al. (2020). Vascular and microvascular dysfunction induced by microgravity and its analogs in humans: mechanisms and countermeasures. *Front. Physiol.* 11:952. doi: 10.3389/fphys.2020.00952

Navasiolava, N. M., Custaud, M.-A., Tomilovskaya, E. S., Larina, I. M., Mano, T., Gauquelin-Koch, G., et al. (2011). Long-term dry immersion: review and prospects. *Eur. J. Appl. Physiol.* 111, 1235–1260. doi: 10.1007/s00421-010-1750-x

Nutt, J. G., Burchiel, K. J., Comella, C. L., Lang, A. E., Laws, Jr E. R. (2003). Randomized, double-blind trial of glial cell line-derived neurotrophic factor (GDNF) in PD. *Neurology* (2003) 60, 69–73. doi: 10.1212/WNL.60.1.69

Ogoh, S., Hirasawa, A., de Abreu, S., Denise, P., and Normand, H. (2017). Internal carotid, external carotid and vertebral artery blood flow responses

to 3 days of head-out dry immersion. *Exp. Physiol.* (2017) 102, 1278–1287. doi: 10.1113/EP086507

Palma, J. A., and Kaufmann, H. (2018). Treatment of autonomic dysfunction in Parkinson disease and other synucleinopathies. *Mov. Disord.* 33, 372–390. doi: 10.1002/mds.27344

Pandiarajan, M., and Hargens, A. R. (2020). Ground-based analogs for human spaceflight. *Front. Physiol.* 11:716. doi: 10.3389/fphys.2020.00716

Parker, R., Higgins, Z., Mlombile, Z. N. P., Mohr, M. J., and Wagner, T. L. (2018). The effects of warm water immersion on blood pressure, heart rate and heart rate variability in people with chronic fatigue syndrome. *S. Afr. J. Physiother.* 74:442. doi: 10.4102/sajp.v74i1.442

Postuma, R. B., Gagnon, J. F., Pelletier, A., and Montplaisir, J. (2013). Prodromal autonomic symptoms and signs in Parkinson's disease and dementia with Lewy bodies. *Mov. Disord.* 28, 597–604. doi: 10.1002/mds.25445

Pursiainen, V., Haapaniemi, T. H., Korpelainen, J. T., Huikuri, H. V., Sotaniemi, K. A., and Myllylä, V. V. (2002). Circadian heart rate variability in Parkinson's disease. *J. Neurol.* 249, 1535–1540. doi: 10.1007/s00415-002-0884-0

Reich, S. G., and Savitt, J. M. (2019). Parkinson's disease. *Med. Clin. North Am.* 103, 337–350. doi: 10.1016/j.mcna.2018.10.014

Rocha, R. S. B., De Oliveira Rocha, L. S., Pena, E. S. M., Caldas, L. C. P., Moreno, M. A. (2018). Analysis of autonomic modulation of heart rate in patients with Parkinson's disease and elderly individuals submitted to game therapy training. *Geriatr Gerontol Int.* (2018) 18:20–25. doi: 10.1111/ggi.13130

Rodriguez-Oroz, M. C., Jahanshahi, M., Krack, P., Litvan, I., Macias, R., and Bezard, E. (2009). Initial clinical manifestations of Parkinson's disease: features and pathophysiological mechanisms. *Lancet Neurol.* 8, 1128–1139. doi: 10.1016/S1474-4422(09)70293-5

Sabino-Carvalho, J. L., Falquetto, B., Takakura, A. C., and Vianna, L. C. (2021). Baroreflex dysfunction in Parkinson's disease: integration of central and peripheral mechanisms. *J. Neurophysiol.* 125, 1425–1439. doi: 10.1152/jn.00548.2020

Sato, D., Yamashiro, K., Yamazaki, Y., Ikarashi, K., Onishi, H., Baba, Y., et al. (2019). Priming effects of water immersion on paired associative stimulation-induced neural plasticity in the primary motor cortex. *Int. J. Environ. Res. Public Health* 17:215. doi: 10.3390/ijerph17010215

Schaeffer, E., Kluge, A., Böttner, M., Zunke, F., Cossais, F., Berg, D., et al. (2020). Alpha synuclein connects the gut-brain axis in Parkinson's disease patients - a view on clinical aspects, cellular pathology and analytical methodology. *Front. Cell Dev. Biol.* 8:573696. doi: 10.3389/fcell.2020.573696

Schulz, S., Adochiei, F. C., Edu, I. R., Schroeder, R., Costin, H., Bär, K. J., et al. (2013). Cardiovascular and cardiorespiratory coupling analyses: a review. *Philos. Trans. A Math. Phys. Eng. Sci.* 371:20120191. doi: 10.1098/rsta.2012.0191

Shaffer, F., and Ginsberg, J. P. (2017). An overview of heart rate variability metrics and norms. *Front. Public Health* 5:258. doi: 10.3389/fpubh.2017.00258

Soares, F. H. R., Rebouças, G. M., Lopes, P. F. F., Felipe, T. R., Bezerra, J. C. L., de Albuquerque Filho, N. J. B., et al. (2013). Measures of heart rate variability in patients with idiopathic Parkinson's disease. *J. Alzheimers Dis. Parkinsonism* 3:130. doi: 10.4172/2161-0460.1000130

Sugawara, J., and Tomoto, T. (2020). Effects of short-term warm water immersion on cardiac baroreflex sensitivity in healthy men. *J. Physiol. Sci.* 70:34. doi: 10.1186/s12576-020-00762-1

Tarvainen, M. P., Niskanen, J. P., Lipponen, J. A., Ranta-Aho, P. O., and Karjalainen, P. A. (2014). Kubios HRV–heart rate variability analysis software. *Comput. Methods Programs Biomed.* 113, 210–220. doi: 10.1016/j.cmpb.2013.07.024

Tomilovskaya, E., Shigueva, T., Sayenko, D., Rukavishnikov, I., and Kozlovskaya, I. (2019). Dry immersion as a ground-based model of microgravity physiological effects. *Front. Physiol.* 10:284. doi: 10.3389/fphys.2019.00284

Turroni, S., Magnani, M., K. C. P., Lesnik, P., Vidal, H., and Heer M (2020). Gut microbiome and space travelers' health: state of the art and possible pro/prebiotic strategies for long-term space missions. *Front. Physiol.* 11:553929. doi: 10.3389/fphys.2020.553929

Voss, A., Schulz, S., Schroeder, R., Baumert, M., and Caminal, P. (2009). Methods derived from nonlinear dynamics for analysing heart rate variability. *Philos. Trans. A Math. Phys. Eng. Sci.* 367, 277–296. doi: 10.1098/rsta.2008.0232

Ward, E. J., McIntyre, A., van Kessel, G., and Hague, W. M. (2005). Immediate blood pressure changes and aquatic physiotherapy. *Hypert. Pregn.* 24, 93–102. doi: 10.1081/PRG-200059828

Watenpaugh, D. E. (2016). Analogs of microgravity: head-down tilt and water immersion. *J. Appl. Physiol.* 120, 904–914. doi: 10.1152/japplphysiol.00986.2015

Wattles, J. (2021a). *An 82-Year-Old Woman Trained to Be an Astronaut Sixty Years Ago. Now She's Going to Space With Jeff Bezos, July 1, 2021.* Available online at: https://edition.cnn.com/2021/07/01/tech/jeff-bezos-blue-origin-flight-wally-funk-mercury-scn/index.html (accessed July 8, 2021).

Wattles, J. (2021b). *Virgin Galactic Founder Richard Branson Successfully Rockets to Outer Space. July 12, 2021.* Available online at: https://edition.cnn.com/2021/07/11/tech/richard-branson-virgin-galactic-space-flight-scn/index.html (accessed July 13, 2021).

Conflict of Interest: The authors declare that the research was conducted in the absence of any commercial or financial relationships that could be construed as a potential conflict of interest.

Publisher's Note: All claims expressed in this article are solely those of the authors and do not necessarily represent those of their affiliated organizations, or those of the publisher, the editors and the reviewers. Any product that may be evaluated in this article, or claim that may be made by its manufacturer, is not guaranteed or endorsed by the publisher.

frontiers in Physiology

ORIGINAL RESEARCH
published: 12 February 2020
doi: 10.3389/fphys.2020.00071

Evaluation of an Antioxidant and Anti-inflammatory Cocktail Against Human Hypoactivity-Induced Skeletal Muscle Deconditioning

Coralie Arc-Chagnaud[1,2], Guillaume Py[1], Théo Fovet[1], Rémi Roumanille[1], Rémi Demangel[1], Allan F. Pagano[3,4], Pierre Delobel[1], Stéphane Blanc[5], Bernard J. Jasmin[4], Dieter Blottner[6], Michele Salanova[6], Mari-Carmen Gomez-Cabrera[2], José Viña[2], Thomas Brioche[1†] and Angèle Chopard[1†]*

[1]DMEM, Université Montpellier, INRAE, Montpellier, France, [2]Freshage Research Group, Department of Physiology, Faculty of Medicine, CIBERFES, Fundación Investigación Hospital Clínico Universitario/INCLIVA, University of Valencia, Valencia, Spain, [3]Faculté des Sciences du Sport, Mitochondries, Stress Oxydant et Protection Musculaire, Université de Strasbourg, Strasbourg, France, [4]Department of Cellular and Molecular Medicine and Centre for Neuromuscular Disease, Faculty of Medicine, University of Ottawa, Ottawa, ON, Canada, [5]IPHC, CNRS, Université de Strasbourg, Strasbourg, France, [6]Berlin Center for Space Medicine, Integrative Neuroanatomy, Charité Universitätsmedizin Berlin, Berlin, Germany

OPEN ACCESS

Edited by:
Marc-Antoine Custaud, Université d'Angers, France

Reviewed by:
Satoshi Iwase, Aichi Medical University, Japan
Laurence Stevens, Lille University of Science and Technology, France

***Correspondence:**
Thomas Brioche
thomas.brioche@umontpellier.fr

[†]These authors have contributed equally to this work

Specialty section:
This article was submitted to Environmental, Aviation and Space Physiology, a section of the journal Frontiers in Physiology

Received: *02 October 2019*
Accepted: *22 January 2020*
Published: *12 February 2020*

Citation:
Arc-Chagnaud C, Py G, Fovet T, Roumanille R, Demangel R, Pagano AF, Delobel P, Blanc S, Jasmin BJ, Blottner D, Salanova M, Gomez-Cabrera M-C, Viña J, Brioche T and Chopard A (2020) Evaluation of an Antioxidant and Anti-inflammatory Cocktail Against Human Hypoactivity-Induced Skeletal Muscle Deconditioning. Front. Physiol. 11:71. doi: 10.3389/fphys.2020.00071

Understanding the molecular pathways involved in the loss of skeletal muscle mass and function induced by muscle disuse is a crucial issue in the context of spaceflight as well as in the clinical field, and development of efficient countermeasures is needed. Recent studies have reported the importance of redox balance dysregulation as a major mechanism leading to muscle wasting. Our study aimed to evaluate the effects of an antioxidant/anti-inflammatory cocktail (741 mg of polyphenols, 138 mg of vitamin E, 80 μg of selenium, and 2.1 g of omega-3) in the prevention of muscle deconditioning induced by long-term inactivity. The study consisted of 60 days of hypoactivity using the head-down bed rest (HDBR) model. Twenty healthy men were recruited; half of them received a daily antioxidant/anti-inflammatory supplementation, whereas the other half received a placebo. Muscle biopsies were collected from the vastus lateralis muscles before and after bedrest and 10 days after remobilization. After 2 months of HDBR, all subjects presented muscle deconditioning characterized by a loss of muscle strength and an atrophy of muscle fibers, which was not prevented by cocktail supplementation. Our results regarding muscle oxidative damage, mitochondrial content, and protein balance actors refuted the potential protection of the cocktail during long-term inactivity and showed a disturbance of essential signaling pathways (protein balance and mitochondriogenesis) during the remobilization period. This study demonstrated the ineffectiveness of our cocktail supplementation and underlines the complexity of redox balance mechanisms. It raises interrogations regarding the appropriate nutritional intervention to fight against muscle deconditioning.

Keywords: muscle wasting, inactivity, oxidative stress, antioxidants, cell signaling

INTRODUCTION

Skeletal muscle is a plastic tissue able to adapt to intrinsic and environmental stresses (Harridge, 2007). While physical exercise and training reinforce our muscles, in contrast, situations of hypoactivity such as immobilization, sedentary lifestyle, or microgravity environments lead to skeletal muscle deconditioning. In this context, space agencies must always work on the optimization of countermeasures, especially in astronaut training programs and supplementation to preserve their work capacity and health. Muscle deconditioning is the consequence of a dysregulation of muscle homeostasis that triggers structural and functional alterations (Jackman and Kandarian, 2004; Chopard et al., 2009a; Baldwin et al., 2013). It translates mainly to a loss of muscle mass and myofiber atrophy, largely induced by a dysregulation of protein balance signaling pathways (Kandarian and Stevenson, 2002; Glass, 2005; Degens and Alway, 2006; Ventadour and Attaix, 2006). Amyotrophy is also accompanied by a greater loss of strength and power (Brioche et al., 2016). Inactive skeletal muscles are also exposed to metabolic remodeling, affecting the myofiber typology and their contractile properties. Indeed, alteration of some actors of the oxidative system (mitochondria and enzymes) contributes to the shift toward a glycolytic profile to the detriment of the oxidative one (Widrick et al., 1999; Fitts et al., 2010).

Another important element influenced by hypoactivity situations is the redox balance. It consists of an equilibrium between pro-oxidant molecules and antioxidant defenses (Powers et al., 2016). In skeletal muscle, mitochondria, NADPH oxidase, and xanthine oxidase are the main sources of the reactive oxygen and nitrogen species (RONS) (Murphy, 2009; Gomez-Cabrera et al., 2013). The antioxidant defenses are composed of two systems, an endogenous one that relies on enzyme actions (superoxide dismutase, catalase, and glutathione peroxidase) and an exogenous one that relies on various actors (glutathione, vitamins C and E, polyphenols, and carotenoids). The steady state of the redox balance is essential for the healthy function of organisms. For example, energy production, cellular proliferation, gene expression, and immunity are some of the functions that it regulates (Sies, 2017). In prolonged muscle-disuse situations, this balance shifts in favor of pro-oxidants and triggers oxidative stress. It translates into a dysregulation of various signaling pathways in the cells, including those linked to protein balance, apoptosis, and regeneration or excitation-contraction coupling (Zerba et al., 1990; Powers et al., 2011a,b; Salanova et al., 2013). On the other hand, inflammatory processes play a role in RONS production and contribute to the alteration of protein balance pathways (Flohé et al., 1997; Li and Karin, 1999; Stamler and Meissner, 2001). In this context, microgravity and hypoactivity-induced high inflammation levels associated with oxidative stress accentuate the muscle deconditioning phenomenon (Reid et al., 1993; Powers et al., 2011b).

The head-down bed rest (HDBR) model is one of the most commonly used models in space physiology, as it mimics weightlessness conditions (Pavy-Le Traon et al., 2007). In addition to involving chronic hypoactivity and muscle unloading, the −6° tilt of the subjects induces fluid redistribution similar to that observed in spaceflight (Hargens and Vico, 2016). Nonetheless, apart from the aerospace context, HDBR represents a strong experimental model in the study of various situations linked to immobilization and reduced activity (sport field, clinical stay, etc.).

The present study relates to the "cocktail study" carried out under the aegis of the European Space Agency (ESA), with the aim of evaluating the effect of an antioxidant/anti-inflammatory cocktail as a countermeasure during a 2-month bedrest experiment. Considering previous knowledge about cellular alterations induced by inactivity, it is legitimate to think that limiting cellular oxidative stress and inflammation levels could be an appropriate strategy. The currently available literature highlights the interesting roles of some molecules in muscle deconditioning prevention. Omega-3 fatty acids, known for their anti-inflammatory action, could decrease atrophy and low-grade inflammation levels and activate the protein synthesis pathway during unloading situations (You et al., 2010; Jeromson et al., 2015). Moreover, in a model of cachexia in rodent cancer-induced cachexia, omega-3 fatty acid supplementation has shown a preventive on muscle atrophy, and data in elderly people showed that omega-3 fatty acids can activate the protein synthesis mTOR pathway (Smith et al., 2011a,b). In animals, vitamin E supplementation was able to decrease proteolysis and muscular atrophy (Servais et al., 2007). Vitamin E is also known for its anti-inflammatory properties through inhibition of the NF-kB pathway which is well described in disuse atrophy models to activate proteolytic pathways (Huey et al., 2008; Khor et al., 2014). Vitamin E is often coupled with Selenium as this latter scavenges RONS and boosts the intracellular effects of vitamin E. Combined with selenium oligo element, vitamin E administration in rats demonstrated positive effects on oxidative stress markers *via* the activation of the endogenous antioxidant system (Beytut et al., 2018). Vitamin E and selenium combination also showed beneficial effect in patients with facioscapulohumeral dystrophy (Passerieux et al., 2015). Polyphenols known for their antioxidant properties given as pure molecules such as quercetin, epigallocatechin 3, resveratrol or as natural plant extracts (green tea or grape seed extracts) showed beneficial effect on rodent muscle atrophy (Alway et al., 1985; Momken et al., 2011; Lambert et al., 2015; Meador et al., 2015; Mukai et al., 2016). For example, during mechanical unloading, Momken et al. (2011) tested a nutritional countermeasure based on resveratrol administration. Its administration in rats was able to maintain protein balance, soleus muscle mass, and maximal force contraction. While current data suggest that some bio-active compounds, taken alone or as natural extracts, enhance several aspects of muscle and whole-body metabolic control, a single micronutrient is unlikely to be strong enough to reverse the wide range of deleterious effects induced by physical inactivity. Recently, the notion of nutrient cocktails, to trigger additive and/or synergistic effects between bio-active compounds, has been proposed (Damiot et al., 2019). In this recent study, we examined the capacity of a nutrient cocktail composed of polyphenols, omega-3 fatty acids, vitamin E, and selenium to prevent the expected metabolic alterations induced by physical inactivity and sedentary behaviors.

The cocktail used in the study of Damiot et al. fully prevented the hypertriglyceridemia, the drop in fasting HDL and total fat oxidation, and the increase in *de novo* lipogenesis. Moreover, the cocktail limited the decrease in type-IIa muscle fiber cross-sectional area and decreased protein ubiquitination content.

This human study is the first to focus on cocktail supplementation with antioxidant/anti-inflammatory molecules as a countermeasure to the deleterious effects of a prolonged simulated microgravity period, and our aim was to evaluate the effects of the oral supplement on muscle deconditioning.

MATERIALS AND METHODS

Subjects and Ethics Statement

Twenty healthy, active (between 10,000 and 15,000 steps per day) males were selected for this experiment (age: 34 ± 8; height: 176 ± 5 cm; weight: 73.5 ± 6.1 kg; BMI: 23.7 ± 1.5). The subjects had no medical history or physical signs of neuromuscular disorders. They were nonsmokers and were not taking any drugs or medications. All subjects gave informed consent to the experimental procedures, which were approved by the local ethics committee (CPP Sud-Ouest et Outre-Mer I, France, number ID RCB: 2016-A00401–50) in accordance with the Declaration of Helsinki. All experiments were conducted at the Space Clinic of the Institute of Space Medicine and Physiology (Medes-IMPS, Rangueil Hospital) in Toulouse (France) and were sponsored by the European Space Agency (ESA) and the French National Space Agency (CNES).

Overall Study Design

This experiment consisted of a 2-month HDBR period with a 14-day baseline data collection period before HDBR and a 14-day recovery period after it. During the 2-month HDBR period, the subjects laid in a supine position with a −6° tilt to preserve simulated microgravity effects. Participants were randomly assigned to two groups on a double-blind basis. Ten of the participants were part of the "Placebo" group, whereas the ten others were part of the "Cocktail" group and received a daily antioxidant/anti-inflammatory cocktail during the 2-month bedrest period. All pills were taken at mealtimes to reduce the risks of secondary effects affecting the gastrointestinal area. Each subject had a daily medical examination, and the MEDES team took several standardized measurements. Room lighting was on between 07.00 and 23.00 h. During the entire hospitalization phase, the diet was monitored, and the meals were defined by the MEDES nutritionist and provided by Toulouse Hospital. During the HDBR period, the subjects remained in a supine position with a −6° tilt continuously, even during a daily 20-min extraction for toilet procedures and weighing (to preserve as much as possible the effects of simulated microgravity) and were instructed not to produce any unnecessary movements with their limbs.

Cocktail Composition

The nutrient cocktail composition was based on a previous study (Damiot et al., 2019). The daily dose administered was composed of a 741 mg of bioactive polyphenol compound mix (XXS-2A-BR2 mix, Spiral Company, Dijon, France), 138 mg of vitamin E coupled with 80 μg of selenium (Solgar, Marne la Vallée, France), and 2.1 g of omega-3 (Omacor, Pierre Fabre Laboratories, Toulouse France). The daily dose of polyphenols was exactly composed by flavonols (323.4 mg), phenylpropanoides (45.6 mg), oligostilbènes, (78.0 mg), acide hydroxycinnamiques (50.4 mg), flavanols (135.6 mg), and flavanones (108.0 mg) and consisted of six pills per day: two at breakfast, two at lunch and two at diner. As there is no Dietary References Intake (DRI) available for polyphenols, the ~700 mg/day dose was based on several reviews on the bioavailability and bioefficacy of polyphenols in humans and other studies that tested the effects of polyphenols on exercise performance and oxidative stress (Manach et al., 2005; Myburgh, 2014; Somerville et al., 2017; Damiot et al., 2019). Polyphenol nutrient cocktail derived from food sources that consist of Liliaceae, Vernenaceae, Lamiaceae, Vitaceae, Rubiaceae, Theaceae, and Rutaceae Genres consisting of *Allium cepa*, *Lippia citriodora*, *Ajuga reptans*, *Vitis vinifera*, *Coffea robusta*, *Camellia sinensis*, and *Citrus aurantium*. For vitamin E, a single pill was orally ingested per day with breakfast. The daily proposed dose was respectively 6 and 5 times lower than the maximum allowed doses according to the US National academy of sciences. The 3 g daily dose of omega-3 was based on French pharmacopeia recommendations for hypolipemic effects (2–4 g/day) and was provided as 1 pill per meal which is within the daily dose used in most clinical studies (Ng et al., 2014; Hodson et al., 2017). This daily dose thus corresponded to 1.1 g of eicosapentaenoic acid (EPA) and 1 g of docosahexaenoic acid (DHA).

Measurements of Maximal Isometric Voluntary Contraction

To characterize the strength of the subjects' lower limb muscles, the maximal voluntary isometric contraction (MVC) strength was measured using a ConTrex device. The left leg of the participants was used to determine strength in knee and ankle flexors and extensor muscle groups. MVC was determined at an angulation of 80° for the knee and 0° for the ankle compared to the standard referential.

Two measurements were completed, with the first one performed 12 days before the bed rest protocol (see **Figure 1**) and the second one just before the end of bed rest (day of restart of the upright posture). To carry out these tests, each participant was familiarized with the equipment and the standardized protocol before conducting the tests. During the assessments, participants were seated on the chair of the ConTrex device and firmly attached to it to avoid disturbance of movement.

The protocol was similar for each muscle group; after a short warm-up in neutral position, a series of measurements were recorded with a 30-s recovery interval. Each series consisted of a first extension movement followed by an isometric contraction and a flexion movement followed by an isometric contraction. Each one was maintained between 5 and 7 s, and 2 min of recovery was provided every 3 sets of measurements. The total duration of the test was 15 min per pair of agonist/

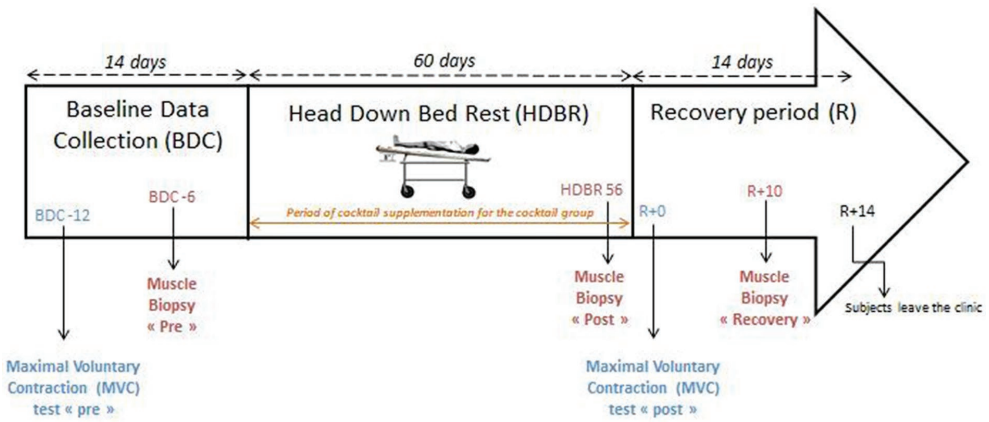

FIGURE 1 | Representative time axis of the experiment.

TABLE 1 | List of primary and secondary antibodies, their reference, provider, and dilution.

Antibody	Reference	Commercial	Dilution
p-4EBP1	9451	Cell signaling	1:1,000
4EBP1	9644	Cell signaling	1:1,000
4-HNE	46545	Abcam	1:1,000
ATG7	8558	Cell signaling	1:1,000
Catalase	110704	Genetex	1:1,000
Citrate synthase	Sc-390693	Santa Cruz	1:200
COX IV	Sc-69360	Santa Cruz	1:200
Cytochrome c	Sc-13560	Santa Cruz	1:200
p-Eif2α	3398	Cell signaling	1:1,000
Eif2α	9722	Cell signaling	1:1,000
Gpx	3206	Cell signaling	1:1,000
LC3	L7543	Sigma	1:400
p-PRAS40	13175	Cell signaling	1:1,000
PRAS40	26915	Cell signaling	1:1,000
PGC1-α	AB3242	Millipore	1:1,000
p-ULK1	6888	Cell signaling	1:1,000
ULK1	4776	Cell signaling	1:1,000
Anti-MyHC1	BA-D5	DSHB	1:10
Anti-MyHC2	M4276	Sigma-Aldrich	1:200
Anti-MyHC2a	SC-71	DSHB	1:10
Anti-mouse - HRP	7076	Cell signaling	1:5,000
Anti-rabbit - HRP	7074	Cell signaling	1:5,000
Anti-goat - HRP	Sc-2953	Santa Cruz	1:4,000
Anti-rabbit - Alexa 488	A11034	Invitrogen	1:800
Anti-mouse - Alexa 588	A11031	Invitrogen	1:800

antagonist muscle groups. To determine the MVC, the maximum strength level (N.m) achieved during the test was retained.

Muscle Biopsy

Skeletal muscle biopsies were performed before (pre), at the end (post), and 10 days after the end of the HDBR period (see **Figure 1**) from the vastus lateralis muscle according to a well-established method using a 5 mm Bergström biopsy needle under sterile conditions and local anesthesia (1% lidocaine). The three biopsies were obtained from the same leg of each subject (the right leg) as near each other as possible because of potential anatomical variations. For each biopsy, one piece was immediately embedded in a small silicone cast filled with a cryoprotectant (OCT, Sakura Finetek), immediately frozen in liquid nitrogen cooled isopentane, and stored at −80°C until further histological analysis. The other piece was rapidly frozen in liquid nitrogen and stored at −80°C for protein content quantification.

Cryosectioning and Immunohistochemistry

To determine cross-sectional area (CSA) and muscle fiber typing, transverse serial cross sections (10 μm thick) of vastus lateralis samples were obtained using a cryostat maintained at −25°C. The same methodology of Demangel et al. (2017) was used for CSA and MyHC (types I, II and IIa) labeling.

Protein Isolation and Western Blotting

Muscle samples were exactly treated as in the study of Pagano et al. (2018). For western blots, we present cropped images of a representative subject of each group.

Carbonylated Protein Determination

Determination of carbonylated protein levels was assessed by immunoblot detection of protein carbonyl groups using the "OxyBlot" protein oxidation kit (Millipore, MA, USA). Total protein carbonyls were quantified with the OxyBlot kit by densitometry of the blotting, relativized by the densitometry of the ponceau red staining of the membrane.

Antibodies

Primary and secondary antibodies used for western blot and immunohistochemistry are presented in **Table 1**, with their respective references and dilutions used.

Statistics

All values are expressed as the mean ± SEM, and the significance level was set at $p < 0.05$. The normal distribution of the samples was assessed by the Shapiro-Wilk test. To compare our two different groups and their different conditions (pre-post-recovery), we used a two-way repeated measure ANOVA associated with

the LSD *post-hoc* test allowing multiple paired comparisons. In the case of a non-normal distribution, we used a Friedman ANOVA. Statistical analysis was performed using Statistica and GraphPad Prism software, and all graphs were created with GraphPad Prism5 software.

RESULTS

Maximum Voluntary Contraction of the Lower Limb

Isometric maximum voluntary contractions represented as torques (N.m) were measured before (pre) and after (post) 2 months of bedrest to evaluate the changes in muscle strength. Torques measured in the knee extension mode were significantly higher in the placebo group at the baseline point compared to the cocktail group (258 versus 195 N.m). However, torques measured in the knee extension mode significantly decreased after the bedrest period in both groups (−32% for the placebo group and −33% for the cocktail group; **Figure 2A**). Torques measured in the ankle extension and flexion modes were equal at baseline in the two groups and significantly decreased after bedrest in both groups (−16 and −25% for the placebo group and −22 and −25% for the cocktail group, in flexion and extension mode, respectively; **Figure 2B**).

These results demonstrated that 2 months of bedrest induced a significant loss of lower limb muscle strength, which was not prevented by cocktail supplementation.

Myofiber Atrophy

Global (all fiber types) and specific fiber type cross-sectional areas (CSAs) were identified from biopsies of pre, post, and recovery conditions. The cocktail group demonstrated a significant decrease of −22.5% in muscle fiber CSA after bedrest (from 3,511 μm^2 before to 2,720 μm^2 after bedrest, $p < 0.01$), while the placebo group showed a −11.7% non-significant decrease (from 3,525 μm^2 before to 3,063 μm^2 after bedrest, $p = 0.08$) (**Figure 3A**). Although the degree of atrophy was higher in the cocktail group compared to the placebo group, this difference was not statistically significant. Looking at the variation of CSA of each specific fiber type (**Figure 3B**), we observed that every type of muscle fiber was atrophied in the cocktail group after 2 months of bedrest (−16, −17, and − 21% for types I, II, and IIa, respectively). For the placebo, a non-significant decrease was observed in all muscle fiber types. After 10 days of recovery, type I fibers of the cocktail group reached the same size observed at baseline, while type II and IIa fibers were still smaller compared to baseline. The fast fiber types (types II and IIa) were more affected and were not recovered at 10 days after bedrest.

These results highlighted that the cocktail was not able to prevent skeletal muscle atrophy. Moreover, subjects that were supplemented with the cocktail were even more affected by myofiber atrophy, particularly type II and IIa muscle fiber atrophy.

Changes in Myofiber Type Distribution

At baseline, the proportions of fibers expressing MyHC I, MyHC IIa, and MyHC IIx were equal in both groups. In the placebo group, 2 months of bedrest induced a significant decrease in the percentage of fibers expressing MyHC I (48 versus 40%; **Figure 4A**). The percentage of fibers expressing MyHC I was still significantly lower after 10 days of recovery compared to baseline. In the cocktail group, no changes in the proportion of type I fibers were observed after the bedrest period compared to baseline. However, we observed a higher proportion of type I fibers at the recovery point compared to the placebo group (56 versus 39%).

In both groups, no changes in the proportion of type IIa fibers were observed after the bed rest period compared to baseline (**Figure 4B**). However, in the placebo group, the proportion of fibers expressing MyHC IIa was significantly higher after 10 days of recovery compared to the end of the bedrest (post) (59 versus 41%) and compared to the values for the cocktail group (59 versus 40%).

Focusing on the fibers expressing MyHC IIx, we observed a dramatic increase in their proportion in the placebo group

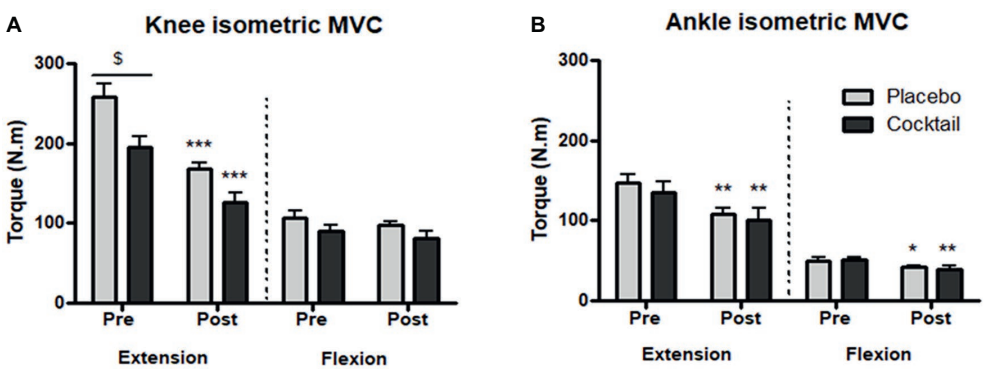

FIGURE 2 | Isometric maximal voluntary contraction (MVC) torques before and after the HDBR experiment: torques (N.m) generated during isometric MVC in **(A)** knee and **(B)** ankle extension and flexion positions. Data bars represent means ± SEM. *$p < 0.05$, **$p < 0.01$, ***$p < 0.001$: difference between time condition (pre vs. post). $^{\$}p < 0.05$: difference between groups (cocktail vs. placebo).

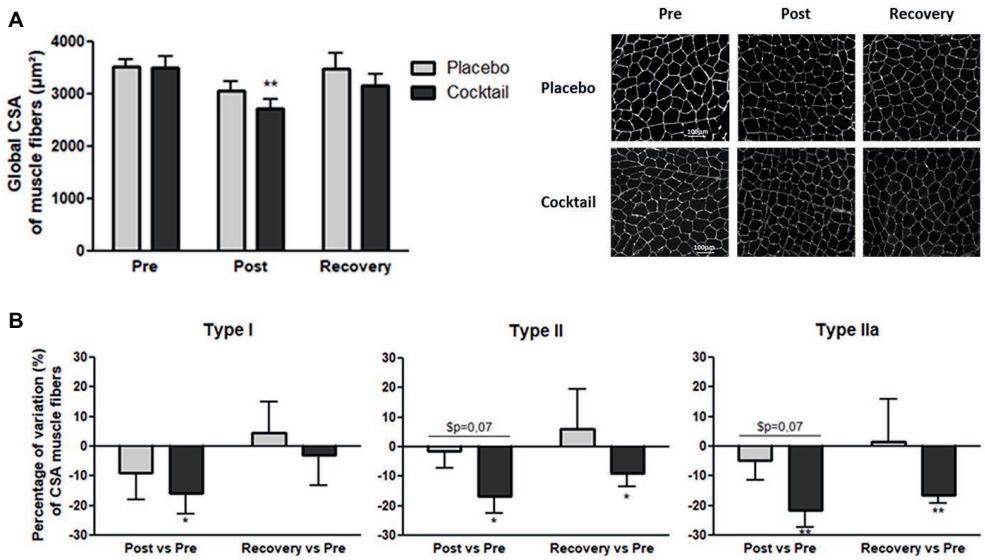

FIGURE 3 | Cross-sectional areas (CSAs) of muscle fibers from vastus lateralis biopsies: **(A)** global CSA of muscle fibers (µm²) before (pre), after (post), and 10 days after the end (recovery) of 2-months HDBR; **(B)** variation of CSA of Type I, Type II, and Type IIa muscle fibers, between different time conditions. Data bars represent means ± SEM. $^{*}p < 0.05$, $^{**}p < 0.01$: difference between time condition. $^{\$}$difference between group treatment (cocktail vs. placebo).

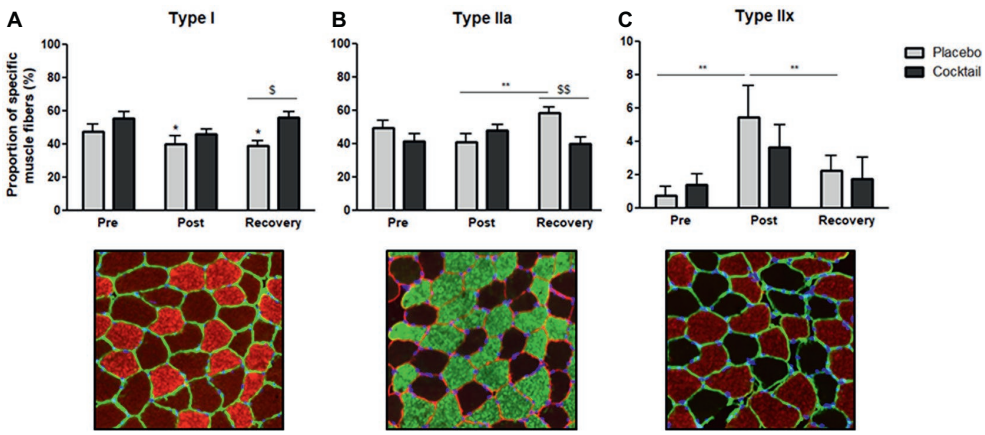

FIGURE 4 | Distribution (%) of muscle fibers in *vastus lateralis* samples, in the different time-points and conditions of the HDBR experiment: proportion of **(A)** Type I, **(B)** Type IIa and **(C)** Type IIx muscle fibers before (pre), after (post), and 10 days after the end (recovery) of 2-months HDBR. Data bars represent means ± SEM. $^{*}p < 0.05$, $^{**}p < 0.01$: difference between time condition. $^{\$}p < 0.05$, $^{\$\$}p < 0.01$: difference between group treatment (cocktail vs. placebo).

between the pre- and post-treatment conditions (0.8 versus 5.5%), which returned to basal values after a short recovery (**Figure 4C**). Conversely, in the placebo group, no changes were observed for the cocktail group during all experiments, which suggests a possible protective effect of the cocktail in the expression of IIx fibers.

The results indicate that prolonged inactivity modulates muscle typology, reducing some of the slow fibers (type I) for the benefit of fibers expressing MyHC IIx and that the cocktail is able to prevent this classical parameter observed in unloading and microgravity situations.

Oxidative Stress Parameters

To evaluate macromolecule ROS-induced damage, we analyzed the levels of 4-hydroxynonenal (4-HNE), a marker of lipid peroxidation, and the levels of carbonylated proteins. No significant change was observed during the experiment in either group for 4-HNE levels. However, 4-HNE levels tended to be increased in placebo subjects after bedrest but not in the cocktail group (**Figure 5A**). Levels of carbonylated proteins did not change after bed rest in the placebo group, while there was a significant decrease in the cocktail group (−19.7%, $p < 0.01$). In both groups, carbonylated protein levels were

significantly decreased after 10 days of recovery compared to baseline (**Figure 5B**).

To explain oxidative damage, we examined the expression of endogen antioxidant defense and measured glutathione peroxidase and catalase protein levels in muscles. No significant differences between groups or time conditions were found (**Figures 5C,D**). However, we observed the same trend for the two enzymes at the recovery y point: the placebo group had lower contents compared to the cocktail group.

These results underline a potential protector effect of cocktail supplementation regarding the oxidative damage in muscle, without impairment of antioxidant enzyme expression after 2 months of hypoactivity and 10 days of recovery.

Oxidative Metabolism Markers

To characterize changes in oxidative metabolism, we analyzed various mitochondrial parameters from vastus lateralis samples. In the cocktail group, two important markers of mitochondrial content, citrate synthase and COX IV, were significantly decreased after bedrest (pre versus post values) and were maintained at the same level after 10 days of recovery (**Figures 6A,B**). For placebo subjects, only citrate synthase protein levels were significantly decreased after bedrest (**Figure 6A**), while a trend to lower levels was observed for COX IV ($p = 0.12$) and cytochrome c ($p = 0.16$), (**Figures 6B,C**). However, cytochrome c protein levels were dramatically decreased after 10 days of recovery in the cocktail group, while values in the placebo group tended to increase (**Figure 6C**). PGC-1α protein levels, the master regulator of mitochondrial biogenesis, were also measured. No changes were observed after the bedrest period in either group. However, the cocktail group showed a drastic significant decrease in PGC-1α protein levels after 10 days of recovery (−61%; **Figure 6D**), while no changes were observed in the placebo group. Lower levels of both proteins were found in cocktail group samples at the recovery point and attested to a rapid loss of oxidative metabolism efficacy (**Figures 6C,D**).

Protein Balance Pathways

We evaluated changes in protein synthesis and degradation pathways under different conditions. We first analyzed markers of the main protein synthesis pathway regulated by mTOR. Levels of phosphorylated Pras40, whose phosphorylation by Akt permits the activation of mTORC1, were increased for the placebo group at the end of bedrest (+66%, $p < 0.05$; post) and 10 days after it (recovery) with respect to the pre values (+64%, $p < 0.05$). For the cocktail group, no changes were observed after bedrest, while a significant increase was observed at the recovery point compared to baseline (+127%, $p < 0.001$) and after bed rest (+72%, $p < 0.01$) (**Figure 7A**). This result demonstrates that mTORC1 is possibly more activated after the immobilization period. The result of phosphorylated 4E-BP1, an activator of elongation processes directly phosphorylated by mTORC1, showed no difference after bed rest in either group. However, a dramatic increase of phosphorylated 4E-BP1 was

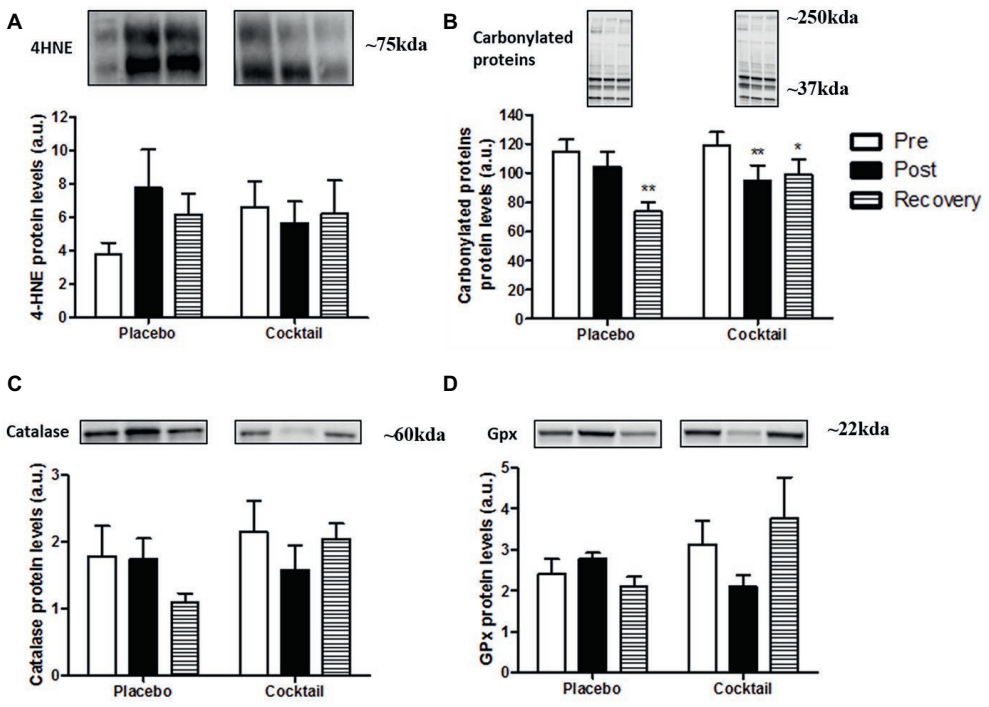

FIGURE 5 | Oxidative stress parameters in the different time-points and conditions of the HDBR experiment: **(A)** determination of oxidative damage to lipids using 4-hydroxynonenal and **(B)** carbonylated protein levels. Protein content of antioxidant enzymes, **(C)** glutathione peroxidase, and **(D)** catalase. Data bars represent means ± SEM. *$p < 0.05$, **$p < 0.01$: difference between time condition.

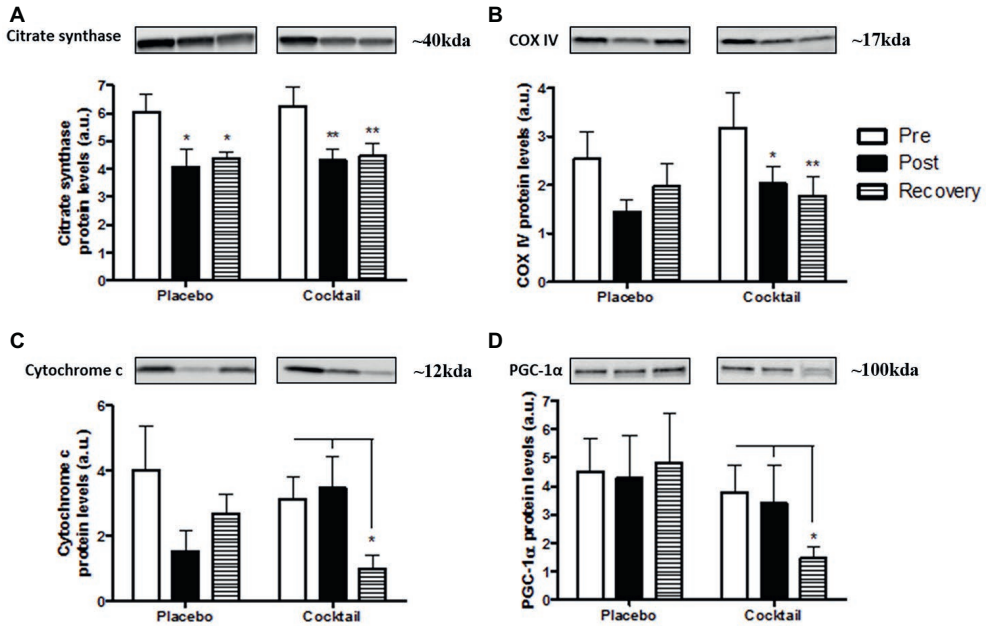

FIGURE 6 | Oxidative metabolism parameters in the different time-points and conditions of the HDBR experiment: determination of **(A)** citrate synthase; **(B)** COX IV; **(C)** cytochrome c, and **(D)** PGC1-α protein levels. Data bars represent means ± SEM. *$p < 0.05$, **$p < 0.01$: difference between time condition.

observed in the placebo group after 10 days of recovery compared to baseline and after bed rest ($p < 0.01$ in both cases). Such an increase was not observed in the cocktail group (**Figure 7B**). The phosphorylation of eIF2α, which is a subunit of the eIF2 initiation factor, has an inhibitory action on protein translation. Its content tended to decrease after bedrest in both groups, which means a lower inhibition of protein translation phenomenon after bedrest (**Figure 7C**). These results support the idea that after a long hypoactivity period, the protein synthesis pathway regulated by mTOR is impaired, while the recovery period is associated with the activation of this latter. However, activation during recovery appears to be impaired by the cocktail.

We studied three markers of the autophagic pathway, one of the main systems responsible for skeletal muscle mass regulation. ULK1, which is phosphorylated and inhibited by mTOR, is considered the first initiator of the autophagic process. No significant differences were observed between conditions and time (**Figure 7D**). However, the protein levels of two actors in autophagosome formation (latter stage of autophagy), ATG7 and LC3 (ratio of LC3 II/LC3 I), were higher at the recovery point with respect to pre- and post-treatment conditions in the placebo group (**Figures 7E,F**). These results suggest that the recovery period is associated with the activation of the autophagic process, which is inhibited by our cocktail.

DISCUSSION

The present study aimed to evaluate the effects of a dietary cocktail supplementation during 60 days of HDBR. It was hypothesized that the antioxidant and anti-inflammatory components of the cocktail would have a protective/preventive action against hypoactivity-induced muscle deconditioning.

After 2 months of HDBR, all subjects presented muscle deconditioning characterized at the functional level by a loss of muscle strength. Isometric MVC of quadriceps and triceps surae muscle groups were decreased in placebo (−32 and −21%, respectively) and cocktail subjects (−33 and −26%, respectively). Previous studies using the same protocol duration (60 days), longer duration (90 days) or shorter duration (28 days) found a loss of lower limb muscle strength (Zachwieja et al., 1999; Alkner and Tesch, 2004; Trappe et al., 2007; Kramer et al., 2017). Recently, using the dry immersion model of simulated microgravity, our research group showed that a few days of hypoactivity induced a decrease of 9% of MVC (Demangel et al., 2017). Concerning this first functional parameter, our results show no effects of cocktail supplementation on muscle strength loss.

It is known that inactivity-induced loss of force is the consequence of a variety of factors: atrophy of muscle cells (Chopard et al., 2009a,b), innervation deficiency (Kawakami et al., 2001), dysregulation of intracellular calcium machinery (Thom et al., 2001), and fatty infiltrations (Delmonico et al., 2009; Pagano et al., 2018). Among these elements, amyotrophy plays a predominant role. In our study, cocktail supplementation did not prevent muscle atrophy and even accentuated the decrease in muscle fiber CSA after 60 days of HDBR compared to the placebo group. Global CSA (−22%), as well as type II (−16% both) and type IIa (−21%), muscle fibers of supplemented subjects exhibited significant atrophy after bedrest. More particularly in this group, fast muscle fibers (type II) were more affected than slow fibers (type I). In humans, the literature has described that fast fibers may be more susceptible to

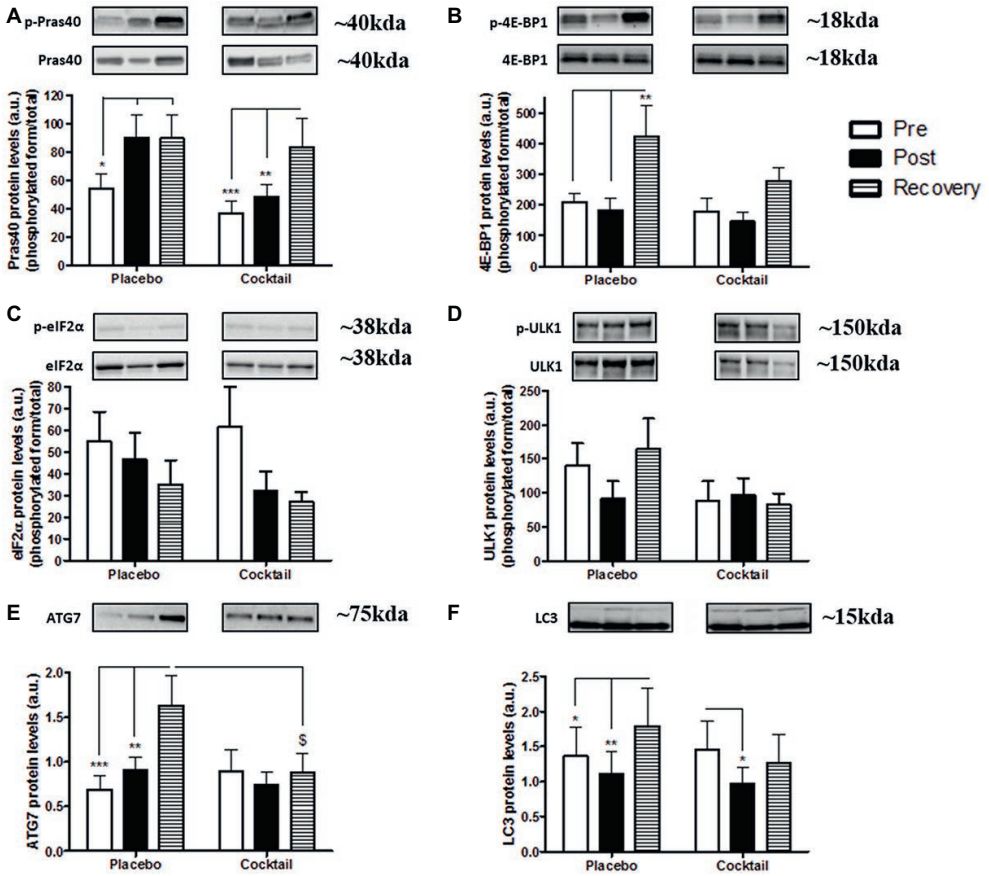

FIGURE 7 | Protein balance parameters in the different time-points and conditions of the HDBR experiment: determination of synthesis pathway markers, **(A)** Pras40; **(B)** 4E-BP1; **(C)** eIF2α and degradation pathway markers **(D)** ULK1; **(E)** ATG7; and **(F)** LC3 protein levels. Data bars represent means ± SEM. *$p < 0.05$, **$p < 0.01$: difference between time condition. $^{\$}p < 0.05$: difference between groups (cocktail vs. placebo) for the same time condition.

microgravity-induced atrophy than oxidative fibers (Edgerton et al., 1995; Widrick et al., 1999; Fitts et al., 2000). Muscle deconditioning is also characterized by changes in muscle fiber typology. In the present study, all subjects exhibited the same fiber type distribution before the experiment. However, 10 days after the end of HDBR (recovery), supplemented subjects presented a higher percentage of type I fibers to the detriment of type IIa (56% of type I and 40% of type IIa) compared to placebo subjects (39% of type I and 58% of type IIa). In the placebo group, the increase of IIx fiber proportion (+718%) after bedrest traduced the contractile properties modification induced by hypoactivity. Interestingly, cocktail supplementation seems to limit the expression of IIx fibers classically observed during muscle deconditioning. The same tendency was also described in human experiments. For example, Edgerton et al. (1995) reported a decrease from 48 to 40% of type I fibers after 11 days of spaceflight. In our study, placebo subjects exhibited the same rate of reduction (47.8% in pre vs. 40% in post condition). We can establish a comparison with the results of Desaphy et al. (2010) who evaluated the effects of antioxidant supplementation during a hindlimb suspension period in mice. The administration of Trolox, a vitamin E analog, was unable to protect disused muscles from atrophy but partially prevented the MHC isoform redistribution in soleus muscles of the supplemented animals. Regarding the loss of muscle mass, our findings are contrary to the initial hypothesis, i.e., a potential supplementation's protection against muscle wasting. Interestingly, although atrophy levels were higher in the cocktail group, the magnitude of strength loss was similar in both groups. This may indicate that antioxidant/anti-inflammatory supplementation would have reduced the relative part of other factors responsible for strength diminution. Extensive investigations are necessary to evaluate the role of every different factor in muscle strength loss contribution.

Situations of reduced activity are known to be sources of inflammation and cellular RONS production (Margaritis et al., 2009; Powers et al., 2011b). In the present study, we decided not to focus on inflammatory processes because of the lack of variation observed in the main marker of inflammation TNF-α in vastus lateralis (data not shown). In skeletal muscles, RONS induced damage to macromolecules such as lipids and proteins. Kondo et al. (1991) was the first study hypothesizing the contribution of redox disturbances to muscle atrophy and reported that prolonged inactivity was associated with high

levels of lipid peroxidation in rats. Here, after 60 days of HDBR, the 4-HNE marker representing lipid peroxidation tended to increase in the placebo group, whereas lower levels of carbonylated proteins were observed in the supplemented group. These results proved that supplementation appears to protect against RONS-induced damage. Nevertheless, these positive effects on macromolecules did not provide better protection against muscle atrophy. To explain this, we hypothesize that the cocktail could be too rich in antioxidants, and it would abolish the beneficial role of RONS. Indeed, minimal amounts of these molecules are necessary for the healthy function of various physiological processes. If RONS are present in large quantities, oxidative stress occurs, whereas the absence of RONS induces "reductive stress" (Narasimhan and Rajasekaran, 2015).

Our results highlight that an imbalance in favor of antioxidant molecules during a prolonged inactivity period could accentuate skeletal muscle wasting. This finding underlines the complexity of redox balance mechanisms and demonstrates that physiological amounts of RONS are essential to activate molecular pathways and preserve positive adaptations. Indeed, a number of studies, particularly in the exercise training context, described that over-supplementation with exogenous antioxidants impairs the molecular signaling required for cellular adaptations (Chang et al., 2007; Gomez-Cabrera et al., 2008; Ristow et al., 2009; Merry and Ristow, 2016).

On the other hand, a body of evidence revealed that prolonged muscle inactivity induces oxidative capacity alteration and mitochondrial dysfunction, leading to activation of atrophic pathways (Hyatt et al., 2019). The major regulator of mitochondrial biogenesis, PGC-1α, and various key mitochondrial proteins is known to be downregulated during muscle inactivity (Chen et al., 2007; Kang et al., 2013). Other studies also demonstrated that hypoactivity leads to oxidative metabolism gene downregulation in animals and in women during bedrest (Chopard et al., 2009a,b; Brocca et al., 2010). In our study, lower protein levels of citrate synthase and COX IV after HDBR indicated a decrease in the mitochondrial content in the skeletal muscles of all subjects. Moreover, 10 days of recovery were not sufficient to recover basal values. Similar results were observed in animals after 2 weeks of immobilization followed by 5 days of recovery (Kang et al., 2013). In addition, the drop of PGC-1α and cytochrome c levels in the recovery point was only observed for the cocktail group. This suggests that the oxidative metabolism of supplemented subjects was more affected than that of the placebo subjects. The sudden stop of antioxidant supplementation after 60 days certainly disturbed the molecular pathways involved in mitochondrial dynamics. This idea is in agreement with the study of Gomez-Cabrera et al. (2012), which indicates that antioxidant supplements were responsible for limited mitochondrial adaptations during aerobic training.

Research has long described that skeletal muscle hypoactivity causes a dysregulation of signaling pathways involved in muscle mass maintenance. Alterations of protein balance mechanisms occur at an early stage, from the first day of hypoactivity, and then tend to stabilize (Kawashima et al., 2004). Due to the long duration of our HDBR protocol, we especially wanted to evaluate the modulation of synthesis and degradation pathways in the days following remobilization. Analyses performed in the recovery point provided information regarding molecular dynamics occurring after long-term inactivity and envisage the rate of muscle recuperation. The PI3K-Akt-mTOR axis is the major pathway activating protein synthesis in skeletal muscle. Here, the elevation of Pras40 protein levels, whose phosphorylation by Akt activates the mTORC1 complex, and the increase of 4E-BP1 levels suggest an activation of the main synthesis pathway in the recovery period. This idea is strengthened by the reduction in eIF2α contents at the same time, knowing that its phosphorylation has an inhibitory action on protein translation. Data in the literature indicate that elevated RONS production can inhibit Akt/mTORC1 signaling (Powers et al., 2016). However, in our study, all subjects, supplemented or not, demonstrated the same dynamic. This indicates that the cocktail does not reduce muscle wasting recovery processes. Our results illustrate the same insight as that described by various studies focusing on antioxidant supplementation and strength training adaptations. All of these studies highlight that additional antioxidants (Vitamin C and/or E) may hamper the optimum activation of important hypertrophic pathways (Makanae et al., 2013; Paulsen et al., 2014; Bjørnsen et al., 2016; Dutra et al., 2018).

We also aimed to investigate the evolution of autophagy parameters. Indeed, autophagy is a major proteolytic pathway whose activation during inactivity accentuates muscle wasting. Numerous reports have evoked the potential of RONS to accelerate protein breakdown *via* this pathway (Navarro-Yepes et al., 2014; Pajares et al., 2015). The mechanisms by which RONS promote autophagy remain unclear, but they could increase ULK1 activity, the initiator of autophagy processes, through the downregulation of mTORC1. In the present study, although no significant differences in ULK1 activation were observed between conditions, and the levels of ATG7 and LC3II/LC3I ratio were significantly higher at recovery points compared with pre- and post-conditions for placebo subjects. These results indicate an increase in key autophagy components after remobilization, but this evolution was not observed in the supplemented subjects. Moreover, the absence of a difference between post- and pre-conditions underlined that autophagy flux was not overstimulated after 2 months of inactivity. If muscle wasting is partly due to an increase of protein degradation pathways, this was not perceptible after such a long time and was certainly detectable in the first days of immobilization. Here, cocktail supplementation seems to abolish autophagy dynamics in skeletal muscle remobilization. At present, there is still a lack of literature available regarding antioxidants and muscle autophagy pathways, but we infer that a dysregulation in favor of pro-oxidants may blunt some molecular mechanisms responsible for the control and the recovery of muscle mass. Further investigations are needed to distinguish the role of exogenous intake of antioxidants on these pathways during immobilization, especially its impact on subsequent recovery.

Previous cited studies showing signaling pathways disturbance using antioxidants were done with direct RONS scavengers (Vitamin C and E) with relative high doses. Similar results have been recently obtained during aerobic adaptations to cycling training in humans with epicatechin, a flavonol which can modulate superoxide dismutase and glutathione peroxidase and activate antioxidant gene such as PGC-1α (Schwarz et al., 2018).

In this study, the dose of epicatechin was very low compared to our study since only 200 mg per day were used. Moreover, it is important to underline that in our present study, the dose of the cocktail's components was the same for each individual, independently of their specific needs. These results show that regardless of the type of antioxidant used alone or combined, if the dose is not personalized, the effects may not be beneficial. Recently, the group of Paschalis et al. published two interesting studies which highlight the importance of adapting antioxidant supplementation to the personalized requirements of the subjects. In these studies, vitamin C and N-acetyl-cysteine (a glutathione precursor) were used alone with individualized doses in regard to blood vitamin C and glutathione levels, respectively. Beneficial effects (increase of maximal oxygen uptake and/or maximal power) were obtained only in people with low blood vitamin C or glutathione levels. These results showed that the effectiveness of antioxidant supplementation largely depends on the redox status of the subjects receiving the treatment (Paschalis et al., 2016, 2018). In our cocktail, vitamin E acts as a RONS scavenger without a specific action. Some studies using Allopurinol, an inhibitor of xanthine oxidase (a major RONS sources during muscle unloading), showed limitation of muscle atrophy in hindlimb suspended rodents and in humans with ankle sprain (Derbré et al., 2014; Ferrando et al., 2018). Compared to our cocktail which does not act on a specific RONS source or RONS family involved during muscle unloading, these studies highlight the importance of choosing an antioxidant strategy with a specific action corresponding to the need of the subject situation (inactivity, aging, microgravity,…). Finally, in the future, antioxidant strategies should be personalized based on the redox status of each subject and should be chosen in function of their action on RONS source and/or RONS family.

CONCLUSIONS

In aerospace applications, understanding muscle deconditioning mechanisms induced by microgravity environments constitutes an essential issue. The results obtained through these studies are also validated in the context of muscle deconditioning prevention, for clinical hospitalization, immobilization post injuries, or more generally chronic hypoactivity. Experimental models provide the opportunity to test countermeasures and strategies and to evaluate their effects on disuse-induced atrophy. Physical exercise is the main intervention that demonstrated positive effects (Fitts et al., 2010; Gao et al., 2018), and some studies combined it with protein or growth factor supplementation (Allen et al., 1997; Brooks et al., 2008). Despite its benefits, exercise training seems insufficient to limit muscle wasting in prolonged hypoactivity periods, and research of an efficient and feasible countermeasure including nutritional intervention is still in progress. The present study was conducted to evaluate the effects of a cocktail enriched in antioxidant/anti-inflammatory molecules in a 2-month HDBR experiment. This countermeasure was expected to limit the effects of muscle deconditioning, but our results clearly demonstrate the ineffectiveness of supplementation in the prevention of muscle mass and strength loss. Moreover, data regarding muscle molecular mechanisms highlight an alteration of recovery processes in the supplemented subjects.

These results can be explained by an inhibition of the beneficial adaptations induced by the presence of RONS and illustrate the necessity of pro-oxidant molecules during long-term inactivity to maintain a certain level of muscle function.

Our conclusions underline the complexity of redox mechanisms and raise interrogations regarding the appropriate nutritional intervention to fight against muscle deconditioning.

DATA AVAILABILITY STATEMENT

The datasets generated for this study are available on request to the corresponding author.

ETHICS STATEMENT

The studies involving human participants were reviewed and approved by CPP Sud-Ouest et Outre-Mer I, France, number ID RCB: 2016-A00401–50. The patients/participants provided their written informed consent to participate in this study.

AUTHOR CONTRIBUTIONS

CA-C, GP, TF, TB, SB, and AC helped in conceptualization and methodology. CA-C, GP, TF, TB, and AC helped in formal analysis, writing original draft preparation, and visualization. CA-C, TB, TF, RR, RD, PD, and AP helped in investigation. DB, MS, M-CG-C, and JV helped in finding resources. CA-C, TF, TB, and GP helped in data curation. CA-C, TB, AC, SB, BJ, MS, M-CG-C, and JV helped in supervision. CA-C, GP, TB, and AC helped in project administration and writing—review and editing. GP, BJ, DB, TB, and AC helped in funding acquisition. All authors read and approved the final manuscript.

FUNDING

This study was funded by The Centre National d'Etudes Spatiales (CNES), Canadian Space Agency (BJ), and by DLR Grant #50WB1121-1421.

ACKNOWLEDGMENTS

We would particularly like to thank all the staff working in the Institute of Space Medicine and Physiology (Medes-IMPS) in Toulouse for having organized and carried out these experiments and especially Marie-Pierre Bareille and Arnaud Beck. We thank Professors Jacques Mercier and Maurice Hayot for their excellent biopsy procedures. We thank Jens Fielitz for the acceptance of sharing the recovery biopsies. We thank Biocampus and RHEM platform for technical support and expertise relating histological image analysis. A special thanks to the subjects for their participation in this project.

REFERENCES

Alkner, B. A., and Tesch, P. A. (2004). Knee extensor and plantar flexor muscle size and function following 90 days of bed rest with or without resistance exercise. *Eur. J. Appl. Physiol.* 93, 294–305. doi: 10.1007/s00421-004-1172-8

Allen, D. L., Linderman, J. K., Roy, R. R., Grindeland, R. E., Mukku, V., and Reggie Edgerton, V. (1997). Growth hormone/IGF-I and/or resistive exercise maintains myonuclear number in hindlimb unweighted muscles. *J. Appl. Physiol.* 83, 1857–1861. doi: 10.1152/jappl.1997.83.6.1857

Alway, S. E., Bennett, B. T., Wilson, J. C., Sperringer, J., Mohamed, J. S., Edens, N. K., et al. (1985). Green tea extract attenuates muscle loss and improves muscle function during disuse, but fails to improve muscle recovery following unloading in aged rats. *J. Appl. Physiol.* 118, 319–330. doi: 10.1152/japplphysiol.00674.2014

Baldwin, K. M., Haddad, F., Pandorf, C. E., Roy, R. R., and Edgerton, V. R. (2013). Alterations in muscle mass and contractile phenotype in response to unloading models: role of transcriptional/pretranslational mechanisms. *Front. Physiol.* 4:284. doi: 10.3389/fphys.2013.00284

Beytut, E., Yilmaz, S., Aksakal, M., and Polat, S. (2018). The possible protective effects of vitamin E and selenium administration in oxidative stress caused by high doses of glucocorticoid administration in the brain of rats. *J. Trace Elem. Med. Biol.* 45, 131–135. doi: 10.1016/j.jtemb.2017.10.005

Bjørnsen, T., Salvesen, S., Berntsen, S., Hetlelid, K. J., Stea, T. H., Lohne-Seiler, H., et al. (2016). Vitamin C and E supplementation blunts increases in total lean body mass in elderly men after strength training. *Scand. J. Med. Sci. Sports* 26, 755–763. doi: 10.1111/sms.12506

Brioche, T., Pagano, A. F., Py, G., and Chopard, A. (2016). Muscle wasting and aging: experimental models, fatty infiltrations, and prevention. *Mol. Asp. Med.* 50, 56–87. doi: 10.1016/j.mam.2016.04.006

Brocca, L., Pellegrino, M. A., Desaphy, J.-F., Pierno, S., Camerino, D. C., and Bottinelli, R. (2010). Is oxidative stress a cause or consequence of disuse muscle atrophy in mice? A proteomic approach in hindlimb-unloaded mice. *Exp. Physiol.* 95, 331–350. doi: 10.1113/expphysiol.2009.050245

Brooks, N., Cloutier, G. J., Cadena, S. M., Layne, J. E., Nelsen, C. A., Freed, A. M., et al. (2008). Resistance training and timed essential amino acids protect against the loss of muscle mass and strength during 28 days of bed rest and energy deficit. *J. Appl. Physiol.* 105, 241–248. doi: 10.1152/japplphysiol.01346.2007

Chang, C.-K., Huang, H.-Y., Tseng, H.-F., Hsuuw, Y.-D., and Tso, T. K. (2007). Interaction of vitamin E and exercise training on oxidative stress and antioxidant enzyme activities in rat skeletal muscles. *J. Nutr. Biochem.* 18, 39–45. doi: 10.1016/j.jnutbio.2006.02.007

Chen, C.-M., Wu, Y.-R., Cheng, M.-L., Liu, J.-L., Lee, Y.-M., Lee, P.-W., et al. (2007). Increased oxidative damage and mitochondrial abnormalities in the peripheral blood of Huntington's disease patients. *Biochem. Biophys. Res. Commun.* 359, 335–340. doi: 10.1016/j.bbrc.2007.05.093

Chopard, A., Hillock, S., and Jasmin, B. J. (2009a). Molecular events and signalling pathways involved in skeletal muscle disuse-induced atrophy and the impact of countermeasures. *J. Cell. Mol. Med.* 13, 3032–3050. doi: 10.1111/j.1582-4934.2009.00864.x

Chopard, A., Lecunff, M., Danger, R., Lamirault, G., Bihouee, A., Teusan, R., et al. (2009b). Large-scale MRNA analysis of female skeletal muscles during 60 days of bed rest with and without exercise or dietary protein supplementation as countermeasures. *Physiol. Genomics* 38, 291–302. doi: 10.1152/physiolgenomics.00036.2009

Damiot, A., Demangel, R., Noone, J., Chery, I., Zahariev, A., Normand, S., et al. (2019). A nutrient cocktail prevents lipid metabolism alterations induced by 20 days of daily steps reduction and fructose overfeeding: result from a randomized study. *J. Appl. Physiol.* 126, 88–101. doi: 10.1152/japplphysiol.00018.2018

Degens, H., and Alway, S. E. (2006). Control of muscle size during disuse, disease, and aging. *Int. J. Sports Med.* 27, 94–99. doi: 10.1055/s-2005-837571

Delmonico, M. J., Harris, T. B., Visser, M., Park, S. W., Conroy, M. B., Velasquez-Mieyer, P., et al. (2009). Longitudinal study of muscle strength, quality, and adipose tissue infiltration. *Am. J. Clin. Nutr.* 90, 1579–1585. doi: 10.3945/ajcn.2009.28047

Demangel, R., Treffel, L., Py, G., Brioche, T., Pagano, A. F., Bareille, M. P., et al. (2017). Early structural and functional signature of 3-day human skeletal muscle disuse using the dry immersion model. *J. Physiol.* 595, 4301–4315. doi: 10.1113/JP273895

Derbré, F., Assi, M., Lefeuvre-Orfila, L., Vincent, S., Chevalier, M., Gueritat, J., et al. (2014). Antioxidants and muscle atrophy in colon cancer: beneficial or deleterious effects? *Free Radic. Biol. Med.* 75(Suppl. 1), S22. doi: 10.1016/j.freeradbiomed.2014.10.735

Desaphy, J.-F., Pierno, S., Liantonio, A., Giannuzzi, V., Digennaro, C., Dinardo, M. M., et al. (2010). Antioxidant treatment of hindlimb-unloaded mouse counteracts fiber type transition but not atrophy of disused muscles. *Pharmacol. Res.* 61, 553–563. doi: 10.1016/j.phrs.2010.01.012

Dutra, M. T., Alex, S., Mota, M. R., Sales, N. B., Brown, L. E., and Bottaro, M. (2018). Effect of strength training combined with antioxidant supplementation on muscular performance. *Appl. Physiol. Nutr. Metab.* 43, 775–781. doi: 10.1139/apnm-2017-0866

Edgerton, V. R., Zhou, M. Y., Ohira, Y., Klitgaard, H., Jiang, B., Bell, G., et al. (1995). Human fiber size and enzymatic properties after 5 and 11 days of spaceflight. *J. Appl. Physiol.* 78, 1733–1739. doi: 10.1152/jappl.1995.78.5.1733

Ferrando, B., Gomez-Cabrera, M. C., Salvador-Pascual, A., Puchades, C., Derbré, F., Gratas-Delamarche, A., et al. (2018). Allopurinol partially prevents disuse muscle atrophy in mice and humans. *Sci. Rep.* 8:3549. doi: 10.1038/s41598-018-21552-1

Fitts, R. H., Riley, D. R., and Widrick, J. J. (2000). Physiology of a microgravity environment invited review: microgravity and skeletal muscle. *J. Appl. Physiol.* 89, 823–839. doi: 10.1152/jappl.2000.89.2.823

Fitts, R. H., Trappe, S. W., Costill, D. L., Gallagher, P. M., Creer, A. C., Colloton, P. A., et al. (2010). Prolonged space flight-induced alterations in the structure and function of human skeletal muscle fibres. *J. Physiol.* 588, 3567–3592. doi: 10.1113/jphysiol.2010.188508

Flohé, L., Brigelius-Flohé, R., Saliou, C., Traber, M. G., and Packer, L. (1997). Redox regulation of NF-Kappa B activation. *Free Radic. Biol. Med.* 22, 1115–1126. doi: 10.1016/S0891-5849(96)00501-1

Gao, Y., Arfat, Y., Wang, H., and Goswami, N. (2018). Muscle atrophy induced by mechanical unloading: mechanisms and potential countermeasures. *Front. Physiol.* 9:235. doi: 10.3389/fphys.2018.00235

Glass, D. J. (2005). Skeletal muscle hypertrophy and atrophy signaling pathways. *Int. J. Biochem. Cell Biol.* 37, 1974–1984. doi: 10.1016/j.biocel.2005.04.018

Gomez-Cabrera, M.-C., Domenech, E., Romagnoli, M., Arduini, A., Borras, C., Pallardo, F. V., et al. (2008). Oral administration of vitamin C decreases muscle mitochondrial biogenesis and Hampers training-induced adaptations in endurance performance. *Am. J. Clin. Nutr.* 87, 142–149. doi: 10.1093/ajcn/87.1.142

Gomez-Cabrera, M. C., Ferrando, B., Brioche, T., Sanchis-Gomar, F., and Viña, J. (2013). Exercise and antioxidant supplements in the elderly. *J. Sport Health Sci.* 2, 94–100. doi: 10.1016/j.jshs.2013.03.007

Gomez-Cabrera, M. C., Ristow, M., and Viña, J. (2012). Antioxidant supplements in exercise: worse than useless? *Am. J. Physiol. Endocrinol. Metab.* 302, E476–E477. doi: 10.1152/ajpendo.00567.2011

Hargens, A. R., and Vico, L. (2016). Long-duration bed rest as an analog to microgravity. *J. Appl. Physiol.* 120, 891–903. doi: 10.1152/japplphysiol.00935.2015

Harridge, S. D. (2007). Plasticity of human skeletal muscle: gene expression to in vivo function. *Exp. Physiol.* 92, 783–797. doi: 10.1113/expphysiol.2006.036525

Hodson, L., Bhatia, L., Scorletti, E., Smith, D. E., Jackson, N. C., Shojaee-Moradie, F., et al. (2017). Docosahexaenoic acid enrichment in NAFLD is associated with improvements in hepatic metabolism and hepatic insulin sensitivity: a pilot study. *Eur. J. Clin. Nutr.* 71, 973–979. doi: 10.1038/ejcn.2017.9

Huey, K. A., Fiscus, G., Richwine, A. F., Johnson, R. W., and Meador, B. M. (2008). In vivo vitamin E administration attenuates interleukin-6 and interleukin-1beta responses to an acute inflammatory insult in mouse skeletal and cardiac muscle. *Exp. Physiol.* 93, 1263–1272. doi: 10.1113/expphysiol.2008.043190

Hyatt, H., Deminice, R., Yoshihara, T., and Powers, S. K. (2019). Mitochondrial dysfunction induces muscle atrophy during prolonged inactivity: a review of the causes and effects. *Arch. Biochem. Biophys.* 662, 49–60. doi: 10.1016/j.abb.2018.11.005

Jackman, R. W., and Kandarian, S. C. (2004). The molecular basis of skeletal muscle atrophy. *Am. J. Phys. Cell Phys.* 287, C834–C843. doi: 10.1152/ajpcell.00579.2003

Jeromson, S., Gallagher, I. J., Galloway, S. D. R., and Hamilton, D. L. (2015). Omega-3 fatty acids and skeletal muscle health. *Mar. Drugs* 13, 6977–7004. doi: 10.3390/md13116977

Kandarian, S. C., and Stevenson, E. J. (2002). Molecular events in skeletal muscle during disuse atrophy. *Exerc. Sport Sci. Rev.* 30, 111–116. doi: 10.1097/00003677-200207000-00004

Kang, C., Chung, E., Diffee, G., and Ji, L. L. (2013). Exercise training attenuates aging-associated mitochondrial dysfunction in rat skeletal muscle: role of PGC-1α. *Exp. Gerontol.* 48, 1343–1350. doi: 10.1016/j.exger.2013.08.004

Kawakami, Y., Akima, H., Kubo, K., Muraoka, Y., Hasegawa, H., Kouzaki, M., et al. (2001). Changes in muscle size, architecture, and neural activation after 20 days of bed rest with and without resistance exercise. *Eur. J. Appl. Physiol.* 84, 7–12. doi: 10.1007/s004210000330

Kawashima, S., Akima, H., Kuno, S. Y., Gunji, A., and Fukunaga, T. (2004). Human adductor muscles atrophy after short duration of unweighting. *Eur. J. Appl. Physiol.* 92, 602–605. doi: 10.1007/s00421-004-1184-4

Khor, S. C., Abdul Karim, N., Ngah, W. Z., Yusof, Y. A., and Makpol, S. (2014). Vitamin E in sarcopenia: current evidences on its role in prevention and treatment. *Oxidative Med. Cell. Longev.* 2014:914853. doi: 10.1155/2014/914853

Kondo, H., Miura, M., and Itokawa, Y. (1991). Oxidative stress in skeletal muscle atrophied by immobilization. *Acta Physiol. Scand.* 142, 527–528. doi: 10.1111/j.1748-1716.1991.tb09191.x

Kramer, A., Kümmel, J., Mulder, E., Gollhofer, A., Frings-Meuthen, P., and Gruber, M. (2017). High-intensity jump training is tolerated during 60 days of bed rest and is very effective in preserving leg power and lean body mass: an overview of the Cologne RSL study. *PLoS One* 12:e0169793. doi: 10.1371/journal.pone.0169793

Lambert, K., Coisy-Quivy, M., Bisbal, C., Sirvent, P., Hugon, G., Mercier, J., et al. (2015). Grape polyphenols supplementation reduces muscle atrophy in a mouse model of chronic inflammation. *Nutrition* 31, 1275–1283. doi: 10.1016/j.nut.2015.04.022

Li, N., and Karin, M. (1999). Is NF-KappaB the sensor of oxidative stress? *FASEB J.* 13, 1137–1143. Available at: http://www.ncbi.nlm.nih.gov/pubmed/10385605

Makanae, Y., Kawada, S., Sasaki, K., Nakazato, K., and Ishii, N. (2013). Vitamin C administration attenuates overload-induced skeletal muscle hypertrophy in rats. *Acta Physiol.* 208, 57–65. doi: 10.1111/apha.12042

Manach, C., Williamson, G., Morand, C., Scalbert, A., and Rémésy, C. (2005). Bioavailability and bioefficacy of polyphenols in humans. I. Review of 97 bioavailability studies. *Am. J. Clin. Nutr.* 81, 230S–242S. doi: 10.1093/ajcn/81.1.230S

Margaritis, I., Rousseau, A. S., Marini, J. F., and Chopard, A. (2009). Does antioxidant system adaptive response alleviate related oxidative damage with long term bed rest? *Clin. Biochem.* 42, 371–379. doi: 10.1016/J.CLINBIOCHEM.2008.10.026

Meador, B. M., Mirza, K. A., Tian, M., Skelding, M. B., Reaves, L. A., Edens, N. K., et al. (2015). The green tea polyphenol epigallocatechin-3-gallate (EGCg) attenuates skeletal muscle atrophy in a rat model of sarcopenia. *J. Frailty Aging* 4, 209–215. doi: 10.14283/jfa.2015.58

Merry, T. L., and Ristow, M. (2016). Do antioxidant supplements interfere with skeletal muscle adaptation to exercise training? *J. Physiol.* 594, 5135–5147. doi: 10.1113/JP270654

Momken, I., Stevens, L., Bergouignan, A., Desplanches, D., Rudwill, F., Chery, I., et al. (2011). Resveratrol prevents the wasting disorders of mechanical unloading by acting as a physical exercise mimetic in the rat. *FASEB J.* 25, 3646–3660. doi: 10.1096/fj.10-177295

Mukai, R., Matsui, N., Fujikura, Y., Matsumoto, N., Hou, D. X., Kanzaki, N., et al. (2016). Preventive effect of dietary quercetin on disuse muscle atrophy by targeting mitochondria in denervated mice. *J. Nutr. Biochem.* 31, 67–76. doi: 10.1016/j.jnutbio.2016.02.001

Murphy, M. P. (2009). How mitochondria produce reactive oxygen species. *Biochem. J.* 417, 1–13. doi: 10.1042/BJ20081386

Myburgh, K. H. (2014). Polyphenol supplementation: benefits for exercise performance or oxidative stress? *Sports Med.* 44(S1), 57–70. doi: 10.1007/s40279-014-0151-4

Narasimhan, M., and Rajasekaran, N. S. (2015). Reductive potential - a savior turns stressor in protein aggregation cardiomyopathy. *Biochim. Biophys. Acta* 1852, 53–60. doi: 10.1016/j.bbadis.2014.11.010

Navarro-Yepes, J., Burns, M., Anandhan, A., Khalimonchuk, O., del Razo, L. M., Quintanilla-Vega, B., et al. (2014). Oxidative stress, redox signaling, and autophagy: cell death versus survival. *Antioxid. Redox Signal.* 21, 66–85. doi: 10.1089/ars.2014.5837

Ng, T. W. K., Ooi, E. M. M., Watts, G. F., Chan, D. C., and Barrett, P. H. R. (2014). Atorvastatin plus Omega-3 fatty acid ethyl ester decreases very-low-density lipoprotein triglyceride production in insulin resistant obese men. *Diabetes. Obes. Metab.* 16, 519–526. doi: 10.1111/dom.12243

Pagano, A. F., Brioche, T., Arc-Chagnaud, C., Demangel, R., Chopard, A., and Py, G. (2018). Short-term disuse promotes fatty acid infiltration into skeletal muscle. *J. Cachexia. Sarcopenia Muscle* 9, 335–347. doi: 10.1002/jcsm.12259

Pajares, M., Jiménez-Moreno, N., Dias, I. H. K., Debelec, B., Vucetic, M., Fladmark, K. E., et al. (2015). Redox control of protein degradation. *Redox Biol.* 6, 409–420. doi: 10.1016/j.redox.2015.07.003

Paschalis, V., Theodorou, A. A., Kyparos, A., Dipla, K., Zafeiridis, A., Panayiotou, G., et al. (2016). Low vitamin C values are linked with decreased physical performance and increased oxidative stress: reversal by vitamin C supplementation. *Eur. J. Nutr.* 55, 45–53. doi: 10.1007/s00394-014-0821-x

Paschalis, V., Theodorou, A. A., Margaritelis, N. V., Kyparos, A., and Nikolaidis, M. G. (2018). N-acetylcysteine supplementation increases exercise performance and reduces oxidative stress only in individuals with low levels of glutathione. *Free Radic. Biol. Med.* 115, 288–297. doi: 10.1016/j.freeradbiomed.2017.12.007

Passerieux, E., Hayot, M., Jaussent, A., Carnac, G., Gouzi, F., Pillard, F., et al. (2015). Effects of vitamin C, vitamin E, zinc gluconate, and selenomethionine supplementation on muscle function and oxidative stress biomarkers in patients with facioscapulohumeral dystrophy: a double-blind randomized controlled clinical trial. *Free Radic. Biol. Med.* 81, 158–169. doi: 10.1016/j.freeradbiomed.2014.09.014

Paulsen, G., Hamarsland, H., Cumming, K. T., Johansen, R. E., Hulmi, J. J., Børsheim, E., et al. (2014). Vitamin C and E supplementation alters protein signalling after a strength training session, but not muscle growth during 10 weeks of training. *J. Physiol.* 592, 5391–5408. doi: 10.1113/jphysiol.2014.279950

Pavy-Le Traon, A., Heer, M., Narici, M. V., Rittweger, J., and Vernikos, J. (2007). From space to earth: advances in human physiology from 20 years of bed rest studies (1986-2006). *Eur. J. Appl. Physiol.* 101, 143–194. doi: 10.1007/s00421-007-0474-z

Powers, S. K., Ji, L. L., Kavazis, A. N., and Jackson, M. J. (2011a). Reactive oxygen species: impact on skeletal muscle. *Compr. Physiol.* 1, 941–969. doi: 10.1002/cphy.c100054

Powers, S. K., Morton, A. B., Ahn, B., and Smuder, A. J. (2016). Redox control of skeletal muscle atrophy. *Free Radic. Biol. Med.* 98, 208–217. doi: 10.1016/j.freeradbiomed.2016.02.021

Powers, S. K., Smuder, A. J., and Criswell, D. S. (2011b). Mechanistic links between oxidative stress and disuse muscle atrophy. *Antioxid. Redox Signal.* 15, 2519–2528. doi: 10.1089/ars.2011.3973

Reid, M. B., Khawli, F. A., and Moody, M. R. (1993). Reactive oxygen in skeletal muscle. III. Contractility of unfatigued muscle. *J. Appl. Physiol.* 75, 1081–1087. doi: 10.1152/jappl.1993.75.3.1081

Ristow, M., Zarse, K., Oberbach, A., Klöting, N., Birringer, M., Kiehntopf, M., et al. (2009). Antioxidants prevent health-promoting effects of physical exercise in humans. *Proc. Natl. Acad. Sci. USA* 106, 8665–8670. doi: 10.1073/pnas.0903485106

Salanova, M., Schiffl, G., Gutsmann, M., Felsenberg, D., Furlan, S., Volpe, P., et al. (2013). Nitrosative stress in human skeletal muscle attenuated by exercise countermeasure after chronic disuse. *Redox Biol.* 1, 514–526. doi: 10.1016/j.redox.2013.10.006

Schwarz, N. A., Blahnik, Z. J., Prahadeeswaran, S., McKinley-Barnard, S. K., Holden, S. L., and Waldhelm, A. (2018). (−)-Epicatechin supplementation inhibits aerobic adaptations to cycling exercise in humans. *Front. Nutr.* 5:132. doi: 10.3389/fnut.2018.00132

Servais, S., Letexier, D., Favier, R., Duchamp, C., and Desplanches, D. (2007). Prevention of unloading-induced atrophy by vitamin E supplementation: links between oxidative stress and soleus muscle proteolysis? *Free Radic. Biol. Med.* 42, 627–635. doi: 10.1016/j.freeradbiomed.2006.12.001

Sies, H. (2017). Hydrogen peroxide as a central redox signaling molecule in physiological oxidative stress: oxidative eustress. *Redox Biol.* 11, 613–619. doi: 10.1016/j.redox.2016.12.035

Smith, G. I., Atherton, P., Reeds, D. N., Mohammed, B. S., Rankin, D., Rennie, M. J., et al (2011a). Omega-3 polyunsaturated fatty acids augment the muscle protein anabolic response to hyperinsulinaemia-hyperaminoacidaemia in healthy young and middle-aged men and women. *Clin. Sci.* 121, 267–278. doi: 10.1042/CS20100597

Smith, G. I., Atherton, P., Reeds, D. N., Mohammed, B. S., Rankin, D., Rennie, M. J., et al. (2011b). Dietary omega-3 fatty acid supplementation increases the rate of muscle protein synthesis in older adults: a randomized controlled trial. *Am. J. Clin. Nutr.* 93, 402–412. doi: 10.3945/ajcn.110.005611

Somerville, V., Bringans, C., and Braakhuis, A. (2017). Polyphenols and performance: a systematic review and meta-analysis. *Sports Med.* 47, 1589–1599. doi: 10.1007/s40279-017-0675-5

Stamler, J. S., and Meissner, G. (2001). Physiology of nitric oxide in skeletal muscle. *Physiol. Rev.* 81, 209–237. doi: 10.1152/physrev.2001.81.1.209

Thom, J. M., Thompson, M. W., Ruell, P. A., Bryant, G. J., Fonda, J. S., Harmer, A. R., et al. (2001). Effect of 10-day cast immobilization on sarcoplasmic reticulum calcium regulation in humans. *Acta Physiol. Scand.* 172, 141–147. doi: 10.1046/j.1365-201X.2001.00853.x

Trappe, T. A., Burd, N. A., Louis, E. S., Lee, G. A., and Trappe, S. W. (2007). Influence of concurrent exercise or nutrition countermeasures on thigh and calf muscle size and function during 60 days of bed rest in women. *Acta Physiol.* 191, 147–159. doi: 10.1111/j.1748-1716.2007.01728.x

Ventadour, S., and Attaix, D. (2006). Mechanisms of skeletal muscle atrophy. *Curr. Opin. Rheumatol.* 18, 631–635. doi: 10.1097/01.bor.0000245731.25383.de

Widrick, J. J., Knuth, S. T., Norenberg, K. M., Romatowski, J. G., Bain, J. L., Riley, D. A., et al. (1999). Effect of a 17 day spaceflight on contractile properties of human soleus muscle fibres. *J. Physiol.* 516, 915–930. doi: 10.1111/j.1469-7793.1999.0915u.x

You, J.-S., Park, M.-N., Song, W., and Lee, Y.-S. (2010). Dietary fish oil alleviates soleus atrophy during immobilization in association with Akt signaling to P70s6k and E3 ubiquitin ligases in rats. *Appl. Physiol. Nutr. Metab.* 35, 310–318. doi: 10.1139/H10-022

Zachwieja, J. J., Smith, S. R., Lovejoy, J. C., Rood, J. C., Windhauser, M. M., and Bray, G. A. (1999). Testosterone administration preserves protein balance but not muscle strength during 28 days of bed rest. *J. Clin. Endocrinol. Metabol.* 84, 207–212. doi: 10.1210/jcem.84.1.5420

Zerba, E., Komorowski, T. E., and Faulkner, J. A. (1990). Free radical injury to skeletal muscles of young, adult, and old mice. *Am. J. Phys. Cell Phys.* 258, C429–C435. doi: 10.1152/ajpcell.1990.258.3.C429

Conflict of Interest: The authors declare that the research was conducted in the absence of any commercial or financial relationships that could be construed as a potential conflict of interest.

frontiers in Physiology

ORIGINAL RESEARCH
published: 16 July 2020
doi: 10.3389/fphys.2020.00812

MNX (Medium Duration Nutrition and Resistance-Vibration Exercise) Bed-Rest: Effect of Resistance Vibration Exercise Alone or Combined With Whey Protein Supplementation on Cardiovascular System in 21-Day Head-Down Bed Rest

Patrick Guinet[1,2†], James Patrick MacNamara[3†], Matthieu Berry[4], Françoise Larcher[5], Marie-Pierre Bareille[6], Marc-Antoine Custaud[7,8], Anne Pavy-Le Traon[9,10], Benjamin D. Levine[3] and Nastassia Navasiolava[7,8]*

[1] Département d'Anesthésie Réanimation, Centre Hospitalier Universitaire de Rennes, Rennes, France, [2] Centre Hospitalier de Fougères, Fougères, France, [3] Institute for Exercise and Environmental Medicine, Texas Health Presbyterian Hospital, The University of Texas Southwestern Medical Center, Dallas, TX, United States, [4] Ramsay Santé, Clinique des Cèdres, Toulouse, France, [5] Laboratoire de Biochimie, Centre Hospitalier Universitaire d'Angers, Angers, France, [6] Institut de Médecine et de Physiologie Spatiales (MEDES), Toulouse, France, [7] Centre de Recherche Clinique, Centre Hospitalier Universitaire d'Angers, Angers, France, [8] Mitovasc UMR INSERM 1083-CNRS 6015, Université d'Angers, Angers, France, [9] Department of Neurology, French Reference Center for MSA, University Hospital of Toulouse, Toulouse, France, [10] Institute of Cardiovascular and Metabolic Diseases INSERM U 1048, Toulouse, France

Current inflight countermeasures do not completely prevent bone and cardiovascular changes induced by microgravity. High load Resistance Exercise combined with whole body Vibration (RVE) demonstrated benefits on bone and cardiovascular system during previous Head-Down Bed Rest (HDBR) studies. We examined the effectiveness of RVE alone or combined with a nutritional supplementation of Whey protein (NeX) on cardiovascular deconditioning. Eight male subjects (age 34 ± 8 years) in a crossover design completed three 21-day HDBR campaigns (Control-CON, RVE, and NeX). Pre and post HDBR Orthostatic Tolerance (OT) was evaluated by a 15-min head-up tilt test followed by increasing levels of Lower Body Negative Pressure (LBNP). Heart rate (HR), blood pressure (BP), and Sympathetic Index (ΣI) through spectral analysis were measured during OT test. Plasma Volume (PV), and Maximal Oxygen Uptake (VO_2max) were measured before and after each campaign. Left ventricular mass, left ventricular end diastolic (LVEDV), end systolic (LVESV), stroke (SV) volumes, and circumferential deformation at rest and during an orthostatic stress simulated by a 30 mmHg LBNP were measured by cardiac MRI. RVE failed to prevent any change in these variables and NeX did not have any additional effect over exercise alone. In the 3 groups, (1) OT time dropped similarly (bed rest $p < 0.001$), (2) HR and ΣI were increased at rest at the end of HDBR and HR increased markedly during LBNP-tilt test, with inability

OPEN ACCESS

Edited by:
Wolfgang Schobersberger, Institut für Sport-, Alpinmedizin & Gesundheitstourismus (ISAG), Austria

Reviewed by:
Dieter Blottner, Charité – Universitätsmedizin Berlin, Germany
Andreas Kramer, University of Konstanz, Germany

***Correspondence:**
Patrick Guinet
patrickguinet@hotmail.com

† These authors have contributed equally to this work

Specialty section:
This article was submitted to Environmental, Aviation and Space Physiology, a section of the journal Frontiers in Physiology

Received: *26 March 2020*
Accepted: *18 June 2020*
Published: *16 July 2020*

Citation:
Guinet P, MacNamara JP, Berry M, Larcher F, Bareille M-P, Custaud M-A, Pavy-Le Traon A, Levine BD and Navasiolava N (2020) MNX (Medium Duration Nutrition and Resistance-Vibration Exercise) Bed-Rest: Effect of Resistance Vibration Exercise Alone or Combined With Whey Protein Supplementation on Cardiovascular System in 21-Day Head-Down Bed Rest. Front. Physiol. 11:812. doi: 10.3389/fphys.2020.00812

to increase further the ΣI, (3) PV dropped (bed rest $p < 0.001$), along with LVEDV, LVESV and SV ($p = 0.08$, $p < 0.001$, and $p = 0.045$, respectively), (4) Left ventricle mass did not change significantly, (5) Deformation of the heart assessed by global circumferential strain was preserved and early diastolic circumferential strain rate was increased during orthostatic stress at the end of HDBR, illustrating preserved systolic and diastolic function respectively, without any difference between groups. Despite the drop in PV and LV volumes, RVE and NeX tended to alleviate the decrease in VO_2max. In conclusion, RVE and NeX failed to prevent the cardiovascular deconditioning induced by a 21 day-HDBR.

Keywords: countermeasures, simulated microgravity, cardiovascular deconditioning, resistance vibration exercise, whey protein supplementation, cardiac MRI, orthostatic tolerance, VO_2max

INTRODUCTION

Head-Down Bed Rest (HDBR) accurately reproduces several of the physiological changes induced by microgravity, including many cardiovascular, muscle and bone alterations (Pavy-Le Traon et al., 2007; Hargens and Vico, 2016; Mulavara et al., 2018). HDBR permits testing potential countermeasures, among which exercise is pivotal. As spaceflight duration may increase with potential missions to the Moon and Mars, new and more effective countermeasures against detrimental adaptations will be needed. Currently, in-flight countermeasures still fail to prevent all bone changes (Rittweger et al., 2018) and cardiovascular deconditioning (Lee et al., 2015).

Cardiovascular deconditioning resulting from spaceflight and HDBR includes increased resting heart rate (HR), orthostatic intolerance (OI), and decreased maximal oxygen uptake (VO_2max) (Bungo et al., 1985; Convertino, 1994; Pavy-Le Traon et al., 2007). Extensive data about mechanisms of OI from previous spaceflight and HDBR studies highlight its multifactorial origin. Blood volume, autonomic function, adrenergic receptor function, vascular compliance, endothelial function, cardio-vestibular interactions, cardiac mass and left ventricular (LV) volumes are all altered by spaceflight or HDBR (Pavy-Le Traon et al., 2007; Hargens and Vico, 2016). Cardiac deconditioning is evidenced by changes in LV morphology, including reduced cardiac mass, end-diastolic volume, and stroke volume (SV) (Levine et al., 1997; Perhonen et al., 2001; Mulavara et al., 2018). Furthermore, LV relaxation is slowed after bed-rest with a presumed reduction in diastolic suction which may further impair ventricular filling, especially in the upright position (Dorfman et al., 2008; Carrick-Ranson et al., 2013). Exercise training has prevented cardiac deconditioning during bed-rest but has not improved orthostatic tolerance (OT) without concurrent volume loading, emphasizing the dual contributions of plasma volume (PV) and cardiac remodeling to the cardiovascular adaptation to microgravity (Shibata and Perhonen, 2010; Hastings et al., 2012; Ploutz-Snyder et al., 2018). Thus, further understanding of cardiac response to orthostatic stress and interventions that can prevent both cardiac deconditioning and OI are needed.

The effect of high intensity resistance exercise on a vibrating plate, so-called Resistive Vibration Exercise (RVE) has been explored during 2 long-term bedrest studies (Berlin BR) (Rittweger et al., 2006; Belavy et al., 2010a). First, a 56-day horizontal BR study explored the impact of 11 RVE sessions per week, and demonstrated a beneficial effect on bone loss, changes in bone metabolism, muscle mass loss, and muscle contractile capacity (Blottner et al., 2006; Belavy et al., 2008, 2009; Armbrecht et al., 2010; Rittweger et al., 2010). Second, a 60-day HDBR compared a high load resistive exercise (RE) to RVE, and with only 3 sessions a week showed an additional effect of RVE on bone (Belavy et al., 2011) but not on muscles (Mulder et al., 2006; Belavy et al., 2010b, 2011; Miokovic et al., 2011; Gast et al., 2012).

During these bedrest studies, cardiovascular deconditioning was not assessed extensively, but interesting vascular effects were observed: RVE attenuated the diameter decrease of leg conduit arteries (1st Berlin BR) (Bleeker et al., 2005) prevented completely (carotid artery) or partially (superficial femoral artery) the increase in wall thickness (2nd Berlin BR, van Duijnhoven et al., 2010a) and abolished the marked increase in flow mediated dilation and decrease in baseline diameter of the superficial femoral artery normally associated with prolonged bed-rest (van Duijnhoven et al., 2010b). Another BR study, using a whole body vibrating device with resistive exercise of lesser intensity, did not protect OT but prevented an increase of the sympathetic index (ΣI) (reflecting the sympathovagal balance of cardiac autonomic control) and limited the decrease of the spontaneous baroreflex sensitivity (Coupé et al., 2011).

Bone, muscle and cardiovascular benefits evidenced in Berlin BR studies motivated European Space Agency's decision to continue the study of this high intensity RVE countermeasure, reducing further the frequency of exercise to 2 sessions per week, while comparing RVE alone to a combination of RVE with a nutritional supplementation in whey protein (Nutritional + Exercise, NeX). High protein intake and essential amino acid supplementation have shown anti-catabolic effects (Phillips et al., 2012), enhanced protein synthesis in human skeletal muscle (Paddon-Jones et al., 2004; Graf et al., 2011) and, when combined with branched chain amino acids, prevented cardiac atrophy if not remodeling during bed-rest (WISE study: Dorfman et al., 2007). Nevertheless such a regimen did not maintain lower limb muscle volume and strength during a long-term bed-rest study in women (WISE study: Trappe et al., 2007;

Lee et al., 2014). Furthermore, a diet high in protein led to a low-grade metabolic acidosis which altered bone metabolism after bed-rest (Zwart et al., 2005). To neutralize these acidogenic effects of whey protein, several authors combined whey protein with potassium bicarbonate supplement in bed-rest studies (Blottner et al., 2014; Bosutti et al., 2016). This combination was not effective on skeletal muscle atrophy (Blottner et al., 2014) but attenuated disuse-induced reductions in muscle fiber oxidative capacity (Bosutti et al., 2016).

The objective of our study was to provide a large exploration of the cardiovascular effects of RVE and NeX countermeasures compared to control (CON). We hypothesized that RVE and NeX would have a beneficial effect on OT, PV, VO_2max, cardiac mass, and cardiac volumes. Furthermore, cardiac MRI was performed during lower body negative pressure (LBNP), for the first time during a HDBR study, to evaluate cardiac volumes and function during an orthostatic stress, and to determine if RVE or NeX could be an effective countermeasure.

MATERIALS AND METHODS

Subjects

A total of twelve healthy men (age 34 ± 8 years, body mass 70 ± 8 kg, height 176 ± 6 cm, BMI 22.4 ± 1.7 kg/m^2, mean ± SD) were included in the study.

Inclusion Criteria

Inclusion criteria were healthy men (according to the performed medical tests plus laboratory analysis), 20–45 years old, BMI 20–26 kg/m^2, height 158–190 cm, no family or personal past record of acute or chronic diseases, no psychological abnormalities, fitness assessment: <35 years: 35 ml/min/kg < VO_2max < 60 ml/min/kg; >35 years: 30 ml/min/kg < VO_2max < 60 ml/min/kg, mobile and active (no orthopedic, musculoskeletal or cardiovascular disorders), and not under medical attendance.

Exclusion Criteria

Exclusion criteria were OI, cardiac rhythm abnormalities, back pain, reported hiatal hernia, thyroid dysfunction, gastro-oesophageal reflux, diabetes, renal stones, migraines, record of thrombophlebitis (personal and family history of thrombosis), claustrophobia, tobacco, drug or alcohol dependence, reported genetic muscle or bone diseases, metallic implants, reported knee problems or joint surgery, BMD: T-score ≤ −1.5, blood collections 8 weeks or less prior the study (more than 8 ml/kg), special diet (vegan, vegetarian), reported lactose intolerance, Hepatitis A, B, C, Anti – HIV1+2 antibodies, inappropriate thoracic acoustic window and any chronic disease.

This study (registered number: 2012-A00337-36) was carried out with the recommendations of the Ethics Committee (CPP Sud-Ouest Outre-Mer I). The protocol was approved by the French Health Authorities. All subjects gave written informed consent in accordance with the Declaration of Helsinki. The study was performed by the Institute for Space Medicine and Physiology (MEDES-IMPS) in Toulouse, France, and supported by the French Spatial Agency [Centre National d'Etudes Spatiales (CNES)] and European Space Agency (ESA).

Study Design

The experiment was organized as a prospective, crossover trial with three campaigns. The campaigns were separated by wash-out periods of 3 months. Volunteers participated in all three campaigns and were assigned in a random order to "Control" (CON), "Exercise and vibration" (RVE), or "Exercise and vibration plus Nutrition" (NeX) group. For each campaign, the subjects remained at MEDES clinic for 35 days, including 7 days of ambulatory control before HDBR (B-#), 21 days of −6° HDBR (D-#), and 7 days of ambulatory recovery period (R-#). Body weight (BW), blood pressure (BP), HR, water intake and urine volume over 24 h were measured daily. Partial water balance, defined as the difference between consumed water and urine volume, was calculated. During HDBR the subjects remained in the head-down tilt position for all activities. For the meal subjects were permitted to lie on their stomach, back or side, however, they were instructed that when in side-lying the trunk and head had to remain in the head-down position, i.e., the head could not be held up with the hand or arm as one commonly does whilst reading. Video monitoring on a 24-h basis permitted further monitoring of subject adherence to the study protocol. A standard controlled diet was followed by all subjects. Individual total energy expenditure (TEE, Kcal) was calculated, based on resting metabolic rate (RMR) measured by indirect calorimetry at B-7 and B-3, and adjusted if necessary during HDBR. TEE was covered by 30–35% total fat, 40–55% carbohydrates, and proteins according to the group. TEE was calculated as followed: during HDBR: TEE = RMR × 1.1 + 10% TEE, during ambulatory control and recovery periods: TEE = RMR × 1.4 + 10% TEE. TEE was adjusted for the training groups, with an increase (in Kcal) of 2.9 × BW on exercise days.

One subject did not complete the Control protocol (withdrawal before the beginning of campaign). All subjects completed the RVE protocol. Four subjects did not complete the NeX protocol [one withdrawal before the beginning of campaign, two during ambulatory control (B-1 and B-6), and one on D-17 of HDBR]. Complete data sets were obtained in eight subjects, therefore those 8 subjects were kept for per-protocol analysis (See **Figure 1**).

This experiment was an integrative international study with several protocols performed on different domains. Some results on this integrative study have already been published: Cvirn et al. (2015) and Waha et al. (2015) (effects of HDBR, RVE, and NeX on the coagulation system), Kenny et al., 2017 (reduction in mitochondrial respiration partially prevented by RVE), Greaves et al., 2019 (echocardiographic study), Kermorgant et al., 2019 (cerebral autoregulation), Owen et al., 2020) (lumbar spinal muscle atrophy reduced by NeX but not by RVE alone), Graf et al., 2014 (no additional effect of whey protein supplementation compared with RVE alone regarding bone turnover markers), Pastushkova et al., 2015 (modification of urine proteome).

Subjects	Campaign 1	Campaign 2	Campaign 3
A	RVE	NeX	CON
B	CON	RVE	NeX
C	RVE	NeX	CON
D	NeX	CON	RVE
E	NeX	CON	RVE
F	CON	RVE	~~NeX~~
G	NeX	CON	RVE
H	CON	RVE	~~NeX~~
I	RVE	~~NeX~~	~~CON~~
J	RVE	NeX	CON
K	NeX	CON	RVE
L	CON	RVE	~~NeX~~

FIGURE 1 | The different allocations of each subject. CON, control condition; RVE, Resistance vibration exercise condition; NeX, Resistance vibration exercise with nutritional supplementation. Campaign 2: I2 withdrawal on B-1. Campaign 3: F3 withdrawal on B-6, H3 withdrawal before the beginning of the campaign, L3 withdrawal on D-17 of HDBR.

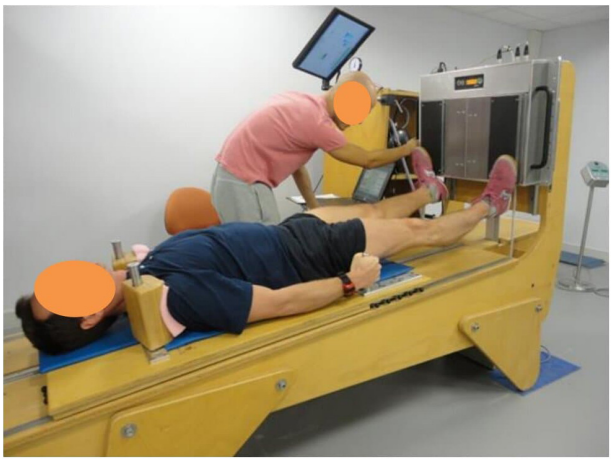

FIGURE 2 | Resistive vibration exercise training (RVE and NeX groups): subjects performed all exercises in the head-down tilt position and were positioned on a moveable platform with shoulder pads and hand grips preventing downward movement and permitting application of force via the platform. A pneumatic system generated the force, applied through the moveable platform, against which the subject needed to resist and move (via the shoulder pads and hand grips). The feet were positioned on either side of a platform which was set to vibrate during high-load resistive exercises. Subjects were given visual feedback of their actual and target position in the exercise via a monitor placed in the subjects' field of view. As the force output was dictated by the exercise device, the feedback focused on ensuring the subjects performing the exercise in the desired range of motion and at the desired speed. During the heel raises the sport scientist monitored the range of movement and encouraged the subject to go to the end of range in each direction. Here the subject is performing toe raises.

Groups and Countermeasures

Control (CON) group

During HDBR, volunteers did not exercise and followed a standard controlled diet. This group served to assess the effect of countermeasures.

Resistive vibration exercise (RVE) group

All training sessions were performed on an integrated training device, manufactured by Novotec Medical (Pforzheim, Germany), combining 2 systems already used in previous studies (Rittweger et al., 2006; Belavy et al., 2010a; **Figure 2**): (1) a moveable platform designed to exercise in a −6° lying position, with shoulder pads and hand grips preventing downward movement and permitting application of force generated by a pneumatic system via the platform, and (2) a vibration system: Galileo Sensor (Vibration Training device including monitoring function and data recording). The load generated by the moveable platform and transmitted by shoulder pads was progressively increased from 1.3 to 1.8 BW.

During each session, the sequence was performed as follows:

- Warm up consisted in bilateral squats from 10° to 90° knee angle during 8 s (four down, four up) controlled by metronome with eight repetitions, load: 50% of the one repetition maximum (1-RM), vibration amplitude: 8 mm, vibration frequency: 24 Hz.
- Bilateral squats from 10° to 90° knee angle during 8 s (four down, four up) controlled by metronome with 10 repetitions, load at study start: 75% of the 1-RM, progression: 5% load increase when more than 10 repetitions were possible, 5% load decrease when six or fewer repetitions were possible, vibration amplitude: 8 mm, vibration frequency: 24 Hz.
- Single leg heel raises were carried out from maximal dorsiflexion to maximal plantar flexion as fast as possible until exhaustion, 1.3 times BW, progression: 5% load increase when more than 50 s were possible, 5% load decrease when 30 s or less were possible, vibration amplitude: 8 mm, vibration frequency: 26 Hz.
- Bilateral heel raises were performed from maximal dorsiflexion to maximal plantar flexion as fast as possible until exhaustion, 1.8 times BW, progression: 5% load increase when more than 55 s were possible, 5% load decrease when 40 s or less were possible; vibration amplitude: 8 mm, vibration frequency: 26 Hz.

Each Exercise session lasted approximately 30 min. The training was performed approximately two times per week (D-2, 5, 12, 16, 21).

Resistive vibration exercise plus Nutrition (NeX) group

During HDBR, volunteers underwent the same physical training as previously described but received a different daily diet with an isocaloric supplementation of whey protein (0.6 g/kg BW/day). The total protein intake was 1.8 g/kg BW/day. The schedule of the protein supplementation was the following: (1) on days without exercise, supplementation was applied in equal amounts

with main meal and (2) on days with exercise, half of the daily amount was taken in a timeframe of 30 min after exercise and the other half equally distributed with main meals. The product was Diaprotein®, a powder supplied by Nephrologische Präparate Dr. Volker Steudle (Linden, Germany). The composition was as follows: Diaprotein® 100 g Powder, calories 1573 kJ (370 kcal), proteins 90 g, fat 0.2 g, lactose 2.5 g, sodium <300 mg, potassium <650 mg, calcium <400 mg, phosphorus <250 mg, and relation phosphorus/protein <3 mg/g. Since whey protein added a certain acid load to the diet, supplementation of 90 mmol potassium bicarbonate per day, applied in six portions (with main meals) was given to compensate for that. Potassium bicarbonate was provided by Krüger GmbH & Co. KG (Bergisch Gladbach, Germany). Carbohydrates and total fat were decreased in NeX subjects in order to obtain a similar caloric intake in RVE and NeX groups, and the decrease was shared between carbohydrates and fat according to the daily menu, without passing beneath 30% total fat.

Tilt LBNP Test (Presyncopal Tilt Test)

Tilt testing with combined LBNP was chosen as the primary outcome for measuring OT. The measurement was conducted in the morning in a temperature-controlled room at baseline on B-2 and immediately following HDBR on R-0 (first rising at the end of HDBR). The subject remained supine for 20 min, after which supine data were recorded for 5 min. The tilt-table was then tilted to 80° for 15 min. After that, LBNP was applied with steps of −10 mmHg every 3 min. The test was stopped at LBNP −80 mmHg or earlier upon appearance of pre-syncopal signs, request to stop, systolic BP ≤80 mmHg, or HR<50 bpm or >170 bpm.

During the tilt-LBNP test, Orthostatic Tolerance Time (OTT, min) was measured. HR was obtained by standard electrocardiography (Biopac, ECG 100C, United States) and SBP and DBP were measured continuously with a non-invasive finger cuff method (Nexfin®, BMeye, United States). MBP was determined as the average value over a complete cardiac cycle. Stroke volume (SV, ml) was estimated from the Modelflow method (Wesseling et al., 1993) which computes an aortic flow waveform from finger pressure, by simulating a non-linear three-element model of the aortic input impedance. An estimate of Total Peripheral Resistance (TPR, dynes.s^{-1}.cm^{-5}) was calculated from Mean blood pressure (MBP)/(SV × HR). Tilt values were calculated as mean values of each variable during the last 3 available minutes of the 15-min −80° head-up tilt test.

The state of autonomic nervous system was estimated via power spectrum analysis of HR variability (HRV) (Task Force et al., 1996; Tank et al., 2004). The power spectral density was estimated using proprietary HRV software. This methodology provides the spectral markers of cardiac sympathetic [low-frequency power (LF): 0.04–0.15 Hz] and vagal [high-frequency power (HF): 0.15–0.4 Hz] modulation of the sinoatrial node activity. LF- and HF-power were determined and normalized by the total power (LF + HF). The LF-to-HF ratio (as sympathetic index, ΣI, arbitrary units – a.u), which reflects the sympathovagal balance of HR control, was calculated (Pagani et al., 1986).

Spontaneous Baroreflex Sensitivity (SBRS, ms.mmHg^{-1}) was estimated using proprietary software. The assessment of baroreflex sensitivity is based on the integrative study of short-term regulation of BP and HR. A spontaneous baroreflex sequence was defined as same-direction changes in R-R interval and SBP for at least three beats. A linear regression was applied to each sequence, and the mean slope was taken as the SBRS.

Plasma Volume Measurement

Plasma volume (PV, ml) was estimated using the optimized Carbon Monoxide Rebreathing Technique (CORT) (Schmidt and Prommer, 2005) in the morning before breakfast before HDBR on B-6 and at the end of HDBR on D-21. Hemoglobin concentration (Hb) and carbon monoxide Hb percentage were determined with a Radiometer OM 3 analyzer (Radiometer, Copenhagen, Denmark), hematocrit (Hct) with a Jouan Hematocrit A 13 centrifuge (Jouan, St. Herblain, France), and exhaled CO with a PAC 7000 analyzer (Draeger, Lübeck, Germany).

Maximal Oxygen Uptake (VO_2max)

An incremental dynamic leg exercise test on a cycle ergometer (Ergometrics 800S, Ergoline, Bitz, Germany) was performed at B-5 and R + 1 to determine maximal oxygen uptake (VO_2max, ml.min^{-1}.kg^{-1}). Breath-by-breath VO_2 was recorded with an Oxycon Pro metabolic cart (E. Jaeger, Hochberg, Germany). VO_2max was determined during the subject selection period. At selection, the initial assessment of aerobic capacity was performed using the following protocol: the subjects cycled for 3 min at 30, 60, 90, 120, and 150 W, followed by an increase of 20 W every min until they could no longer maintain the desired cycling cadence of 75 rotations per minute (rpm) (peak exertion reached) and/or they wanted to stop. Before (B-5) and after the bed-rest period (R + 1), the subjects cycled for 5 min at 25, 50, and 75% of the maximal power measured at selection. At completion of the third stage, the workload increased 25 W every min until exhaustion, when the subject could no longer maintain the required cycling cadence of 75 rpm. HR and BP were monitored continuously. VO_2max was calculated to be the highest 60-s moving average in the VO_2 recording.

Cardiac MRI

Acquisition

Cardiac MRI was performed at B-3 and D-18. Subjects were transported in the supine position and placed into an MRI compatible LBNP chamber (Polyform, La Mézière, France, **Figure 3**). Cardiac MRI was performed on a 1.5T Philips MRI scanner during supine rest and then with LBNP. Protocol included scout and longitudinal axis images as well as short axis cine stack from ventricular apex to left atrium with slice thickness of 6 mm. After supine images without LBNP, negative pressure of −30 mmHg was maintained for 2 min prior to repeating the MRI sequence in order to simulate a mild hypovolemia approximately equivalent to the sitting position and its consequences on myocardial volumes and contractility.

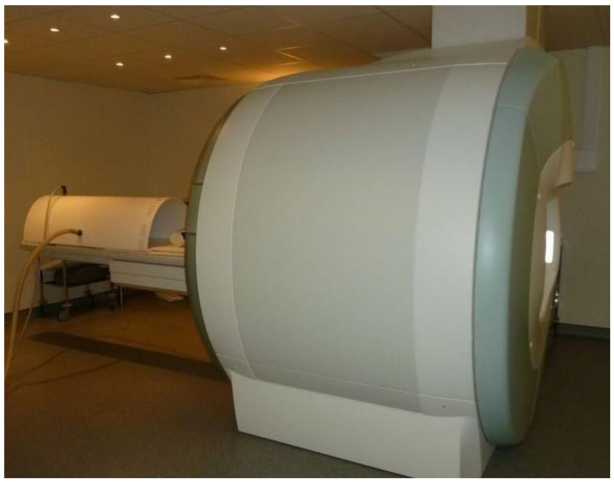

FIGURE 3 | LBNP chamber, made with wood reinforced with plastic resin, especially designed for MRI scanner (Polyform®, La Mézière, France). Chamber was sealed with a neoprene suit. Negative pressure was maintained by air compressor (Mil's, Lyon, France) and controlled by a manometer (ADMI, Noisy Le Grand, France) situated outside the MRI chamber.

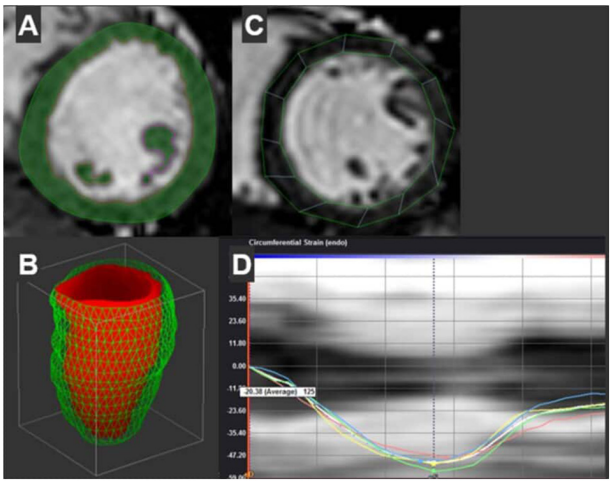

FIGURE 4 | Representative contours of the left ventricle and subsequent measures are shown. **(A)** Semi-automated contours with manual adjustment are combined with Qmass's threshold based mass detection (green shading) for each short axis slice of the ventricle. These slices create a 3D re-construction of the LV volumes by method of discs (Diastolic volume shown in Panel **B**). **(C)** Separate contours at the mid-section of the ventricle are used to measure circumferential strain through the cardiac cycle using Tomtec's semi-automated feature tracking algorithm. **(D)** Shows both segmental strain curves. Peak strain of the mid-section is shown in white.

Negative pressure was maintained by air compressor (Mil's, Lyon, France) and controlled by a manometer (ADMI, Noisy Le Grand, France) situated outside the MRI chamber. All MRIs and LBNP were completed under the supervision of cardiologist (MB) and anaesthesiologist (PG) at Toulouse Rangueil Hospital.

Analysis

Left ventricular volumes were measured by manually tracing the endocardial borders of the short axis stack of cine SSFP images from LV base to apex slices during end-diastole and end-systole using Qmass v8.1 (Medis, Raleigh, NC, United States) in accordance to CMR guidelines (Schulz-Menger et al., 2013). Papillary muscles and significant trabeculae were included in endocardial border. End-diastole was defined as the frame with the largest endocardial area before the aortic valve opened, and end-systole was defined as frame with the smallest endocardial area, after the aortic valve had closed. Care was taken to standardize the basal slice and include the LVOT in the traced blood pool. SV was determined by subtracting end-systolic volume (LVESV) from end-diastolic volume (LVEDV). Cardiac output (Q) was estimated by multiplying SV by HR during the scan. LV mass (LVM) was measured by tracing the epicardial border during end-diastole and using a semi-automated program, MassK: a threshold-based method to estimate cardiac mass (Csecs et al., 2018).

To assess systolic and diastolic ventricular motion, feature tracking analysis was performed using Cardiac Performance Analysis MR v1.3 (Tomtec, Unterschleissheim, Germany) (see **Figure 4**). The left ventricle twists during systole to generate the SV and untwists during diastole to restore the end-diastolic volume. Global circumferential strain (GCS) and early diastolic circumferential strain rate (GCSR-E) measure circumferential fiber shortening during systole and re-lengthening rate during early diastole, respectively. GCS and GCSR-E are similar to, but not interchangeable with, systolic and early diastolic torsion. Changes in GCS occur before changes in ejection fraction in some cardiovascular disease, thus GCS provides a measure of subclinical systolic and diastolic function (Lunning et al., 2015). GCS was measured using short axis stack of cine SSFP images from LV base to apex. The basal slice was identified as the slice closest to the mitral valve with circular myocardium. The apical slice was identified as the slice just proximal to systolic cavitary obliteration. The mid slice was identified between basal and apical slices with papillary muscles clearly defined (Hor et al., 2010; Claus et al., 2015). Endocardial and epicardial borders were manually traced at end-systole and adjusted at end-diastole to ensure adequate tracking. Papillary muscles and trabeculae were excluded. Feature tracking was performed by Tomtec's semi-automated algorithm. GCS was defined as peak strain averaged from all three levels of myocardium. Early diastolic circumferential strain rate (GCSR-E) was defined as the first peak positive strain rate during diastole at the mid-section to capture the opposed untwisting of the base and apex. The observer who performed 2D and feature tracking (JM) was blinded to group assignments. Six studies were randomly selected from the study subjects to evaluate intra-observer variability for GCS and GCSR-E. The measures were repeated by researcher (JM) blinded to initial results and coefficient of variation was calculated as intra-observer variation.

Blood Studies

Antecubital venous blood samples were collected before (B-3) and at the end of HDBR (D-21) in the morning before breakfast.

Plasma and serum samples were analyzed for electrolytes (Na+, K+, Cl−), total CO2, glucose, proteins, albumin, urea and creatinine concentrations, insulin, leptin, renin, aldosterone, brain natriuretic peptide (BNP), triglycerides, total cholesterol and HDL-cholesterol. LDL-cholesterol was calculated using the Friedewald formula. Homeostasis model assessment-insulin resistance index (HOMA-IR) was calculated as fasting insulin concentration (μU/mL) × fasting glucose concentration (mmol/L)/22.5.

Statistical Analysis

Continuous data are expressed as mean ± SD. We first checked whether data passed d'Agostino-Pearson normality test. 3-way ANOVA or 2-way ANOVA for repeated measures were used with bed-rest (pre, post), countermeasure (Control, RVE, NeX), and position (supine, orthostatic stimulation) as within-subject factors. Statistically significant differences were further analyzed by pairwise multiple comparisons with Sidak correction. All statistical analyses were performed with GraphPrism 8.1.2. Differences were considered as statistically significant when adjusted $p < 0.05$.

RESULTS

Body Weight, HR, BP, Water Balance (See Supplementary Data, Appendix 1–5)

Body weight (**Supplementary Data, Appendix 1**) gradually declined during HDBR without significant difference between groups (day*countermeasure $p = 0.07$); at R-0 BW decrease vs. B-1 baseline was 2.3 ± 0.9 kg for CON, 2.1 ± 0.8 kg for RVE, and 1.7 ± 0.9 kg for NEX (day $p < 0.001$, countermeasure $p = 0.66$). HR (**Supplementary Data, Appendix 2**) expectedly increased at recovery without differences between groups (day*countermeasure $p = 0.7$, day $p < 0.001$), systolic and diastolic BPs were not substantially modified (**Supplementary Data, Appendix 3, 4**). Expected changes in water intake and diuresis resulted to about 1L decrease in partial water balance at D-1 and about 0.8 L increase – at R-0 vs. B-1 baseline (**Supplementary Data, Appendix 5**).

Presyncopal Tilt/LBNP Test

Orthostatic Tolerance Time (Figure 5)

Orthostatic tolerance time (min) markedly decreased in all groups without any difference between groups (bed-rest*countermeasure $p = 0.76$), from 29 ± 6 to 15 ± 10 in CON, 29 ± 4 to 13 ± 9 in RVE, 27 ± 5 to 13 ± 8 in NeX (bed-rest $p < 0.001$). Pre-BR, all 8 subjects finished the 15-min upright period in all groups, post-BR there were 4 finishers in CON, 4 in RVE, 3 in NeX.

Hemodynamic and Autonomic Responses to Tilt (Table 1 and Figure 5)

No significant differences were found in RVE and NeX compared with control group and between countermeasures (bed-rest*countermeasure interaction $p = 0.29$ for HR, 0.46 for SBP, 0.57 for DBP, 0.94 for SV, 0.76 for TPR, 0.74 for ΣI, and 0.54 for SBRS, respectively).

Before HDBR, the upright position provoked expected changes in central hemodynamics and cardiac autonomic neural control (increased HR, BP, TPR, and ΣI; decreased SV and SBRS).

Post-BR supine measurements on R0 compared to pre-BR supine showed increase in HR of about 10–12 bpm, from 55 ± 12 to 67 ± 11 in CON, 58 ± 17 to 67 ± 10 in RVE, and 57 ± 10 to 67 ± 11 in NeX (bed rest $p < 0.0001$), a two-fold increase in ΣI, ∼30% decrease in SBRS, and a stable SV with the Modelflow method.

Post-BR upright measurements compared to pre-BR upright showed ∼15% decrease in SBP, ∼20% decrease in SV and more than 2-fold decrease in SBRS, accompanied by pronounced tachycardia. TPR and ΣI, which were already increased in the supine position, failed to further increase with orthostasis.

Plasma Volume (Figure 5)

For technical reasons pre-BR PV test was not performed for the 1st campaign. Mean of pre-BR test of the 2nd and the 3rd campaign for each subject has been used as a common pre-BR baseline. RVE and NeX did not alleviate the drop in PV (interaction bed rest*countermeasure $p = 0.65$). PV decreased significantly pre to post BR in the 3 groups, from 3894 ± 573 ml at baseline to 3301 ± 446 ml (−15 ± 4%) in CON, 3256 ± 519 ml (−16 ± 6%) in RVE, 3332 ± 601 ml (−15 ± 4%) in NeX, (bed rest $p < 0.0001$).

VO_2max (Figure 5)

The differential response to countermeasures on VO_2max did not reach statistical significance (interaction p for bedrest*countermeasure = 0.09). VO_2max (ml/kg/min) declined significantly in CON group (from 38 ± 6 to 31 ± 5, $p < 0.05$, −17 ± 13%), but not in RVE (from 38 ± 5 to 36 ± 5, −4 ± 8%) nor in NeX groups (from 37 ± 7 to 34 ± 6, −7 ± 12%). Peak power (Watts) dropped from 266 ± 49 to 206 ± 37 in CON (−23%) and decreased from 273 ± 73 to 244 ± 46 in RVE (−10%), 248 ± 48 to 229 ± 47 in NeX (−8%).

Cardiac Structure and Function (Figures 6, 7 and Table 2)

After 18 days of HDBR, there was a small reduction in LVM that did not reach statistical significance (CON: Pre: 155 ± 52 g, end 132 ± 17 g, $p = 0.1$) (**Figure 6**). LVEDV decreased with LBNP prior to bedrest, at end-bedrest and with end-bedrest LBNP (LVEDV: bedrest effect $p = 0.0003$, LBNP effect $p = 0.088$) (**Figure 6**). LVESV similarly decreased with LBNP, end-bedrest and end-bedrest LBNP (LVESV: bedrest effect $p = 0.0009$, LBNP effect $p = 0.008$), which resulted in a decrease in SV with LBNP, end-bedrest and end-bedrest LBNP (SV LBNP effect $p = 0.045$). LV ejection fraction did not change with LBNP or bedrest. Cardiac output slightly decreased with both LBNP and bedrest (Q: bedrest effect $p = 0.033$, LBNP effect $p = 0.005$). There was no significant differential response to countermeasures on LV mass (interaction $p = 0.6$), LV volumes (LVEDV $p = 0.26$, LVESV

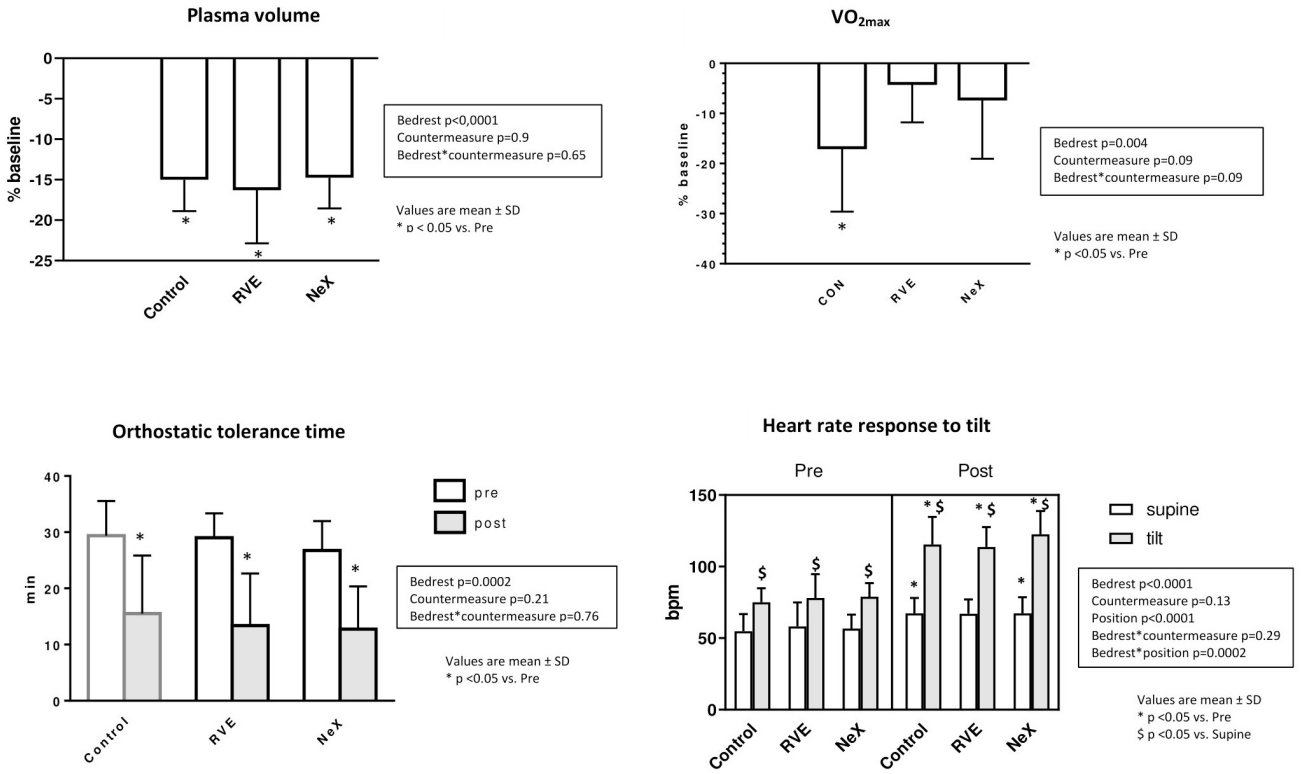

FIGURE 5 | Changes in Plasma Volume (%), $V02_{max}$(%), Orthostatic Tolerance Time (min), and Heart Rate (bpm) (supine and mean during the 3 last available minutes of the 15-min 80° head up tilt test).

$p = 0.63$, SV $p = 0.57$), LV ejection fraction ($p = 0.27$) or cardiac output ($p = 0.32$) (**Table 2**).

Peak GCS and GCSR-E across interventions are represented in **Table 2**. At baseline, GCS was −20.91 ± 3.58%. Across groups, a small reduction in GCS was seen with LBNP ($p = 0.06$), but no differential change occurred after bedrest or with countermeasures (interaction for bedrest*LBNP $p = 0.21$, and bedrest*countermeasure $p = 0.41$) (**Figure 7**). GCSR-E was 1.19 ± 0.36 1/s at baseline. Across groups, GCSR-E did not change with LBNP prior to bedrest (Control pre: 1.19 ± 0.36 1/s, pre LBNP: 1.20 ± 0.27 1/s, $p = 0.11$) or after bedrest (Control pre: 1.19 ± 0.36 1/s, end: 1.20 ± 0.19 1/s, $p = 0.63$). There was a differential change with LBNP after bedrest with a significant increase in GCSR-E (Control end: 1.20 ± 0.19 1/s, end LBNP: 1.46 ± 0.27 1/s, interaction for bedrest*position = 0.02) No differential effect of the countermeasures was seen (interaction $p = 0.92$). Intra-observer typical error was 1.7% for GCS and 4.8% for GCSR-E.

Cardiovascular Hormones, Blood Variables Relevant to Metabolism, Blood Electrolytes (Table 3 and Figure 8)

Blood biochemistry remained in the physiological range. We did not observe any significant differential changes between groups.

At the end of HDBR, aldosterone and renin increased and BNP tended to decrease.

Leptin tended to increase following HDBR ($p = 0.13$). Total cholesterol decreased. HDL-fraction was unmodified. Fasting blood glucose remained stable. Fasting insulin and HOMA-IR increased.

Proteins and albumin were unchanged. Creatinine increased at the end of HDBR. Urea was also increased at the end of HDBR, with significantly more prominent increase for NeX.

Sodium, potassium and chlorine were not significantly modified by HDBR or countermeasures.

DISCUSSION

The Major New Results of This Study Are the Following

(1) RVE countermeasure had no effect on HDBR-induced hypovolemia, orthostatic intolerance, modifications in heart rate and heart rate variability in responses to tilt, hormonal and metabolic changes.

(2) LV volumes (LVEDV, LVESV, SV) decreased during bedrest and orthostatic stress (related to decrease in circulating blood volume), while LV mass tended to decrease slightly. Despite reduction in size during bedrest, deformation of the heart assessed by GCS was preserved and GCSR-E was enhanced during orthostatic stress, illustrating preserved systolic and diastolic function, respectively.

TABLE 1 | Presyncopal tilt/LBNP test: Hemodynamic variables at supine rest and during the 15-min 80°-head up tilt test (mean ± SD during the last 3 available minutes); Heart Rate (HR, bpm), Systolic and Diastolic Blood Pressure (SBP and DBP, mmHg), Stroke Volume (SV, ml), Total Peripheral Resistance (TPR, dynes·s−1·cm^{-5}), Sympathetic Index (ΣI, a.u), i.e., ratio of low-to-high frequency spectral power, Spontaneous Baroreflex Slope (SBRS, ms·mmHg^{-1}).

		CON		RVE		NEX		3-way ANOVA (p)				
Variable	**Position**	**Pre-HDBR**	**Post-HDBR**	**Pre-HDBR**	**Post-HDBR**	**Pre-HDBR**	**Post-HDBR**	**BR**	**CM**	**Position (tilt)**	**BR *CM**	**BR*position**
HR (bpm)	supine	55 ± 12	67 ± 11	58 ± 17	67 ± 10	57 ± 10	67 ± 11	**< 0,0001**	0,13	**< 0,0001**	0,29	**0,0002**
	tilt	75 ± 10	115 ± 9	78 ± 17	114 ± 4	79 ± 9	123 ± 16					
SBP (mmHg)	supine	130 ± 12	134 ± 9	122 ± 7	127 ± 10	124 ± 10	122 ± 9	**0,008**	**0,024**	0,25	0,46	**0,0003**
	tilt	140 ± 12	117 ± 15	128 ± 8	114 ± 11	134 ± 19	109 ± 10					
DBP (mmHg)	supine	75 ± 9	76 ± 3	70 ± 8	75 ± 5	74 ± 6	70 ± 5	0,17	0,2	**< 0,0001**	0,57	**0,046**
	tilt	89 ± 12	80 ± 8	83 ± 7	78 ± 6	87 ± 13	79 ± 6					
SV (ml)	supine	107 ± 14	102 ± 11	110 ± 15	100 ± 15	103 ± 20	104 ± 14	**0,002**	0,47	**< 0,0001**	0,94	0,098
	tilt	78 ± 15	63 ± 14	77 ± 16	66 ± 10	73 ± 16	56 ± 13					
TPR (Dynes.s^{-1}cm^{-5})	supine	1390 ± 409	1164 ± 178	1212 ± 313	1178 ± 320	1333 ± 255	1081 ± 318	**0,003**	0,23	0,16	0,76	**0,006**
	tilt	1568 ± 513	1110 ± 168	1405 ± 284	1006 ± 105	1539 ± 433	1213 ± 302					
ΣI (A.U.)	supine	1, 83 ± 1, 34	4, 04 ± 4, 63	1, 92 ± 1, 51	3, 35 ± 1, 8	2, 27 ± 2, 86	2, 53 ± 3, 07	0,11	0,61	**0,02**	0,47	**0,006**
	tilt	5, 74 ± 4, 6	2, 76 ± 1, 81	6, 82 ± 5, 25	3, 32 ± 2, 55	6, 14 ± 3, 65	2, 05 ± 1, 04					
SBRS (ms.mmHg^{-1})	supine	19, 6 ± 12, 9	12, 8 ± 5	22 ± 13, 6	11, 9 ± 4, 7	17, 3 ± 1, 3	15, 1 ± 6, 2	**0,001**	0,7	**< 0,0001**	0,54	0,39
	tilt	8, 0 ± 3, 1	3, 3 ± 1, 8	9, 0 ± 4, 6	3, 0 ± 1	6, 6 ± 3, 3	3, 1 ± 1, 3					

Significant differences are bolded.

RVE and NeX countermeasures had no effect on cardiac structure and function.

(3) Nutritional supplementation associated with RVE did not provide any additional beneficial effect for studied variables.

(4) However, RVE and NeX countermeasures tended to limit VO_2max loss, although there was no significant bed rest*countermeasure effect.

Plasma Volume, Orthostatic Tolerance

The decrease in PV observed is a well-known consequence of BR, and mimics post-spaceflight hypovolemia. Other BR studies document a decrease of 10–12% (Fortney et al., 1988, 1994; Traon et al., 1995; Custaud et al., 2002; Belin de Chantemele et al., 2004; Hastings et al., 2012).

RVE and NeX countermeasures had no effect on PV and OT. Although several previous studies had documented beneficial vascular effects of RVE during prolonged HDBR, on artery diameter, stiffness or reactivity (Bleeker et al., 2005; van Duijnhoven et al., 2010a), OT nevertheless seemed to be severely altered: at the end of the 2nd Berlin BR, 11 of 23 subjects could not finish a progressive head-up tilt (+10° every 5 min until 60° HUT) on R0 (Belavy et al., 2010b). During this 2nd Berlin BR the last exercise session was scheduled 4 days before the OT evaluation, which may be enough to limit any effect of exercise on OT (Butler et al., 1991; Khan et al., 2002). In the present study, the last exercise session was scheduled on D21, less than 18 h before the tilt/LBNP test, strengthening the conclusion that RVE had no effect on OT.

The low frequency and low duration of exercise and its focus exclusively on resistance type training likely limited the effectiveness of the countermeasures. A negative result on OT had been similarly observed with a high intensity resistive exercise on a flywheel ergometer 2–3 days per week during a longer 90-days BR (Belin de Chantemele et al., 2004). In contrast, prior studies using a greater frequency and duration have demonstrated that exercise can prevent cardiac deconditioning and maintain PV but not necessarily improve OT without concurrent volume loading (Guinet et al., 2009; Shibata and Perhonen, 2010; Hastings et al., 2012). The RVEs that our subjects performed may have failed to stimulate cardiac work or activate the muscle pump sufficiently to prevent beginning cardiac deconditioning and PV loss.

We did not observe any effect of RVE or NeX on the tilt-LBNP autonomic impairment. ΣI was increased in the supine position after HDBR, but could not increase further during tilt-LBNP test, and supine spontaneous baroreflex slope decreased, in all 3 groups with a further decrease in the HUT position after HDBR. After a 60-day HDBR, Coupé et al. (2011) reported that daily RVE prevented the increase in ΣI in standing position and alleviated the decrease in supine SBRS. While the frequencies of vibrations during exercise were close (30 Hz in the study from Coupé et al., 2011, 25 Hz in our study), there were several differences: in the study of Coupé et al. (2011): the frequency of RVE was higher (daily exercise vs. 2 sessions per week in our study), the vibration amplitude was lower (0.1 mm vs. 8 mm in our study), the intensity of exercise was much

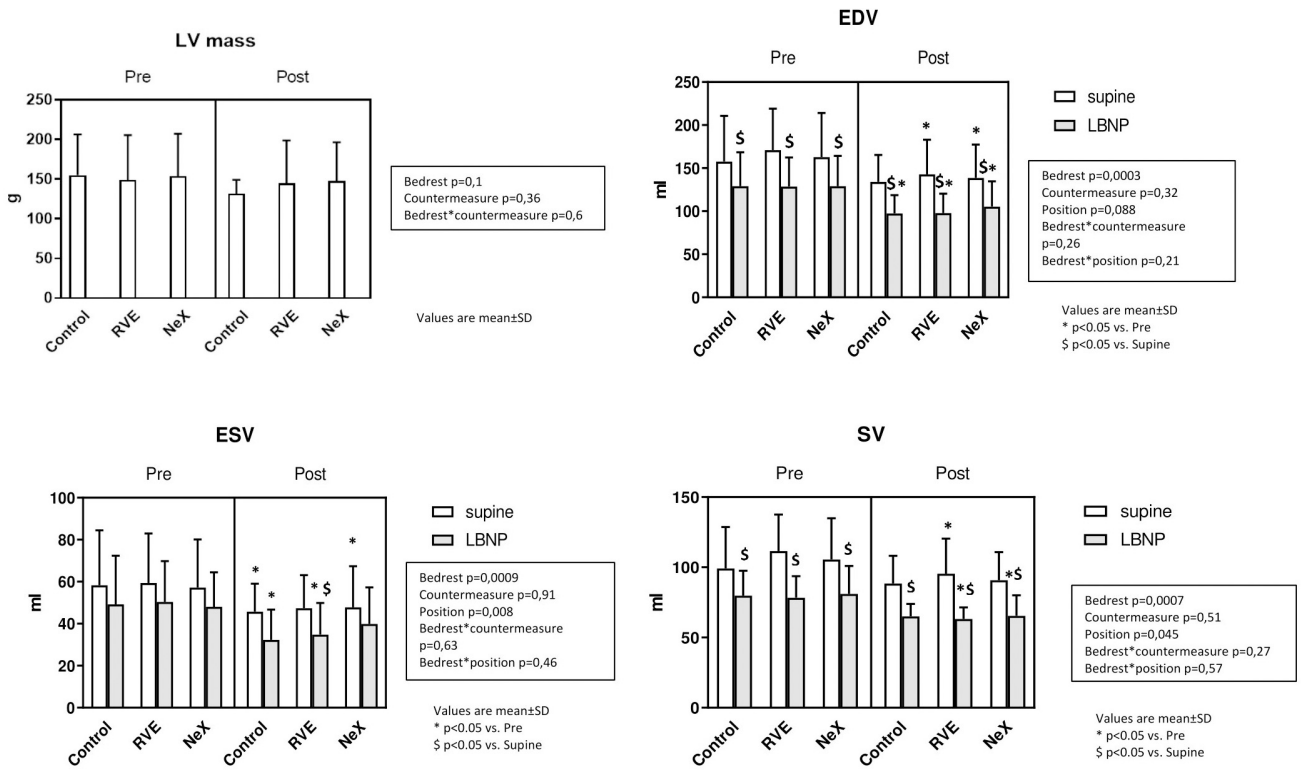

FIGURE 6 | Cardiac MRI main results: Left Ventricle Mass (g), Left ventricle End-Diastolic Volume (LVEDV, ml) and End-Systolic Volume (LVESV, ml), and Stroke Volume (SV, ml).

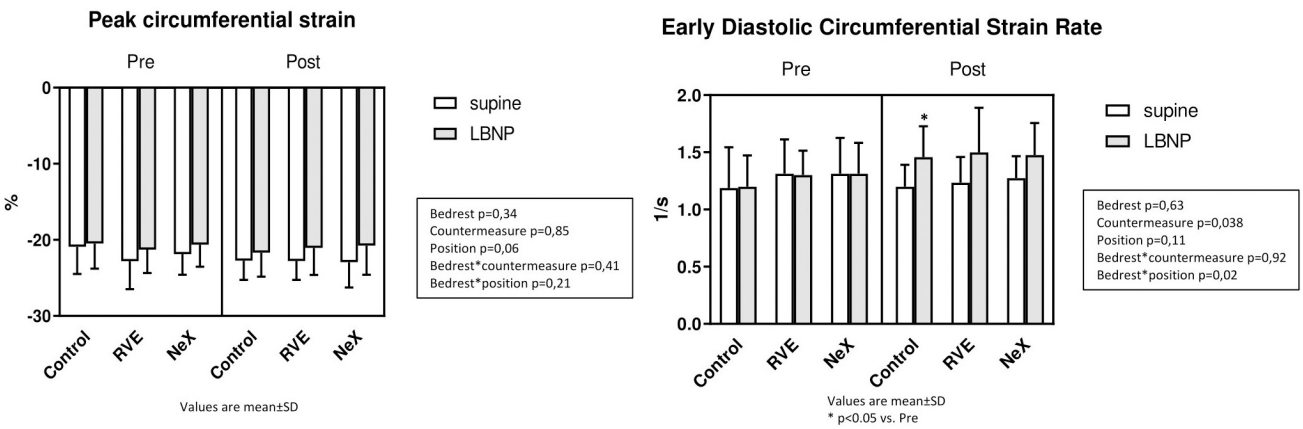

FIGURE 7 | Cardiac MRI main results: Peak circumferential Strain *(%)* and Early Diastolic Circumferential Strain Rate (1/s).

lower (low intensity resistive exercise vs. exhausting exercise in the present study), and HDBR was longer and could induce more pronounced deconditioning (60 days vs. 21 days in our study). As resistive exercise alone does not result in decreased sympathetic activity, unlike endurance training (Fagard, 2006), whole body vibration was hypothesized to act on the autonomic nervous system through plantar and muscular mechanoreceptors (Gladwell and Coote, 2002). This hypothetical effect was not observed in our study.

Biochemical Markers

We observed an increase in Renin and Aldosterone at the end of HDBR, without any difference between groups. Such results have been consistently described during BR studies and in flight, once the initial change in PV (taking 24 h) related to headward fluid shift is achieved (Gharib et al., 1992; Maillet et al., 1996). The decrease in PV, perceived by atrial and kidney receptors, triggers activation of Renin-Angiotensin-Aldosterone System (RAAS) and inhibition of Atrial Natriuretic Factor (ANF)

TABLE 2 | Cardiac parameters pre-bedrest and at end-best with and without −30 mm Hg lower body negative pressure (LBNP).

		Control		RVE		NeX		3-way ANOVA (p)				
Variable	**LBNP Level**	**Pre-HDBR**	**End-HDBR**	**Pre-HDBR**	**End-HDBR**	**Pre-HDBR**	**End-HDBR**	**BR**	**CM**	**Position (LBNP)**	**BR*CM**	**BR*Position**
LVM (g)	0 mm Hg	155 ± 52	132 ± 17	149 ± 57	145 ± 54	154 ± 53	148 ± 49	0.1	0.36		0.6	
LVEDV (ml)	0 mm Hg	158 ± 53	134 ± 31	171 ± 48	143 ± 40	163 ± 51	139 ± 39	**0.0003**	0.32	0.088	0.26	0.21
	−30 mm Hg	129 ± 39	97 ± 21	129 ± 34	98 ± 22	129 ± 35	105 ± 29					
LVESV (ml)	0 mm Hg	58 ± 26	46 ± 13	59 ± 24	47 ± 16	57 ± 23	48 ± 20	**0.0009**	0.91	**0.008**	0.63	0.46
	−30 mm Hg	49 ± 23	32 ± 14	50 ± 19	35 ± 15	48 ± 16	40 ± 17					
SV (ml)	0 mm Hg	99 ± 29	88 ± 20	112 ± 26	95 ± 25	106 ± 29	91 ± 20	**0.0007**	0.51	**0.045**	0.27	0.57
	−30 mm Hg	80 ± 18	65 ± 9	78 ± 15	63 ± 8	81 ± 20	65 ± 15					
Ejection	0 mm Hg	0.64 ± 0.06	0.66 ± 0.04	0.66 ± 0.05	0.67 ± 0.03	0.66 ± 0.04	0.67 ± 0.06	0.32	0.97	0.32	0.27	0.63
Fraction	−30 mm Hg	0.64 ± 0.08	0.66 ± 0.04	0.66 ± 0.05	0.67 ± 0.03	0.66 ± 0.04	0.67 ± 0.06					
Cardiac Output	0 mm Hg	5.28 ± 1.2	4.97 ± 0.51	6.16 ± 1.65	5.16 ± 1.18	5.64 ± 0.68	5.1 ± 0.81	**0.033**	0.23	**0.005**	0.32	0.18
(L/min)	−30 mm Hg	4.77 ± 0.79	4.54 ± 0.46	4.86 ± 0.92	4.59 ± 0.65	4.97 ± 0.61	4.6 ± 0.67					
GCS (%)	0 mm Hg	−20.91 ± 3.58	−22.74 ± 2.53	−22.82 ± 3.67	−22.78 ± 2.48	−21.88 ± 2.72	−22.95 ± 3.31	0.34	0.85	0.06	0.41	0.21
	−30 mm Hg	−20.49 ± 3.31	−21.7 ± 3.14	−21.28 ± 3.07	−21.06 ± 3.55	−20.64 ± 2.9	−20.76 ± 3.82					
GCSR-E (1/s)	0 mm Hg	1.19 ± 0.36	1.2 ± 0.19	1.31 ± 0.3	1.23 ± 0.23	1.31 ± 0.31	1.28 ± 0.19	0.63	**0.038**	0.11	0.92	**0.02**
	−30 mm Hg	1.2 ± 0.27	1.46 ± 0.27	1.3 ± 0.21	1.5 ± 0.39	1.31 ± 0.27	1.48 ± 0.28					

LVM, left ventricular mass; LVEDV, left ventricular end-diastolic volume; LVESV, left ventricular end-systolic volume; SV, stroke volume; GCS, global circumferential strain; GCSR-E, early diastolic circumferential strain rate. Significant differences are bolded.

(Gharib et al., 1992). These adaptations lead to a new steady state of PV, stabilized at about 15% less than preBR levels.

Brain natriuretic peptide tended to decrease in the 3 groups, presumably reflecting decreased cardiac load due to inactivity, and in line with documented cardiac atrophy. ANF and BNP share most biological properties including diuretic, natriuretic, cardiac antihypertrophic and antifibrotic properties, and vasodilation through inhibition of sympathetic nervous system and RAAS (Nishikimi et al., 2006). BNP and its more stable split-mate, NT-proBNP, released by ventricular walls in case of volumetric or barometric stimulus, are used as markers of cardiac load in clinical practice (Chen and Burnett, 2006; Ogawa and de Bold, 2012). BNP or NT-proBNP had not been previously measured during HDBR in humans. As ANF and BNP share the same triggering stimulus in the heart wall, the decrease observed in this 21-day HDBR is in line with the decrease in ANF observed in previous BR studies (Gharib et al., 1993; Belin de Chantemele et al., 2004).

Increase in insulin resistance presumably due to inactivity-related metabolic impairment is typically observed in protocols of simulated microgravity (Pavy-Le Traon et al., 2007). Increase in creatinine evidences increased muscle catabolism. As for increase in urea in NeX group, it may be related to increased protein intake. However, these metabolic changes remained in physiological range.

Cardiac Structure and Function

To our knowledge, this study is the first time that MRI, the gold standard for cardiac structure, has been used to assess bedrest-induced cardiac deconditioning during orthostatic stress. The subjects lost 14.8% of their cardiac mass during the control bedrest campaign, consistent with the cardiac atrophy seen in prior studies (Levine et al., 1996; Perhonen et al., 2001; Dorfman et al., 2008; Carrick-Ranson et al., 2013; Mulavara et al., 2018). The cardiac volumes, including LVEDV, LVESV, and SV, all decreased with bedrest to levels similar to pre-bedrest LBNP. This observation suggests that the upright, sitting position may well be the "regulated" position for the circulation during prolonged absence of gravitational gradients, as has been hypothesized by us and others (Norsk et al., 1995; Pancheva et al., 2006). Moreover LBNP at the end of bedrest (simulating the effect of orthostasis on cardiac morphology) amplified the reduction in cardiac volumes to levels far below the pre-bedrest baseline, consistent with a prior echocardiographic study (Carrick-Ranson et al., 2013). This finding emphasizes why orthostatic stress after bedrest results in an amplification of the reduction in SV induced by gravity, serving as the primary stimulus for post-bedrest OI.

NeX results on OT, PV, and cardiac mass and volumes were not different from RVE. While whey protein supplementation combined with resistance vibrations has prevented skeletal muscle loss in other populations (Pennings et al., 2011; Chale et al., 2013) it did not have statistical impact of cardiac mass loss in our study, though the relative drop was much less (14.8% in control arm, 3.9% in NeX arm). Thus, the impact of whey protein on cardiac mass loss, particularly if combined with more intensive exercise, may be of further interest. Addition

TABLE 3 | Blood biochemistry.

Parameters	Ref range	Control		RVE		NeX		3 way ANOVA (p)		
		Before	End	Before	End	Before	End	Bed Rest	Countermeasure	BR*CM
Aldosterone, ng/L	30-355	53 ± 42	76 ± 31	38 ± 23	106 ± 53*	44 ± 27	93 ± 54*	**0.008**	0.77	0.13
BNP, ng/L	≤ 35	16 ± 12	6 ± 2	14 ± 13	6 ± 2	12 ± 11	6 ± 2	0.06	0.38	0.07
Renin, ng/L	2.0-25.0	15 ± 17	39 ± 20*	16 ± 12	43 ± 18*	13 ± 10	38 ± 14*	**0.0001**	0.43	0.85
Leptin, ng/ml	1.2-9.5	1.49 ± 1.39	2.75 ± 3.09	2.00 ± 2.09	2.46 ± 2.37	1.71 ± 1.68	2.38 ± 2.21	0.13	0.8	0.35
Fasting glucose, mmol/L	4.1-6.1	5.0 ± 0.4	5.0 ± 0.2	4.9 ± 0.4	4.7 ± 0.3	4.8 ± 0.4	4.8 ± 0.4	0.15	0.24	0.8
Fasting insulin, μU/ml	5.0-25.0	4.3 ± 0.9	5.9 ± 1.7	4.4 ± 1.9	6.2 ± 1.9*	4.1 ± 1.6	5.2 ± 1.1	**0.005**	0.4	0.7
HOMA- IR	< 2	0.97 ± 0.22	1.29 ± 0.36	0.98 ± 0.50	1.29 ± 0.36	0.89 ± 0.38	1.11 ± 0.26	**0.005**	0.06	0.99
Proteins, g/L	65-80	64 ± 8	68 ± 4	63 ± 8	64 ± 8	64 ± 5	63 ± 6	0.33	0.73	0.21
Albumin, g/L	35-50	40 ± 2	42 ± 2	40 ± 5	40 ± 5	40 ± 2	39 ± 3	0.71	0.87	0.17
Urea, mmol/L	2.7-7.9	4.1 ± 0.4	4.9 ± 0.2*	4.1 ± 0.2	4.9 ± 0.4*	4.2 ± 0.8	6.4 ± 0.9*#	**0.001**	**0.005**	**0.0001**
Creatinine, μmol/L	65-105	79 ± 7	86 ± 9*	78 ± 9	83 ± 12*	76 ± 9	82 ± 8*	**0.004**	0.47	0.82
Na^+, mmol/L	135-145	138 ± 5	141 ± 3	139 ± 5	139 ± 7	139 ± 4	136 ± 6	0.74	0.62	0.24
Cl^-, mmol/L	95-105	102 ± 3	103 ± 2	101 ± 3	102 ± 4	102 ± 4	99 ± 5	0.37	0.34	0.13
K^+, mmol/L	3.5-5.0	4.0 ± 0.3	3.9 ± 0.2	4.0 ± 0.4	3.9 ± 0.3	4.0 ± 0.2	4.0 ± 0.4	0.38	0.62	0.67
Total CO_2, mmol/L	23-29	25 ± 2	26 ± 1	24 ± 3	26 ± 2	25 ± 1	26 ± 1	0.054	0.45	0.98
Cholesterol, mmol/L	3.9-5.1	4.4 ± 0.6	4.0 ± 0.6*	4.6 ± 0.7	3.8 ± 0.7*	4.8 ± 0.8#	3.8 ± 0.8*	**0.004**	0.97	**0.01**
HDL, mmol/L	0.9-2.3	1.2 ± 0.2	1 ± 0.2*	1.2 ± 0.3	0.9 ± 0.2*	1.2 ± 0.2	0.9 ± 0.2*	**0.001**	0.95	0.22
LDL, mmol/L	< 4.1	2.8 ± 0.3	2.6 ± 0.4	2.9 ± 0.4	2.4 ± 0.5*	3.0 ± 0.6	2.4 ± 0.6*	**0.006**	0.92	0.12
Triglycerides, mmol/L	0.3-2.3	1.10 ± 0.47	1.05 ± 0.31	1.16 ± 0.46	1.05 ± 0.41	1.28 ± 0.73	0.88 ± 0.21	0.17	0.8	0.09

*Values are mean ± SD; BR*CM, bedrest*countermeasure. *p < 0.05 vs. Before; #p < 0.05 vs. Control. Significant differences are bolded.*

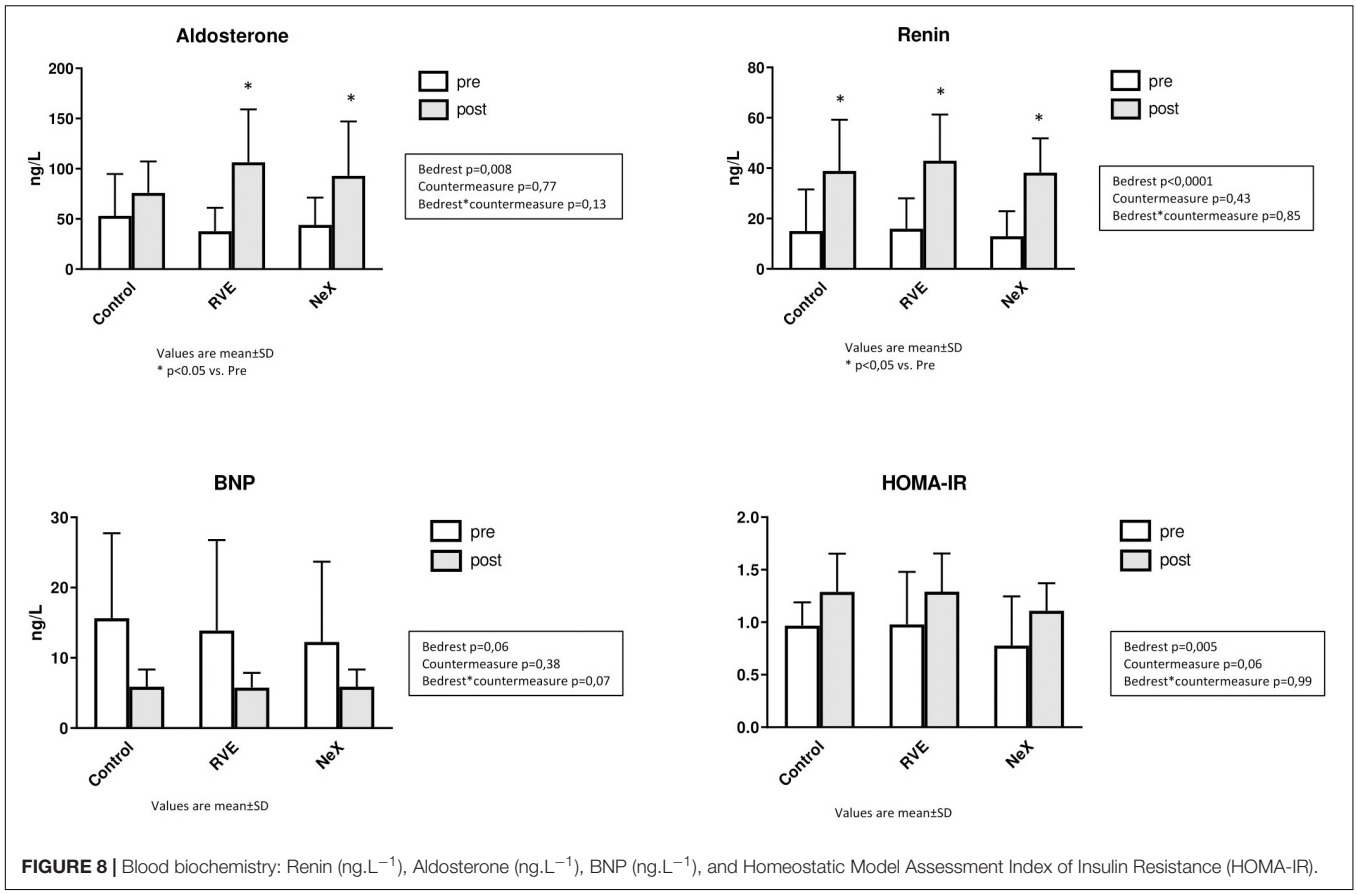

FIGURE 8 | Blood biochemistry: Renin (ng.L^{-1}), Aldosterone (ng.L^{-1}), BNP (ng.L^{-1}), and Homeostatic Model Assessment Index of Insulin Resistance (HOMA-IR).

of branched chain amino acids to the protein supplementation might also help maintaining left and right ventricle masses, as previously demonstrated during a long term bed-rest in women in the WISE study (Dorfman et al., 2007).

This study has two novel findings: first, while a small reduction in GCS was seen with LBNP, a similar reduction was not seen after bedrest. A decrease in GCS with gravitational stress has been shown before, and if cardiac adaptation to bedrest is solely due to loss of PV and cardiac preload, a similar reduction would be expected (Negishi et al., 2017). Yet, the reduction in GCS is limited to LBNP, suggesting that the actual twisting deformation of the heart is preserved despite its reduction in size. Second, cardiac untwisting has been shown to slow after bedrest, as assessed by MRI tagged analysis, but the cardiac response to orthostatic stress was unknown (Dorfman et al., 2008). In our study, we found no difference in the untwisting deformation (GCSR-E) with bedrest, but found a significant increase during orthostatic stress. This increase was likely a result of the higher HR and sympathetic activation increasing contractility (Fredholm et al., 2017). Yet the deconditioned heart was able to mount an appropriate deformation to maintain adequate, if slightly decreased, cardiac output. Both these findings would suggest the deformation of the heart adapts to preserve systolic and diastolic function during bedrest. While both torsion and circumferential strain aim to assess similar cardiac motion, the resulting measure (twisting/untwisting and deformation, respectively) are not interchangeable, and to our knowledge have not been directly compared. Thus, it remains unknown if the slowed untwisting demonstrated by Dorfman et al. (2008) and the increased deformation rate in our study are compatible findings, particularly since our finding occurred during orthostatic stress.

VO_2max

The decreased VO2max in CON ($-17 \pm 13\%$) compared to pre HDBR levels is in line with previous studies of similar duration. A decrease of 1% per day until 30 days of HDBR is usually observed in absence of CM (Convertino, 1996; Watenpaugh et al., 2000), although a smaller reduction of 0.3% per day is reported by Ried-Larsen et al. in a recent meta-analysis (Ried-Larsen et al., 2017).

Interestingly the decrease in VO_2max tended to be alleviated in RVE and NeX groups (respectively $-4 \pm 8\%$ and $-7 \pm 12\%$, interaction $p = 0.09$), although the frequency and duration of training was quite low, e.g., 2 sessions per week with a total of 5 sessions along the 21 days of BR. Each exercise session lasted about 30 min, but the cumulative loading duration did not exceed 5–6 min. During the 1st Berlin BR, this high load RVE achieved lactate levels after exercise of 9–10 mmol/l, attesting to the high level of intensity (Rittweger et al., 2006). This intensity was accomplished by increasing

progressively the load from 1.3 to 1.8 BW, and the frequency of vibration from 19 to 26 Hz at the end of BR. The relative protection of VO_2max during this study suggests that this high intensity resistive exercise has additional benefit to the musculoskeletal gains seen in previous studies (Mulder et al., 2006; Armbrecht et al., 2010). Considering the marked decreases in PV and LV volumes evidenced in this study, the lower VO_2max decrease in RVE and NeX might still represent a true finding despite the absence of a significant interaction effect, but studies with a larger sample size would be required to confirm this.

Considering those results in a whole, it is clear that the RVE countermeasure two times a week, alone or combined with whey protein supplementation, did not have any significant effect on most of the cardiovascular changes induced by 21 days of HDBR.

Regarding our cardiovascular variables, supplementation in whey protein did not show any benefit, except for a potential effect on cardiac mass as mentioned above. Conversely, some positive impact on muscle was observed before: whey protein supplementation alone alleviated disuse-induced reduction in fiber oxidative capacity during a 21-days HDBR (Bosutti et al., 2016) even if it did not attenuate lower limb muscle atrophy nor fiber type transition (Blottner et al., 2014). Furthermore, Owen et al. have recently shown in the same MNX bed rest, a reduction in paralumbar spinal atrophy with NeX countermeasure but not RVE alone (Owen et al., 2020).

Though RVE did not prevent cardiovascular deconditioning in this study, it does not preclude the interest of high intensity resistive training. Hastings et al., with a daily rowing exercise and biweekly strength training, prevented myocardial changes and maintained OT with an added oral volume load (Hastings et al., 2012). When a high intensity exercise provides a high loading impact, for example with plyometric exercises like series of jumps, noteworthy beneficial effects on bone and some aspects of the cardiovascular system are observed. During a 60-day-HDBR, a jump countermeasure consisting of 5–6 sessions per week, each session lasting 8–17 min, maintained bone mass and maximal muscle force (Kramer et al., 2017a) and also preserved resting HR and peak oxygen consumption (Kramer et al., 2017b), two major criteria of cardiovascular deconditioning. Nevertheless in this latter study the decrease in PV was not prevented (Kramer et al., 2017a), and neither OT nor cardiac mass and volumes were assessed. Integration of this jumping countermeasure with other ones especially effective on cardiac and vascular deconditioning, such as artificial gravity or LBNP, may be of further interest.

LIMITATIONS

This study has several limitations that are worth noting: First, the sample size in our study was limited to 8 subjects who completed testing. While the crossover design allowed to reduce confounding covariates, we have "lost" 4 subjects out of 12, with unfortunately the withdrawal of 3 subjects in the NeX group during the 3rd campaign. There were potential effects of the countermeasures that did not reach conventional level of significance, namely cardiac mass and VO_2max. Second, the duration and frequency of exercise were reduced compared to prior studies. This was done to assess the effect of twice weekly exercise, but likely limited the impact of the countermeasures. The only effects that a longer or larger study may clarify are the impact of countermeasures on VO_2max and cardiac mass discussed above. Third, our study only included males and thus may not be generalizable to females undergoing spaceflight or bedrest. Finally, cardiac torsion and untwisting could not be assessed and thus our results are not directly comparable to prior studies that showed slowed untwisting after bedrest. We substituted it by circumferential strain and found no impact of countermeasures.

CONCLUSION

During this 21-day HDBR RVE and NeX countermeasures did not limit losses in PV, OT and cardiac volumes. RVE and NeX might alleviate VO_2max loss, and whey protein supplementation might be beneficial on myocardial mass but this would require further studies with larger sample size. Despite the reduction in left ventricle volumes during bedrest, deformation of the heart assessed by GCS was preserved and untwisting deformation was enhanced during orthostatic stress, illustrating the ability of the deconditioned heart to preserve systolic and diastolic functions.

DATA AVAILABILITY STATEMENT

The datasets generated for this study are available on request to the corresponding author.

ETHICS STATEMENT

This study was reviewed and approved by French Health Authorities (Comité de Protection des Personnes Sud-Ouest Outre-Mer I). The subjects provided their written informed consent to participate in this study.

AUTHOR CONTRIBUTIONS

PG designed the study, acquired and analyzed the data, and wrote the manuscript. JM analyzed MRI data, wrote and reviewed the manuscript. MB acquired MRI data and reviewed the manuscript. FL performed and analyzed biochemical data and reviewed the manuscript. M-PB designed the study and acquired data. M-AC designed the study, acquired and analyzed the data and reviewed the manuscript. AP-L acquired data and reviewed the manuscript. BL designed the study, analyzed MRI data and reviewed the manuscript. NN designed the study, analyzed data, performed statistical analysis and reviewed the manuscript. All authors contributed to the article and approved the submitted version.

FUNDING

This experiment was proposed and sponsored by the European Space Agency (ESA) and the French Spatial Agency (CNES). In addition, the authors have been supported by their respective research organizations.

ACKNOWLEDGMENTS

This study was performed at MEDES (Toulouse, France). We acknowledge the dedication and time of the participants in this study. We would also like to thank all the staff at MEDES Institute for Space Medicine and Physiology (Toulouse, France), and particularly A. Beck, for the medical supervision throughout the study.

SUPPLEMENTARY MATERIAL

The Supplementary Material for this article can be found online at: https://www.frontiersin.org/articles/10.3389/fphys.2020.00812/full#supplementary-material

REFERENCES

Armbrecht, G., Belavı, D. L., Gast, G., Bongrazio, M., Touby, F., Beller, G., et al. (2010). Resistive vibration exercise attenuates bone and muscle atrophy in 56 days of bed rest: biochemical markers of bone metabolism. *Osteoporos. Int.* 21, 597–607. doi: 10.1007/s00198-009-0985-z

Belavy, D. L., Armbrecht, G., Gast, U., Richardson, C. A., Hides, J. A., and Felsenberg, D. (2010a). Countermeasures against lumbar spine deconditioning in prolonged bed rest: resistive exercise with and without whole body vibration. *J. Appl. Physiol.* 109, 1801–1811. doi: 10.1152/japplphysiol.00707.2010

Belavy, D. L., Bock, O., Börst, H., Armbrecht, G., Gast, U., Degner, C., et al. (2010b). The 2nd Berlin BedRest Study: protocol and implementation. *J. Musculoskelet. Neuronal. Interact.* 10, 207–219.

Belavy, D. L., Beller, G., Armbrecht, G., and Perschel, F. H. (2011). Fitzner Evidence for an additional effect of whole-body vibration above resistive exercise alone in preventing bone loss during prolonged bed rest. *Osteoporos. Int.* 22, 1581–1591. doi: 10.1007/s00198-010-1371-6

Belavy, D. L., Hides, J. A., Wilson, S. J., Stanton, W., Dimeo, F. C., Rittweger, J., et al. (2008). Resistive simulated weightbearing exercise with whole body vibration reduces lumbar spine deconditioning in bed-rest. *Spine* 33, E121–E131. doi: 10.1097/BRS.0b013e3181657f98

Belavy, D. L., Miokovic, T., Armbrecht, G., Rittweger, J., and Felsenberg, D. (2009). Resistive vibration exercise reduces lower limb muscle atrophy during 56-day bed-rest. *J. Musculoskelet. Neuronal Interact.* 9, 225–235.

Belin de Chantemele, E., Blanc, S., Pellet, N., Duvareille, M., Ferretti, G., and Gauquelin-Koch, G. (2004). Does resistance exercise prevent body fluid changes after a 90-day bed rest? *Eur. J. Appl. Physiol.* 92, 555–564.

Bleeker, M. W., De Groot, P. C., Rongen, G. A., Rittweger, J., Felsenberg, D., Smits, P., et al. (2005). Vascular adaptation to deconditioning and the effect of an exercise countermeasure: results of the Berlin Bed Rest study. *J. Appl. Physiol.* 99, 1293–1300. doi: 10.1152/japplphysiol.00118.2005

Blottner, D., Bosutti, A., Degens, H., Schiffl, G., Gutsmann, M., and Buehlmeier, J. (2014). Whey protein plus bicarbonate supplement has little effects on structural atrophy and proteolysis marker immunopatterns in skeletal muscle disuse during 21 days of bed rest. *J. Musculoskelet. Neuronal Interact.* 14, 432–444.

Blottner, D., Salanova, M., Puttmann, B., Schiffl, G., Felsenberg, D., Buehring, B., et al. (2006). Human skeletal muscle structure and function preserved by vibration muscle exercise following 55 days of bed rest. *Eur. J. Appl. Physiol.* 97, 261–271. doi: 10.1007/s00421-006-0160-6

Bosutti, A., Salanova, M., Blottner, D., Buehlmeier, J., Mulder, E., Rittweger, J., et al. (2016). Whey protein with potassium bicarbonate supplement attenuates the reduction in muscle oxidative capacity during 19 days of bed rest. *J. Appl. Physiol.* 121, 838–848. doi: 10.1152/japplphysiol.00936.2015

Bungo, M. W., Charles, J. B., and Johnson, P. C. (1985). Cardiovascular deconditioning during space flight and the use of saline as a countermeasure to orthostatic intolerance. *Aviat. Space Environ. Med.* 56, 985–990.

Butler, G. C., Xing, H. C., Northey, D. R., and Hughson, R. L. (1991). Reduced orthostatic tolerance following 4 h head-down tilt. *Eur. J. Appl. Physiol. Occup. Physiol.* 62, 26–30. doi: 10.1007/bf00635629

Carrick-Ranson, G., Hastings, J. L., Bhella, P. S., Shibata, S., and Levine, B. D. (2013). The effect of exercise training on left ventricular relaxation and diastolic suction at rest and during orthostatic stress after bed rest. *Exp. Physiol.* 98, 501–513. doi: 10.1113/expphysiol.2012.067488

Chale, A., Cloutier, G. J., Hau, C., Phillips, E. M., Dallal, G. E., and Fielding, R. A. (2013). Efficacy of whey protein supplementation on resistance exercise-induced changes in lean mass, muscle strength, and physical function in mobility-limited older adults. *J. Gerontol. A Biol. Sci. Med. Sci.* 68, 682–690. doi: 10.1093/gerona/gls221

Chen, H. H., and Burnett, J. C. (2006). Therapeutic potential for existing and novel forms of natriuretic peptides. *Heart Fail Clin.* 2, 365–373. doi: 10.1016/j.hfc.2006.09.003

Claus, P., Omar, A. M. S., Pedrizzetti, G., Sengupta, P. P., and Nagel, E. (2015). Tissue tracking technology for assessing cardiac mechanics: principles, normal values, and clinical applications. *JACC Cardiovasc. Imaging* 8, 1444–1460. doi: 10.1016/j.jcmg.2015.11.001

Convertino, V. (1996). "Exercise and adaptation to microgravity environments," in *Handbook of Physiology: Section 4. Environmental Physiology*, Vol. 3, eds M. J. Fregly and C. M. Blatteis (New York, NY: Oxford University), 815–843.

Convertino, V. A. (1994). Countermeasures against cardiovascular deconditioning. *J. Gravit. Physiol.* 1, 125–128.

Coupé, M., Yuan, M., Demiot, C., Bai, Y. Q., Jiang, S. Z., Li, Y. Z., et al. (2011). Low-magnitude whole body vibration with resistive exercise as a countermeasure against cardiovascular deconditioning after 60 days of head-down bed rest. *Am. J. Physiol. Regul. Integr. Comp. Physiol.* 301, R1748–R1754.

Csecs, I., Czimbalmos, C., Suhai, F. I., Mikle, R., Mirzahosseini, A., Dohy, Z., et al. (2018). Left and right ventricular parameters corrected with threshold-based quantification method in a normal cohort analyzed by three independent observers with various training-degree. *Int. J. Cardiovasc. Imaging* 34, 1127–1133. doi: 10.1007/s10554-018-1322-4

Custaud, M. A., de Souza, E. P., Abry, P., Flandrin, P., Millet, C., Duvareille, M., et al. (2002). Orthostatic tolerance and spontaneous baroreflex sensitivity in men versus women after 7 days of head-down bed rest. *Auton. Neurosci.* 100, 66–76. doi: 10.1016/s1566-0702(02)00132-7

Cvirn, G., Waha, J. E., Ledinski, G., Schlagenhauf, A., Leschnik, B., and Koestenberger, M. (2015). Bed rest does not induce hypercoagulability. *Eur. J. Clin. Invest.* 45, 63–69. doi: 10.1111/eci.12383

Dorfman, T. A., Levine, B. D., Tillery, T., Peshock, R. M., Hastings, J. L., and Schneider, S. M. (2007). Cardiac atrophy in women following bed rest. *J. Appl. Physiol.* 103, 8–16. doi: 10.1152/japplphysiol.01162.2006

Dorfman, T. A., Smith, S. M., Watenpaugh, D. E., and Hargens, A. R. (2008). Diastolic suction is impaired by bed rest: MRI tagging studies of diastolic untwisting. *J. Appl. Physiol.* 104, 1037–1044. doi: 10.1152/japplphysiol.00858.2006

Fagard, R. H. (2006). Exercise is good for your blood pressure: effects of endurance training and resistance training. *Clin. Exp. Pharmacol. Physiol.* 33, 853–856. doi: 10.1111/j.1440-1681.2006.04453.x

Fortney, S. M., Beckett, W. S., Carpenter, A. J., Davis, J., Drew, H., and LaFrance, N. D. (1988). Changes in plasma volume during bed rest: effects of menstrual cycle and estrogen administration. *J. Appl. Physiol.* 65, 525–533. doi: 10.1152/jappl.1988.65.2.525

Fortney, S. M., Turner, C., Steinmann, L., Driscoll, T., and Alfrey, C. (1994). Blood volume responses of men and women to bed rest. *J. Clin. Pharmacol.* 34, 434–439. doi: 10.1002/j.1552-4604.1994.tb04984.x

Fredholm, M., Rock, J. A., Tankersley, C. G., and Vroman, N. B. (2017). Load-dependence of myocardial deformation variables - a clinical strain-echocardiographic study. *Acta Anaesthesiol. Scand.* 61, 1155–1165. doi: 10.1111/aas.12954

Gast, U., John, S., Runge, M., Rawer, R., Felsenberg, D., and Belavı, D. L. (2012). Short-duration resistive exercise sustains neuromuscular function after bed rest. *Med. Sci. Sports Exerc.* 44, 1764–1772. doi: 10.1249/mss.0b013e318256b53b

Gharib, C., Bansard, J. Y., Hargens, A. R., and Hughson, R. L. (1993). "Fluid and electrolytes regulation in space," in *Advances in Space Biology and Medicine*, Vol. 2, ed. S. L. Bontings (Greenwich: JAI Press Inc), 113–130. doi: 10.1016/s1569-2574(08)60019-2

Gharib, C., Maillet, A., Gauquelin, G., Allevard, A. M., Güell, A., Cartier, R., et al. (1992). Results of a 4-week head-down tilt with and without LBNP countermeasure: I. Volume regulating hormones. *Aviat. Space Environ. Med.* 63, 3–8.

Gladwell, V. F., and Coote, J. H. (2002). Heart rate at the onset of muscle contraction and during passive muscle stretch in humans: a role for mechanoreceptors. *J. Physiol.* 540, 1095–1102. doi: 10.1113/jphysiol.2001.013486

Graf, S., Baecker, N., Buehlmeier, J., Annelie, F., Scott, M., Smith, M., et al. (2014). "Effects of resistive vibration exercise combined with whey protein and KHCO3 on bone thurnover markers in head-down tilt bed rest (MTBR-MNX Study)," in *Proceedings of the Aerospace Medicine Conference paper*, (Paris: International Astronautical Federation).

Graf, S., Egert, S., and Heer, M. (2011). Effects of whey protein supplements on metabolism: evidence from human intervention studies. *Curr. Opin. Clin. Nutr. Metab. Care* 14, 569–580. doi: 10.1097/mco.0b013e32834b89da

Greaves, D., Arbeille, P., Guillon, L., Zuj, K., and Caiani, E. G. (2019). Effects of exercise countermeasure on myocardial contractility measured by 4D speckle tracking during a 21-day head-down bed rest. *Eur. J. Appl. Physiol.* 119, 2477–2486. doi: 10.1007/s00421-019-04228-0

Guinet, P., Schneider, S. M., Macias, B. R., Watenpaugh, D. E., Hughson, R. L., and Le Traon, A. P. (2009). WISE-2005: effect of aerobic and resistive exercises on orthostatic tolerance during 60 days bed rest in women. *Eur. J. Appl. Physiol.* 106, 217–227. doi: 10.1007/s00421-009-1009-6

Hargens, A. R., and Vico, L. (2016). Long-duration bed rest as an analog to microgravity. *J. Appl. Physiol.* 120, 891–903. doi: 10.1152/japplphysiol.00935.2015

Hastings, J. L., Krainski, F., Snell, P. G., Pacini, E. L., Jain, M., and Bhella, P. S. (2012). Effect of rowing ergometry and oral volume loading on cardiovascular structure and function during bed rest. *J. Appl. Physiol.* 112, 1735–1743. doi: 10.1152/japplphysiol.00019.2012

Hor, K. N., Gottliebson, W. M., Carson, C., Wash, E., Cnota, J., Fleck, R., et al. (2010). Comparison of magnetic resonance feature tracking for strain calculation with harmonic phase imaging analysis. *JACC Cardiovasc. Imaging* 3, 144–151. doi: 10.1016/j.jcmg.2009.11.006

Kenny, H. C., Rudwill, F., Breen, L., Salanova, M., Blottner, D., Heise, T., et al. (2017). Bed rest and resistive vibration exercise unveil novel links between skeletal muscle mitochondrial function and insulin resistance. *Diabetologia* 60, 1491–1501. doi: 10.1007/s00125-017-4298-z

Kermorgant, M., Nasr, N., Custaud, M. A., Navasiolava, N., Arbeille, P., Guinet, P., et al. (2019). Effects of resistance exercise and nutritional supplementation on dynamic cerebral autoregulation in head-down bed rest. *Front. Physiol.* 10:1114. doi: 10.3389/fphys.2019.01114

Khan, M. H., Kunselman, A. R., Leuenberger, U. A., Davidson, W. R., Ray, C. A., Gray, K. S., et al. (2002). Attenuated sympathetic nerve responses after 24 hours of bed rest. *Am. J. Physiol. Heart Circ. Physiol.* 282, H2210–H2215.

Kramer, A., Gollhofer, A., Armbrecht, G., Felsenberg, D., and Gruber, M. (2017a). How to prevent the detrimental effects of two months of bed-rest on muscle, bone and cardiovascular system: an RCT. *Sci Rep.* 7:13177.

Kramer, A., Kümmel, J., Mulder, E., Gollhofer, A., Frings-Meuthen, P., and Gruber, M. (2017b). High-intensity jump training is tolerated during 60 days of bed rest and is very effective in preserving leg power and lean body mass: an overview of the cologne RSL study. *PLoS One* 12:e0169793. doi: 10.1371/journal.pone.0169793

Lee, S. M. C., Feiveson, A. H., Stein, S., Stenger, M. B., and Platts, S. H. (2015). Orthostatic intolerance after ISS and space shuttle missions. *Aerosp. Med. Hum. Perform.* 86, A54–A67.

Lee, S. M. C., Schneider, S. M., Feiveson, A. H., Macias, B. R., Smith, S. M., and Watenpaugh, D. E. (2014). WISE-2005: countermeasures to Prevent Muscle Deconditioning During Bed Rest in Women. *J. Appl. Physiol.* 116, 654–667. doi: 10.1152/japplphysiol.00590.2013

Levine, B. D., Lane, L. D., Watenpaugh, D. E., Gaffney, F. A., Buckey, J. C., and Blomqvist, C. G. (1996). Maximal exercise performance after adaptation to microgravity. *J. Appl. Physiol.* 81, 686–694. doi: 10.1152/jappl.1996.81.2.686

Levine, B. D., Zuckerman, H., and Pawelczyk, J. A. (1997). Cardiac atrophy after bed-rest deconditioning: a nonneural mechanism for orthostatic intolerance. *Circulation* 96, 517–525. doi: 10.1161/01.cir.96.2.517

Lunning, M. A., Kutty, S., Rome, E. T., Li, L., Padiyath, A., Loberiza, F., et al. (2015). Cardiac magnetic resonance imaging for the assessment of the myocadium following doxorubicin-based chemotherapy. *Am. J. Clin. Oncol.* 38, 377–381. doi: 10.1097/coc.0b013e31829e19be

Maillet, A., Fagette, S., Allevard, A. M., Pavy-Le Traon, A., Guell, A., and Gharib, C. (1996). Cardiovascular and hormonal response during a 4-week head-down tilt with and without exercise and LBNP countermeasures. *J. Gravit. Physiol.* 3, 37–48.

Miokovic, T., Armbrecht, G., Felsenberg, D., and Belavy, D. L. (2011). Differential atrophy of the postero-lateral hip musculature during prolonged bedrest and the influence of exercise countermeasures. *J. Appl. Physiol.* 110, 926–934. doi: 10.1152/japplphysiol.01105.2010

Mulavara, A. P., Peters, B. T., Miller, C. A., Kofman, I. S., Reschke, M. F., Taylor, L. C., et al. (2018). Physiological and functional alterations after spaceflight and bed rest. *Med. Sci. Sports Exerc.* 50, 1961–1980. doi: 10.1249/mss.0000000000001615

Mulder, E. R., Stegeman, D. F., Gerrits, K. H., Paalman, M. I., Rittweger Felsenberg, D., et al. (2006). Strength, size and activation of knee extensors followed during 8 weeks of horizontal bed rest and the influence of a countermeasure. *Eur. J. Appl. Physiol.* 97, 706–715. doi: 10.1007/s00421-006-0241-6

Negishi, K., Borowski, A. G., Popoviæ, Z. B., Greenberg, N. L., Martin, D. S., and Bungo, M. W. (2017). Effect of gravitational gradients on cardiac filling and performance. *J. Am. Soc. Echocardiogr.* 30, 1180–1188. doi: 10.1016/j.echo.2017.08.005

Nishikimi, T., Maeda, N., and Matsuoka, H. (2006). The role of natriuretic peptides in cardioprotection. *Cardiovasc. Res.* 69, 318–328. doi: 10.1016/j.cardiores.2005.10.001

Norsk, P., Drummer, C., Röcker, L., Strollo, F., Christensen, N. J., Warberg, J., et al. (1995). Renal and endocrine responses in humans to isotonic saline infusion during microgravity. *J. Appl. Physiol.* 78, 2253–2259. doi: 10.1152/jappl.1995.78.6.2253

Ogawa, T., and de Bold, A. J. (2012). Brain natriuretic Peptide production and secretion in inflammation. *J. Transplant. Epub* 2012:28.

Owen, P. J., Ambrecht, G., Bansmann, M., Zange, J., Pohle-Fröhlich, R., Felsenberg, D., et al. (2020). Whey protein supplementation with vibration exercise ameliorates lumbar paraspinal muscle atrophy in prolonged bed-rest. *J. Appl. Physiol.* 128, 1568–1578. doi: 10.1152/japplphysiol.00125.2020

Paddon-Jones, D., Sheffield-Moore, M., Zhang, X. J., Volpi, E., Wolf, S. E., Aarsland, A., et al. (2004). Amino acid ingestion improves muscle protein synthesis in the young and elderly. *Am. J. Physiol. Endocrinol. Metab.* 286, E321-E328. doi: 10.1152/ajpendo.00368.2003

Pagani, M., Lombardi, F., Guzzetti, S., Rimoldi, O., Furlan, R., Pizzinelli, P., et al. (1986). Power spectral analysis of heart rate and arterial pressure variabilities as a marker of sympatho-vagal interaction in man and conscious dog. *Circ. Res.* 59, 178–193. doi: 10.1161/01.res.59.2.178

Pancheva, M. V., Panchev, V. S., and Suvandjieva, A. V. (2006). Lower body negative pressure vs. lower body positive pressure to prevent cardiac atrophy after bed rest and spaceflight. What caused the controversy?. *J. Appl. Physiol.* 100, 1091–1092.

Pastushkova, LKh, Custaud, M. A., Kononikhin, A. S., Brzhozovsky, A. G., Dmitrieva, L. E., and Dobrokhotov, I. V. (2015). Modification of urine proteome in healthy human during 21-day bed rest. *Aviakosm. Ekolog. Med.* 49, 11–16.

Pavy-Le Traon, A., Heer, M., Narici, M. V., Rittweger, J., and Vernikos, J. (2007). From space to Earth: advances in human physiology from 20 years of bed rest

studies (1986–2006). *Eur. J. Appl. Physiol.* 101, 143–194. doi: 10.1007/s00421-007-0474-z

Pennings, B., Boirie, Y., Senden, J. M., Gijsen, A. P., Kuipers, H., and van Loon, L. J. (2011). Whey protein stimulates postprandial muscle protein accretion more effectively than do casein and casein hydrolysate in older men. *Am. J. Clin. Nutr.* 93, 997–1005. doi: 10.3945/ajcn.110.008102

Perhonen, M. A., Franco, F., Lane, L. D., Buckey, J. C., Blomqvist, C. G., Zerwekh, J. E., et al. (2001). Cardiac atrophy after bed rest and spaceflight. *J. Appl. Physiol.* 91, 645–653. doi: 10.1152/jappl.2001.91.2.645

Phillips, B. E., Hill, D. S., and Atherton, P. J. (2012). Regulation of muscle protein synthesis in humans. *Curr. Opin. Clin. Nutr. Metab. Care* 15, 58–63. doi: 10.1097/mco.0b013e32834d19bc

Ploutz-Snyder, L. L., Downs, M., Goetchius, E., Crowell, B., English, K. L., Ploutz-Snyder, R., et al. (2018). Exercise training mitigates multisystem deconditioning during bed rest. *Med. Sci. Sports Exerc.* 50, 1920–1928. doi: 10.1249/mss.0000000000001618

Ried-Larsen, M., Aarts, H. M., and Joyner, M. J. (2017). Effects of strict prolonged bed rest on cardiorespiratory fitness: systematic review and meta-analysis. *J. Appl. Physiol.* 123, 790–799. doi: 10.1152/japplphysiol.00415.2017

Rittweger, J., Albracht, K., Flück, M., Ruoss, S., Brocca, L., Longa, E., et al. (2018). Sarcolab pilot study into skeletal muscle's adaptation to long-term spaceflight. *NPJ Microgravity* 4:18.

Rittweger, J., Belavy, D., Hunek, P., Gast, U., Boerst, H., Feilcke, B., et al. (2006). Highly demanding resistive vibration exercise program is tolerated during 56 days of strict bed-rest. *Int. J. Sports Med.* 27, 553–559. doi: 10.1055/s-2005-872903

Rittweger, J., Beller, G., Armbrecht, G., Mulder, E., Buehring, B., Gast, U., et al. (2010). Prevention of bone loss during 56 days of strict bed rest by side-alternating resistive vibration exercise. *Bone* 46, 137–147. doi: 10.1016/j.bone.2009.08.051

Schmidt, W., and Prommer, N. (2005). The optimised CO-rebreathing method: a new tool to determine total haemoglobin mass routinely. *Eur. J. Appl. Physiol.* 95, 486–495. doi: 10.1007/s00421-005-0050-3

Schulz-Menger, J., Bluemke, D. A., Bremerich, J., Flamm, S. D., Fogel, M. A., Friedrich, M. G., et al. (2013). Standardized image interpretation and post processing in cardiovascular magnetic resonance: Society for Cardiovascular Magnetic Resonance (SCMR) board of trustees task force on standardized post processing. *J. Cardiovasc. Magn. Reson.* 15:35.

Shibata, S. M., and Perhonen, B. D. (2010). Supine cycling plus volume loading prevent cardiovascular deconditioning during bed rest. *J. Appl. Physiol.* 108, 1177–1186. doi: 10.1152/japplphysiol.01408.2009

Tank, J., Diedrich, A., Szczech, E., Luft, F. C., and Jordan, J. (2004). 2-Adrenergic transmission and human baroreflex regulation. *Hypertension* 43, 1035–1041. doi: 10.1161/01.hyp.0000125729.90521.94

Task Force, A., Esc, and Asc. (1996). European Society of Cardiology and the North American Society of Pacing and Electrophysiology. Heart rate variability: standards of measurement, physiological interpretation, and clinical use. *Circulation* 93, 1043–1065. doi: 10.1161/01.cir.93.5.1043

Traon, A. P., Vasseur, P., Arbeille, P., Guell, A., Bes, A., and Gharib, C. (1995). Effects of 28-day head-down tilt with and without countermeasures on lower body negative pressure responses. *Aviat. Space Environ. Med.* 66, 982–991.

Trappe, T. A., Burd, N. A., Louis, E. S., Lee, G. A., and Trappe, S. W. (2007). Influence of Concurrent Exercise or Nutrition Countermeasures on Thigh and Calf Muscle Size and Function During 60 Days of Bed Rest in Women. *Acta Physiol.* 191, 147–159. doi: 10.1111/j.1748-1716.2007.01728.x

van Duijnhoven, N. T., Green, D. J., Felsenberg, D., Belavy, D. L., Hopman, M. T., and Thijssen, D. H. (2010a). Impact of bed rest on conduit artery remodeling: effect of exercise countermeasures. *Hypertension* 56, 240–246. doi: 10.1161/hypertensionaha.110.152868

van Duijnhoven, N. T., Thijssen, D. H., Green, D. J., Felsenberg, D., Belavy, D. L., and Hopman, M. T. (2010b). Resistive exercise versus resistive vibration exercise to counteract vascular adaptations to bed rest. *J. Appl. Physiol.* 108, 28–33. doi: 10.1152/japplphysiol.00760.2009

Waha, J. E., Goswami, N., Schlagenhauf, A., Leschnik, B., Koestenberger, M., Reibnegger, G., et al. (2015). Effects of exercise and nutrition on the coagulation system during bedrest immobilization. *Medicine* 94:e1555. doi: 10.1097/md.0000000000001555

Watenpaugh, D. E., Ballard, R. E., Schneider, S. M., Lee, S. M., Ertl, A. C., and William, J. M. (2000). Supine lower body negative pressure exercise during bed rest maintains upright exercise capacity. *J. Appl. Physiol.* 89, 218–227. doi: 10.1152/jappl.2000.89.1.218

Wesseling, K. H., Jansen, J. R., Settels, J. J., and Schreuder, J. J. (1993). Computation of aortic flow from pressure in humans using a nonlinear, three-element model. *J. Appl. Physiol.* 74, 2566–2573. doi: 10.1152/jappl.1993.74.5.2566

Zwart, S. R., Davis-Street, J. E., Paddon-Jones, D., Ferrando, A. A., Wolfe, R. R., and Smith, S. M. (2005). Amino acid supplementation alters bone metabolism during simulated weightlessness. *J. Appl. Physiol.* 99, 134–140. doi: 10.1152/japplphysiol.01406.2004

Conflict of Interest: The authors declare that the research was conducted in the absence of any commercial or financial relationships that could be construed as a potential conflict of interest.

frontiers in Physiology

DATA REPORT
published: 24 July 2020
doi: 10.3389/fphys.2020.00678

Semiquantitative Proteomic Research of Protein Plasma Profile of Volunteers in 21-Day Head-Down Bed Rest

Daria N. Kashirina[1], Alexander G. Brzhozovskiy[1,2], Ludmila Kh. Pastushkova[1], Alexey S. Kononikhin[1,2], Christoph H. Borchers[2,3], Evgeny N. Nikolaev[2] and Irina M. Larina[1]**

[1] Institute of Biomedical Problems–Russian Federation State Scientific Research Center, Russian Academy of Sciences, Moscow, Russia, [2] CDISE, Skolkovo Institute of Science and Technology, Moscow, Russia, [3] Department Oncology, Faculty of Medicine, McGill University, Montreal, QC, Canada

OPEN ACCESS

Edited by:
François Guerrero, Université de Bretagne Occidentale, France

Reviewed by:
Jochen Zange, Helmholtz Association of German Research Centers (HZ), Germany
Zhili Li, China Astronaut Research and Training Center, China

***Correspondence:**
Evgeny N. Nikolaev
e.nikolaev@skoltech.ru
Irina M. Larina
irina.larina@gmail.com

Specialty section:
This article was submitted to Environmental, Aviation and Space Physiology, a section of the journal Frontiers in Physiology

Received: 31 January 2020
Accepted: 26 May 2020
Published: 24 July 2020

Citation:
Kashirina DN, Brzhozovskiy AG, Pastushkova LK, Kononikhin AS, Borchers CH, Nikolaev EN and Larina IM (2020) Semiquantitative Proteomic Research of Protein Plasma Profile of Volunteers in 21-Day Head-Down Bed Rest. Front. Physiol. 11:678. doi: 10.3389/fphys.2020.00678

Keywords: bed rest, proteomics, label free analysis, blood plasma, resistive vibration exercise

INTRODUCTION

During spaceflight, a complex of spaceflight factors impacts on the human organism (such as radiation, weightlessness, artificial habitat, etc.) causing various adaptive changes to occur in the human body, including changing of gene expression and protein synthesis. Due to certain ethical restrictions and complexity associated with the delivery of biological samples (costliness, lack of free space on board the descent module), there is a relatively small number of the opportunity to study these factors, one of which is a ground-based model experiment such as head-down bed rest (HDBR). HDBR is a ground-based experiment that is widely used to model the microgravity effects of spaceflight. During HDBR, human mobility is limited by strict bed rest; the longitudinal axis of the body is tilted so that the head is below the legs. Under these conditions, interdependent reactions from various body systems occur. It is noted that as a result of this, adaptation mechanisms are activated, in particular of the cardiovascular, endocrine, central nervous, and peripheral nervous systems (Larina et al., 1999; Batchu et al., 2015). The negative effect of HDBR on the cardiovascular system is realized with a decrease in the volume of circulating plasma and redistribution of vasoconstrictor and pressor influences in the vessels of various regions of the body (Baranov et al., 2016). HDBR often leads to orthostatic intolerance. Orthostatic intolerance develops as a result of hypovolemia, increased vasoconstriction response of cerebral vessels, decreased sensitivity to vasoconstrictors of resistance vessels, and decreased myocardial contractility.

For deceleration of the adaptive changes to spaceflight conditions, as well as for the astronaut's organism preparation for the ground conditions, a set of recovery measures and trainings is used, the effectiveness of which can be estimated at the molecular level using the proteomic approach in model experiments. Numerous bed rest studies of various durations have been conducted without or with specific countermeasures, such as exercises and vibrations (Pavy-Le Traon et al., 2007). The studies were mainly aimed at studying changes in the expression of muscle proteins and analyzing of the signaling pathways for proteins changed under the influence of chronic unloading.

It was shown that resistive vibration exercises (RVEs) preserved the mass and diastolic volume of the left ventricle and the contractility of the heart during HDBR (Greaves et al., 2019). It was demonstrated that this countermeasure prevented changes in the autonomic nervous system associated with deconditioning of the cardiovascular system (Coupé et al., 2011), though RVE did not effectively prevent orthostatic intolerance (Coupé et al., 2011).

Nowadays, proteomic methods allow us to expand our understanding of the mechanisms of the adaptive processes occurring under the influence of various extreme conditions. Understanding protein expression is the key to deciphering the mechanisms of action of microgravity and ultimately to finding effective countermeasures to prevent negative changes. Untargeted proteomic approach based on mass spectrometry allows to study a huge amount of proteins in a sample (the dynamic range of plasma protein concentrations is up to 10–11 orders of magnitude) (Wu and Han, 2006) and to find proteins specific for the studied effects.

Moriggi et al. (2010) revealed a substantial downregulation of proteins involved in aerobic metabolism when investigated in biopsies of the calf soleus (SOL) and the vastus lateralis (VL) in a 55-days bed rest experiment. They also showed that proteins involved in anaerobic glycolysis were upregulated when RVE countermeasures were used. Proteomic analysis of biopsy samples from the volunteers of bed rest showed that both RVE and resistive exercise led to a differential regulation of various skeletal muscle proteins (Salanova et al., 2014). RVE has been shown to prevent muscle atrophy and ultrastructural muscle changes in chronic unloading.

Dillon et al. (2019) showed that HDBR led to alterations in the expression and phosphorylation of several metabolic and structural proteins. Inclusion of exercise modulated the proteomic responses toward cellular reorganization.

Salanova et al. (2015) showed that 60 days of bed rest resulted in gene transcription and proteomic changes in the human soleus muscle. These changes were associated with various key metabolic pathways (glycolysis, tricarboxylic acid cycle, oxidative phosphorylation, lipid metabolism) and functional contractile structures. It was demonstrated that RVE countermeasures helped to reduce key signs of maladaptation and atrophy, as well as maintain normal skeletal muscle quality after chronic unloading in bed rest (Salanova et al., 2015). So, the proteomics of muscles have already been studied well, but no one has analyzed proteome changes in the blood. This can provide additional information about changes at the system level.

A blood test using a panoramic proteomic method will help to identify the effects of HDBR in a comprehensive manner, without reference to any one organ or tissue. All tissues are washed with blood, so any physiological changes are reflected in changes in the proteomic composition of the blood. Thus, the aim of the study was to compare proteomic data on the effects of HDBR with or without countermeasures on the human body. To identify protein changes, estimate the rehabilitation measures' effectiveness, and evaluate their contribution at the molecular level, a semiquantitative proteomic analysis of blood plasma samples obtained from eight volunteers who participated in HDBR with and without RVEs was performed.

MATERIALS AND METHODS

Head-Down Bed Rest Design

Eight healthy men (20–45 years old) participated in the experiment with HDBR for 21 days with an angle of inclination of the longitudinal axis of the body relative to the horizontal position of 6°. Volunteers did not suffer from any orthopedic, musculoskeletal, and cardiovascular diseases, while there was neither excess weight nor chronic or acute diseases.

HDBR was organized by the Institute of Space Medicine and Physiology (MEDES-IMPS) in Toulouse, France, and supported by the French Spatial Agency. Samples were collected 1 day before the experiment and on the 21st day of HDBR. The subjects were in controlled conditions of life, and the diet was balanced. The volunteers were not permitted to get up or to sit up during the experiment.

All the volunteers participated in the control session of HDBR without countermeasures and in the second session with RVEs comprising of squats, single leg heel, and bilateral heel raises. Between sessions, the break was 4 months.

For exercises, a special vibration platform (Galileo® Fitness, Novotec, Germany) with an angle of inclination of 6°, combined with a training device from Novotec Medical (Pforzheim, Germany), was used. The training was carried out twice a week with an interval of 3–4 days. The first workout was on the second day of the HDBR.

Physical trainings were as follows: the warm-up consisted of bilateral squats with a knee angle from 10 to 90° for 8 s with eight repetitions; bilateral squats with a knee angle from 10 to 90° for 8 s with 10 repetitions; elevations of the heel of one leg carried out from maximal dorsiflexion to maximal plantar flexion as quickly as possible until exhaustion, and the same bilateral heel raises. The vibration frequency during exercise was 24–26 Hz with an amplitude of 8 mm. More detailed characteristics of volunteers, medical examinations, and physical training design have been described previously (Kermorgant et al., 2019).

This study (registered number: 2012-A00337-36) was carried out with the recommendations of the Ethics Committee (CPP Sud-Ouest Outre-Mer I). The protocol of the experiment was approved by the French Health Authorities. All volunteers gave written informed consent in accordance with the Declaration of Helsinki.

Blood Sampling

Blood samples were taken from a vein in the cubital fossa and were harvested in commercial Monovette tubes (SARSTEDT, Germany) containing EDTA as an anticoagulant. Immediately after collection, the samples were centrifuged, and the obtained plasma was frozen at −80°C and stored before further sample preparation for light chromatography (LC)–mass spectrometry (MS) analysis.

Light Chromatography–Tandem Mass Spectrometry Proteomic Analysis

To prepare for proteomic analysis, 10 μl of blood plasma was depleted using Top 12 columns (Pierce). The samples were prepared via the filter-aided sample preparation (FASP) (Wiśniewski et al., 2009) using Amicon Ultra centrifugal 10-kDa filter devices. Protein mixture was reduced using 0.1 mol/L dithiothreitol (DTT) in buffer containing 8 mol/L urea and 0.2 mol/L Tris (pH 8.5), alkylated with 0.55 mol/L iodoacetamide in buffer containing 8 mol/L urea, and 0.1 mol/L Tris (pH 8.5) and digested using trypsin with a final concentration of 1:100

enzyme:protein (w/w) in 0.05 mol/L ammonium bicarbonate (17 h, 37°C).

The resulting peptide mixture was analyzed in triplicate using LC-MS method based on a nano-HPLC Dionex UltiMate 3000 system (Thermo Fisher Scientific, USA) and a timsTOF Pro (Bruker Daltonics, Germany) equipped with a nanospray ion source (positive ion mode, 1,600 V). A C18 capillary column (75 μm × 50 cm, C18, 3 μm, 100 A) (Thermo Fisher Scientific,

TABLE 1 | Proteins are significantly different from the summary background during head-down bed rest without countermeasures (HDBR) and with resistive vibration exercises (HDBR+RVE).

Gene names	Protein names	HDBR			HDBR+RVE		
		p-value	Welch's *t*-test difference		*p*-value	Welch's *t*-test difference	
IGKC	Ig kappa chain C region	1.41E-03	−3.0	↓			
AMBP	Alpha-1-microglobulin	2.56E-04	−1.4	↓	1.62E-08	2.1	↑
F2	Prothrombin	1.48E-05	−1.3	↓			
AFM	Afamin	1.15E-05	−0.9	↓			
C6	Complement component C6	8.05E-04	−0.7	↓			
GPX3	Glutathione peroxidase 3	8.41E-03	−0.6	↓			
CFI	Complement factor I	7.42E-03	−0.6	↓			
BCHE	Cholinesterase	3.87E-03	−0.5	↓			
AGT	Angiotensinogen	3.47E-03	−0.5	↓			
CP	Ceruloplasmin	2.53E-05	−0.5	↓			
SERPINC1	Antithrombin-III	4.62E-05	−0.5	↓			
PCYOX1	Prenylcysteine oxidase 1	3.98E-03	−0.4	↓			
MCAM	Cell surface glycoprotein MUC18	1.95E-03	−0.2	↓			
SERPINF2	Alpha-2-antiplasmin	2.32E-03	0.4	↑			
APOE	Apolipoprotein E	2.42E-03	0.4	↑			
CPN1	Carboxypeptidase N catalytic chain	1.98E-03	0.4	↑			
C4A	Complement C4-A	1.36E-03	0.4	↑			
C5	Complement C5	1.41E-03	0.4	↑			
ITIH4	Inter-alpha-trypsin inhibitor heavy chain H4	1.96E-03	0.5	↑			
ITIH2	Inter-alpha-trypsin inhibitor heavy chain H2	2.51E-04	0.5	↑			
PROS1	Vitamin K-dependent protein S	2.37E-03	0.5	↑			
SERPIND1	Heparin cofactor 2	3.78E-04	0.5	↑	3.19E-03	−0.4	↓
SERPINA4	Kallistatin	1.26E-03	0.6	↑			
HP	Haptoglobin	4.67E-03	0.7	↑			
C1QB	Complement C1q subcomponent subunit B	2.36E-06	0.7	↑			
IGHG1	Ig gamma-1 chain C region	4.65E-03	0.7	↑			
FGA	Fibrinogen alpha chain	2.54E-03	0.7	↑	4.38E-03	0.7	↑
FGG	Fibrinogen gamma chain	4.68E-05	0.7	↑			
FGB	Fibrinogen beta chain	2.07E-06	0.8	↑			
C1QC	Complement C1q subcomponent subunit C	5.59E-08	0.8	↑			
APOM	Apolipoprotein M	1.05E-05	0.9	↑			
AZGP1	Zinc-alpha-2-glycoprotein	5.35E-04	0.9	↑			
IGHG2	Ig gamma-2 chain C region	2.24E-03	1.6	↑			
APOA1	Apolipoprotein A-I				4.03E-05	−0.6	↓
MST1	Hepatocyte growth factor-like protein				4.96E-03	0.5	↑
ECM1	Extracellular matrix protein 1				2.73E-04	0.5	↑
C1S	Complement C1s subcomponent				1.86E-04	0.5	↑
ITIH3	Inter-alpha-trypsin inhibitor heavy chain H3				1.27E-03	0.5	↑
KLKB1	Plasma kallikrein				6.88E-03	0.5	↑
CFB	Complement factor B				3.58E-05	0.6	↑
GPLD1	Phosphatidylinositol-glycan-specific phospholipase D				1.11E-03	0.6	↑
ATRN	Attractin				2.19E-04	0.6	↑
PLG	Plasminogen				9.26E-03	0.9	↑
GC	Vitamin D-binding protein				7.73E-03	1.2	↑

TABLE 2 | Comparison of the biological processes enriched in two sessions of head-down bed rest (HDBR).

Term ID	Term description	HDBR				HDBR+RVE			
		Observed gene count	Background gene count	FDR	Proteins	Observed gene count	Background gene count	FDR	Proteins
GO:0030162	Regulation of proteolysis	18	742	1.27e-15	AGT, AMBP, APOE, C1QB, C1QC, C4A, C5, C6, CFI, CPN1, F2, ITIH2, ITIH4, PROS1, SERPINA4, SERPINC1, SERPIND1, SERPINF2	8	742	9.18e-06	AMBP, C1S, CFB, ECM1, GPLD1, ITIH3, KLKB1, SERPIND1
GO:0030449	Regulation of complement activation	9	52	7.04e-14	C1QB, C1QC, C4A, C5, C6, CFI, CPN1, F2, PROS1	2	52	0.0072	C1S, CFB
GO:0002673	Regulation of acute inflammatory response	9	92	3.63e-12	C1QB, C1QC, C4A, C5, C6, CFI, CPN1, F2, PROS1	3	92	0.0013	C1S, CFB, KLKB1
GO:0031347	Regulation of defense response	14	676	3.67e-11	AGT, APOE, C1QB, C1QC, C4A, C5, C6, CFI, CPN1, F2, FGA, FGB, FGG, PROS1	5	676	0.0020	APOA1, C1S, CFB, FGA, KLKB1
GO:0080134	Regulation of response to stress	17	1,299	4.84e-11	AGT, AMBP, APOE, C1QB, C1QC, C4A, C5, C6, CFI, CPN1, F2, FGA, FGB, FGG, PROS1, SERPINC1, SERPINF2	7	1,299	0.00073	AMBP, APOA1, C1S, CFB, FGA, KLKB1, PLG
GO:0042730	Fibrinolysis	6	21	1.46e-10	F2, FGA, FGB, FGG, PROS1, SERPINF2	3	21	9.81e-05	FGA, KLKB1, PLG
GO:0051246	Regulation of protein metabolic process	21	2,668	1.79e-10	AGT, AMBP, APOE, C1QB, C1QC, C4A, C5, C6, CFI, CPN1, F2, FGA, FGB, FGG, ITIH2, ITIH4, PROS1, SERPINA4, SERPINC1, SERPIND1, SERPINF2	11	2,668	2.11e-05	AMBP, APOA1, C1S, CFB, ECM1, FGA, GPLD1, ITIH3, KLKB1, MST1, SERPIND1
GO:0050776	Regulation of immune response	13	873	6.89e-09	AMBP, C1QB, C1QC, C4A, C5, C6, CFI, CPN1, F2, FGA, FGB, FGG, PROS1	7	873	0.00013	AMBP, APOA1, C1S, CFB, ECM1, FGA, GPLD1
GO:0002576	Platelet degranulation	7	129	4.24e-08	FGA, FGB, FGG, ITIH4, PROS1, SERPINA4, SERPINF2	5	129	1.11e-05	APOA1, ECM1, FGA, ITIH3, PLG

(Continued)

TABLE 2 | Continued

Term ID	Term description	HDBR				HDBR+RVE			
		Observed gene count	Background gene count	FDR	Proteins	Observed gene count	Background gene count	FDR	Proteins
GO:0097746	Regulation of blood vessel diameter	6	129	1.31e-06	AGT, APOE, FGA, FGB, FGG, SERPINF2				
GO:0007596	Blood coagulation	7	288	5.23e-06	F2, FGA, FGB, FGG, PROS1, SERPINC1, SERPIND1	4	288	0.0013	FGA, KLKB1, PLG, SERPIND1
GO:0042060	Wound healing	8	461	7.47e-06	F2, FGA, FGB, FGG, MCAM, PROS1, SERPINC1, SERPIND1				
GO:0009611	Response to wounding					5	547	0.0011	APOA1, FGA, KLKB1, PLG, SERPIND1
GO:0006810	transport	19	4,130	1.39e-05	AFM, AGT, AMBP, APOE, APOM, AZGP1, CFI, CP, F2, FGA, FGB, FGG, HP, ITIH4, PCYOX1, PROS1, SERPINA4, SERPINC1, SERPINF2	8	4,130	0.0257	AMBP, APOA1, ECM1, FGA, GC, GPLD1, ITIH3, PLG
GO:0045834	Positive regulation of lipid metabolic process	3	135	0.0074	AGT, APOE, F2				
GO:0046889	Positive regulation of lipid biosynthetic process					2	73	0.0115	APOA1, GPLD1
GO:0045765	Regulation of angiogenesis	3	277	0.0403	AGT, C5, C6				
GO:0010906	Regulation of glucose metabolic process					2	100	0.0188	GPLD1, MST1
GO:0051346	Negative regulation of hydrolase activity					5	438	0.00071	AMBP, APOA1, ECM1, ITIH3, SERPIND1
GO:0043534	Blood vessel endothelial cell migration					2	26	0.0029	APOA1, GPLD1

USA) was used to separate peptides at a flow rate of 0.3 µl/min by gradient elution from 3 to 90% of phase B during 120 min. The mobile phase A consisted of 0.1% formic acid in water and mobile phase B consisting of 0.1% formic acid in acetonitrile.

Data Analysis

LC-MS data were searched using a MaxQuant software search engine to identify proteins from the human SwissProt database. The following parameters were used: enzyme-trypsin; missed cleavage-2; taxonomy-Human; fixed

modifications-Carbamidomethyl (C); variable modifications-Oxidation (M), Acetylation (N-term); peptide tolerance ± 10 ppm; MS/MS (fragments) tolerance ± 0.5 Da. A prerequisite for identifying a protein was the presence in the spectrum of at least one unique peptide of the protein. The cutoff FDR was specified to 0.01. For semiquantitative analysis, the "no label" method with the additional "match between the runs" option was used in Perseus software package that generated normalized label-free quantification (LFQ) intensities of peptides according to the algorithms described by Cox et al. (Tyanova et al., 2016). Analysis of proteomic changes was performed using logarithmized LFQ intensities. More data on analysis parameters can be found in the article (Brzhozovskiy et al., 2019).

For identification of significantly changed proteins in two sessions of HDBR, a two-sample Welch's *t*-test ($p < 0.05$) with Benjamini–Hochberg correction was used. The String web resource (v 11.0) was used to analyze proteins with a significantly changed concentration to identify GO biological processes that were reliably presented for this set of proteins. Only associations with $p < 0.05$ were included in the table. From similar processes, more general ones were selected, which were more reliable. The mass spectrometric data were uploaded to the ProteomeXchange Consortium through the PRIDE partner repository with the dataset identifier PXD013305.

Comparative Plasma Proteome Profiling

Using MaxQuant and Perseus programs, 239 proteins were quantified in blood plasma samples of volunteers of both HDBR sessions. By using the statistical parameters reported in the *Materials and Methods* section, we recovered 33 proteins whose peak intensities significantly differed between background and 21st day of HDBR without the use of countermeasures (**Table 1**). Concentrations of 20 proteins were increased, while 13 proteins were decreased. According to the Gene Ontology (GO) database, most of these proteins were involved in the regulation of proteolysis, complement activation, acute inflammatory response, defense response, response to stress, fibrinolysis, blood coagulation, etc. (**Table 2**).

Previously, it was shown that under the impact of + GX overloads after long-term spaceflights (186–380 days), petechial hemorrhages occur in the skin integument of the back, supposedly by a marked decrease in the tone of arterial and venous vessels (Kotovskaya et al., 2005). It was also reported that 21-days HDBR can cause hemorrhages in the tissues of the lower extremities during the test for orthostatic resistance (Ganse et al., 2013). Authors reported that this volunteer did not have avascular diseases, thrombosis, or thrombophlebitis in anamnesis; therefore, the prolonged bed rest can reduce the threshold for the formation of petechiae due to a decrease in vascular tone. Also, regarding thrombophography and thromboelastometry results, hypercoagulation does not occur during HDBR (Cvirn et al., 2015). Proteins that change their level at 21 days of HDBR (F2, FGA, FGB, FGG, PROS1, SERPINC1, SERPIND1) can be involved in the negative regulation of the coagulation process.

In the study of the effect of countermeasures used in HDBR on the protein composition of the blood, it was found that the use of a set of preventive measures modified the plasma proteome, as compared with HDBR as such. So, the total number of significantly changing proteins decreased, which indicated the clinical effectiveness of this complex of preventive measures. Thirteen proteins were determined (**Table 1**), the concentrations of which significantly changed at the end of HDBR with exercises. Eleven proteins increased, and two proteins decreased. These proteins, according to the GO database, were involved in such processes like regulation of proteolysis, fibrinolysis, platelet degranulation, complement activation, inflammatory response, and other processes similar to HDBR processes described above. The difference between the processes of the two sessions of HDBR was the appearance of such processes like regulation of glucose metabolic process, negative regulation of hydrolase activity, blood vessel endothelial cell migration, and disappearance of such processes like regulation of blood vessel diameter and regulation of angiogenesis in the second session of HDBR with RVE (**Table 2**).

During HDBR experiments, muscle mass loss occurs, based on the decrease of protein synthesis (Crucian and Sams, 2009), while there was no increase in the rate of proteolysis of myofibrils or activation of the ubiquitin–proteasome pathway of protein degradation (Ogawa et al., 2006). Changing of the level of the proteins involved in extracellular matrix (ECM) organization was registered at 21 days of HDBR. Such proteins were not changed during HDBR with RVEs; at the same time, the level of the other proteins involved in ECM organization was changed (FGA, KLKB1, PLG). This indicates that RVE can reduce the influence of the hypodynamic factor on changes in ECM remodeling and loss of muscle mass. In general, a similar, although less pronounced, response of the physiological systems of the body to the effects of HDBR is observed, despite the use of preventive measures for adverse effects. The main difference in the regulation of metabolism was a predominant effect on the processes of regulation of carbohydrate metabolism in the group with the use of preventive measures (physical activity). It is worth noting that this is a pilot study, and the identified proteins will need to be validated more carefully in the future.

DATA AVAILABILITY STATEMENT

The datasets generated for this study can be found in the mass spectrometric proteomic data have been deposited to the ProteomeXchange Consortium via the PRIDE partner repository with the dataset identifier PXD013305.

ETHICS STATEMENT

The studies involving human participants were reviewed and approved by CPP Sud-Ouest Outre-Mer I. The patients/participants provided their written informed consent to participate in this study.

AUTHOR CONTRIBUTIONS

LP performed the head-down bed rest. DK and AB performed the sample preparation to mass spectrometry. AK and AB conducted mass spectrometric analysis. IL, CB, EN, and DK wrote the

article. All authors contributed to the article and approved the submitted version.

FUNDING

This study was supported by the Megagrant of the Ministry of Science and Higher Education of the Russian Federation (Agreement with Skolkovo Institute of Science and Technology on December 11, 2019, No. 075-10-2019-083).

ACKNOWLEDGMENTS

The team of authors expresses gratitude to Dr. Marc-Antoine Custaud for the opportunity to participate in the HDBR experiment.

REFERENCES

Baranov, M. V., Katuntsev, V. P., and Shpakov, A. V. (2016). A method of ground simulation of physiological effects of hypogravity on humans. *Bull. Exp. Biol. Med*. 160, 401–405. doi: 10.1007/s10517-016-3181-0

Batchu, S. N., Smolock, E. M., Dyachenko, I. A., Murashev, A. N., and Korshunov, V. A. (2015). Autonomic dysfunction determines stress-induced cardiovascular and immune complications in mice. *J. Am. Heart. Assoc*. 4:e001952. doi: 10.1161/JAHA.115.001952

Brzhozovskiy, A. G., Kononikhin, A. S., Pastushkova, L., Ch., Kashirina, D. N., Indeykina, M. I., et al. (2019). The effects of spaceflight factors on the human plasma proteome, including both real space missions and ground-based experiments. *Int. J. Mol. Sci*. 20:3194. doi: 10.3390/ijms20133194

Coupé, M., Yuan, M., Demiot, C., Bai, Y. Q., Jiang, S. Z., Li, Y. Z., et al. (2011). Low-magnitude whole body vibration with resistive exercise as a countermeasure against cardiovascular deconditioning after 60 days of head-down bed rest. *Am. J. Physiol. Regul. Integr. Comp. Physiol*. 301, R1748–R1754. doi: 10.1152/ajpregu.00234.2011

Crucian, B., and Sams, C. (2009). Immune system dysregulation during spaceflight : clinical risk for exploration-class missions. *J. Leukocyte Biol*. 86, 1017–1018. doi: 10.1189/jlb.0709500

Cvirn, G., Waha, J. E., Ledinski, G., Schlagenhauf, A., Leschnik, B., Koestenberger, M., et al. (2015). Bed rest does not induce hypercoagulability. *Eur. J. Clin. Investig*. 45, 63–69. doi: 10.1111/eci.12383

Dillon, E. L., Soman, K. V., Wiktorowicz, J. E., Sur, R., Jupiter, D., Danesi, C. P., et al. (2019). Proteomic investigation of human skeletal muscle before and after 70 days of head down bed rest with or without exercise and testosterone countermeasures. *PLoS ONE* 14:e0217690. doi: 10.1371/journal.pone.0217690

Ganse, B., Limper, U., Bühlmeier, J., and Rittweger, J. (2013). Petechiae: reproducible pattern of distribution and increased appearance after bed rest. *Aviation Space Environ. Med*. 84, 864–866. doi: 10.3357/ASEM.3567.2013

Greaves, D., Arbeille, P., Guillon, L., Zuj, K., and Caiani, E. G. (2019). Effects of exercise countermeasure on myocardial contractility measured by 4D speckle tracking during a 21-day head-down bed rest. *Eur. J. Appl. Physiol*. 119, 2477–2486. doi: 10.1007/s00421-019-04228-0

Kermorgant, M., Nasr, N., Custaud, M. A., Navasiolava, N., Arbeille, P., Guinet, P., et al. (2019). Effects of resistance exercise and nutritional supplementation on dynamic cerebral autoregulation in head-down bed rest. *Front. Physiol*. 10:1114. doi: 10.3389/fphys.2019.01114

Kotovskaya, A. R., Wil-Williams, I. F., and Fomina, G. A. (2005). The relationship of physiological reactions of astronauts with current overload + GX on the descent from orbit to earth with hemodynamic rearrangements in the conditions of short-term weightlessness. *Aerospace Environ. Med*. 39, 9–15.

Larina, I. M., Popova, I. A., Mikhailov, V. M., and Buravkova, L. B. (1999). The hormonal mechanisms supporting muscle work during prolonged head-down tile hypokinesia. *Fiziol Cheloveka* 25, 117–124.

Moriggi, M., Vasso, M., Fania, C., Capitanio, D., and Bonifacio, G., Salanova, et al. (2010). Long term bed rest with and without vibration exercise countermeasures: effects on human muscle protein dysregulation. *Proteomics* 10, 3756–3774. doi: 10.1002/pmic.200900817

Ogawa, T., Furochi, H., Mameoka, M., Hirasaka, K., Onishi, Y., Suzue, N., et al. (2006). Ubiquitin ligase gene expression in healthy volunteers with 20-day bedrest. *Muscle Nerve* 34, 463–469. doi: 10.1002/mus.20611

Pavy-Le Traon, A., Heer, M., Narici, M. V., Rittweger, J., Vernikos, J. (2007). From space to Earth: advances in human physiology from 20 years of bed rest studies (1986-2006). *Eur. J. Appl. Physiol.* 101, 143–194. doi: 10.1007/s00421-007-0474-z

Salanova, M., Gambara, G., Moriggi, M., Vasso, M., Ungethuem, U., Belavý, D. L., et al. (2015). Vibration mechanosignals superimposed to resistive exercise result in baseline skeletal muscle transcriptome profiles following chronic disuse in bed rest. *Sci. Rep*. 24:17027. doi: 10.1038/srep17027

Salanova, M., Gelfi, C., Moriggi, M., Vasso, M., Viganò, A., Minafra, L., et al. (2014). Disuse deterioration of human skeletal muscle challenged by resistive exercise superimposed with vibration: evidence from structural and proteomic analysis. *FASEB J.* 28, 4748–4763. doi: 10.1096/fj.14-252825

Tyanova, S., Temu, T., and Cox, J. (2016). The MaxQuant computational platform for mass spectrometry-based shotgun proteomics. *Nat. Protoc.* 11, 2301–2319. doi: 10.1038/nprot.2016.136

Wiśniewski, J. R., Zougman, A., Nagaraj, N., and Mann, M. (2009). Universal sample preparation method for proteome analysis. *Nat. Methods* 6, 359–362. doi: 10.1038/nmeth.1322

Wu, L., and Han, D. K. (2006). Overcoming the dynamic range problem in mass spectrometry-based shotgun proteomics. *Expert. Rev. Proteom.* 3, 611–619. doi: 10.1586/14789450.3.6.611

Conflict of Interest: The authors declare that the research was conducted in the absence of any commercial or financial relationships that could be construed as a potential conflict of interest.

frontiers in Physiology

ORIGINAL RESEARCH
published: 13 August 2021
doi: 10.3389/fphys.2021.656527

The Relationship Between Blood Perfusion in the Lower Extremities and Heart Rate Variability at Different Positions

Shuyong Jia[1†], Qizhen Wang[2†], Hongyan Li[1], Xiaojing Song[1], Shuyou Wang[1], Weibo Zhang[1] and Guangjun Wang[1]*

[1]*Institute of Acupuncture and Moxibustion, China Academy of Chinese Medical Sciences, Beijing, China,* [2]*Institute of Basic Research in Clinical Medicine, China Academy of Chinese Medical Sciences, Beijing, China*

OPEN ACCESS

Edited by:
Olga Vinogradova, Russian Academy of Sciences, Russia

Reviewed by:
Roland Pittman, Virginia Commonwealth University, United States
Eiich Watanabe, Fujita Health University, Japan

****Correspondence:***
Guangjun Wang
tjuwgj@gmail.com

[†]These authors have contributed equally to this work

Specialty section:
This article was submitted to Vascular Physiology, a section of the journal Frontiers in Physiology

Received: *21 January 2021*
Accepted: *23 July 2021*
Published: *13 August 2021*

Citation:
Jia S, Wang Q, Li H, Song X, Wang S, Zhang W and Wang G (2021) The Relationship Between Blood Perfusion in the Lower Extremities and Heart Rate Variability at Different Positions. Front. Physiol. 12:656527. doi: 10.3389/fphys.2021.656527

Previous studies have explored the relationship between the complexity of local blood flow signals and heart rate variability (HRV) under different thermal stimulations. However, the relationship between the complexity of local blood flow signals and HRV in different positions is not clear. In this study, healthy participants were placed in different body positions. The bilateral blood flux and ECG were monitored, and refined composite multiscale entropy (RC MSE) and refined composite multiscale fuzzy entropy (RC MFE) were used to measure the complexity of the local blood flux. The sample entropy was calculated to evaluate the HRV complexity. The change of body position did not affect the time domain or frequency domain of HRV, but did reverse the blood flux laterality of the lower extremities. Furthermore, there was a negative correlation between the complexity of right-side blood flux and sample entropy of HRV when the participant was in the -10 degrees position. These results provide a new perspective of the relationship between skin blood flux signals and cardiac function.

Keywords: laser doppler blood perfusion, electrocardiogram, RMSSD, refined composite multiscale entropy, refined composite multiscale fuzzy entropy, positions

INTRODUCTION

Previous studies have shown that there is a correlation between the skin blood flux perfusion of the left and right sides of the body. Whether due to thermal (Kubo et al., 2011), physical (Guangjun et al., 2012), or laser (Wang et al., 2012) stimulation, an increase in the blood perfusion of the body part contralateral to the stimulation occurs, suggesting that the skin blood flux regulation of bilateral body parts is internally correlated under certain conditions. Further studies have shown that the skin blood flux distribution in the same parts of the body exhibits laterality, whether at the body surface (Wang et al., 2012) or in the viscera (Mezentseva and Pertsov, 2019). Preliminary studies have shown that this laterality can be used to quantitatively evaluate the microcirculation perfusion status of different age groups (Wang et al., 2017). When the digestive tract was stimulated by cold water load, the laterality changed (Wang et al., 2017). As skin blood flux regulation is controlled by the autonomic nervous system, we believe that the laterality of skin blood flux distribution may be a result of autonomic

nerve regulation. This suggests that autonomic nerve function regulation may differ between the two sides of the body; the function is lateralized. Recent studies have shown that autonomic nerve function is lateralized under specific stimulation conditions (Aghababaei Ziarati et al., 2020), which provides direct evidence for the lateralization of skin blood flux regulation.

In contrast, there is more and more evidence that microcirculation can be used to assess vascular function at the systemic level (IJzerman et al., 2003; Holowatz et al., 2008), and there is a close relationship between heart and vessel functions (Debbabi et al., 2010; Pinter et al., 2012). A correlation between regional skin blood flux and heart rate variability (HRV) when the body surface was stimulated by different temperatures has been reported (Wang et al., 2018, 2019). However, there are no reports focusing on the laterality of blood perfusion from the perspective of complexity measurement. The purpose of this study is to analyze the relationship between blood perfusion and HRV in healthy participants in different body positions.

MATERIALS AND METHODS

Inclusion and Exclusion Criteria

Participants were required to be 18–60 years of age and healthy (no history of any medical conditions). Patients receiving medication affecting the cardiovascular system or autonomic regulation were excluded from this study. The participants were asked to avoid coffee, tea, and alcohol for 24 h prior to the study.

Participants and Positions

A total of 32 healthy participants were enrolled in current study, and 28 were included in the final statistical analysis. Each subject was paid for the participation. The characteristics of the participants are presented in **Table 1**. The study was conducted in a quiet, temperature-controlled (24–26°C) laboratory. Participants were instructed to lay flat on a multifunctional electric nursing bed (DB-3, Daermonda Medical Equipment Co., Ltd., Wuxi, China). As shown in **Figure 1**, the angle of the bed is adjustable. Following a 40-min period of cardiovascular stability, 15-min baseline ECG and bilateral Zusanli skin blood flux recordings were obtained with the participant in the horizontal position (Pre). The participant was then positioned at an angle of 10 degrees (up position) for 15 min before returning to a horizontal position. After a rest period of 15 min, the body position was changed to −10 degrees (down position) for 15 min before returning to horizontal. Both ECG and bilateral Zusanli skin blood flux were recorded at each body position. The changes in body position are shown in **Figure 1**.

TABLE 1 | Participants' characteristics.

n	Sex (female/male)	Age (years, mean ± SD)	Height (cm, mean ± SD)	Weight (kg, mean ± SD)
28	19/9	25.75 ± 2.35	166.54 ± 7.12	61.46 ± 10.97

Measurement and Analysis of ECG Data

The participants maintained a supine position throughout the study. The ECG data was analyzed as previously described (Wang et al., 2013, 2015; Guangjun et al., 2014). Briefly, the ECG signals were recorded with standard II leads using the NeurOne system (NeurOne, MEGA electronics Ltd., Finland). The data were digitized at a sampling rate of 1,000 Hz. The raw data was exported in the EDF format and imported into Kubio HRV Premium software (Kubios Oy, Finland) for analysis (Niskanen et al., 2004). The length of analysis data was 15 min, and other analysis parameters were default. In the frequency domain, the power spectrum density was analyzed using the AR spectrum method in normalized units. Very low frequency (VLF) and low frequency (LF) were defined as 0–0.04 Hz and 0.04–0.15 Hz, respectively.

Measurement and Analysis of Blood Perfusion Data

Both sides Zusanli acupoints (ST 36) were marked by senior acupuncture physicians. Blood perfusion signals were recorded using a PeriFlux System 5,000 (Perimed AB, Stockholm, Sweden) at a sample rate of 64 Hz and a time constant of 0.2 s. An optical fiber probe connected with a Periflux 5,000 was used to illuminate and collect the scattered light from the skin tissue. The probe was attached to the surface of interest with two-sided adhesive tape. The data were viewed using PeriSoft software for Windows (version 2.5.5, Perimed, Sweden), then exported in txt format and imported into MATLAB software (MathWorks, Natick, Massachusetts, United States) for analysis. The unit of blood perfusion is PU, which is the product of the number of moving blood cells in the measurement area and the average movement rate of blood cells. In consideration of sex-related differences in forearm skin microvascular reactivity (Stupin et al., 2019), male and female subjects were analyzed, respectively.

Complexity of Blood Flux Signal

Refined composite multiscale entropy (RC MSE) and refined composite multiscale fuzzy entropy (RC MFE) were used to measure the complexity of the blood flux signal. The analytical methods of the MATLAB toolbox were used as previously described (Ahmed and Mandic, 2012; Azami and Escudero, 2017). A total of 15 min of blood flux data was used for the complexity analysis. The analysis parameters were N = 57,600 and scale = 20. The other parameters were default. A single index named complexity area index (CA) was calculated as the area under the multiscale entropy curve (Manor et al., 2010; Lu et al., 2012).

Statistical Analysis

Data are presented as mean ± SE. Paired t-test was used to compare different positions and horizontal positions. The correlation between HRV and complexity of skin blood flow was calculated by Spearman's correlation coefficient (SCC). All statistical analyses

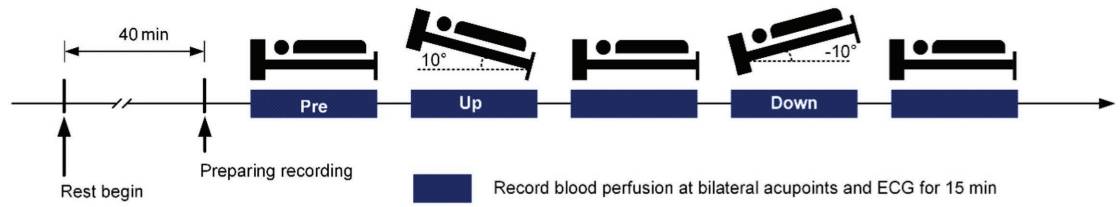

FIGURE 1 | Schematic diagram of positions and recordings.

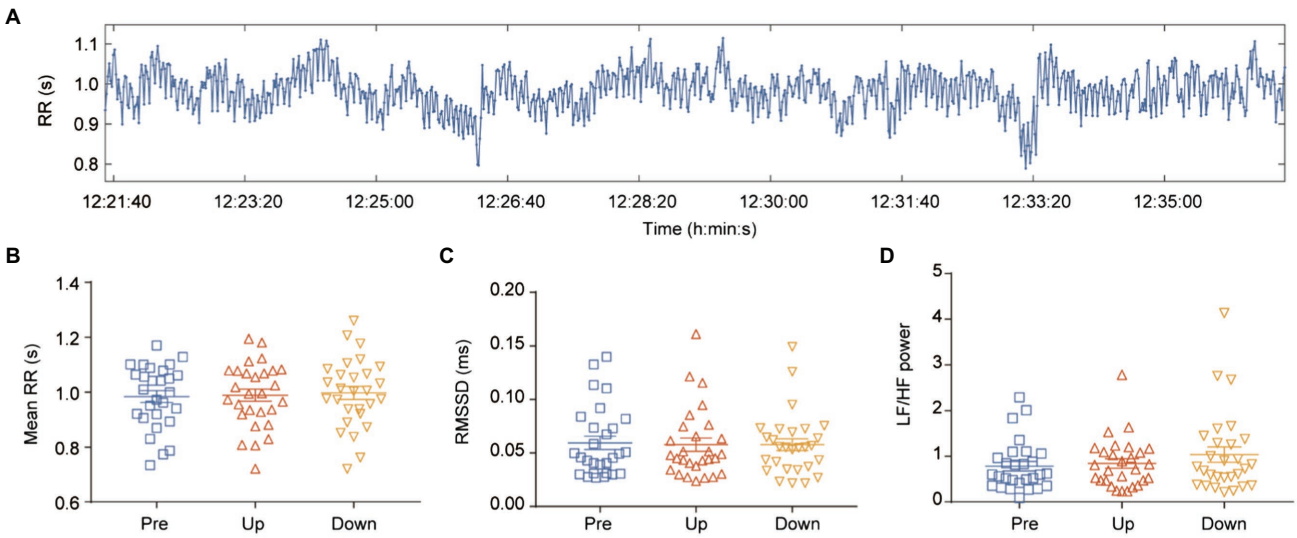

FIGURE 2 | Change in heart rate variability (HRV). **(A)** RR intervals of the ECGs. **(B)** Mean RR intervals at each body position. **(C)** RMSSD at each body position. **(D)** LF/HF power ratio at each body position.

were conducted using MATLAB software. All reported p values are two-sided. Statistical significance was set at $p < 0.05$.

RESULTS

A total of 32 participants were recruited for this study; however, two participants did not complete the study and two had abnormal ECGs. The final analysis included 28 participants (**Table 1**).

ECG Results

The RR interval signals are shown in **Figure 2A**. There was no significant difference in RR interval (**Figure 2B; Supplementary Figures 1A, 2A**), RMSSD (**Figure 2C; Supplementary Figures 1B, 2B**), and LF/HF ratio (**Figure 2D; Supplementary Figures 1C, 2C**) between the different body positions.

Skin Blood Flux

The average responses of blood perfusion to different body positions are shown in **Figure 3**. There was a significant difference in the skin blood flux between the left and right lower extremities in the horizontal position (**Figure 3C**); however, there was no difference in the skin blood flux between the left and right lower extremities in the up or down positions (**Figures 3D,E**). Subgroup analysis showed that regardless of female (**Supplementary Figures 3A–C**) or male (**Supplementary Figures 4A–C**), there was no significant difference in left and right blood perfusion.

Relationship Between HRV and Blood Flux Signals

To discriminate the local blood flux pattern at different body positions, a time series of blood flux signals was analyzed using two methods of complexity analysis. There was no significant difference in local blood flux patterns between the different body positions on the RC MSE (**Figure 4A**) or RC MFE (**Figure 5A**) analyses in either lower extremity. However, the complexity of HRV was negatively correlated with the complexity of the right skin blood flux signal in the down position but not in other positions (**Figures 4B, 5B**).

DISCUSSION

This study found a negative correlation between the HRV and the right limb skin blood flux when the body was inclined

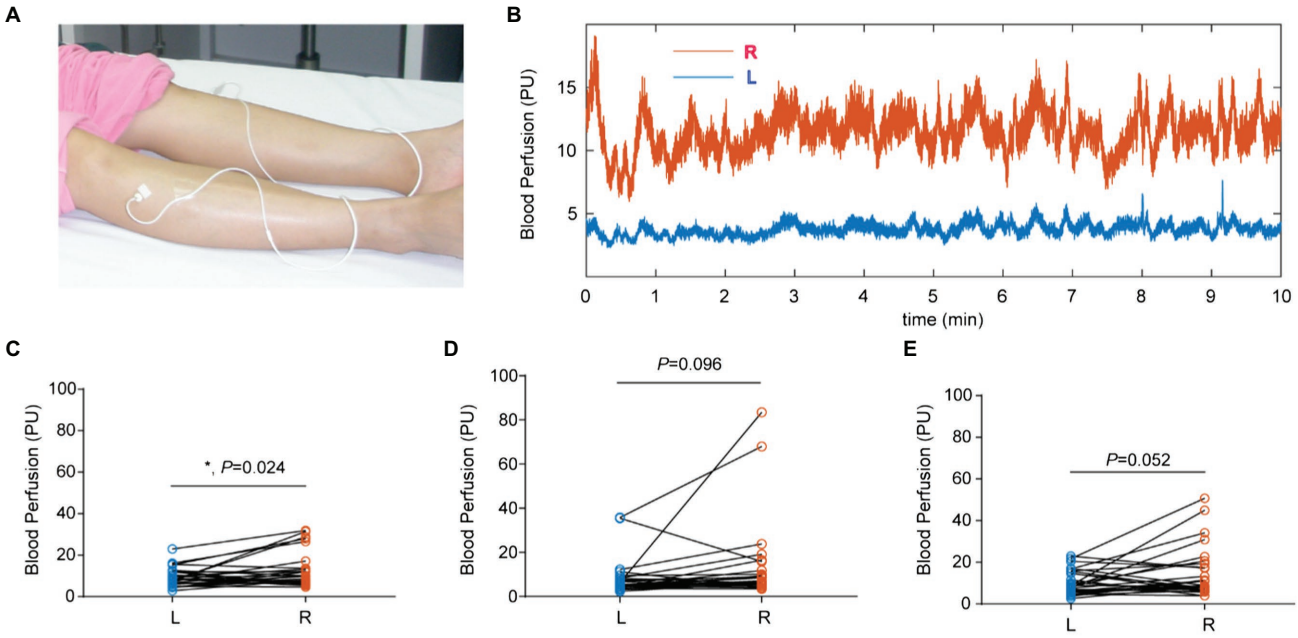

FIGURE 3 | Blood perfusion in both lower extremities at different body positions. **(A)** Recording position at ST 36. **(B)** Raw data of blood flux in the left (blue) and right (red) lower extremities. **(C)** The blood flux was significantly different between the right (R) and left (L) sides in the horizontal position. **(D)** The blood flux was not significantly different between the R and L sides in the up position. **(E)** The blood flux was not significantly different between the R and L sides in the down position.

at −10 degrees. However, there was no correlation between left blood flow and HRV in the same position. These results suggest that the regulation of bilateral blood flow is lateralized. Moreover, this correlation only occurred at the down position, indicating that certain conditions are required for the emergence of the laterality of the regulation of bilateral blood flow. These results are consistent with those of previous studies (Wang et al., 2018, 2019) that reported no correlation between HRV and skin blood flux under normal or near normal conditions, but a correlation between HRV and skin blood flux when the thermal stimulation reached a specific temperature.

The change of HRV in the up or down position is subtle and difficult to distinguish with traditional time domain or frequency domain analyses. Therefore, HRV is maintained within a normal range when the external stimulation does not exceed a certain threshold. However, different body positions can cause changes in tissue perfusion (Tapar et al., 2018). The results of this study suggest that the change of body position directly reversed the laterality of bilateral blood flow, indicating that although the heart and vascular system are a whole, they are relatively independent when controlled by the autonomic nervous system. In normal state or near normal state, there is no significant correlation between HRV and peripheral blood flow; this correlation is only observed when the external stimuli reach a certain threshold. The integration of the heart rate and vascular response indicate a correlation between HRV and peripheral blood flow in these conditions.

The regulation of the circulatory system is believed to be a nonlinear process (Liao et al., 2010); therefore, nonlinear dynamic analyses can provide information regarding the variability of skin blood flow oscillations (Liao et al., 2010; Jan et al., 2012). An MSE analysis provides a more powerful method for analyzing complexity measurements (Costa et al., 2002, 2005; Liao et al., 2020) of vascular dynamics. Heart rate signal is also believed to be a nonlinear process. The complexity of HR contains information beyond conventional time- and frequency-domain parameters, which could be sensitive to special conditions. It seems that some complexity parameters have higher regularity and predictability during environmental challenges (Young and Benton, 2015; Schneider et al., 2021). In current study, the intervention method is posture change, and the maximum tilt angle is 10 degrees. This method has little disturbance to the body, and it is more difficult to detect this change by conventional HRV related indicators. Therefore, The complexity of blood flow and heart rate signals is measured and the correlation between them is analyzed.

In this study, the RC MSE analysis results were less sensitive to the signal length than the RC MFE analysis results, suggesting that RC MSE should be used to assess the perfusion of the skin in different positions. Similarly, among irregular time series data in a wide range of time scales, the data with larger entropy are considered to be more complex (Kang et al., 2009). No correlations between the complexity of blood flow and HRV were observed in the horizontal or up positions in this study. A negative correlation between HRV and the complexity of the blood flow signal was observed in the right lower limb in the down position. These results highlight the laterality of the blood flow regulation.

Several studies have addressed the lateral distribution of blood flow (Wong et al., 1988; Yao et al., 2001; Ceylan et al., 2016).

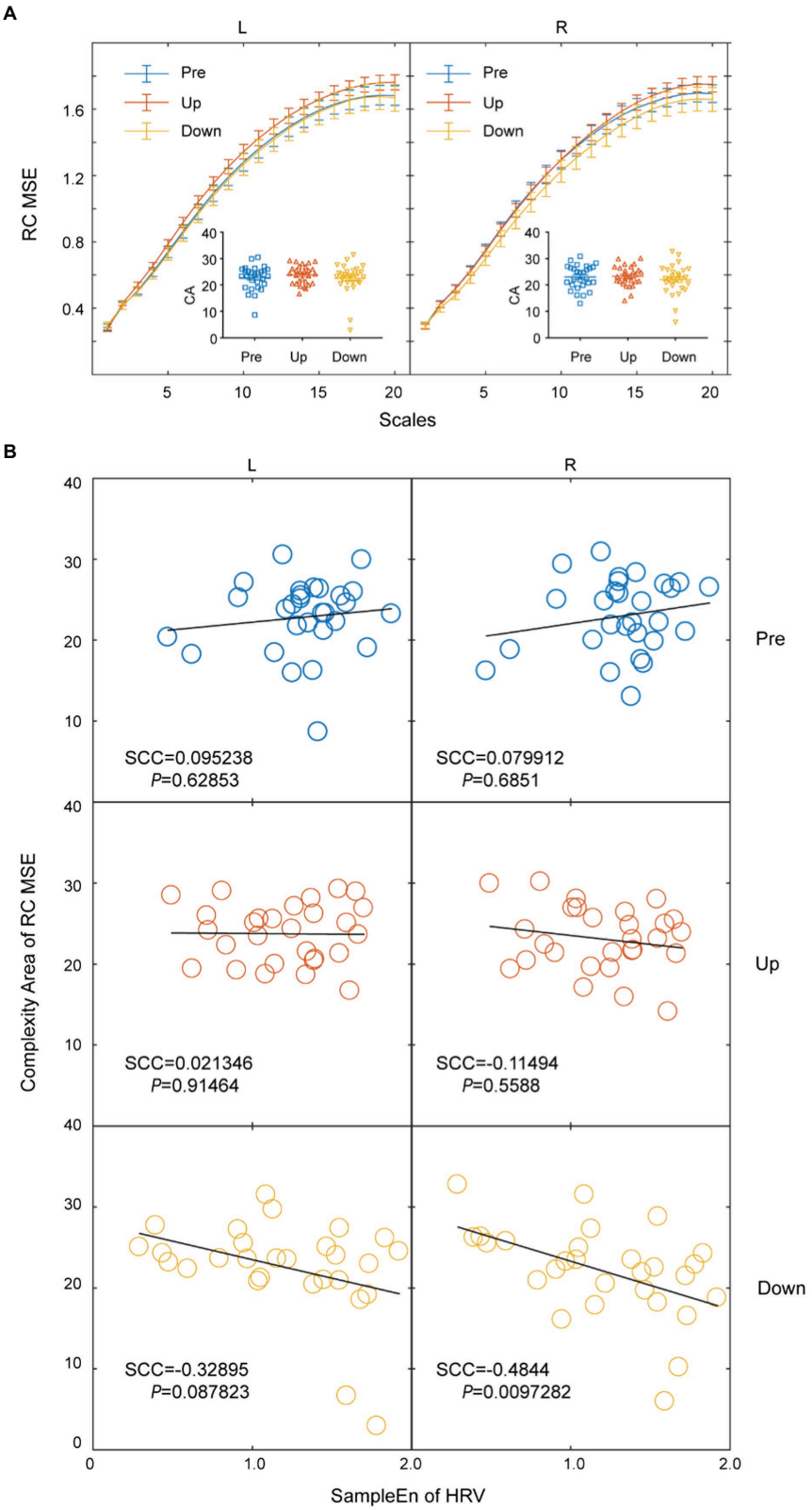

FIGURE 4 | Relationship between sample entropy of HRV and refined composite multiscale entropy (RC MSE) of blood flux signals. **(A)**. There were no significant differences in the RC MSE of blood flux signals at different positions between the left and right lower extremities. **(B)**. The HRV is negatively correlated to the complexity area of the RC MSE blood flux signal in the right lower extremity in the down position, Spearman's correlation coefficient (SCC).

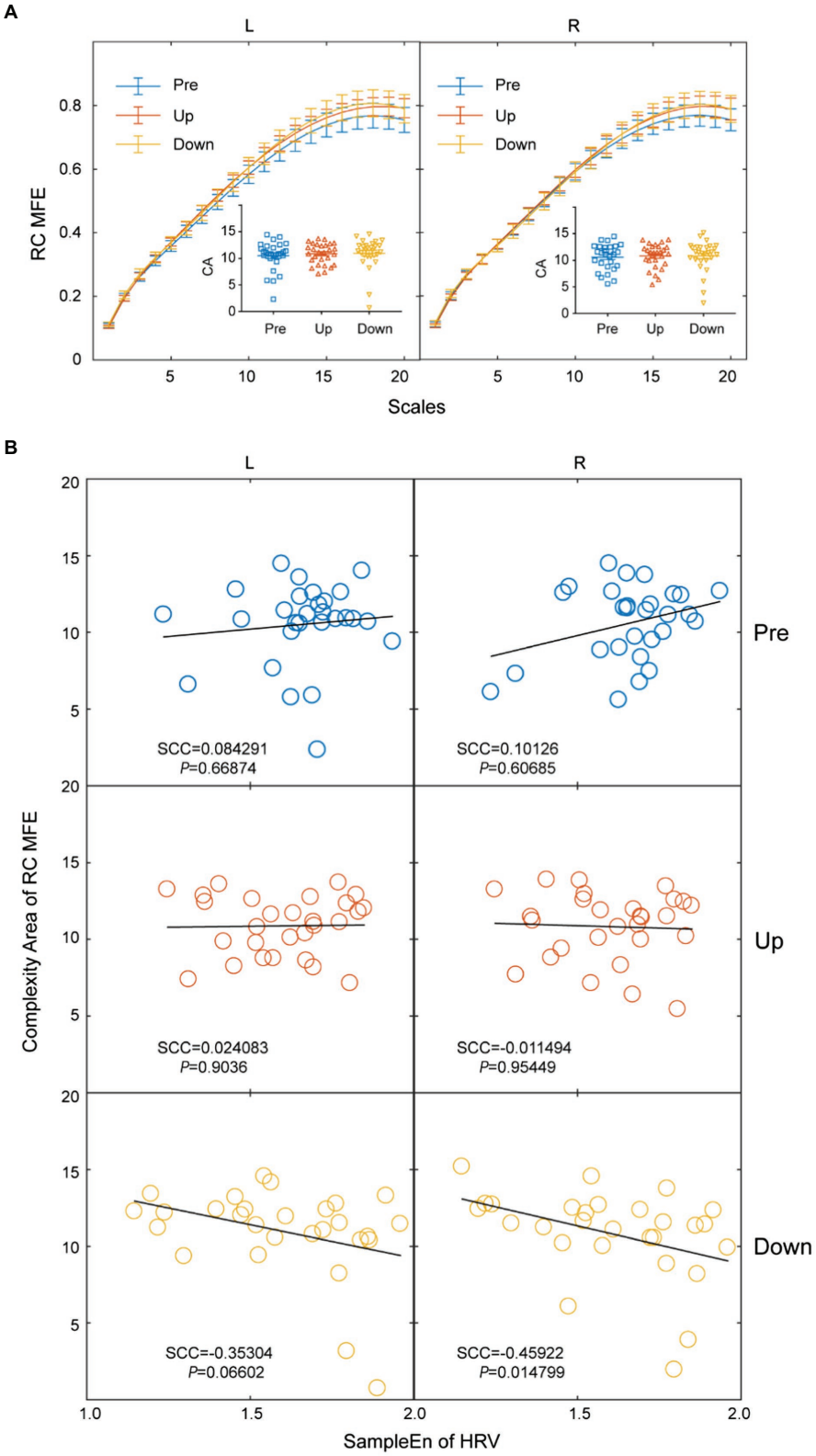

FIGURE 5 | Relationship between sample entropy of HRV and refined composite multiscale fuzzy entropy (RC MFE) of blood flux signals **(A)** There were no significant differences in the RC MFE of blood flux signals at different positions between the left and right lower extremities **(B)** The HRV is negatively correlated to the complexity area of the RC MFE blood flux signal in the right lower extremity in the down position, SCC.

Significant differences in the distribution and regulation of skin blood flux in bilateral parts of the body have been reported (Wang et al., 2012; Mezentseva and Pertsov, 2019). Together, these studies confirm that the distribution of bilateral skin blood flux and its variation are asymmetric.

Generally, asymmetric or lateralization is considering as a fundamental characteristic in vertebrates (Vallortigara and Rogers, 2005) and invertebrate (Frasnelli, 2013). It is well known as hemispheric or cerebral laterality (Vallortigara and Rogers, 2005). Although, there is some evidence to support the existence of laterality in circulating blood flow signals (Wang et al., 2012; Mezentseva and Pertsov, 2019), this phenomenon is still not paid attention enough. We do not know whether this lateralization is an independent character or not associated with the handedness. This study seems to suggest that the laterality of microcirculation blood flow signal changes with the change of body position, especially in abnormal position. It means that laterality and that changes are closely related to systemic regulation. From the relevant perspective (Jia et al., 2020), the laterality of blood flow signal is closely related to autonomic nervous system, and the occurrence of some diseases of circulatory system, such as hypertension, is also the result of autonomic nervous dysfunction (Zubcevic et al., 2019; Yoo and Fu, 2020). Therefore, we speculate that the laterality of peripheral blood flow signals may be a window for understanding the regulation of autonomic nervous system.

Our research also has some shortcomings. The first limitation is that at each side, only one part blood flow was recorded. If blood flow of multiple parts on bilateral were recorded at the same time, the conclusion will be more representative and more reliable. The second disadvantage is that the blood flow and ECG were recorded only at two different positions. The third limitation is that the blood flow signal and HRV of a few subjects appear outlier data in abnormal posture, which indicates that the state of the subjects is not very well. The fourth deficiency is that there is a serious imbalance in the ratio of male to female, which leads to bias in the subgroup analysis of gender.

CONCLUSION

Changes in body position can affect the correlation between skin blood flow and HRV.

DATA AVAILABILITY STATEMENT

The datasets presented in this study can be found in online repositories. The names of the repository/repositories and accession number(s) can be found at: https://doi.org/10.6084/m9.figshare.14907972.v1

ETHICS STATMENT

The studies involving human participants were reviewed and approved by Institutional Research Ethics Boards of Acupuncture & Moxibustion, China Academy of Chinese Medical Sciences. The patients/participants provided their written informed consent to participate in this study.

AUTHOR CONTRIBUTIONS

GW: conceptualization and funding acquisition. GW, SJ, and QW: methodology. GW and QW: software, formal analysis, and visualization. SJ, HL, XS, SW, WZ, and GW: resources. WZ and GW: data curation and supervision. SJ and GW: writing—original draft preparation, writing—review and editing, and project administration. All authors have read and agreed to the published version of the manuscript.

FUNDING

This research was funded by the Ministry of Science and Technology of the People's Republic of China (2015CB554502) and the Fundamental Research Funds for the Central Public Welfare Research Institutes (ZZ11098).

ACKNOWLEDGMENTS

We would like to thank Editage (www.editage.cn) for English language editing.

SUPPLEMENTARY MATERIAL

The Supplementary Material for this article can be found online at https://www.frontiersin.org/articles/10.3389/fphys.2021.656527/full#supplementary-material

REFERENCES

Aghababaei Ziarati, M., Taziki, M. H., and Hosseini, S. M. (2020). Autonomic laterality in caloric vestibular stimulation. *World J. Cardiol.* 12, 144–154. doi: 10.4330/wjc.v12.i4.144

Ahmed, M. U., and Mandic, D. P. (2012). Multivariate multiscale entropy analysis. *Ieee Signal Proces. Lett.* 19, 91–94. doi: 10.1109/LSP.2011.2180713

Azami, H., and Escudero, J. (2017). Refined composite multivariate generalized multiscale fuzzy entropy: a tool for complexity analysis of multichannel signals. *Physica a-Stat. Mech.Appl.* 465, 261–276. doi: 10.1016/j.physa.2016.07.077

Ceylan, B., Khorshid, L., Gunes, U. Y., and Zaybak, A. (2016). Evaluation of oxygen saturation values in different body positions in healthy individuals. *J. Clin. Nurs.* 25, 1095–1100. doi: 10.1111/jocn.13189

Costa, M., Goldberger, A. L., and Peng, C. K. (2002). Multiscale entropy analysis of complex physiologic time series. *Phys. Rev. Lett.* 89:068102. doi: 10.1103/PhysRevLett.89.068102

Costa, M., Goldberger, A. L., and Peng, C. K. (2005). Multiscale entropy analysis of biological signals. *Phys. Rev. E Stat. Nonlinear Soft Matter Phys.* 71:021906. doi: 10.1103/PhysRevE.71.021906

Debbabi, H., Bonnin, P., Ducluzeau, P. H., Leftheriotis, G., and Levy, B. I. (2010). Noninvasive assessment of endothelial function in the skin microcirculation. *Am. J. Hypertens.* 23, 541–546. doi: 10.1038/ajh.2010.10

Frasnelli, E. (2013). Brain and behavioral lateralization in invertebrates. *Front. Psychol.* 4:939. doi: 10.3389/fpsyg.2013.00939

Guangjun, W., Yuying, T., Shuyong, J., Tao, H., and Weibo, Z. (2012). Change of blood perfusion in Hegu acupoint after contralateral Hegu acupoint was stimulated. *J. Altern. Complement. Med.* 18, 784–788. doi: 10.1089/acm.2011.0440

Guangjun, W., Yuying, T., Shuyong, J., Wenting, Z., and Weibo, Z. (2014). Bilateral hegu acupoints have the same effect on the heart rate variability of the healthy subjects. *Evid. Based Complement. Alternat. Med.* 2014:106940. doi: 10.1155/2014/106940

Holowatz, L. A., Thompson-Torgerson, C. S., and Kenney, W. L. (2008). The human cutaneous circulation as a model of generalized microvascular function. *J. Appl. Physiol.* 105, 370–372. doi: 10.1152/japplphysiol.00858.2007

IJzerman, R. G., de Jongh, R. T., Beijk, M. A., van Weissenbruch, M. M., de Waal, H. A. D.-v., Serne, E. H., et al. (2003). Individuals at increased coronary heart disease risk are characterized by an impaired microvascular function in skin. *Eur. J. Clin. Investig.* 33, 536–542. doi: 10.1046/j.1365-2362.2003.01179.x

Jan, Y. K., Lee, B., Liao, F., and Foreman, R. D. (2012). Local cooling reduces skin ischemia under surface pressure in rats: an assessment by wavelet analysis of laser Doppler blood flow oscillations. *Physiol. Meas.* 33, 1733–1745. doi: 10.1088/0967-3334/33/10/1733

Jia, S., Wang, Q., Li, H., Song, X., Wang, S., Zhang, W., et al. (2020). Laterality of Blood Perfusion in the Lower Extremities after Drinking Saline at Different Temperatures. *(Version 4) available at Research Square* [Preprint]. doi:10.21203/rs.3.rs-112441/v4

Kang, H. G., Costa, M. D., Priplata, A. A., Starobinets, O. V., Goldberger, A. L., Peng, C. K., et al. (2009). Frailty and the degradation of complex balance dynamics during a dual-task protocol. *J. Gerontol. A Biol. Sci. Med. Sci.* 64, 1304–1311. doi: 10.1093/gerona/glp113

Kubo, K., Yajima, H., Takayama, M., Ikebukuro, T., Mizoguchi, H., and Takakura, N. (2011). Changes in blood circulation of the contralateral Achilles tendon during and after acupuncture and heating. *Int. J. Sports Med.* 32, 807–813. doi: 10.1055/s-0031-1277213

Liao, F., Garrison, D. W., and Jan, Y. K. (2010). Relationship between nonlinear properties of sacral skin blood flow oscillations and vasodilatory function in people at risk for pressure ulcers. *Microvasc. Res.* 80, 44–53. doi: 10.1016/j.mvr.2010.03.009

Liao, F., Zhang, K., Zhou, L., Chen, Y., Elliott, J., and Jan, Y. K. (2020). Effect of different local vibration frequencies on the multiscale regularity of plantar skin blood flow. *Entropy* 22:1288. doi: 10.3390/e22111288

Lu, C. W., Czosnyka, M., Shieh, J. S., Smielewska, A., Pickard, J. D., and Smielewski, P. (2012). Complexity of intracranial pressure correlates with outcome after traumatic brain injury. *Brain* 135, 2399–2408. doi: 10.1093/brain/aws155

Manor, B., Costa, M. D., Hu, K., Newton, E., Starobinets, O., Kang, H. G., et al. (2010). Physiological complexity and system adaptability: evidence from postural control dynamics of older adults. *J. Appl. Physiol.* 109, 1786–1791. doi: 10.1152/japplphysiol.00390.2010

Mezentseva, L. V., and Pertsov, S. S. (2019). Correlation-and-spectral analysis of time series for microcirculatory parameters in vessels of symmetrical organs. *Bull. Exp. Biol. Med.* 166, 301–305. doi: 10.1007/s10517-019-04337-y

Niskanen, J. P., Tarvainen, M. P., Ranta-Aho, P. O., and Karjalainen, P. A. (2004). Software for advanced HRV analysis. *Comput. Methods Prog. Biomed.* 76, 73–81. doi: 10.1016/j.cmpb.2004.03.004

Pinter, A., Horvath, T., Sarkozi, A., and Kollai, M. (2012). Relationship between heart rate variability and endothelial function in healthy subjects. *Auton. Neurosci.-Basic Clin.* 169, 107–112. doi: 10.1016/j.autneu.2012.05.005

Schneider, M., Kraemmer, M. M., Weber, B., and Schwerdtfeger, A. R. (2021). Life events are associated with elevated heart rate and reduced heart complexity to acute psychological stress. *Biol. Psychol.* 163:108116. doi: 10.1016/j.biopsycho.2021.108116

Stupin, A., Stupin, M., Baric, L., Matic, A., Kolar, L., and Drenjancevic, I. (2019). Sex-related differences in forearm skin microvascular reactivity of young healthy subjects. *Clin. Hemorheol. Microcirc.* 72, 339–351. doi: 10.3233/CH-180483

Tapar, H., Karaman, S., Dogru, S., Karaman, T., Sahin, A., Tapar, G. G., et al. (2018). The effect of patient positions on perfusion index. *BMC Anesthesiol.* 18:111. doi: 10.1186/s12871-018-0571-z

Vallortigara, G., and Rogers, L. J. (2005). Survival with an asymmetrical brain: advantages and disadvantages of cerebral lateralization. *Behav. Brain Sci.* 28, 575–589. doi: 10.1017/S0140525X05000105

Wang, G., Han, J., Litscher, G., and Zhang, W. (2012). System identification algorithm analysis of acupuncture effect on mean blood flux of contralateral hegu acupoint. *Evid. Based Complement. Alternat. Med.* 2012:951928. doi: 10.1155/2012/951928

Wang, G., Jia, S., Li, H., Song, X., and Zhang, W. (2019). Exploring the relationship between the speed-resolved perfusion of blood flux and HRV following different thermal stimulations using MSE and MFE analyses. *PLoS One* 14:e0217973. doi: 10.1371/journal.pone.0217973

Wang, G., Jia, S., Li, H., Wang, Z., Tian, Y., and Zhang, W. (2017). Response of blood perfusion at ST 36 Acupoint after drinking cold glucose or saline injection. *Evid. Based Complement. Alternat. Med.* 2017:4212534. doi: 10.1155/2017/4212534

Wang, G., Jia, S., Li, H., Wang, Z., and Zhang, W. (2018). Exploring the relationship between blood flux signals and HRV following different thermal stimulations using complexity analysis. *Sci. Rep.* 8:8982. doi: 10.1038/s41598-018-27374-5

Wang, G., Tian, Y., Jia, S., Litscher, G., and Zhang, W. (2012). Evaluate laser needle effect on blood perfusion signals of contralateral hegu acupoint with wavelet analysis. *Evid. Based Complement. Alternat. Med.* 2012:103729. doi: 10.1155/2012/103729

Wang, G., Tian, Y., Jia, S., Wang, Z., and Zhang, W. (2017). Laterality and coherence analysis of laser Doppler Flowmetry signals in bilateral Nèi guān (内关 PC 6): a potential non-invasive method to assess microdrculatory changes of people in different ages. *World J. Acupuncture - Moxibustion* 27, 47–52. doi: 10.1016/S1003-5257(17)30099-5

Wang, G., Tian, Y., Jia, S., Zhou, W., and Zhang, W. (2013). Pilot study of acupuncture point laterality: evidence from heart rate variability. *Evid. Based Complement. Alternat. Med.* 2013:476064. doi: 10.1155/2013/476064

Wang, G., Tian, Y., Jia, S., Zhou, W., and Zhang, W. (2015). Acupuncture regulates the heart rate variability. *J. Acupunct. Meridian Stud.* 8, 94–98. doi: 10.1016/j.jams.2014.10.009

Wong, D. H., Tremper, K. K., Zaccari, J., Hajduczek, J., Konchigeri, H. N., and Hufstedler, S. M. (1988). Acute cardiovascular response to passive leg raising. *Crit. Care Med.* 16, 123–125. doi: 10.1097/00003246-198802000-00005

Yao, Y. J., Wu, X. Y., Sun, X. Q., Wang, Z. B., Jiang, C. L., and Jiang, S. Z. (2001). Changes in blood flow mechanics of arteries in the brain during 21d head low bed. *Space Med. Med. Eng.* 14, 11–16. doi: 10.16289/j.cnki.1002-0837.2001.01.003

Yoo, J. K., and Fu, Q. (2020). Impact of sex and age on metabolism, sympathetic activity, and hypertension. *FASEB J.* 34, 11337–11346. doi: 10.1096/fj.202001006RR

Young, H., and Benton, D. (2015). We should be using nonlinear indices when relating heart-rate dynamics to cognition and mood. *Sci. Rep.* 5:16619. doi: 10.1038/srep16619

Zubcevic, J., Richards, E. M., Yang, T., Kim, S., Sumners, C., Pepine, C. J., et al. (2019). Impaired autonomic nervous system-microbiome circuit in hypertension. *Circ. Res.* 125, 104–116. doi: 10.1161/CIRCRESAHA.119.313965

Conflict of Interest: The authors declare that the research was conducted in the absence of any commercial or financial relationships that could be construed as a potential conflict of interest.

Publisher's Note: All claims expressed in this article are solely those of the authors and do not necessarily represent those of their affiliated organizations, or those of the publisher, the editors and the reviewers. Any product that may be evaluated in this article, or claim that may be made by its manufacturer, is not guaranteed or endorsed by the publisher.

frontiers in Physiology

ORIGINAL RESEARCH
published: 23 June 2021
doi: 10.3389/fphys.2021.670640

Gravity-Induced Lower-Leg Swelling Can Be Ameliorated by Ingestion of α-Glucosyl Hesperidin Beverage

Naoki Nishimura[1], Satoshi Iwase[2], Hiroko Takumi[3] and Keiko Yamamoto[4]*

[1] Department of Sport Sciences, Faculty of Sport Sciences, Nihon Fukushi University, Mihama, Japan, [2] Department of Physiology, School of Medicine, Aichi Medical University, Nagakute, Japan, [3] Institute of Health Sciences, Ezaki Glico Co., Ltd., Osaka, Japan, [4] Okinawa Prefectural College of Nursing, Naha, Japan

The most likely cause of lower-leg swelling is prolonged sitting, which sometimes induces deep vein thrombosis, also known as, economy class syndrome. We aimed to clarify the influence of intake of 4^G-α-glucopyranosyl hesperidin (G-Hsp) beverage on the lower-leg swelling caused by 6 h of sitting in six healthy women. All subjects ingested 100 mL of G-Hsp or Placebo beverages with 100 mL of mineral water after 10 min of rest in a chair. Subsequently, subjects were requested to sit in the chair in a relaxed position for 6 h with two breaks to walk for urination. Calf water content measured by impedance plethysmography, calf circumference, and calf skin temperature by infrared thermography were measured, along with assessment of calf swelling sensation on a visual analog scale. Increase in ankle % circumference was significantly less after the G-Hsp ingestion (101.8 ± 1.5%) than after placebo (103.3 ± 0.8%; $P = 0.004$). A significant difference was found between percent circumference after the G-Hsp and the placebo, that is, the calf swelling after the placebo was significantly larger ($P = 0.043$). A gradual increase in skin temperature at the lower limb was observed after G-Hsp ingestion, while there was no change after placebo. Gravity-induced calf and ankle swelling resulted by prolonged sitting can be ameliorated by oral ingestion of hesperidin-derived G-Hsp through production of nitric oxide. It might be helpful in preventing economy-class syndrome caused by enforced sitting for a long duration.

Keywords: 4^G-α-glucopyranosyl hesperidin, lower leg swelling, vascular permeability, gravity, skin surface temperature

OPEN ACCESS

Edited by:
Airong Qian, Northwestern Polytechnical University, China

Reviewed by:
Jochen Zange, German Aerospace Center, Helmholtz Association of German Research Centers (HZ), Germany
Ronan Padraic Murphy, Dublin City University, Ireland

****Correspondence:***
Naoki Nishimura
nnaoki@n-fukushi.ac.jp

Specialty section:
This article was submitted to Environmental, Aviation and Space Physiology, a section of the journal Frontiers in Physiology

Received: *22 February 2021*
Accepted: *30 April 2021*
Published: *23 June 2021*

Citation:
Nishimura N, Iwase S, Takumi H and Yamamoto K (2021) Gravity-Induced Lower-Leg Swelling Can Be Ameliorated by Ingestion of α-Glucosyl Hesperidin Beverage. Front. Physiol. 12:670640. doi: 10.3389/fphys.2021.670640

INTRODUCTION

Foot, ankle, and lower-leg swelling refers to an accumulation of interstitial fluid in the lowest part of the body. It is a type of edema, which is an abnormal accumulation of interstitial fluid (Weber, 1932). Clinically, edema is significant swelling; the amount of interstitial fluid is determined by the balance of fluid homeostasis and the increased secretion of fluid into the interstitium, and the most likely cause of lower-leg swelling is prolonged sitting, which sometimes induces pulmonary embolism or deep vein thrombosis when blood clots leave and move to the lungs (Cruickshank et al., 1977; Lapostolle et al., 2001; Abunnaja et al., 2014). This lower-leg swelling is likely to occur in the lower limb in the daily lives of normal subjects (Yoneyama et al., 2007). In order to prevent this lower-leg swelling, several physical techniques have been implemented including dynamic action (Stick et al., 1992) and compression (Khoshgoftar et al., 2009) of the lower-leg muscles (the tibialis

anterior, the soleus, and the gastrocnemius). However, oral ingestion of beverages has not been well examined yet.

The flavonoids including flavanones, flavone, and isoflavon are polyphenols present in the peel of such fruits as the mandarin orange (*Citrus unshiu* Marc.) in the form of glycosides. Hesperidin, one of the flavanone glycosides, is contained in the skin and flesh of some citrus fruits, and is considered to protect the fruit from ultraviolet rays, namely through vitamin P (Bentsáth et al., 1936). It has been shown to exert many biological activities, including reducing blood cholesterol levels and enhancing blood circulation (Garg et al., 2001). Hesperidin is one of the primary constituents of *Citrus unshiu* peel but is of limited use because of its low water solubility (Yamada et al., 2006). A hesperidin-derived compound, 4^G-α-glucopyranosyl hesperidin (G-Hsp), by transglucosylation using cyclodextrin glucano-transferase (**Figure 1**) is much more soluble than conventional hesperidin (Kometani et al., 1994). Its absorbance rate to the human body is three times higher than that of hesperidin (Kometani et al., 2008). Moreover, it has been reported that G-Hsp can treat capillary fragility and permeability decrease (Garg et al., 2001; Liu et al., 2008), has an antioxidant effect (Hijiya and Miyake, 1991), and acts as an antiallergic (Galati et al., 1994) and antihypertensive (Galati et al., 1996). Thus, by enhancing the permeability of interstitial fluid into the blood vessel, G-Hsp might reduce lower-leg swelling.

We measured calf water content and calf circumference to examine the effect of G-Hsp ingestion on the prevention of the lower-leg swelling caused by prolonged sitting in healthy women. We hypothesized that the oral ingestion of a beverage containing dissolved G-Hsp would suppress water congestion at the lower leg in middle-aged women during prolonged sitting.

MATERIALS AND METHODS

Subjects

Six healthy women served as the subjects. Their ages were 43 ± 2 years. They were all non-smokers and were taking no medications. They were given sufficient explanation and provided written informed consent. The protocol of the present study was approved by the institutional review board of Aichi Medical University. The study was conducted in accordance with the principles of the Declaration of Helsinki. Subjects were requested to abstain from caffeinated beverages, alcohol, citrus, and spices for at least 12 h before experimental sessions.

Experimental Protocol

The subjects were requested to come to the laboratory at 10:00 h, at least 2 h after a light meal. All subjects were familiarized with the equipment and procedures before any experimental sessions. The experiments were carried out in an artificial climate chamber at an ambient temperature of 26°C and 50% relative humidity. The subjects change clothes a long-sleeved shirt and shorts pants after urination before start of experiments. After measuring of the circumference of the lower leg at the 1/2 and 1/4 sites between the patella and the malleolus of the subjects in a relaxed sitting position at the chair, an impedance electrode was applied halfway between the patella and the first toe. After 10 min of control reading, the subjects ingested 100 mL of test beverage with 100 mL of mineral water (total 200 mL) within a minute. The test beverage either contained dissolved G-Hsp or a placebo. The subjects were requested to come to the laboratory twice on other days, and the order of the beverages was selected at random (double blind study). After ingestion, they sat on a chair in a relaxed position for 6 h. At 2 h and 4 h after ingestion, they were requested to ingest 200 mL of mineral water, and they were allowed to walk for 30 s to the toilet next to the climatic chamber to urinate. During the 6 h of sitting, they were instructed to move as little as possible.

Measurements

Calf water content was measured by impedance plethysmography using the bioelectrical impedance analysis (BIA) method (Kyle et al., 2004a,b) to analyze the body composition at the lower leg. This method measures the impedance between the two electrodes using an impedance plethysmograph (Nihon Koden AI-601G, Tokyo). Skin temperature at the lower limb was assessed by infrared thermography (Avio TVS-200EX, Tokyo Japan) every 30 min. The calf and ankle perimeters were measured every 30 min using a measuring tape. Subjective symptoms of calf swelling were rated every 30 min using a visual analog scale (VAS) between 0 and 100. Subjective symptoms of calf swelling were rated every 30 min using a VAS. This uses a 100 mm VAS, ranging from 0 (no swelling) to 100 (very severe swelling).

Test Beverage

Each subject ingested 100 mL of a beverage containing 1,000 mg of G-Hsp with 100 mL of mineral water. The sweetness (sucrose) and acidic (citric acid) had been added to the beverage for taste the same to placebo beverage. A placebo beverage not containing G-Hsp was used for comparison. G-Hsp and placebo beverage were ingested on the other days in a random order.

Statistics

All data are shown as the mean ± SE. Statistical significances between G-Hsp and placebo were calculated using two-way analysis of variance (ANOVA) followed by Greenhouse-Geisser or Huynh-Feldt multiple comparison tests. A p-value < 0.05 was considered significant. The VAS assessment was analyzed using the t-test.

RESULTS

Changes in Calf Water Content During Sitting

Since the impedance of biological tissue is a reciprocal of its water content, a decrease in impedance reflects an increase in water content. The calf impedance decreased gradually during sitting for 6 h after beverage ingestion. The percent difference from the control reading (taken as 100%), impedance tended to be smaller after G-Hsp ingestion than after the placebo ($P = 0.053$; **Figure 2**).

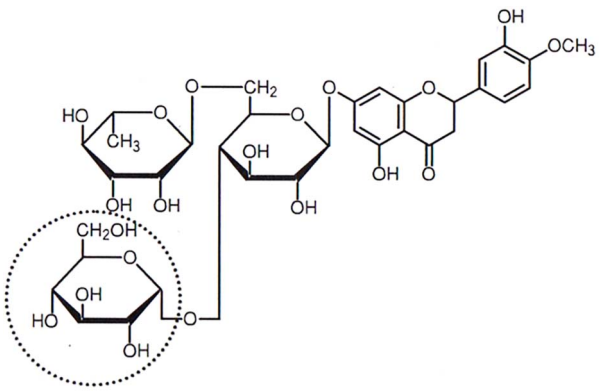

FIGURE 1 | Structure of 4^G-α-D-glucosylhesperidin.

Changes in Ankle Circumferences During Prolonged Sitting

The ankle circumference was increased with sitting time, and the absolute values of ankle circumference exhibited significant difference between G-Hsp and placebo ($P = 0.002$; **Figure 3**). Furthermore, there was a significant difference between the percent changes in circumference from the control reading after the G-Hsp beverage ingestion and after placebo. The increase in ankle percent circumference was significantly less after the G-Hsp ingestion ($101.8 \pm 1.5\%$) than after placebo ($103.3 \pm 0.8\%$; $P = 0.004$; **Figure 3**).

Changes in Calf Circumferences During Prolonged Sitting

The calf circumference also increased with sitting time. A significant difference was found between percent circumference after the G-Hsp and the placebo, that is, the calf swelling after placebo was significantly larger ($P = 0.043$; **Figure 4**).

Changes in Skin Surface Temperature During Prolonged Sitting

A typical case of the skin surface temperature change shown by the infrared thermography is illustrated in **Figure 5**. In the lower-leg area, a gradual increase in the skin surface temperature was observed up to 6 h after G-Hsp ingestion. In contrast, a gradual decrease in the skin surface temperature was seen after placebo ingestion.

Changes in Subjective Symptoms of Swelling During Prolonged Sitting

The VAS score for subjective symptoms of calf swelling is illustrated in **Figure 6**. The VAS score for subjective symptoms over time tended to be reduced by G-Hsp ingestion. However, the difference from the placebo was not significant.

DISCUSSION

The present study confirmed that the ankle swelling caused by prolonged sitting was ameliorated by the ingestion of a hesperidin derived compound, G-Hsp. This means that the ankle swelling was significantly larger after placebo ingestion.

The main findings of the present study were as follows: (1) the increase in calf water content induced by prolonged sitting as measured by bioimpedance analysis was suppressed by G-Hsp ingestion (**Figure 2**), (2) increases in the calf and the ankle circumference and subjective symptoms of swelling were suppressed by G-Hsp ingestion (**Figures 3**, **4**, **6**) and, (3) increases in skin temperature were facilitated by G-Hsp ingestion (**Figure 5**).

Symptoms of calf swelling are observed during and after prolonged standing or sitting, especially in women, and especially during pregnancy (Yoneyama et al., 2007). Venous clotting, especially pulmonary embolism or deep vein thrombosis, also known as, economy class syndrome, is one of the serious problems associated with prolonged sitting

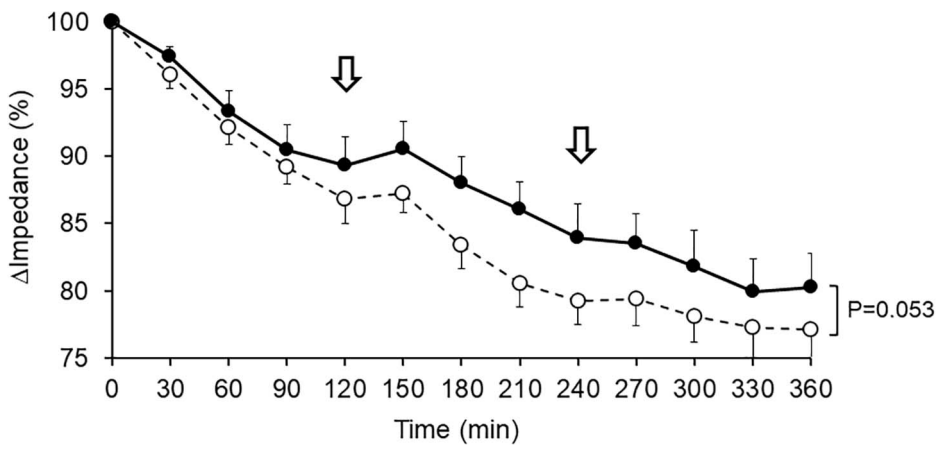

FIGURE 2 | Changes in impedance of the lower leg after 1,000 mg of G-Hsp (●) and Placebo (○) beverage ingestion. The arrow indicates the walking for urination, mean and SE, $n = 6$.

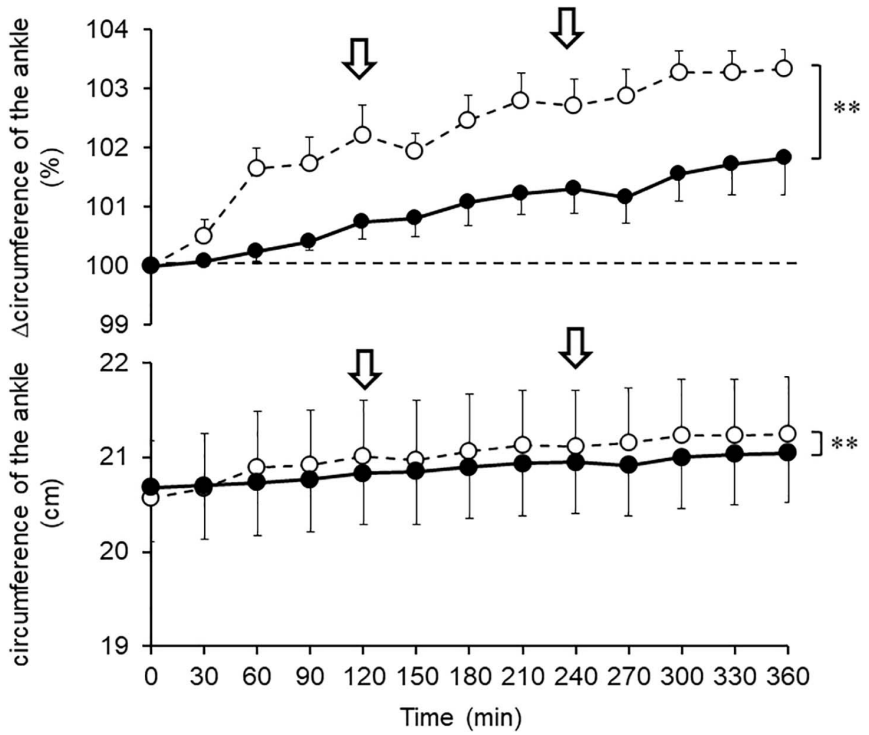

FIGURE 3 | Changes in circumference of the ankle after 1,000 mg of G-Hsp (•) and Placebo (○) beverage ingestion. The arrow indicates the walking for urination, mean and SE, $n = 6$, Asterisks indicate significant differences (**$P < 0.01$).

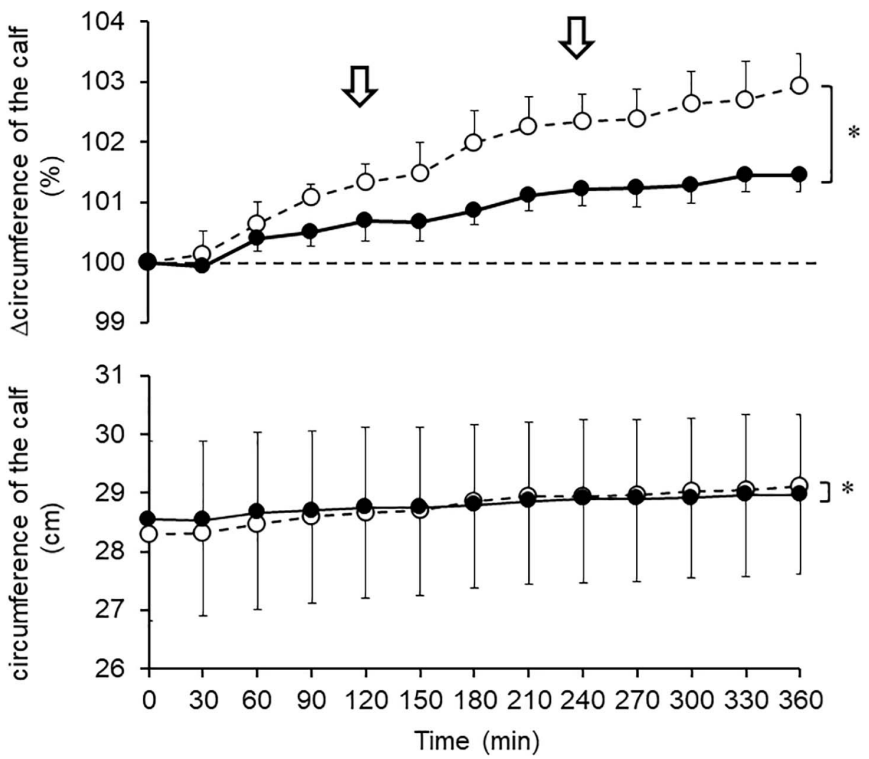

FIGURE 4 | Changes in circumference of the calf after 1,000 mg of G-Hsp (•) and Placebo (○) beverage ingestion. The arrow indicates the walking for urination, mean and SE, $n = 6$, Asterisks indicate significant differences (*$P < 0.05$).

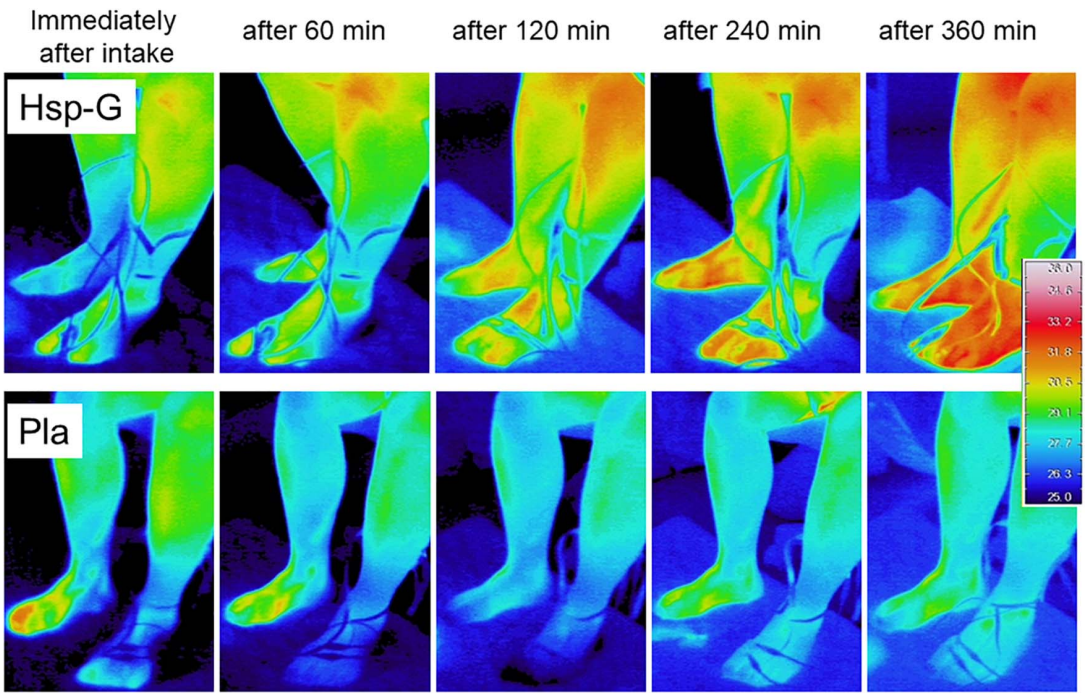

FIGURE 5 | Comparison of skin temperature in the lower leg after 1,000 mg of G-Hsp (*upper panel*) and Placebo (lower panel) beverage ingestion in a subject.

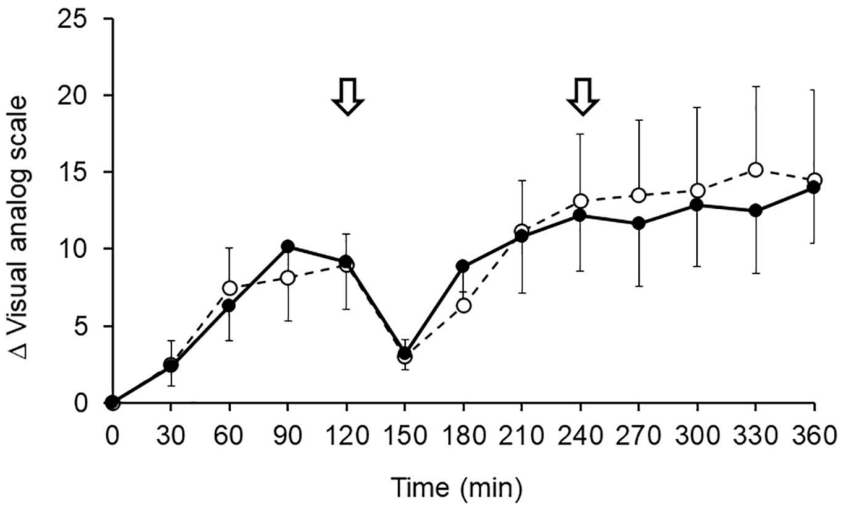

FIGURE 6 | Changes in subjective symptoms of calf swelling using VAS scale after 1,000 mg of G-Hsp (•) and Placebo (○) beverage ingestion. The arrow indicates the walking for urination, mean and SE, $n = 6$.

(Cruickshank et al., 1977; Lapostolle et al., 2001; Abunnaja et al., 2014), and dehydration caused by hypovolemia also contributes to this syndrome (Eklof et al., 1996). Hamada et al. (2002) reported that ionized beverage ingestion significantly ameliorates the condition. However, there has been no report on what kinds of supplement can facilitate the reduction of calf swelling.

4^G-α-glucopyranosyl hesperidin is hydrolyzed into hesperidin by intestinal mucosal α-glucosidases, followed by its hydrolysis into aglycone hesperetin by β-glucosidase found in cytoplasm, and its absorption into the human body (Ohtsuki et al., 2002, 2003; Nielsen et al., 2006). It has been reported that G-Hsp is absorbed more efficiently and functions more effectively than hesperidin (Yamada et al., 2006). Various physiological functions of G-Hsp have been reported including serum lipid improvement (Miwa et al., 2005), bone metabolism improvement (Chiba et al., 2013), blood pressure decrease (Yamamoto et al., 2008), and reduced inflammation (Kometani et al., 2008).

In the present study, the calf and ankle swelling caused by prolonged sitting was possibly contributed to by femoral compression that reduced venous return and the effect of hydrostatic congestion in the lower extremities. This increased venous pressure can induce blood plasma to leak out of the vessels, eventually resulting in water retention in the interstitium. This calf and ankle swelling and subjective symptoms of swelling were ameliorated by ingestion of G-Hsp contained beverage.

The skin temperature was increased at 6 h after the G-Hsp ingestion, reflecting improved peripheral circulation through G-Hsp intake. A recent study on the suppression of tympanic and skin temperature decrease by exposure to cold confirmed the vasodilative effect and heat production caused by a G-Hsp ingestion, as well as a warmer sensation, particularly in women with high sensitivity to cold in the lower legs (Takumi et al., 2010). They administrated oral G-Hsp to the women for 4 weeks, and the subjects' discomfort related to blood circulation and autonomic nervous system was ameliorated. In addition to this chronic administration study, the present acute administration study confirmed the effectiveness of G-Hsp on prevention of calf and ankle swelling as well as skin temperature maintenance.

The mechanism of blood circulatory improvement is considered to be dependent on nitric oxide production, inducing vascular dilatation (Takumi et al., 2011), since oral administration of G-Hsp for 3 weeks has been proved to promote nitric oxide production, reduced inflammation, and improved vascular endothelial cells (Rizza et al., 2011). In animal studies, administration of G-Hsp to spontaneous hypertensive rats were found to increase the bioavailability of smooth muscles, resulting in an increase in peripheral circulation and a decrease in systemic blood pressure (Yamamoto et al., 2008). Another study on the autonomic nervous system showed that G-Hsp administration to healthy women led to a significantly lower LF/HF ratio and higher HF component in heart rate variability, indicating vagal tone increase after ingestion of G-Hsp (Takumi et al., 2010).

In conclusion, gravity-induced calf and ankle swelling resulted by prolonged sitting can be ameliorated by oral ingestion of hesperidin-derived G-Hsp through production of nitric oxide. This may help people who complain of discomfort from lower-leg swelling and may provide a good measure for preventing economy-class syndrome.

DATA AVAILABILITY STATEMENT

The raw data supporting the conclusions of this article will be made available by the authors, without undue reservation.

ETHICS STATEMENT

The studies involving human participants were reviewed and approved by the Aichi Medical University. The patients/participants provided their written informed consent to participate in this study.

AUTHOR CONTRIBUTIONS

NN and HT decided on the conception and design of the research. NN drafted the manuscript. NN, HT, and KY performed the experiments, analyzed the data, and interpreted the results of the experiments. All authors edited and revised the manuscript and read and approved the final manuscript.

FUNDING

This study was funded by the Ezaki Glico Co., Ltd. (to SI). The funding body had no role in the design of this study, data collection, interpretation of data, or in writing of the manuscript.

ACKNOWLEDGMENTS

We appreciate the effort spent by volunteer subjects in this study. This study was performed as the cooperative research between Aichi Medical University and Ezaki Glico Co., Ltd.

REFERENCES

Abunnaja, S., Clyde, M., Cuviello, Brenes, R. A., and Tripodi, G. (2014). Concomitant deep venous thrombosis, femoral artery thrombosis, and pulmonary embolism after air travel. *Case Rep. Vasc. Med.* 2014, 1–4. doi: 10.1155/2014/174147

Bentsáth, A., Rusznyák, S. T., and Szent-Györgyi, A. (1936). Vitamin nature of flavones. *Nature* 138:798.

Chiba, H., Uehara, M., Wu, J., Wang, X., Masuyama, K., Suzuki, K., et al. (2013). Hesperidin, a citrus flavonoid, inhibits bone loss and decreases serum and hepatic lipids in ovariectomized mice. *J. Nutr.* 133, 1892–1897. doi: 10.1093/jn/133.6.1892

Cruickshank, J. M., Gorlin, R., and Jennett, B. (1977). Air travel and thrombotic episodes: the economy class syndrome. *Lancet* 332, 497–498. doi: 10.1016/s0140-6736(88)90134-1

Eklof, B., Kistner, R. L., Masuda, E. M., Sonntag, B. V., and Wong, H. P. (1996). Venous thromboembolism in association with prolonged air travel. *Dermatol. Surg.* 22, 637–641. doi: 10.1111/j.1524-4725.1996.tb00610.x

Galati, E. M., Monforte, M. T., Kirjavainenm, S., Forestieri, A. M., Trovato, A., and Tripodo, M. M. (1994). Biological effects of hesperidin, a citrus flavonoid. (Note I): anti-inflammatory and analgesic activity. *Farmaco* 40, 709–712.

Galati, E. M., Trovato, A., Kirjavainenm, S., Forestieri, A. M., Rossitto, A., and Monforte, M. T. (1996). Biological effects of hesperidin, a citrus flavonoid. (Note III): antihypertensive and diuretic activity in rat. *Farmaco* 51, 219–221.

Garg, A., Garg, S., Zaneveld, L. J., and Singla, A. K. (2001). Chemistry and pharmacology of the citrus bioflavonoid hesperidin. *Phytother. Res.* 15, 655–669. doi: 10.1002/ptr.1074

Hamada, K., Doi, T., Sakurai, M., Matsumoto, K., Yanagisawa, K., Suzuki, T., et al. (2002). Effects of hydration on fluid balance and lower-extremity blood viscosity during long airplane flights. *JAMA* 287, 844–845. doi: 10.1001/jama.287.7.844-a

Hijiya, H., and Miyake, T. (1991). *Alpha-glycosyl hesperidin, and its preparation and uses. European Patent Publication. No 0402049*. Munich: European Patent Office.

Khoshgoftar, Z., Esfahani, A. F., Marzban, M., Omran, A. S., Ghasemi, A. H., Movaghar, S., et al. (2009). Comparison of compression stocking with elastic

bandage in reducing postoperative edema in coronary artery bypass graft patient. *J. Vasc. Nurs.* 27, 103–106. doi: 10.1016/j.jvn.2009.09.004

Kometani, T., Terada, Y., Nishimura, T., Takii, H., and Okada, S. (1994). Transglycosylation to Hesperidin by Cyclodextrin Glucanotransferase from an Alkalophilic Bacillus Species in Alkaline pH and Properties of Hesperidin Glycosides. *Biosci. Biotechnol. Biochem.* 58, 1990–1994. doi: 10.1271/bbb.58.1990

Kometani, T., Fukuda, T., Kakuma, T., Kawaguchi, K., Tamura, W., Kumazawa, Y., et al. (2008). Effects of α-glucosylhesperidin, a bioactive food material, on collagen induced arthritis in mice and rheumatoid arthritis in humans. *Immnopharmacol. Immunotoxicol.* 30, 117–134. doi: 10.1080/08923970701812688

Kyle, U. G., Bosaeus, I., De Lorenzo, A. D., Deurenberg, P., Elia, M., Gómez, J. M., et al. (2004a). Bioelectrical impedance analysis- part I: review of principles and methods. *Clin. Nutr.* 23, 1226–1243. doi: 10.1016/j.clnu.2004.06.004

Kyle, U. G., Bosaeus, I., De Lorenzo, A. D., Deurenberg, P., Elia, M., Gómez, J. M., et al. (2004b). Bioelectrical impedance analysis-part II: utilization in clinical practice. *Clin. Nutr.* 23, 1430–1453. doi: 10.1016/j.clnu.2004.09.012

Lapostolle, F., Surget, V., Borron, S. W., Desmaizières, M., Sordelet, D., Lapandry, C., et al. (2001). Severe pulmonary embolism associated with air travel. *N. Engl. J. Med.* 345, 779–783. doi: 10.1056/NEJMoa010378

Liu, L., Xu, D. M., and Cheng, Y. Y. (2008). Distinct effects of naringenin and hesperetin on nitric oxide production from endothelial cells. *J. Agric. Food. Chem.* 56, 824–829. doi: 10.1021/jf0723007

Miwa, Y., Mitsuzumi, T., Sunayama, T., Yamada, M., Okada, K., Kubota, M., et al. (2005). Glucosyl hesperidin lowers serum triglyceride level in hypertriglyceridemic subjects through the improvement of very low-density lipoprotein metabolic abnormality. *J. Nutr. Sci. Vitaminol.* 51, 460–470. doi: 10.3177/jnsv.51.460

Nielsen, I. L., Chee, W. S., Poulsen, L., Offord-Cavin, E., Rasmussen, S. E., Frederiksen, H., et al. (2006). Bioavailability is improved by enzymatic modification of the citrus flavonoid hesperidin in humans: a randomized, double-blind, crossover trial. *J. Nutr.* 136, 404–408. doi: 10.1093/jn/136.2.404

Ohtsuki, K., Abe, A., Mitsuzuwi, H., Kondo, M., Uemura, K., Iwasaki, Y., et al. (2002). Effects of long-term administration of hesperidin and glucosyl hesperidin to spontaneously hypertensive rats. *J. Nutr. Sci. Vitaminol.* 48, 420–422. doi: 10.3177/jnsv.48.420

Ohtsuki, K., Abe, A., Mitsuzuwi, H., Kondo, M., Uemura, K., Iwasaki, Y., et al. (2003). Glucosyl hesperidin improves serum cholesterol composition and inhibits hypertrophy in vasculature. *J. Nutr. Sci. Vitaminol.* 49, 447–450. doi: 10.3177/jnsv.49.447

Rizza, S., Muniyappa, R., Iantorno, M., Kim, J. A., Chen, H., Pullikotil, P., et al. (2011). Citrus polyphenol hesperidin stimulates production of nitric oxide in endothelial cells while improving endothelial function and reducing inflammatory markers in patients with metabolic syndrome. *J. Clin. Endcrinol. Metab.* 96, E782–E792. doi: 10.1210/jc.2010-2879

Stick, C., Jaeger, H., and Witzleb, E. (1992). Measurements of volume changes and venous pressure in the human lower leg during walking and running. *J. Appl. Physiol.* 72, 2063–2068. doi: 10.1152/jappl.1992.72.6.2063

Takumi, H., Fujishima, N., Shiraishi, K., Mori, Y., Ariyama, A., Kometani, T., et al. (2010). Effects of alpha-glucosylhesperidin on the peripheral body temperature and autonomic nervous system. *Biosci. Biotechnol. Biochem.* 74, 707–715. doi: 10.1271/bbb.90742

Takumi, H., Nakamura, H., Kamasaka, H., Kometani, T., Nadamoto, T., Terao, J., et al. (2011). Effects of α-Glucosyl hesperidin on the blood circulation. *Bull. Appl. Glycosci.* 1, 186–193.

Yamada, M., Tanabe, F., Arai, N., Mitsuzumi, H., Miwa, Y., Kubota, M., et al. (2006). Bioavailability of glucosyl hesperidin in rats. *Biosci. Biochnol. Biochem.* 70, 1386–1394. doi: 10.1271/bbb.50657

Yamamoto, M., Suzuki, A., and Hase, T. (2008). Short-term effects of glucosyl hesperidin and hesperetin on blood pressure and vascular endothelial function in spontaneously hypertensive rats. *J. Nutr. Sci. Vitaminol.* 54, 95–98. doi: 10.3177/jnsv.54.95

Yoneyama, M., Yatsuzuka, M., Ishida, Y., Shinmen, N., Hara, Y., and Matsui, A. (2007). The present status of the foot trouble and its care in college students. *J. Nurs. Soc. Univ. Toyama* 6, 27–35. doi: 10.15099/00002602

Weber, F. P. (1932). Persistent oedema of right lower limb. *Proc. R. Soc. Med.* 26, 53–54.

Conflict of Interest: HT was employed by the Ezaki Glico Co., Ltd., Osaka, Japan.

The remaining authors declare that the research was conducted in the absence of any commercial or financial relationships that could be construed as a potential conflict of interest.

frontiers in Physiology

ORIGINAL RESEARCH
published: 27 October 2021
doi: 10.3389/fphys.2021.712422

Orthostatic Resiliency During Successive Hypoxic, Hypoxic Orthostatic Challenge: Successful vs. Unsuccessful Cardiovascular and Oxygenation Strategies

Michael Nordine[1], Sascha Treskatsch[1], Helmut Habazettl[2], Hanns-Christian Gunga[2], Katharins Brauns[2], Petr Dosel[3], Jan Petricek[3] and Oliver Opatz[2]*

[1] Department of Anaesthesiology and Intensive Care Medicine, Berlin Institute of Health, Charité – Universitätsmedizin Berlin, Corporate Member of Freie Universität Berlin, Humboldt-Universität zu Berlin, Berlin, Germany, [2] Center for Space Medicine and Extreme Environments Berlin, Berlin Institute of Health, Institute of Physiology, Charité – Universitätsmedizin Berlin, Corporate Member of Freie Universität Berlin, Humboldt-Universität zu Berlin, Berlin, Germany, [3] Military University Hospital, Institute of Aviation Medicine, Prague, Czechia

OPEN ACCESS

Edited by:
Ronan Padraic Murphy, Dublin City University, Ireland

Reviewed by:
Martin Burtscher, University of Innsbruck, Austria
Richard D. Boyle, National Aeronautics and Space Administration (NASA), United States

***Correspondence:**
Michael Nordine
michael.nordine@charite.de

Specialty section:
This article was submitted to Environmental, Aviation and Space Physiology, a section of the journal Frontiers in Physiology

Received: *20 May 2021*
Accepted: *06 October 2021*
Published: *27 October 2021*

Citation:
Nordine M, Treskatsch S, Habazettl H, Gunga H-C, Brauns K, Dosel P, Petricek J and Opatz O (2021) Orthostatic Resiliency During Successive Hypoxic, Hypoxic Orthostatic Challenge: Successful vs. Unsuccessful Cardiovascular and Oxygenation Strategies. Front. Physiol. 12:712422. doi: 10.3389/fphys.2021.712422

Introduction: Rapid environmental changes, such as successive hypoxic-hypoxic orthostatic challenges (SHHOC) occur in the aerospace environment, and the ability to remain orthostatically resilient (OR) relies upon orchestration of physiological counter-responses. Counter-responses adjusting for hypoxia may conflict with orthostatic responses, and a misorchestration can lead to orthostatic intolerance (OI). The goal of this study was to pinpoint specific cardiovascular and oxygenation factors associated with OR during a simulated SHHOC.

Methods: Thirty one men underwent a simulated SHHOC consisting of baseline (P0), normobaric hypoxia (Fi02 = 12%, P1), and max 60 s of hypoxic lower body negative pressure (LBNP, P2). Alongside anthropometric variables, non-invasive cardiovascular, central and peripheral tissue oxygenation parameters, were recorded. OI was defined as hemodynamic collapse during SHHOC. Comparison of anthropometric, cardiovascular, and oxygenation parameters between OR and OI was performed via Student's *t*-test. Within groups, a repeated measures ANOVA test with Holm-Sidak *post hoc* test was performed. Performance diagnostics were performed to assess factors associated with OR/OI (sensitivity, specificity, positive predictive value PPV, and odd's ratio OR).

Results: Only 9/31 were OR, and 22/31 were OI. OR had significantly greater body mass index (BMI), weight, peripheral Sp02, longer R-R Interval (RRI) and lower heart rate (HR) at P0. During P1 OR exhibited significantly higher cardiac index (CI), stroke volume index (SVI), and lower systemic vascular resistance index (SVRI) than OI. Both groups exhibited a significant decrease in cerebral oxygenation (TOIc) with an increase in cerebral deoxygenated hemoglobin (dHbc), while the OI group showed a significant decrease in cerebral oxygenated hemoglobin (02Hbc) and peripheral oxygenation (TOIp) with an increase in peripheral deoxygenated hemoglobin (dHbp). During P2, OR

maintained significantly greater CI, systolic, mean, and diastolic pressure (SAP, MAP, DAP), with a shortened RRI compared to the OI group, while central and peripheral oxygenation were not different. Body weight and BMI both showed high sensitivity (0.95), low specificity (0.33), a PPV of 0.78, with an OR of 0.92, and 0.61. P0 RRI showed a sensitivity of 0.95, specificity of 0.22, PPV 0.75, and OR of 0.99. Delta SVI had the highest performance diagnostics during P1 (sensitivity 0.91, specificity 0.44, PPV 0.79, and OR 0.8). Delta SAP had the highest overall performance diagnostics for P2 (sensitivity 0.95, specificity 0.67, PPV 0.87, and OR 0.9).

Discussion: Maintaining OR during SHHOC is reliant upon greater BMI, body weight, longer RRI, and lower HR at baseline, while increasing CI and SVI, minimizing peripheral 02 utilization and decreasing SVRI during hypoxia. During hypoxic LBNP, the ability to remain OR is dependent upon maintaining SAP, via CI increases rather than SVRI. Cerebral oxygenation parameters, beyond 02Hbc during P1 did not differ between groups, suggesting that the during acute hypoxia, an increase in cerebral 02 consumption, coupled with increased peripheral 02 utilization does seem to play a role in OI risk during SHHOC. However, cardiovascular factors such as SVI are of more value in assessing OR/OI risk. The results can be used to implement effective aerospace crew physiological monitoring strategies.

Keywords: LBNP, hypoxia, cardiovascular, oxygenation, aerospace

INTRODUCTION

Rapid environmental changes can occur during aerospace travel, which can have significant consequences for crew health and safety. Specific environmental changes include acute alterations in atmospheric composition, such as hypoxia during sudden loss of cabin pressure for example, as well as orthostatic challenges, such as during take-off, orbital re-entry, and aerobraking maneuvers. Taken as solitary events, innate physiological counter-responses can compensate for these challenges, allowing the crew enough time to enact exogenous countermeasures, such as utilizing supplemental oxygen, or adjusting the approach vector to lessen the degree of hyper-gravity. Combined hypoxia and orthostatic challenge would present as a significant challenge for the innate physiological mechanisms to overcome, as these challenges require unique responses. Remaining orthostatically resilient (OR) during such intense environmental challenges, is essential, and any crew member that exhibited orthostatic intolerance (OI) during an acute onset hypoxic orthostatic challenge would be unable to perform complex motor or cognitive tasks, thereby increasing the risk of critical mission failure.

OR during a successive hypoxic-hypoxic orthostatic challenge (SHHOC) is dependent upon precise orchestration of physiological counter-responses to ensure cerebral perfusion and oxygenation. Under normal atmospheric conditions, cerebral blood flow and oxygenation are maintained via cerebral autoregulation. Cerebral autoregulation is, however, sensitive to changes in 02/C02. During acute hypoxia, vasodilation of the cerebral vessels is known to occur (Hoiland et al., 2016). This cerebral vasodilation increases cerebral blood flow, and thus provides the brain with an ample supply of oxygenated blood to maintain an optimal 02 extraction/utilization (Van Mil et al., 2002). States of hypoxia can alter cerebral autoregulation, so that optimal cerebral perfusion is impaired, despite compensatory cardiovascular reactions (Iwasaki et al., 2011). In the macro-circulation, hypoxia induces a compensatory increase in cardiac output (CO) via increases in stroke volume (SV) and heart rate (HR), with reductions in systemic vascular resistance (SVR) (Paparde et al., 2015; Siebenmann and Lundby, 2015). This response is modulated by the peripheral chemoreceptor system, located in the carotid bodies and aortic arch (Kane et al., 2020) and ensures adequate cerebral 02 delivery (D02) (Siebenmann and Lundby, 2015). Furthermore, a compensatory capillary recruitment occurs during acute hypoxia, leading to a significant decrease in SVR, thus allowing for increased tissue perfusion and 02 extraction (Mirna et al., 2020). A non-optimal response to hypoxia would include a decrease in CO, and an upsurge in SVR, which would lead to an increased peripheral 02 consumption, and inadequate blood flow. This non-optimal response could lead to compromised cerebral perfusion and oxygenation, thus increasing the risk for an OI event during an orthostatic challenge.

During acute orthostatic challenges, a sudden decrease in central blood volume, via cranial to caudal shifts, occurs. This in turn activates the baroreceptor reflex (Melchior et al., 1992), which activates a compensatory increase in SVR and HR, to maintain mean arterial pressure (MAP) and cerebral perfusion. Maintaining MAP above 65 mmHg is presumed to be the critical threshold that can preserve cerebral autoregulation, however, once MAP is below < 65 mmHg, cerebral autoregulation fails, and cerebral blood flow is then compromised (Rickards, 2015).

To remain OR during an orthostatic challenge, a balanced HR and SVR response are needed, which preserve CO and critical MAP. If these HR and SVR increases are not optimal nor carefully orchestrated, a critical decrease in cerebral perfusion can occur, thus leading to OI (Manuel et al., 2020).

The number of studies examining successful/unsuccessful response patterns during SHHOC are few. The only study to our knowledge, found that hypoxia blunts an effective SVR response during hypoxic orthostatic challenge, and the maintenance of cerebral perfusion is thus reliant upon maintaining CO to maintain MAP (Shepherd et al., 2020). Other studies have found that acute hypoxia can augment baroreflex responses as well as increase sympathetic outflow, meaning that acute hypoxic exposure, prior to and during orthostatic stress, would increase the chance of OR (Halliwill et al., 2003). Aarts et al. (2017) found a 70% OI occurrence during hypoxic LBNP, and that OR during hypoxic LBNP is reliant upon maintaining a MAP above 70 mmHg. Furthermore, that study found that the OI group was unable to mount an effective HR response during hypoxic LBNP (Aarts et al., 2017). Other working groups have concluded that the ability to maintain OR during SHHOC is dependent upon appropriately timed and orchestrated neural recruitment strategies (Badrov et al., 2015), and a misguided activation of the endogenous physiological counter-measure reactions could lead to OI. The ability to remain OR during a hypoxic orthostatic challenge would be dependent upon a robust cardiac (HR and CO) response, as hypoxia can attenuate any effective SVR counter-response. Finally, no study has examined both cardiovascular and central/peripheral oxygenation reactions during a SHHOC, so any successful/unsuccessful cerebral and peripheral oxygenation strategies are unknown at this time.

This study was performed to comprehensive analyze and catalog successful vs. unsuccessful cardiovascular and oxygenation strategies involved in maintaining OR during SHHOC. Given the findings of previous studies and the degree of orthostatic stress, we expected an OI rate of at least 50%, and that crew members exhibiting increases in CO (via HR increases and preserved SV) and decreases in SVR during hypoxia would exhibit a greater degree of OR during subsequent hypoxic orthostatic challenge. Also, the ability to remain OR during hypoxic orthostatic stress should primarily rely on maintaining CO as opposed to increases in SVR, to preserve cerebral oxygenation and perfusion. We further hypothesized that cerebral oxygenation and peripheral oxygenation parameters such as 02 utilization/extraction, could offer unique insights into OR/OI status. Finally, our goal was to determine which baseline factors, as well as physiological factors could be used as a predictive factor in pinpointing OR/OI status. The results would be therefore highly beneficial for, implementing appropriate physiological monitoring strategies for aerospace crews.

MATERIALS AND METHODS

Environmental Challenge Simulation

This study took place in September–October 2013, at the Prague military hospital, division of aerospace medicine, Prague, Czech Republic. A total of 31 Czech military aviation students underwent this SHHOC trial as part of their advanced military aviation training curriculum. Since this course was a mandatory part of the curriculum, no recruitment of volunteers was needed. All participants gave their informed consent for additional monitoring as part of this study, and the division of aerospace medicine approved of the study. The SHHOC consisted of a three-stage environmental challenge course. Phase 0 (P0), a 5-min sitting upright baseline phase, was followed by a normobaric hypoxic phase (P1). Normobaric hypoxia (Fi02 12%) was induced via facemask and a hypoxic gas mixture containing 12% Fi02. P1 lasted until central oxygen saturation (Sp02c) fell to 85%. Phase 2 (P2) consisted of a rapid onset of −70 mmHg lower body negative pressure (LBNP) for either 60 s or until OI occurred. OI was defined as either a narrowing of pulse pressure (PP), a 20% decrease in baseline mean arterial of systolic arterial pressure (MAP/SAP), a significant decrease in heart rate (HR < 60 bpm), loss of consciousness (LOC) or responsiveness (LOR), as well as reports of blurred vision, slurred speech, or vegetative symptoms such as sweating. The LBNP was turned off, mask removed, and normal atmospheric conditions were re-established if any participant exhibited any OI criteria. OR was classified as 60 s of hypoxic LBNP exposure without incident. The flight physician sat next to the participant the entire time and could stop the LBNP at any point.

On the day of testing, which was assigned randomly to each participant, a "check-in" was performed, which included acquiring the height and weight of each subject. Also, each participant had to dress down to boxer shorts, and the LBNP-seal was fitted across the waist, superior to the iliac crest. Then, each participant sat at a 90-degree upright position in the LBNP device while all monitoring equipment was attached.

Anthropometric Measurements

A height in centimeters (cm) and weight in kilograms (kg) was recorded for each participant. From this, a body mass index (BMI kg/cm^2), body surface according to Dubois (BSA cm^2), along with an estimated lean body mass according to Boer (LBM kg) were all calculated.

Hemodynamic Monitoring

Hemodynamic monitoring was performed non-invasively using the Finapress device using Beatscope software (®Finapres Medical Systems, Netherlands). SAP, DAP, and MAP were continuously measured via the dominant hand via a pneumatic pump placed on the index and middle finger. HR was measured via 3 Lead ECG, with R-R Interval (RRI) being taken from Lead II from each participant. Stroke volume (SV) was measured using pulse contour analysis, through which a cardiac output (CO) was calculated. Systemic vascular resistance (SVR) was calculated via MAP/CO. CO, SV, and SVR were all divided by BSA to give cardiac index (CI), stroke volume index (SVI), and systemic vascular resistance index (SVRI).

Central and Peripheral Oxygenation Parameters

Central 02 oxygenation (Sp02c) was measured via ear clip, while a finger probe was used to measure Sp02 peripherally from the non/dominant finger (Sp02p). Central and peripheral oxygenation was measured via near infrared spectroscopy (NIRS) (NIRO 200, Hamamatsu Instruments, Hamamatsu, Japan). Cerebral oxygenation was measured with a NIRS probe fixated to the right forehead, while peripheral oxygenation was measured with a second NIRS probe affixed to the right lateral thigh, bisecting the vastus lateralis muscle. The complete NIRS measurement included central and peripheral tissue oxygen index (TOIc/TOIp), delta central and peripheral total (tHbc/tHbp), oxygenated (02Hbc/02Hbp), and deoxygenated hemoglobin (dHbc/dHbp).

Data Analysis

Upon conclusion of the study, cardiovascular and oxygenation parameters were synchronized, compressed into a data table, and grouped according to the corresponding phases. Beyond baseline, all values except Sp02c/p were converted to delta from P0 to highlight the magnitude of physiological adaptation during P1 and P2, and to reduce the effect of inter-individual variability. Groups were classified as OR and OI based on LBNP time (< 60 s = OI, 60 s = OR). P0 values were averaged over a 5-min time span. P1 values were averaged from the point of reaching Sp02c of circa 85%. P2 values were taken from the last 10 s of LBNP exposure, to highlight maximal effect. Group comparison was performed via Student's *t*-test on a phase per phase basis. Within group analysis was performed via repeated measures ANOVA with Holm-Sidak *post hoc* test. Cardiovascular and NIRS data was synchronized using R software (© The R Foundation). Statistics were performed via JASP statistical software (Version 0.13.1), and graphics were created using Data graph software for Mac OS (Version 4.6.1). All parameters are reported as mean ± SEM. This study was exploratory in nature, so that a specific power test was not performed prior to statistical analysis. A significance level of $p < 0.05$ was used for all statistical testing. A sensitivity, specificity, positive predictive value (PPV), and odd's ratio analysis (OR) were performed for parameters that were significantly different between OR/OI, and from P0, to assess the predictive capability of these parameters to predict OR/OI.

Results: Overall and Baseline

From the 31 participants, 9 (29%) could be classified as OR, whereas 22 (71%), were classified as OI. One participant exhibited LOC during P1, and had his exposure terminated by the flight physician prior to P2. This data from this participant was used for baseline and P1 analysis. Average LBNP exposure time for the OI group was 25.1 ± 3.5 vs. 60 s for the OR group. At baseline, the OR group had significantly greater BMI, weight, RRI, and Sp02p, and significantly lower HR. No other significant differences at baseline were revealed between both groups. Baseline values are displayed in **Table 1**.

TABLE 1 | Baseline (P0) anthropometric, cardiovascular, and central/peripheral oxygenation parameters between OR and OI.

Parameter	OR (*n* = 9)	OI (*n* = 22)
Age (years)	25 ± 2.0	24 ± 1.2
Height (cm)	183 ± 3.1	182 ± 1.6
Weight (kg)	82 ± 4.6*	73 ± 1.9
BMI (kg/m^2)	24 ± 1.0*	22 ± 0.4
BSA (m^2)	2.0 ± 0.7	1.9 ± 0.03
Est. LBM (kg)	63 ± 2.7	59 ± 1.2
MAP (mmHg)	104 ± 3.6	105 ± 2.3
SAP (mmHg)	137 ± 4.0	138 ± 3.4
DAP (mmHg)	83 ± 2.9	84 ± 1.7
CI (L/min/m^2)	4.0 ± 0.3	4.5 ± 0.2
SVI (ml/m^2)	47 ± 2.3	46 ± 1.6
HR (beats/min)	86 ± 5.4	100 ± 3.1*
RRI (ms)	722 ± 48.1*	622 ± 18.8
SVRI (mmHg/min/L/m^2)	27.0 ± 2.2	24.0 ± 1.3
Sp02c (%)	98 ± 0.4	98 ± 0.2
Sp02p (%)	98 ± 0.3*	97 ± 0.3
TOIc (%)	69 ± 1.6	70 ± 1.1
TOIp (%)	66 ± 1.8	69 ± 1.2

*$p < 0.05$.

Orthostatically Resilient vs. Orthostatic Intolerance: P1 and P2 Differences

Upon reaching peak hypoxia (circa 85% Sp02c), the OR group exhibited a significantly greater increases in CI, SVI, and decrease in SVRI compared with the OI group. No other significant differences between the groups were observed during P1. During P2, the OR group exhibited a significantly greater delta SAP, DAP, MAP, and CI as well as a stronger decrease in RRI compared to the OI group. No differences in central or peripheral oxygenation were found between both groups throughout the SHHOC. **Figures 1**, **2** highlight cardiovascular trends throughout the study for OR/OI groups, while information regarding central and peripheral oxygenation is found in **Table 2**.

Orthostatically Resilient and Orthostatic Intolerance: Within Group Reactions, P1 and P2

Taken as a group, cardiovascular reactions amongst the OR group during P1 included significant HR upsurges, leading to a significant CI increase, with stable SVI, as well as a significant decrease in RRI. TOIc significantly decreased, while dHbc increased. All other central and peripheral oxygenation parameters did not significantly deviate from baseline levels during P1. Cardiovascular changes during P2 for the OR group included a further significant HR increase, while CI, SVI, and RRI decreased from P0. MAP, SAP, DAP, and SVRI did not significantly change from P0. During P2, TOIc, 02Hbc, and TOIp all decreased significantly from P0, while dHbc, 02Hbp, dHbp, and tHbp all increased significantly from P0. Sp02c/p were significantly lower in P1 and P2 compared to P0.

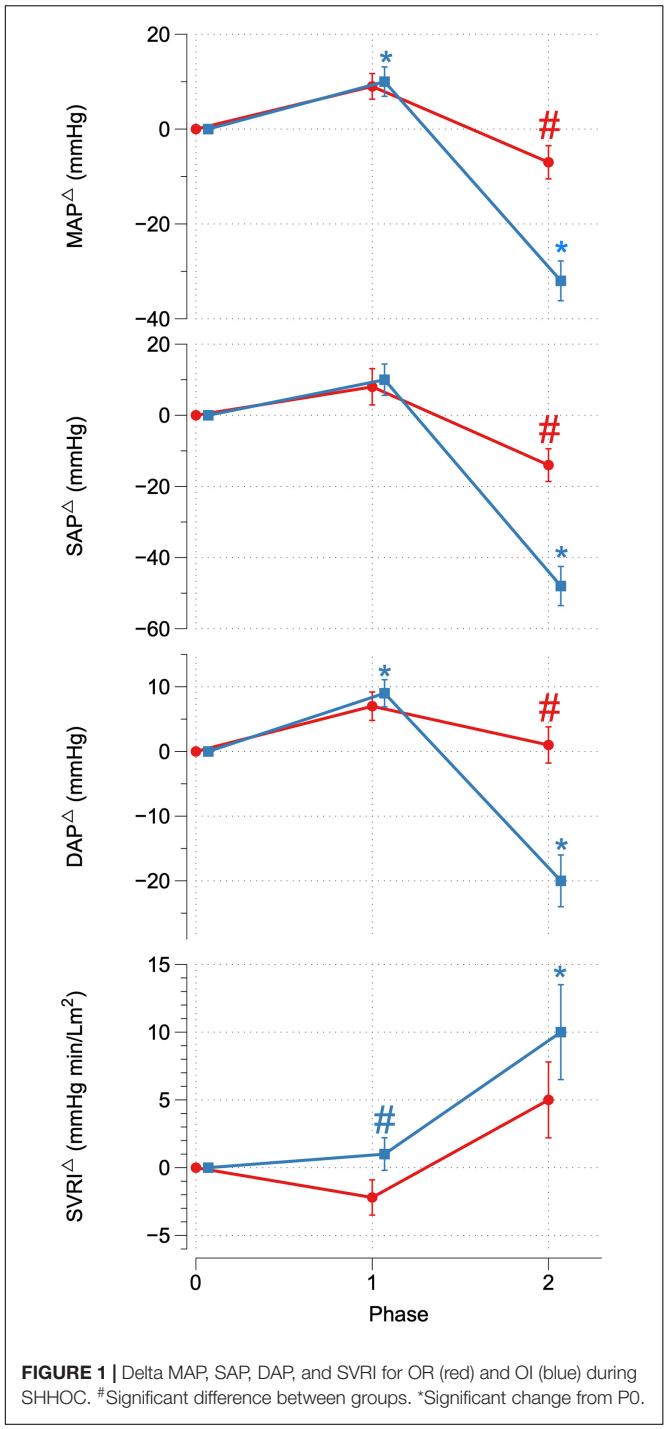

FIGURE 1 | Delta MAP, SAP, DAP, and SVRI for OR (red) and OI (blue) during SHHOC. #Significant difference between groups. *Significant change from P0.

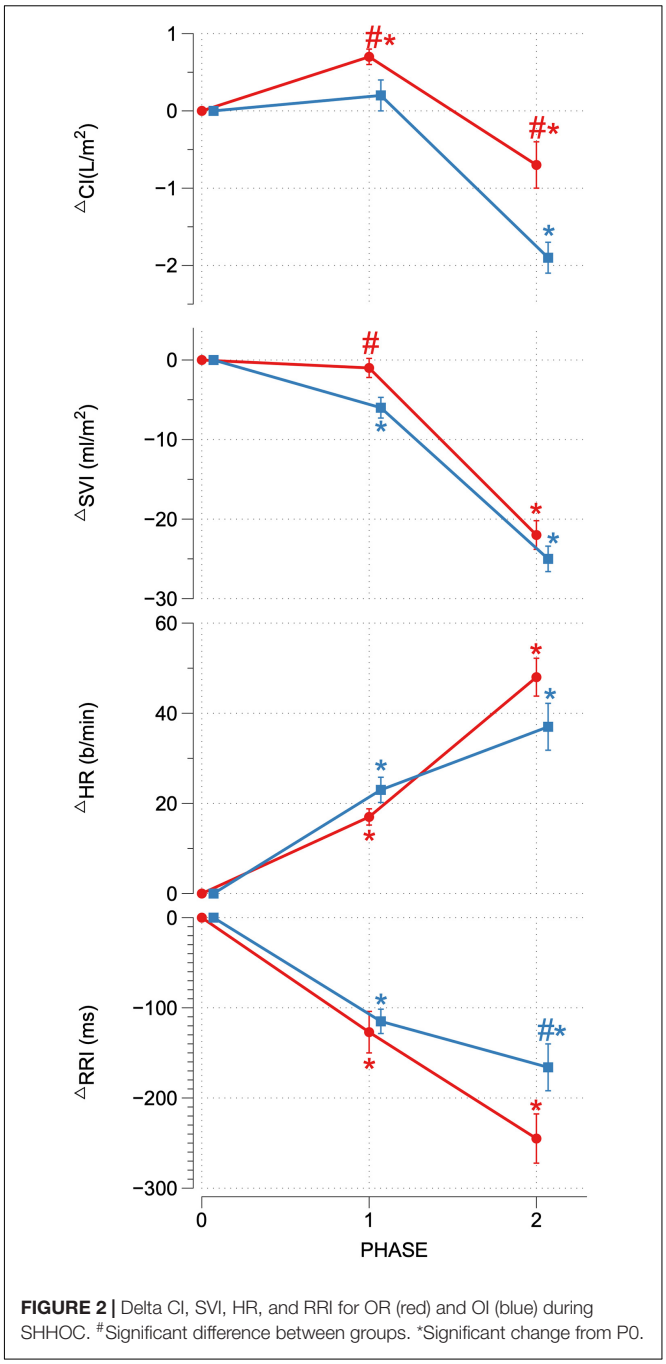

FIGURE 2 | Delta CI, SVI, HR, and RRI for OR (red) and OI (blue) during SHHOC. #Significant difference between groups. *Significant change from P0.

For OI, the following cardiovascular changes occurred during SHHOC: a significant increase in MAP, DAP, and HR, with a concomitant significant decrease in SVI and RRI during P1. Amongst oxygenation parameters, TOIc, 02HBc, and TOIp all significantly decreased, while dHbc, and dHbp all increased significantly from baseline. During P2, MAP, SAP, DAP, CI, SVI, and RRI all significantly decreased from baseline, while HR and SVRI significantly increased from P0. TOIc, TOIp, and 02Hbc continued to decrease from P0 levels. 02Hbc did not change significantly from baseline, while dHbc remained elevated from P0 levels. Sp02c/p were significantly lower during P1 and P2 compared with P0.

Orthostatically Resilient/Orthostatic Intolerance Performance Diagnostics

Performance diagnostics performed for significant factors between groups and within groups per phase are displayed in **Tables 3–5**. From the baseline anthropometric factors, body

TABLE 2 | Central and peripheral oxygenation trends for OR/OI during P1 and P2.

Parameter	OR P1	OI P1	OR P2	OI P2
ΔTOIc (%)	−5.3 ± 0.5*	−6.4 ± 0.5*	−10.8 ± 2.6*	−9.4 ± 0.8*
ΔtHbc (μmol/L)	2.4 ± 1.1	2.7 ± 0.6	−0.9 ± 1.0	−1.5 ± 1.1
Δ02Hbc (μmol/L)	−2.3 ± 1.1	−3.0 ± 0.4*	−6.9 ± 1.1*	−7.6 ± 0.8*
ΔdHbc (μmol/L)	4.7 ± 0.3*	5.6 ± 0.4*	6.1 ± 0.6*	6.1 ± 0.7*
Sp02c (%)	83 ± 0.4*	83 ± 0.4*	81 ± 0.7*	81 ± 0.8*
ΔTOIp (%)	−1.4 ± 0.5	−2.3 ± 0.5*	−5.1 ± 1.1*	−4.8 ± 0.7*
ΔtHbp (μmol/L)	0.5 ± 0.6	0.9 ± 0.5	13.4 ± 1.4*	13.5 ± 1.4*
Δ02Hbp (μmol/L)	−0.3 ± 0.9	−1.2 ± 0.6	5.2 ± 1.8*	4.4 ± 0.8*
ΔdHbp (μmol/L)	0.8 ± 0.5	2.1 ± 0.5*	8.2 ± 0.5*	9.1 ± 1.1*
Sp02p (%)	81 ± 0.9*	80 ± 0.9*	82 ± 1.2*	80 ± 1.1*

**Significant change from baseline.*

TABLE 3 | Performance diagnostics and odd's ratio for P0 significant factors.

Parameter	Sensitivity	Specificity	Positive predictive value	Odds ratio	*P*-value	Confidence interval
Weight (kg)	0.95	0.33	0.78	0.92	0.06	0.84–1.00
BMI (kg/m^2)	0.95	0.33	0.78	0.61	0.04	0.4–0.97
HR (b/min)	0.91	0.22	0.74	1.07	0.05	1.0–1.14
RRI (ms)	0.95	0.22	0.75	0.99	0.05	0.98–1.0
Sp02p (%)	0.90	0.33	0.76	0.37	0.04	0.14–0.95

TABLE 4 | Performance diagnostics and odd's ratio for P1 significant factors.

Parameter	Sensitivity	Specificity	Positive predictive value	Odds Ratio	*p*-value	Confidence interval
ΔCI (L/min)	0.91	0.44	0.80	0.09	0.03	0.0–0.79
ΔSVI (ml/m^2)	0.91	0.44	0.80	0.8	0.03	0.65–0.98
ΔSVRI (mmHg/L/m^2)	0.91	0.22	0.74	1.33	0.05	1.00–1.77
ΔdHbp (μmol/L)	0.91	0.00	0.71	1.36	0.17	0.88–2.11

TABLE 5 | Performance diagnostics and odd's ratio for P2 significant factors.

Parameter	Sensitivity	Specificity	Positive predictive value	Odds ratio	*P*-value	Confidence interval
ΔMAP (mmHg)	0.86	0.67	0.86	0.86	0.02	0.76–0.97
ΔSAP (mmHg)	0.95	0.67	0.87	0.90	0.02	0.83–0.98
ΔDAP (mmHg)	0.86	0.44	0.78	0.88	0.02	0.8–0.98
ΔCI (L/min/m^2)	0.90	0.67	0.86	0.14	0.02	0.03–0.70
ΔRRI (ms)	0.86	0.22	0.72	1.01	0.07	1.0–1.02

weight and BMI showed identical sensitivity, specificity, and PPV, with weight having a greater OR (0.92) than BMI (0.61). Baseline hemodynamic and oxygenation factors of importance were, RRI, HR, and Sp02p, with RRI showing the highest sensitivity (0.95), Sp02p the highest specificity (0.33), comparable PPV (0.74, 0.74, and 0.76), while HR and RRI having the highest OR (1.07 vs. 0.99). During P1, delta SVI, CI, SVRI, and dHbp showed high sensitivity (0.95), while specificity was higher in CI and SVI (0.44). Both delta CI and SVI exhibited a PPV of 0.80, Delta SVRI and dHbp had a sensitivity of 0.91, however, low specificity and PPV, with albeit higher OR (1.33 and 1.36). Performance diagnostics for P2 revealed that delta SAP had the highest sensitivity, specificity, PPV, and odd's ratio compared to delta MAP, DAP, CI, and RRI.

DISCUSSION

Overall Results

Upon conclusion of this SHHOC study, it was found that 71% (n = 22) of the crew experienced OI during SHHOC, whereas 29% (n = 9) remained OR. The OR group had a greater body weight, BMI, Sp02p, lower HR, and longer RRI than the OI group at P0. During P1, the OR group exhibited a significantly greater increase in CI, SVI, and lower SVRI, compared to the OI group. During P2, the OR group maintained a significantly greater MAP, SAP, DAP, CI, with a shorter RRI than their OI counterparts. No central or peripheral oxygenation differences were found between groups. The only distinguishing oxygenation factors, was that of significant decrease in 02Hbc and TOIp, as well as an increase in dHbp in the OI group during P1. This finding suggests a decreased cerebral 02 supply combined with an increased cerebral 02 utilization, and an increased peripheral oxygenation usage in this group during P1, which may have predisposed this group for a OI during P2. Total body weight and BMI at baseline had the highest sensitivity, PPV, and odd's ratio of the significant baseline factors, although a low specificity was observed. Furthermore, delta SVI during P1 was the factor that had the highest sensitivity, specificity, and PPV compared with delta CI and SVRI. Finally, delta SAP was the main cardiovascular factor most associated with OR during hypoxic LBNP.

The results of this study can confirm that the ability to maintain OR during combined hypoxic orthostatic stress presents as a formidable challenge to the innate physiological counter-response system, and our results are in line with other studies showing that OI occurrence during such an event range from 30 to 70% (Rowell and Seals, 1990; Crandall et al., 2019). The physiological basis of this is thought to be due to excess concentrations of serum adrenaline, as opposed to noradrenaline, which in turn lead to a misorchestration of autonomic responses (Ainslie et al., 2007). To our knowledge, there is only one study that directly compared OI vs. OR during hypoxic tilt table test. That study found that OI is due to failure of vascular adjustment during hypoxic orthostatic stress, and not due to baroreflex misorchestration (Halliwill and Minson, 2005). Furthermore, 70% of that cohort remained OR, which is directly opposite of our findings, although both study protocols were radically different, so a direct comparison cannot be made. In this study, it appeared that the OI group expressed a dramatic increase, albeit unsuccessful, in SVRI during P2 which was not a successful strategy for maintaining MAP. It appears that CI is decisive in maintaining critical MAP during hypoxic orthostatic stress.

Baseline Factors

At baseline, the OR group had a greater BMI, body weight, and Sp02p, with a lower HR as well as a prolonged RRI than the OI group. These findings strengthen the evidence that anthropometric factors such as BMI and body weight are associated with OR (Halliwill and Minson, 2005; Nordine et al., 2015; Christou and Kiortsis, 2017). While both BMI and body weight showed a high sensitivity and moderate PPV, the specificity was low. The physiological basis as to why an increased body size contributes to OR is due to greater and cardiac size and contractility function (Dewey et al., 2008).

The significant baseline HR difference between both groups could indicate discrepancies in hydration status, or baseline autonomic excitability. Prior investigations have also found that a higher resting HR is associated with OI (Lee et al., 2013). The high HR amongst the OI group may have been due to anxiety/excitability prior to the exposure. A heightened level of anxiety would have led to a pre-mature increase in sympathetic activation, thereby contributing to cardiac reserve exhaustion prior to P2. The presence of a longer RRI in the OR group would suggest decreased autonomic activity at baseline, which would support the previous statement. A previous study examining high/low tolerance to −60 mmHg LBNP found that high tolerant subjects had a significantly longer RRI vs. low tolerant participants, while high tolerant individuals had a lower baseline HR (Hinojosa-Laborde et al., 2011). Our study supports these prior results, showing that baseline HR and RRI offer valuable predictive information regarding baseline autonomic activity and OI/OR risk Also, although not tested prior to the study, dehydration or low plasma volume may have contributed to the baseline tachycardia, although no difference in SVI or CI were apparent. The significant difference in Sp02p between both groups may further indicate that the OI group had suboptimal hydration status, as a lower Sp02 may reflect this (Secher and Van Lieshout, 2005). Between these two factors, HR had a higher odd's ratio than Sp02p, and thus may be more of a useful baseline predictor of OR/OI status.

Orthostatically Resilient vs. Orthostatic Intolerance: Cardiovascular and Oxygenation Strategies During P1

During P1, the key cardiovascular differences between OR and OI were the change in CI, SVI, and SVRI. Specifically, the OR group responded to hypoxia via increasing CI, preserving SVI, increasing HR, while decreasing SVRI. This type of cardiovascular response during hypoxia would increase blood flow and ensure adequate cerebral oxygenation. The inability for the OI group to preserve SVI during this during hypoxia, would lead to a decrease in blood flow, and possible compromised tissue oxygenation. Also, as the OI group began with an elevated resting HR, the increases in HR during P1, may have further compromised SVI, thereby necessitating additional SVRI support. A decrease in SVI during hypoxia may also indicate reduced venous return (Siebenmann and Lundby, 2015), thereby triggering compensatory SVRI activity. The inability to decrease SVRI would further lead to additional 02 usage in the periphery thus further limiting available 02 reserves to the cerebral and myocardial tissues. Amongst these cardiovascular factors, the change in SVI during hypoxia exhibited the highest sensitivity, specificity, and PPV compared to delta CI and SVRI.

Cerebral oxygenation (TOIc) decreased and dHbc increased significantly amongst both groups, however, the OI group exhibited a significant decrease in 02Hbc. The reduction in 02Hbc and increase in dHbc amongst the OI group would suggest either an increase in cerebral 02 extraction, a reduction in cerebral 02 supply, or a combination of both. Given the significant decrease in SVI during P1, this may have led to a decrease in cerebral 02 supply, which may have triggered a greater increase in 02 extraction, thus increasing dHbc. The counter-measures enacted by the OI group were not sufficient enough to maintain cerebral oxygenation, while it appears that cerebral auto regulation was left largely unaffected. This trend of cerebral oxygenation in the OI group may have increased the risk for OI during subsequent orthostatic challenge. While no exact comparable study could be found to expand on this finding, prior results have demonstrated a link between sympathetic failure and falling cerebral oxygenation (Harms et al., 2000), which could indicate that the falling cerebral oxygenation in the OI group contributed to the cardiovascular collapse in P2. Clearly, further studies of this nature need to be performed to examine the link between OI and 02Hbc.

Prior evidence suggests that increases in cerebral blood flow during normobaric hypoxia may operate independently of respiratory or systemic cardiovascular reactions (AlSalahi et al., 2021). Other groups have not observed increased cerebral blood flow during hypoxia, suggesting that autoregulation remains intact (Cheng et al., 2017; Ogoh et al., 2018; van Helmond et al., 2018). Wilson et al. (2011) performed a multifaceted study examining cerebral oxygenation and blood flow during simulated and real-world hypoxic environments and found that at moderate hypoxia (Sp02 85% equivalent to 4250 meters of altitude), cerebral oxygenation significantly decreases, while at the same time, cerebral perfusion, and 02 delivery are not compromised. While doppler was not used in this study, no significant increase in tHbc could be found amongst our cohort, hinting that cerebral auto regulation remained largely intact during P1. The increase in dHbc amongst the OR group, while maintaining 02Hbc, would suggest an optimal cerebral 02 extraction and optimal 02 delivery, while a non-significant increase in tHbc would indicate a stable autoregulation during P1. In summary, cerebral oxygenation did not differ between groups, with only OI showing a significant 02Hbc decrease amongst the OI group, which may have contributed to cardiovascular collapse in P2.

In the peripheral tissues, changes in oxygenation were not significantly different between groups, however, group specific reactions were seen. TOIp decreased in both groups, however, this decrease was significant in the OI group, suggesting either a decrease in 02 flow to the periphery or increased 02 usage. Our evidence hints to an increased 02 utilization in the peripheral tissues amongst the OI group, as evidenced by a significant dHbp increase. An increase in dHbp would equate to increased 02 utilization. Local tissue hypoxia may have been further exacerbated by the SVI decrease amongst the OI group, which

should have led to a refractory decrease in vascular activity (Hansen et al., 2000) however, this did not occur.

These findings can be summarized as the following: as the supply of 02 decreases during normobaric hypoxia, delivery of 02 to the critical organ systems is reliant upon increasing flow (Kane et al., 2020), via selective peripheral vasodilation, increasing CI via careful increases in HR, while maintaining SVI. In response to a falling 02, the OR group was able to down-tune SVRI, and increase CI (flow), thereby ensuring cerebral 02 supply, and minimizing excess 02 consumption in the peripheral tissues.

Ainslie et al., found that during acute normobaric hypoxia (Fi02 12%), 02Hb decreased, and dHb increased to a greater extent in the frontal cortex than in the vastus lateralis muscle, however, they found no difference in total hemoglobin change (Ainslie et al., 2007). These same trends were seen in our study, which would suggest that cerebral 02 supply and extraction are increased during hypoxia to shield the brain from hypoxic damage. The increase in tHbc amongst both groups suggest cerebral vasodilation, compared to the peripheral tissues, which runs in contrast to the findings of Ainsle.

Although no differences between groups with regards to central and peripheral oxygenation were observed, performance diagnostics for within group oxygenation patterns revealed that only dHbp did show a high sensitivity for OR/OI prediction, however, with a specificity of 0.0, and a PPV of 0.71. This suggest that rate of peripheral 02 utilization may have limited utility in revealing the propensity for an orthostatic event. A higher utilization of 02 during hypoxia could also be due to individual metabolic states, as well as a higher local metabolic rate in these regions, for example increases in vascular activity. Prior studies have suggested the use of peripheral oxygenation as an early detection system for OI predisposition during hypoxia (Soller et al., 2008; Rupp et al., 2013; Ovadia-Blechman et al., 2015; Schlotman et al., 2020). Based on the results of our study, the use of central and peripheral oxygenation via NIRS, especially dHb, may be used to pinpoint differences between high and low tolerant individuals during hypoxic orthostatic challenges, however, the predictive power is minimal.

Orthostatically Resilient vs. Orthostatic Intolerance: Cardiovascular and Oxygenation Strategies During P2

During P2, the key differences between groups was that the OR group exhibited a greater MAP, SAP, DAP, and CI, and shortened RRI compared to the OI group, while no differences with regards to oxygenation were found. Despite significant decreases in SVI and CI during P2, increases in HR and SVRI were able to uphold critical MAP amongst the OR group, while these same increases in the OI group were not sufficient to maintain critical MAP. Although not specifically investigating hypoxic orthostatic stress, Convertino (2014), found that individuals exhibiting heightened increases in HR during orthostatic stress were more resilient, and that this increase in HR is associated with a greater sympathetic nervous system recruitment. The harnessing of sympathetic reserves could be supported by the significantly shortened RRI amongst OR, which would signal higher autonomic functioning. Furthermore, Hachiya et al. (2010), found that successful OR strategies involve delayed activation of SVRI, and gradual HR increases during graded orthostatic stress. While not directly comparable to our study, the OR group did show a heightened HR response during P2 and did exhibit a delayed SVRI activation. Therefore, we can confirm the findings from these studies, that successful cardiovascular OR strategies involve the harnessing of HR reserves, and delaying SVRI activity, either in normoxic or hypoxic orthostatic challenges. Davis et al. (2013), found that the ability to remain OR during hypoxic stand-test is dependent upon HR increases to maintain MAP. Work done by Fox et al. (2006), suggested that hypoxia exposure increases baroreflex sensitivity during LBNP, and that this advantage is expressed in individuals with innate hypoxic tolerance. Baroreflex sensitivity amongst the OR cohort may in fact have been heightened during P1, although this was not measured in this study. An increased baroreflex sensitivity as a response to acute onset hypoxia is known to occur, and is independent of respiratory factors (Halliwill et al., 2003). Furthermore, hypoxia can initiate full sympathetic activation, while withdrawing parasympathetic function (Halliwill and Minson, 2002; Blaber et al., 2003). The OR group may have exhibited a timely and balanced sympathetic activation during P2, whereas the OI group seems to have had a premature maximal sympathetic activation in P1, leading to a sympathetic overreaction, and collapse in P2. Furthermore, based on performance diagnostics, SAP showed the highest sensitivity, specificity, PPV, and odd's ratio, compared to MAP, DAP, and CI. SAP is influenced by factors such as blood volume, SVI, and CI, and cardiac contractility. Although blood and plasma volume were not measured in this study, the increased CI in the OR group contributed to higher SAP in this study, as well as optimal cardiac contractility. Furthermore, SAP has been shown to be linked to higher BMI, and body weight, which may have further contributed to OR status (Das, 2017).

Cerebral oxygenation parameters, such as TOIc, and 02HBc further decreased significantly from baseline amongst both groups, while dHBc further increased. No differences in cerebral oxygenation could be pinpointed between both groups, meaning that cerebral oxygenation index during P2 did not play a role in OR/OI status in this study. The decisive factor for OR/OI is due to the maintenance of cerebral perfusion pressure, which is strongly correlated to maintaining MAP at a critical threshold (Kharraziha et al., 2019). Cerebral blood flow velocity is impaired in syncopal astronauts upon return to Earth under normoxic conditions, and although not measured in our study, the significant decrease in MAD, SAP, and CI, may have decreased cerebral blood flow velocity to a critical degree amongst the OI group (Blaber et al., 2011). Although not directly comparable to this study, similar patterns of cerebral oxygenation were found during G-Force exposure via human centrifuge under normoxic conditions, and that these decreases in cerebral oxygenation did not correlate with cortical activity (Smith et al., 2013). A loss of cerebral perfusion pressure may also be due to complete sympathetic failure (Harms et al., 2000). Cognitive ability during hypoxic hyper-gravity may not be solely dependent upon cerebral oxygenation, the maintenance of cerebral perfusion pressure would be paramount for crew health.

The significant increase in tHbp, 02Hbp, dHbp, and decrease in TOIp were not different between groups, and are a result of significant venous pooling during LBNP. At a level of −70 mmHg, a cranial to caudal shift of 25% of blood volume is expected (Hinojosa-Laborde et al., 2014). Also, despite a significant degree of venous pooling, arteriolar vasoconstriction is not impaired at this level of orthostatic stress (Habazettl et al., 2015).

It appears from our data, that a successful OR strategy during combined hypoxic orthostatic stress relies on mobilizing sympathetic reserves (RRI, HR, and SVRI), during a significant fall in blood volume, which maintains CI, thus contributing to the maintenance of stable MAP and SAP. Secondarily, it appears that a delayed and balanced SVRI, combined with this HR response, can maintain MAD, SAP, and DAP at critical levels which maintains cerebral perfusion pressure. An exaggerated SVRI response, amongst the OI group was not sufficient to maintain MAP, despite further increases in HR. Based on these results, OR is dependent upon the maintenance of cerebral perfusion, rather than that of cerebral oxygenation (Kharraziha et al., 2019). Finally, it appears that the change in SAP during P2 was strongly associated with LBNP OR status, and that SAP may contribute to maintaining cerebral perfusion more than MAD.

Limitations

Despite having a good sample size and being only one of a few studies that directly examined the differences between OR and OI subjects, there are a few limitations to this study. Primarily is the omission of respiratory parameters. Respiratory rate, tidal volume, and minute ventilation were unfortunately not measured. An increase in minute ventilation is expected during hypoxia, however, this change in ventilation does not seem to influence cerebral perfusion (AlSalahi et al., 2021). Also, no comparison was performed using normoxic LBNP. A cross-over design could have directly compared LBNP responses to the 2 conditions (normoxic and hypoxic). One study found that the HR response during a normoxic vs. a hypoxic orthostatic challenge did not differ (Koelwyn et al., 2013), and that during any orthostatic challenge, the baroreceptor response overrides the peripheral chemoreceptor response (Shepherd et al., 2020). To solidify this finding, a cross-over study design would have been useful. Another drawback is the homogenous pool of exclusively men. Aerospace crews are composed of women and men, and gender specific countermeasures will be needed, as there appears to be a varying gender specific response to orthostatic stress (Barnes and Charkoudian, 2020). Another limitation is the use of NIRS for measuring cerebral and peripheral oxygenation. NIRS, although a useful instrument, can relay information only regarding the change in oxygenation, and not perfusion. To better solidify the findings of our study, doppler images of the middle cerebral artery could have been obtained to estimate the degree of cerebral perfusion. Also, it is difficult to estimate if our NIRS recordings reflected a more venous or arterial aspect of oxygenation. Recent evidence suggests that NIRS is composed of 50% arterial, and 50% venous concentrations, as opposed to the previously suggested 25% arterial, and 75% venous (Sørensen et al., 2014). And finally, no serum values of hemoglobin, noradrenaline, adrenaline, creatinine, of hematocrit were analyzed. Prior reports have suggested that OF is associated with excess serum adrenaline during simulated hypoxic hypovolemia (Crandall et al., 2019). Given the scant number of studies on this topic, we missed an opportunity to verify this evidence. Hemoglobin can play a role in the hypoxic response, and although we did not measure hemoglobin, one can assume that any symptoms of anemia would have been detected during the rigorous military pilot program. Hematocrit and creatinine were not measured at baseline, and thus, there is speculation as to the hydration status of our cohort. Dehydration can affect the response to hypoxia (Richardson et al., 2009), as well as tolerance to an orthostatic stimulus (Schroeder et al., 2002). Surrogate baseline factors such as an elevated HR and decreased Sp02d may suggest that the OI group began the run in a dehydrated state, however, this is purely speculation.

CONCLUSION

In conclusion, successful OR strategies during SHHOC depend upon baseline anthropometric (greater body weight and BMI), lower baseline HR with higher RRI and Sp02p. Furthermore, responding to hypoxia via elevations in CI, maintaining SVI, and decreasing SVRI, with the minimization of central/peripheral 02 usage is also a key strategy. During hypoxic orthostatic challenge, a mobilization of HR reserves and delayed SVRI activation, leading to the maintenance a higher CI which maintains MAP, DAP, and SAP above critical levels, are key OR strategies. The utilization of central and peripheral oxygenation parameters did not reveal any differences between OR/OI during the SHHOC, although inter-group trends did show a trend amongst the OI group for higher peripheral 02 utilization/extraction during hypoxia along with a decrease in cerebral 02 supply.

The results of this study can be useful for developing effective non-invasive monitoring strategies for future aerospace crews and for establishing crew medical support to pinpoint which crew members are predisposed to an orthostatic event during critical periods such as acute atmospheric changes combined with increases in gravitational vector. Maintaining body weight, and the use of SVI tracking may enhance crew-health to prevent an orthostatic event, and better ensure the continued success of human aerospace travel.

DATA AVAILABILITY STATEMENT

The original contributions presented in the study are included in the article/supplementary material, further inquiries can be directed to the corresponding author/s.

ETHICS STATEMENT

Ethical review and approval was not required for the study on human participants in accordance with the local legislation and institutional requirements. The patients/participants provided their written informed consent to participate in this study.

AUTHOR CONTRIBUTIONS

MN, HH, H-CG, and OO devised, financed, and performed the study. PD and JP supervised and assisted in performing the study. KB performed statistical analysis. MN, OO, and ST wrote the manuscript. All authors contributed to the article and approved the submitted version.

REFERENCES

Aarts, H. M., PetersenJones, H. G., Johnson, B. D., Curry, T. B., and Joyner, M. J. (2017). Cardiac baroreflex sensitivity during lower body negative pressure and acute hypoxia: fainters vs. nonfainters. *FASEB J.* 31, 1087–1091. doi: 10.1096/faebj.31.1_supplement.1087.1

Ainslie, P. N., Barach, A., Murrell, C., Hamlin, M., Hellemans, J., and Ogoh, S. (2007). Alterations in cerebral autoregulation and cerebral blood flow velocity during acute hypoxia: rest and exercise. *Am. J. Physiol. Heart Circul. Physiol.* 292, H976–H983. doi: 10.1152/ajpheart.00639.2006

AlSalahi, S. E., Junejo, R. T., Bradley, C., Balanos, G. M., Siebenmann, C., and Fisher, J. P. (2021). The middle cerebral artery blood velocity response to acute normobaric hypoxia occurs independently of changes in ventilation in humans. *Experim. Physiol.* 106, 861–867. doi: 10.1113/ep089127

Badrov, M. B., Usselman, C. W., and Shoemaker, J. K. (2015). Sympathetic neural recruitment strategies: responses to severe chemoreflex and baroreflex stress. *Am. J. Physiol. Regulatory, integrative and comparative physiology* 309, R160–R168. doi: 10.1152/ajpregu.00077.2015

Barnes, J. N., and Charkoudian, N. (2020). Integrative cardiovascular control in women: Regulation of blood pressure, body temperature, and cerebrovascular responsiveness. *FASEB J.* 35:1387. doi: 10.1096/fj.202001387R

Blaber, A. P., Goswami, N., Bondar, R. L., and Kassam, M. S. (2011). Impairment of cerebral blood flow regulation in astronauts with orthostatic intolerance after flight. *Stroke* 42, 1844–1850. doi: 10.1161/strokeaha.110.610576

Blaber, A. P., Hartley, T., and Pretorius, P. J. (2003). Effect of acute exposure to 3,660 m altitude on orthostatic responses and tolerance. *J. Appl. Physiol.* 95, 591–601. doi: 10.1152/japplphysiol.00749.2002

Cheng, X., Wszedybyl-Winklewska, M., Wolf, J., Swierblewska, E., Kunicka, K., Gruszecka, A., et al. (2017). Acute hypoxia diminishes the relationship between blood pressure and subarachnoid space width oscillations at the human cardiac frequency. *Plos One* 12:172842. doi: 10.1371/journal.pone.0172842

Christou, G. A., and Kiortsis, D. N. (2017). The effects of body weight status on orthostatic intolerance and predisposition to noncardiac syncope. *Obes. Rev.* 18, 370–379. doi: 10.1111/obr.12501

Convertino, V. A. (2014). Neurohumoral mechanisms associated with orthostasis: reaffirmation of the significant contribution of the heart rate response. *Front. Physiol.* 5:236. doi: 10.3389/fphys.2014.00236

Crandall, C. G., Rickards, C. A., and Johnson, B. D. (2019). Impact of environmental stressors on tolerance to hemorrhage in humans. *Am. J. Physiol. Regul. Integr. Comp. Physiol.* 316, R88–R100. doi: 10.1152/ajpregu.00235.2018

Das, R. N. (2017). Systolic blood pressure determinants. *Ann. Clin. Hyperten.* 1, 32–38. doi: 10.29328/journal.ach.1001004

Davis, J. E., Wagner, D. R., Thorington, J., and Schall, C. (2013). Orthostatic responses at 4860m in low, moderate, and high altitude residents. *High Altit. Med. Biol.* 14, 251–255. doi: 10.1089/ham.2012.1069

Dewey, F. E., Rosenthal, D., Murphy, D. J. Jr., Froelicher, V. F., and Ashley, E. A. (2008). Does size matter? Clinical applications of scaling cardiac size and function for body size. *Circulation* 117, 2279–2287. doi: 10.1161/CIRCULATIONAHA.107.736785

Fox, W. C., Watson, R., and Lockette, W. (2006). Acute hypoxemia increases cardiovascular baroreceptor sensitivity in humans. *Am. J. Hyperten.* 19, 958–963. doi: 10.1016/j.amjhyper.2006.02.005

Habazettl, H., Stahn, A., Nitsche, A., Nordine, M., Pries, A. R., Gunga, H. C., et al. (2015). Microvascular responses to (hyper-)gravitational stress by short-arm human centrifuge: arteriolar vasoconstriction and venous pooling. *Eur. J. Appl. Physiol.* 116, 57–65. doi: 10.1007/s00421-015-3241-6

Hachiya, T., Walsh, M. L., Saito, M., and Blaber, A. P. (2010). Delayed vasoconstrictor response to venous pooling in the calf is associated with high orthostatic tolerance to LBNP. *J. Appl. Physiol.* 109, 996–1001. doi: 10.1152/japplphysiol.00593.2009

Halliwill, J. R., and Minson, C. T. (2002). Effect of hypoxia on arterial baroreflex control of heart rate and muscle sympathetic nerve activity in humans. *J. Appl. Physiol.* 93, 857–864. doi: 10.1152/japplphysiol.01103.2001

Halliwill, J. R., and Minson, C. T. (2005). Cardiovagal regulation during combined hypoxic and orthostatic stress: fainters vs. nonfainters. *J. Appl. Physiol.* 98, 1050–1056. doi: 10.1152/japplphysiol.00871.2004

Halliwill, J. R., Morgan, B. J., and Charkoudian, N. (2003). Peripheral Chemoreflex and Baroreflex Interactions in Cardiovascular Regulation in Humans. *J. Physiol.* 552, 295–302. doi: 10.1113/jphysiol.2003.050708

Hansen, J., Sander, M., Hald, C. F., Victor, R. G., and Thomas, G. D. (2000). Metabolic modulation of sympathetic vasoconstriction in human skeletal muscle: role of tissue hypoxia. *J. Physiol.* 527, 387–396. doi: 10.1111/j.1469-7793.2000.00387.x

Harms, M. P. M., Colier, W. N. J. M., Wieling, W., Lenders, J. W. M., Secher, N. H., and van Lieshout, J. J. (2000). Orthostatic tolerance. cerebral oxygenation, and blood velocity in humans with sympathetic failure. *Stroke* 31, 1608–1614. doi: 10.1161/01.Str.31.7.1608

Hinojosa-Laborde, C., Rickards, C. A., Ryan, K. L., and Convertino, V. A. (2011). Heart Rate Variability during simulated hemorrhage with lower body negative pressure in high and low tolerant subjects. *Front. Physiol.* 2:85. doi: 10.3389/fphys.2011.00085

Hinojosa-Laborde, C., Shade, R. E., Muniz, G. W., Bauer, C., Goei, K. A., Pidcoke, H. F., et al. (2014). Validation of lower body negative pressure as an experimental model of hemorrhage. *J. Appl. Physiol.* 116, 406–415. doi: 10.1152/japplphysiol.00640.2013

Hoiland, R. L., Bain, A. R., Rieger, M. G., Bailey, D. M., and Ainslie, P. N. (2016). Hypoxemia, oxygen content, and the regulation of cerebral blood flow. *Am. J. Physiol. Regul. Integr. Comp. Physiol.* 310, R398–R413. doi: 10.1152/ajpregu.00270.2015

Iwasaki, K., Zhang, R., Zuckerman, J. H., Ogawa, Y., Hansen, L. H., and Levine, B. D. (2011). Impaired dynamic cerebral autoregulation at extreme high altitude even after acclimatization. *J. Cereb. Blood Flow Metab.* 31, 283–292. doi: 10.1038/jcbfm.2010.88

Kane, A. D., Kothmann, E., and Giussani, D. A. (2020). Detection and response to acute systemic hypoxia. *BJA Edu.* 20, 58–64. doi: 10.1016/j.bjae.2019.10.004

Kharraziha, I., Holm, H., Bachus, E., Ricci, F., Sutton, R., Fedorowski, A., et al. (2019). Cerebral oximetry in syncope and syndromes of orthostatic intolerance. *Front. Cardiovasc. Med.* 6:171. doi: 10.3389/fcvm.2019.00171

Koelwyn, G. J., Wong, L. E., Kennedy, M. D., and Eves, N. D. (2013). The effect of hypoxia and exercise on heart rate variability, immune response, and orthostatic stress. *Scand. J. Med. Sci. Sports* 23, e1–e8. doi: 10.1111/sms.12003

Lee, J. F., Harrison, M. L., Christmas, K. M., Kim, K., Hurr, C., and Brothers, R. M. (2013). Elevated resting heart rate and reduced orthostatic tolerance in obese humans. *Clin. Auto. Res.* 24, 39–46. doi: 10.1007/s10286-013-0222-x

Manuel, J., Färber, N., Gerlach, D. A., Heusser, K., Jordan, J., Tank, J., et al. (2020). Deciphering the neural signature of human cardiovascular regulation. *eLife*, 9:e55316. doi: 10.7554/eLife.55316

Melchior, F. M., Srinivasan, R. S., and Charles, J. B. (1992). Mathematical modeling of human cardiovascular system for simulation of orthostatic response. *Am. J. Physiol.* 262, H1920–H1933. doi: 10.1152/ajpheart.1992.262.6.H1920

Mirna, M., Bimpong-Buta, N. Y., and Hoffmann, F. (2020). Exposure to acute normobaric hypoxia results in adaptions of both the macro- and microcirculatory system. *Sci. Rep.* 10:20938. doi: 10.1038/s41598-020-77724-5

Nordine, M., Maggioni, M. A., Stahn, A., Mendt, S., Brauns, K., Gunga, H. C., et al. (2015). Form influences function: Anthropometry and orthostatic stability during sustained acceleration in a short arm human centrifuge. *Acta Astron.* 115, 138–146. doi: 10.1016/j.actaastro.2015.05.025

Ogoh, S., Nakata, H., Miyamoto, T., Bailey, D. M., and Shibasaki, M. (2018). Dynamic cerebral autoregulation during cognitive task: effect of hypoxia. *J. Appl. Physiol.* 124, 1413–1419. doi: 10.1152/japplphysiol.00909.2017

Ovadia-Blechman, Z., Meilin, A., Rabin, N., Eldar, M., and Castel, D. (2015). Noninvasive monitoring of peripheral microcirculatory hemodynamics under varying degrees of hypoxia. *Resp. Physiol. Neurobiol.* 216, 23–27. doi: 10.1016/j.resp.2015.05.011

Paparde, A., Plakane, L., Circenis, K., and Aivars, J. I. (2015). Effect of acute systemic hypoxia on human cutaneous microcirculation and endothelial, sympathetic and myogenic activity. *Microvas. Res.* 102, 1–5. doi: 10.1016/j.mvr.2015.07.005

Richardson, A., Watt, P., and Maxwell, N. (2009). Hydration and the Physiological Responses to Acute Normobaric Hypoxia. *Wilder. Environ. Med.* 20, 212–220. doi: 10.1580/09-weme-or-272r1.1

Rickards, C. A. (2015). Cerebral blood-flow regulation during hemorrhage. *Compr. Physiol.* 5, 1585–1621. doi: 10.1002/cphy.c140058

Rowell, L. B., and Seals, D. R. (1990). Sympathetic activity during graded central hypovolemia in hypoxemic humans. *Am. J. Physiol.* 259, H1197–H1206. doi: 10.1152/ajpheart.1990.259.4.H1197

Rupp, T., Leti, T., Jubeau, M., Millet, G. Y., Bricout, V. A., Levy, P., et al. (2013). Tissue deoxygenation kinetics induced by prolonged hypoxic exposure in healthy humans at rest. *J. Biomed. Optics* 18:2. doi: 10.1117/1.Jbo.18.9.095002

Schlotman, T. E., Akers, K. S., Cardin, S., Morris, M. J., Le, T., and Convertino, V. A. (2020). Evidence for misleading decision support in characterizing differences in tolerance to reduced central blood volume using measurements of tissue oxygenation. *Transfusion* 2020:15648. doi: 10.1111/trf.15648

Schroeder, C., Bush, V. E., Norcliffe, L. J., Luft, F. C., Tank, J., Jordan, J., et al. (2002). Water Drinking acutely improves orthostatic tolerance in healthy subjects. *Circulation* 106, 2806–2811. doi: 10.1161/01.Cir.0000038921.64575.D0

Secher, N. H., and Van Lieshout, J. J. (2005). Normovolaemia defined by central blood volume and venous oxygen saturation. *Clin. Exp. Pharmacol. Physiol.* 32, 901–910. doi: 10.1111/j.1440-1681.2005.04283.x

Shepherd, J. R. A., Baker, S. E., Holbein, W. W., Limberg, J. K., Johnson, B. D., Schroeder, D. J., et al. (2020). Peripheral chemoreceptors hemodynamic responses during simulated hemorrhage under hypoxia conditions. *FASEB J.* 34:8935. doi: 10.1096/fasebj.2020.34.s1.08935

Siebenmann, C., and Lundby, C. (2015). Regulation of cardiac output in hypoxia. *Scand. J. Med. Sci. Sports* 25, 53–59. doi: 10.1111/sms.12619

Smith, C., Goswami, N., Robinson, R., von der Wiesche, M., and Schneider, S. (2013). The relationship between brain cortical activity and brain oxygenation in the prefrontal cortex during hypergravity exposure. *J. Appl. Physiol.* 114, 905–910. doi: 10.1152/japplphysiol.01426.2012

Soller, B. R., Yang, Y., Soyemi, O. O., Ryan, K. L., Rickards, C. A., Walz, J. M., et al. (2008). Noninvasively determined muscle oxygen saturation is an early indicator of central hypovolemia in humans. *J. Appl. Physiol.* 104, 475–481. doi: 10.1152/japplphysiol.00600.2007

Sørensen, H., Secher, N. H., and Rasmussen, P. (2014). A note on arterial to venous oxygen saturation as reference for NIRS-determined frontal lobe oxygen saturation in healthy humans. *Front. Physiol.* 4:403. doi: 10.3389/fphys.2013.00403

van Helmond, N., Johnson, B. D., Holbein, W. W., Petersen-Jones, H. G., Harvey, R. E., Ranadive, S. M., et al. (2018). Effect of acute hypoxemia on cerebral blood flow velocity control during lower body negative pressure. *Physiol. Rep.* 6:13594. doi: 10.14814/phy2.13594

Van Mil, A. H., Spilt, A., Van Buchem, M. A., Bollen, E. L., Teppema, L., Westendorp, R. G., et al. (2002). Nitric oxide mediates hypoxia-induced cerebral vasodilation in humans. *J. Appl. Physiol. (Bethesda, Md.: 1985)* 92, 962–966. doi: 10.1152/japplphysiol.00616.2001

Wilson, M. H., Edsell, M. E. G., Davagnanam, I., Hirani, S. P., Martin, D. S., Levett, D. Z. H., et al. (2011). Cerebral artery dilatation maintains cerebral oxygenation at extreme altitude and in acute hypoxia—an ultrasound and MRI Study. *J. Cereb. Blood Flow Metabol.* 31, 2019–2029. doi: 10.1038/jcbfm.2011.81

Conflict of Interest: The authors declare that the research was conducted in the absence of any commercial or financial relationships that could be construed as a potential conflict of interest.

Publisher's Note: All claims expressed in this article are solely those of the authors and do not necessarily represent those of their affiliated organizations, or those of the publisher, the editors and the reviewers. Any product that may be evaluated in this article, or claim that may be made by its manufacturer, is not guaranteed or endorsed by the publisher.

frontiers in Physiology

ORIGINAL RESEARCH
published: 11 February 2020
doi: 10.3389/fphys.2020.00097

Hyperoxia During Exercise: Impact on Adenosine Plasma Levels and Hemodynamic Data

Alain Boussuges[1,2], Sarah Rives[1,2], Marion Marlinge[2], Guillaume Chaumet[3], Nicolas Vallée[1], Régis Guieu[2] and Olivier Gavarry[4]*

[1] ERRSO, Institut de Recherche Biomédicale des Armées (IRBA), Toulon, France, [2] Center for Cardiovascular and Nutrition Research (C2VN), Aix-Marseille Université, INSERM, INRA, Marseille, France, [3] AltraBio, Lyon, France, [4] Laboratoire Impact de l'Activité Physique sur la Santé, UFR STAPS, Université de Toulon, La Garde, France

Introduction: Adenosine is an ATP derivative that is strongly implicated in the cardiovascular adaptive response to exercise. In this study, we hypothesized that during exercise the hyperemia, commonly observed during exercise in air, was counteracted by the downregulation of the adenosinergic pathway during hyperoxic exposure.

Methods: Ten healthy volunteers performed two randomized sessions including gas exposure (Medical air or Oxygen) at rest and during exercise performed at 40% of maximal intensity, according to the individual fitness of the volunteers. Investigations included the measurement of adenosine plasma level (APL) and the recording of hemodynamic data [i.e., cardiac output (CO) and systemic vascular resistances (SVR) using pulsed Doppler and echocardiography].

Results: Hyperoxia significantly decreased APL (from 0.58 ± 0.06 to 0.21 ± 0.05 μmol L^{-1}, $p < 0.001$) heart rate and CO and increased SVR in healthy volunteers at rest. During exercise, an increase in APL was recorded in the two sessions when compared with measurements at rest (+0.4 ± 0.4 vs. +0.3 ± 0.2 μmol L^{-1} for medical air and oxygen exposures, respectively). APL was lower during the exercise performed under hyperoxia when compared with medical air exposure (0.5 ± 0.06 vs. 1.03 ± 0.2 μmol L^{-1}, respectively $p < 0.001$). This result could contribute to the hemodynamic differences between the two conditions, such as the increase in SVR and the decrease in both heart rate and CO when exercises were performed during oxygen exposure as compared to medical air.

Conclusion: Hyperoxia decreased APLs in healthy volunteers at rest but did not eliminate the increase in APL and the decrease in SVR during low intensity exercise.

Keywords: oxygen, circulatory system, hyperemia, echocardiography, cardiac output, systemic vascular resistances

OPEN ACCESS

Edited by:
François Guerrero, Université de Bretagne Occidentale, France

Reviewed by:
Costantino Balestra, Haute École Bruxelles-Brabant (HE2B), Belgium
Satoshi Iwase, Aichi Medical University, Japan

****Correspondence:***
Alain Boussuges
alain.boussuges@univ-amu.fr;
alain.boussuges@gmail.com

Specialty section:
This article was submitted to Environmental, Aviation and Space Physiology, a section of the journal Frontiers in Physiology

Received: *26 September 2019*
Accepted: *27 January 2020*
Published: *11 February 2020*

Citation:
Boussuges A, Rives S, Marlinge M, Chaumet G, Vallée N, Guieu R and Gavarry O (2020) Hyperoxia During Exercise: Impact on Adenosine Plasma Levels and Hemodynamic Data. Front. Physiol. 11:97. doi: 10.3389/fphys.2020.00097

INTRODUCTION

Subjects experienced physical effort under an ambient hyperoxic environment during various professional or recreational activities. In ambient hyperbaric environment, such as the environment experienced by divers or by professional workers in a tunnel boring machine hyperbaric chamber, hyperoxia is secondary to the increase in ambient pressure and its consequence on oxygen partial

pressure. In hypoxic environments, enriched oxygen mixtures are used and can lead to an increase in oxygen partial pressure. Lastly, some athletes used hyperoxic exposure during their exercise training to improve physical performance.

In healthy volunteers at rest, the impact of hyperoxia on the cardio-vascular system has been studied. A decrease in cardiac output (CO) secondary to a slowing of the heart rate has been observed (Waring et al., 2003; Thomson et al., 2006; Gole et al., 2011). Furthermore, an increase in systemic vascular resistances (SVR) and a decrease in arterial compliance induced by an arterial vasoconstriction have been commonly reported (Milone et al., 1999; Rossi and Boussuges, 2005; Gole et al., 2011).

Various mechanisms have been implicated in the alteration of vasomotion in an ambient hyperoxic environment. An increase in the endothelin I plasma level might contribute to the vasoconstriction of the cerebral arteries under hyperoxia (Armstead, 1999). Alterations to endothelial function including action of nitric oxide (NO) being impeded by reactive oxygen species have been reported (Rubanyi and Vanhoutte, 1986; Pasgaard et al., 2007). A decrease in muscle sympathetic nerve activity has been reported at rest but not during exercise (Seals et al., 1991). Recently, a decrease in adenosine plasma levels (APLs) has been reported in rats subjected to normobaric or hyperbaric hyperoxia (Bruzzese et al., 2015). Adenosine is an ATP derivative which strongly impacts heart rate and blood pressure through its G-protein coupled receptors known as A1, A2A, A2B, or A3R, depending on their pharmacological properties (Burnstock, 2017).

During exercise on land, hemodynamic changes include an increase in CO secondary to the increase in both heart rate and stroke volume and a decrease in SVR. Exercise-induced hyperemia has been attributed to various factors such as NO, prostacyclin (PGI2), and endothelium-derived hyperpolarizing factor (Sarelius and Pohl, 2010). Furthermore, it has been reported that adenosine was responsible for a part of the maintained phase of the muscle vasodilation that accompanies muscle hyperemia during exercise (Marshall, 2007).

In this study, we hypothesized that during exercise in hyperoxia, the hyperemia commonly observed during exercise in air was counteracted by the downregulation of the adenosinergic pathway secondary to the increase in oxygen partial pressure.

MATERIALS AND METHODS

Subjects

Ten healthy male volunteers participated in this study. Mean age, weight, height, and body surface area were 35 ± 6 years, 73 ± 12 kg, 177 ± 7 cm, and 1.9 ± 0.2 m^2, respectively. All volunteers gave their written informed consent to participation in the experiment, which was approved by the Regional Ethics Committee (Aix Marseille University, CPP-1, ID RCB: 2008-AOO171-54). The research was conducted according to the Helsinki Declaration. All the exercise bouts were performed on the same ergobike (Tunturi Endurance E80R Recumbent Bike). This recumbent bike was used to make the ultrasonographic examinations easier. Prior the main experiment, the volunteers performed an incremental maximal cycling exercise to assess maximal aerobic fitness (peak VO_2) and the power corresponding to 40% intensity exercise on this ergometer.

Main Experiment

The experimental session consisted of a sequence of four measurement periods: baseline, gas exposure (medical air or oxygen), cycling exercise at a workload corresponding to 40% of VO_2 peak (breathing air or oxygen), and recovery period, 30 min after the end of exercise.

To determine data at rest, participants were in a sitting position, in a quiet and air-conditioned room (50% humidity, temperature: 25°C). During exercises, ambient temperature was lowered to 22°C.

During the baseline period, volunteers breathed ambient air without a face mask for 10 min of quiet rest. After the baseline investigations, each subject underwent two sessions in a randomized order. The volunteers at rest were exposed during 1 h to a medical gases supplied by the society Air Liquide (AL Healthcare, Paris, France), i.e., medical air (21% oxygen and 79% nitrogen) or pure oxygen (inspired oxygen fraction = 1) delivered in a Douglas bag, to be breathed at atmospheric pressure. Subjects received either medical air or pure oxygen through a face mask connected to two-way low-resistance *T* valve (Hans Rudolph Inc., Shawnee, KS, United States). The facemask was fixed firmly around the mouth and nose to prevent air leaks. An oxygen analyzer (Servomex Oxygen Analyzer 570A; Servomex Group Ltd, Crowborough, United Kingdom) was used to control FiO_2.

Volunteers and investigators were blinded to the gas mixture used. Thereafter, all participants performed a 30-min constant-load exercise on the recumbent bike, breathing medical air or oxygen. The pedaling rate was fixed at 60 rotations per minute. The workload was adjusted to represent 40% of the VO_2 peak according to the individual maximal incremental exercise. There were a minimum of 3 days and a maximum of 7 days between the two sessions. The two sessions were performed in a random order, at the same time of day for each subject. At each measurement period, the investigations included venous blood sampling, and an ultrasonographic study.

Investigations

All procedures were undertaken after 10 min of rest as baseline measurements, 1 h after the exposure to medical air or oxygen at rest, 20 min after the beginning of the exercises, and during recovery, 30 min after the return to ambient air. During the experiment, oxygen saturation level (SpO_2) was measured using a pulse oximeter (NPB 40; Nellcor Puritan Bennett, Pleasanton, CA, United States) fixed on the left median finger.

Echocardiographic and Doppler Study

The ultrasonographic examinations were carried out by an experienced investigator using a Doppler cardiovascular ultrasound (Mylab 25CV, Esaote SpA, Genova, Italy) connected to a 2.5–3.5 MHz transducer array. The mean duration for each examination was 10 min. All Doppler recordings were performed at the end of a normal expiration in order to eliminate the effects

of breathing on the parameters studied. Measurements were averaged from at least three different beats.

The left ventricular outflow tract (LVOT) was first measured by 2D echocardiography from the left parasternal long axis view. The aortic systolic flow velocity time integral (AoVTI) was measured by computer-assisted determination from the pulsed-wave Doppler profile of the aortic blood flow from the apical four chamber view, allowing stroke volume (SV) and CO to be calculated: SV = AoVTI × LVOT, CO = SV × HR. SVR were calculated as mean arterial pressure (MAP) divided by CO.

Blood Pressure Measurement

Sphygmomanometer blood pressure measurements on the right arm were obtained at the end of each echographic examination. MAP was calculated as DAP + 1/3 (SAP – DAP), where SAP and DAP were respectively the systolic and diastolic arterial blood pressures.

Adenosine Plasma Level Measurement

Blood sample collection for adenosine plasma measurement was performed through a catheter inserted in a vein in the elbow folds, at baseline, during gas exposure at rest and during exercise (at the end of each period) and after recovery as described above. Since adenosine has a short half-life, we used a stop solution to block adenosine metabolism and uptake by red blood cells as previously described (Guieu et al., 1994; Maille et al., 2019). After centrifugation (1500 × *g*, 10 min, 4°C), supernatants were pipetted off and frozen (−80°C) until analysis. APL measurement was performed by LC-MS/MS as previously described (Maille et al., 2019).

Statistical Analysis

Data are expressed as mean ± SEM. Statistical tests were run on Sigma Stat software.

The cohorts for comparison consisted of the ten subjects at 4 time points during the two sessions, i.e., under medical air or oxygen exposure: baseline, during gas exposure at rest, during exercise and 30 min after the end of exercise. Comparison between cohorts of continuous variables having normal distribution was carried out with the parametric analysis of variance (repeated measurements, ANOVA); multiple pairwise comparison procedures were done using the Holm-Sidak method. In the case of variable cohorts not having normal distribution, comparisons were performed with a non-parametric univariate analysis (Friedman's test); comparison of dichotomous variables was carried out using the Student-Newman–Keuls Method. Differences between groups were considered significant at $p < 0.05$.

RESULTS

Exercise Testing

The peak of VO_2 and maximal workload recorded by the incremental exercise testing were 47 ± 6 mL kg^{-1} min^{-1} (115 ± 15% of the predicted value) and 263 ± 45 Watts, respectively. According to these results, the workload used for the cycling exercise performed under medical air and oxygen exposure was 115 ± 10 W. This workload corresponded to an intensity that was under the ventilatory threshold (in mean 167 ± 32 W) in all volunteers.

SpO_2 Measurement

SpO_2 varied between 99 and 100% during oxygen session (at rest and exercise). During air medical session, mean SpO_2 was 97 ± 1%.

Adenosine Plasma Level Measurement

Figure 1 reports the changes in APL during the two sessions. During the medical air session, APL significantly increased during exercise and returned to the baseline value during recovery. During oxygen exposure at rest, APL was significantly lower when compared with medical air exposure ($p < 0.001$). During exercise, APL significantly increased but remained significantly lower during oxygen exposure in comparison with medical air exposure ($p < 0.001$). After exercise, APL returned to the baseline values.

There is no significant difference between the increase in APL during exercises between the two sessions (+0.4 ± 0.4 μmol L^{-1} vs. +0.3 ± 0.2 μmol L^{-1} for medical air and oxygen exposures, respectively). Interestingly, APL at the end of exercise in O_2 ambiance was similar than APL at rest in medical air ambiance.

Blood Pressure Measurement

Systolic blood pressure increased during exercise, this increase was significantly larger during oxygen rather than medical air exposure ($p < 0.05$). Mean and diastolic blood pressure significantly increased during exercise without a significant difference between the two sessions (**Table 1**).

Hemodynamic Data

During medical air exposure at rest, hemodynamic data were similar to measurements performed at baseline. During exercise, an increase in CO secondary to an increase in both heart rate and stroke volume was observed. Blood pressure (systolic, mean, diastolic, and pulse pressure) increased during exercise whereas SVR decreased significantly. During recovery, heart rate decreased ($p < 0.05$) but remained significantly accelerated when compared with baseline values (**Table 1**).

A decrease in heart rate leading to a decrease in CO was recorded during oxygen exposure at rest (**Figure 2**). The difference was significant with measurements performed both at baseline and during medical air exposure. SVR significantly increased during hyperoxia when compared with medical air (**Figure 3**).

During exercise, heart rate and CO increased but remained lower during oxygen exposure when compared with medical air, in contrast stroke volume was not significantly different between the two conditions (**Table 1**). During exercise SVR decreased and was lower during medical air when compared with exercise performed during oxygen exposure (**Figure 3**).

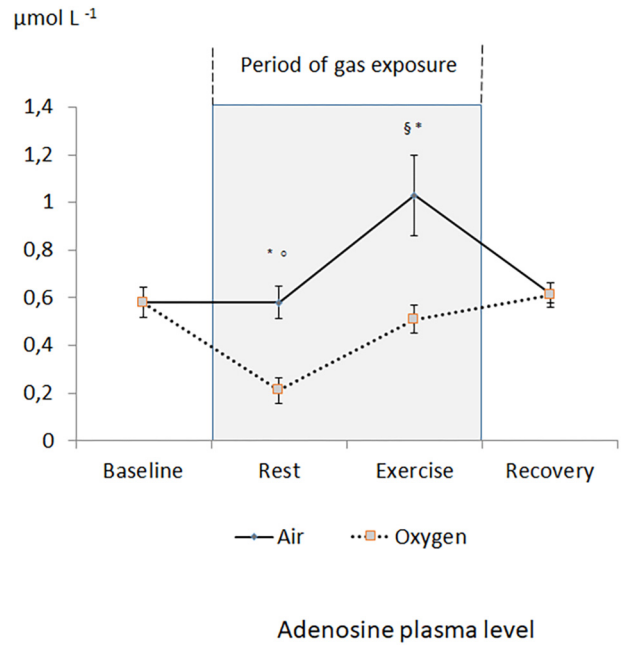

FIGURE 1 | Evolution of adenosine plasma level during the two sessions. $^{§}p < 0.05$ oxygen vs. medical air. $^{*}p < 0.05$ exercise vs. measurement at rest of the same session. $^{\circ}p < 0.05$ oxygen vs. baseline.

DISCUSSION

This study reports, for the first time, the impact of hyperoxia on both APL and hemodynamic status in healthy volunteers at rest and during exercise. The main result of the study was that hyperoxia decreased APL in men, both at rest and during exercise. Our results and previous studies support the fact that APL is generated in an oxygen-dependent manner (Schrader et al., 1990). Indeed, it has been reported that hypoxia induced an increase in APL (Eltzschig et al., 2006; Joulia et al., 2013) whereas hyperoxia lead to a decrease in APL (Bruzzese et al., 2015; Fromonot et al., 2016).

The impact of adenosine on the hemodynamic status is well recognized and could contribute to the cardio-vascular changes observed in our healthy volunteers. In agreement with previous work, a decrease in CO secondary to a slowing of the heart rate was observed during hyperoxia (Waring et al., 2003; Gole et al., 2011). Furthermore, a significant increase in SVR was reported in healthy volunteers at rest during hyperoxia. The increase in oxygen partial pressure and the production of reactive oxygen species can be implicated in arterial vasoconstriction through an alteration in endothelial function or a direct effect on vascular smooth muscle (Welsh et al., 1998; Pasgaard et al., 2007). It has been shown that endothelial function was impaired after SCUBA diving, involving exposure to elevated partial pressures of oxygen at depth (Lambrechts et al., 2013). Pre-ingestion of nutritional antioxidants such as red orange extract (Balestra et al., 2016) or dark chocolate (Theunissen et al., 2015) prevented endothelial dysfunction. This improvement has been attributed, by the authors, to an increase in activity and expression of endothelial NO synthase. The decrease in APL might contribute to the vasomotor action of hyperoxia. Indeed, APL is recognized as having an impact on vasomotor tone, an increase in APL leading to vasodilation (Duza and Sarelius, 2003; Mortensen et al., 2009). The vasodilatory properties of adenosine are mediated by several physiological factors including an increase in NO production by endothelial cells (Li et al., 1995).

In our study, the slowing of the heart rate under hyperoxia might be secondary to the baroreflex stimulation induced by vasoconstriction (Waring et al., 2003; Demchenko et al., 2013). During exercise breathing medical air, the hemodynamic changes were common, including an increase in CO associated with a decrease in SVR. Furthermore, a significant increase in APL was observed, which could participate in the hyperemia induced by exercise through the action on arterial function (Hellsten et al., 2012).

TABLE 1 | Blood pressure and hemodynamic data.

Parameters	Session	Baseline (AA)	Gas exposure	Exercise	Recovery (AA)
SBP (mmHg)	Medical air	115 ± 5	107 ± 4	136 ± 6*	110 ± 3
	Oxygen	117+/2	116 ± 2	145 ± 5*§	107 ± 4#
MBP (mmHg)	Medical air	88 ± 4	82 ± 3	97 ± 4*	85 ± 3
	Oxygen	90 ± 3	85 ± 2	102 ± 4*	81 ± 4#
DBP (mmHg)	Medical air	75 ± 4	70 ± 3	78 ± 3*	73 ± 4
	Oxygen	76 ± 3	70 ± 3	81 ± 5*	69 ± 5#
PP (mmHg)	Medical air	41 ± 2	37 ± 2	59 ± 5*	38 ± 4
	Oxygen	42 ± 2	45 ± 3	65 ± 5*	38 ± 2
SV (mL)	Medical air	68 ± 3	73 ± 4	91 ± 8*	56 ± 5£#
	Oxygen	67 ± 4	65 ± 5	90 ± 10*	58 ± 5#
CO (L min^{-1})	Medical air	4.4 ± 0.3	4.6 ± 0.3	10.1 ± 0.7*	4.2 ± 0.4
	Oxygen	4.4 ± 0.3	3.6 ± 0.3§°	9.2 ± 0.7*§	4 ± 0.3

Results are reported as mean ± SEM. AA, ambient air; SBP, systolic blood pressure; MBP, mean blood pressure; DBP, diastolic blood pressure; PP, pulse pressure; SV, stroke volume; CO, cardiac output. $^{*}p < 0.05$ exercise vs. other measurement times in the same session, $^{§}p < 0.05$ oxygen vs. medical air, $^{£}p < 0.05$ recovery vs. gas exposure, $\#p < 0.05$ recovery vs. baseline, $^{\circ}p < 0.05$ gas exposure vs. baseline.

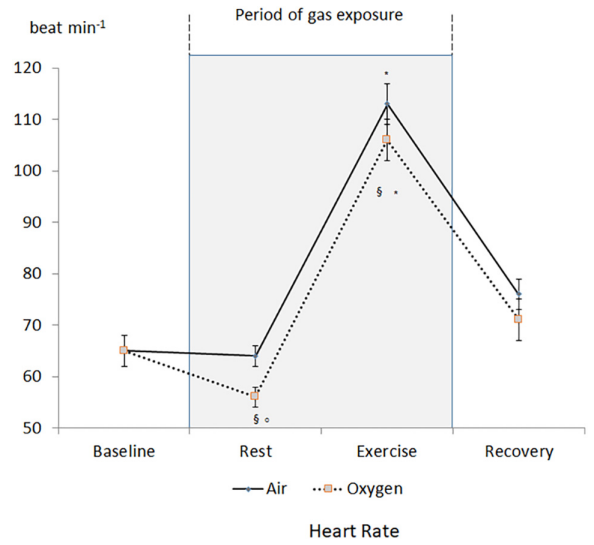

FIGURE 2 | Changes in heart rate during the two sessions. $^{\S}p < 0.05$ oxygen vs. medical air. $^{*}p < 0.05$ exercise vs. measurement at rest of the same session. $^{\circ}p < 0.05$ oxygen vs. baseline.

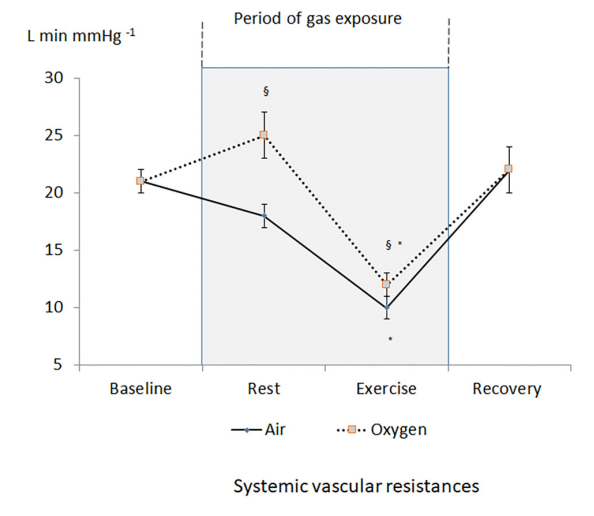

FIGURE 3 | Changes in systemic vascular resistances during the two sessions. $^{\S}p < 0.05$ oxygen vs. medical air. $^{*}p < 0.05$ exercise vs. measurement at rest of the same session.

In the session breathing pure oxygen, a significant increase in APL was recorded during exercise when compared with the resting condition. Nevertheless, APL remained lower than during exercise performed with medical air exposure. APL was comparable to the baseline measurements (in ambient air or during medical air exposure). Hemodynamic status was also significantly different between the two sessions. Hyperoxia-induced vasoconstriction could explain the increase in both systolic blood pressure and SVR. It could also explain the decrease in heart rate recorded in healthy volunteers during oxygen exposure when compared with medical air exposure, through baroreflex stimulation. Consequently, our findings supported previous observations that breathing pure oxygen induced vasoconstriction and attenuated hyperemia secondary to dynamic exercise (Welch et al., 1977; González-Alonso et al., 2002).

Nevertheless, there was no difference between the increases in APL recorded during exercise between the two sessions. In our study, exercise bouts were performed at low intensity (40% of VO_2 peak), under the ventilatory threshold. Such exercises are recognized not inducing cellular hypoxia. Previous studies have attributed hyperemia to the release of oxygen-dependent factors secondary to the cellular hypoxia induced by anaerobic exercise (Marshall, 2007). Our study did not support this single mechanism since, although the exercises were performed in aerobic conditions, an increase in APL associated with a decrease in SVR was observed. Furthermore, the magnitude of the changes in these two parameters was reduced but not eliminated during exercise with oxygen exposure. In these circumstances, the increase in intravascular purines should not be secondary to hypoxia but to mechanical stressors induced by exercise. Indeed, it has been reported that shear stress and mechanical compression could induce a release of ATP from endothelial cells, erythrocytes and skeletal muscle cells (Sprague et al., 1996; Buvinic et al., 2009; Mortensen et al., 2011; Crecelius et al., 2013). The dephosphorylation of ATP by ectoenzymes CD39 and CD73 could explain the increase in APL (Borea et al., 2018).

Study Limits

It is recognized that hyperoxic exposure during exercise impacted on both gas exchanges and minute ventilation (Ulrich et al., 2017). Cardiovascular function can be modified through the heart-lung interactions. Consequently, it would be interesting to perform a supplementary study on this topic.

CONCLUSION

In our study, hyperoxia decreased APL in resting healthy volunteers but did not eliminate the increase in APL and the decrease in SVR during low intensity exercise. Further studies are needed to improve knowledge about the factors regulating the increase in APL during exercise according to the modalities (endurance or resistance, intensity) and its contribution to hyperemia.

DATA AVAILABILITY STATEMENT

The datasets generated for this study are available on request to the corresponding author.

ETHICS STATEMENT

The studies involving human participants were reviewed and approved by Aix Marseille University, CPP-1, ID RCB: 2008-AOO171-54. The patients/participants provided their written informed consent to participate in this study.

AUTHOR CONTRIBUTIONS

AB, RG, and OG conceived and designed the study. NV and SR assisted with the technical aspects of the protocol, recruited all the participants, and involved in the acquisition of the data. MM and RG performed the biological study. AB and GC analyzed the data and performed the statistical analysis. AB, GC, and OG have drafted the manuscript while NV and RG revised it critically for important intellectual content. All authors have given final approval of the version to be published.

FUNDING

This study was supported by a French Ministry of Defense research grant (Direction Générale de l'Armement, PDH-1-SMO-2-0701).

ACKNOWLEDGMENTS

The authors gratefully acknowledge the volunteers.

REFERENCES

Armstead, W. M. (1999). Endothelin-1 contributes to normocapnic hyperoxic pial artery vasoconstriction. *Brain Res.* 842, 252–255. doi: 10.1016/s0006-8993(99)01825-9

Balestra, C., Cimino, F., Theunissen, S., Snoeck, T., Provyn, S., Canali, R., et al. (2016). A red orange extract modulates the vascular response to a recreational dive: a pilot study on the effect of anthocyanins on the physiological consequences of scuba diving. *Nat. Prod. Res.* 30, 2101–2106. doi: 10.1080/14786419.2015

Borea, P. A., Gessi, S., Merighi, S., Vincenzi, F., and Varani, K. (2018). Pharmacology of adenosine receptors the state of the art. *Physiol. Rev.* 98, 1591–1625. doi: 10.1152/physrev.00049.2017

Bruzzese, L., Rostain, J. C., Née, L., Condo, J., Mottola, G., Adjriou, N., et al. (2015). Effect of hyperoxic and hyperbaric conditions on the adenosinergic pathway and CD26 expression in rat. *J. Appl. Physiol.* 119, 140–147. doi: 10.1152/japplphysiol.00223.2015

Burnstock, G. (2017). Purinergic signaling in the cardiovascular system. *Circ. Res.* 120, 207–228. doi: 10.1161/CIRCRESAHA.116.309726

Buvinic, S., Almarza, G., Bustamante, M., Casas, M., López, J., Riquelme, M., et al. (2009). ATP released by electrical stimuli elicits calcium transients and gene expression in skeletal muscle. *J. Biol. Chem.* 284, 34490–34505. doi: 10.1074/jbc.M109.057315

Crecelius, A. R., Kirby, B. S., Richards, J. C., and Dinenno, F. A. (2013). Mechanical effects of muscle contraction increase intravascular ATP draining quiescent and active skeletal muscle in humans. *J. Appl. Physiol.* 114, 1085–1093. doi: 10.1152/japplphysiol.01465.2012

Demchenko, I. T., Zhilyaev, S. Y., Moskvin, A. N., Krivchenko, A. I., Piantadosi, C. A., and Allen, B. W. (2013). Baroreflex-mediated cardiovascular responses to hyperbaric oxygen. *J. Appl. Physiol.* 115, 819–828. doi: 10.1152/japplphysiol.00625.2013

Duza, T., and Sarelius, I. H. (2003). Conducted dilations initiated by purines in arterioles are endothelium dependent and require endothelial Ca2+. *Am. J. Physiol. Heart Circ. Physiol.* 285, H26–H37. doi: 10.1152/ajpheart.00788.2002

Eltzschig, H. K., Karhausen, J., and Kempf, V. A. (2006). Acute oxygen-sensing mechanisms. *N. Engl. J. Med.* 2006, 975–977. doi: 10.1056/nejmc053396

Fromonot, J., Chaumet, G., Gavarry, O., Rostain, J. C., Lucciano, M., Joulia, F., et al. (2016). Hyperoxia improves hemodynamic status during head-up tilt testing in healthy volunteers: a randomized study. *Medicine* 95:e2876. doi: 10.1097/MD.0000000000002876

Gole, Y., Gargne, O., Coulange, M., Steinberg, J. G., Bouhaddi, M., Jammes, Y., et al. (2011). Hyperoxia-induced alterations in cardiovascular function and autonomic control during return to normoxic breathing. *Eur. J. Appl. Physiol.* 111, 937–946. doi: 10.1007/s00421-010-1711-4

González-Alonso, J., Olsen, D. B., and Saltin, B. (2002). Erythrocyte and the regulation of human skeletal muscle blood flow and oxygen delivery: role of circulating ATP. *Circ. Res.* 91, 1046–1055. doi: 10.1161/01.res.0000044939.73286.e2

Guieu, R., Sampieri, F., Bechis, G., and Rochat, H. (1994). Use of HPLC to measure circulating adenosine levels in migrainous patients. *Clin. Chim. Acta* 227, 185–194. doi: 10.1016/0009-8981(94)90146-5

Hellsten, Y., Nyberg, M., and Mortensen, S. P. (2012). Contribution of intravascular versus interstitial purines and nitric oxide in the regulation of exercise hyperaemia in humans. *J. Physiol.* 590, 5015–5023. doi: 10.1113/jphysiol.2012.234963

Joulia, F., Coulange, M., Lemaitre, F., Costalat, G., Franceschi, F., Gariboldi, V., et al. (2013). Plasma adenosine release is associated with bradycardia and transient loss of consciousness during experimental breath-hold diving. *Int. J. Cardiol.* 168:e00138-41. doi: 10.1016/j.ijcard.2013.08.053

Lambrechts, K., Pontier, J. M., Balestra, C., Mazur, A., Wang, Q., Buzzacott, P., et al. (2013). Effect of a single, open-sea, air scuba dive on human micro- and macrovascular function. *Eur. J. Appl. Physiol.* 113, 2637–2645. doi: 10.1007/s00421-013-2676-x

Li, J. M., Fenton, R. A., Cutler, B. S., and Dobson, J. G. Jr. (1995). Adenosine enhances nitric oxide production by vascular endothelial cells. *Am. J. Physiol.* 269, C519–C523.

Maille, B., Marlinge, M., Vairo, D., Mottola, G., Koutbi, L., Deharo, P., et al. (2019). Adenosine plasma level in patients with paroxysmal or persistent atrial fibrillation and normal heart during ablation procedure and/or cardioversion. *Purinergic Signal.* 15, 45–52. doi: 10.1007/s11302-018-9636-1

Marshall, J. M. (2007). The roles of adenosine and related substances in exercise hyperaemia. *J. Physiol.* 583, 835–845. doi: 10.1113/jphysiol.2007.136416

Milone, S., Newton, G., and Parker, J. (1999). Hemodynamic and biochemical effects of 100% oxygen breathing in humans. *Can. J. Physiol. Pharmacol.* 77, 124–130. doi: 10.1139/y99-010

Mortensen, S. P., Nyberg, M., Thaning, P., Saltin, B., and Hellsten, Y. (2009). Adenosine contributes to blood flow regulation in the exercising human leg by increasing prostaglandin and nitric oxide formation. *Hypertension* 53, 993–999. doi: 10.1161/HYPERTENSIONAHA.109.130880

Mortensen, S. P., Thaning, P., Nyberg, M., Saltin, B., and Hellsten, Y. (2011). Local release of ATP into the arterial inflow and venous drainage of human skeletal muscle: insight from ATP determination with the intravascular microdialysis technique. *J. Physiol.* 589, 1847–1857. doi: 10.1113/jphysiol.2010.203034

Pasgaard, T., Stankevicius, E., Jorgensen, M., Ostergaard, L., Simonsen, U., and Frobert, O. (2007). Hyperoxia reduces basal release of nitric oxide and contracts porcine coronary arteries. *Acta Physiol.* 191, 285–296. doi: 10.1111/j.1748-1716.2007.01745.x

Rossi, P., and Boussuges, A. (2005). Hyperoxia-induced arterial compliance decrease in healthy man. *Clin. Physiol. Funct. Imag.* 25, 10–15. doi: 10.1111/j.1475-097X.2004.00572.x

Rubanyi, G. M., and Vanhoutte, P. M. (1986). Superoxide anions and hyperoxia inactivate endothelium-derived relaxing factor. *Am. J. Physiol.* 250, H822–H827.

Sarelius, I., and Pohl, U. (2010). Control of muscle blood flow during exercise: local factors and integrative mechanisms. *Acta Physiol.* 199, 349–365. doi: 10.1111/j.1748-1716.2010.02129.x

Schrader, J., Deussen, A., and Smolenski, R. T. (1990). Adenosine is a sensitive oxygen sensor in the heart. *Experientia* 46, 1172–1175. doi: 10.1007/bf01936930

Seals, D., Johnson, G., and Fregosi, R. (1991). Hyperoxia lowers sympathetic activity at rest but not during exercise in humans. *Am. J. Physiol.* 260, R873–R878.

Sprague, R. S., Ellsworth, M. L., Stephenson, A. H., and Lonigro, A. J. (1996). ATP: the red blood cell link to NO and local control of the pulmonary circulation. *Am. J. Physiol.* 271, H2717–H2722.

Theunissen, S., Balestra, C., Boutros, A., De Bels, D., Guerrero, F., and Germonpre, P. (2015). The effect of pre-dive ingestion of dark chocolate on endothelial function after a scuba dive. *Diving Hyperb. Med.* 45, 4–9.

Thomson, A. J., Drummond, G. B., Waring, W. S., Webb, D. J., and Maxwell, S. R. J. (2006). Effects of short-term isocapnic hyperoxia and hypoxia on cardiovascular function. *J. Appl. Physiol.* 101, 809–816. doi: 10.1152/japplphysiol.01185.2005

Ulrich, S., Hasler, E. D., Muller-Mottet, S., Keusch, S., Furian, M., Latshang, T. D., et al. (2017). Mechanisms of improved exercise performance under hyperoxia. *Respiration* 93, 90–98. doi: 10.1159/000453620

Waring, W., Thomson, A., Adwani, S., Rosseel, A., Potter, J., Webb, D., et al. (2003). Cardiovascular effects of acute oxygen administration in healthy adults. *J. Cardiovasc. Pharmacol.* 42, 245–250. doi: 10.1097/00005344-200308000-00014

Welch, H. G., Bonde-Petersen, F., Graham, T., Klausen, K., and Secher, N. (1977). Effects of hyperoxia on leg blood flow and metabolism during exercise. *J. Appl. Physiol. Respir. Environ. Exerc. Physiol.* 42, 385–390. doi: 10.1152/jappl.1977.42.3.385

Welsh, D. G., Jackson, W. F., and Segal, S. S. (1998). Oxygen induces electromechanical coupling in arteriolar smooth muscle cells: a role for L-type Ca2+ channels. *Am. J. Physiol.* 274, H2018–H2024. doi: 10.1152/ajpheart.1998.274.6.H2018

Conflict of Interest: The authors declare that the research was conducted in the absence of any commercial or financial relationships that could be construed as a potential conflict of interest.

frontiers in Physiology

PERSPECTIVE
published: 19 July 2021
doi: 10.3389/fphys.2021.699493

The Circulatory Effects of Increased Hydrostatic Pressure Due to Immersion and Submersion

Robert P. Weenink[1,2] and Thijs T. Wingelaar[1,2]*

[1]Diving Medical Center, Royal Netherlands Navy, Den Helder, Netherlands, [2]Department of Anesthesiology, Amsterdam University Medical Centers, Location AMC, Amsterdam, Netherlands

Increased hydrostatic pressure as experienced during immersion and submersion has effects on the circulation. The main effect is counteracting of gravity by buoyancy, which results in reduced extravasation of fluid. Immersion in a cold liquid leads to peripheral vasoconstriction, which centralizes the circulation. Additionally, a pressure difference usually exists between the lungs and the rest of the body, promoting pulmonary edema. However, hydrostatic pressure does not exert an external compressing force that counteracts extravasation, since the increased pressure is transmitted equally throughout all tissues immersed at the same level. Moreover, the vertical gradient of hydrostatic pressure down an immersed body part does not act as a resistance to blood flow. The occurrence of cardiovascular collapse when an immersed person is rescued from the water is not explained by removal of hydrostatic squeeze, but by sudden reinstitution of the effect of gravity in a cold and vasoplegic subject.

Keywords: hydrostatic pressure, immersion, blood circulation, hyperbaric oxygenation, swimming, diving, immersion pulmonary edema, rescue collapse

OPEN ACCESS

Edited by:
François Guerrero, Université de Bretagne Occidentale, France

Reviewed by:
Tiago Peçanha, University of São Paulo, Brazil
Brett Wong, Georgia State University, United States

****Correspondence:***
Robert Paul Weenink
r.p.weenink@amsterdamumc.nl

Specialty section:
This article was submitted to Environmental, Aviation and Space Physiology, a section of the journal Frontiers in Physiology

Received: *23 April 2021*
Accepted: *02 July 2021*
Published: *19 July 2021*

Citation:
Weenink RP and Wingelaar TT (2021) The Circulatory Effects of Increased Hydrostatic Pressure Due to Immersion and Submersion. Front. Physiol. 12:699493. doi: 10.3389/fphys.2021.699493

INTRODUCTION

Humans are generally subjected to a rather constant environmental pressure, but may experience changes in ambient pressure during activities such as flying and diving. One of the most common activities that involve increased environmental pressure is immersion (when the body is partially surrounded by liquid) as occurs during bathing or swimming, or submersion (when the body is fully surrounded by liquid), when snorkeling, diving, or swimming under water. When reviewing the literature on the circulatory effects of immersion and submersion one frequently encounters misconceptions, which seem to result from an incorrect application of physical principles. A regularly encountered misconception concerns the phenomenon of cardiovascular collapse when an immersed or submerged person is removed from the water (Tipton and Ducharme, 2014). This is frequently attributed to the removal of "hydrostatic squeeze," i.e., the supposed compressing effect of hydrostatic pressure on the immersed tissue (Pendergast et al., 2015; Bierens et al., 2016). At first glance, this explanation, which suggests that hydrostatic pressure may act similarly to an elastic stocking around the leg (Tipton et al., 2017), may seem convincing. However, it does not comply with the physics involved in hydrostatic pressure. In this perspective, we will provide an overview of the effects of immersion and submersion on the circulation, address frequently encountered misconceptions, and thereby

hope to encourage the correct application of physical principles and use of appropriate terminology.

PHYSIOLOGY OF INCREASED HYDROSTATIC PRESSURE

Firstly, it should be appreciated that Pascal's law dictates that hydrostatic pressure acting on an immersed body part is transmitted equally through all tissues. In other words, the pressure at a certain depth of immersion will be equal in all tissues immersed at that level. This means that there is no pressure gradient between – for instance – the blood vessels and the surrounding tissues. Therefore, no force is squeezing the vessels, pushing interstitial fluid into the vessels, or counteracting extravasation. This is best demonstrated by regarding the effects of increasing pressure in a hyperbaric chamber. A person subjected to increased ambient pressure in a dry chamber, the pressure is equal all around and inside the body, i.e., the increased atmospheric pressure in the chamber is transmitted throughout the body. Hence, there is no pressure gradient to cause a circulatory effect. This is in line with the experience of anyone working in hyperbaric medicine: in the range of pressures encountered in the hyperbaric chamber – usually up to three atmospheres (304 kPa), equivalent to immersion in water to a depth of 20 m – the pressure *per se* has no effect (Welslau, 2006). For sake of completeness, it should be noted that other components of hyperbaric medicine can have circulatory effects, such as vasoconstriction caused by increased partial oxygen tensions (Mathieu et al., 2006), but this is not the topic of the current paper.

So far, we can conclude that the amount of pressure increase is equal in all tissues at the same level of immersion. Increased hydrostatic pressure is not the same as an elastic stocking. What then are the causes of circulatory effects due to increased hydrostatic pressure during immersion or submersion? In order to understand these, we must consider the differences between compression in a dry hyperbaric chamber and immersion or submersion in a liquid:

1. Counteracting of gravity by buoyancy.
2. Vertical pressure gradient of hydrostatic pressure.
3. Pressure gradient between the lungs and the rest of the body.
4. Effects due to temperature.
5. Miscellaneous other effects.

Buoyancy

Archimedes' law states that an object submerged in a liquid experiences an upward force equal to the weight of the displaced liquid. This is caused by the upward force exerted on the object by the liquid below the object being greater than the downward force exerted by the liquid above the object. As the density of the human body is quite comparable to the density of water, this upward force is almost equal to the weight of the body, and therefore humans experience "weightlessness" during submersion. In a standing, non-immersed person there is a considerable intravascular pressure gradient down the body due to gravity. If we assume a mean blood pressure of 74 mmHg (100 cm H_2O, 9.81 kPa) in the aortic root, the mean intravascular pressure 1 m lower in the legs will be 200 cm H_2O (19.6 kPa), promoting extravasation of fluid. During immersion, the buoyancy caused by the upward force of the liquid on the body counteracts gravity and thereby reduces the gradient for extravasation. Decreased extravasation means more fluid is retained in the circulation, and this accounts for the approximately 500–700 ml increase in circulating volume as measured during submersion (Weston et al., 1987). The increased urine output that follows will tend to normalize circulating volume over time.

Pressure Gradient of Hydrostatic Pressure

In a hyperbaric chamber, the pressure increase is equal all around the body. During immersion and submersion, this is not the case. Non-immersed parts of the body experience the atmospheric pressure of the air above the water, while immersed parts experience higher pressures, depending on the level of immersion. If the immersion is in water, the pressure gradient will be 100 cm H_2O (9.81 kPa) for each meter of immersion. It is exactly this pressure gradient that causes buoyancy as explained above. What now is the effect of this vertical pressure gradient, reiterating that at every given level of immersion, the pressure inside the tissues at that level is equal?

One might be inclined to think of this increase in pressure in the blood vessels and tissues as acting as a resistance to blood flow. During submersion in a vertical position, on its way from the heart to the legs the blood encounters increasingly greater pressures, resulting in incremental decreases of flow. This would then lead to preferential perfusion of the least immersed parts of the body. However, this is not the case. The reason for this is that the circulation is a siphon, i.e., a closed loop of flowing liquid without any air. In a siphon, flow is determined by the difference between the inlet and the outlet pressure and the resistance of the system; intermediary pressure has no effect (Munis and Lozada, 2000). Consider a garden hose through which water flows at a specific rate. If a portion of the hose is now lowered (or elevated) while inlet and outlet remain at the same level, the flow rate will not change. If the pressure inside the hose would be measured, it would be greater in the lower portion of the hose, but this increase in intermediate pressure does not affect flow rate.

It should be borne in mind that lowering part of the hose is not the same as squeezing the hose. Squeezing the hose is equivalent to external compression on the dependent body parts. As explained above, this is not what happens during immersion. Also, it is important to realize that the gradient of hydrostatic pressure due to immersion is different from the gradient of intravascular pressure in a standing non-immersed person. As mentioned above, in a standing non-immersed person, intravascular pressure increases on the way down from the heart, due to the effect of gravity on the blood. This has no effect on flow (again, because the circulation is a siphon) but since in this case, a pressure difference between the blood

in the vessel and extravascular tissues does exist, it promotes extravasation of fluid.

Pressure Gradient Between the Lung and the Rest of the Body

In most situations of submersion and immersion, there will be a pressure difference between the air in the lung and the rest of the body. For instance, during immersion with the head above the water (head-out-water-immersion) and snorkeling, air pressure in the lung is equal to the atmospheric pressure of the air breathed, and the pressure in the tissue surrounding the lung depends on the level of immersion (**Figure 1**). With head-out-water-immersion, the lung will be some 20 cm below the water, resulting in a pressure differential of 20 cm H_2O (2.0 kPa). The pressure gradient between the air in the lungs and the surrounding tissues promotes extravasation of fluid from the pulmonary vasculature. This is one of the supposed mechanisms in immersion pulmonary edema (Koehle et al., 2005; Wilmshurst, 2019) and is also a reason why snorkels cannot be longer than a few decimeters, or the large pressure difference would lead to pulmonary edema.

Of note, a pressure difference between the lungs and the surrounding tissues is absent when a person is fully submerged and not breathing, such as when swimming below the surface. In this case, pressure in the lung equalizes with surrounding pressure, again following Pascal's law. During diving a pressure difference between lung and surrounding tissues may exist, depending on the pressure at which the breathing gases are delivered to the diver. Usually, some amount of resistance has to be overcome in order to draw breathing gas into the lung and expel it out of the lungs. If this resistance is too high, excessive negative airway pressure will exist during inspiration, again promoting pulmonary extravasation of fluid. Through this and other mechanisms, immersion pulmonary edema can also occur during diving (Coulange et al., 2010).

The special case of breath-hold diving must be briefly mentioned here. This is basically submersion while holding one's breath, and therefore no pressure difference between lungs and surroundings exists. However, the volume of the air in the lungs will decrease as the diver goes deeper, per Boyle's law. At a certain point, lung volume will reach the residual volume so the lung cannot collapse any further. Further descent causes extravasation of fluid from the pulmonary vasculature, which is a cause of pulmonary edema in extreme breath-hold diving (Lindholm and Lundgren, 2009).

Effects Due to Temperature

All of the abovementioned changes in hydrostatic pressure have been assumed to occur in a thermoneutral environment (water of approximately 35°C). However, in most cases of immersion or submersion, this is not a realistic assumption. When immersion or submersion occurs in cold water, stimulation of autonomic nerve fibers will result in peripheral vasoconstriction in order to prevent heat loss. This will – together with the effect of buoyancy as explained above – increase centralization of circulating volume. If, on the other hand, peripheral vasodilation occurs, such as during bathing in hot water, this may counteract the centralization of circulation volume as seen in thermoneutral or cold water.

Additional Factors to Consider

For the sake of completeness, we will briefly mention two circulatory effects that may occur during immersion or submersion, although they are not due to hydrostatic pressure and therefore not the aim of this paper. The first is the mammalian diving reflex, which consists of parasympathetic stimulation leading to bradycardia, apnea, and vasoconstriction upon facial contact with liquid (Bosco et al., 2018). Mean arterial pressure is usually increased due to the vasoconstriction, despite bradycardia. There is an inverse relationship with water temperature: the effect is stronger in cold water. The effects are transient, dissolving after approximately 5–10 min (Lundell et al., 2020).

Secondly, when a tightly fitting suit is worn, the elastic compression may exert external compression on the tissue. In this case, an active compression counteracting the extravasation of fluid is present. The amount of pressure

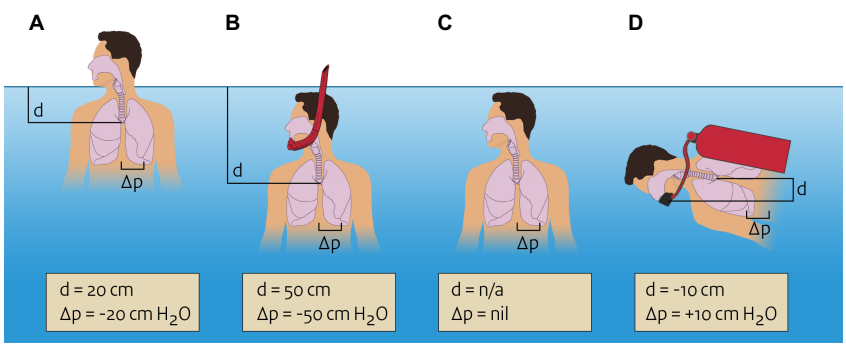

FIGURE 1 | Pressures in and around the lung during various types of immersion or submersion. Negative pressure differential means the pressure in the lung is lower than the pressure in the surrounding tissue. **(A)** Head-out-water-immersion, pressure differential of –20 cm H_2O. **(B)** snorkeling, pressure differential of –50 cm H_2O. **(C)** Swimming under water (breath holding), no pressure differential. **(D)** Diving with mouthpiece 10 cm below the lung, pressure differential of +10 cm H_2O.

caused by swimming or diving suits has, to our knowledge, not been scientifically determined. We estimate this could be compared to the pressure of a mild compression stocking [20–25 cm H_2O (2.0–2.5 kPa)].

DISCUSSION

In summary, a few conclusions can be drawn. Firstly, immersion and submersion affect the circulation. This is caused by buoyancy, which abolishes the effect of gravity and therefore reduces extravasation that normally occurs in dependent parts of the body. This results in increased circulating volume. Peripheral vasoconstriction decreases peripheral perfusion and leads to a more centralized circulation. Additionally, when the pressure in the lungs is lower than the pressure in the surrounding tissues, there is a gradient for extravasation from the lung which may cause pulmonary edema. However, the increased hydrostatic pressure does not act as an external compressing force on immersed body parts. Even when there is a vertical pressure gradient of pressure down the body, these increased intermediary pressures encountered by the blood when flowing from the heart to the dependent parts of the body do not act to reduce blood flow.

As for the phenomenon of rescue collapse, this is not explained by the removal of a squeezing effect of hydrostatic pressure on the body. Instead, it can be explained by the sudden return of the effect of gravity. After prolonged immersion, the subject is cold and vasoplegic. After an initial increase, the circulating volume has been normalized by increased diuresis. It is not hard to imagine the profound effect that sudden reinstitution of the effect of gravity may have on such a person. Additionally, removal of a tightly fitting suit may remove its compressing effect. These effects more than suffice to explain rescue collapse and no supposed removal of hydrostatic squeeze are needed.

DATA AVAILABILITY STATEMENT

The original contributions presented in the study are included in the article/supplementary material, further inquiries can be directed to the corresponding author.

AUTHOR CONTRIBUTIONS

Both authors contributed to the conception of the manuscript as well as writing of the initial and subsequent versions.

REFERENCES

Bierens, J. J. L. M., Lunetta, P., Tipton, M., and Warner, D. S. (2016). Physiology of drowning: A review. *Physiology* 31, 147–166. doi: 10.1152/physiol.00002.2015

Bosco, G., Rizzato, A., Moon, R. E., and Camporesi, E. M. (2018). Environmental physiology and diving medicine. *Front. Psychol.* 9:72. doi: 10.3389/fpsyg.2018.00072

Coulange, M., Rossi, P., Gargne, O., Gole, Y., Bessereau, J., Regnard, J., et al. (2010). Pulmonary oedema in healthy SCUBA divers: new physiopathological pathways. *Clin. Physiol. Funct. Imaging* 30, 181–186. doi: 10.1111/j.1475-097X.2010.00922.x

Koehle, M. S., Lepawsky, M., and McKenzie, D. C. (2005). Pulmonary oedema of immersion. *Sports Med.* 35, 183–190. doi: 10.2165/00007256-200535030-00001

Lindholm, P., and Lundgren, C. E. G. (2009). The physiology and pathophysiology of human breath-hold diving. *J. Appl. Physiol.* 106, 284–292. doi: 10.1152/japplphysiol.90991.2008

Lundell, R. V., Räisänen-Sokolowski, A. K., Wuorimaa, T. K., Ojanen, T., and Parkkola, K. I. (2020). Diving in the Arctic: Cold water immersion's effects on heart rate variability in navy divers. *Front. Physiol.* 10:1600. doi: 10.3389/fphys.2019.01600

Mathieu, D., Favory, R., Collet, F., Linke, J.-C., and Wattel, F. (2006). "Physiologic effects of hyperbaric oxygen on hemodynamics and microcirculation," in *Handbook on Hyperbaric Medicine*. ed. D. Mathieu (Dordrecht, The Netherlands: Springer), 75–101.

Munis, J. R., and Lozada, L. J. (2000). Giraffes, siphons, and starling resistors: Cerebral perfusion pressure revisited. *J. Neurosurg. Anesthesiol.* 12, 290–296. doi: 10.1097/00008506-200007000-00029

Pendergast, D. R., Moon, R. E., Krasney, J. J., Held, H. E., and Zamparo, P. (2015). Human physiology in an aquatic environment. *Compr. Physiol.* 5, 1705–1750. doi: 10.1002/cphy.c140018

Tipton, M. J., Collier, N., Massey, H., Corbett, J., and Harper, M. (2017). Cold water immersion: kill or cure? *Exp. Physiol.* 102, 1335–1355. doi: 10.1113/EP086283

Tipton, M., and Ducharme, M. (2014). "Rescue collapse following cold water immersion," in *Drowning: Prevention, Rescue, Treatment*. ed. J. J. L. M. Bierens (Berlin, Heidelberg: Springer), 855–858.

Welslau, W. (2006). "Physiological effects of increased barometric pressure," in *Handbook on Hyperbaric Medicine*. ed. D. Mathieu (Dordrecht, The Netherlands: Springer), 31–47.

Weston, C. F. M., O'Hare, J. P., Evans, J. M., and Corrall, R. J. M. (1987). Haemodynamic changes in man during immersion in water at different temperatures. *Clin. Sci.* 73, 613–616. doi: 10.1042/cs0730613

Wilmshurst, P. T. (2019). Immersion pulmonary oedema: a cardiological perspective. *Diving Hyperb. Med.* 49, 30–40. doi: 10.28920/dhm49.1.30-40

Conflict of Interest: The authors declare that the research was conducted in the absence of any commercial or financial relationships that could be construed as a potential conflict of interest.

frontiers in Physiology

ORIGINAL RESEARCH
published: 31 January 2020
doi: 10.3389/fphys.2019.01600

Diving in the Arctic: Cold Water Immersion's Effects on Heart Rate Variability in Navy Divers

Richard V. Lundell[1,2], Anne K. Räisänen-Sokolowski[3,4], Tomi K. Wuorimaa[5], Tommi Ojanen[6] and Kai I. Parkkola[7,8]*

[1] Diving Medical Centre, Centre for Military Medicine, The Finnish Defence Forces, Helsinki, Finland, [2] Doctoral Programme in Clinical Research, University of Helsinki, Helsinki, Finland, [3] Department of Pathology, HUSLAB, Helsinki University Hospital, University of Helsinki, Helsinki, Finland, [4] Centre for Military Medicine, The Finnish Defence Forces, Kirkkonummi, Finland, [5] Diving Medical Centre, Centre for Military Medicine, The Finnish Defence Forces, Kirkkonummi, Finland, [6] Human Performance Division, Finnish Defence Research Agency, The Finnish Defence Forces, Tuusula, Finland, [7] Faculty of Medicine and Health Technology, Tampere University, Tampere, Finland, [8] National Defence University, Helsinki, Finland

OPEN ACCESS

Edited by:
François Guerrero, Université de Bretagne Occidentale, France

Reviewed by:
Ki Chon, University of Connecticut, United States
Alain Boussuges, Aix-Marseille Université, France

****Correspondence:***
Richard V. Lundell
richard.lundell@fimnet.fi

Specialty section:
This article was submitted to Environmental, Aviation and Space Physiology, a section of the journal Frontiers in Physiology

Received: *03 November 2019*
Accepted: *20 December 2019*
Published: *31 January 2020*

Citation:
Lundell RV, Räisänen-Sokolowski AK, Wuorimaa TK, Ojanen T and Parkkola KI (2020) Diving in the Arctic: Cold Water Immersion's Effects on Heart Rate Variability in Navy Divers. Front. Physiol. 10:1600. doi: 10.3389/fphys.2019.01600

Introduction: Diving close to the Arctic circle means diving in cold water regardless of the time of year. The human body reacts to cold through autonomous nervous system (ANS)-mediated thermoregulatory mechanisms. Diving also induces ANS responses as a result of the diving reflex.

Materials and Methods: In order to study ANS responses during diving in Arctic water temperatures, we retrospectively analyzed repeated 5-min heart rate variability (HRV) measures and the mean body temperature from dives at regular intervals using naval diving equipment measurement tests in 0°C water. Three divers performed seven dives without physical activity (81–91 min), and two divers performed four dives with physical activity after 10 min of diving (0–10 min HRV recordings were included in the study).

Results: Our study showed a significant increase in parasympathetic activity (PNS) at the beginning of the dives, after which PNS activity decreased significantly (measure 5–10 min). Subsequent measurements (15–20 min and onward) showed a significant increase in PNS activity over time.

Conclusion: Our results suggest that the first PNS responses of the human diving reflex decrease quickly. Adverse effects of PNS activity should be considered on long and cold dives. To avoid concurrent sympathetic (SNS) and PNS activity at the beginning of dives, which in turn may increase the risk of arrhythmia in cold water, we suggest a short adaptation phase before physical activity. Moreover, we suggest it is prudent to give special attention to cardiovascular risk factors during pre-dive examinations for cold water divers.

Keywords: diving reflex, diving response, sympathetic response, parasympathetic response, Arctic diving, cold water immersion

INTRODUCTION

Arctic water conditions induce special risk factors for divers. At a depth of 20 meters or deeper, water temperatures are 4°C throughout the year in Finland. For 4 months per year, the surface of the water is frozen, and, just below the layer of ice, water temperatures vary from −2 to 0°C in saltwater. Heat loss is uncomfortable for the divers, but it also impairs physical and cognitive performance (Davis et al., 1975; Bridgman, 1990), increases the risk of decompression illness (DCI), (Gerth, 2015; Pendergast et al., 2015) and may lead to hypothermia. These factors increase the risk of fatal diving accidents.

Both recreational and occupational divers in Northern Europe dive throughout the year. Even with the best efforts to keep divers warm, heat loss is unavoidable during Arctic diving. The human body reacts to cold through autonomous nervous system (ANS)-mediated thermoregulation mechanisms, (Morrison, 2016) such as vasoconstriction and shivering. The ANS responses to cold are well understood, but, to the best of our knowledge, there is no published data on these responses when measured during diving in Arctic water temperatures.

The aim of this study was to evaluate ANS responses in Finnish Navy divers when diving in 0°C water and with special emphasis on the first responses of the diving reflex. To achieve this, we analyzed short-term recordings (5 min) of heart rate variability (HRV) as values for ANS activity as well as mean body temperature (MBT) as a measure of body thermal balance during diving.

MATERIALS AND METHODS

Subjects

The demographics of the Navy divers are shown in **Table 1** and **Supplementary Table S1**. All divers (n = 4) volunteered for the study and gave their written consent. The data was collected during regular Naval diving equipment development tests and analyzed retrospectively. Approval from the Ethical Committee of Tampere University Hospital was obtained. The study protocol was accepted by The Logistic Department of the Defence Command Finland (2018), and it adhered to the Declaration of Helsinki.

Diving Equipment

The divers used standard military SCUBA diving equipment for Arctic conditions: standard regulator mask, standard dry suit, standard diving hood, standard diving gloves, standard diving underwear, 70% merino wool socks, and elbow and knee warmers. In addition to this, the divers wore Merinot 100% merino wool polo skirts and pants. All divers used air as their breathing gas.

Diving Procedure

The tests were performed over the course of 3 days in January near the Arctic Circle. Four divers performed 11 dives in total during the tests [dives for each diver (D1–D4)]: D1 two dives, D2 three dives, and D3 three dives (of these, one 0–10 min dive was included in study because after this the diver could move freely and physical activity was not controlled), D4 three dives (all three 0–10 min dives were included in study because after this the diver could move freely and physical activity was not controlled). Subjects dived only once a day. During the diving days the divers had their normal 6–8 h a night of sleep, and no exercise was permitted for the 4 h prior to the dives.

During the tests, air temperature varied from −13 to −24°C. Water temperature in the diving depth was 0°C during all dives. Diving equipment and sensors were donned with the assistance of staff members in a consistent room temperature of 18–19°C. After this, the divers walked about 30 meters to the river where an ice hole had been bored and performed their dive without further delay. The participants dived to the bottom of the river to a depth of 6 meters (160 kPa) where they remained still in a horizontal prone position for 80–91 min (n = 7). Other dives (n = 4) had the same protocol at the beginning of the dives (0–10 min). After this, staying still was not required, and the amount of physical activity was therefore not controlled.

Measurements

Divers' fat and muscle mass were measured with the InBody 720 composition analyzer (Biospace Ltd., Seoul, South Korea).

We recorded the heart rate (R to R wave measures at a 1000 Hz sampling frequency) with the HRV Bodyguard device (Firstbeat Technologies Ltd., Jyväskylä, Finland). Using these recordings, the HRV was analyzed with the Kubios HRV Standard program (Ver. 3.1, Kubios Ltd., Kuopio, Finland) from the recordings on diving subjects for the following measurement time intervals (M1–M9 and MR). We used the program's automatic artifact correction to correct corruption in data and the program's time series trend removal tool for each subject before analysis (Lipponen and Tarvainen, 2019). The start of the dive is defined as time point 0 min:

M1 0–5 min (11 dives),
M2 5–10 min (11 dives),
M3 15–20 min (7 dives),
M4 25–30 min (7 dives),
M5 35–40 min (7 dives),
M6 45–50 min (7 dives),

TABLE 1 | Demographics of the four study subjects.

Age in years range and (mean)	Height in meters range and (mean)	Weight in kg range and (mean)	BMI in kg/m^2 range and (mean)	Body Fat Mass in kg range and (mean)	Body Muscle Mass in kg range and (mean)
25 – 43 (39)	1.78 – 1.81 (1.78)	79.2 – 86.8 (83.2)	24.8 – 29.2 (26.4)	4.9 – 14.5 (11.5)	37.2 – 43.3 (41.2)

M7 55–60 min (7 dives),
M8 65–70 min (7 dives),
M9 75–80 min (7 dives).

MR: 5-min recordings for each diving day of HRV in the morning at 0600 and in the evening at 2400 to get a HRV baseline at rest (MR) (2 × 11 measures = 22).

We used three time-domain measures and five frequency-domain measures.

Time-domain measures were recorded: (a) Mean heart rate (HR_{mean}) (bpm), (b) Standard deviation of NN intervals (SDNN) (ms), and (c) Root mean square of successive RR interval differences (RMSSD) (ms).

Frequency-domain measures were recorded: (d) Absolute total power (TP) (ms^2), (e) Absolute power of the very low frequency band (VLF) (ms^2), (f) Absolute power of the low frequency band (LF) (ms^2), (g) Absolute power of the high frequency band (HF) (ms^2), and (h) Ratio of LF to HF power (LF/HF) (%).

For all 81–91 min of diving (n = 7), we also recorded deep body temperature (Trect), measured rectally with the Data Storage Tags (DST) sensor (Star-Oddi Ltd., Gardabaer, Iceland), and skin temperature (T_{skin}), measured with the Smartreader Plus 8-system (ACR Systems Inc., Vancouver, BC, Canada) from eight standardized skin spots (left calf, right anterior thigh, right scapula, left upper chest, forehead, right arm in upper location, left arm in lower location, and left hand) (The International Organization for Standardization, 2004), for the whole duration of the dives.

We used the temperature values at the beginning of the HRV measurements (M1 0 min, M2 5 min, M3 15 min, M4 25 min, M5 35 min, M6 45 min, M7 55 min, M8 65 min, and M9 75 min) and calculated for each time point the MBT with Burtons formula:

$$MBT = \text{Trect} \times 0,65 + \text{Tskin} \times 0,35^{9}$$

where T_{rect} is deep body temperature and T_{skin} is area weighted skin temperature (Burton, 1935).

T_{skin} was calculated with the ISO-standard weighting coefficients [0,2 × left calf, 0,19 × right anterior thigh, 0,175 × (right scapula + left upper chest), 0,07 × (forehead + right arm in upper location + left arm in lower location), 0,05 × left hand] (The International Organization for Standardization, 2004).

Interpretation of used HRV-measures:

(a) Heart rate was regulated by ANS input to the sinoatrial node. Sympathetic activity increased the heart while parasympathetic activity decreased the heart rate (Schmidt-Nielsen, 1997).
(b) Both the sympathetic nervous system and parasympathetic nervous system activity contributes to the SDNN. In short-term recordings, as in this project, the greatest source of the SDNN was the parasympathetically mediated respiratory sinus arrhythmia (Shaffer et al., 2014).
(c) The RMSSD illustrated the variance in the beat-to-beat heart rate and was the golden standard HRV measure for vagally mediated changes (Shaffer et al., 2014).
(d) The total power is the sum of power of ultra-low frequency (ULF), VLF, LF, and HF bands (Shaffer et al., 2014). An increase in T power was linked with parasympathetic activity, whereas a decrease was mostly seen as a result of sympathetic activity.
(e) The VLF band (0.0033–0.04 Hz) was influenced by many factors. The intrinsic nervous system of the heart seemed to contribute to it (Shaffer et al., 2014). Moreover, physical activity, thermoregulatory, renin-angiotensin, and endothelial influences on the heart contributed to it (Akselrod et al., 1981; Claydon and Krassioukov, 2008). PNS activity contributed strongly to VLF power (Taylor et al., 1998).

The LF band (0.04–0.15 Hz) was produced by both the SNS and the PNS (Akselrod et al., 1981; Heart Rate Variability, 1996; Berntson et al., 2007). It also reflected baroreceptor activity in resting individuals (McCraty and Shaffer, 2015), primarily PNS activity via baroreceptors (Reyes del Paso et al., 2013) or baroreflex activity alone (Moak et al., 2007) contributed to LF power. Slow respiration rates, especially when one takes a deep breath or sighs, may have, through vagal activity, contributed to the LF band (Ahmed et al., 1982; Brown et al., 1993; Tiller et al., 1996; Lehrer et al., 2003).
(f) The HF band (0.15–0.40 Hz), also called the respiratory band, reflected parasympathetic activity and corresponded to heart rate variations related to the respiratory sinus arrhythmia (Grossman and Taylor, 2007). Low HF power was correlated with stress, worry, or anxiety.
(g) Under controlled conditions, LF/HF has been used to estimate the relation between the SNS and the PNS activity. In fact, as great portions of the LF band power is caused by the PNS and baroreceptor activity and smaller portions by other factors, the use of this ratio is challenged (Pagani et al., 1984, 1986). Also, SNS contribution to the LF band varies greatly depending on different testing conditions (Eckberg, 1983; Kember et al., 2001; Shaffer et al., 2014).

Statistics

For evaluating changes, a linear mixed-effects model was performed. The analyses were performed with the R program (R Core Team, 2014).

Heart rate variability analyses were performed for all subjects for the beginnings of dives MR–M1 and M1–M2. For the 81–91 min of diving (n = 7), analyses were performed for M2–M9. Temperature analyses (n = 7) were performed for M1–M9, except for T_{rect}, which seemed to show an increase from M1–M3 (M1–M3 and M3–M9 were analyzed separately).

RESULTS

Results for various HRV parameters are shown in **Figures 1A–H**. Temperature measures are shown in **Figures 2A–C**.

HRV measures:

(a) HR_{mean}: From MR–M1, the heart rate increased significantly of 25 bpm (Standard error (SE) = 1.86,

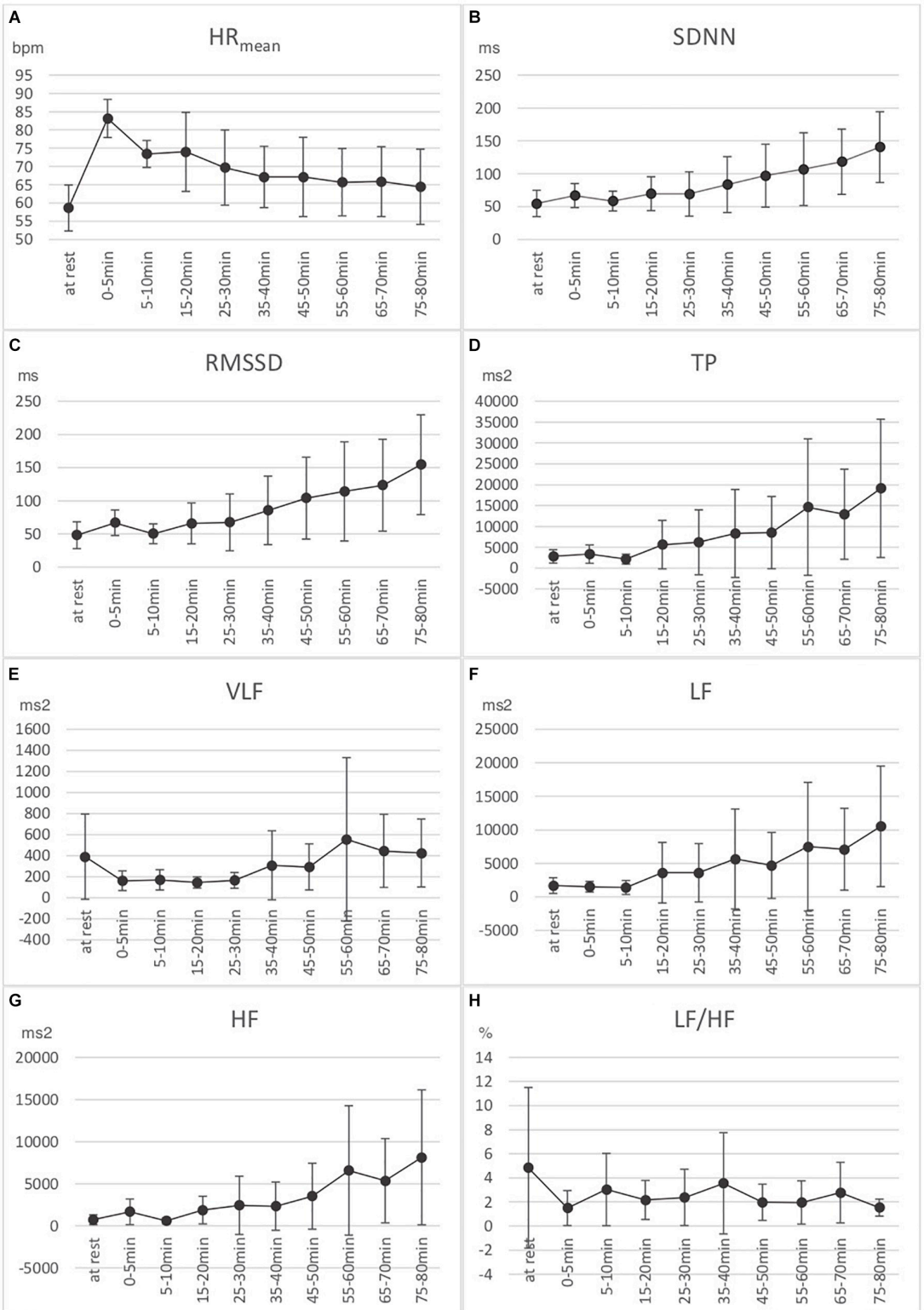

FIGURE 1 | Eight HRV measures: three time-domain measures [**(A)** Mean heart rate (HR_{mean}), **(B)** Standard deviation of NN intervals (SDNN), and **(C)** Root mean square of successive RR interval differences (RMSSD)], and five frequency-domain measures [**(D)** Absolute power of the very low frequency band (VLF power), **(E)** Absolute power of the low frequency band (LF), **(F)** Absolute power of the high frequency band (HF), **(G)** Absolute total power (TP), and **(H)** Ratio of LF to HF power (LF/HF)]. Measures are presented at rest (n = 22), 0–5 min (n = 11), 5–10 min (n = 11), 15–20 min (n = 7), 25–30 min (n = 7), 35–40 min (n = 7), 45–50 min (n = 7), 55–60 min (n = 7), 65–70 min (n = 7), and 75–80 min (n = 7). Means and standard errors shown.

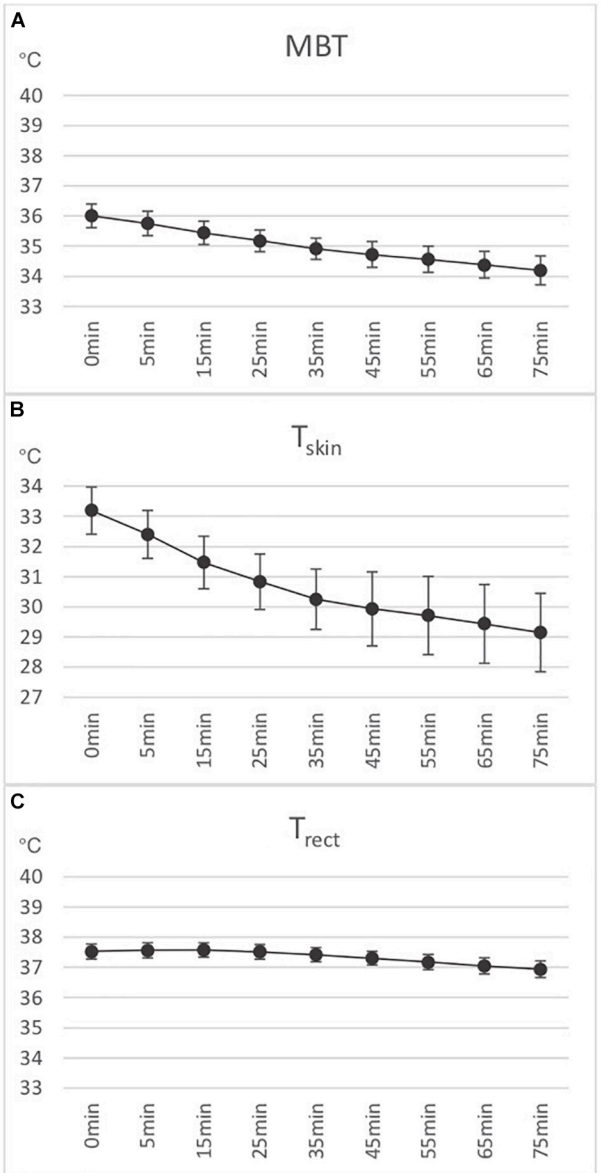

FIGURE 2 | (A) Calculated mean body temperature (MBT) (n = 7). **(B)** Area weighted skin temperature (T_{skin}) (n = 7). **(C)** Rectally measured deep body temperature (T_{rect}) (n = 7). Means and standard errors shown.

$p < 0.001$). From M1–M2, the heart rate decreased significantly of 9.08 bpm (SE = 1.86, $p < 0.001$). From M2–M9 (n = 7), the heart rate decreased significantly of 9.66 bpm (SE = 0.36, $p < 0.001$).

(b) SDNN: From MR–M1, there was a significant increase of 12.22 ms (SE = 5.79, p = 0.04). From M1–M2, there was a non-significant decrease of 6.99 ms (SE = 5.79, p = 0.23). From M2–M9 (n = 7), there was a significant increase of 78.61 ms (SE = 1.87, $p < 0.001$).

(c) RMSSD: From MR–M1, there was a significant increase of 14.67 ms (SE = 6.09, p = 0.02). From M1–M2, there was a significant decrease of 12.92 ms (SE = 6.09, p = 0.04). From M2–M9 (n = 7), there was a significant increase of 97.86 ms (SE = 2.28, $p < 0.001$).

(d) TP: From MR-M1 and M1–M2, there was no significant change. From M2–M9 (n = 7), there was a significant increase of 15044.61 ms^2 (SE = 441.67, $p < 0.001$).

(e) VLF: From MR–M1, there was a significant decrease of 172.90 ms^2 (SE = 60.98, p = 0.008). From M1–M2, there was no significant change (increase 6.27 ms^2, SE = 60.98, p = 0.91). From M2–M9, there was no linear significant change.

(f) LF: From MR-M1 and M1–M2, there was no significant change. From M2–M9 (n = 7), there was a significant increase of 7675.92 ms^2 (SE = 273.75, $p < 0.001$).

(g) HF: From MR–M1, there was a near-significant increase of 678.63 ms^2 (SE = 344.48, p = 0.059). From M1–M2, there was a significant decrease of 835.73 ms^2 (SE = 344.48, p = 0.022). From M2–M9, there was a significant increase of 6983.41 ms^2 (SE = 208.23, $p < 0.001$).

(h) LF/HF: From MR–M1, there was a near-significant decrease of 2.46% (SE = 1.45, p = 0.10). From M1–M2, there was a significant increase of 3.05% (SE = 1.45, p = 0.045). From M2–M9 (n = 7), there was no significant linear change.

Temperatures:

(a) T_{skin}: From M1–M9, there was a significant decrease of 3.92°C (SE = 0.05, $p < 0.001$).

(b) T_{rect}: From M1–M3, there was a non-significant increase of 0.051°C (SE = 0.068, p = 0.46). From M3–M9, there was a significant decrease of 0.66°C (SE = 0.009, $p < 0.001$).

(c) MBT: From M1–M9, there was a significant decrease of 1.84°C (SE = 0.02, $p < 0.001$).

DISCUSSION

The novelty of our study is the observation that in these freezing water conditions, after a quick increase at the beginning of the dives, parasympathetic (PNS) activity actually decreased for HRV measures at 5–0 min. The first PNS response (M1) could be explained with a strong diving reflex at the beginning of the dives (Konishi et al., 2016; Schaller et al., 2017; Vega, 2017; McCulloch et al., 2018; Schlader et al., 2018). The next measure (M2) may suggest that, in humans, the diving reflex-induced PNS response actually decreased after a while. To the best of our knowledge, this finding has not been described in earlier studies. Our hypothesis is that the trigeminocardiac part of the diving reflex was lost quickly while the baroreceptor- and body temperature-induced PNS responses increased more slowly. This, most likely, has not been noticed because of other ANS responses covering the decrease in the trigeminocardiac part of the diving reflex, longer measurement intervals, and the usage of heart rate as the only measure. As we used short heart rate variability measures (5-min HRV) with a close measurement interval, the decrease in parasympathetic activity could be observed. Otherwise, for example, the increase in parasympathetic activity during immersion, correlates well with earlier observations from

HRV studies in diving (Lund et al., 2000; Schipke and Pelzer, 2001; Kurita et al., 2002; Chouchou et al., 2009; Flouris and Scott, 2009; Noh et al., 2018).

After 15 min, PNS activity shown in HRV measures most likely increased because of hemodynamic changes through baroreceptors and a decrease in body temperature. The deep body temperature increased or stayed the same (no significant change) from 0 to 15 min because of a centralization of the blood volume. Both the hyperbaric pressure and the body's thermoregulatory mechanisms contributed to this. MBT is a good measure for the heat loss of the body. It is a combination of both surface and deep body temperature, and it takes into account changes in blood redistribution. Cold is a known promoter of PNS activity (Vesoulis et al., 2017; Hodges et al., 2019). Since MBT decreased during the dives we would assume that temperature is an important factor in inducing the increase in PNS activity over time. Hyperbaric pressure was constant during dives since the divers were at a depth of six meters for the entire duration of the dives. Based on earlier studies, one could speculate that a change in PNS activity would be more dependent on the pressure and not as much on time in hyperbaric conditions (Barbosa et al., 2010). Only limited knowledge on the topic is available. On the other hand, throughout the dives we have seen a strong increase in the power of the LF-band, which would suggest ongoing baroreceptor activity. This would support the hypothesis of pressure-induced PNS activity over time. After the previously described short decrease in PNS activity at the beginning of the dives, PNS activity increased, according to our measurements, up to 80 min of diving (our last measurement). Our study did not determine how long diving in similar conditions induced PNS activity for. In theory, strong PNS activity may have possible adverse effects that could jeopardize diving safety, for example through an atrioventricular block, arrhythmia, syncope, or even sudden death (Aste and Brignole, 2017; Vaseghi et al., 2017; Japundzic-Zigon et al., 2018; Benito-Gomez et al., 2019).

When estimating the SNS activity of the diver from the LF-band and the LF/LH ratio, these did not show a significant increase at the beginning of the dives. This finding is in line with an earlier finding with experienced divers (Schipke and Pelzer, 2001). On the other hand, SNS activity is only one of the factors that contribute to the LF band. The significant increase in mean heart rate at the beginning of the dives suggests that there actually was a strong activation of the SNS. This is in line with most earlier observations of the diving reflex and sensation of cold also causing an SNS activation (Boussuges et al., 2007; Buchholz et al., 2017). After the first SNS response, the mean heart rate and LF/LH ratio suggested that SNS activity actually decreased over time. Our finding indicated that, for our experienced subjects, cold was, after the first responses to diving, neither a physiological nor a psychological stress factor. On the other hand, the dives were not deep nor demanding. Physical stress at the beginning of a cold-water dive, together with the diving reflex and cold stress-induced SNS activation, leads to a quick concurrent increase in both PNS and SNS activity. This, in turn, is a known risk factor for arrhythmia and sudden death (Buchholz et al., 2017; Kane and Davis, 2018). For this reason, at the beginning of a cold-water dive, we recommend an adaptation phase before tasks requiring physical stress. Furthermore, we recommend that special emphasis be placed on evaluating cardiovascular risk factors and incipient signs of heart disease for persons who dive in Arctic conditions. In the fit-to-dive evaluations of Naval divers, we recommend strict cardiovascular criteria.

Our study had some limitations. First, it was a field study, with results gathered during regular diving equipment development tests and not in a more controlled environment, such as in a wet chamber. However, as diving was performed under the ice cover, the weather did not affect diving conditions, which were constant during all dives.

Secondly, the number of divers and dives was limited in our study. However, a small amount of measurements is not unusual in similar experimental field studies made in extreme conditions. Even with this small number of dives, results were statistically significant.

Thirdly, for a better HRV baseline and for evaluating the ANS changes caused by the diving reflex, we recommend measuring 5-min resting values before diving, 5 min-values after immersion, 5-min values directly after submersion, and the next 5-min measure 5–10 min after submersion for future studies. In our study, we have taken the resting HRV baseline from when the divers were in bed in the mornings and in the evenings. These are not necessarily exact HRV resting values because possible sleep may influence HRV (Penzel et al., 2016; Balasubramanian et al., 2017).

Our results received in a limited number of shallow dives in resting individuals cannot automatically be extrapolated to all types of SCUBA diving. During open-sea diving, in addition to water immersion and cold exposure, divers face supplementary stressors such as heart–lung interaction, induced by breathing a hyperbaric mixture through the regulator and hyperoxia. The increase in ambient pressure at depth leads to an increase in both the work of breathing and the oxygen partial pressure. All these stressors have been recognized to influence ANS and HRV.

CONCLUSION

The first PNS response as a result of the human diving reflex decreased quickly. Our interpretation of this finding is that the trigeminocardiac part of the reflex declined quickly.

Both cold and hyperbaric pressure contributing to parasympathetic activity increased up to 80 min when diving in very cold water under constant hyperbaric pressure. Our study did not determine whether the increase in parasympathetic activity will reach a plateau at some point, which is why we feel that possible adverse effects of strong parasympathetic activity should be considered on long and cold dives.

Although our small study involved cold-adapted, experienced divers, we suggest an adaptation phase before physical activity at the beginning of dives in very cold water in order to reduce the risk of arrhythmia. Furthermore, it is prudent for special emphasis on cardiovascular risk factors to be placed on pre-dive evaluation of potential cold-water divers.

DATA AVAILABILITY STATEMENT

The datasets generated for this study are available on request to the corresponding author.

ETHICS STATEMENT

The studies involving human participants were reviewed and approved by Ethical Committee of Tampere University Hospital Nr 2/2018. The patients/participants provided their written informed consent to participate in this study.

AUTHOR CONTRIBUTIONS

RL planned the study, took part in the data analysis, and was the main writer of the manuscript. AR-S planned the study, supervised RL during the data analysis, and was a writer of the manuscript. TW was present at the data-gathering phase, planned the study, and was a writer of the manuscript. TO planned the study, helped and worked with the HRV method, and was a writer of the manuscript. KP planned the study, supervised RL during the data analysis, and was a writer of the manuscript.

FUNDING

The study was funded by The Finnish Defence Forces Joint Healthcare. We have cooperated with the company Ursuk Ltd., during equipment development tests by receiving the equipment for testing. However, there was no direct, financial funding.

ACKNOWLEDGMENTS

We thank Mr. Harri Mäkitalo and Mr. Petri Pekkala for their great work in planning and performing the equipment development tests. The guidance of Dr. Janne Tikkinen has been greatly valued. We also thank Prof. Hannu Rintamäki and Dr. Sirkka Rissanen for all the advice on the methodology of cold research. Statistical analysis by Ville Korhonen, M.Sc., is also greatly appreciated.

SUPPLEMENTARY MATERIAL

The Supplementary Material for this article can be found online at: https://www.frontiersin.org/articles/10.3389/fphys.2019.01600/full#supplementary-material

REFERENCES

Ahmed, A. K., Harness, J. B., and Mearns, A. J. (1982). Respiratory control of heart rate. *Eur. J. Appl. Physiol. Occup. Physiol.* 50, 95–104.

Akselrod, S., Gordon, D., Ubel, F. A., Shannon, D. C., Berger, A. C., and Cohen, R. J. (1981). Power spectrum analysis of heart rate fluctuation: a quantitative probe of beat-to-beat cardiovascular control. *Science* 213, 220–222. doi: 10.1126/science.6166045

Aste, M., and Brignole, M. (2017). Syncope and paroxysmal atrioventricular block. *J. Arrhythm.* 33, 562–567. doi: 10.1016/j.joa.2017.03.008

Balasubramanian, K., Harikumar, K., Nagaraj, N., and Pati, S. (2017). Vagus nerve stimulation modulates complexity of heart rate variability differently during sleep and wakefulness. *Ann. Ind. Acad. Neurol.* 20, 403–407. doi: 10.4103/aian.AIAN_148_17

Barbosa, E., Garcia-Manso, J. M., Martin-Gonzalez, J. M., Sarmiento, S., Calderon, F. J., and Da Silva-Grigoletto, M. E. (2010). Effect of hyperbaric pressure during scuba diving on autonomic modulation of the cardiac response: application of the continuous wavelet transform to the analysis of heart rate variability. *Mil. Med.* 175, 61–64. doi: 10.7205/milmed-d-02-00808

Benito-Gomez, M., Fletcher, A. C., and Buehler, C. (2019). Sympathetic and parasympathetic nervous system functioning and experiences of peer exclusion: links to internalizing problems in early adolescence. *J. Abnorm. Child Psychol.* 47, 633–644. doi: 10.1007/s10802-018-0472-0

Berntson, G. G., Cacioppo, J. T., and Grossman, P. (2007). Whither vagal tone. *Biol. Psychol.* 74, 295–300. doi: 10.1016/j.biopsycho.2006.08.006

Boussuges, A., Molenat, F., Grandfond, A., Regnard, J., Wolf, J. P., Galland, F., et al. (2007). Cardiovascular changes induced by cold water immersion during hyperbaric hyperoxic exposure. *Clin. Physiol. Funct. Imag.* 27, 268–274. doi: 10.1111/j.1475-097x.2007.00747.x

Bridgman, S. A. (1990). Thermal status of antarctic divers. *Aviat. Space Environ. Med.* 61, 795–801.

Brown, T. E., Beightol, L. A., Koh, J., and Eckberg, D. L. (1993). Important influence of respiration on human R-R interval power spectra is largely ignored. *J. Appl. Physiol.* 75, 2310–2317. doi: 10.1152/jappl.1993.75.5.2310

Buchholz, B., Kelly, J., Bernatene, E. A., Mendez Diodati, N., and Gelpi, R. J. (2017). Antagonistic and synergistic activation of cardiovascular vagal and sympathetic motor outflows in trigeminal reflexes. *Front. Neurol.* 8:52. doi: 10.3389/fneur.2017.00052

Burton, A. C. (1935). Human calorimetry 2. The average temperature of the tissues of the body. *J. Nutr.* 9, 261–280.

Chouchou, F., Pichot, V., Garet, M., Barthélémy, J. C., and Roche, F. (2009). Dominance in cardiac parasympathetic activity during real recreational SCUBA diving. *Eur. J. Appl. Physiol.* 106, 345–352. doi: 10.1007/s00421-009-1010-0

Claydon, V. E., and Krassioukov, A. V. (2008). Clinical correlates of frequency analyses of cardiovascular control after spinal cord injury. *Am. J. Physiol. Heart Circ. Physiol.* 294:668.

Davis, F. M., Baddeley, A. D., and Hancock, T. R. (1975). Diver performance: the effect of cold. *Undersea Biomed. Res.* 2, 195–213.

Eckberg, D. L. (1983). Human sinus arrhythmia as an index of vagal cardiac outflow. *J. Appl. Physiol. Respir. Environ. Exerc. Physiol.* 54, 961–966. doi: 10.1152/jappl.1983.54.4.961

Flouris, A. D., and Scott, J. M. (2009). Heart rate variability responses to a psychologically challenging scuba dive. *J. Sports Med. Phys. Fitness* 49, 382–386.

Gerth, W. A. (2015). On diver thermal status and susceptibility to decompression sickness. *Diving Hyperb. Med.* 45:208.

Grossman, P., and Taylor, E. W. (2007). Toward understanding respiratory sinus arrhythmia: relations to cardiac vagal tone, evolution and biobehavioral functions. *Biol. Psychol.* 74, 263–285. doi: 10.1016/j.biopsycho.2005.11.014

Heart Rate Variability (1996). Standards of measurement, physiological interpretation, and clinical use. Task force of the european society of cardiology and the north american society of pacing and electrophysiology. *Eur. Heart J.* 17, 354–381.

Hodges, G. J., Ferguson, S. A., and Cheung, S. S. V. (2019). Cardiac autonomic function during hypothermia and its measurement repeatability. *Appl. Physiol. Nutr. Metab.* 44, 31–36. doi: 10.1139/apnm-2018-0248

Japundzic-Zigon, N., Sarenac, O., Lozic, M., Vasič, M., Tasič, T., Bajič, D., et al. (2018). Sudden death: neurogenic causes, prediction and prevention. *Eur. J. Prev. Cardiol.* 25, 29–39. doi: 10.1177/2047487317736827

Kane, S. M., and Davis, J. (2018). Cardiac arrest and death attributable to the diving respons triggered during incision and debridement of an abscess of the forehead. *J. Craniofac. Surg.* 29:e509. doi: 10.1097/SCS.0000000000004555

Kember, G. C., Fenton, G. A., Armour, J. A., and Kalyaniwalla, N. (2001). Competition model for aperiodic stochastic resonance in a fitzhugh-nagumo

model of cardiac sensory neurons. *Phys. Rev. E Stat. Nonlin. Soft. Matter. Phys.* 63(4 Pt 1):041911.

Konishi, M., Kawano, H., Xiang, M., Kim, H. K., Ando, K., Tabata, H., et al. (2016). Diurnal variation in the diving bradycardia response in young men. *Clin. Auton. Res.* 26, 135–140. doi: 10.1007/s10286-016-0342-1

Kurita, A., Nagayoshi, H., Okamoto, Y., Takase, B., Ishizuka, T., and Oiwa, H. (2002). Effects of severe hyperbaric pressure on autonomic nerve functions. *Mil. Med.* 167, 934–938. doi: 10.1093/milmed/167.11.934

Lehrer, P. M., Vaschillo, E., Vaschillo, B., Lu, S. E., Eckberg, D. L., Edelberg, R., et al. (2003). Heart rate variability biofeedback increases baroreflex gain and peak expiratory flow. *Psychosom. Med.* 65, 796–805. doi: 10.1097/01.psy.0000089200.81962.19

Lipponen, J. A., and Tarvainen, M. P. (2019). A robust algorithm for heart rate variability time series artefact correction using novel beat classification. *J. Med. Eng. Technol.* 43, 173–181. doi: 10.1080/03091902.2019.1640306

Lund, V., Kentala, E., Scheinin, H., Klossner, J., Sariola-Heinonen, K., and Jalonen, J. (2000). Hyperbaric oxygen increases parasympathetic activity in professional divers. *Acta Physiol. Scand.* 170, 39–44. doi: 10.1046/j.1365-201x.2000.00761.x

McCraty, R., and Shaffer, F. (2015). Heart rate variability: new perspectives on physiological mechanisms, assessment of self-regulatory capacity, and health risk. *Glob. Adv. Health Med.* 4, 46–61. doi: 10.7453/gahmj.2014.073

McCulloch, P. F., Lahrman, K. A., DelPrete, B., and DiNovo, K. M. (2018). Innervation of the nose and nasal region of the rat: implications for initiating the mammalian diving response. *Front. Neuroanat.* 12:85. doi: 10.3389/fnana.2018.00085

Moak, J. P., Goldstein, D. S., and Eldadah, B. A. (2007). Supine low-frequency power of heart rate variability reflects baroreflex function, not cardiac sympathetic innervation. *Heart Rhythm.* 4, 1523–1529. doi: 10.1016/j.hrthm.2007.07.019

Morrison, S. F. (2016). Central control of body temperature. *F1000Research* 5:F1000FacultyRev–880.

Noh, Y., Posada-Quintero, H. F., Bai, Y., White, J., Florian, J. P., Brink, P. R., et al. (2018). Effect of shallow and deep SCUBA dives on heart rate variability. *Front. Physiol.* 9:110. doi: 10.3389/fphys.2018.00110

Pagani, M., Lombardi, F., Guzzetti, S., Rimoldi, O., Furlan, R., Pizzinelli, P., et al. (1986). Power spectral analysis of heart rate and arterial pressure variabilities as a marker of sympatho-vagal interaction in man and conscious dog. *Circ. Res.* 59, 178–193. doi: 10.1161/01.res.59.2.178

Pagani, M., Lombardi, F., Guzzetti, S., Sandrone, G., Rimoldi, O., Malfatto, G., et al. (1984). Power spectral density of heart rate variability as an index of sympatho-vagal interaction in normal and hypertensive subjects. *J. Hypertens. Suppl.* 2:383.

Pendergast, D. R., Senf, C. J., Fletcher, M. C., and Lundgren, C. E. (2015). Effects of ambient temperature on nitrogen uptake and elimination in humans. *Undersea Hyperb. Med.* 42, 85–94.

Penzel, T., Kantelhardt, J. W., Bartsch, R. P., Riedl, M., Kraemer, J. F., Wessel, N., et al. (2016). Modulations of heart rate, ECG, and cardio-respiratory coupling observed in polysomnography. *Front. Physiol.* 7:460.

R Core Team, (2014). *R: A Language and Environment for Statistical Computing*. Vienna: R Foundation for Statistical Computing.

Reyes del Paso, G. A., Langewitz, W., Mulder, L. J., van Roon, A., and Duschek, S. (2013). The utility of low frequency heart rate variability as an index of sympathetic cardiac tone: a review with emphasis on a reanalysis of previous studies. *Psychophysiology* 50, 477–487. doi: 10.1111/psyp.12027

Schaller, B., Chowdhury, T., and Rosemann, T. (2017). Editorial: the trigeminocardiac reflex: beyond the diving reflex. *Front. Neurosci.* 11:673.

Schipke, J. D., and Pelzer, M. (2001). Effect of immersion, submersion, and scuba diving on heart rate variability. *Br. J. Sports Med.* 35, 174–180. doi: 10.1136/bjsm.35.3.174

Schlader, Z. J., O'Leary, M. C., Sackett, J. R., and Johnson, B. D. (2018). Face cooling reveals a relative inability to increase cardiac parasympathetic activation during passive heat stress. *Exp. Physiol.* 103, 701–713. doi: 10.1113/EP086865

Schmidt-Nielsen, K. (1997). *Animal Physiology: Adaptation and Environment*, 5th Edn, Cambridge: Cambridge University Press.

Shaffer, F., McCraty, R., and Zerr, C. L. (2014). A healthy heart is not a metronome: an integrative review of the heart's anatomy and heart rate variability. *Front. Psychol.* 5:1040. doi: 10.3389/fpsyg.2014.01040

Taylor, J. A., Carr, D. L., Myers, C. W., and Eckberg, D. L. (1998). Mechanisms underlying very-low-frequency RR-interval oscillations in humans. *Circulation* 98, 547–555. doi: 10.1161/01.cir.98.6.547

The International Organization for Standardization, (2004). *Ergonomics – Evaluation of Thermal Strain by Physiological Measurements, B.2 Measurement of Skin Temperature, Table B.1 – Measuring Sites and Weighing Coefficients*. Geneva: The International Organization for Standardization.

The Logistic Department of the Defence Command Finland (2018). Permission AO3867,28.2.2018, 1650/12.04.01/2018.

Tiller, W. A., McCraty, R., and Atkinson, M. (1996). Cardiac coherence: a new, noninvasive measure of autonomic nervous system order. *Altern. Ther. Health Med.* 2, 52–65.

Vaseghi, M., Salavatian, S., Rajendran, P. S., Yagishita, D., Woodward, W. R., Hamon, D., et al. (2017). Parasympathetic dysfunction and antiarrhythmic effect of vagal nerve stimulation following myocardial infarction. *JCI Insight* 2:16.

Vega, J. L. (2017). Edmund goodwyn and the first description of diving bradycardia. *J. Appl. Physiol.* 123, 275–277. doi: 10.1152/japplphysiol.00221.2017

Vesoulis, Z. A., Rao, R., Trivedi, S. B., and Mathur, A. M. (2017). The effect of therapeutic hypothermia on heart rate variability. *J. Perinatol.* 37, 679–683. doi: 10.1038/jp.2017.42

Conflict of Interest: The authors declare that the research was conducted in the absence of any commercial or financial relationships that could be construed as a potential conflict of interest.

frontiers in Physiology

ORIGINAL RESEARCH
published: 20 June 2019
doi: 10.3389/fphys.2019.00749

High Bubble Grade After Diving: The Role of the Blood Pressure Regimen

Alain Boussuges[1,2], Guillaume Chaumet[3], Nicolas Vallée[1], Jean Jacques Risso[1] and Jean Michel Pontier[4]*

[1]ERRSO, Institut de Recherche Biomédicale des Armées (IRBA), Toulon, France, [2]Center for Cardiovascular and Nutrition Research (C2VN), INSERM, INRA, Aix Marseille Université, Marseille, France, [3]Altra Bio SA, Lyon, France, [4]Cephismer, Centre d'expertise plongée pour la Marine Nationale, Toulon, France

Introduction: Previous studies have suggested that the circulatory system was involved in the production of circulatory bubbles after diving. This study was designed to research the cardio-vascular function characteristics related to the production of high bubble grades after diving.

Methods: Thirty trained divers were investigated both at baseline and after a 30-msw SCUBA dive. At baseline, the investigations included blood pressure measurement, echocardiography, and assessment of aerobic fitness using VO_2 peak measurement. Blood samples were taken at rest, to measure the plasma concentration of NOx and endothelin-1. After diving, circulating bubbles were detected in the pulmonary artery by pulsed Doppler at 20-min intervals during the 90 min after surfacing. The global bubble quantity production was estimated by the KISS index.

Results: Divers with a high bubble grade (KISS > 7.5) had systolic blood pressure, pulse pressure, weight, and height significantly higher than divers with a low bubble grade. By contrast, total arterial compliance, plasma NOx level, and percentage of predicted value of peak oxygen uptake were significantly lower in divers with a high bubble grade. Cardiac dimensions, left ventricular function, and plasma endothelin-1 concentration were not significantly different between groups. The multivariate analysis identified blood pressure as the main contributor of the quantity of bubble production. The model including pulse pressure, plasma NOx level, and percentage of predicted value of peak oxygen uptake has an explanatory power of 49.22%.

Conclusion: The viscoelastic properties of the arterial tree appeared to be an important contributor to the circulating bubble production after a dive.

Keywords: circulatory system, decompression, endothelial function, SCUBA diving, venous gas emboli

OPEN ACCESS

Edited by:
François Guerrero, Université de Bretagne Occidentale, France

Reviewed by:
Costantino Balestra, Haute École Bruxelles-Brabant (HE2B), Belgium
Weigang Xu, The Second Military Medical University, China

****Correspondence:***
Alain Boussuges
alain.boussuges@univ-amu.fr;
alain.boussuges@gmail.com

Specialty section:
This article was submitted to Vascular Physiology, a section of the journal Frontiers in Physiology

Received: *08 April 2019*
Accepted: *31 May 2019*
Published: *20 June 2019*

Citation:
Boussuges A, Chaumet G, Vallée N, Risso JJ and Pontier JM (2019) High Bubble Grade After Diving: The Role of the Blood Pressure Regimen. Front. Physiol. 10:749. doi: 10.3389/fphys.2019.00749

During the decompression stage after a dive, circulating bubbles are commonly observed in the venous system. Since the 1970s, venous gas emboli (VGE) can be screened by ultrasonography and Doppler. To quantify the number of bubbles, it is usual to rate the number and frequency of bubbles compared with the heartbeat. Using this method, bubble grades have been proposed (Spencer, 1976; Kisman et al., 1978; Boussuges et al., 1998). Previous studies have researched the correlation between the venous bubble quantity and the probability of decompression sickness

(Nashimoto and Gotoh, 1978; Nishi et al., 1981; Eatock, 1984; Bayne et al., 1985). The correlation is debatable, but all authors have observed that, when the quantity of circulating bubbles is low, the risk is also low. Consequently, bubble screening has been used as a safety indicator for diving profiles (Eatock and Nishi, 1987). A decompression profile producing a small quantity of circulating bubbles in a large population of divers is recognized as a low risk dive. A conservative decompression profile is particularly important in divers with patent foramen ovale (Boussuges et al., 2014; Honek et al., 2014). Furthermore, a wide inter-individual susceptibility to bubble formation has been reported (Papadopoulou et al., 2018). Indeed, for the same given dive profile, no circulating bubbles were detected in some divers whereas other individuals presented a large quantity of circulating bubbles. The mechanism explaining this variability remains largely unknown. VGE are made up from pre-existing gas nuclei and enriched by the neutral gas in the breathing mixture, which is in a supersaturated state in blood and tissues, when the ambient pressure drops. The sites and mechanisms for the formation of gas nuclei remain uncertain (Blatteau et al., 2006). Some authors have suggested that gas nuclei might be trapped in hydrophobic crevices. These hydrophobic sites might be present on the surface of the endothelium in the form of caveolae (Brubakk, 2004). The impact of vasomotor tone and endothelial function on bubble formation has also been supported by previous studies (Dujic et al., 2006). An increase in nitric oxide (NO)-dependent relaxation leads to a decrease in bubble grade (Wisløff et al., 2004). In contrast to this finding, in animals subjected to a hyperbaric exposure, an inhibition of NO induced both an increase in bubble grade and mortality (Wisløff et al., 2003). Lastly, in volunteers, Cialoni et al. reported an increase in nitric oxide levels during a SCUBA dive (Cialoni et al., 2019), suggesting an endothelial stimulation at the bottom.

According to the previous studies, we hypothesized that the viscoelastic properties of the circulatory system of healthy volunteers studied at baseline before a dive, differed between bubble-prone divers and bubble-resistant divers.

MATERIALS AND METHODS

All the procedures were conducted in accordance with the Declaration of Helsinki and were approved by the local Ethics Committee (CCPPRB 1 Aix Marseille No. 20062103). Each method and the potential risks were explained to the participants in detail, and they gave written informed consent before the experiment.

Subjects

Thirty trained male divers, aged 37 ± 7 years, weight 77 ± 8 kg, height 175 ± 8 cm, BMI 25 ± 2 kg m^{-2}, and body surface area 1.93 ± 0.14 m^2, volunteered to participate in this experiment. All of them were regular recreational or professional SCUBA divers with 100–4,000 dives and without a past history of diving injury. Each participant underwent a physical examination and a full medical history. The subjects were non-smokers and were included if they had no hypertension, cardiovascular or kidney disease, and no medication during the study.

Baseline Investigations

During the inclusion visit, it was verified that volunteers had a similar arterial pressure on both upper limbs.

Assessment of Aerobic Fitness

To assess individual aerobic fitness, each volunteer performed an incremental fatigue treadmill test. Ventilatory and gas-exchange parameters were measured using a breath-by-breath system (Cosmed Quark PFT ergo, Rome, Italy) which was calibrated before each test. The subjects spent 3 min at rest to reach a steady-state gas exchange condition. Thereafter, all participants carried out a 4-min warm-up running session at 8 km h^{-1} with an elevation of 2%, after which the treadmill speed was increased by 1 km h^{-1} every 1 min until volitional fatigue was reached. The data were averaged for 20 s and the VO_2 peak was defined as the highest value of oxygen uptake despite increased workload. The criteria indicating maximal exercise were as follows: plateauing of oxygen consumption, respiratory gas exchange ratio ≥1.1, and heart rate (HR) ≥95% age-predicted maximal HR. The results were reported in VO_2 peak (ml kg^{-1} min^{-1}) and in percent-predicted peak VO_2 calculated according to the equation [weight (kg) × 56.36 − (0.413 × age)] proposed by Wasserman et al. (1987). No diver was considered to be overweight, according to the formula: weight (kg) > 0.79 × height (cm) − 60.7.

Echocardiographic Study

Divers underwent the echocardiographic examinations in basal conditions 1 h before the dives. The subjects were placed in left lateral decubitus. HR was recorded by echocardiogram and the rate was averaged over 60 s. The cardiac ultrasound examinations were carried out by an experienced investigator (AB) using a commercially available echocardiograph (Mylab 25, Genoa, Italy) connected to a transducer array of 2.5–3.5 MHz. At this time, any cardiac abnormalities resulted in the exclusion of the subject from the study. Doppler recordings were performed at the end of a normal expiration in order to eliminate the effects of respiration on the parameters studied. Measurements were averaged from at least three different beats.

Left Heart Study

Left atrial (LA) diameter, left ventricle (LV) end systolic and end diastolic diameters (ESD, EDD), left ventricle end systolic and end diastolic interventricular septal thickness, and left ventricle end systolic and end diastolic posterior wall thickness were measured by M-mode echocardiography from the left short and long axis views. Left ventricular mass (LVM) was assessed by M mode echocardiography and the application of Devereux's formula (Devereux and Reichek, 1977). The standard index of global LV systolic performance was LV percent fractional shortening (%FS) as the ratio (LV EDD − LV ESD)/LV EDD.

Left ventricular filling was studied using transmitral blood flow velocities recorded by pulsed Doppler. Transmitral blood flow velocities were obtained from the apical four-chamber view, positioning the sample volume at the mitral valve leaflet tips.

Doppler velocity curves were recorded at 100 mm s^{-1}. Peak velocity and velocity-time integral (VTI) of the initial flow (E wave), representing the early filling phase, and of the late flow (A wave), representing the atrial contraction, were measured. The peak velocities ratio (*E*/*A*) and the ratio of the A wave VTI to the total VTI (relative contribution of atrial contraction to the total LV filling) were calculated. The interval from the aortic valve closure signal to the mitral valve opening signal (IVRT) was also measured.

Tissue Doppler imaging (TDI) of the mitral annulus during diastole was recorded. The ratio of transmitral early diastolic velocity (*E*) to TDI early diastolic velocity of the mitral annulus (*E*′) was calculated as an index of LV filling pressures (Nagueh et al., 1997).

Right Heart Study

Right ventricle end-diastolic diameter (RVEDD) was measured by M-mode echocardiography from the left parasternal long axis views. The measurement of the peak of the tricuspid regurgitation velocity (TRV) was performed using continuous wave Doppler.

The RV outflow tract time-velocity integral (TVI_{RVOT}) was recorded from the parasternal short axis view. Pulmonary vascular resistance (PVR) was estimated by the formula [(TRV/TVI_{RVOT} × 10) + 0.16] in Wood units (WU) according to the method proposed by Abbas et al. (2003). Furthermore, the acceleration time/RV ejection time ratio of the pulmonary artery blood flow (AcT/RVET) was calculated to assess the pulmonary artery pressure (PAP) regimen owing to the negative correlation between the AcT/RVET and the mean PAP (Kitabatake et al., 1983). The inferior vena cava diameter was measured at the end of the expiration from a subcostal view.

Hemodynamic Data

Cardiac output (CO) was derived from the aortic blood flow. The aortic cross-sectional diameter was measured by 2D echocardiography from the left parasternal short axis view at the level of the aortic root. Aortic cross-sectional area (ACSA) was calculated as: ACSA = 3.14 × d^2/4.

The aortic systolic flow velocity -time integral (VTI Ao) was measured using the pulsed wave Doppler profile of aortic blood flow from the apical four chamber view making it possible to calculate LV stroke volume (LV SV = VTI Ao × ACSA) and cardiac output (LV CO = LV SV × HR).

Systemic vascular resistance and total arterial compliance were calculated as mean arterial pressure/CO and LV SV/pulse pressure (PP), respectively (Chemla et al., 1998).

Blood Pressure Measurement

Sphygmomanometric blood pressure measurements on the right arm were obtained using an automatic device (Omron HEM-705CP, Bannockburn, IL, USA) at the end of each echocardiographic examination. This automated device was validated by the British Hypertension Society and the Association for the Advancement of Medical Instrumentation (Asmar and Zanchetti, 2000).

Biological Study

Blood samples were taken before the dives. The tubes were immediately placed in iced water and centrifuged for 15 min at 4,000 $rmin^{-1}$ at 4°C. Plasma was then stored at −70°C until analysis. Nitric oxide (NO) is rapidly converted in plasma; consequently to estimate NO bioavailability, the sum of stable metabolites of NO, i.e., nitrate and nitrite (NOx) was used. Plasma NOx was determined using a spectrophotometric kit (Cayman Chemical, Ann Arbor, MI, USA). Plasma concentration of endothelin-1 was measured using a commercially available ELISA kit (R&D Systems, Minneapolis, MN, USA).

Dives

The day before the dives it was recommended that no intense physical activity was performed and a low-nitrate diet was followed. All the dives were performed 3–4 h after a light meal between 10 and 11 a.m. The volunteers were weighed both before and after the dives. The divers breathed air during the dives. They were equipped with neoprene diving wet suits, the thickness of which was in accordance with the temperature of the sea (from 15 to 20°C at the surface). The dive profile was the same for all divers. They performed the SCUBA dives in open seawater at 30 m of seawater (msw) on a regular flat bottom. The bottom time including the descent time (velocity of the descent time from 10 to 15 msw min^{-1}) was 30 min. At the bottom, the divers performed a regular finning action for a distance to 400 m. After 30 min, the ascent rate up to the decompression stop was 9–10 msw min^{-1}. Decompression stop (9 min at 3 msw) was in accordance with the French Navy procedure (Marine Nationale 90). After the dives, they were instructed to reduce activity as much as possible.

Examinations After the Dives

The duration of the transfer to the laboratory was around 25 min (the return of the boat to port and the route from the port to the laboratory); consequently, the investigations began 30 min after the end of the dive. Examiners were blinded to the results of the other investigations (previous examinations or investigations performed by the other examiners). Investigations were undertaken in a quiet room with a controlled environmental temperature (28°C).

Circulating Bubble Detection

Circulating vascular bubble detections were performed by an experienced investigator (JMP) using a pulsed Doppler equipped with a 2-MHz probe (Pioneer-Siemens, Malvern, USA). The screening tests were performed in the laboratory at 20-min intervals during the 90 min after surfacing (30, 50, 70, and 90 min). The subjects were in the left lateral position and rested for 1 min before the test. The Doppler probe was placed along the left edge of the sternum to record the pulmonary artery blood flow. VGE were monitored in the pericardial area with the divers at rest, during muscle contraction of the quadriceps (the patients were told to contract the quadriceps

to pull the patella superiorly tightly during 10 s) and during flexion of the lower limb (hip and knee flexion to 90°). Each maneuver was repeated twice. The Spencer scale was used to quantify the bubble amount (Spencer, 1976). The quality of the screening was assessed for each recording and rated as satisfactory, average, or poor. The screening sessions were recorded and then analyzed by two independent investigators. If any discrepancy in the interpretation of the signals occurred, the recording was studied again in order to reach a consensus. When a consensus was lacking the diver was excluded from the study.

Furthermore, after diving, an echocardiographic examination has been repeated 1 h after emersion. During this examination, it was performed both the study of the cardiac function (results not reported in the present work) and the assessment of the circulating bubbles quantity.

The Kisman-Masurel integrated severity score (KISS) was calculated from bubble detections performed at rest, to estimate the magnitude of the evolved gas phase induced by the decompression stress (Nishi et al., 1981).

Thereafter, the population was divided in two groups according to their bubble production:

- Divers with a low bubble grade (LBG) producing few bubbles, i.e., with a maximal bubble grade ≤2 and a KISS index <7.5.
- Divers with a high bubble grade (HBG) producing an important circulating bubble quantity, i.e., with a maximal bubble grade >2 and a KISS index >7.5.

Statistical Analysis

Data are expressed as mean ± standard deviation. All the statistical analyses were performed with R statistical software (Lagani et al., 2016). The distribution of the variables was studied by a Kolmogorov-Smirnov test. To compare the characteristics of the cardio-vascular function in divers with HBG and LBG, a t-test was used. When the variables were not normally distributed a Mann-Whitney test was performed. Significance was $p < 0.05$.

We then searched for the factors associated with the bubble production assessed by the KISS index. First, the relationship between the KISS index and variables was described by using Spearman's correlation. Second, we selected the set of variables that could explain the high bubble grade, using a logistic regression model. Because we suspected multicollinearity between our explanatory variables, we excluded variables with the highest variance inflation factor (VIF) *via* a stepwise method: the algorithm calculates the VIF score for all explanatory variables and removes the variable with the highest value, then recalculates the VIF scores on the remaining values, until there are no variables with a VIF greater than the threshold (10 here) (Naimi et al., 2014). On these selected variables, we then used the variable selection method. Among the various methods of variable selection, we chose the adaptation for logistic regression (Lozano et al., 2011) of the generalized orthogonal matching pursuit algorithm (Pati et al., 1993). This algorithm was implemented in R (Lagani et al., 2016).

RESULTS

Baseline Investigations

All divers had a normal left ventricular systolic and diastolic function. Left ventricular mass was measured as a mean of 198 ± 52 g (104 ± 27 g m^{-2}). The quality of the echocardiographic examinations was considered to be poor in two divers. These volunteers were excluded from the subsequent analysis. VO_2 peak was measured as a mean of 49 ± 6 ml kg^{-1} min^{-1} (120 ± 14% of the predicted value).

Plasma NOx level was 30 ± 8 μmol L^{-1}. Plasma endothelin-1 concentration was 1.4 ± 0.7 pg ml^{-1}.

Examinations After the Dives

None of the divers presented any disorders suggesting a decompression accident.

Study of the Whole Population

Significant weight loss was found after the dives (as a mean 590 ± 390 g – 0.8% of body mass).

One hour after the dive, the quantity of circulating bubbles assessed by pulsed Doppler and echocardiography were closely related.

A significant inter-individual variability in the production of VGE was observed in the population. In some divers ($n = 3$), no bubbles were detected whereas in other individuals Grade 3 (**Figure 1**) was recorded over the whole detection period. Mean KISS index was calculated as 17.4 ± 16 (ranging from 0 to 42). The muscle contractions of the lower limbs led to an increase in circulating bubbles (**Figure 2**).

According to the criteria previously mentioned in section "Methods," the population was divided into divers with a high bubble grade (13 divers) and divers with a low bubble grade (15 divers).

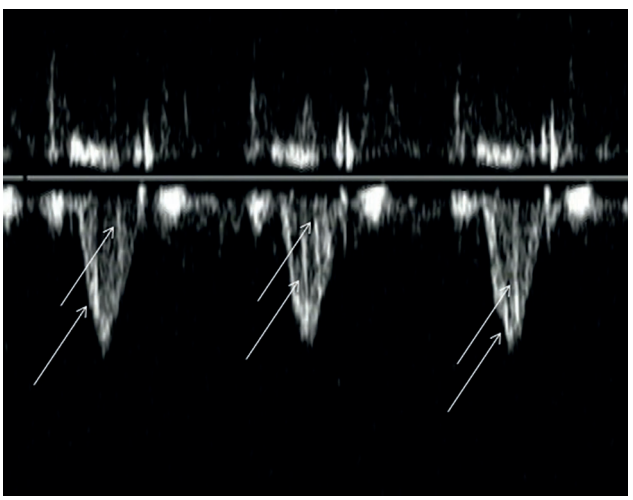

FIGURE 1 | Circulating bubbles detected in the pulmonary artery blood flow: the arrows indicate bubble signals in each cycle (Grade 3: the majority of the cardiac periods contain bubble signals singularly or in group).

FIGURE 2 | Time course of the bubble grade recorded after the dive, at rest and during muscle contraction of the lower limbs (data are expressed as median).

Comparison Between Divers With an HBG and Divers With an LBG

The mean age of the two groups of divers with an LBG and an HBG was not significantly different (38 ± 6 vs. 36 ± 7 years, respectively).

Divers with an HBG had a weight (80 ± 7 vs. 73 ± 9 kg – $p < 0.05$) and a height (179 ± 6 vs. 172 ± 7 cm – $p < 0.05$) significantly higher than divers with an LBG. In total, the body surface area of the divers with an HBG was larger than divers with an LBG (1.99 ± 0.1 vs. 1.86 ± 0.14 m^2). BMI was not significantly different between the two groups (25 ± 1.9 vs. 24.9 ± 1.8 kg m^{-2}).

The VO_2 peak was not significantly different between groups (LBG divers 50 ± 6 vs. HBG divers 48 ± 7 ml kg^{-1} min^{-1}). Nevertheless, when the result was expressed as the percentage of the predicted value [according to the equation proposed by Wasserman et al. (1987)], the difference reached significance (LBG divers: 126 ± 13% vs. HBG divers: 115 ± 14% of the predicted value – $p < 0.05$).

Echocardiographic parameters including left ventricular systolic and diastolic function and right heart study were not significantly different between the two groups (**Tables 1** and **2**).

Hemodynamic data did not report differences in HR and cardiac output between groups (**Table 3**). However, brachial blood pressure was different between the two groups. Systolic arterial pressure and pulse pressure were significantly higher in divers with an HBG when compared with LBG divers. Total arterial compliance estimated by the ratio SV/PP was lower in divers with an HBG when compared with divers with an LBG.

Biological Study

The plasma endothelin-1 concentration was not significantly different between the two groups (divers with an LBG 1.2 ± 0.1 pg ml^{-1} vs. divers with an HBG 1.7 ± 1 pg ml^{-1}).

TABLE 1 | Left ventricular systolic and diastolic function.

	Divers with an LBG	Divers with an HBG	
LA (mm)	35 ± 4	34 ± 3	NS
LV EDD (mm)	53 ± 3	54 ± 2	NS
LV ESD (mm)	33 ± 3	34 ± 3	NS
LV mass/BSA (g m^{-2})	104 ± 31	103 ± 21	NS
LV FS (%)	38 ± 5	36 ± 4	NS
E (cm s^{-1})	70 ± 17	71 ± 11	NS
A (cm s^{-1})	46 ± 9	49 ± 16	NS
E/A ratio	1.6 ± 0.4	1.6 ± 0.6	NS
IVRT (ms)	74 ± 8	76 ± 8	NS
LA contribution (%)	25 ± 6	26 ± 8	NS
E' (cm s^{-1})	16 ± 3	16 ± 3	NS
E/E' ratio	5 ± 2	5 ± 1	NS

LBG, low bubble grade; HBG, high bubble grade; LA, left atrium; LV, left ventricle; EDD, end diastolic diameter; ESD, end systolic diameter; BSA, body surface area; LV FS, left ventricle fraction shortening; E, peak velocity of the initial trans mitral flow; A, peak velocity of the late flow; IVRT, isovolumetric relaxation time; LA contribution, contribution of atrial contraction to the LV filling; E´, early diastolic velocity of the mitral annulus.

TABLE 2 | Right heart study.

	Divers with an LBG	Divers with an HBG	
IVC (mm)	19 ± 3	21 ± 5	NS
RVEDD (mm)	22 ± 1	21 ± 3	NS
TRV (cm s^{-1})	2 ± 0.2	2 ± 0.1	NS
PVR (WU)	0.1 ± 0.02	0.1 ± 0.02	NS
AcT/RVET (%)	47 ± 4	47 ± 6	NS

LBG, low bubble grade; HBG, high bubble grade; IVC, diameter of the inferior vena cava at expiration; RVEDD, right ventricle end-diastolic diameter; TRV, peak of the tricuspid regurgitation velocity; PVR, pulmonary vascular resistance; WU, Woods unit; AcT/RVET, acceleration time/RV ejection time ratio of the pulmonary artery blood flow.

TABLE 3 | Hemodynamic data.

	Divers with an LBG	Divers with an HBG	
SBP (mmHg)	118 ± 7	126 ± 7	$p < 0.01$
DBP (mmHg)	70 ± 7	71 ± 6	NS
MBP (mmHg)	86 ± 6	90 ± 6	NS
PP (mmHg)	48 ± 6	54 ± 6	P < 0.01
Heart rate (beat min^{-1})	65 ± 7	65 ± 8	NS
Ao VTI (cm)	21 ± 3	20 ± 2	NS
SV (ml)	90 ± 16	89 ± 10	NS
Cardiac output (L min^{-1})	5.8 ± 1.1	5.8 ± 1	NS
SVR (dyne s^{-1} cm^{-1})	1,236 ± 250	1,260 ± 156	NS
SV/PP (ml $mmHg^{-1}$)	1.9 ± 0.3	1.6 ± 0.3	<0.05

LBG, low bubble grade; HBG, high bubble grade; SBP, systolic blood pressure; DBP, diastolic blood pressure; MBP, mean blood pressure; PP, pulse pressure; Ao VTI, velocity-time integral of the aortic blood flow; SV, stroke volume; SVR, systemic vascular resistance; SV/PP, total arterial compliance.

Plasma NOx level was higher in divers with an LBG (34.5 ± 6 µmol L^{-1}) when compared with divers with an HBG (23.3 ± 4 µmol L^{-1} – $p < 0.05$).

Results of the Multivariate Analysis

Correlation result was represented in the correlogram (**Figure 3**).

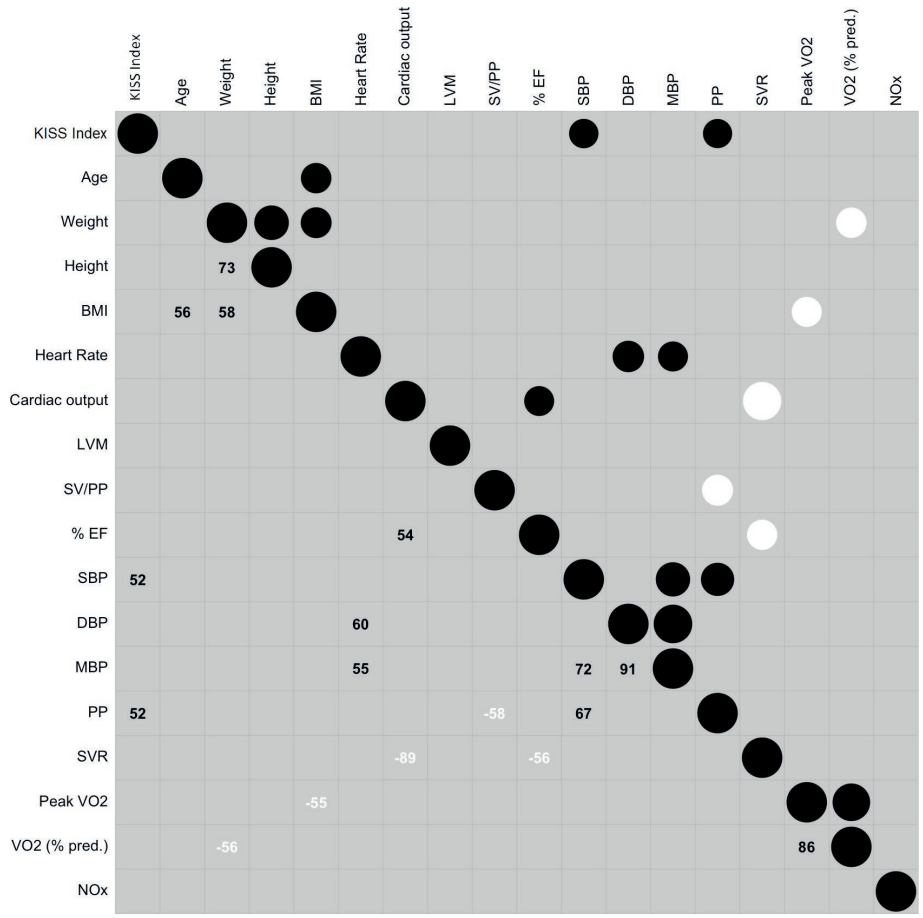

FIGURE 3 | Correlogram reporting the relationship between the variables. The circles in the upper part contain two information: the size reports the absolute value of the relation: the bigger the size is, the higher the strength is. Positive relationship is in black and negative relationship is in white. The larger number in the lower part is r in percentage ($r \times 100$). Abbreviations: KISS, Kisman-Masurel integrated severity score; BMI, body mass index; LVM, left ventricular mass; SV, stroke volume; SV/PP, total arterial compliance; LV FS, left ventricle fraction shortening (%EF); SBP, systolic blood pressure; DBP, diastolic blood pressure; MBP, mean blood pressure; PP, pulse pressure; SVR, systemic vascular resistance; peak VO_2, highest value of oxygen uptake; VO_2 (% pred.), percentage of predicted peak VO_2; NOx, metabolites of nitric oxide.

The variable inflation factor step procedure kept the following variables: age, height, BMI, HR, left ventricular mass, % EF, PP, SVR, VO_2 (% predicted), and plasma NOx level.

The generalized orthogonal pursuit algorithm selected the following model: PP, VO_2 (% predicted, and plasma NOx level with the following results: this model had an explanatory power of 49.22%. The model's intercept was at 3.26 (SE = 6.83, 95% CI [−9.63, 18.75]). Within this model:

- The effect of PP was significant (beta = 0.23, SE = 0.095, 95% CI [0.067, 0.45], $z = 2.38$, $p = 0.0171$) and can be considered as large (std. beta = 1.56, std. SE = 0.65).
- The effect of VO_2 (% predicted) tended to be significant (beta = −0.093, SE = 0.052, 95% CI [−0.22, −0.0094], $z = -1.79$, $p = 0.07$) and could be considered as medium (std. beta = −1.31, std. SE = 0.73).
- The effect of the plasma NOx level was not significant (beta = −0.12, SE = 0.088, 95% CI [−0.36, −0.0053], $z = -1.34$, $p = 0.1815$) and could be considered as medium (std. beta = −1.32, std. SE = 0.99).

The Likelihood ratio test result of PP + VO_2 (% predicted) + plasma NOx level model was the following log Lik = −19.337 (Df = −3), Chisq = 17.071, $p = 0.0006833$.

As expected, both correlogram and VIF algorithm results showed that most of the hemodynamic and blood pressure variables were correlated and collinear. In the final model, we observed that plasma NOx was not significantly related to the high bubble grade state but when plasma NOx variable was dropped, the new model had a decrease of the explanatory power (from 49.2 to 38.52%).

DISCUSSION

The main result of this study was that volunteers with an HBG after the dive presented both higher SBP and PP at

baseline when compared with divers with an LBG. The multivariate analysis supported this finding. Indeed, the main contributor to the bubble quantity assessed by the KISS index was the blood pressure regimen.

It is recognized that the determinants of systolic blood pressure are stroke volume, HR, and the distensibility of the arterial tree (Smulyan and Safar, 1997). In our study, since there was no difference in cardiac output, stroke volume, and HR between groups, the higher SBP in divers with an HBG could be attributed to a reduced arterial distensibility in this group. This interpretation was supported by the wider pulse pressure recorded in divers with an HBG. Indeed, it has been demonstrated that an increased stiffness of the central arteries led to an increase in PP through an impairment in arterial compliance and an increase of the impact of the wave reflection on the blood pressure (Dart and Kingwell, 2001). Some anthropometric characteristics are recognized as risk factors for decompression sickness and HBG after diving (Cialoni et al., 2017). In our population, anthropometric data reported differences between groups. Divers with an HBG had a larger body surface area than divers with an LBG. It is recognized that the intensity of arterial wave reflections are positively correlated with height (Asmar et al., 1997). Furthermore, it has been reported a significant positive correlation between systolic blood pressure and body size (weight, height, or BSA) in healthy young adults (Evans et al., 2017). Consequently, the difference in body size could have contributed to the higher pulse pressure in divers with an HBG.

Estimating the total arterial compliance by the ratio stroke volume divided by pulse pressure (Chemla et al., 1998) has been proposed. When compared with divers with an LBG, SV/PP was significantly lower in divers with an HBG supporting an increased stiffness of the central arteries in this group. Arterial compliance varies according to several factors such as age, physical fitness, and pathophysiological states such as hypercholesterolemia, diabetes, and hypertension. In this study, the divers were healthy non-smoker volunteers, and divers with an HBG had a similar age and VO_2 peak to divers with an LBG. Nevertheless, the percentage of predicted VO_2 peak was significantly higher in divers with an LBG, suggesting that aerobic fitness was higher in this group when compared with divers with an HBG. This result was supported by the multivariate analysis. Indeed, the percentage of predicted VO_2 peak was retained in the model. The impact of aerobic fitness on the production of VGE after a dive has been previously reported by some studies (Carturan et al., 2000; Schellart et al., 2012). Furthermore, it has been demonstrated that aerobic exercise training, was able to improve central arterial compliance in middle-aged men (Hayashi et al., 2005). Consequently, the physiological mechanism explaining the impact of aerobic fitness on VGE production after a dive might be the viscoelastic properties of the vascular tree. Endothelial function is implicated in the improvement in arterial compliance induced by aerobic exercise training. A single bout of physical exercise leads to an elevation in cardiac output, pulse pressure, and arterial blood flow and subsequently to an increase in laminar shear stress on vessel walls. Repetitive endothelial stressors induced by endurance physical training are able to increase plasma nitric oxide (NO) concentration and NO bioavailability (Green et al., 2004; Higashi and Yoshizumi, 2004; Rush et al., 2005; Goto et al., 2007). In our work, the results for the plasma NOx level agreed with these previous studies. Indeed, the plasma NOx level was higher in divers with an LBG, suggesting a higher NO bioavailability in this group. In the multivariate analysis, the effect of plasma NOx level on the bubble production was considered as medium: the integration of plasma NOx level in the model improved the explanatory power from 38.5 to 49.2%. The main contributor of high bubble grade was the blood pressure regimen.

A number of factors are known to influence arterial wall behavior and, therefore, blood pressure. Arterial compliance varies with the physical properties of the arterial media which contains smooth muscle cells, elastin, and collagen. Smooth muscle tone is affected by nervous activity, by hormones, and by locally produced vasoactive substances. Endothelial cells produce several important vasoactive substances including nitric oxide, and other factors such as prostacyclin, endothelium-derived hyperpolarizing factor, carbon monoxide, endothelin, and vasoactive prostanoids. The number of factors affecting the mechanical properties of the arterial wall explains that arterial compliance cannot be assessed by the sole measurement of NO production.

A negative relationship has been reported between endothelin-1 and aerobic physical fitness (Otsuki et al., 2006). Nevertheless, in our population, a significant difference in plasma endothelin-1 concentration in divers with an LBG and an HBG was not found.

In total, the viscoelastic properties of the arterial tree appeared to be an important contributor to circulating bubble production after a dive. This finding makes it possible to explain the results of some previously published studies.

It has been observed that older divers produced more bubbles than younger divers (Carturan et al., 2002; Schellart et al., 2012). This result could be attributed to the decrease in arterial compliance commonly observed with increasing age.

Higher NO biosynthesis has been reported in pre-menopausal women when compared with men (Forte et al., 1998). This difference is probably related to sex hormones (Cicinelli et al., 1996) because NO production decreases after menopause. After diving, less bubble production in premenopausal women has been observed in comparison with postmenopausal women and male divers (Boussuges et al., 2009).

Lastly, it has been demonstrated that a single bout of aerobic exercise reduced central and peripheral blood pressure and increased arterial compliance (Kingwell et al., 1997). Post-exercise hypotension can persist for several hours. The impact of exercise on the arterial tree might explain why an endurance exercise performed many hours before a dive could decrease the circulating bubble quantity after the dive (Dujic et al., 2004; Blatteau et al., 2007).

Study Limits and Hypotheses

The interpretation of the present study should be cautious: indeed some study limits can be stressed.

The interest of plasma NOx concentration in assessing NO bioavailability has been questioned (Kim-Shapiro and Gladwin, 2015). Nevertheless, in our work, the contribution of the arterial

function in venous gas bubble production after the dive was supported by several independent or combined data such as blood pressure measurements, ultrasonography study (assessment of total arterial compliance) and biological parameters (plasma NOx concentration).

The method of bubble detection followed the guidelines (Mollerlokken et al., 2016). To improve the assessment of the circulating bubbles quantity, we have used repeated detections. Screening Doppler tests began 30 min after the dive and were conducted every 20 min for 90 min. The KISS index was used as a semi quantitative method to estimate the whole bubble production. After a similar dive profile, the maximal bubble grade has been assessed to be around 40–50 min (Boussuges et al., 2009). On the other hand, VGE can be detected for several hours after diving (Masurel et al., 1976). To assess the total bubble activity prolonged monitoring would be better. Furthermore, to distinguish bubble-prone divers and bubble-resistant divers, we have chosen to separate the population in two groups; divers with LBG, i.e., with bubble grades 0, 1, or 2 leading to a KISS index <7.5 and divers with HBG, i.e., with bubble grades 3 or 4 with a KISS index >7.5. In further studies, for a better assessment of the whole bubble production for each diver, the use of two dimensional echocardiography combined with a computerized automatic counting of the circulating bubbles would be advantageous (Germonpré et al., 2014).

Lastly, in this study some factors known to impact bubble production such as age and BMI were not observed (Carturan et al., 2002). Our study included professional or recreational divers with good physical fitness (VO_2 peak from 36 to 62 ml kg^{-1} min^{-1}). None of the divers were overweight. Furthermore, most divers were middle-aged (24 out of 30 were from 30 and 45 years). A larger range for age and BMI could be more appropriate to study these factors.

The mechanism explaining the impact of arterial compliance on the circulating bubbles quantity remains hypothetical. The visco-elastic properties of the arterial wall might affect the diffusion of inert gas. Indeed, it has been reported that the systemic infusion of an endogenous nitric oxide synthase inhibitor lead to an increase in vascular stiffness and a decrease in cerebral blood flow in healthy subjects (Kielstein et al., 2006). As suggested by Arieli and Marmur (2017), the reduction of peripheral blood flow, in divers with low arterial compliance, might enhance the diffusion of inert gas into the artery and therefore the expansion of microbubbles.

CONCLUSION

In the present study, arterial compliance appeared to be a major factor in the circulating bubble quantity after a dive. The measurement of blood pressure including pulse pressure can provide the dive medical doctors with a simple means of estimating the risk of a high quantity of circulating bubbles after diving. It is therefore important to check blood pressure regularly in professional divers. When an increase in systolic blood pressure and pulse pressure is recorded, it should be recommended that dietary changes are made and the duration of endurance exercise training increased. These recommendations can be beneficial for reducing both the cardio-vascular risk factors and the quantity of bubble production after diving.

DATA AVAILABILITY

The raw data supporting the conclusions of this manuscript will be made available by the authors, without undue reservation, to any qualified researcher.

ETHICS STATEMENT

All the procedures were conducted in accordance with the Declaration of Helsinki and were approved by the local Ethics Committee (CCPPRB 1 Aix Marseille No. 20062103). Each method and the potential risks were explained to the participants in detail and they gave written informed consent before the experiment.

AUTHOR CONTRIBUTIONS

AB and JP conceived and designed the study. NV and JR assisted with the technical aspects of the protocol, recruited all the participants, and were involved in the acquisition of the data. AB and GC analyzed the data and performed the statistical analysis. AB, GC, and JP have drafted the article, while NV and JR revised it critically for important intellectual content. All the authors have given final approval of the version to be published.

FUNDING

This study was supported by a French Ministry of Defense research grant (Direction Générale de l'Armement, PDH-1-SMO-2-0701).

ACKNOWLEDGMENTS

The authors gratefully acknowledge the volunteers.

REFERENCES

Abbas, A. E., Fortuin, F. D., Schiller, N. B., Appleton, C. P., Moreno, C. A., and Lester, S. J. (2003). A simple method for noninvasive estimation of pulmonary vascular resistance. *J. Am. Coll. Cardiol.* 41, 1021–1027. doi: 10.1016/s0735-1097(02)02973-x

Arieli, R., and Marmur, A. (2017). A biophysical vascular bubble model for devising decompression procedures. *Physiol. Rep.* 5:e13191. doi: 10.14814/phy2.13191

Asmar, R., Brisac, A. M., Courivaud, J. M., Lecor, B., London, G. M., and Safar, M. E. (1997). Influence of gender on the level of pulse pressure: the role of large conduit arteries. *Clin. Exp. Hypertens.* 19, 793–811.

Asmar, R., and Zanchetti, A. (2000). Guidelines for the use of self-blood pressure monitoring: a summary report of the first international consensus conference. Groupe evaluation & measure of the french society of hypertension. *J. Hypertens.* 18, 493–508. doi: 10.1097/00004872-200018050-00001

Bayne, C. G., Hunt, W. S., Johanson, D. C., Flynn, E. T., and Weathersby, P. K. (1985). Doppler bubble detection and decompression sickness: a prospective clinical trial. *Undersea Biomed. Res.* 12, 327–332.

Blatteau, J. E., Boussuges, A., Gempp, E., Pontier, J. M., Castagna, O., Robinet, C., et al. (2007). Haemodynamic changes induced by submaximal exercise before a dive and its consequences on bubble formation. *Br. J. Sports Med.* 41, 375–379. doi: 10.1136/bjsm.2006.032359

Blatteau, J. E., Souraud, J. B., Gempp, E., and Boussuges, A. (2006). Gas nuclei, their origin, and their role in bubble formation. *Aviat. Space Environ. Med.* 77, 1068–1076.

Boussuges, A., Carturan, D., Ambrosi, P., Habib, G., Sainty, J. M., and Luccioni, R. (1998). Decompression induced venous gas emboli in sport diving: detection with 2D echocardiography and pulsed Doppler. *Int. J. Sports Med.* 19, 7–11. doi: 10.1055/s-2007-971871

Boussuges, A., Pontier, J. M., Schmid, B. and Dussault, C. (2014). Paradoxical gas embolism after SCUBA diving: hemodynamic changes studied by echocardiography. *Scand. J. Med. Sci. Sports* 24, 111–116. doi: 10.1111/j.1600-0838.2012.01474.x

Boussuges, A., Retali, G., Bodere-Melin, M., Gardette, B., and Carturan, D. (2009). Gender differences in circulating bubble production after SCUBA diving. *Clin. Physiol. Funct. Imaging* 29, 400–405. doi: 10.1111/j.1475-097X.2009.00884.x

Brubakk, A. (2004). "Endothelium and bubble injury: the role of endothelium in decompression illness" in *Proceedings of the 30th Annual Meeting of the European Underwater Baromedical Society*. eds. B. Grandjean and J. L. Meliet (Ajaccio, France), 17–22.

Carturan, D., Boussuges, A., Molenat, F., Burnet, H., Fondarai, J., and Gardette, B. (2000). Ascent rate and circulating venous bubbles in recreational diving. *Int. J. Sports Med.* 21, 459–462. doi: 10.1055/s-2000-7411

Carturan, D., Boussuges, A., Vanuxem, P., Bar-Hen, A., Burnet, H., and Gardette, B. (2002). Ascent rate, age, maximal oxygen uptake, adiposity, and circulating venous bubbles after diving. *J. Appl. Physiol.* 93, 1349–1356. doi: 10.1152/japplphysiol.00723.1999

Chemla, D., Hebert, J. L., Coirault, C., Zamani, K., Suard, I., Colin, P., et al. (1998). Total arterial compliance estimated by stroke volume-to-aortic pulse pressure ratio in humans. *Am. J. Phys.* 274, H500–H505. doi: 10.1152/ajpheart.1998.274.2.H500

Cialoni, D., Brizzolari, A., Samaja, M., Pieri, M., and Marroni, A. (2019). Altered venous blood nitric oxide levels at depth and related bubble formation during scuba diving. *Front. Physiol.* 10, 1–8. doi: 10.3389/fphys.2019.00057

Cialoni, D., Pieri, M., Balestra, C., and Marroni, A. (2017). Dive risk factors, gas bubble formation, and decompression illness in recreational SCUBA diving: analysis of DAN Europe DSL data base. *Front. Psychol.* 8:1587. doi: 10.3389/fpsyg.2017.01587

Cicinelli, E., Ignarro, L. J., Lograno, M., Galantino, P., Balzano, G., and Schonauer, L. M. (1996). Circulating levels of nitric oxide in fertile women in relation to the menstrual cycle. *Fertil. Steril.* 66, 1036–1038. doi: 10.1016/S0015-0282(16)58706-8

Dart, A. M., and Kingwell, B. A. (2001). Pulse pressure – a review of mechanisms and clinical relevance. *J. Am. Coll. Cardiol.* 37, 975–984. doi: 10.1016/s0735-1097(01)01108-1

Devereux, R. B., and Reichek, N. (1977). Echocardiographic determination of left ventricular mass in man. Anatomic validation of the method. *Circulation* 55, 613–618. doi: 10.1161/01.CIR.55.4.613

Dujic, Z., Duplancic, D., Marinovic-Terzic, I., Bakovic, D., Ivancev, V., Valic, Z., et al. (2004). Aerobic exercise before diving reduces venous gas bubble formation in humans. *J. Physiol.* 555, 637–642. doi: 10.1113/jphysiol.2003.059360

Dujic, Z., Palada, I., Valic, Z., Duplancic, D., Obad, A., Wisloff, U., et al. (2006). Exogenous nitric oxide and bubble formation in divers. *Med. Sci. Sports Exerc.* 38, 1432–1435. doi: 10.1249/01.mss.0000228936.78916.23

Eatock, B. (1984). Correspondence between intravascular bubbles and symptoms of decompression sickness. *Undersea Biomed. Res.* 11, 326–329.

Eatock, B. C., and Nishi, R. Y. (1987). "Analysis of Doppler ultrasonic data for the evaluation of dive profiles" in *IXth international symposium on underwater and hyperbaric physiology*. eds. A. A. Bove, A. J. Bachrach, and L. J. Greenbaum (Bethesda), 183–195.

Evans, J. M., Wang, S., Greb, C., Kostas, V., Knapp, C. F., Zhang, Q., et al. (2017). Body size predicts cardiac and vascular resistance effects on Men's and Women's blood pressure. *Front. Physiol.* 8:561. doi: 10.3389/fphys.2017.00561

Forte, P., Kneale, B. J., Milne, E., Chowienczyk, P. J., Johnston, A., Benjamin, N., et al. (1998). Evidence for a difference in nitric oxide biosynthesis between healthy women and men. *Hypertension* 32, 730–734. doi: 10.1161/01.HYP.32.4.730

Germonpré, P., Papadopoulou, V., Hemelryck, W., Obeid, G., Eckersley, R. J., Tang, M. X., et al. (2014). The use of portable 2D echocardiography and "frame-based" bubble counting as a tool to evaluate diving decompression stress. *Diving Hyperb. Med.* 44, 5–13.

Goto, C., Nishioka, K., Umemura, T., Jitsuiki, D., Sakagutchi, A., Kawamura, M., et al. (2007). Acute moderate-intensity exercise induces vasodilation through an increase in nitric oxide bioavailiability in humans. *Am. J. Hypertens.* 20, 825–830. doi: 10.1016/j.amjhyper.2007.02.014

Green, D. J., Maiorana, A., O'driscoll, G., and Taylor, R. (2004). Effect of exercise training on endothelium-derived nitric oxide function in humans. *J. Physiol.* 561, 1–25. doi: 10.1113/jphysiol.2004.068197

Hayashi, K., Sugawara, J., Komine, H., Maeda, S., and Yokoi, T. (2005). Effects of aerobic exercise training on the stiffness of central and peripheral arteries in middle-aged sedentary men. *Jpn. J. Physiol.* 55, 235–239. doi: 10.2170/jjphysiol.S2116

Higashi, Y., and Yoshizumi, M. (2004). Exercise and endothelial function: role of endothelium-derived nitric oxide and oxidative stress in healthy subjects and hypertensive patients. *Pharmacol. Ther.* 102, 87–96. doi: 10.1016/j.pharmthera.2004.02.003

Honek, J., Sramek, M., Sefc, L., Januska, J., Fiedler, J., Horvath, M., et al. (2014). Effect of conservative dive profiles on the occurrence of venous and arterial bubbles in divers with a patent foramen ovale: a pilot study. *Int. J. Cardiol.* 176, 1001–1002. doi: 10.1016/j.ijcard.2014.04.218

Kielstein, J. T., Donnerstag, F., Gasper, S., Menne, J., Kielstein, A., Martens-Lobenhoffer, J., et al. (2006). ADMA increases arterial stiffness and decreases cerebral blood flow in humans. *Stroke* 8, 2024–2029. doi: 10.1161/01.STR.0000231640.32543.11

Kim-Shapiro, D. B., and Gladwin, M. T. (2015). Pitfalls in measuring NO bioavailability using NOx. *Nitric Oxide* 44, 1–2. doi: 10.1016/j.niox.2014.10.003

Kingwell, B. A., Berry, K. L., Cameron, J. D., Jennings, G. L., and Dart, A. M. (1997). Arterial compliance increases after moderate-intensity cycling. *Am. J. Phys. Heart Circ. Phys.* 273, H2186–H2191. doi: 10.1152/ajpheart.1997.273.5.H2186

Kisman, K., Masurel, G., Lagrue, D., and Lepechon, J. (1978). Evaluation de la qualité d'une décompression basée sur la détection ultrasonore de bulles. *Méd. Aéro. Spat. Méd. Sub. Hyp.* 17, 293–297.

Kitabatake, A., Inoue, M., Asao, M., Masuyama, T., Tanouchi, J., Morita, T., et al. (1983). Noninvasive evaluation of pulmonary hypertension by a pulsed Doppler technique. *Circulation* 68, 302–309. doi: 10.1161/01.CIR.68.2.302

Lagani, V., Athineou, G., Farcomeni, A., Tsagris, M., and Tsamardinos, I. (2016). Feature selection with the r package mxm: Discovering statistically-equivalent feature subsets. *arXiv preprint arXiv:1611.03227* [Preprint].

Lozano, A., Swirszcz, G., and Abe, N. (2011). "Group orthogonal matching pursuit for logistic regression" in *Proceedings of the fourteenth international conference on artificial intelligence and statistics*. eds. G. Gordon, D. Dunson, and M. Dudík (Fort Lauderdale, USA), 452–460.

Masurel, G., Guillerm, R., and Cavenel, P. (1976). Détection ultrasonore par effet Doppler de bulles circulantes chez l'homme lors de 98 plongées à l'air. *Méd. Aero. Spat. Méd. Sub. Hyp.* 156, 199–202.

Mollerlokken, A., Blogg, S. L., Doolette, D. J., Nishi, R. Y., and Pollock, N. W. (2016). Consensus guidelines for the use of ultrasound for diving research. *Diving Hyperb. Med.* 46, 26–32.

Nagueh, S. F., Middleton, K. J., Kopelen, H. A., Zoghbi, W. A., and Quiñones, M. A. (1997). Doppler tissue imaging: a noninvasive technique for evaluation of left ventricular relaxation and estimation of filling pressures. *J. Am. Coll. Cardiol.* 30, 1527–1533. doi: 10.1016/S0735-1097(97)00344-6

Naimi, B., Hamm, N. A., Groen, T. A., Skidmore, A. K., and Toxopeus, A. G. (2014). Where is positional uncertainty a problem for species distribution modelling? *Ecography* 37, 191–203. doi: 10.1111/j.1600-0587.2013.00205.x

Nashimoto, I., and Gotoh, Y. (1978). "Relationship between precordial doppler ultrasound records and decompression sickness" in *VIth international symposium*

on underwater and hyperbaric physiology. eds. C. W. Shilling and M. W. Beckett (Bethesda: Undersea Medical Society), 497–501.

Nishi, R., Kisman, K., Eatock, B., Buckingham, I., and Masurel, G. (1981). "Assessment of decompression profiles and divers by Doppler ultrasonic monitoring" in *Underwater physiology VII, proceedings of the seventh symposium on underwater physiology*. (Bethesda, MD: Undersea Medical Society), 717–727.

Otsuki, T., Maeda, S., Iemitsu, M., Saito, Y., Tanimura, Y., Ajisaka, R., et al. (2006). Effects of athletic strength and endurance exercise training in young humans on plasma endothelin-1 concentration and arterial distensibility. *Exp. Biol. Med.* 231, 789–793.

Papadopoulou, V., Germonpre, P., Cosgrove, D., Eckersley, R. J., Dayton, P. A., Obeid, G., et al. (2018). Variability in circulating gas emboli after a same scuba diving exposure. *Eur. J. Appl. Physiol.* 118, 1255–1264. doi: 10.1007/s00421-018-3854-7

Pati, Y. C., Rezaiifar, R., and Krishnaprasad, P. S. (1993). "Orthogonal matching pursuit: recursive function approximation with applications to wavelet decomposition" in *Signals, Systems and Computers, Proceedings of 27th Asilomar Conference on Signals, Systems and Computers* (Pacific Grove, California: IEEE Xplore Digital Library), 40–44.

Rush, J. W., Denniss, S. G., and Graham, D. A. (2005). Vascular nitric oxide and oxidative stress: determinants of endothelial adaptations to cardiovascular disease and to physical activity. *Can. J. Appl. Physiol.* 30, 442–474. doi: 10.1139/h05-133

Schellart, N. A., Van Rees, V., Tjeerd, P., Van Dijk, F. J., and Sterk, W. (2012). Doppler bubble grades after diving and relevance of body fat. *Aviat. Space Environ. Med.* 83, 951–957. doi: 10.3357/ASEM.3189.2012

Smulyan, H., and Safar, M. E. (1997). Systolic blood pressure revisited. *J. Am. Coll. Cardiol.* 29, 1407–1413. doi: 10.1016/S0735-1097(97)00081-8

Spencer, M. P. (1976). Decompression limits for compressed air determined by ultrasonically detected blood bubbles. *J. Appl. Physiol.* 40, 229–235. doi: 10.1152/jappl.1976.40.2.229

Wasserman, K., Hansen, J. E., Sue, D. Y., Whipp, B. J., and Froelicher, V. F. (1987). Principles of exercise testing and interpretation. *J. Cardiopulm. Rehabil. Prev.* 7, 189–199. doi: 10.1097/00008483-198704000-00014

Wisløff, U., Richardson, R. S., and Brubakk, A. O. (2003). NOS inhibition increases bubble formation and reduces survival in sedentary but not exercised rats. *J. Physiol.* 546, 577–582. doi: 10.1113/jphysiol.2002.030338

Wisløff, U., Richardson, R. S., and Brubakk, A. O. (2004). Exercise and nitric oxide prevent bubble formation: a novel approach to the prevention of decompression sickness? *J. Physiol.* 555, 825–829. doi: 10.1113/jphysiol.2003.055467

Conflict of Interest Statement: The authors declare that the research was conducted in the absence of any commercial or financial relationships that could be construed as a potential conflict of interest.

frontiers in Physiology

ORIGINAL RESEARCH
published: 26 March 2020
doi: 10.3389/fphys.2020.00273

Ulinastatin: A Potential Alternative to Glucocorticoid in the Treatment of Severe Decompression Sickness

Wen-tao Meng[1†], Long Qing[2†], Chun-zhen Li[3†], Kun Zhang[1], Hong-jie Yi[1], Xu-peng Zhao[1] and Wei-gang Xu[1]*

[1] Department of Diving and Hyperbaric Medicine, Naval Special Medicine Center, Naval Medical University, Shanghai, China, [2] Naval Diving Medical Discipline, Naval Special Medicine Center, Naval Medical University, Shanghai, China, [3] School of Basic Medicines, Naval Medical University, Shanghai, China

Inflammatory reaction is the crux in various clinical critical diseases including decompression sickness (DCS). Ulinastatin (UTI), a potent anti-inflammatory agent, has been used clinically, including as a substitution for steroids. This study aimed to explore the potential effects of UTI upon DCS in a rabbit model. Eighty-eight rabbits were subjected to simulated diving to 6 atmospheres absolute (ATA) for 60 min with 2.5-minute decompression. Three doses of UTI (15/7.5/3.75 × 10^5 U/kg) or saline were intravenously administered immediately following decompression. Circulating bubbles were monitored for 3 h following decompression and DCS signs were evaluated for 24 h. Blood was sampled 8 times during 72 h after decompression for inflammatory, endothelial, oxidative and routine blood indices. Lung tissues were also sampled for evaluating endothelial function. Another six rabbits were used as Normal controls. In the high dose UTI group the mortality, general morbidity and incidence of severe DCS was decreased from 31.25 to 9.38% (P = 0.030), 84.38 to 62.50% (P = 0.048) and 46.88 to 21.88% (P = 0.035), respectively. The high dose of UTI significantly postponed the occurrence of DCS (P = 0.030) and prolonged survival time (P = 0.009) compared with the Saline group, and significantly ameliorated inflammation responses, endothelial injuries and oxidative damage. The results strongly suggest the benefit of UTI on DCS, especially for severe cases. Large doses are needed to achieve significant effects. UTI may be a potential ideal pharmacological candidate for the treatment of severe DCS.

Keywords: ulinastatin, decompression sickness, inflammation, endothelial injury, rabbit

OPEN ACCESS

Edited by:
François Guerrero, Université de Bretagne Occidentale, France

Reviewed by:
Jacek Kot, Medical University of Gdańsk, Poland
Jacky Lautridou, Norwegian University of Science and Technology, Norway

****Correspondence:***
Wei-gang Xu
wg_hsu@163.com

† These authors have contributed equally to this work

Specialty section:
This article was submitted to Vascular Physiology, a section of the journal Frontiers in Physiology

Received: *01 February 2020*
Accepted: *10 March 2020*
Published: *26 March 2020*

Citation:
Meng W, Qing L, Li C, Zhang K, Yi H, Zhao X and Xu W (2020) Ulinastatin: A Potential Alternative to Glucocorticoid in the Treatment of Severe Decompression Sickness. Front. Physiol. 11:273. doi: 10.3389/fphys.2020.00273

INTRODUCTION

Urinary trypsin inhibitor (Ulinastatin, UTI) is a nonspecific and multivalent Kunitz-type serine protease inhibitor purified from human urine (Yano et al., 2003). It is capable of suppressing various serine proteases such as trypsin, plasmin, neutrophil elastase and chymotrypsin (Nishiyama et al., 1996; Nakatani et al., 2001), and can also effectively stabilize lysosomal and cellular membranes (Nakahama et al., 1999). UTI has confirmed powerful efficacy in inhibiting the release of inflammatory factors, removing oxygen free radicals, improving microcirculation and tissue perfusion, and alleviating endothelial injuries (Takada et al., 2003; Tanaka et al., 2010; We et al., 2017; Fang et al., 2018). Clinically, UTI has been applied effectively in treating acute pancreatitis,

acute circulatory failure, and ischemia-reperfusion injury with few adverse events (Yoo et al., 2008; Li et al., 2017). Recently, UTI was demonstrated to exert protective effects in shock (Li et al., 2019). These clinical indications are similar to those of many steroids.

Decompression sickness (DCS) is one major concern for divers, astronauts and other personnel engaging in barometric operations, and bubble formation in tissue and circulation is the underlying mechanism (Arieli, 2018). As foreign bodies, bubbles can activate inflammatory cascade reactions, and induce cell irritation and tissue injuries (Papadopoulo et al., 2014). In the severe forms of DCS, significant neurological, respiratory and circulatory deficits or failure are frequently involved, and steroids are routinely used due to their potency on inhibiting systemic inflammation, reducing capillary permeability, maintaining cell membrane and reducing tissue edema (Kizer, 1981). However, many studies have shown no significant improvement of DCS when treated with steroids (Dromsk et al., 2003; Montcalm-Smith et al., 2008), and may even worsen the outcome of central nervous system injury due to their adverse effect of elevating blood glucose (Chikani et al., 2017). Hence, there has been a decline in the use of steroids for the treatment of severe DCS as well as other critical diseases due to their adverse effects and uncertainty of outcomes (Dromsk et al., 2003; Felleiter et al., 2012; Gibbison et al., 2017; Walje et al., 2017; Oh et al., 2019). Since 2008, the United States Navy no longer recommends steroids for DCS treatment. In consideration of UTI's unique pharmacological properties, we speculated that UTI would have therapeutic effects on DCS, and the underlying mechanisms are also explored in the present study.

MATERIALS AND METHODS

Animals

Ninety-four male *New Zealand White* rabbits weighing 2.0∼2.3 kg were obtained from Shanghai Shengwang Laboratory Animal Co., Ltd. The current study was performed at the laboratory of Diving and Hyperbaric Medicine at the Naval Medical University. All experimental procedures in this study were reviewed and approved by the Ethics Committee for Animal Experiment of the university. The rabbits were housed, and standard chow and water were given *ad libitum* in a room with controlled humidity (50∼60%), temperature (24∼26°C) and a 12-hour light-dark cycle.

Experimental Procedure and Design

After acclimation to the laboratory environment for one week, 88 rabbits were randomly divided into 4 groups and subjected to simulated diving and rapid decompression. After surfacing, either a single intravenous injection of UTI (Techpool Biopharma Co., Ltd., Guangdong, China) at 15×10^5 U/kg (High dose, UTI-H, $n = 32$), 7.5×10^5 U/kg (Median dose, UTI-M, $n = 12$) and 3.75×10^5 U/kg (Low dose, UTI-L, $n = 12$) or a same volume of saline ($n = 32$) were immediately administered. UTI was dissolved in saline (1 ml/kg body weight) and injected via the marginal ear veins. All of the animals were under continuous observation for 24 h after decompression to evaluate DCS signs. Blood was sampled before the simulated diving and at 1, 6, 12, 24, 36, 48, and 72 h following decompression to determine serum levels of biochemical indices. Twelve rabbits in each group underwent bubble detection at 10, 20, 30, 40, 60, 90, 120, and 180 min following decompression, and were then euthanized by intraperitoneal injection of pentobarbital (200 mg/kg) for sampling lung tissues and bronchoalveolar lavage fluid (BALF). Another six rabbits were sham exposed at normobaric air in the chamber as normal controls and were similarly sampled.

Hyperbaric Exposure Protocol

The rabbits were subjected to simulated diving in pairs as designated in **Table 1** in an animal hyperbaric chamber (DWC150, Yangyuan, Shanghai, China). The pressure was increased to six atmospheres absolute (ATA) in 5 min, slowly at the beginning to minimize any possible discomfort, and maintained for 60 min before decompressing linearly at two ATA/min to ambient pressure. Our previous research showed this profile could produce an incidence of DCS in rabbits of around 75% (Meng et al., 2018). During exposure, the temperature inside the chamber was maintained between 23 and 25°C, and the chamber was ventilated continuously for timely removal of metabolic generated carbon dioxide (CO_2).

DCS Symptoms Observation and Functional Evaluation

Following decompression, DCS was evaluated by two observers who were blinded to the treatments. The appearance and onset time of DCS signs were recorded. Severe DCS was defined as individuals with at least one of the signs including paralysis, dyspnea, seizure and death. Respiratory function was monitored

TABLE 1 | The matching scheme of rabbits from different groups for simulated diving.

Group	UTI-H	UTI-M	UTI-L	Saline	Sum
UTI-H	–	4	4	24	32
UTI-M	4	–	4	4	12
UTI-L	4	4	–	4	12
Saline	24	4	4	–	32

TABLE 2 | Modified Eftedal-Brubakk score for ultrasound-detected bubbles.

Score	Definition
0	No visible bubbles
1	Occasional bubbles
2	At least 1 bubble every 4 heart cycles
3	At least 1 bubble every heart cycle
4	Not more than one third of every image
5	Not more than two thirds of every image
6	Near whiteout; individual bubbles still discerned
7	Whiteout; individual bubbles can't be discerned

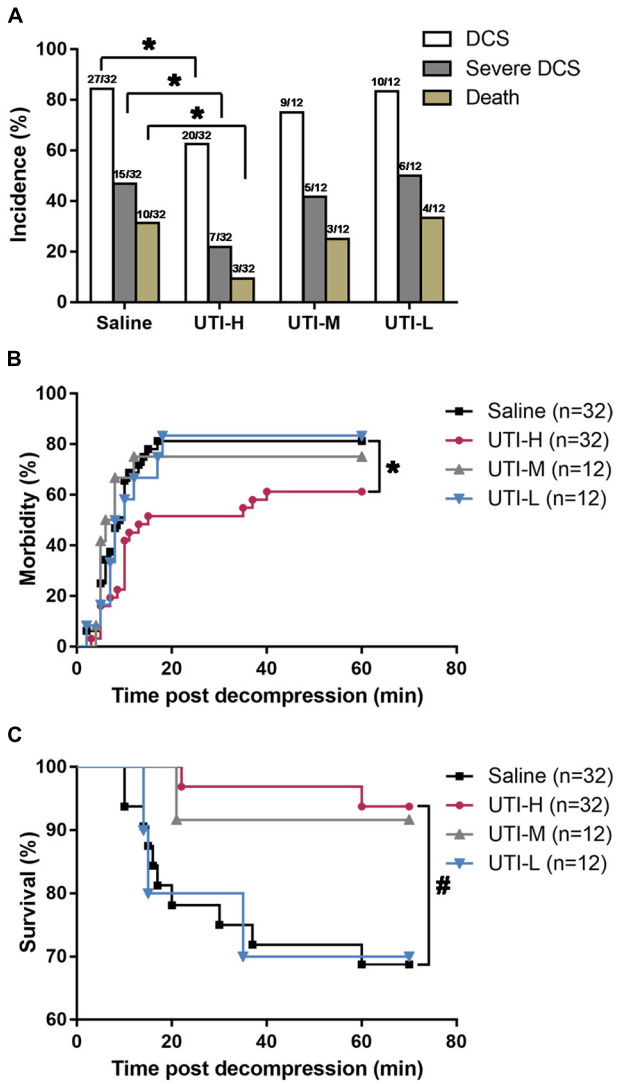

FIGURE 1 | Effects of different doses of UTI on DCS morbidity and mortality in rabbits. Rabbits were subjected to a simulated dive to six atmospheres absolute (ATA) for 60 min with 2.5-minute decompression, and received intravenous injection of different doses of UTI or saline immediately following decompression. **(A)** The mortality, general morbidity and incidence of severe DCS. **(B)** The incidence of DCS with time. **(C)** Survival curve of rapid decompressed rabbits. $^{*}P < 0.05$, $^{\#}P < 0.01$ vs. Saline group.

and scored at 10, 20, 30, 40, 60, 90, and 120 min post decompression using a 0–4 grading system as following (Atkins et al., 1988): 0, normal breathing; 1, mild labored breathing; 2, restlessness and labored breathing; 3, severely labored breathing, recumbent posture; 4, collapse, stupor and death. Motor function was evaluated before simulated diving and at 1, 6, 12, and 24 h after surfacing using Tarlov score (Kertmen et al., 2013), and each rabbit was scored 0 to 5 as following: 0, normal hind-limb function; 1, able to hop but uncoordinated; 2, able to sit but unable to hop; 3, active movement but unable to sit without assistance; 4, movement of joints perceptible; and 5, no voluntary hind-limb movement.

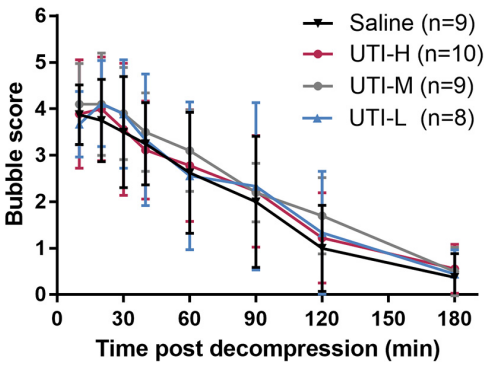

FIGURE 2 | Bubble load in rabbits after simulated diving and UTI treatments. After a simulated dive, rabbits immediately received an intravenous injection of different doses of UTI or saline. Bubbles were detected by ultrasound at multiple time points following decompression and were scored using the modified Eftedal-Brubakk grading scale. No statistical difference existed between groups ($P = 0.895$).

Bubble Detection

After surfacing, rabbits were placed in a supine position for bubble detection using a 10 MHz transducer connected to an ultrasound scanner (Mylab 30CV, Esaote, Italy). Bubbles were recognized as bright spots in heart chambers, and were scored by optimized Eftedal-Brubakk (EB) grading scale (Møllerløkken et al., 2016), with the modification shown in **Table 2**.

Blood Routine Examination

Half milliliter venous blood samples were taken from the marginal ear veins and collected into EDTA-anticoagulated tubes for blood routine examination using an automatic hematology analyzer (BC-2800Vet, Mindray, China).

Determination of Serum Biochemical Indices

Another 2 ml venous blood was obtained and centrifuged at 4°C and 2500 rpm for 10 min. Serum levels of intercellular cell adhesion molecule-1 (ICAM-1), endothelin-1 (ET-1), monocyte chemoattractant protein-1 (MCP-1) and interleukin-1beta (IL-1β) were determined by respective enzyme-linked immunosorbent assay (ELISA) kits (Jiancheng Bioengineering Institute, Nanjing, China). Levels of malondialdehyde (MDA) and myeloperoxidase (MPO) were determined by ELISA using respective assay kits (Melian Biological Technology Co., Shanghai, China). All assays were performed according to the manufacturers' instructions.

Lung Wet/Dry Weight Ratio Assay and BALF Analysis

After euthanasia at 24 h following decompression, fresh specimens of the right lung lobes were removed and weighed as wet weight and placed in an oven at 60°C for 72 h to measure dry weight. Lung water content was assayed by Wet/Dry (W/D)

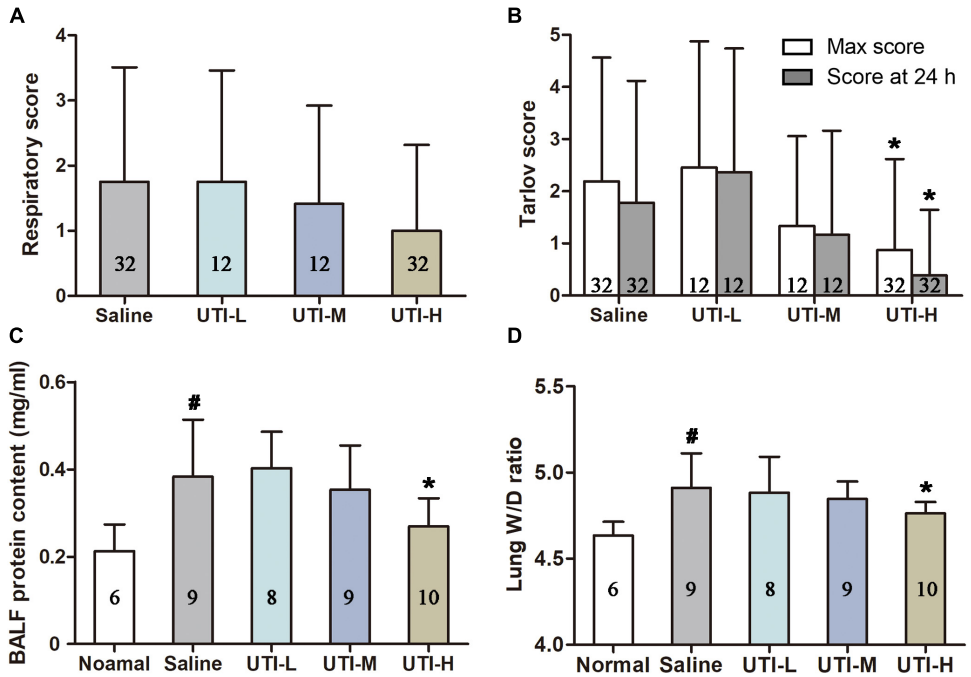

FIGURE 3 | Protective effects of UTI against lung injuries and neurological disorders. Respiratory function was monitored and scored for 2 h following simulated diving. The maximum observed respiratory scores are shown in panel **(A)**. Motor function was evaluated using Tarlov score for 24 h, and UTI-H significantly lowered both the maximal observed scores and scores assessed at 24 h after surfacing **(B)**. The high dose of UTI reduced the elevated BALF protein content and lung W/D ratio **(C,D)**. $^{\#}P < 0.01$ vs. Normal controls, $^{*}P < 0.05$ vs. Saline group.

weight ratio. A plastic tube was tied into the trachea and the left lung lavage was performed by flushing the airways with 3 × 10 ml 0.9% saline, and BALF recovery was approximately 80%. Total BALF protein was measured by bicinchoninic acid (BCA) using enhanced BCA protein assay kit (Beyotime Institute of Biotechology, Nantong, China).

Statistical Analysis

Where applicable, parametric data are expressed as mean ± s.d. Morbidity and mortality from different treatments were compared by Chi-square test. Normal distribution was determined by Shapiro-Wilk test. Comparisons of latency to DCS and survival curves were performed with the log-rank test. Bubble loads were analyzed by the generalized estimation equation. The mean differences between groups were assessed using an LSD test or Dunnett's test. Respiratory and Tarlov scores were compared between UTI and Saline groups by Mann-Whitney *U* test. *P* values less than 0.05 were considered statistically significant.

RESULTS

Morbidity and Mortality of DCS

The rabbits weighted 2.16 ± 0.12 kg before simulated diving, and there was no significant difference between groups. In 95% animals, DCS occurred within 30 min following decompression. The morbidity of DCS and severe DCS in the UTI-H group were significantly lower than in the Saline group (62.50% vs. 84.38%, $\chi^2 = 3.925$, $P = 0.048$ and 21.88% vs. 46.88%, $\chi^2 = 4.433$, $P = 0.035$; **Figure 1A**), and the occurrence of DCS was significantly postponed ($\chi^2 = 4.724$, $P = 0.030$, **Figure 1B**). The majority of deaths occurred following ∼1 min severe dyspnea and a transient convulsion. The high dose of UTI significantly decreased mortality from 31.25 to 9.38% ($\chi^2 = 4.730$, $P = 0.030$, **Figure 1A**), and survival time was also obviously extended ($\chi^2 = 6.838$, $P = 0.009$, **Figure 1C**). No statistical significance was found in DCS signs between UTI-M, UTI-L and Saline groups.

Bubble Load Following Decompression

Abundant bubbles were detected as bright spots in the right heart chambers. Bubbles peaked within 30 min following decompression, and diminished gradually thereafter (**Figure 2**). There was no obvious difference between bubble scores in rabbits treated with UTI and saline ($F = 0.201$ and $P = 0.895$).

Protective Effects of UTI Against Lung Injuries and Neurological Disorders

In the Saline group, 37.50% of individuals underwent a short period of fast or difficult breathing following decompression. Though no obvious difference existed in UTI treated animals when compared with those treated with saline, the high dose of UTI showed a tendency to decrease maximum respiratory scores observed during the 2 h following decompression ($Z = -1.684$, $P = 0.092$, **Figure 3A**). Protein content in BALF and lung W/D

weight ratio were significantly decreased in the UTI-H group compared with the Saline group (P = 0.025, **Figure 3C** and P = 0.042, **Figure 3D**), and detailed statistical results are shown in **Table 3**. There was no statistical difference in UTI-M and UTI-L with regard to BALF protein (P = 0.592 and P = 0.727, **Figure 3C**) or lung W/D weight ratio (P = 0.402 and P = 0.781, **Figure 3D**). 46.88% of individuals in the Saline group developed neurological disorders, which were accompanied with different degrees of paralysis. The high dose of UTI significantly lowered maximal observed Tarlov scores and scores assessed at 24 h following decompression ($Z = -2.220$, $P = 0.026$, and $Z = -2.592$, P = 0.010, **Figure 3B**). The median or low doses of UTI did not show a statistical difference.

Protective Effects of UTI on Blood Routine

As shown in **Figure 4**, counts of white blood cells (WBC) and platelet (PLT) decreased rapidly 1 h following decompression, and returned to normal gradually around 24 h following decompression. The high dose of UTI significantly inhibited the reduction of WBC and PLT (P = 0.006, **Figure 4B** and P = 0.005, **Figure 4D**). No statistical difference existed in UTI-M and UTI-L in terms of WBC (P = 0.066 and P = 0.134, **Figure 4B**) and PLT (P = 0.065 and P = 0.160, **Figure 4D**).

Anti-inflammatory, Anti-oxidative, Endothelial Protective Effects of UTI Against DCS

Levels of IL-1β, MCP-1, ET-1, ICAM-1, MDA, and MPO increased following decompression, peaked at 6, 12, 12, 12, 6, and 1 h, and gradually decreased to normal around 72, 72, 48, 48, 24, and 24 h, respectively (**Figures 5A1–A3**). As shown in **Figures 5B1–B3**, both the high and median doses of UTI reduced the peak levels of all the determined biochemical indices ($P < 0.05$ or $P < 0.01$) except median dose of UTI on MCP-1, MDA and MPO, which did not reach statistical significance. The low dose of UTI decreased MCP-1, ET-1, ICAM-1 and MPO levels, but only reached statistical significance on ICAM-1 ($P < 0.05$). Statistical results in detail are shown in **Table 3**.

TABLE 3 | Results of ANOVA and multiple comparisons.

Parameters	Testing time (time post de-compression)	ANOVA			*Post Hoc* Tests	
		df	*F*	*P*	Groups (vs. Saline group)	*P*
W/D weight ratio	24 h	4	4.120	0.007	UTI-H	0.034
					UTI-M	0.352
					UTI-L	0.693
					Normal	0.001
BALF Protein	24 h	4	5.492	0.001	UTI-H	0.012
					UTI-M	0.498
					UTI-L	0.675
					Normal	0.001
WBC	1 h	3	2.928	0.049	UTI-H	0.006
					UTI-M	0.066
					UTI-L	0.134
PLT	1 h	3	3.047	0.043	UTI-H	0.005
					UTI-M	0.065
					UTI-L	0.160
IL-1β	6 h	3	7.195	0.000	UTI-H	0.001
					UTI-M	0.018
					UTI-L	0.999
MCP-1	12 h	3	6.897	0.000	UTI-H	0.002
					UTI-M	0.106
					UTI-L	0.181
ET-1	12 h	3	9.554	0.000	UTI-H	0.001
					UTI-M	0.011
					UTI-L	0.340
ICAM-1	12 h	3	13.733	0.000	UTI-H	0.000
					UTI-M	0.000
					UTI-L	0.022
MDA	6 h	3	5.560	0.002	UTI-H	0.001
					UTI-M	0.174
					UTI-L	0.806
MPO	1 h	3	2.799	0.047	UTI-H	0.006
					UTI-M	0.083
					UTI-L	0.273

Rabbits were subjected to simulated diving to 6 atmospheres absolute (ATA) for 60 min with 2.5-minute decompression, and received intravenous injection of different doses of UTI or saline immediately following decompression. Lung tissues and BALF were sampled for determination of W/D weight ratio and protein content, respectively. Blood was sampled for WBC, PLT and serum indices including IL-1β, MCP-1, ET-1, ICAM-1, MDA, and MPO. Values of the indices were compared between the Saline group and UTI groups at different time points.

DISCUSSION

Inflammation is an adaptive and evolving process, which can be triggered by pernicious stimuli and conditions, such as infection and tissue injury (Medzhitov, 2008). Generally, it is supposed to be beneficial when it's under control, such as by exerting protective effects against infection. However, it becomes detrimental when out of control and may progress into a vicious cycle. Decompression bubbles formed in tissues and the circulatory system trigger inflammatory cascades, and play an extremely important role in the pathophysiology of DCS, especially in severe cases, in which systemic inflammatory responses continue despite the disappearance of bubbles, and further worsen the outcomes of DCS (Levin et al., 1981; Dennison et al., 2012). The inhibition of inflammation cascade responses is of great importance to stop the progression of DCS (Papadopoulo et al., 2014).

Ulinastatin is a multivalent serine protease inhibitor extracted from human urine. It exerts protective effects via suppressing various serine proteases (Nishiyama et al., 1996; Park et al., 2010) and stabilizing lysosomes and cellular membranes (Kanayama et al., 1997). Various clinical and animal experiments have demonstrated its anti-inflammatory, anti-oxidative, anticoagulant properties, and it can also improve the microcirculatory environment and reduce tissue damage (Tsujimura et al., 2008; Xu et al., 2012; Li et al., 2017; Liu et al., 2018). Clinically, it has been adopted successfully in the treatment

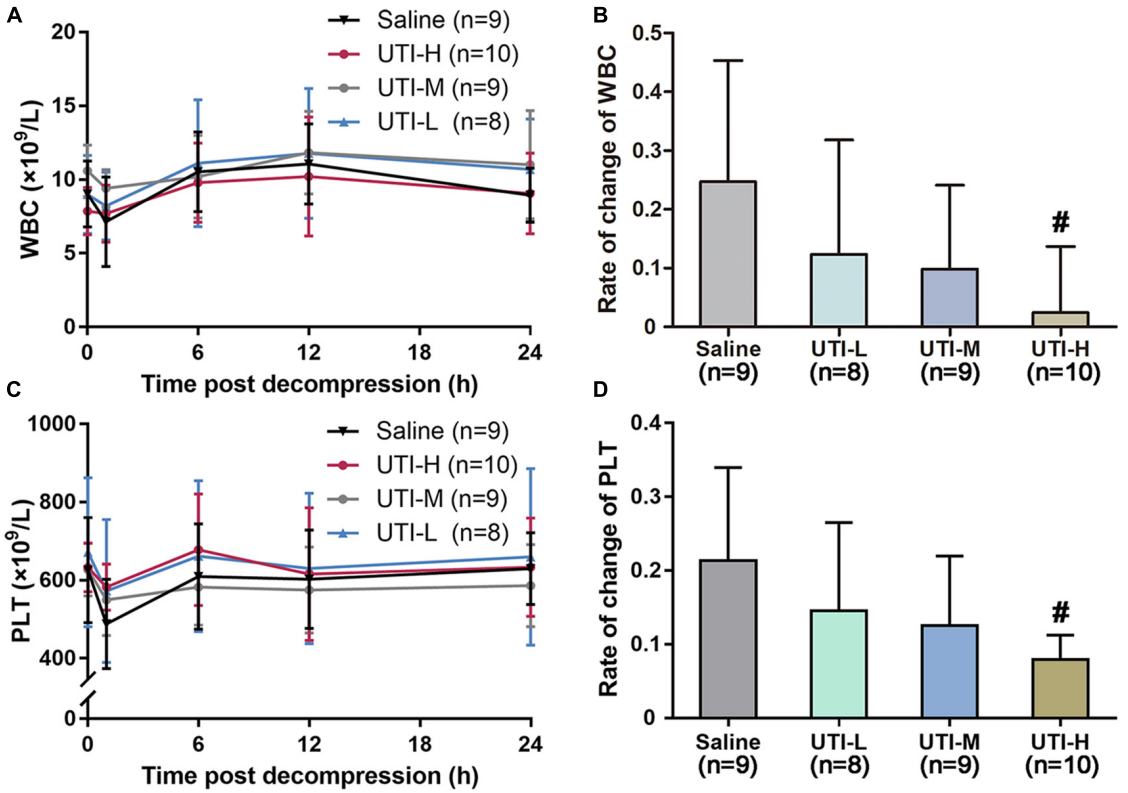

FIGURE 4 | Protective effects of different doses of UTI on blood routine. Blood was sampled from marginal ear veins in rabbits treated with saline or UTI before and after a simulated dive. Changes of WBC and PLT with time are shown **(A,C)**, and respective changes rates of different groups at 1 h following decompression are shown in panels **(B,D)**. The change rates of WBC and PLT were compared between UTI and Saline groups, respectively. $^{\#}P < 0.01$ vs. Saline group.

of life-threatening inflammation such as acute pancreatitis and sepsis (Tsujino et al., 2005; Zhang et al., 2008). Previously, steroids were routinely recommended and administered for severe DCS considering their benefits of decreasing tissue edema, reducing inflammation, alleviating leakage of blood vessels, and preventing histamine release (Kizer, 1981; Halpern et al., 1982; Dutka et al., 1992; Montcalm-Smith et al., 2008). However, even a high dose of steroids showed no improvement (Francis and Dutka, 1989; Montcalm-Smith et al., 2008) and even worsened the outcomes of DCS in animals (Dromsk et al., 2003). Side effects including the elevation of blood sugar were observed and steroids are no longer recommended for treating DCS in divers (Moon, 2009). Since UTI is regarded as an exciting alternative for steroids clinically (Linder and Russell, 2014), research into the potential protective effects of UTI on DCS is warranted.

In this study, the median dose of 7.5×10^5 U/kg was derived from the effective dosage commonly used in experimental acute pancreatitis (Ohbishi et al., 1984), and a dose gradient of $3.75/7.5/15 \times 10^5$ U/kg was adopted to explore possible dose-effect responses. Based on our preliminary experiments, the morbidity of DCS was around 75% for the saline treated rabbits and 40% for high dose of UTI treated ones, and a sample size of 32 for the two groups would provide 80% power to reach statistical significance concerning DCS morbidity based on a two-tailed significance level of 0.05. To minimize the use of animals, 12 rabbits were chosen for the other two dosage groups, which were designed to compare mainly biochemical indices with a concurrent observation of morbidity and mortality.

Autochthonous or circulating bubbles formed after rapid decompression play an important role in the progress of DCS (Qing et al., 2017; Zhang et al., 2017). The bubbles can not only cause mechanical damages and blockage, but also act as foreign bodies that trigger a cascade of inflammatory responses (Levett and Millar, 2008). As a powerful serine protease inhibitor, UTI is capable of reducing the release of inflammatory factors (Liu et al., 2017). IL-1β is one proximal factor responsible for downstream cytokine production and vascular injuries induced by decompression (Thom et al., 2018). MCP-1 is another proinflammatory cytokine in the process of disease resistance, which is related to decompression stress (Qing et al., 2018). UTI treatment significantly decreased the elevated serum levels of IL-1β and MCP-1 and, hence, in this study relieved inflammation cascade reactions induced by DCS.

In addition to its anti-inflammation property, UTI also effectively relieves endothelial injuries in DCS, probably through protecting endothelial glycocalyx (Wang et al., 2017). Besides, UTI can reduce the permeability of pulmonary capillary endothelial cells through the protection of endothelial junctional proteins (Fang et al., 2018). UTI may also protect endothelial cells from neutrophil-mediated injury not only by inactivation

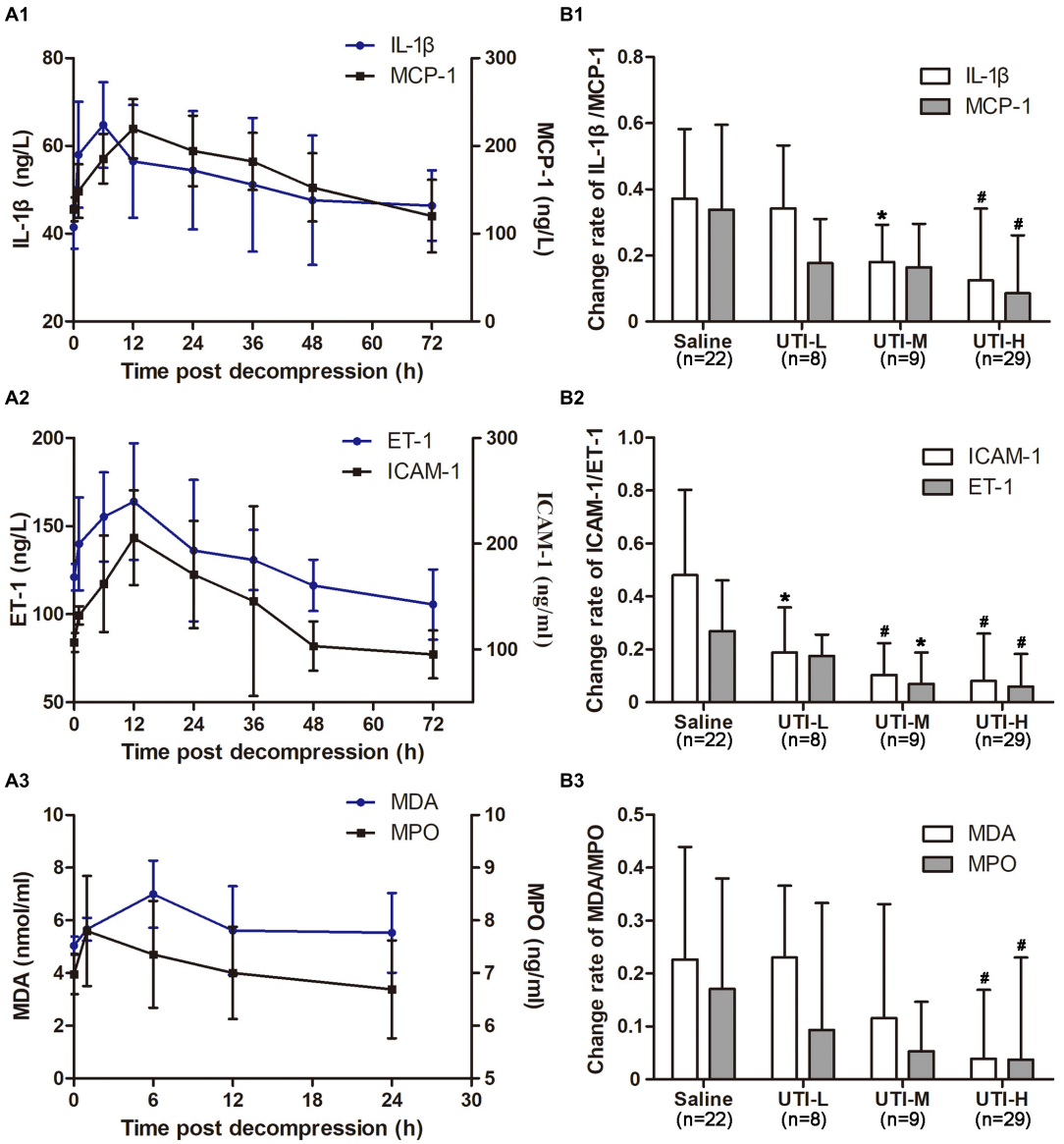

FIGURE 5 | Effects of different doses of UTI on inflammatory, endothelial and oxidative indicators. Before simulated diving and 1, 6, 12, 24, 36, 48, and 72 h following decompression, blood was sampled via marginal ear veins in rabbits treated with different doses of UTI or saline. Six rabbits in the Saline group were used to monitor changes in biochemical indices over time to determine their respective peak time points **(A1–A3)**, and the change rates were compared between UTI and Saline groups at the respective peak time points **(B1–B3)**. $^{*}P < 0.05$ and $^{\#}P < 0.01$ vs. Saline group.

of the extracellular elastase excreted from neutrophils, but also by suppressing the production of activated elastase (Nakatani et al., 2001). These pathways ultimately lowered the degrees of endothelial injuries and high permeability. Since the endothelial system is one of the vulnerable organs of DCS, UTI may hence alleviate DCS injuries. The effectiveness on reducing BALF protein content and lung W/D weight ratio, and serum levels of ET-1 and ICAM-1 provide evidence that endothelial injuries and microvascular permeability were ameliorated by UTI.

Bubbles interact with blood cells and plasma proteins, which may cause platelet activation and deposition, as well as leucocyte-endothelial adhesion, which are further enhanced by the increased expression of ICAM-1 (Aosasa et al., 1998; Levett and Millar, 2008; Vann et al., 2011). UTI has been confirmed to be effective in inhibiting neutrophil accumulation caused by the ischemia/reperfusion injury (Okuhama et al., 1999), and suppressing reduction of PLT induced by lipopolysaccharide (Inoue and Takano, 2010). Similarly, in this study UTI effectively counteracted the reduction of WBC and PLT post decompression. Apart from the properties mentioned above, UTI has also been demonstrated to inhibit oxidative stress and acts as a potent reactive oxygen scavenger (Du and Ko, 2005). Levels of oxidative stress, which were correlated with the severity of decompression (Lambrechts et al., 2015), were significantly

lowered in UTI-H as exhibited by the changes of MDA and MPO. As oxidative stress is likely to trigger endothelial responses (Eftedal et al., 2012), endothelial injuries may be relieved in turn due to alleviated oxidative stress.

The inflammatory, endothelial and oxidative indices in this study were mainly selected based on our previous studies in rat and swine DCS models (Zhang et al., 2017; Qing et al., 2018, 2019). In accordance with our swine model, all biochemical indices showed similar changes to those seen in rats except for E-selectin, which showed no change in the rabbit and swine DCS model. Considering the time course following decompression of these indices between different species, there was a general trend showing that the peak time points in rabbits were earlier than that of swine, then that of rats. These time courses supply indispensable information to determine the severity of DCS at different times following decompression. Another trend observed was that the change rates of indices were contrary to animal size.

The present results also confirm the protective effects of UTI against lung injuries and neurological disorders induced by DCS. There is strong evidence indicating protective effects of UTI against sepsis-induced multiorgan injuries, such as acute lung injury (Fang et al., 2018). It has been demonstrated that UTI relieves TNF-α induced hyperpermeability of vascular endothelial cells (We et al., 2017). In addition, UTI can effectively inhibit inflammation and reduce protein expression of AQP-4 (Cui and Zhu, 2015), which helps to attenuate capillary permeability and, as a result, alleviates lung and neural injuries.

The results of the present study show that a high dose of UTI (15×10^5 U/kg) significantly lowered the morbidity and mortality of DCS. Because no obvious difference in circulating bubbles between groups were found, the protective effects of UTI relied mainly on its anti-inflammatory, anti-oxidative, endothelial protective properties, as well as hematology stabilization. These features led to the alleviation of lung injuries and neurologic disorders, and significant improvement of DCS prognosis.

Clinically, UTI has already been adopted in treating diseases such as acute pancreatitis, circulatory shock, and systemic inflammatory response syndrome conditions including burns and acute respiratory distress syndrome (ARDS) in China and Japan (Nakahama et al., 1999; Tsujimura et al., 2008; Wang et al., 2016). The results in the present study not only confirm the protective effects of UTI in treating DCS, especially for severe cases, but also prove UTI is powerful in coping with the inflammation cascade response and endothelium related injuries. These evidences provide additional support for replacing steroids with UTI, at least partially, in the treatment of critical diseases characterized by inflammatory responses. No obvious side effect has been observed in past observations, either clinically or experimentally. All these properties favor applying UTI in treating various critical diseases.

In conclusion, this is the first study to explore the potential effects of UTI on DCS using a rabbit model. A single intravenous injection of UTI immediately following decompression exerted significant protective effects against DCS in a dose-response manner, especially for severe cases. The beneficial effects of UTI on DCS were attributed to its anti-inflammatory, anti-oxidative, endothelial protective properties, as well as inhibition of cell adhesion. Depending on the clinical routine in using UTI, it is thought repeated administrations will likely gain further benefits. Regarding that steroids are no longer recommended for the treatment of DCS, UTI may be an ideal substitute. Further explorations in large animals and divers are encouraged.

DATA AVAILABILITY STATEMENT

The raw data supporting the conclusions of this manuscript will be made available by the authors, without undue reservation, to any qualified researcher.

ETHICS STATEMENT

The animal study was reviewed and approved by the Ethics Committee for Animal Experiment of the Naval Medical University.

AUTHOR CONTRIBUTIONS

WX, WM, and LQ designed the experiments. WM, LQ, CL, and HY conducted the experiments. WM, LQ, and XZ contributed to data analyses and interpretation of the results. WX, WM, LQ, and CL wrote the manuscript and prepared all the figures and tables. KZ revised the manuscript.

FUNDING

The study was partly supported by the Natural Science Foundation of China (grant number: 81571846).

ACKNOWLEDGMENTS

The authors thank Dr. Peter Buzzacott for language polishing.

REFERENCES

Aosasa, S., Ono, S., Seki, S., Takayama, E., Tadakuma, T., Hirdide, H., et al. (1998). Inhibitory effect of protease inhibitor on endothelial cell activation. *J. Surg .Res.* 80, 182–187. doi: 10.1006/jsre.1998.5474

Arieli, R. (2018). Extravascular hydrophobic surfaces, fat droplets, and the connection with decompression illness spinal, joint pain, and dysbaric osteonecrosis. *Front. Physiol.* 9:305. doi: 10.3389/fphys.2018.00305

Atkins, C. E., Lehner, C. E., Beck, K. A., Dubielzig, R. R., Nordheim, E. V., and Lanphier, E. H. (1988). Experimental respiratory decompression sickness in sheep. *J. Appl .Physiol.* 65, 1163–1171. doi: 10.1152/jappl.1988.65.3.1163

Chikani, U. N., Ibekwe, M. U., Oguonu, T., Mungai, L., Bisi-Onyemaechi, A. I., Ugege, O. M., et al. (2017). Steroid-induced impairment of glucose tolerance: prevalence among pediatric patients on long-term

steroid use in Nigeria. *Pediatr Diabetes.* 18, 942–946. doi: 10.1111/pedi.12514

Cui, T., and Zhu, G. (2015). Ulinastatin attenuates brain edema after traumatic brain injury in rats. *Cell Biochem. Biophys.* 71, 595–600. doi: 10.1007/s12013-014-0239-3

Dennison, S., Moore, M., Fahlman, A., Moore, K., Sharp, S., Harry, C. T., et al. (2012). Bubbles in live-stranded dolphins. *Proc. Biol. Sci.* 279, 1396–1404. doi: 10.1098/rspb.2011.1754

Dromsk, D. M., Weathersby, P. K., and Fahlman, A. (2003). Prophylactic high dose methylprednisolone fails to treat severe decompression sickness in swine. *Aviat Space Environ. Med.* 74, 21–28.

Du, Y., and Ko, K. M. (2005). Effects of emodin treatment on mitochondrial ATP generation capacity and antioxidant components as well as susceptibility to ischemia-reperfusion injury in rat hearts: single versus multiple doses and gender difference. *Life Sci.* 77, 2770–2782. doi: 10.1016/j.lfs.2005.03.027

Dutka, A. J., Mink, R. B., Pearson, R. R., and Hallenbeck, J. M. (1992). Effects of treatment with dexamethasone on recovery from experimental cerebral arterial gas embolism. *Undersea Biomed. Res.* 19, 131–141.

Eftedal, I., Jørgensen, A., Røsbjørgen, R., Flatberg, A., and Brubakk, A. O. (2012). Early genetic responses in rat vascular tissue after simulated diving. *Physiol. Genomics.* 44, 1201–1207. doi: 10.1152/physiolgenomics.00073.2012

Fang, M., Zhong, W. H., Song, W. L., Deng, Y. Y., Yang, D. M., Xiong, B., et al. (2018). Ulinastatin ameliorates pulmonary capillary endothelial permeability induced by sepsis through protection of tight junctions via inhibition of TNF-α and related pathways. *Front. Pharmacol.* 9:823. doi: 10.3389/fphar.2018.00823

Felleiter, P., Müller, N., Schumann, F., Felix, O., and Lierz, P. (2012). Changes in the use of the methylprednisolone protocol for traumatic spinal cord injury in Switzerland. *Spine* 37, 953–956. doi: 10.1097/BRS.0b013e31823a07a2

Francis, T., and Dutka, A. (1989). Methyl prednisolone in the treatment of acute spinal cord decompression sickness. *Undersea Biomed. Res.* 16, 165–174.

Gibbison, B., Lopez-Lopez, J. A., Higgins, J. P., Miller, T., Angelini, G. D., Lightman, S. L., et al. (2017). Corticosteroids in septic shock: a systematic review and network meta-analysis. *Crit Care* 21:78. doi: 10.1186/s13054-017-1659-4

Halpern, P., Greenstein, A., Melamed, Y., Margulies, J. Y., and Robin, G. C. (1982). Spinal decompression sickness with delayed onset, delayed treatment, and full recovery. *Br. Med. J.* 284, 1014. doi: 10.1136/bmj.284.6321.1014

Inoue, K., and Takano, H. (2010). Urinary trypsin inhibitor as a therapeutic option for endotoxin-related inflammatory disorders. *Expert Opin. Investig Drugs.* 19, 513–520. doi: 10.1517/13543781003649533

Kanayama, N., Mashara, K., Suzuki, M., Fujise, Y., and Terao, T. (1997). The role of chondroitin sulfate chains of urinary trypsin inhibitor in inhibition of LPS-induced increase of cytosolic free Ca2+ in HL60 cells and HUVEC cells. *Biochem. Biophys. Res. Commun.* 238, 560–564. doi: 10.1006/bbrc.1997.7344

Kertmen, H., Gürer, B., Yılmaz, E. R., Sanlı, A. M., Sorar, M., Arıkök, A. T., et al. (2013). The protective effect of low-dose methotrexate on ischemia-reperfusion injury of the rabbit spinal cord. *Eur. J. Pharmacol.* 714, 148–156. doi: 10.1016/j.ejphar.2013.05.012

Kizer, K. W. (1981). Corticosteroids in treatment of serious decompression sickness. *Ann. Emerg. Med.* 10, 485–488. doi: 10.1016/s0196-0644(81)80285-5

Lambrechts, K., Pontier, J. M., Mazur, A., Theron, M., Buzzacott, P., Wang, Q., et al. (2015). Mechanism of action of antiplatelet drugs on decompression sickness in rats: a protective effect of anti-GPIIbIIIa therapy. *J. Appl. Physiol.* 118, 1234–1239. doi: 10.1152/japplphysiol.00125.2015

Levett, D. Z., and Millar, I. L. (2008). Bubble trouble: a review of diving physiology and disease. *Postgrad Med. J.* 84, 571–578. doi: 10.1136/pgmj.2008.068320

Levin, L. L., Stewart, G. J., Lynch, P. R., and Bove, A. A. (1981). Blood and blood vessel wall changes induced by decompression sickness in dogs. *J. Appl. Physiol* 50, 944–949. doi: 10.1152/jappl.1981.50.5.944

Li, M., Shen, J., Zou, F., Li, B., and Fan, M. (2017). Effect of ulinastatin on the permeability of the blood-brain barrier on rats with global cerebral ischemia/reperfusion injury as assessed by MRI. *Biomed. Pharmacother.* 85, 412–417. doi: 10.1016/j.biopha.2016.11.044

Li, S., Yang, W., Zhou, L., Nie, D., and Yu, H. (2019). Vascular permeability and hemodynamic effects of ulinastatin on organs affected by shock during early burn injury. *Am. J. Emerg. Med.* 37, 249–253. doi: 10.1016/j.ajem.2018.05.038

Linder, A., and Russell, J. A. (2014). An exciting candidate therapy for sepsis: ulinastatin, a urinary protease inhibitor. *Intensive Care Med.* 40, 1164–1167. doi: 10.1007/s00134-014-3366-9

Liu, S., Xu, J., Gao, Y., Shen, P., Xia, S., Li, Z., et al. (2018). Multi-organ protection of ulinastatin in traumatic cardiac arrest model. *World J. Emerg Surg.* 13:51. doi: 10.1186/s13017-018-0212-3

Liu, W., Pang, G., Wang, S., and Sun, A. (2017). Protective effect of ulinastatin on severe pulmonary infection under immunosuppression and its molecular mechanism. *Exp. Ther. Med.* 14, 3583–3588. doi: 10.3892/etm.2017.4993

Medzhitov, R. (2008). Origin and physiological roles of inflammation. *Nature* 454, 428–435. doi: 10.1038/nature07201

Meng, W. T., Qing, L., Yi, H. J., and Xu, W. G. (2018). Establishment of a rabbit decompression sickness model and its evaluation system. *Acad. J. Second Milit. Med. Univ.* 39, 33–39.

Møllerløkken, A., Blogg, S. L., Doolette, D. J., Nishi, R. Y., and Pollock, N. W. (2016). Consensus guidelines for the use of ultrasound for diving research. *Diving Hyperb. Med.* 46, 26–32.

Montcalm-Smith, E. A., Fahlman, A., and Kayar, S. R. (2008). Pharmacological interventions to decompression sickness in rats: comparison of five agents. *Aviat Space Environ. Med.* 79, 7–13. doi: 10.3357/asem.2071.2008

Moon, R. E. (2009). Adjunctive therapy for decompression illness: a review and update. *Diving Hyperb. Med.* 39, 81–87.

Nakahama, H., Kuribayashi, K., Sugita, M., and Shinkawa, T. (1999). Cytoprotective effect of ulinastatin, a Kunitz-type protease inhibitor, on hypoxic injury in L2 cells treated with antimycin A via stabilization of lysosomal fragility. *Pulm. Pharmacol. Ther.* 12, 1–6. doi: 10.1006/pupt.1998.9998

Nakatani, K., Takeshita, S., Tsujimoto, H., Kawamura, Y., and Sekine, I. (2001). Inhibitory effect of serine protease inhibitors on neutrophil-mediated endothelial cell injury. *J. Leukoc Biolo.* 69, 241–247. doi: 10.1189/jlb.69.2.241

Nishiyama, T., Aibike, M., and Hanaoka, K. (1996). The effect of ulinastatin, a human protease inhibitor, on the transfusion-induced increase of plasma polymorphonuclear granulocyte elastase. *Anesth Analg.* 82, 108–112. doi: 10.1097/00000539-199601000-00019

Oh, T. K., Song, I. A., Lee, J. H., Lim, C., Jeon, Y. T., Bae, H. J., et al. (2019). Effect of preadmission glucocorticoid therapy on 30-day mortality in critically ill patients: a retrospective study of a mixed ICU population in a tertiary hospital. *Ann. Intensive Care* 9:8. doi: 10.1186/s13613-019-0489-8

Ohbishi, H., Kosuzume, H., Ashida, Y., Kato, K., and Honjo, I. (1984). Effects of urinary trypsin inhibitor on pancreatic enzymes and experimental acute pancreatitis. *Dig Dis Sci.* 29, 26–32. doi: 10.1007/bf01296858

Okuhama, Y., Shiraishi, M., Higa, T., Tomori, H., Taira, K., Mamadi, T., et al. (1999). Protective effects of ulinastatin against ischemia-reperfusion injury. *J. Surg Res.* 82, 34–42. doi: 10.1006/jsre.1998.5496

Papadopoulo, P., Tan, M. X., Balestra, C., Eckersley, R. J., and Karapantsios, T. D. (2014). Circulatory bubble dynamics: from physical to biological aspects. *Adv. Colloid. Interface Sci.* 206, 239–249. doi: 10.1016/j.cis.2014.01.017

Park, K. H., Lee, K. H., Kim, H., and Hwang, S. O. (2010). The anti-inflammatory effects of ulinastatin in trauma patients with hemorrh shock. *J. Korean Med. Sci.* 25, 128–134. doi: 10.3346/jkms.2010.25.1.128

Qing, L., Ariyadewa, D. K., Yi, H., Wang, Y., Zhou, Q., and Xu, W. (2017). Skin lesions in swine with decompression sickness: clinical appearance and pathogenesis. *Front. Physiol.* 8:540. doi: 10.3389/fphys.2017.00540

Qing, L., Meng, W., Zhang, W., Yi, H. J., Zhang, K., Ariyadewa, D. K., et al. (2019). Benefits of escin for decompression sickness in bama pigs by endothelial-targeting protection. *Front. Physiol.* 10:605. doi: 10.3389/fphys.2019.00605

Qing, L., Yi, H. J., Wang, Y. W., Zhou, Q., Ariyadewa, D. K., and Xu, W. G. (2018). Benefits of hyperbaric oxygen pretreatment for decompression sickness in Bama pigs. *J. Exp. Biol.* 221:jeb171066. doi: 10.1242/jeb.171066

Takada, K., Komori, M., Notoya, A., Tomizawa, Y., and Ozaki, M. (2003). Effect of ulinastatin on microcirculation during excessive hemorrhage using fluid therapy. *In vivo* 17, 129–135. doi: 10.1159/000346205

Tanaka, R., Fujita, M., Tsuruta, R., Fujimoto, K., Aki, H. S., Kumagai, K., et al. (2010). Urinary trypsin inhibitor suppresses excessive generation of superoxide anion radical, systemic inflammation, oxidative stress, and endothelial injury in endotoxemic rats. *Inflamm Res.* 59, 597–596. doi: 10.1007/s00011-010-0166-8

Thom, S. R., Bhopale, V. M., Yu, K., and Yang, M. (2018). Provocative decompression causes diffuse vascular injury in mice mediated by

microparticles containing interleukin-1β. *J. Appl. Physiol.* [Epub ahead of print].

Tsujimura, S., Saito, K., Nakayamada, S., and Tanaka, Y. (2008). Bolus infusion of human urinary trypsin inhibitor improves intractable interstitial pneumonia in patients with connective tissue diseases. *Rheumatology* 47, 907–913. doi: 10.1093/rheumatology/ken067

Tsujino, T., Komatsu, Y., Isayama, H., Hirano, K., Sasahira, N., Yamamoto, N., et al. (2005). Ulinastatin for pancreatitis after endoscopic retrograde cholangiopancreatography: a randomized, controlled trial. *Clin. Gastroenterol. Hepatol.* 3, 376–383. doi: 10.1016/s1542-3565(04)00671-8

Vann, R. D., Butler, F. K., Mitchell, S. J., and Moon, R. E. (2011). Decompression illness. *Lancet* 377, 153–164. doi: 10.1016/S0140-6736(10)61085-9

Walje, A. K., Rogers, M. A., Lin, P., Singal, A. G., Stein, J. D., Marks, R. M., et al. (2017). Short term use of oral corticosteroids and related harms among adults in the United States: population based cohort study. *BMJ* 357:j1415. doi: 10.1136/bmj.j1415

Wang, J., Wu, A., and Wu, Y. (2017). Endothelial glycocalyx layer: a possible therapeutic target for acute lung injury during lung resection. *Biomed. Res. Int.* 2017:5969657. doi: 10.1155/2017/5969657

Wang, L. Z., Luo, M. Y., Zhang, J. S., Ge, F. G., Chen, J. L., and Zheng, C. Q. (2016). Effect of ulinastatin on serum inflammatory factors in Asian patients with acute pancreatitis before and after treatment: a meta-analysis. *Int. J. Clin. Pharmacol. Ther.* 54, 890–898. doi: 10.5414/CP202454

We, F., Liu, S., Luo, L., Gu, N., Zeng, Y., Chen, X., et al. (2017). Anti-inflammatory mechanism of ulinastatin: Inhibiting the hyperpermeability of vascular endothelial cells induced by TNF-α via the RhoA/ROCK signal pathway. *Int. Immunopharmacol.* 46, 220–227. doi: 10.1016/j.intimp.2017.03.007

Xu, C. E., Zhang, M. Y., Zou, C. W., and Guo, L. (2012). Evaluation of the pharmacological function of ulinastatin in experimental animals. *Molecules* 17, 9070–9080. doi: 10.3390/molecules17089070

Yano, T., Anraku, S., Nakayama, R., and Ushijima, K. (2003). Neuroprotective effect of urinary trypsin inhibitor against focal cerebral ischemia-reperfusion injury in rats. *Anesthesiology* 98, 465–473. doi: 10.1097/00000542-200302000-00028

Yoo, J. W., Ryu, J. K., Lee, S. H., Woo, S. M., Park, J. K., Yoon, W. J., et al. (2008). Preventive effects of ulinastatin on post-endoscopic retrograde cholangiopancreatography pancreatitis in high-risk patients: a prospective, randomized, placebo-controlled trial. *Pancreas* 37, 366–370. doi: 10.1097/MPA.0b013e31817f528f

Zhang, K., Wang, M., Wang, H., Liu, Y., Buzzacott, P., and Xu, W. (2017). Time course of endothelial dysfunction induced by decompression bubbles in rats. *Front. Physiol.* 8:181. doi: 10.3389/fphys.2017.00181

Zhang, Y., Chen, H., Li, Y. M., Zheng, S. S., Chen, Y. G., Li, L. G., et al. (2008). Thymosin alpha1- and ulinastatin-based immunomodulatory strategy for sepsis arising from intra-abdominal infection due to carbapenem-resistant bacteria. *J. Infect. Dis.* 198, 723–730. doi: 10.1086/590500

Conflict of Interest: The authors declare that the research was conducted in the absence of any commercial or financial relationships that could be construed as a potential conflict of interest.

frontiers in Physiology

ORIGINAL RESEARCH
published: 30 June 2020
doi: 10.3389/fphys.2020.00675

Simulated Microgravity Induces Regionally Distinct Neurovascular and Structural Remodeling of Skeletal Muscle and Cutaneous Arteries in the Rat

Olga S. Tarasova[1,2], Vjatcheslav U. Kalenchuk[3], Anatoly S. Borovik[1], Veronika O. Golubinskaya[2†], Michael D. Delp[4] and Olga L. Vinogradova[1,3]*

[1]State Research Center of the Russian Federation, Institute of Biomedical Problems, Russian Academy of Sciences, Moscow, Russia, [2]Faculty of Biology, M.V. Lomonosov Moscow State University, Moscow, Russia, [3]Faculty of Basic Medicine, M.V. Lomonosov Moscow State University, Moscow, Russia, [4]Department of Nutrition, Food and Exercise Sciences, College of Human Sciences, Florida State University, Tallahassee, FL, United States

OPEN ACCESS

Edited by:
Dieter Blottner,
Charité – Universitätsmedizin Berlin, Germany

Reviewed by:
Nicholas Gregory Jendzjowsky, University of Calgary, Canada
Satoshi Iwase, Aichi Medical University, Japan

***Correspondence:**
Olga S. Tarasova
ost.msu@gmail.com

†Present address:
Veronika O. Golubinskaya, Department of Physiology, Institute of Neuroscience and Physiology, The Sahlgrenska Academy, University of Gothenburg, Gothenburg, Sweden

Specialty section:
This article was submitted to Environmental, Aviation, and Space Physiology, a section of the journal Frontiers in Physiology

Received: 16 March 2020
Accepted: 26 May 2020
Published: 30 June 2020

Citation:
Tarasova OS, Kalenchuk VU, Borovik AS, Golubinskaya VO, Delp MD and Vinogradova OL (2020) Simulated Microgravity Induces Regionally Distinct Neurovascular and Structural Remodeling of Skeletal Muscle and Cutaneous Arteries in the Rat. Front. Physiol. 11:675. doi: 10.3389/fphys.2020.00675

Introduction: Mechanical forces and sympathetic influences are key determinants of vascular structure and function. This study tested the hypothesis that hindlimb unloading (HU) exerts diverse effects on forelimb and hindlimb small arteries of rats in functionally different regions of the skeletal muscle and skin.

Methods: Male Wistar rats were subjected to HU for 2 weeks, then skeletal muscle arteries (deep brachial and sural) and skin arteries (median and saphenous) were examined *in vitro* using wire myography or isobaric perfusion and glyoxylic acid staining.

Results: HU increased lumen diameter of both forelimb arteries but decreased diameter of the sural artery; the saphenous artery diameter was not affected. Following HU, maximal contractile responses to noradrenaline and serotonin increased in the forelimb but decreased in the hindlimb skeletal muscle feed arteries with no change in skin arteries; all region-specific alterations persisted after endothelium removal. HU increased the sensitivity to vasoconstrictors in the saphenous artery but not in the sural artery. In the saphenous artery, initially high sympathetic innervation density was reduced by HU, sparse innervation in the sural artery was not affected. Electrical stimulation of periarterial sympathetic nerves in isobarically perfused segments of the saphenous artery demonstrated a two-fold decrease of the contractile responses in HU rats compared to that of controls.

Conclusion: HU induces contrasting structural and functional adaptations in forelimb and hindlimb skeletal muscle arteries. Additionally, HU had diverse effects in two hindlimb vascular regions. Hyper-sensitivity of the saphenous artery to vasoconstrictors appears to result from the shortage of trophic sympathetic influence. Importantly, HU impaired sympathetically induced arterial vasoconstriction, consistent with the decreased sympathetic constrictor response in humans following space flight.

Keywords: microgravity, hindlimb unloading, rat, small arteries, remodeling, sympathetic innervation, noradrenaline, serotonin

INTRODUCTION

The vascular system is constantly exposed to mechanical forces such as transmural pressure and shear stress, the latter of which is created by flowing blood on the endothelial cell lining of the vessel. Prolonged changes in these factors govern gross structural remodeling of blood vessels, which in turn affects their functional characteristics. For example, previous work has shown that chronic increases in transmural pressure induce hypertrophy of the vascular wall and increases in vessel contractility, while decreases in pressure result in the opposite changes (Folkow, 1982). Chronic increases in shear stress, in turn, lead to structural increases in maximal diameter, whereas decreases in shear result in a narrowing of the vessel lumen (Langille, 1993; Pourageaud and De Mey, 1997).

The cardiovascular system of all terrestrial inhabitants is adapted to the gravitational field of the Earth and changes significantly in conditions of weightlessness (Watenpaugh and Hargens, 1996). Importantly, redistribution of transmural pressures and flows within the arterial vasculature during space flight or simulated microgravity is known to initiate different adaptations in vessels from different anatomic regions (Zhang, 2001, 2013). In humans, exposure to long term head-down bed rest was shown to reduce intimal-medial thickness and lumen diameter of arterial vessels in lower extremities, in contrast to upper extremity and cranial arteries (Bleeker et al., 2005; Platts et al., 2009).

The model of hindlimb unloading (HU) in rats is commonly used to study the mechanisms of microgravity effects on different body systems, including vasculature (Globus and Morey-Holton, 2016). Even relatively small change in hydrostatic pressure gradient, as observed in the rat body with this model (Colleran et al., 2000), results in different vascular alterations in rostral and caudal parts of the body. Similar to microgravity effects in human vascular system, rat hindlimb arteries commonly demonstrate wall thinning and lumen reduction, in contrast to cranial arteries (Wilkerson et al., 1999; Delp et al., 2000; Sun et al., 2004; Stabley et al., 2013).

Data from the literature also provide the evidence that transmural pressure shifts cannot explain all effects of simulated microgravity on vascular characteristics, because vascular alterations in HU rats may differ in functionally different vascular beds within the same part of the body. This was shown in studies of vascular dimensions and reactivity of arterioles from postural (soleus) and phasic (gastrocnemius) hindlimb muscles (Delp et al., 2000), as well as arterioles from white (glycolytic) and red (oxidative) parts from the same gastrocnemius muscle (Heaps and Bowles, 2002) of HU rats. Obviously, such diverse effects of HU on the arterial vasculature within and among postural and phasic muscles are largely the result of differential alterations in muscle activity and blood flow during the conditions of disuse (McDonald et al., 1992).

Structural and functional changes in the vascular bed could also result from the influence of sympathetic nervous system. In addition to acute control of vessel diameter and blood flow, neurotransmitters from the sympathetic nerves exert a trophic effect on the vasculature (Bevan, 1984; Puzdrova et al., 2014; Adeoye et al., 2015). The severity of trophic sympathetic influence in certain vascular bed may depend on the density of its innervation and/or on the efferent sympathetic traffic it receives. In addition, the state of the vascular neuroeffector apparatus has been shown to depend on the prevailing level of transmural pressure and, therefore, may be affected in the conditions of microgravity (Monos et al., 2001; Zhang, 2001; Puzdrova et al., 2009).

In contrast to the skeletal muscle circulation, the cutaneous circulation is regulated by a smaller contribution from metabolic vasomotor mechanisms and a higher role of sympathetic control, including a greater sympathetic vasoconstriction of small cutaneous arteries relative to that in skeletal muscle (Tarasova et al., 2003). However, to our knowledge, no study has examined the effects of simulated microgravity *via* HU on the structural and functional properties of cutaneous arteries, nor contrasted these effects in the forelimb and hindlimb circulations. Therefore, this study tested the hypothesis that HU exerts diverse effects on the neurovascular density, structural properties, and functional vasoconstrictor responsiveness of skeletal muscle and cutaneous feed arteries in the rat forelimb and hindlimb regions.

MATERIALS AND METHODS

All the procedures were conducted in accordance with the European Convention for the Protection of Vertebrate Animals used for experimental and other scientific purposes and conformed to the Guide for the Care and Use of Laboratory Animals published by the US National Institutes of Health (Eighth edition, 2011). The procedures were approved by the Biomedical Ethics Committee of the Institute of Biomedical Problems, Russian Academy of Sciences (protocol N224).

Animals

Male Wistar rats (2.5–3-month-old) were obtained from the breeder of the Institute of Biomedical Problems and housed in laboratory animal unit at the Faculty of Biology, M.V. Lomonosov Moscow State University in controlled conditions of temperature (22–24°C) and light-dark cycle (12–12 h) with *ad libitum* access to water and standard chow diet (Laboratorkorm, Russia). After 1-week acclimatization to the environment, the rats were randomly assigned to the cage control (n = 10) and HU (n = 10) groups. In HU group, the hindlimbs of the rat were elevated with a hook attached to the proximal third of the tail with adhesive material. The hook was connected by a harness to a swivel apparatus at the top of the cage. The height of the hindquarter elevation was adjusted to prevent the hindlimbs from touching the supporting surfaces, resulting in a suspension angle of 35–40°. The forelimbs maintained the contact with the floor surface, which allowed the animals full range of motion. The animals were housed individually in cages of 50 cm × 50 cm × 50 cm. Animals remained under HU or control conditions for a total of 14 days. This duration of HU was shown to provide the stable changes in muscle weight and blood flow in rats (McDonald et al., 1992). No signs of ischemia or damage of the tail skin were observed during HU.

After 2 weeks of HU, the animals were sacrificed by decapitation under CO_2 anesthesia and the arteries were dissected free from surrounding tissue. Two arteries were isolated from the forelimb (deep brachial artery and median artery) and two arteries from the hindlimb (sural artery and saphenous artery). These feed arteries provide blood flow to skeletal muscle (brachial and sural arteries) and predominantly to the skin (median and saphenous arteries). Brachial and median arteries were dissected from the right forelimb for myography experiments. Sural arteries from right and left hindlimbs were used for myography experiments and histochemical examination, respectively. Right saphenous artery from each rat was used for wire myography (distal part) and histochemical examination (proximal part), while the artery from the left hindlimb was studied in perfusion experiments.

Wire Myography

Two neighboring segments with a length of 2 mm were cut from each type of artery and mounted in wire myograph system (DMT, Denmark, 410A or 620 model) for isometric force recoding at well-defined internal circumferences. Endothelium was gently removed from one of the segments by rubbing with a rat whisker. The preparations were kept at 37°C in physiological salt solution containing (in mM): 120 NaCl, 26 $NaHCO_3$, 4.5 KCl, 1.2 NaH_2PO_4, 1.0 $MgSO_4$, 1.6 $CaCl_2$, 5.5 D-glucose, 0.025 EDTA, and 5 HEPES, equilibrated with gas mixture 5% CO_2 + 95% O_2 to maintain pH 7.4. Force readings were continuously recorded at 10 Hz sampling rate using E14-140 analog-to-digital data converter (L-Card, Russia) and PowerGraph 3.3 software (DISoft, Russia). Fully relaxed arterial segments were gradually stretched to d_{100}, the inner diameter equivalent to a transmural pressure of 100 mmHg, and then set to $0.9d_{100}$, where maximal active force is developed (Mulvany and Halpern, 1977).

The arteries were activated three times with noradrenaline (10^{-6} M, Sigma). Functional integrity of the endothelium was checked by application of acetylcholine (10^{-6} M, Sigma) on top of noradrenaline-induced contraction (3×10^{-7} M). Endothelium-intact preparations relaxed in response to acetylcholine by at least 50% of the precontraction level and the relaxation response of endothelium-denuded preparations was not larger than 10%. The experimental protocol included consecutively performed concentration-response relationships to noradrenaline (10^{-8} – 3×10^{-5} M, Sigma) and serotonin (3×10^{-8} – 3×10^{-5} M, Sigma) with 30-min washout interval between them. The agonists were given cumulatively in half-log increments. The responses to noradrenaline were studied in the presence of propranolol (10^{-6} M, Sigma), to prevent relaxation mediated by β-adrenoceptors.

During data analysis, active force values were calculated by subtracting the passive force value (recorded in the preparation with fully relaxed smooth muscle) from all recorded force values (before the first and at each noradrenaline or serotonin concentration). Then, respective values of active wall tension were calculated as $T = F / 2l$, where T is tension, F is active force and l is the segment length. The concentration-response relationships were fitted to a sigmoidal function with variable slope using GraphPad Prism 7.0 software (La Jolla, CA, USA) to calculate pD_2 values (the negative logarithm of EC_{50}). Inner diameter of each artery (d_{100}) was estimated from its passive length-tension relationship.

Constant-Pressure Perfusion

A segment of the saphenous artery was isolated, placed into the tissue bath, and cannulated at both ends. The vessel fragment length between the cannulae was about 5–6 mm. Krebs-Henseleit physiological salt solution was used for perfusion and superfusion (NaCl 119 mM, KCl 4.7 mM, $CaCl_2$ 2.5 mM, $MgSO_4$ 1.17 mM, $NaHCO_3$ 25 mM, KH_2PO_4 1.18 mM, D-glucose 5.5 mM, EDTA 0.026 mM, 37°C, and 95% O_2 + 5% CO_2). Artery was perfused under a constant pressure; input and output pressures were measured continuously using two pressure transducers (BLPR2, World Precision Instruments, USA) and kept at 60 and 50 mmHg, respectively. Volume flow rate was measured with 1N type transducer connected to transit-time flowmeter (Transonic Systems Inc., USA). All parameters were permanently recorded at 20 Hz sampling rate using E14-140 analog-to-digital data converter (L-Card, Russia) and PowerGraph 3.3 software (DISoft, Russia).

Intramural nerves were stimulated with rectangular electric pulses of changing polarity, with amplitude of 200–300 mA and 0.2 ms duration. All the effects of electrical stimulation could be blocked by tetrodotoxin (3 μM, Sigma), thus indicating the neurogenic origin of the response. Electric pulse frequency was 4, 8, or 12 Hz, the stimulation lasted for 30 s, and 3-min intervals were applied between the stimulations. Data analysis was performed using a custom program working under MATLAB (MathWorks Inc., USA). The constrictor response was evaluated as a relative change of the intralumen diameter (D), which was calculated by Poiseuille equation: $D = \sqrt[4]{(l \cdot Q) / \Delta P}$, l, length of the vessel segment between canulae; Q, volume flow rate; and ΔP, the difference between input and output pressures.

Glyoxylic Acid Staining for Periarterial Adrenergic Innervation

Segments of saphenous and sural arteries were cut lengthwise and placed in 0.1 M PBS (pH 7.2) supplemented with 2% glyoxylic acid, 10% sucrose, and 0.03% Pontamine Sky Blue (Puzdrova et al., 2009). After a 30-min incubation, the preparation was flattened on the slide with the adventitia upward, dried (30 min in jet of warm air and 5 min at 100°C), and overlaid with mineral oil and covered with a cover glass.

A LUMAM R3 microscope (LOMO, USSR; eyepiece ×7, objective lens ×40) was used for visualization. The exciting light wavelength was 380–440 nm; the luminescence wavelength was 480–700 nm. The plexus density was estimated with a grid that covered a field of 300 × 300 μm on the preparation and consisted of 24 rows, each containing 22–23 round markers (the ratio of marker diameter to space between markers was 1:2.5). Counting was performed in three randomly selected fields and the results were averaged.

Statistical Data Analysis

Statistical analysis was performed in GraphPad Prism 7.0. The normality of the data distribution was confirmed using D'Agostino-Pearson test. Unpaired Student's *t*-test or Repeated Measures ANOVA with Bonferroni *post hoc* test was used, as appropriate. Statistical significance was reached at $p < 0.05$. All data are given as mean ± S.E.M. and *n* represents the number of animals.

RESULTS

Body Weight

At the beginning of the experiment, body weights of rats from control and HU groups were 316 ± 6 g ($n = 10$) and 310 ± 9 g ($n = 10$), respectively ($p > 0.05$). Within 2 weeks, control group increased body weight to 376 ± 14 g ($n = 10$) and HU group to 353 ± 6 g ($n = 10$). No difference in body weight was observed between the two experimental groups at the end of the experiment ($p > 0.05$, control vs. HU).

Inner Diameter of the Arteries

Both forelimb arteries from HU rats had larger inner diameters compared to the respective arteries from control rats (**Table 1**). However, when calculated as percentage of the mean value in control group, the increment of diameter in the brachial artery was more prominent compared to the median artery: 22.5 ± 3.0 and 10.2 ± 3.8%, respectively ($p < 0.05$).

TABLE 1 | Relaxed inner diameter (d_{100}, μm) of endothelium-intact forelimb and hindlimb arteries from control and hindlimb-unloaded (HU) rats.

Organ	Arteries	Control	Hindlimb unloaded
Forelimb	Brachial (*n* = 9; 9)	213 ± 15	261 ± 6*
	Median (*n* = 10; 10)	375 ± 10	413 ± 14*
Hindlimb	Sural (*n* = 10; 10)	250 ± 11	208 ± 11*
	Saphenous (*n* = 10; 9)	418 ± 20	424 ± 20

*The numbers in parentheses indicates the numbers of animals in the groups.*p < 0.05 HU vs. control.*

In contrast, sural arteries of HU rats demonstrated a decrease of inner diameter (by 17.9 ± 4.7%) compared to the arteries of control rats (**Table 1**). The diameter of saphenous artery was not affected by HU (**Table 1**).

Contractile Responses of Forelimb Arteries

Contractile responses of brachial arteries were greater in HU rats compared to that in control rats. This was observed when endothelium-intact segments of brachial arteries were exposed to noradrenaline (**Figure 1A**) or serotonin (**Figure 1B**). Endothelium removal did not change the differences in brachial artery contractile responses between HU and control rats (**Figures 1C,D**). Most prominent effects of HU on brachial artery contractility were observed when the agonists were applied in near-maximal to maximal concentrations. The sensitivity of endothelium-intact and endothelium-denuded brachial artery preparations to vasoconstrictors was not altered by HU (**Table 2**).

Contractile responses of median artery segments to noradrenaline and serotonin were not different in HU rats compared to control rats regardless of the presence of the endothelium (**Figure 2**). The sensitivity of median artery segments to both vasoconstrictors was also similar in control and HU rats (**Table 2**).

Contractile Responses of Hindlimb Arteries

Sural arteries of HU rats developed less contractile tension to noradrenaline and serotonin. This decrease was observed in both endothelium-intact (**Figures 3A,B**) and endothelium-denuded (**Figures 3C,D**) segments of sural artery from HU rats compared to control rats. Again, most prominent effect of HU on contractile responses was observed with the higher concentrations of the agonists, while the sensitivity of sural arteries to contractile stimuli was not altered by HU (**Table 2**).

In contrast to sural arteries, saphenous arteries from HU rats developed stronger contractile responses compared to the arteries from control rats, regardless of the type of agonist

TABLE 2 | Sensitivity to noradrenaline and serotonin (pD_2 values) of endothelium-intact (Endo+) and endothelium-denuded (Endo–) hindlimb and forelimb arteries from control and HU rats.

Arteries		Noradrenaline		Serotonin	
		Control	Hindlimb unloaded	Control	Hindlimb unloaded
Brachial	Endo (+)	5.93 ± 0.14	5.93 ± 0.13	6.02 ± 0.06	6.10 ± 0.05
	Endo (–)	5.71 ± 0.22	6.05 ± 0.13	5.92 ± 0.07	5.97 ± 0.06
Median	Endo (+)	n.d.	n.d.	6.34 ± 0.14	6.45 ± 0.07
	Endo (–)	n.d.	n.d.	5.99 ± 0.15	6.01 ± 0.09
Sural	Endo (+)	6.18 ± 0.05	5.90 ± 0.13	5.97 ± 0.10	5.86 ± 0.10
	Endo (–)	6.07 ± 0.07	5.95 ± 0.16	5.97 ± 0.13	5.77 ± 0.07
Saphenous	Endo (+)	5.50 ± 0.08	5.77 ± 0.10*	6.00 ± 0.09	6.44 ± 0.14*
	Endo (–)	5.50 ± 0.08	5.82 ± 0.09*	5.99 ± 0.08	6.45 ± 0.18*

*The numbers of animals in the groups are shown in **Figures 1–4**.*
n.d., not determined, because of non-saturated concentration-response relationship.
**p < 0.05 HU vs. control.*

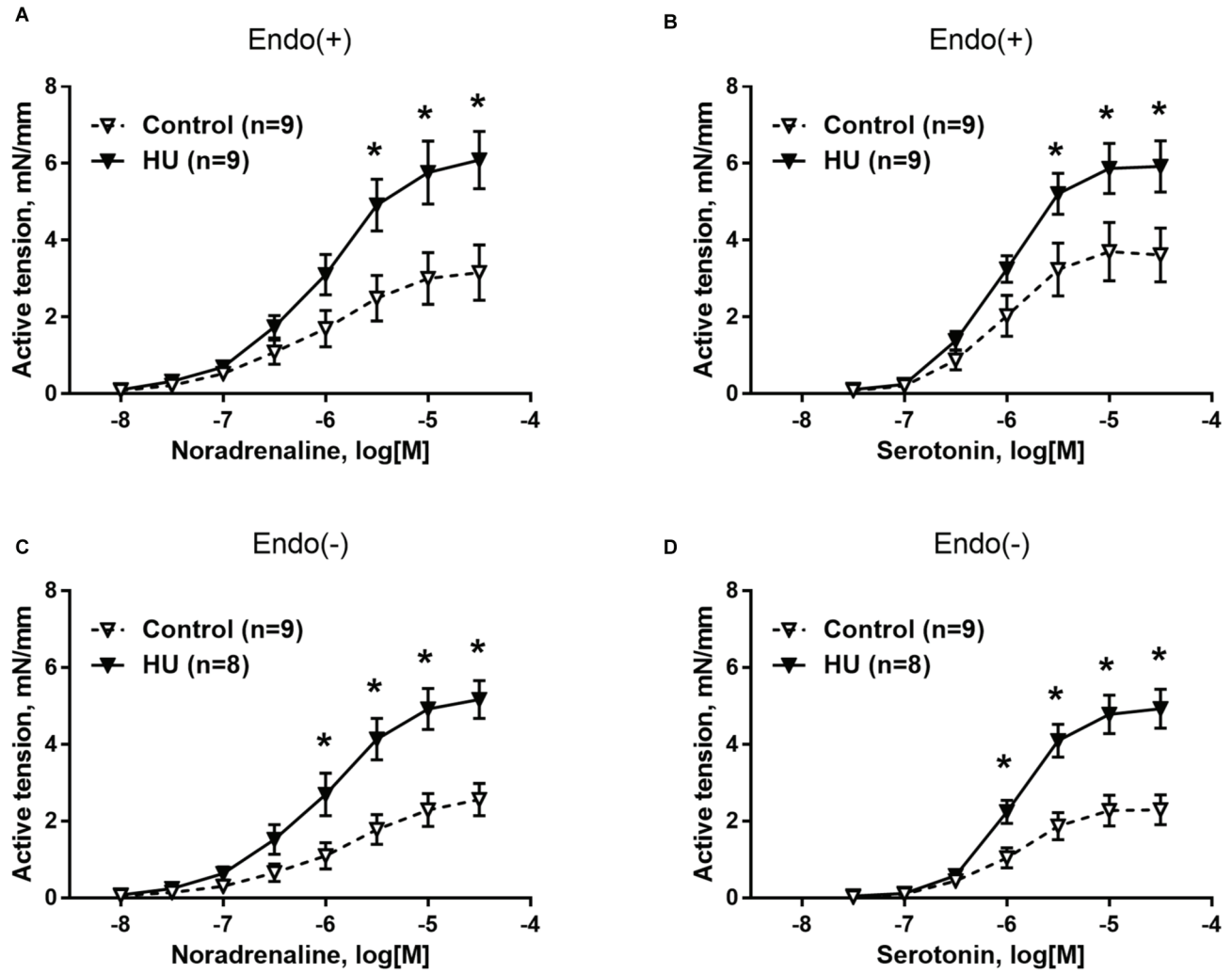

FIGURE 1 | HU increases contractile responses of skeletal muscle feed arteries from the rat forelimb. Concentration-response relationships to noradrenaline **(A,C)** and serotonin **(B,D)** of endothelium-intact **(A,B)** and endothelium-denuded **(C,D)** deep brachial arteries in control and HU rats. The number in parentheses indicates the number of animals in the group. *$p < 0.05$ HU vs. control.

and the presence of the endothelium (**Figure 4**). HU did not alter saphenous artery maximum contractile responses to noradrenaline and serotonin (**Figure 4**), but rather elevated the sensitivity of this artery to vasoconstrictors (**Table 2**).

Sympathetic Neurotransmission in Saphenous Artery

In control rats, adrenergic fiber plexus was dense in the saphenous artery, but sparse in the sural artery (**Figure 5A**). HU had no effect on innervation density in the sural artery (**Figure 5A**) but decreased it by about 20% in the saphenous artery (**Figures 5A,B**).

The effects of HU on sympathetic control of the saphenous artery were studied with the use of perfusion technique. In the absence of nerve stimulation, solution flow rate values did not differ in control and HU rats: 3.9 ± 0.18 and 4.1 ± 0.18 ml/min, respectively. The relative decreases of arterial inner diameter caused by 8 and 12 Hz stimulation were lower in HU rats compared to that in controls (**Figure 5C**).

DISCUSSION

The purpose of this study was to compare the effects of 2 weeks of simulated microgravity on skeletal muscle and skin feed arteries from the rat forelimb and hindlimb regions. We hypothesized that HU exerts diverse effects on the sympathetic innervation density, structural properties, and functional vasoconstrictor responsiveness of skeletal muscle and cutaneous feed arteries. The data indicate that HU induces increases in maximal lumen diameter and vasoconstrictor

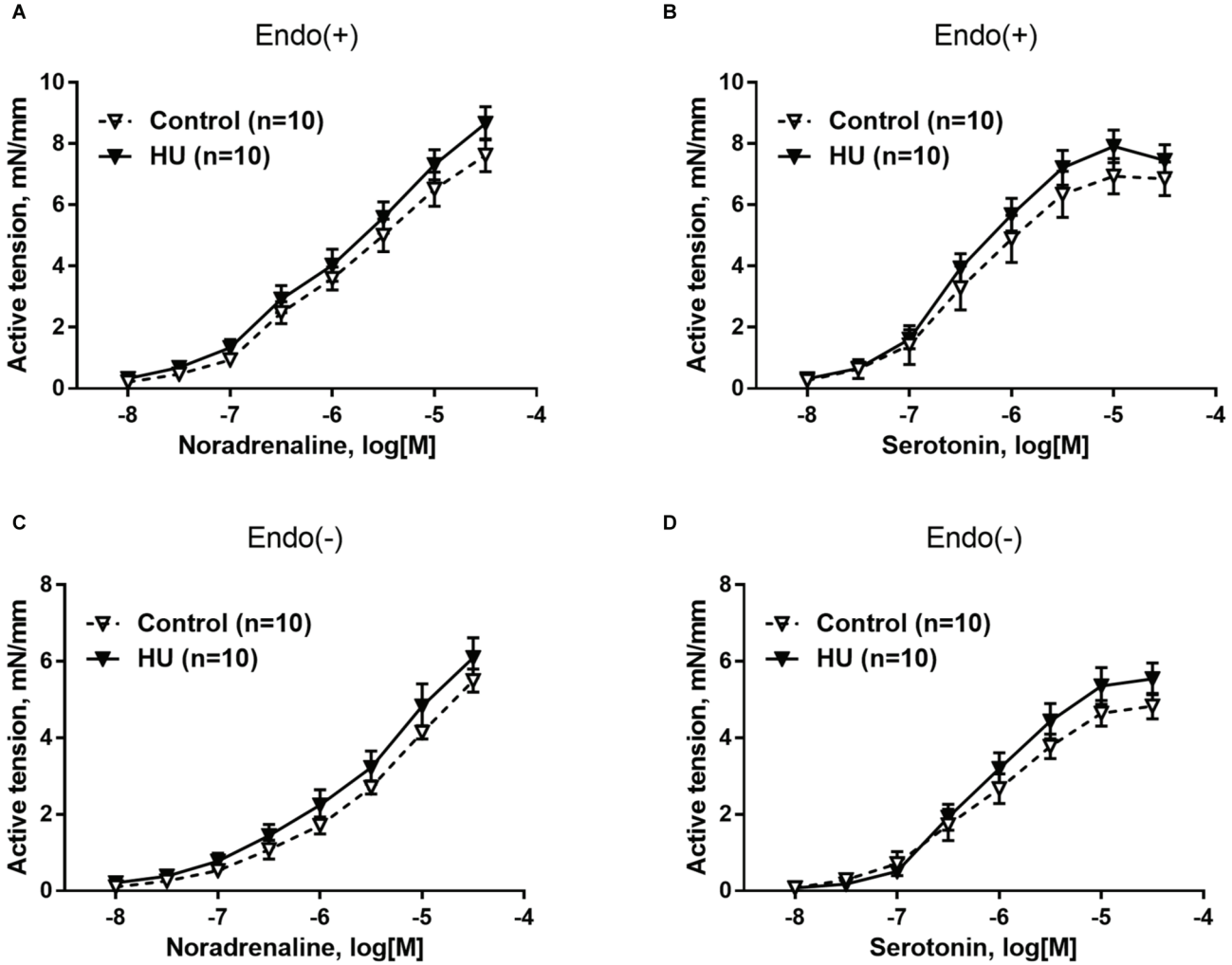

FIGURE 2 | HU does not change contractile responses of skin feed arteries from the rat forelimb. Concentration-response relationships to noradrenaline **(A,C)** and serotonin **(B,D)** of endothelium-intact **(A,B)** and endothelium-denuded **(C,D)** median arteries in control and HU rats. The number in parentheses indicates the number of animals in the group.

responsiveness in forelimb skeletal muscle arteries, but decreases in these structural and functional properties in hindlimb skeletal muscle arteries. In the cutaneous vasculature of the forelimbs and hindlimbs, alterations in the structure and vasoconstrictor properties either did not occur or were of smaller magnitude than that occurring in the skeletal muscle arteries from the same region of the body. Exposure to HU also diminished sympathetic nerve density and impaired vasoconstriction induced by sympathetic nerve stimulation in hindlimb cutaneous, but not skeletal muscle arteries. However, vasoconstrictor responses of hindlimb cutaneous arteries to direct smooth muscle stimulation by vasoconstrictor agonists exhibited greater sensitivity in the HU rats. Collectively, these results demonstrate that the complexity of vascular adaptations to simulated microgravity is much greater than previously described. Vascular alterations not only differentially occur between regions of the body, but also within those regions, and can be functionally related to physical alterations in sympathetic nerve density and gross structural remodeling of resistance arteries.

Both the forelimbs and hindlimbs of the rat perform functions of support and locomotion, which suggest these two different anatomical regions of the body share similar inherent characteristics that include skeletal muscle and cutaneous circulations. Additionally, systemic humoral influences would not differ in forelimb and hindlimb arteries of the same rat. Alterations in nerve traffic during HU exposure would also likely be equalized between the same-type arteries in the forelimbs and hindlimbs, since functional specialization of efferent sympathetic pathways is organotypic rather than

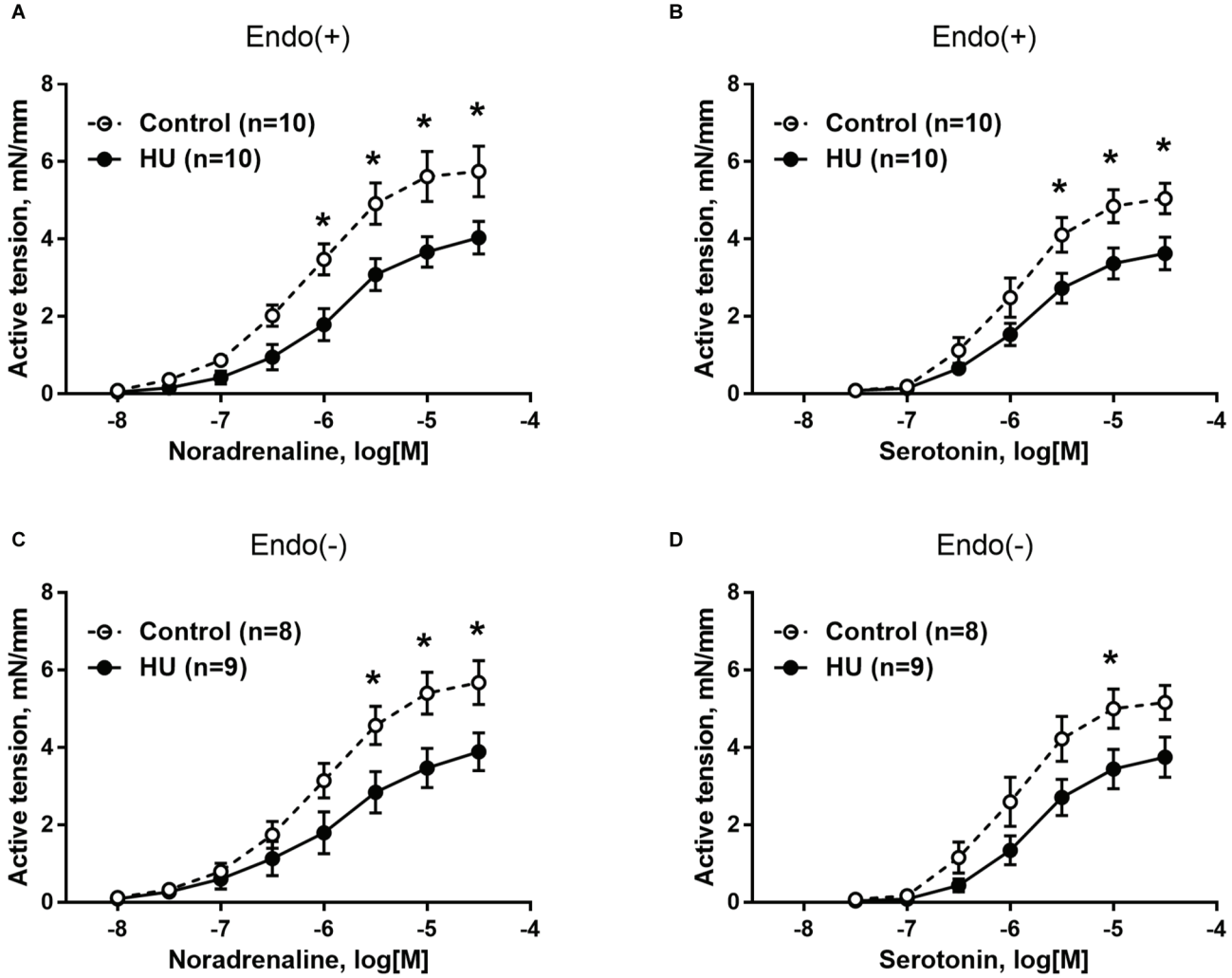

FIGURE 3 | HU decreases contractile responses of skeletal muscle feed arteries from the rat hindlimb. Concentration-response relationships to noradrenaline **(A,C)** and serotonin **(B,D)** of endothelium-intact **(A,B)** and endothelium-denuded **(C,D)** sural arteries in control and HU rats. The number in parentheses indicates the number of animals in the group. *$p < 0.05$ HU vs. control.

somatotopic (Jänig and McLachlan, 1992; Jänig and Häbler, 2003). Therefore, the design of this study allowed us to separate adaptive arterial responses to the anti-orthostatic body position and redistribution of support and muscle activity from other effects associated with the HU model, including social isolation, restraint, and the development of neuroendocrine stress (Tsvirkun et al., 2012).

Hindlimb Unloading Induces Contrasting Structural and Functional Adaptations in Forelimb and Hindlimb Skeletal Muscle Arteries

HU exposure resulted in divergent alterations of forelimb and hindlimb skeletal muscle arteries, i.e., lumen diameter and wall contractility (maximal active tension) increased in the forelimb but decreased in the hindlimb. The changes in contractility were independent of the vascular endothelium and not associated with the change in smooth muscle sensitivity to contractile stimulation by noradrenaline or serotonin. These data point to non-specific amplification of smooth muscle contractile responses in forelimb arteries, presumably resulting from smooth muscle hypertrophy and media wall thickening. In contrast, non-specific attenuation of smooth muscle contractile responses takes place in hindlimb arteries, presumably resulting from smooth muscle atrophy and a thinning of the medial wall (Delp et al., 2000).

Previous work has shown that HU in rats is associated with ~10 mmHg gradient between aortic and hindlimb arterial pressures (Colleran et al., 2000). Therefore, arterial transmural pressure in HU rats is elevated in the forelimb region and

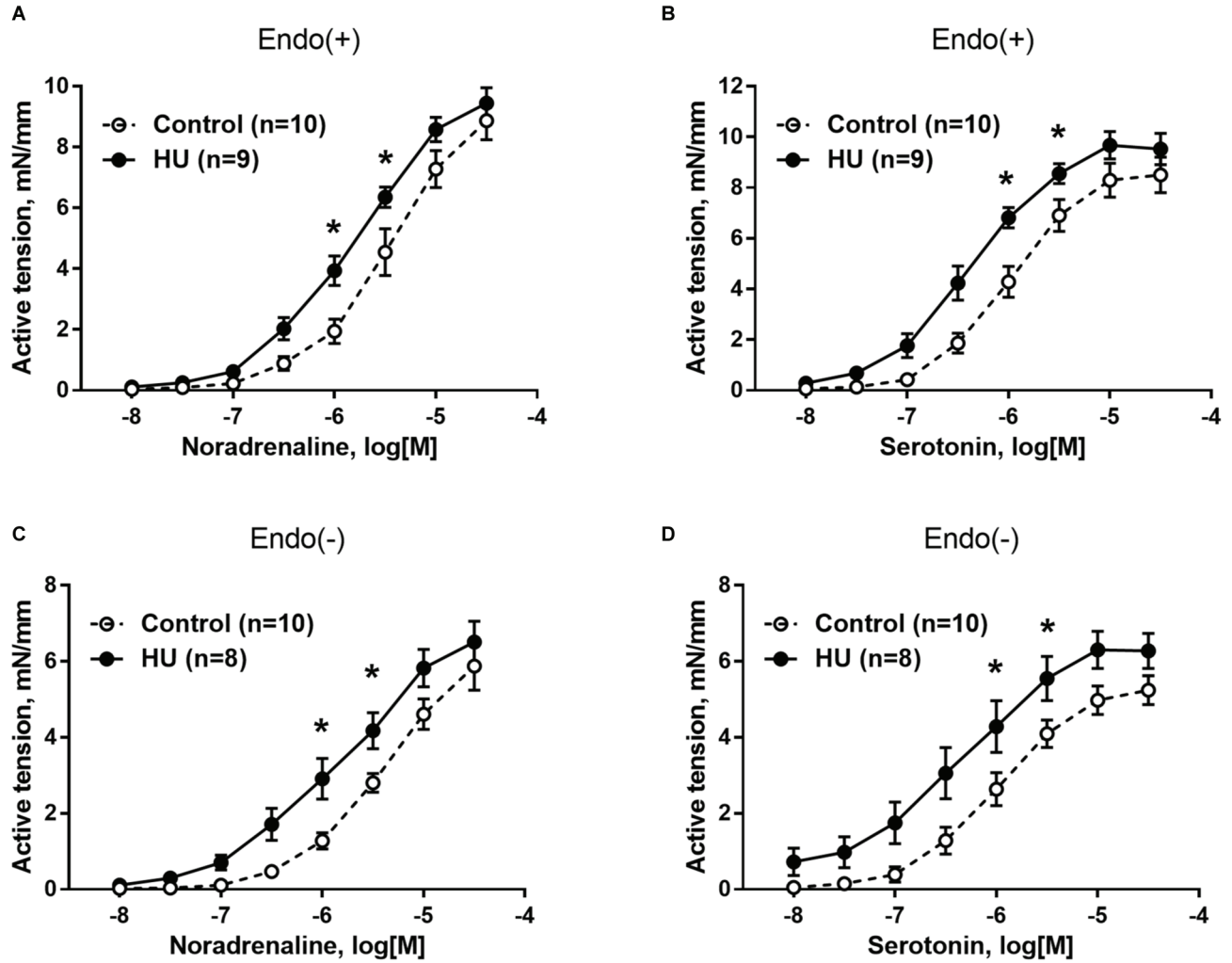

FIGURE 4 | HU increases contractile responses of skin feed arteries from the rat hindlimb. Concentration-response relationships to noradrenaline **(A,C)** and serotonin **(B,D)** of endothelium-intact **(A,B)** and endothelium-denuded **(C,D)** sural arteries in control and HU rats. The number in parentheses indicates the number of animals in the group. *$p < 0.05$ HU vs. control.

reduced in the hindlimbs; this pressure differential presumably governs the divergent alterations in media thickness (Wilkerson et al., 1999; Stabley et al., 2012). The mechanisms which mediate the effects of transmural pressure on media remodeling may include the secretion of angiotensin II from vascular smooth muscle cells with further stimulation of MAPK cascades (Eskildsen-Helmond and Mulvany, 2003). Importantly, HU was shown to stimulate the activity of vascular renin-angiotensin system in cranial arteries, but depress it in femoral arteries (Bao et al., 2007; Zhang, 2013). In support of the present data, wall thickness and medial cross-section area were shown to be diminished in resistance arteries associated with the anterior tibial (Sun et al., 2004) and gastrocnemius (Delp et al., 2000) muscles in the hindlimbs of HU rats. In addition, chronic increases in blood flow/shear stress in loaded forelimb muscles and chronic decreases in unloaded hindlimb muscles induce divergent changes in maximal passive diameter of arteries (Delp et al., 2000; Stabley et al., 2013). Similar results have also been found in human models used to simulate microgravity. For instance, long-duration (up to 60 days) head-down bed rest has been reported to reduce intimal-medial thickness in the anterior tibial artery (Platts et al., 2009), as well as lumen diameter of the femoral artery and its branch (Bleeker et al., 2005). Therefore, these results indicate that the gross structural adaptations of skeletal muscle arteries in HU rats and humans undergoing head-down bed rest are mainly induced by the influence of mechanical forces.

In both the forelimbs and hindlimbs, cutaneous arteries were less affected by HU, as compared to skeletal muscle

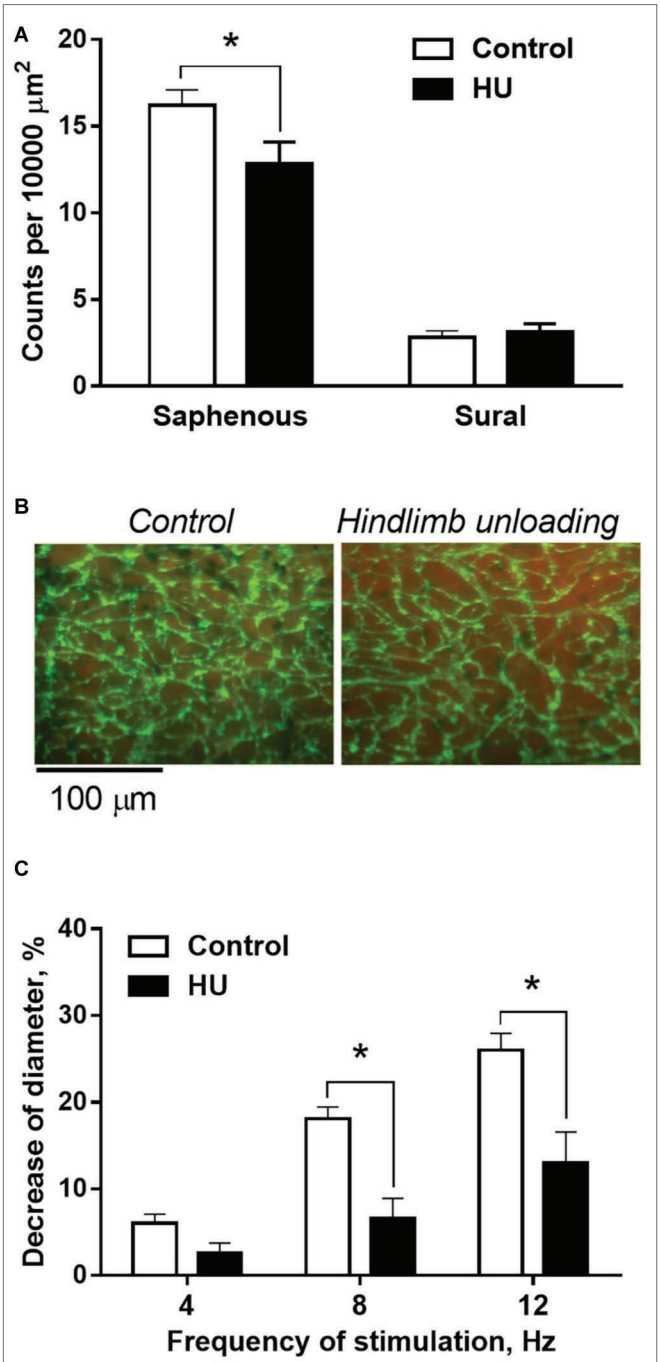

FIGURE 5 | HU worsens sympathetic control in skin but not skeletal muscle feed arteries from rat hindlimb. **(A)** The density of periarterial adrenergic plexus in saphenous and sural arteries from control (n = 10; 10) and HU (n = 8; 7) rats. **(B)** Representative staining for adrenergic nerves with glyoxylic acid in whole-mount preparations of saphenous arteries. **(C)** Constrictor responses of isobarically perfused saphenous arteries from control (n = 5) and HU (n = 5) rats to electrical field stimulation of intramural nerves with graded frequencies. *p < 0.05 HU vs. control.

arteries from the same region of the body. These results may be attributed to several factors. First, cutaneous blood flow would not be as greatly affected by changes in postural support and low level physical activity as that of the skeletal muscle, particularly given the rapid and profound changes in skeletal muscle vascular resistance associated with increases and decreases in muscle activity (Delp, 1999). Second, the profile of blood pressure changes within the cutaneous vasculature may differ from that within the skeletal muscle vascular tree. A prominent constriction of proximal cutaneous arteries during sympathetic activation (Tarasova et al., 2003) would decrease transmural pressure in more distal arteries (Abboud and Eckstein, 1966) and protect them from redistribution of transmural pressure during HU.

Hindlimb Unloading Had Diverse Effects in Two Functionally Different Vascular Beds of the Rat Hindlimb

In the hindlimb, 2-week exposure to HU impaired sympathetic nerve-mediated vasoconstriction while enhancing the sensitivity of smooth muscle to the adrenergic agonist noradrenaline in cutaneous arteries. The higher constrictor sensitivity of cutaneous arteries was also observed after endothelium removal and with the application of the non-adrenergic agonist serotonin, pointing to its independence of the type of activated receptors in smooth muscle cells. These data suggest the development of non-specific hyper-sensitivity of the saphenous artery to constrictor stimulation, which may result from the deficiency in its sympathetic control. This suggestion is based on several observations from the present and earlier published studies: (1) the higher sensitivity to constrictors was observed in densely innervated saphenous artery but not in the sparsely innervated sural artery; (2) HU reduced the density of adrenergic plexus in saphenous arteries; and (3) denervated vessels are well-known to become hyper-sensitive to various constrictor agonists and high-K^+ depolarization (Bevan, 1984; Bentzer et al., 1997; Tarasova et al., 2006). Post-denervation hyper-sensitivity occurs without changes in total density or affinity of post-junctional α_1-adrenoceptors (Dalessandri et al., 1991; Taki et al., 2004), indicating its mechanisms of effect are downstream to the receptors and may include depolarization of smooth muscle cells (Fleming, 1999), facilitation of L-type Ca^{2+}-channel-dependent signaling (Heumann et al., 2016), Ca^{2+}-sensitization of smooth muscle contractile machinery (Puzdrova et al., 2014), and altered cell-to-cell coupling (Slovut et al., 2004). Taken together, these observations allow the conclusion that the shortage of sympathetic influences may govern functional remodeling of arteries subjected to gravitational unloading.

In our opinion, the effect of HU on saphenous artery sympathetic innervation is due in part to a drop in transmural pressure in hindlimb arteries during long-term anti-orthostasis (Colleran et al., 2000). It is well-known that the functional state of postganglionic nerve fibers and the density of sympathetic innervation is controlled by target tissue-derived trophic factors, including nerve growth factor (NGF) (Creedon and Tuttle, 1991; Thrasivoulou and Cowen, 1995). For example, it has been shown that NGF secretion by vascular smooth muscle cells in cell culture increases with stretch

(Clemow et al., 2000). Presumably, the production of NGF under *in vivo* conditions is also dependent on the stretch induced by the transmural pressure. A chronic decrease in transmural pressure in the saphenous artery of HU rats could suppress NGF production and, therefore, result in the decrease of adrenergic nerve plexus density. We have shown previously that chronic hindquarter hypotension (induced by partial occlusion of the abdominal aorta distal to the renal arteries) has negative effects on sympathetic innervation of the rat saphenous artery (Tarasova et al., 2006). Interestingly, an opposite change of innervation density was demonstrated in the rat saphenous artery after the 2-week experimental orthostatic body position (Monos et al., 2001). Results from the present study thus indicate that chronic decreases in transmural pressure worsens sympathetic vasomotor control at the prejunctional level, but at the same time, increases vessel reactivity to noradrenaline, a principal transmitter of the sympathetic nerves. Further work should be conducted to determine whether noradrenaline release during activation of the sympathetic nerves in skin arteries differs between control and HU rats to better characterize how sympathetic neural control of peripheral resistance is altered.

In contrast to cutaneous arteries, we did not find any effect of transmural pressure changes on the adrenergic nerve plexus in the sural artery, probably due to the already low density of its innervation in control rats. However, we suggest that such effects of pressure to decrease the innervation density at distal part of skeletal muscle arterial tree may occur, since the more distal resistance arteries have a higher density of innervation. Indeed, a decrease in the innervation density was observed in hindlimb muscle arterioles in rats after a 4-week HU (Zhang, 2001). This suggestion is supported by our findings of a reduced integral response of perfused rat hindlimb vascular bed to the stimulation of sympathetic nerves (Rodionov et al., 1999).

Our findings indicate that the precision in which the sympathetic nervous system controls peripheral resistance and cutaneous perfusion is compromised in HU rats. Importantly, a decreased vascular sensitivity to sympathetic influences has been observed in humans following space flight (Fu et al., 2002). A smaller increase in lower limb arterial resistance was observed in cosmonauts during infight and postflight lower body negative pressure (LBNP) test (Herault et al., 2000). In contrast, forelimb subcutaneous vascular response to LBNP was more pronounced after 10-day-long space flight than during preflight (Gabrielsen et al., 1995). Although the present study is limited to an animal model used to simulate spaceflight, it provides a mechanistic explanation of the link between the state of sympathetic vascular control with the prevailing changes in transmural pressure thought to occur in astronauts and cosmonauts.

CONCLUSION

A novel result of this study is that simulated microgravity differentially affects the skin and skeletal muscle arteries in the hindlimb. Functional alterations in the vasoconstrictor responses of sparsely innervated skeletal muscle arteries appear to primarily result from the direct effects of physical forces acting on smooth muscle or endothelial cells to induce a gross structural remodeling of these arteries. However, functional changes in the densely innervated cutaneous arteries appear to be mainly governed by the effect of transmural pressure on periarterial sympathetic innervation. If similar adaptations occur in the peripheral vasculature of human cosmonauts and astronauts, such changes could underlie the weaker arterial vasoconstriction during activation of the sympathetic nerves, as well as serve as a mechanism of reduced vascular resistance and orthostatic intolerance following a return to Earth.

DATA AVAILABILITY STATEMENT

The datasets generated for this study are available on request to the corresponding author.

ETHICS STATEMENT

The animal study was reviewed and approved by Biomedical Ethics Committee of the Institute of Biomedical Problems, Russian Academy of Sciences.

AUTHOR CONTRIBUTIONS

OT, AB, VG, MD, and OV conceived and designed the study. OT, VK, AB, and VG were involved in laboratory work, data collection, and analysis. OT, AB, MD, and OV drafted the manuscript. All the authors contributed in the final writing.

FUNDING

The study was performed according to the Plan for Fundamental research of State Research Center of the Russian Federation, Institute of Biomedical Problems, Russian Academy of Sciences (N 64.1).

REFERENCES

Abboud, F. M., and Eckstein, J. W. (1966). Comparative changes in segmental vascular resistance in response to nerve stimulation and to norepinephrine. *Circ. Res.* 18, 263–277. doi: 10.1161/01.RES.18.3.263

Adeoye, O. O., Silpanisong, J., Williams, J. M., and Pearce, W. J. (2015). Role of the sympathetic autonomic nervous system in hypoxic remodeling of the fetal cerebral vasculature. *J. Cardiovasc. Pharmacol.* 65, 308–316. doi: 10.1097/FJC.0000000000000192

Bao, J.-X., Zhang, L.-F., and Ma, J. (2007). Angiotensinogen and AT1R expression in cerebral and femoral arteries during hindlimb unloading in rats. *Aviat. Space Environ. Med.* 78, 852–858.

Bentzer, P., Nielsen, N., Arner, M., Danielsen, N., Ekblad, E., Lundborg, G., et al. (1997). Supersensitivity in rat micro-arteries after short-term

denervation. *Acta Physiol. Scand.* 161, 125–133. doi: 10.1046/j.1365-201X.1997.00177.x

Bevan, R. D. (1984). Trophic effects of peripheral adrenergic nerves on vascular structure. *Hypertension* 6, 19–26. doi: 10.1161/01.hyp.6.6_pt_2.iii19

Bleeker, M. W. P., De Groot, P. C. E., Rongen, G. A., Rittweger, J., Felsenberg, D., Smits, P., et al. (2005). Vascular adaptation to deconditioning and the effect of an exercise countermeasure: results of the Berlin Bed Rest study. *J. Appl. Physiol.* 99, 1293–1300. doi: 10.1152/japplphysiol.00118.2005

Clemow, D. B., Steers, W. D., and Tuttle, J. B. (2000). Stretch-activated signaling of nerve growth factor secretion in bladder and vascular smooth muscle cells from hypertensive and hyperactive rats. *J. Cell. Physiol.* 183, 289–300. doi: 10.1002/(SICI)1097-4652(200006)183:3<289::AID-JCP1>3.0.CO;2-6

Colleran, P. N., Wilkerson, M. K., Bloomfield, S. A., Suva, L. J., Turner, R. T., and Delp, M. D. (2000). Alterations in skeletal perfusion with simulated microgravity: a possible mechanism for bone remodeling. *J. Appl. Physiol.* 89, 1046–1054. doi: 10.1152/jappl.2000.89.3.1046

Creedon, D., and Tuttle, J. B. (1991). Nerve growth factor synthesis in vascular smooth muscle. *Hypertension* 18, 730–741. doi: 10.1161/01.hyp.18.6.730

Dalessandri, K. M., Giri, S. R., Robison, T. W., Hayashi, H. H., and Talken, L. (1991). No change in alpha 1 adrenoceptors in canine femoral arteries after lumbar sympathectomy. *J. Investig. Surg.* 4, 137–140. doi: 10.3109/08941939109140773

Delp, M. D. (1999). Control of skeletal muscle perfusion at the onset of dynamic exercise. *Med. Sci. Sports Exerc.* 31, 1011–1018. doi: 10.1097/00005768-199907000-00014

Delp, M. D., Colleran, P. N., Wilkerson, M. K., McCurdy, M. R., and Muller-Delp, J. (2000). Structural and functional remodeling of skeletal muscle microvasculature is induced by simulated microgravity. *Am. J. Physiol. Heart Circ. Physiol.* 278, H1866–H1873. doi: 10.1152/ajpheart.2000.278.6.H1866

Eskildsen-Helmond, Y. E. G., and Mulvany, M. J. (2003). Pressure-induced activation of extracellular signal-regulated kinase 1/2 in small arteries. *Hypertension* 41, 891–897. doi: 10.1161/01.HYP.0000058701.11991.C4

Fleming, W. W. (1999). Cellular adaptation: journey from smooth muscle cells to neurons. *J. Pharmacol. Exp. Ther.* 291, 925–931.

Folkow, B. (1982). Physiological aspects of primary hypertension. *Physiol. Rev.* 62, 347–504. doi: 10.1152/physrev.1982.62.2.347

Fu, Q., Levine, B. D., Pawelczyk, J. A., Ertl, A. C., Diedrich, A., Cox, J. F., et al. (2002). Cardiovascular and sympathetic neural responses to handgrip and cold pressor stimuli in humans before, during and after spaceflight. *J. Physiol.* 544, 653–664. doi: 10.1113/jphysiol.2002.025098

Gabrielsen, A., Norsk, P., Videbaek, R., and Henriksen, O. (1995). Effect of microgravity on forearm subcutaneous vascular resistance in humans. *J. Appl. Physiol.* 79, 434–438. doi: 10.1152/jappl.1995.79.2.434

Globus, R. K., and Morey-Holton, E. (2016). Hindlimb unloading: rodent analog for microgravity. *J. Appl. Physiol.* 120, 1196–1206. doi: 10.1152/japplphysiol.00997.2015

Heaps, C. L., and Bowles, D. K. (2002). Nonuniform changes in arteriolar myogenic tone within skeletal muscle following hindlimb unweighting. *J. Appl. Physiol.* 92, 1145–1151. doi: 10.1152/japplphysiol.01031.2000

Herault, S., Fomina, G., Alferova, I., Kotovskaya, A., Poliakov, V., and Arbeille, P. (2000). Cardiac, arterial and venous adaptation to weightlessness during 6-month MIR spaceflights with and without thigh cuffs (bracelets). *Eur. J. Appl. Physiol.* 81, 384–390. doi: 10.1007/s004210050058

Heumann, P., Koenen, A., Zavaritskaya, O., Schütze, K., Ramm, A., Schlüter, T., et al. (2016). Sympathetic denervation facilitates L-type Ca^{2+} channel activation in renal but not in mesenteric resistance arteries. *J. Hypertens.* 34, 692–703. doi: 10.1097/HJH.0000000000000856

Jänig, W., and Häbler, H.-J. (2003). Neurophysiological analysis of target-related sympathetic pathways--from animal to human: similarities and differences. *Acta Physiol. Scand.* 177, 255–274. doi: 10.1046/j.1365-201X.2003.01088.x

Jänig, W., and McLachlan, E. M. (1992). Specialized functional pathways are the building blocks of the autonomic nervous system. *J. Auton. Nerv. Syst.* 41, 3–13. doi: 10.1097/00005344-199321001-00003

Langille, B. L. (1993). Remodeling of developing and mature arteries: endothelium, smooth muscle, and matrix. *J. Cardiovasc. Pharmacol.* 21, S11–S17. doi: 10.1097/00005344-199321001-00003

McDonald, K. S., Delp, M. D., and Fitts, R. H. (1992). Effect of hindlimb unweighting on tissue blood flow in the rat. *J. Appl. Physiol.* 72, 2210–2218. doi: 10.1152/jappl.1992.72.6.2210

Monos, E., Lóránt, M., and Fehér, E. (2001). Influence of long-term experimental orthostatic body position on innervation density in extremity vessels. *Am. J. Physiol. Heart Circ. Physiol.* 281, H1606–H1612. doi: 10.1152/ajpheart.2001.281.4.H1606

Mulvany, M. J., and Halpern, W. (1977). Contractile properties of small arterial resistance vessels in spontaneously hypertensive and normotensive rats. *Circ. Res.* 41, 19–26. doi: 10.1161/01.RES.41.1.19

Platts, S. H., Martin, D. S., Stenger, M. B., Perez, S. A., Ribeiro, L. C., Summers, R., et al. (2009). Cardiovascular adaptations to long-duration head-down bed rest. *Aviat. Space Environ. Med.* 80, A29–A36. doi: 10.3357/asem.br03.2009

Pourageaud, F., and De Mey, J. G. R. (1997). Structural properties of rat mesenteric small arteries after 4-wk exposure to elevated or reduced blood flow. *Am. J. Physiol. Heart Circ. Physiol.* 273, H1699–H1706. doi: 10.1152/ajpheart.1997.273.4.h1699

Puzdrova, V. A., Kargina-Terent'eva, R. A., and Tarasova, O. S. (2009). Effects of chronic hypotension on the adrenergic nervous plexus of the saphenous artery in rats and its regeneration after femoral nerve injury. *Neurosci. Behav. Physiol.* 39, 757–761. doi: 10.1007/s11055-009-9194-7

Puzdrova, V. A., Kudryashova, T. V., Gaynullina, D. K., Mochalov, S. V., Aalkjaer, C., Nilsson, H., et al. (2014). Trophic action of sympathetic nerves reduces arterial smooth muscle $Ca^{(2+)}$ sensitivity during early post-natal development in rats. *Acta Physiol.* 212, 128–141. doi: 10.1111/apha.12331

Rodionov, I. M., Timin, E. N., Matchkov, V. V., Tarasova, O. S., and Vinogradova, O. L. (1999). An experimental study and mathematical simulation of adrenergic control of hindlimb vessels in rats after 3-week tail suspension. *Environ. Med.* 43, 1–9.

Slovut, D. P., Mehta, S. H., Dorrance, A. M., Brosius, F. C., Watts, S. W., and Webb, R. C. (2004). Increased vascular sensitivity and connexin43 expression after sympathetic denervation. *Cardiovasc. Res.* 62, 388–396. doi: 10.1016/j.cardiores.2003.12.024

Stabley, J. N., Dominguez, J. M., Dominguez, C. E., Mora Solis, F. R., Ahlgren, J., Behnke, B. J., et al. (2012). Spaceflight reduces vasoconstrictor responsiveness of skeletal muscle resistance arteries in mice. *J. Appl. Physiol.* 113, 1439–1445. doi: 10.1152/japplphysiol.00772.2012

Stabley, J. N., Prisby, R. D., Behnke, B. J., and Delp, M. D. (2013). Chronic skeletal unloading of the rat femur: mechanisms and functional consequences of vascular remodeling. *Bone* 57, 355–360. doi: 10.1016/j.bone.2013.09.003

Sun, B., Zhang, L.-F., Gao, F., Ma, X.-W., Zhang, M.-L., Liu, J., et al. (2004). Daily short-period gravitation can prevent functional and structural changes in arteries of simulated microgravity rats. *J. Appl. Physiol.* 97, 1022–1031. doi: 10.1152/japplphysiol.00188.2004

Taki, N., Tanaka, T., Zhang, L., Suzuki, F., Israilova, M., Taniguchi, T., et al. (2004). Alpha-1D adrenoceptors are involved in reserpine-induced supersensitivity of rat tail artery. *Br. J. Pharmacol.* 142, 647–656. doi: 10.1038/sj.bjp.0705817

Tarasova, O. S., Puzdrova, V. A., Kalenchuk, V. U., and Koshelev, V. B. (2006). Increase in the sensitivity of the vascular smooth muscle to constrictor factors after denervation and with a decrease in blood pressure. *Biophysics* 51, 805–810. doi: 10.1134/S000635090605023X

Tarasova, O., Sjöblom-Widfeldt, N., and Nilsson, H. (2003). Transmitter characteristics of cutaneous, renal and skeletal muscle small arteries in the rat. *Acta Physiol. Scand.* 177, 157–166. doi: 10.1046/j.1365-201X.2003.01057.x

Thrasivoulou, C., and Cowen, T. (1995). Regulation of rat sympathetic nerve density by target tissues and NGF in maturity and old age. *Eur. J. Neurosci.* 7, 381–387. doi: 10.1111/j.1460-9568.1995.tb00333.x

Tsvirkun, D., Bourreau, J., Mieuset, A., Garo, F., Vinogradova, O., Larina, I., et al. (2012). Contribution of social isolation, restraint, and hindlimb unloading to changes in hemodynamic parameters and motion activity in rats. *PLoS One* 7:e39923. doi: 10.1371/journal.pone.0039923

Watenpaugh, D., and Hargens, A. (1996). "The cardiovascular system in microgravity" in *Handbook of physiology vol. environmental physiology*. eds. M. J. Fregly and C. M. Blatteis (Bethesda, MD: American Physiological Society), 631–674.

Wilkerson, M. K., Muller-Delp, J., Colleran, P. N., and Delp, M. D. (1999). Effects of hindlimb unloading on rat cerebral, splenic, and mesenteric resistance artery morphology. *J. Appl. Physiol.* 87, 2115–2121. doi: 10.1152/jappl.1999.87.6.2115

Zhang, L. F. (2001). Vascular adaptation to microgravity: what have we learned? *J. Appl. Physiol.* 91, 2415–2430. doi: 10.1152/jappl.2001.91.6.2415

Zhang, L.-F. (2013). Region-specific vascular remodeling and its prevention by artificial gravity in weightless environment. *Eur. J. Appl. Physiol.* 113, 2873–2895. doi: 10.1007/s00421-013-2597-8

Conflict of Interest: The authors declare that the research was conducted in the absence of any commercial or financial relationships that could be construed as a potential conflict of interest.

frontiers in Physiology

BRIEF RESEARCH REPORT
published: 13 January 2020
doi: 10.3389/fphys.2019.01597

Continuous Hemodynamic Monitoring in an Intact Rat Model of Simulated Diving

Svein E. Gaustad[1,2,3], Timofei V. Kondratiev[2,4], Ingrid Eftedal[3] and Torkjel Tveita[2,4,5]*

[1] Møreforskning AS, Ålesund, Norway, [2] Cardiovascular Research Group, Department of Medical Biology, UiT, The Arctic University of Norway, Tromsø, Norway, [3] Department of Circulation and Medical Imaging, Norwegian University of Science and Technology, Trondheim, Norway, [4] Anesthesia and Critical Care Research Group, Department of Clinical Medicine, UiT, The Arctic University of Norway, Tromsø, Norway, [5] Division of Surgical Medicine and Intensive Care, University Hospital of North Norway, Tromsø, Norway

Cardiovascular risk is elevated in divers, but detailed information of cardiac function during diving is missing. The aim of this study was to apply an intact rat model with continuous monitoring of cardiac left ventricular (LV) function in a simulated diving experiment. Thirteen rats were inserted with a LV pressure–volume catheter and a pressure transducer in the femoral artery to measure hemodynamic variables, and randomly assigned to diving (n = 9) and control (n = 4) groups. The diving group was compressed to 600 kPa in air, maintained at pressure for 45 min (bottom phase), and decompressed to surface at 50 kPa/min. Data was collected before, during, and up to 60 min after exposure in the diving group, and at similar times in non-diving controls. During the bottom phase, stroke volume (SV) (−29%) and cardiac output (−30%) decreased, whereas LV end-systolic volume (+13%), mean arterial pressure (MAP) (+29%), and total peripheral resistance (TPR) (+72%) increased. There were no changes in LV contractility, stroke work, or diastolic function. All hemodynamic variables returned to baseline values within 60 min after diving. In conclusion, our simulated dive experiment to 600 kPa increased MAP and TPR to levels which caused a substantial reduction in SV and LV volume output. The increase in cardiac afterload demonstrated to take place during a dive is well tolerated by the healthy heart in our model, whereas in a failing heart this abrupt change in afterload may lead to acute cardiac decompensation.

Keywords: cardiac function, decompression, diving, hyperbaric, left ventricular, rattus norvegicus

OPEN ACCESS

Edited by:
François Guerrero, Université de Bretagne Occidentale, France

Reviewed by:
Marko Ljubkovic, University of Split, Croatia
Danilo Cialoni, Dan Europe Foundation, Italy

****Correspondence:***
Ingrid Eftedal
ingrid.eftedal@ntnu.no

Specialty section:
This article was submitted to Environmental, Aviation and Space Physiology, a section of the journal Frontiers in Physiology

Received: *07 November 2019*
Accepted: *19 December 2019*
Published: *13 January 2020*

Citation:
Gaustad SE, Kondratiev TV, Eftedal I and Tveita T (2020) Continuous Hemodynamic Monitoring in an Intact Rat Model of Simulated Diving. Front. Physiol. 10:1597. doi: 10.3389/fphys.2019.01597

INTRODUCTION

In diving, the body must adjust to hyperbaric environments. There are changes in ambient pressure and breathing gas density, partial gas pressures and thermal conductivity, and added strain from physical exertion, psychological stress, and immersion (Mack and Lin, 1986; Lango et al., 1996; Leffler, 2001; Bennett and Rostain, 2003; Boussuges et al., 2007). As a consequence cardiovascular

function is altered and the diver is exposed to; bradycardia, altered stroke volume (SV), reduced cardiac output (CO) and increased vascular resistance (Bove et al., 1974; Wilson et al., 1977; Shida and Lin, 1981; Molenat et al., 2004; Boussuges et al., 2006; Dujic et al., 2006). Human experiments have reported increased afterload, decrease in LV preload, and decrease in systolic performance after diving (Molenat et al., 2004; Boussuges et al., 2006). Animal experiments have documented increased cardiac contractility when assessed as maximal velocities of LV pressure rise (Stuhr et al., 1989; Risberg et al., 1995).

The sum of environmental stress factors encountered in diving can augment cardiovascular risk (Bove, 2011). While the vast majority of divers have no history of heart disease and active divers score better than the general population on known risk factors (Buzzacott et al., 2018), cardiovascular problems were reported as being prominent – second only to drowning – as cause of diver fatalities in the Divers Alert Network's annual diving report (Buzzacott and Denoble, 2018). Prior human experimental studies of dive-induced cardiovascular changes have largely been limited to recording of baseline and post-dive data (Marabotti et al., 1999; Boussuges et al., 2006; Dujic et al., 2006). Thus, limited knowledge of functional parameters exist to describe the progression of cardiovascular changes taking place during the dive, which may be important for the tolerance of diving stress and outcome.

In this study, we report the set-up and application of a method for continuous monitoring of hemodynamic parameters in an intact, spontaneously breathing rat model. Simulated diving tests were done in an air-filled hyperbaric chamber for animal research. In this model we monitored LV pressure–volume relationship during all phases of a 600-kPa dry air dive: pre-dive, bottom phase, decompression, and post-dive.

MATERIALS AND METHODS

Ethics

The research protocol was approved in advance by the Norwegian Council for Animal Research (approval ID 2111). All experimental procedures conformed to The European Convention for the Protection of Vertebrate Animals used for Experimental and Other Scientific Purposes (ETS 123).

Animals

Adult female Sprague Dawley rats (Weight 259 ± 6.3 g) were obtained from Charles River Laboratories (Charles River Laboratories Inc., Sulzfeld, Germany). The animals were controlled at a 12 h dark-12 h light cycle with access to a standard rodent diet and water *ad libitum*. In order to limit stress, the same person handled the animals throughout the study and all experimental procedures were performed during the animals' dark cycle.

Anesthesia

Anesthesia was induced by an i.p. bolus injection of sodium pentobarbital (50 mg/kg + Fentanyl 0.05 mg/kg body weight). One hour later, a second bolus injection (25 mg/kg + Fentanyl 0.025 mg/kg body weight i.p.) was given. The rats remained under anesthesia for the duration of the invasive procedures and the experimental diving protocol, after which they were sacrificed by decapitation.

Respiratory Support

To secure patent airways, the trachea was opened and a small-size metal tube (13G) inserted. Following surgery, the animals rested for 60 min to regain hemodynamic stability before the simulated diving commenced. All animals maintained spontaneous ventilation throughout the experiment.

Catheterization for Hemodynamic Monitoring

A microtip pressure–volume (P–V) catheter (SPR-838, 2.0 F, Millar Instruments, Houston, TX, United States) was inserted into the right carotid artery and gently advanced into the LV under pressure guidance. A similar microtip catheter measuring the mean arterial pressure (MAP) was positioned in the left femoral artery. MAP, and pressure–volume signals were digitized at 1 kHz and recorded using ADInstruments LabChart DAQ software (AD Instruments, Hastings, United Kingdom). This software displays P–V raw data in a scrolling strip chart format and plots parameters against each other in real-time, ensuring continuous monitoring of P–V loop data. Data is saved to a hard disk on request. The recorded data; HR, maximal LV systolic pressure, LV end-diastolic pressure, maximal slope of LV systolic pressure increment (dP/dt_{max}) and diastolic pressure decrement (dP/dt_{min}), time constant of LV pressure decay, Tau (τ), SV, end-diastolic volume, end-systolic volume, CO, and stroke work were analyzed off-line using a cardiac pressure–volume analysis program (PVAN 3.6, Millar Instruments, Houston, TX, United States). Data were collected during steady-state baseline conditions, and during transient inferior vena cava occlusions performed to vary LV preload for determination of load-independent indices of systolic function such as preload recruitable stroke work (PRSW). Respiration frequency was determined by analyzing respiration-dependent, cyclic changes in the LV pressure curve.

Temperature Monitoring

The animals were placed in a supine position on an electric heat pad to maintain appropriate temperature (37°C) throughout the experiment. Their core temperature was continuously monitored using a thermocouple wire with the sensor tip positioned in the lower 1/3 of the esophagus and connected to a digital thermometer (Thermoalert, Columbus Instruments, Columbus, OH, United States). For diving animals, the thermocouple controller was placed inside the hyperbaric chamber and monitored through an armored window.

Simulated Diving Protocol

On each day of simulated diving, individual rats were randomly assigned to one of two groups: one diving (n = 9) and one

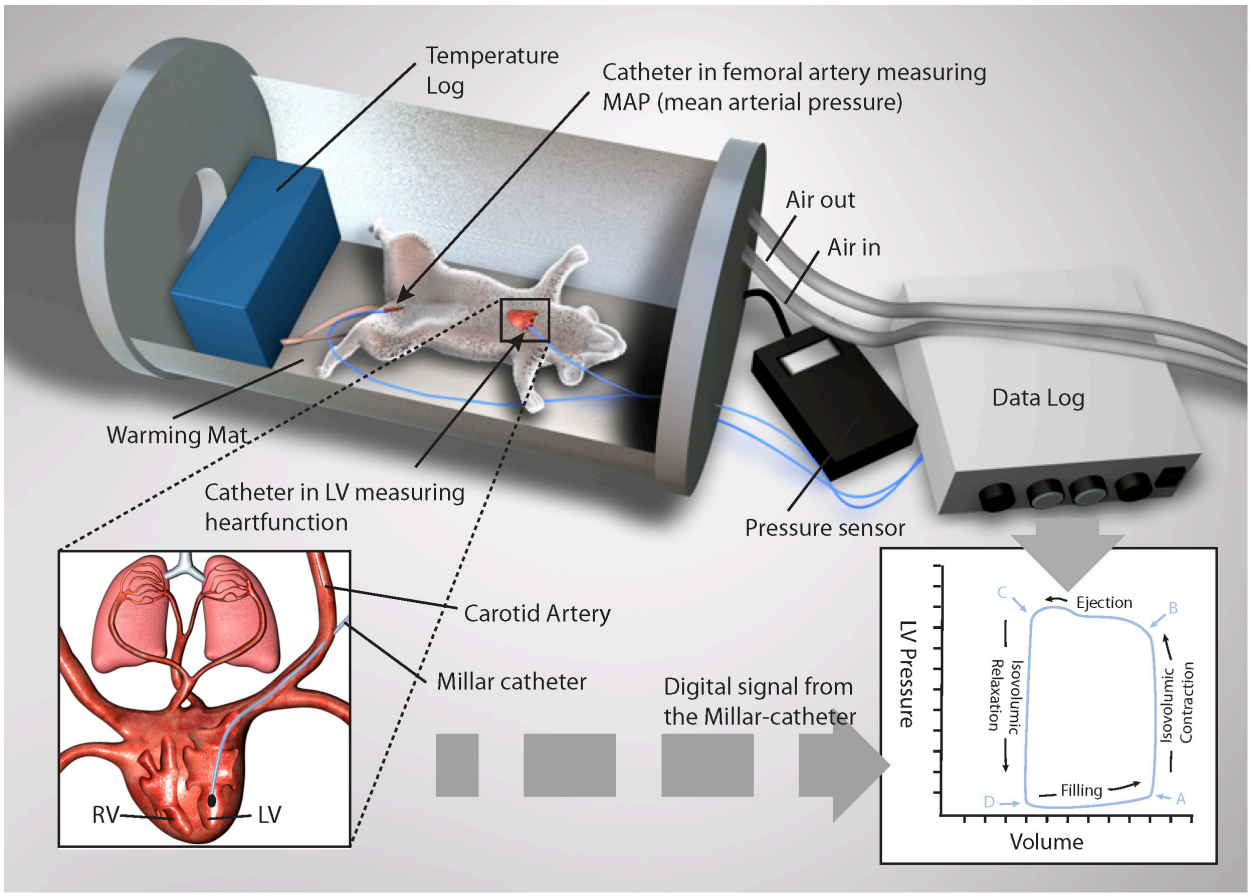

FIGURE 1 | Depiction of pressure volume loop (PV-loop) recordings in an anesthetized rat during simulated diving. A Millar catheter was inserted into the left ventricle and femoral artery. Illustration made on request by MGS studios.

non-diving control group ($n = 4$). Anesthetized rats were exposed to simulated diving one at a time in hyperbaric air in a pressure chamber for animal research (Sira Engineering, Trondheim, Norway). The experimental set-up is illustrated in **Figure 1**. Compression was done at a rate of 200 kPa min^{-1} to a pressure of 600 kPa (corresponding to 50 m water depth). The rat was maintained at pressure for 45 min while breathing air, before being decompressed to the surface over 10 min at a linear rate of 50 kPa min^{-1}. The decompression was followed by a 60 min observation phase at surface pressure.

Hemodynamic Data Recording

In the diving group, hemodynamic data were recorded at baseline (pre-dive), at 1, 2, 2.5, 5 min during the bottom phase, and subsequently every 10 min until 45 min when the bottom phase ended. During the decompression, recordings were done every 2 min, and during the post-dive observation phase, the rats were monitored after 2 min and then every 10 min up to 60 min. In the control group, hemodynamic parameters were recorded 60 (baseline), 120 and 180 min after the trachea surgery and hemodynamic catheterization.

Vascular Bubble Detection

Immediately after the completion of decompression, the pulmonary artery and aorta of diving rats were insonated using a GE Vingmed Vivid i ultrasonic scanner (GE Vingmed Ultrasound, Horten, Norway), with a 10 MHz transducer as previously described (Wisloff and Brubakk, 2001). Ultrasound images were graded according to a method described previously (Eftedal and Brubakk, 1997). The insonation was repeated at 10-min intervals up 60 min post-dive.

Statistics

Statistical analysis was done in SigmaPlot software (Systat Software Inc., San Jose, CA, United States). Normal distribution was checked using Shapiro–Wilk test. Within groups, hemodynamic data were analyzed by one-way repeated measures ANOVA for normal distributed variables and by Friedman repeated measures ANOVA on ranks for non-normal distributed variables. If the intragroup difference among values was greater than would be expected by chance, Dunnett's test was used to evaluate differences between baseline value and responses to simulated diving at different time points. Differences were

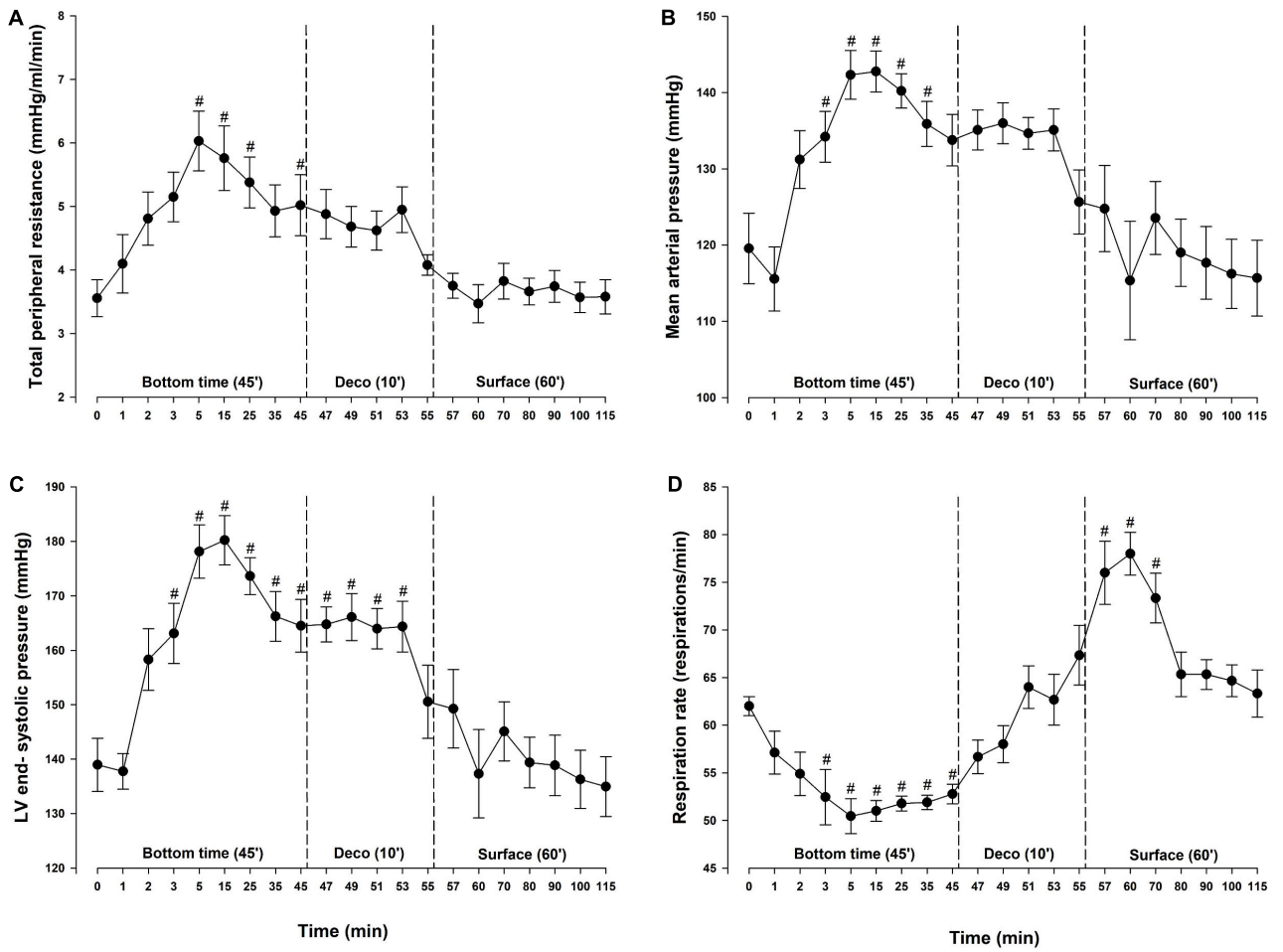

FIGURE 2 | Determinants of cardiac afterload and respiration. **(A)** Total peripheral resistance (TPR), **(B)** mean arterial pressure (MAP), **(C)** left ventricular (LV) end-systolic pressure and **(D)** respiration rate (RR) in rats exposed to simulated diving (n = 9). Data were assessed using one-way repeated measures ANOVA for normal distributed variables and Friedman repeated measures ANOVA on ranks for non-normal distributed variables. Values are mean ± SEM. #$p < 0.05$ compared to intragroup baseline.

considered significant at $p < 0.05$. Results are presented as means ± SEM.

RESULTS

At baseline, after surgery and 60 min rest, there were no differences in hemodynamic variables between diving and non-diving animals. The stability of the model was demonstrated as no change in hemodynamic variables in time-matched, non-diving controls. All animals survived the experimental protocol.

General Stress Assessment

For diving animals, respiration rate (RR) was significantly decreased 2.5 min after reaching the bottom pressure at 600 kPa and remained below baseline throughout the bottom phase (**Figure 2D**). At surface, after decompression, RR exceeded baseline values before returning to normal within 15 min. Vascular bubbles were observed in two rats during the post-dive observation period; both with max bubble grade 2 on the Eftedal-Brubakk scale (Eftedal and Brubakk, 1997).

LV Hemodynamic Function

During diving, MAP and total peripheral resistance (TPR) increased by 29 and 72%, respectively, and remained elevated throughout the bottom phase (**Figures 2A,B**). During the bottom phase a linear reduction in SV took place in parallel with a reduction in CO. At 5 min bottom time SV was decreased by 29% (**Figure 3B**). Heart rate remained stable throughout the experiment (**Figure 3C**) and thus the concurrent 30% reduction in CO (**Figure 3A**) was due to the decrease in SV only. During compression, following the abrupt increase in MAP and TPR, LV end-systolic volume increased to levels reaching significance at 5 (+13%) and 35 (+10%) -min bottom time, but remained unaltered during decompression (**Figure 3E**). A simultaneous elevation of LV end-systolic pressure (+29%) was measured during the bottom phase (**Figure 2C**). It remained

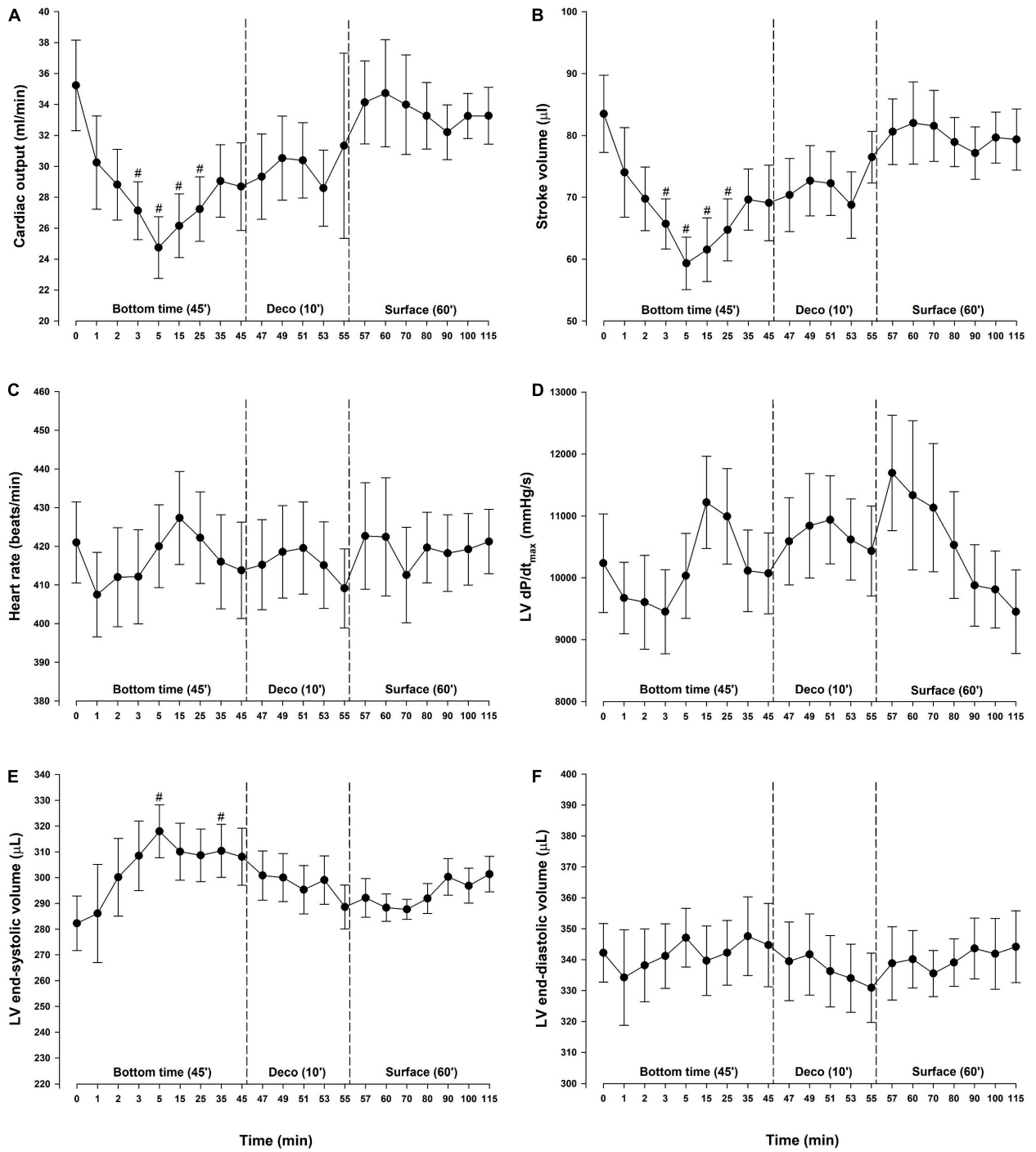

FIGURE 3 | Cardiac output and its determinants. **(A)** Cardiac output (CO), **(B)** stroke volume (SV), **(C)** heart rate (HR), **(D)** maximal slope of left ventricular systolic pressure increment (LV dP/dt_{max}), **(E)** left ventricular (LV) end-systolic volume and **(F)** left ventricular (LV) end-diastolic volume in rats exposed to simulated diving ($n = 9$). Data were assessed using one-way repeated measures ANOVA for normal distributed variables and Friedman repeated measures ANOVA on ranks for non-normal distributed variables. Values are mean ± SEM. #$p < 0.05$ compared to intragroup baseline.

elevated during decompression, before returning to normal at the surface. LV end-diastolic volume was unchanged throughout the simulated dive (**Figure 3F**). Stroke work (mmHg·µL), LV dP/dt_{min} (mmHg/s) and LV end-diastolic pressure (mmHg) were unchanged (data not shown). No change in cardiac contractility was detected when determined by calculating PRSW before compression (76.2 ± 5.9) and after decompression (68.5 ± 9.7) (data not shown). Another determinant of cardiac

contractility, dP/dt_{max}, was continuously measured but showed no change (**Figure 3D**).

DISCUSSION

The present experiment demonstrated an abrupt increase in LV cardiac afterload occuring already in the first 5 min of a 600-kPa simulated air dive, to an extent which reduced both SV and CO by ∼30%. The increase in afterload was substantiated as increases in MAP and TPR which caused a physiologic increase in LV end-systolic pressure and volume and a subsequent reduction in SV. The LV volume output remained reduced during the bottom phase but was reversed within 60 min post-dive. To the best of our knowledge, this is the first report of real-time hemodynamic monitoring in response to changes in ambient pressure.

Most studies of dive-induced cardiovascular changes have recorded hemodynamic variables at baseline and after the dive only. Some have reported cardiovascular responses to increased ambient pressures at discreet time points during the bottom phase, but not measured LV function continuously (Stuhr et al., 1989; Risberg et al., 1995; Molenat et al., 2004; Boussuges et al., 2007). In man, hyperbaric hyperoxic exposure up to 300 kPa air pressure produced no change in CO after 15 min, but a decrease was seen after 5 h (Molenat et al., 2004; Boussuges et al., 2007). In the present study, we observed a rapid and significant decrease in CO after 2.5 min at 600 kPa. Since heart rate remained unchanged, the reduction of CO in our study was explained by a decrease in SV, in accordance with the earlier findings (Molenat et al., 2004). Our observations are supported by Stuhr et al. (1989) who observed pronounced changes in cardiac function at an ambient pressure of 500 kPa. The reduced SV took place in parallel with the increase in LV end-systolic volume, whereas LV end-diastolic volume remained unchanged. This in support of our interpretation that the reduced SV was a consequence of the abrupt increase in afterload. Further, the unchanged LV end-diastolic volume indicated that pulmonary artery pressure did not increase (Valic et al., 2005) to a level which compromised LV filling. This may imply that right ventricular function and LV preload remained unaltered at pressure in our experiment.

Due to a 70% increase in vascular resistance during the bottom phase, MAP, and thus cardiac afterload, increased significantly. The product of HR and MAP, also termed the double product, is often used to determine stress put on the cardiac muscle during exercise as it correlates with changes in myocardial oxygen consumption (MVO_2) (Amsterdam and Mason, 1977). Due to physiologic baroreflex stabilization during exercise; if afterload is increased abruptly, HR will fall, and vice versa (van Vliet and Montani, 1999). In general, the double product remains relatively unchanged during exercise, interpreted as a way to save MVO_2 during cardiac stress. In the present experiment, however, the 30% increase in MAP is not compensated by a fall in HR. This may represent an abrupt increase in MVO_2, which is well tolerated by the healthy heart, but could be a risk factor in the presence of coronary artery disease or myocardial failure. The partial pressure of oxygen at the bottom phase in our study was 120 kPa, and the increased MAP could be caused by hyperoxia-induced vasoconstriction (Mak et al., 2001; Waring et al., 2003) leading to an increased in vascular resistance (Milone et al., 1999; Waring et al., 2003). This is in line with increased MAP accompanied with increased TPR and LV end systolic pressure in the present study, indicating increased LV afterload.

By monitoring LV dP/dt_{max}, some have reported increased myocardial contractility with increase in ambient pressure (Stuhr et al., 1989; Risberg et al., 1995). However, LV dP/dt_{max} is sensitive to changes in pre- and after-load, which can vary considerably during compression/decompression. This was observed in response to diving in our experiment, making this variable a less reliable index of LV contractility under the present circumstances. But, based on continuous measurements of LV dP/dt_{max} and on PRSW calculated before and after the simulated diving exposure, we are able to conclude that in our experiment all changes in LV function were reversible by decompression.

The protocol for the current study required the animals to be anesthetized, and anesthesia affects vascular tone (Matsukawa et al., 1995). In pilot studies at our laboratory, anesthetized rats did not survive decompression from our usual air dive protocol to 700 kPa. Thus, since we wanted to observe the rats for 60 min after decompression, bottom pressure was reduced to 600 kPa. Future studies are needed to determine why anesthetized rats are more vulnerable to decompression stress.

Our diving rats experienced a drop in respiratory rate during the bottom phase. At high ambient pressure, respiratory function is affected by increased resistive and elastic load, and increased partial pressures of inert gas and oxygen (Moon et al., 2009). As we did not perform respiratory functional measurements we have no additional data to explain the observed decrease in respiratory rate, but other studies have reported decreased alveolar-arterial partial pressure of oxygen difference at high gas densities (Christopherson and Hlastala, 1982; Moon et al., 2009), possibly caused by altered blood flow distribution resulting in a more efficient ventilation perfusion ratio.

Our experiments were performed in a dry pressure chamber, which limits the general interpretation of the result. Dry dives are not directly comparable to SCUBA diving where water immersion induces prolonged cardiovascular changes (Marabotti et al., 1999, 2013; Boussuges et al., 2009), and influences bubble production and DCS risk (Obad et al., 2007; Gaustad et al., 2010). To improve the understanding of cardiovascular responses to wet diving, future studies should include LV pressure–volume recording in immersed animals. It should also be noted that only female rats were included our study. While cardiovascular anatomy is similar for females and males, there are sex differences in cardiovascular function (Huxley, 2007), and we cannot speculate whether the responses would be identical in males.

CONCLUSION

In conclusions, our simulated dive experiment to 600 kPa increased MAP and TRP to levels which caused a substantial reduction in SV and LV volume output. The elevated cardiac stress which takes place during a dive, here demonstrated by the increase in afterload, is well tolerated by the healthy heart but may lead to acute cardiac decompensation in a failing heart.

DATA AVAILABILITY STATEMENT

The datasets generated for this study are available on request to the corresponding author.

ETHICS STATEMENT

The animal study was reviewed and approved by the Norwegian Animal Research Authority.

AUTHOR CONTRIBUTIONS

SG designed the study, and contributed to the experimental work and manuscript writing. TK contributed to the experimental work and statistical analysis. IE contributed to the manuscript writing. TT contributed to the study design and manuscript writing. All authors contributed and approved the final version of the manuscript.

FUNDING

The study was generously supported by the Norwegian Petroleum Directorate, Statoil (now Equinor), ExxonMobil and Gassco under the Competence Program Diving, the Research Council of Norway's Large-scale Programme for Petroleum Research (Petromaks2), and The Norwegian Ministry of Foreign Affairs' (Barents 2020). The funders were not involved in the study design, collection, analysis, interpretation of data, the writing of this article or the decision to submit it for publication.

REFERENCES

Amsterdam, E. A., and Mason, D. T. (1977). Exercise testing and indirect assessment of myocardial oxygen consumption in evaluation of angina pectoris. *Cardiology* 62, 174–189. doi: 10.1159/000169852

Bennett, P. B., and Rostain, J. C. (2003). "Inert gas narcosis," in *Bennett and Elliott's Physiology and Medicine of Diving*, 5th Edn, eds A. O. Brubakk, and T. S. Neumann (Amsterdam: Elsevier Science Limited), 300–322.

Boussuges, A., Blanc, F., and Carturan, D. (2006). Hemodynamic changes induced by recreational scuba diving. *Chest* 129, 1337–1343. doi: 10.1378/chest.129.5.1337

Boussuges, A., Gole, Y., Mourot, L., Jammes, Y., Melin, B., Regnard, J., et al. (2009). Haemodynamic changes after prolonged water immersion. *J. Sports Sci.* 27, 641–649. doi: 10.1080/02640410902717001

Boussuges, A., Molenat, F., Grandfond, A., Regnard, J., Wolf, J. P., Galland, F., et al. (2007). Cardiovascular changes induced by cold water immersion during hyperbaric hyperoxic exposure. *Clin. Physiol. Funct. Imaging* 27, 268–274. doi: 10.1111/j.1475-097x.2007.00747.x

Bove, A. (2011). The cardiovascular system and diving risk. *Undersea Hyperb. Med.* 38, 261–269.

Bove, A. A., Hallenbeck, J. M., and Elliott, D. H. (1974). Circulatory responses to venous air embolism and decompression sickness in dogs. *Undersea Biomed. Res.* 1, 207–220.

Buzzacott, P., and Denoble, P. J. (eds) (2018). *DAN Annual Diving Report 2018 Edition: A Report on 2016 Diving Fatalities, Injuries, and Incidents*. Durham NC: Divers Alert Network.

Buzzacott, P., Edelson, C., Bennett, C. M., and Denoble, P. J. (2018). Risk factors for cardiovascular disease among active adult US scuba divers. *Eur. J. Prev. Cardiol.* 25, 1406–1408. doi: 10.1177/2047487318790290

Christopherson, S. K., and Hlastala, M. P. (1982). Pulmonary gas exchange during altered density gas breathing. *J. Appl. Physiol. Respir. Environ. Exerc. Physiol.* 52, 221–225. doi: 10.1152/jappl.1982.52.1.221

Dujic, Z., Obad, A., Palada, I., Valic, Z., and Brubakk, A. O. (2006). A single open sea air dive increases pulmonary artery pressure and reduces right ventricular function in professional divers. *Eur. J. Appl. Physiol.* 97, 478–485. doi: 10.1007/s00421-006-0203-z

Eftedal, O., and Brubakk, A. O. (1997). Agreement between trained and untrained observers in grading intravascular bubble signals in ultrasonic images. *Undersea Hyperb. Med.* 24, 293–299.

Gaustad, S. E., Brubakk, A. O., Hoydal, M., Catalucci, D., Condorelli, G., Dujic, Z., et al. (2010). Immersion before dry simulated dive reduces cardiomyocyte function and increases mortality after decompression. *J. Appl. Physiol.* 109, 752–757. doi: 10.1152/japplphysiol.01257.2009

Huxley, V. H. (2007). Sex and the cardiovascular system: the intriguing tale of how women and men regulate cardiovascular function differently. *Adv. Physiol. Educ.* 31, 17–22. doi: 10.1152/advan.00099.2006

Lango, T., Morland, T., and Brubakk, A. O. (1996). Diffusion coefficients and solubility coefficients for gases in biological fluids and tissues: a review. *Undersea Hyperb. Med.* 23, 247–272.

Leffler, C. T. (2001). Effect of ambient temperature on the risk of decompression sickness in surface decompression divers. *Aviat. Space Environ. Med.* 72, 477–483.

Mack, G. W., and Lin, Y. C. (1986). Hypothermia impairs but hyperthermia does not promote inert gas elimination in the rat. *Undersea Biomed. Res.* 13, 133–145.

Mak, S., Azevedo, E. R., Liu, P. P., and Newton, G. E. (2001). Effect of hyperoxia on left ventricular function and filling pressures in patients with and without congestive heart failure. *Chest* 120, 467–473. doi: 10.1378/chest.120.2.467

Marabotti, C., Chiesa, F., Scalzini, A., Antonelli, F., Lari, R., Franchini, C., et al. (1999). Cardiac and humoral changes induced by recreational scuba diving. *Undersea Hyperb. Med.* 26, 151–158.

Marabotti, C., Scalzini, A., Menicucci, D., Passera, M., Bedini, R., and L'Abbate, A. (2013). Cardiovascular changes during SCUBA diving: an underwater doppler echocardiographic study. *Acta Physiol.* 209, 62–68. doi: 10.1111/apha.12112

Matsukawa, T., Sessler, D. I., Sessler, A. M., Schroeder, M., Ozaki, M., Kurz, A., et al. (1995). Heat flow and distribution during induction of general anesthesia. *Anesthesiology* 82, 662–673. doi: 10.1097/00000542-199503000-0008

Milone, S. D., Newton, G. E., and Parker, J. D. (1999). Hemodynamic and biochemical effects of 100% oxygen breathing in humans. *Can. J. Physiol. Pharmacol.* 77, 124–130. doi: 10.1139/y99-010

Molenat, F., Boussuges, A., Grandfond, A., Rostain, J. C., Sainty, J. M., Robinet, C., et al. (2004). Haemodynamic effects of hyperbaric hyperoxia in healthy volunteers: an echocardiographic and Doppler study. *Clin. Sci.* 106, 389–395. doi: 10.1042/cs20030293

Moon, R. E., Cherry, A. D., Stolp, B. W., and Camporesi, E. M. (2009). Pulmonary gas exchange in diving. *J. Appl. Physiol.* 106, 668–677. doi: 10.1152/japplphysiol.91104.2008

Obad, A., Palada, I., Valic, Z., Ivanèev, V., Bakoviæ, D., Wisløff, U., et al. (2007). The effects of acute oral antioxidants on diving-induced alterations in human cardiovascular function. *J. Physiol.* 578, 859–870. doi: 10.1113/jphysiol.2006.122218

Risberg, J., Skei, S., and Tyssebotn, I. (1995). Effects of gas density and ambient pressure on myocardial contractility in the rat. *Aviat. Space Environ. Med.* 66, 1159–1168.

Shida, K. K., and Lin, Y. C. (1981). Contribution of environmental factors in development of hyperbaric bradycardia. *J. Appl. Physiol.* 50, 731–735. doi: 10.1152/jappl.1981.50.4.731

Stuhr, L. E., Ask, J. A., and Tyssebotn, I. (1989). Increased cardiac contractility in rats exposed to 5 bar. *Acta Physiol. Scand.* 136, 167–176. doi: 10.1111/j.1748-1716.1989.tb08649.x

Valic, Z., Duplancic, D., Bakovic, D., Ivancev, V., Eterovic, D., Wisloff, U., et al. (2005). Diving-induced venous gas emboli do not increase pulmonary artery pressure. *Int. J. Sports Med.* 26, 626–631. doi: 10.1055/s-2004-830379

van Vliet, B. N., and Montani, J. P. (1999). Baroreflex stabilization of the double product. *Am. J. Physiol.* 277, H1679–H1689. doi: 10.1152/ajpheart.1999.277.5.H1679

Waring, W. S., Thomson, A. J., Adwani, S. H., Rosseel, A. J., Potter, J. F., Webb, D. J., et al. (2003). Cardiovascular effects of acute oxygen administration in healthy adults. *J. Cardiovasc. Pharmacol.* 42, 245–250. doi: 10.1097/00005344-200308000-00014

Wilson, J. M., Kligfield, P. D., Adams, G. M., Harvey, C., and Schaefer, K. E. (1977). Human tecg changes during prolonged hyperbaric exposures breathing N2-O2 mixtures. *J. Appl. Physiol.* 42, 614–623. doi: 10.1152/jappl.1977.42.4.614

Wisloff, U., and Brubakk, A. O. (2001). Aerobic endurance training reduces bubble formation and increases survival in rats exposed to hyperbaric pressure. *J. Physiol.* 537(Pt 2), 607–611. doi: 10.1111/j.1469-7793.2001.00607.x

Conflict of Interest: SG was employed by the company Møreforskning AS.

The remaining authors declare that the research was conducted in the absence of any commercial or financial relationships that could be construed as a potential conflict of interest.

frontiers in Physiology

ORIGINAL RESEARCH
published: 22 October 2019
doi: 10.3389/fphys.2019.01342

A Single Simulated Heliox Dive Modifies Endothelial Function in the Vascular Wall of ApoE Knockout Male Rats More Than Females

Simin Berenji Ardestani[1,2], Vladimir V. Matchkov[3], Ingrid Eftedal[2,4] and Michael Pedersen[1]*

[1] Department of Clinical Medicine, Comparative Medicine Lab, Aarhus University, Aarhus, Denmark, [2] Department of Circulation and Medical Imaging, Faculty of Medicine and Health Sciences, NTNU: Norwegian University of Science and Technology, Trondheim, Norway, [3] Department of Biomedicine, Aarhus University, Aarhus, Denmark, [4] Faculty of Nursing and Health Sciences, Nord University, Bodø, Norway

OPEN ACCESS

Edited by:
François Guerrero, Université de Bretagne Occidentale, France

Reviewed by:
Nicolas Vallée, Institut de Recherche Biomédicale des Armées, France
Marc-Antoine Custaud, Université d'Angers, France
Aleksandra Mazur, Novo Nordisk (Denmark), Denmark

***Correspondence:**
Simin Berenji Ardestani
Simin.berenji@clin.au.dk

Specialty section:
This article was submitted to Vascular Physiology, a section of the journal Frontiers in Physiology

Received: *18 June 2019*
Accepted: *09 October 2019*
Published: *22 October 2019*

Citation:
Berenji Ardestani S, Matchkov VV, Eftedal I and Pedersen M (2019) A Single Simulated Heliox Dive Modifies Endothelial Function in the Vascular Wall of ApoE Knockout Male Rats More Than Females. Front. Physiol. 10:1342. doi: 10.3389/fphys.2019.01342

Introduction: The number of divers is rising every year, including an increasing number of aging persons with impaired endothelial function and concomitant atherosclerosis. While diving is an independent modulator of endothelial function, little is known about how diving affects already impaired endothelium. In this study, we questioned whether diving exposure leads to further damage of an already impaired endothelium.

Methods: A total of 5 male and 5 female ApoE knockout (KO) rats were exposed to simulated diving to an absolute pressure of 600 kPa in heliox gas (80% helium, 20% oxygen) for 1 h in a dry pressure chamber. 10 ApoE KO rats (5 males, 5 females) and 8 male Sprague-Dawley rats served as controls. Endothelial function was examined *in vitro* by isometric myography of pulmonary and mesenteric arteries. Lipid peroxidation in blood plasma, heart and lung tissue was used as measures of oxidative stress. Expression and phosphorylation of endothelial NO synthase were quantified by Western blot.

Results and Conclusion: A single simulated dive was found to induce endothelial dysfunction in the pulmonary arteries of ApoE KO rats, and this was more profound in male than female rats. Endothelial dysfunction in males was associated with changing in production or bioavailability of NO; while in female pulmonary arteries an imbalance in prostanoid signaling was observed. No effect of diving was found on mesenteric arteries from rats of either sex. Our findings suggest that changes in endothelial dysfunction were specific for pulmonary circulation. In future, human translation of these findings may suggest caution for divers who are elderly or have prior reduced endothelial function.

Keywords: endothelial dysfunction, apolipoprotein E, atherosclerosis, cardiovascular, saturation diving

INTRODUCTION

Diving is a popular physical activity, and the number of divers is increasing worldwide. In recent years, the average age of the recreational diving population has increased (Denoble et al., 2012; Berenji Ardestani et al., 2015). One-third of active United States scuba divers are reported >50 years old and exposed to several cardiovascular risk factors (Buzzacott et al., 2018). According to the International Marine Contractors Association, commercial divers at work must hold a valid certificate of medical fitness but no upper age limit is stated in the requirements. In the general population, endothelial dysfunction progresses with age and is associated with various cardiovascular diseases (Lakatta and Levy, 2003). Experimental and clinical evidence links endothelial dysfunction to oxidative stress, in which redox balances are disturbed by an imbalance of reactive oxygen species (ROS) and nitric oxide (NO) production (Cai and Harrison, 2000; El Assar et al., 2013; Higashi et al., 2014). In diving, excess oxidative stress is a prominent trait due to physical and chemical stress factors in the hyperbaric environment (Nossum et al., 1999, 2002; Brubakk et al., 2005; Obad et al., 2007; Eftedal et al., 2012, 2013; Mazur et al., 2014b). However, little is known about the effect of diving on the endothelial function in individuals who already are burdened with endothelial dysfunction.

Deficient apolipoprotein E (ApoE) expression impairs plasma lipoprotein metabolism and promotes the development of atherosclerosis (Davignon et al., 1988). ApoE knockout (KO) mice have frequently been used in studies of endothelial dysfunction associated with atherosclerosis and oxidative stress (Plump et al., 1992). These mice suffer from hypercholesterolemia even when they are fed a low-fat diet, and they develop atherosclerotic lesions in the aorta and large arteries already at 10 weeks of age (Plump et al., 1992). ApoE KO rats are now available and develop dyslipidemia and atherosclerotic plaques in carotid arteries already 12 weeks after onset of high-fat diet (Wei et al., 2015; Rune et al., 2018; Lee et al., 2019). This suggests endothelial dysfunction at early age of ApoE KO rats although this was not studied yet. In comparative studies that simulate human diving, rats have been used more than any other species (Lillo et al., 1985; Lillo and Parker, 2000; Bjorkum et al., 2017). In compressed gas diving, the pulmonary vasculature is exposed to oxidative stress and oxygen toxicity due to high partial pressure of oxygen and inert gas bubbles that develop during the decompression (ascent) phase (Butler and Hills, 1979; Wingelaar et al., 2017). Thus, pulmonary arteries may become susceptible to endothelial dysfunction mediated by diving procedures.

In this study, we hypothesized that simulated diving in arteriosclerosis-prone ApoE KO rats would cause endothelial dysfunction in pulmonary circulation, and that this deterioration would be larger in pulmonary than in peripheral, e.g., mesenteric, arteries (Mulvany and Aalkjaer, 1990). Since endothelial characteristics differ between the sexes, males and females were separately assessed in this study (Villar et al., 2008; Mazur et al., 2014a).

MATERIALS AND METHODS

Experiments were conducted in accordance with Animal Research: Reporting of *In Vivo* Experiments (ARRIVE) and the European Convention for the Protection of Vertebrate Animals used for experimental and other scientific purposes, and after permissions from the Norwegian ethical committee for animal experiments, approval number 16/210914; and Ministry of Environment and Food of Denmark, approval number 2018-15-0201-01477.

Animals

A total of 10 male and 10 female ApoE KO rats (Horizon Discovery, Saint Louis, MO, United States) at the age of 6–9 weeks were used. This age can be considered as pre-atherosclerotic (Wei et al., 2015; Rune et al., 2018; Lee et al., 2019) with putative disturbance in endothelial function but no atherosclerotic plaques. All animals arrived to the facility at the age of 4 weeks old and were giving 2 weeks to acclimatize. 8 male Sprague-Dawley (SD) rats (210.1 ± 10.0 g) were included as controls. The ApoE KO rats are produced on the Sprague Dawley background (Rune et al., 2018). The animals were housed 5 per cage (temperature 21 ± 1°C, 12–12 h light-dark cycle) with *ad libitum* access to water and standard chow diet (Special diet service (SDS); Scanbur, Copenhagen, Denmark). The ApoE animals were randomly divided into diving and control groups; male diving (213.4 ± 18.9 g), male control (203.8 ± 23.9 g), female diving (178.2 ± 5.5 g) and female control (201.2 ± 9.5 g). Both diving and control animals were caged in the same cage in the weeks prior to experiment.

Simulated Diving Protocol

Each diving rat was exposed to a hyperbaric heliox gas mixture (80% He and 20% O_2) in a 22 L hyperbaric chamber, starting at 8:00 am. The compression rate was 200 kPa/min until reaching an absolute pressure of 600 kPa, corresponding to 50 meters of seawater (msw). Conscious freely moving rats were exposed to the hyperbaric condition for 60 min, followed by a decompression stage to return to surface pressure at a decompression rate of 50 kP/min (**Figure 1**). Non-diving groups were not exposed to any sham diving.

Post-diving Observation

After decompression, the animals were observed for 15 min to identify signs of decompression sickness, including abnormal walking, paralysis and twitching/convulsions (Pontier et al., 2009). Each rat was then anesthetized with a mixture of midazolam (0.5 mg/100 g), fentanyl (5 mg/100 g) and haldol (0.33 mg/100 g), euthanized by decapitation.

Blood Sampling and Tissue Dissections

Blood samples from the right heart ventricle were collected immediately following anesthesia, in vacutainer 4 mL plastic lithium heparin tubes. The blood was centrifuged at 2200 g for

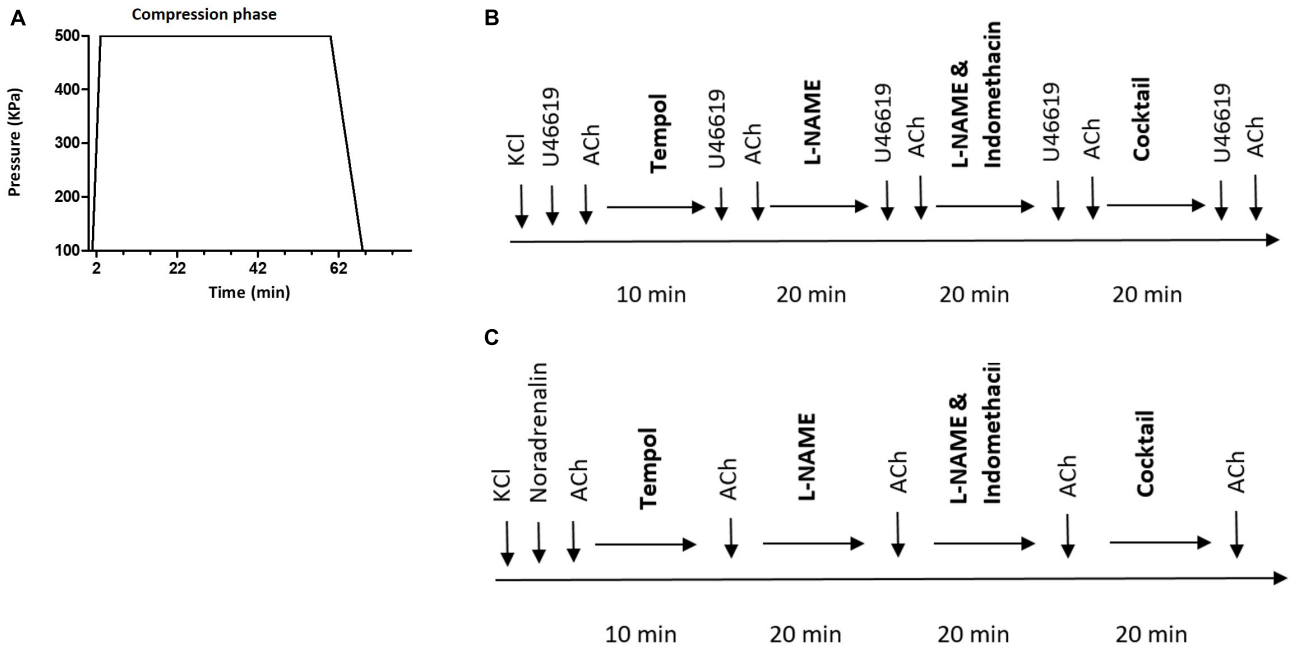

FIGURE 1 | (A) Diving protocol. Each diving rat was exposed to hyperbaric heliox gas mixture (80% He and 20% O_2) with compression rate of 200 kPa/min until it reached an absolute pressure of 600 kPa. The rat was exposed to hyperbaric conditions for 60 min followed by decompression at 50 kP/min; **(B)** schematic presentation of the protocol for myograph experiments on pulmonary and **(C)** mesenteric arteries. Cocktail, a mixture of L-NAME, indomethacin, Tram-34 and apamin; ACh, acetylcholine.

10 min at 20°C within 30 min of collection. Aspirated blood plasma was stored at −80°C until it was assayed. Heart ventricles and right lung were dissected and snap-frozen in liquid N_2, before being stored at −80°C. The pulmonary artery (first bronchial artery in right lobe) and third order branch of the mesenteric artery were dissected. The arteries were transferred to cold physiological saline solution (PSS): NaCl, 119 mM; KCl, 4.7 mM; KH_2PO4, 1.18 mM; MgSO4, 1.17 mM; $NaHCO_3$, 25 mM; $CaCl_2$, 1.6 mM; EDTA, 0.026 mM; and glucose, 5.5 mM, gassed with air, and pH adjusted to 7.4.

Isometric Force Measurement

Immediately after dissection, each vessel was cleaned under a dissection microscope to remove surrounding connective tissues, cut into 2 mm pieces, and mounted in an isometric myograph (Danish Myo Technology, Aarhus, Denmark). The myograph chamber was filled with PSS, heated to 37°C, and constantly gassed with 5% CO_2 in air. Force (in units of mN) was recorded with a PowerLab 4SP and Chart5 acquisition system (ADInstruments, Dunedin, New Zealand) and converted to wall tension (in units of N/m) by dividing the force with twice of vessel segment length.

After a 30 min equilibration period, the arteries were normalized to a passive wall tension where maximal contractile response was measured. This passive wall tension was equivalent to a lumen pressure of 3.9 kPa for the pulmonary artery (Nielsen et al., 2013) while the mesenteric artery segment was stretched to values corresponding 90% of the internal circumference of relaxed artery at 13.3 kPa (Mulvany et al., 1978). Maximal contractile response was assessed in the presence of 100 mM K^+ ions in the bath solution (substituting Na^+ ions with K^+ ions in PSS). Contractility of pulmonary and mesenteric arteries were tested by cumulative applications of U46619, thromboxane analog (10^{-8} to 3×10^{-6} M) and noradrenaline (NA, 10^{-8} to 3×10^{-5} M), respectively. Endothelial function was assessed by relaxing pre-constricted arteries with acetylcholine (ACh: 10^{-7}, 10^{-6} and 10^{-5} M). Pre-constrictions to approximately 80% of maximal constriction were obtained with either U46619 or NA-stimulations of the pulmonary and mesenteric arteries, respectively. Different components of the endothelium-dependent relaxation were inhibited by pre-incubation with inhibitors; arteries were pre-incubated for 20 min with non-selective inhibitor of NO synthase, 100 μM of N(G)-Nitro-*L*-arginine methyl-ester (L-NAME); with non-selective cyclooxygenase inhibitor, indomethacin (3 μM) and with a combination of small and intermittent Ca^{2+}-activated K^+ channel inhibitors, TRAM-34 (1 μM) and apamin (50nM), which have been shown to inhibit the endothelium-dependent hyperpolarizing factor (EDHF) response. Tempol (100 μM, 10 min pre-incubation) was used as superoxide scavenger. At the end of each experiment, endothelial-independent relaxation was tested by adding cumulative doses of sodium nitroprusside (SNP, 10^{-8}–3×10^{-5} M). All drugs were purchased from Sigma-Aldrich (Oslo, Norway).

The experimental protocol is schematically shown in **Figure 1**. No time effect was observed in the separate time-control experiments (data not shown).

Western Blot

Lung tissue was homogenized in lysis buffer (Tris–HCl 20 mM, ethylene glycol tetraacetic acid (5 mM), NaCl (150 mM), glycerophosphate (20 mM), NaF (10 mM), Triton X-100 (1%), Tween-20 (0.1%) and one tablet of protease inhibitor per 10 mL, pH adjusted to 7.5). 10 μg protein was loaded on gel (Criterion TGX gels 4–15%, cat #567-1085) and the gel was run for 1 h at 200 V, and then electrotransferred for 1 h at 100 V to nitrocellulose membranes. The membranes were blocked with 0.3% i-block in TBS-T and incubated with primary antibody overnight at 4°C, and, after washout, with horseradish-peroxidase (HRP)-conjugated secondary antibody (1:5000; Dako, Copenhagen, Denmark) for 2 h at room temperature. Excess antibody was removed by 4 times × 15 min washing, and bound antibody was detected by an enhanced chemiluminiscence kit (ECL, Amersham, United Kingdom). Protein amount was quantified using the ImageJ program (National Institutes of Health, Bethesda, MD, United States) (Bouzinova et al., 2014).

Different primary antibodies were used; e-NOS antibody (1:1.000; ab5589; Abcam, Cambridge, United Kingdom) and phospho-eNOS antibody (1:500; Ser1177; Cell Signaling Technology, Danvers, MA, United States). Pan-actin (1:1.000; #4968; Cell Signaling Technolog) served as loading reference.

Lipid Peroxidation

Oxidative stress was evaluated by measuring the level of lipid peroxidation in heart and lung tissues. Formation of malondialdehyde (MDA) was measured using a thiobarbituric acid reactive substances (TBARS) kit (R&D System, Minneapolis, MN, United States). 10 mg of heart and lung tissue were lysed in 400 μl and 300 μl of lysis buffer (Tris–HCl 10 mM, sucrose 250 mM, EDTA 1 mM, EGTA 1 mM, Triton X-100 2%, pH adjusted to 7.4), respectively. Lung and heart lysates and plasma samples were prepared in accordance with the manufacturer's protocol, and loaded onto a 96-well microplate. The plate was incubated for 2 h at 40–45°C, and MDA absorbance was measured at 532 nm (PHERAstar; BMG Labtech, Ortenberg, Germany). The results were calculated using the standard curve of TBARS Standard and normalized to the total protein content. Total protein content in blood plasma, lung and heart lysates was quantified by bicinchoninic acid (BCA) protein assay kit (Thermo Fisher Scientific, MA, United States) with loading 100 μl of working solution and 1 μl of sample to a 96-well microplate. Samples were measured at 562 nm (PHERAstar; BMG Labtech, Ortenberg, Germany) after 30 min of incubation at 37°C.

Total Cholesterol

Total cholesterol was measured in blood plasma using cholesterol-reagents (Randox CH201; Randox Laboratories, Crumlin, United Kingdom). A volume of 1 μl plasma was mixed with 300 μl cholesterol reagents (1:100) in room temperature and transferred to a spectrophotometer 96-well microplate. Absorbance was measured at 500 nm and 37°C (PHERAstar; BMG Labtech, Ortenberg, Germany). The results were analyzed using a standard curve made with cholesterol standards and cholesterol reagent.

DATA ANALYSES

Vessel contraction was expressed relative to the maximal contraction of KCl (100% of contraction). Vessel relaxation was expressed in percentage of pre-constricted level (0% relaxation) to passive wall tension (100% relaxation). The effect of inhibitors was calculated as a comparison of difference in concentration-response curves before and after administration of the drug. Concentration–response curves were fitted to experimental data using four-parameter, non-linear regression curve fitting. From these curves, $-\log EC_{50}$, where EC_{50} was the concentration required to produce a half-maximal response, and maximal response were derived and compared using an extra sum-of-squares F test. Differences between means were tested by one-way ANOVA followed by Bonferroni *post hoc*-test or by t-test statistics. Results are presented as means ± SEM (standard error of the mean) for all analyses. Based on previous studies, a sample size of five rats per group was expected to give a power of 80%. $P < 0.05$ was considered statistically significant.

RESULTS

All diving rats completed the diving intervention without abnormal walking, paralysis or twitching/convulsions that would signify decompression sickness.

Total Cholesterol Was Elevated in Blood Plasma of ApoE KO Rats

Plasma cholesterol level was significantly elevated in both male and female ApoE KO rats compared to normal plasma cholesterol in Sprague Dawley rats (**Figure 2**). There was no statistical difference in total plasma cholesterol between diving and non-diving groups, although there was a tendency for elevated cholesterol in males compared to females (**Figure 2**, $P = 0.06$).

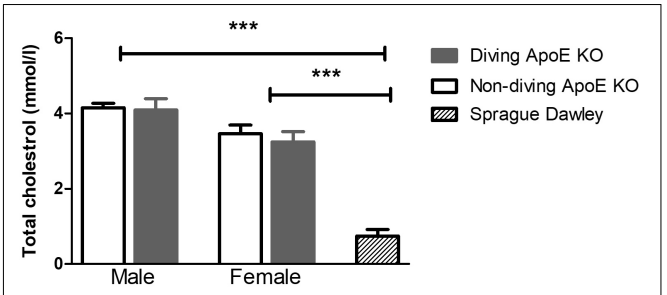

FIGURE 2 | The total cholesterol in blood plasma from ApoE KO male and female rats was significantly higher than in Sprague Dawley rats that form a genetic background for ApoE KO rats, ***$P < 0.001$, ANOVA, $n = 5$.

Pulmonary Arteries From Diving Rats Had Reduced no Production, While Only the Arteries From Female Non-diving Rats Had Increased Contribution of Pro-contractile Prostanoids

Detailed are available in the **Supplementary Figure S1**. Contractile responses of pulmonary arteries to increasing concentrations of U46619 were compared between the experimental groups (**Figure 3**). There was no gender difference between contractile responses of pulmonary arteries from non-diving groups (**Figure 3**). A single diving simulation potentiated contractile responses under control conditions in pulmonary arteries from male, but not female rats (**Figure 3**). Diving significantly potentiated U46619 sensitivity of the arteries from male ApoE KO (**Figure 3**; -logEC$_{50}$ was 7.08 ± 0.08 vs. 6.89 ± 0.14; $n = 5$, $P < 0.001$) and Sprague Dawley rats (**Figure 3**; -logEC$_{50}$ was 7.36 ± 0.11 vs. 7.26 ± 0.08; $n = 4$, $P < 0.001$) in comparison with non-diving groups.

Incubation with tempol, a superoxide scavenger, had no effects on contractions of pulmonary arteries from male non-diving and diving ApoE KO rats (**Figure 3**). In the presence of tempol, pulmonary arteries from diving ApoE KO male still contracted stronger than non-diving ApoE KO controls (**Figure 3**; -logEC$_{50}$ 7.20 ± 0.09 vs. 6.88 ± 0.07, respectively, $n = 5$, $P < 0.001$). In Sprague Dawley males, incubation with tempol significantly suppressed the contraction response in both diving and non-diving group (**Figure 3**; -logEC50 7.20 ± 0.12 vs. 7.23 ± 0.08, respectively, $n = 4$, $P < 0.001$). Contraction of pulmonary arteries from ApoE KO female rats was unaffected by tempol.

Incubation with L-NAME significantly potentiated contraction of pulmonary arteries from all experimental groups in ApoE rats (**Figure 3**; $P < 0.01$). In the presence of L-NAME, the difference between contractile responses of pulmonary arteries from male diving and non-diving ApoE KO was abolished (**Figure 3**; -logEC$_{50}$, 7.32 ± 0.27 vs. 7.40 ± 0.06; $n = 5$, $P = 0.69$). Accordingly, L-NAME also potentiated the contraction of pulmonary arteries from non-diving female rats significantly stronger than the diving females (**Figure 3**; -logEC$_{50}$, 7.30 ± 0.08 vs. 7.18 ± 0.08, $n = 5$, $P < 0.0001$). However, in Sprague Dawley males, incubation with L-NAME significantly suppressed the contraction response in diving pulmonary artery (**Figure 3**; -logEC50, 7.36 ± 0.11 vs. 7.61 ± 0.20, $n = 4$, $P < 0.01$).

Pulmonary artery contractile responses of diving and non-diving males were not changed by addition of indomethacin (**Figure 3**). Pre-incubation with L-NAME and indomethacin significantly suppressed contraction of female pulmonary arteries only from non-diving rats (**Figure 3**; -logEC$_{50}$, 7.05 ± 0.17, $n = 5$, $P < 0.01$). After pharmacological inhibition of all major pathways for endothelium-dependent relaxation,

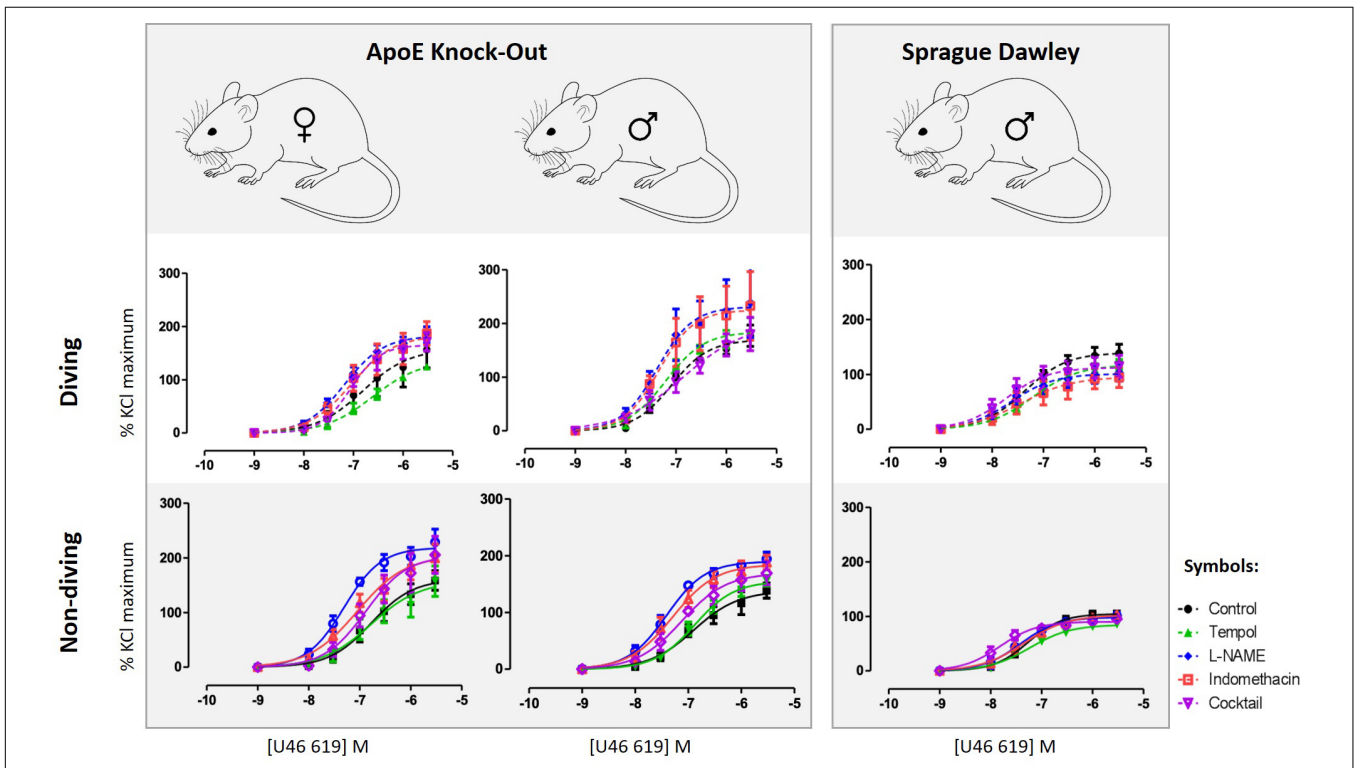

FIGURE 3 | U46619 concentration-response curves of pulmonary arteries from different experimental groups under different experimental conditions; control conditions, following 10 min treatment with superoxide scavenger, Tempol (100 μM), incubation for 20 min with non-selective inhibitor of NO synthase, L-NAME (100 μM), incubation for 20 min with both L-NAME (100 μM) and indomethacin (3 μM); (e) 20 min incubation with L-NAME, indomethacin, TRAM-34 and apamin, i.e., pharmacological inhibition of all major pathways for endothelium-dependent relaxation. *F* test, $n = 5$.

i.e., pre-incubation with L-NAME, indomethacin, TRAM-34 and apamin, no difference between contractile responses of ApoE KO diving and non-diving males, and diving and non-diving females was found. The incubation potentiated the contractile response in male diving Sprague Dawley rats while significantly suppressed the response in ApoE KO male diving rats (**Figure 3**; -logEC50, 7.33 ± 0.02 vs. 6.84 ± 0.30, $n = 5$, $P < 0.02$).

When pre-constricted pulmonary arteries were compared for their ACh-induced relaxation responses, we found no difference between diving and non-diving rats (**Figure 4**). Accordingly, when endothelial-independent relaxation was tested by SNP, no difference between diving and non-diving groups or across sexes was found (**Figure 5**).

No Differences Between Relaxation Responses of Mesentery Arteries to Increasing Concentrations of ACh

Maximal contractile responses to NA of mesenteric arteries from female diving rats were significantly larger in comparison with non-diving females and diving males (**Figure 6**; $P < 0.001$). There was no difference between diving and non-diving ApoE KO groups in NA-induced contraction of mesenteric small arteries from male rats (**Figure 6**; -logEC_{50} 5.28 ± 0.06 vs. 5.03 ± 0.2, $n = 5$).

No differences between the experimental groups after pre-incubation with inhibitors for endothelium-dependent relaxing factors was observed (**Figure 7**). The endothelial-independent relaxation in response to SNP was similar in mesenteric arteries from all experimental groups (**Figure 8**).

No Association Between Diving Simulation and Phosphorylation of eNOS and Oxidative Stress

Our functional study suggested that diving affected NO production in the pulmonary artery of ApoE KO rats. This finding might be due to either changes in eNOS expression, changes in its activation by phosphorylation or NO scavenging in the vascular wall. However, we found no difference in eNOS expression between the groups (**Figure 9**). The relative amount of phosphorylated eNOS (p-eNOS) tended toward an increase in the male diving group (**Figure 9**; 56.17 ± 36.57 vs. 65.08 ± 35.84, $n = 5$), suggesting that reduced NO production was not the reason for observed changes in the vascular tone of pulmonary arteries from diving male rats.

Free radicals might scavenge NO in the vascular wall, and for this reason, we evaluated oxidative stress by measuring lipid peroxidation level in blood plasma, lung and heart tissues. However, no differences were observed between the groups (**Figure 10**).

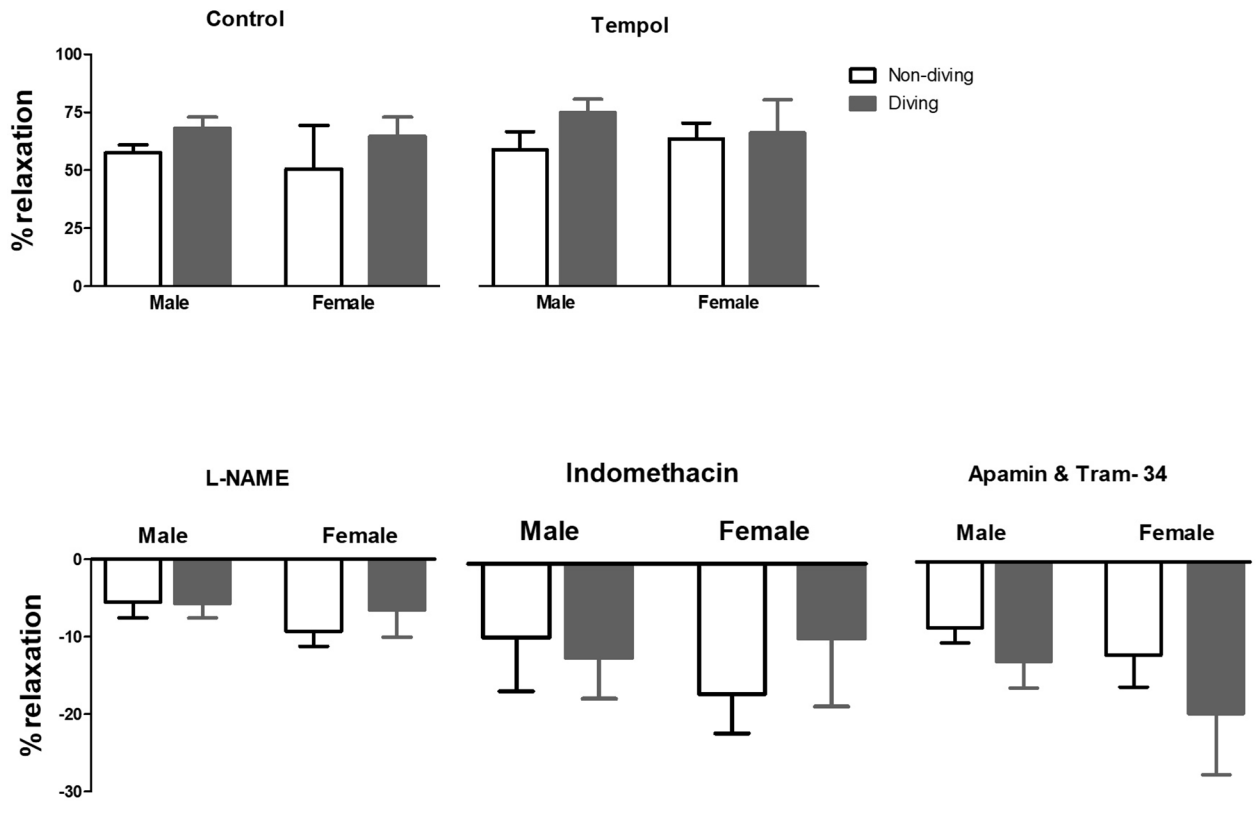

FIGURE 4 | Percentage of relaxation in pulmonary arteries of ApoE KO rats in response to 10–5 M concentration of ACh in the presence of inhibitors for different endothelium-dependent relaxing pathways, ANOVA, $n = 5$.

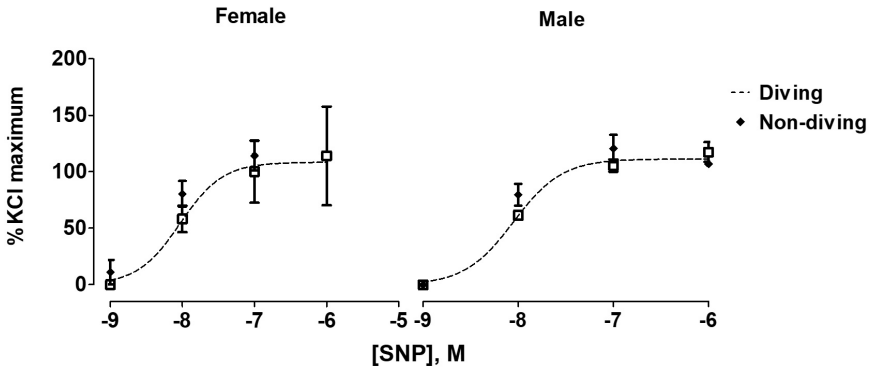

FIGURE 5 | Concentration-response curves to endothelial-independent relaxation by SNP in pulmonary arteries of ApoE KO rats, *F* test.

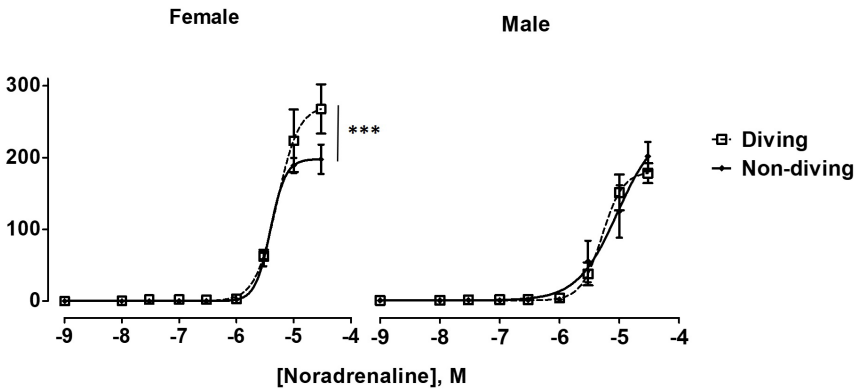

FIGURE 6 | Noradrenaline concentration-response curves of mesentery arteries in ApoE KO rats from different experimental groups under control condition. To fit the experimental data to non-linear regression curves, noradrenaline concentration of 3×10^{-5} M was assumed to induce maximal contractile response in non-diving male rats. ***$P < 0.001$, diving vs. non-diving female rats, *F* test, $n = 5$.

DISCUSSION

The main finding of this study was that simulated diving caused endothelial dysfunction in the pulmonary arteries of ApoE KO rats. In mesenteric arteries from female rats, the contractile response to NA was potentiated after a single diving simulation but does not confirm any endothelial dysfunction since no difference after pre-incubation with endothelium-dependent relaxation inhibitors was observed. This is the first study to include rats that are genetically prone to atherosclerosis, and it supports previous reports on both humans and animals (Nossum et al., 1999; Brubakk et al., 2005). Interestingly, we found that endothelial dysfunction after diving was more severe in male than in female ApoE KO rats. Endothelial dysfunction in males' pulmonary arteries was associated with changing in production or bioavailability of NO. We also observed an imbalance in prostanoid signaling in female pulmonary arteries (**Figure 11**).

Previous studies on humans and animal models have shown that diving causes endothelial dysfunction. An early study on rabbits exposed to simulated diving suggested that endothelial dysfunction in the pulmonary artery arose from mechanical disruption caused by decompression-induced vascular bubbles (Nossum et al., 1999). Later, the endothelial dysfunction and reduction of flow-mediated dilatation (FMD) in the human brachial artery was reported after SCUBA dives with few bubbles (Brubakk et al., 2005). SCUBA diving has since then been shown to affect endothelium-dependent relaxation responses in micro and macro vasculature (Lambrechts et al., 2013). Accordingly, an impaired contractile response to phenylephrine in aorta and mesentery arteries from male rats has been reported as a result of vascular smooth muscle injury without any changes in endothelium-dependent relaxation (Mazur et al., 2014b, 2016). In the present study, we also found no difference in ACh-induced relaxations in neither pulmonary or mesentery arteries. However, the U46619 induced contraction was potentiated in male ApoE KO diving rats compared to the non-diving groups, which is contrary to previous *ex vivo* studies (Mazur et al., 2016). We observed similar results in the Sprague Dawley diving rat suggesting that these changes were due to the diving exposure itself and not the nature of ApoE KOs.

ApoE plays a major physiological role in lipoprotein metabolism; ApoE deficiency is associated with hypercholesterolemia. This makes ApoE KO animals appropriate models for studies of atherosclerotic diseases, which are usually

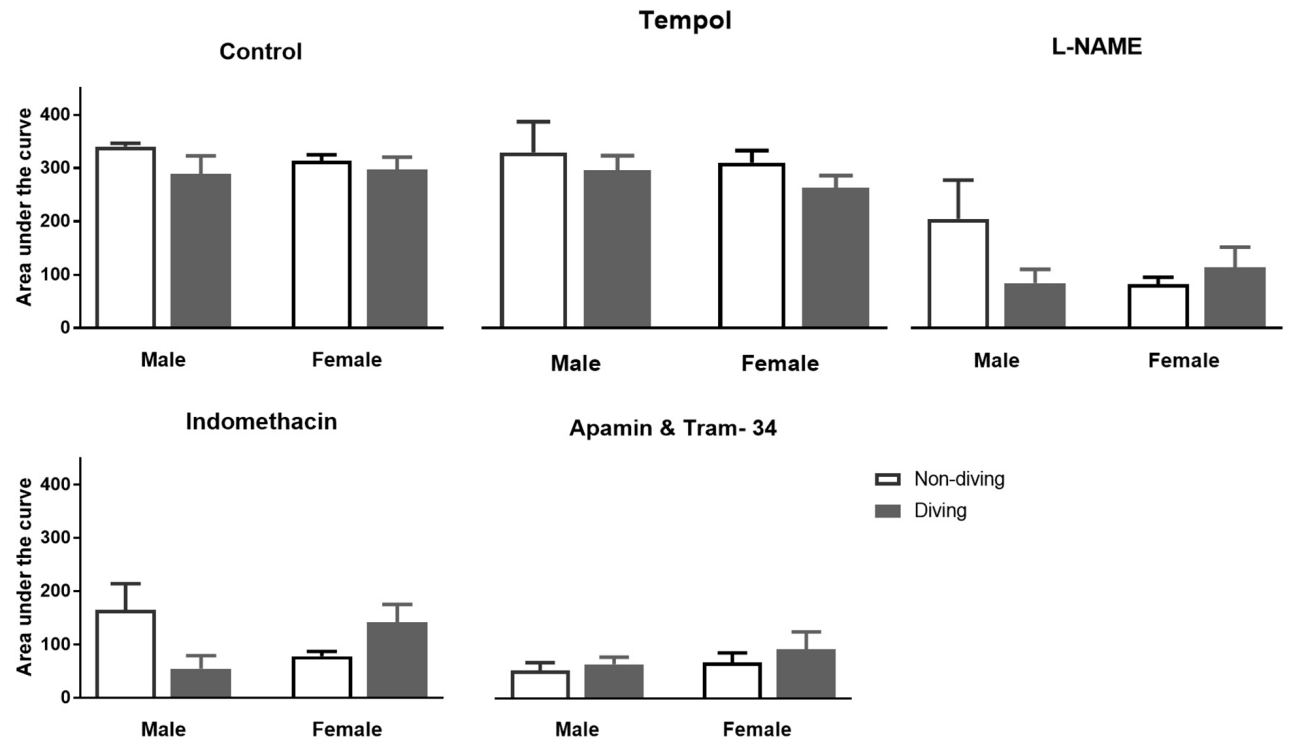

FIGURE 7 | Area under curve for relaxation responses of mesenteric arteries in ApoE KO rats to acetylcholine (ACh) in the presence of inhibitors for different endothelium-dependent relaxing pathways; ANOVA and *t*-test.

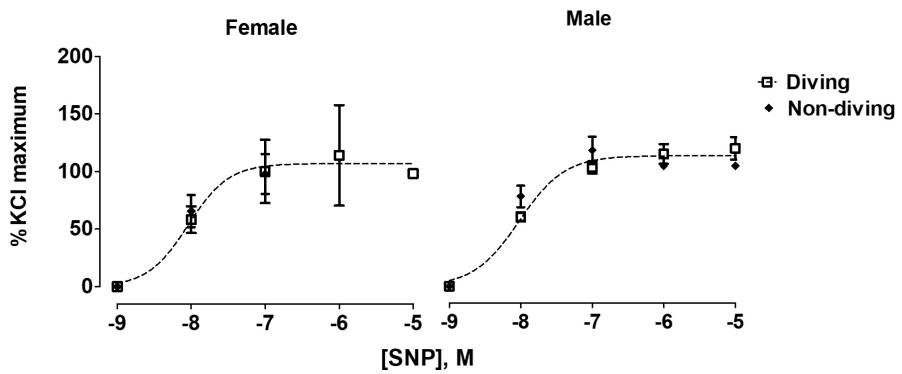

FIGURE 8 | Concentration-response curves for endothelial-independent relaxations to SNP of mesentery arteries of ApoE KO rats from different experimental groups; *F* test, $n = 5$.

absent in rodents (Meir and Leitersdorf, 2004; Rune et al., 2018; Lee et al., 2019). In present study, the rats were fed a chow diet, allowing investigations of the endothelial function at early stage of atherosclerosis and before development of atherosclerotic lesions (d'Uscio et al., 2001; Van Assche et al., 2007). However, ApoE KO rats still had remarkably higher amounts of total cholesterol compared to the Sprague Dawley rats that form the genetic background for the ApoE KOs. Hypercholesterolemia triggers oxidative stress due to increased production of O_2^- and degradation and/or inactivation of NO, leading to endothelium-dependent relaxation dysfunction in ApoE KO animals (Rosenfeld et al., 2002). Importantly, in cardiovascular disease, there is often imbalance between endothelium-derived relaxing factors and endothelium-derived contracting factors, and this shift is usually in favor of the endothelium-derived contracting factors (Gluais et al., 2005; Félétou et al., 2011). This finding could explain the differences between the non-diving ApoE KO and Sprague Dawley rats in this study.

We should emphasize that while we chose to study the pulmonary artery, most of previous *ex vivo* diving studies have examined mesenteric artery and/or aorta. This could explain some of the differences between the current and previously

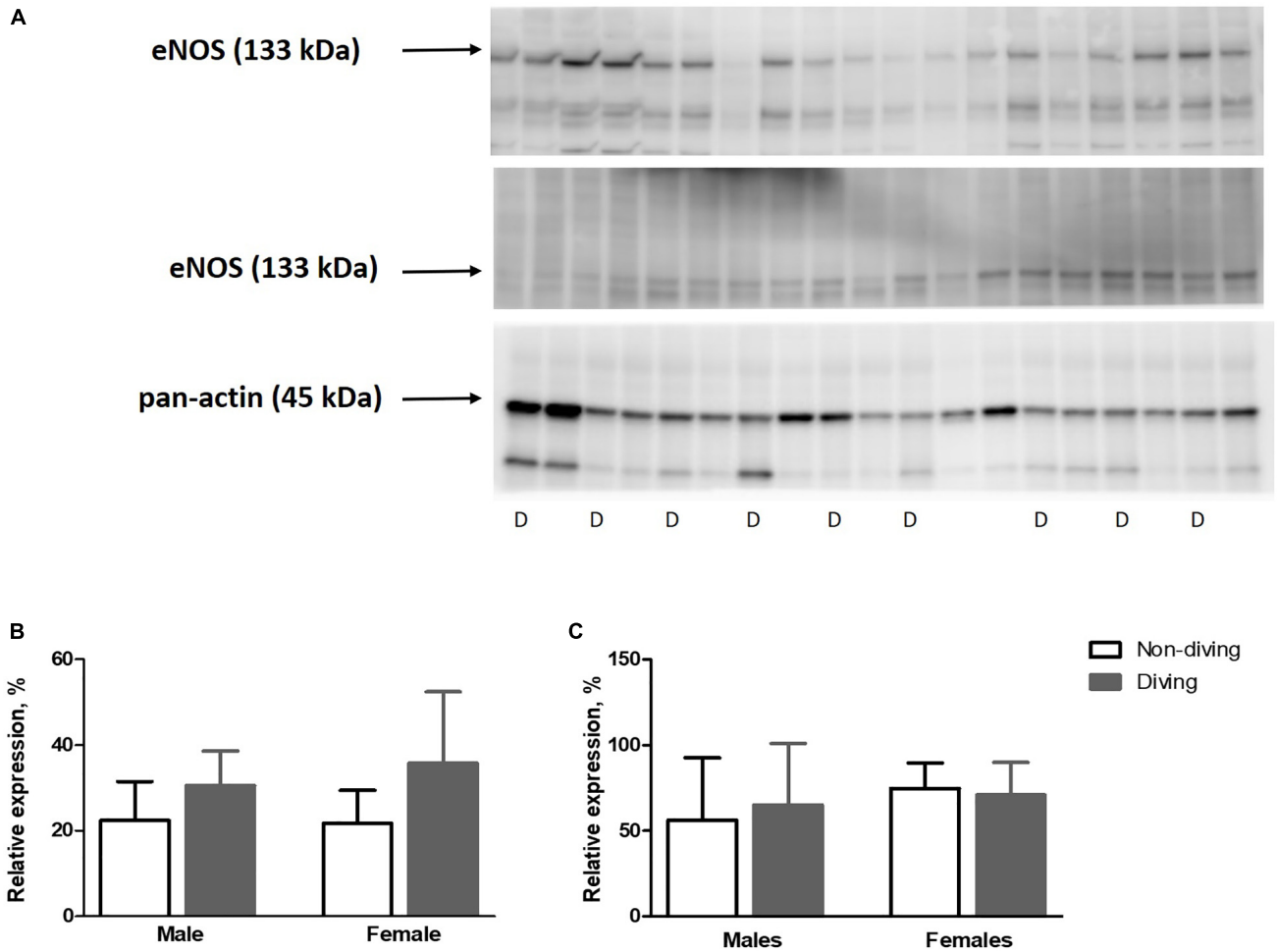

FIGURE 9 | (A) Relative expression of eNOS and p-eNOS proteins quantified by Western blot and normalized to pan-actin as housekeeping protein ApoE KO rats, **(B)**, relative expression of eNOS normalized to pan-actin **(C)**, p-eNOS/eNOS in lung tissue, $n = 5$. eNOS, endothelial nitric oxide synthase; p-eNOS, phosphorylated eNOS; D, diving; ANOVA and *t*-test.

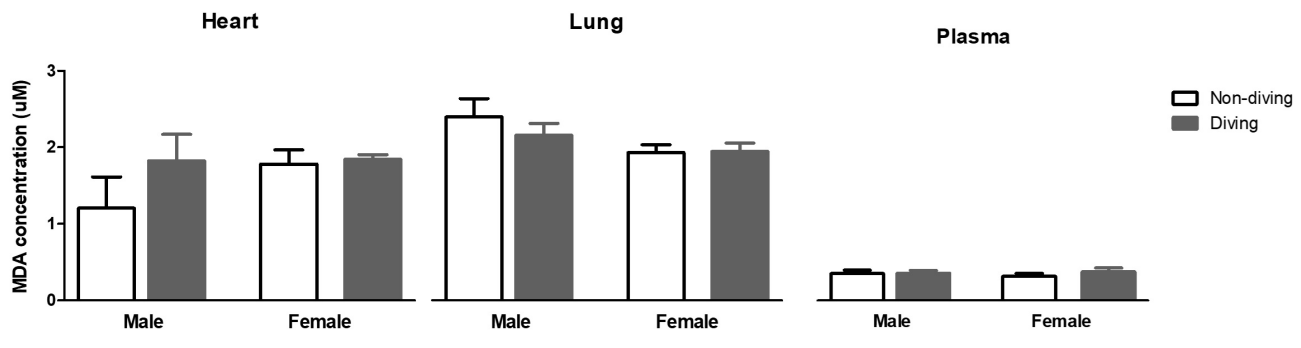

FIGURE 10 | Lipid peroxidation in blood plasma, lung and heart measured as malondialdehyde (MDA) concentration, and normalized to total protein content in ApoE KO rats; ANOVA and *t*-test.

reported results. Due to low pulmonary resistance the pressure in pulmonary artery is much lower than in the systemic arteries. In compressed gas diving, the pulmonary vasculature is exposed to high partial pressure of oxygen levels that border on oxygen toxicity, and causing high levels of oxidative stress (Butler and Hills, 1979; Malik, 2016; Wingelaar et al., 2017). Therefore, we consider the pulmonary artery to be highly relevant in diving studies. We assessed oxidative stress by both MDA

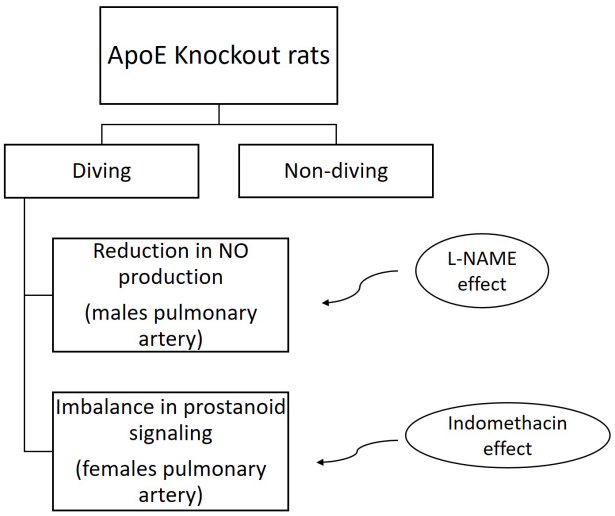

FIGURE 11 | Summery chart of main results.

production measurement and as a contraction to U46619 in the presence of antioxidant tempol. However, we found no indication of increased ROS production that could explain the differences between diving and non-diving rats. It may be worth noting that ventilation with helium has been reported to have an anti-inflammatory effect (Brubakk et al., 2014; Rocco et al., 2019), which may have reduced any side effect of potential O_2 toxicity.

We found no difference in ACh responses in the pulmonary arteries between diving or non-diving groups in this study. This could however be due to technical issues. Pulmonary arteries show tachyphylaxis when accumulatively stimulated with increasing concentrations of ACh. We chose therefore to test the relaxation of pulmonary arteries with applying a single dose of ACh (Boedtkjer et al., 2011). The endothelium-independent relaxation was tested by SNP and found to be unaffected in any groups, in agreement with a previous report (Mazur et al., 2014b). The incubation with L-NAME caused the differences between ApoE KO diving/non-diving and Sprague Dawley rats in U46619 induced contraction. The contraction was potentiated in ApoE KO rats while it was suppressed in Sprague Dawley. L-NAME is a non-selective NO inhibitor, and the observed differences between diving and non-diving ApoE KO rats could be due to changing in production or bioavailability of NO (Okon et al., 2003). However, the mechanism behind suppression of contraction by L-NAME in Sprague Dawley rats is surprising but this could be some indirect effect as it was previously been shown for inhibiting effect of L-NAME on hypoxia-induced contraction (Terraz et al., 1999). As mentioned above, due to hypercholesterolemia, NO production was impaired in APoE KOs compared to the Sprague Dawley rats (Rosenfeld et al., 2002), and we hypothesized that it was even further damaged in diving ApoE KOs. We did not observe any difference in contractile responses to U46619 in pulmonary arteries after inhibition of all endothelium-dependent relaxation factors suggesting that smooth muscle cell function was not affected.

The diving female ApoE KO rats' pulmonary arteries were not affected by L-NAME incubation. U46619 induced contraction was significantly suppressed following incubation with both L-NAME and indomethacin which could be a consequence of changes in prostanoid signaling. We suggest that female APoE KO rats were not affected by diving but this is not surprising; previous studies have shown that endothelium-dependent relaxation is more severely impaired in atherosclerosis arteries of males compared to females, both in humans and animals (Bossaller et al., 1987; Bonthu et al., 1997).

CONCLUSION

In summary, endothelial dysfunction after a single dry heliox dive was associated with changing in bioavailability of NO in males, and altered prostanoid signaling in female ApoE KO rats. Whether repeated diving over time causes persistent changes in endothelial function in divers with atherosclerosis, either worsening from excess oxidative stress or improving via acclimatization, should be evaluated in future studies.

LIMITATIONS

In this study, we focused on the function of the vascular endothelium. Since the changes in vascular smooth muscle cell function after simulated diving were previously reported (Mazur et al., 2014b) we cannot rule out that this may also been the case in this study. We did not assess decompression-induced microbubbles as we prioritized measuring endothelial function as soon as possible without exposure to prolonged anesthesia, which is necessary for ultrasound imaging. Future studies could benefit from the assessment of bubble formation.

DATA AVAILABILITY STATEMENT

All datasets generated for this study are included in the manuscript/**Supplementary Files**.

ETHICS STATEMENT

The animal study was reviewed and approved by Norwegian ethical committee for animal experiments, approval number 16/210914 and Ministry of Environment and Food of Denmark, approval number 2018-15-0201-01477.

AUTHOR CONTRIBUTIONS

All authors designed the study. SB managed the data collection, laboratory work and analysis, and drafted the manuscript. SB and VM conducted the statistical analysis. All the co-authors contributed in the final correction and writing.

FUNDING

This project was funded by the Graduate School of Health, Aarhus University, the Department of Circulation and Medical Imaging, NTNU, and the Norwegian Research Council (Grant Numbers 220546 and 280425).

ACKNOWLEDGMENTS

The authors wish to thank Jane Holbaek Rønn, Astrid Hjelde, and Ragnhild Elisabet Nyhus Røsbjørgen for their laboratory guidance. The rodents housing was provided by the Comparative medicine Core Facility (CoMed), Norwegian University of Science and Technology (NTNU). CoMed is funded by the Faculty of Medicine at NTNU and Central Norway Regional Health Authority.

SUPPLEMENTARY MATERIAL

The Supplementary Material for this article can be found online at: https://www.frontiersin.org/articles/10.3389/fphys.2019.01342/full#supplementary-material

REFERENCES

Berenji Ardestani, S., Buzzacott, P., and Eftedal, I. (2015). The aging diver: endothelial biochemistry and its potential implications for cardiovascular health. *Diving Hyperb. Med.* 45, 235–239.

Bjorkum, A. A., Oveland, E., Stuhr, L., Havnes, M. B., Berven, F., Gronning, M., et al. (2017). Fast hyperbaric decompression after heliox saturation altered the brain proteome in rats. *PLoS One* 12:e0185765. doi: 10.1371/journal.pone.0185765

Boedtkjer, E., Praetorius, J., Matchkov, V. V., Stankevicius, E., Mogensen, S., Fuchtbauer, A. C., et al. (2011). Disruption of Na+,HCO(3)(-) cotransporter NBCn1 (slc4a7) inhibits NO-mediated vasorelaxation, smooth muscle Ca(2)(+) sensitivity, and hypertension development in mice. *Circulation* 124, 1819–1829. doi: 10.1161/circulationaha.110.015974

Bonthu, S., Heistad, D. D., Chappell, D. A., Lamping, K. G., and Faraci, F. M. (1997). Atherosclerosis, vascular remodeling, and impairment of endothelium-dependent relaxation in genetically altered hyperlipidemic mice. *Arterioscler. Thromb. Vasc. Biol.* 17, 2333–2340. doi: 10.1161/01.atv.17.11.2333

Bossaller, C., Habib, G. B., Yamamoto, H., Williams, C., Wells, S., and Henry, P. D. (1987). Impaired muscarinic endothelium-dependent relaxation and cyclic guanosine 5'-monophosphate formation in atherosclerotic human coronary artery and rabbit aorta. *J. Clin. Invest.* 79, 170–174. doi: 10.1172/jci112779

Bouzinova, E. V., Norregaard, R., Boedtkjer, D. M., Razgovorova, I. A., Moeller, A. M., Kudryavtseva, O., et al. (2014). Association between endothelial dysfunction and depression-like symptoms in chronic mild stress model of depression. *Psychosom. Med.* 76, 268–276. doi: 10.1097/psy.0000000000000062

Brubakk, A. O., Duplancic, D., Valic, Z., Palada, I., Obad, A., Bakovic, D., et al. (2005). A single air dive reduces arterial endothelial function in man. *J. Physiol.* 566(Pt 3), 901–906. doi: 10.1113/jphysiol.2005.089862

Brubakk, A. O., Ross, J. A., and Thom, S. R. (2014). Saturation diving; physiology and pathophysiology. *Compr. Physiol.* 4, 1229–1272. doi: 10.1002/cphy.c130048

Butler, B. D., and Hills, B. A. (1979). The lung as a filter for microbubbles. *J. Appl. Physiol. Respir. Environ. Exerc. Physiol.* 47, 537–543. doi: 10.1152/jappl.1979.47.3.537

Buzzacott, P., Edelson, C., Bennett, C. M., and Denoble, P. J. (2018). Risk factors for cardiovascular disease among active adult US scuba divers. *Eur. J. Prev. Cardiol.* 25, 1406–1408. doi: 10.1177/2047487318790290

Cai, H., and Harrison, D. G. (2000). Endothelial dysfunction in cardiovascular diseases: the role of oxidant stress. *Circ. Res.* 87, 840–844. doi: 10.1161/01.res.87.10.840

Davignon, J., Gregg, R. E., and Sing, C. F. (1988). Apolipoprotein E polymorphism and atherosclerosis. *Arteriosclerosis* 8, 1–21.

Denoble, P. J., Ranapurwala, S. I., Vaithiyanathan, P., Clarke, R. E., and Vann, R. D. (2012). Per-capita claims rates for decompression sickness among insured divers alert network members. *Undersea Hyperb. Med.* 39, 709–715.

d'Uscio, L. V., Baker, T. A., Mantilla, C. B., Smith, L., Weiler, D., Sieck, G. C., et al. (2001). Mechanism of endothelial dysfunction in apolipoprotein E-deficient mice. *Arterioscler. Thromb. Vasc. Biol.* 21, 1017–1022. doi: 10.1161/01.atv.21.6.1017

Eftedal, I., Jorgensen, A., Rosbjorgen, R., Flatberg, A., and Brubakk, A. O. (2012). Early genetic responses in rat vascular tissue after simulated diving. *Physiol. Genom.* 44, 1201–1207. doi: 10.1152/physiolgenomics.00073.2012

Eftedal, I., Ljubkovic, M., Flatberg, A., Jorgensen, A., Brubakk, A. O., and Dujic, Z. (2013). Acute and potentially persistent effects of scuba diving on the blood transcriptome of experienced divers. *Physiol. Genom.* 45, 965–972. doi: 10.1152/physiolgenomics.00164.2012

El Assar, M., Angulo, J., and Rodriguez-Manas, L. (2013). Oxidative stress and vascular inflammation in aging. *Free Radic. Biol. Med.* 65, 380–401. doi: 10.1016/j.freeradbiomed.2013.07.003

Félétou, M., Huang, Y., and Vanhoutte, P. M. (2011). Endothelium-mediated control of vascular tone: COX-1 and COX-2 products. *Br. J. Pharmacol.* 164, 894–912. doi: 10.1111/j.1476-5381.2011.01276.x

Gluais, P., Lonchampt, M., Morrow, J. D., Vanhoutte, P. M., and Feletou, M. (2005). Acetylcholine-induced endothelium-dependent contractions in the SHR aorta: the Janus face of prostacyclin. *Br. J. Pharmacol.* 146, 834–845. doi: 10.1038/sj.bjp.0706390

Higashi, Y., Maruhashi, T., Noma, K., and Kihara, Y. (2014). Oxidative stress and endothelial dysfunction: clinical evidence and therapeutic implications. *Trends Cardiovasc. Med.* 24, 165–169. doi: 10.1016/j.tcm.2013.12.001

Lakatta, E. G., and Levy, D. (2003). Arterial and cardiac aging: major shareholders in cardiovascular disease enterprises: part I: aging arteries: a "set up" for vascular disease. *Circulation* 107, 139–146. doi: 10.1161/01.cir.0000048892.83521.58

Lambrechts, K., Pontier, J. M., Balestra, C., Mazur, A., Wang, Q., Buzzacott, P., et al. (2013). Effect of a single, open-sea, air scuba dive on human micro- and macrovascular function. *Eur. J. Appl. Physiol.* 113, 2637–2645. doi: 10.1007/s00421-013-2676-x

Lee, J. G., Ha, C. H., Yoon, B., Cheong, S. A., Kim, G., Lee, D. J., et al. (2019). Knockout rat models mimicking human atherosclerosis created by Cpf1-mediated gene targeting. *Sci. Rep.* 9:2628. doi: 10.1038/s41598-019-38732-2

Lillo, R. S., Flynn, E. T., and Homer, L. D. (1985). Decompression outcome following saturation dives with multiple inert gases in rats. *J. Appl. Physiol.* 59, 1503–1514. doi: 10.1152/jappl.1985.59.5.1503

Lillo, R. S., and Parker, E. C. (2000). Mixed-gas model for predicting decompression sickness in rats. *J. Appl. Physiol.* 89, 2107–2116. doi: 10.1152/jappl.2000.89.6.2107

Malik, A. R. (2016). Association of increased lipid peroxide levels in the aorta in comparison to the pulmonary artery with the presence of coronary artery disease. *Biomed. Rep.* 4, 479–484. doi: 10.3892/br.2016.614

Mazur, A., Buzzacott, P., Lambrechts, K., Wang, Q., Belhomme, M., Theron, M., et al. (2014a). Different effect of l-NAME treatment on susceptibility to decompression sickness in male and female rats. *Appl. Physiol. Nutr. Metab.* 39, 1280–1285. doi: 10.1139/apnm-2014-8

Mazur, A., Lambrechts, K., Buzzacott, P., Wang, Q., Belhomme, M., Theron, M., et al. (2014b). Influence of decompression sickness on vasomotion of isolated rat vessels. *Int. J. Sports Med.* 35, 551–558. doi: 10.1055/s-0033-1358472

Mazur, A., Lambrechts, K., Wang, Q., Belhomme, M., Theron, M., Buzzacott, P., et al. (2016). Influence of decompression sickness on vasocontraction of isolated rat vessels. *J. Appl. Physiol.* 120, 784–791. doi: 10.1152/japplphysiol.00139.2015

Meir, K. S., and Leitersdorf, E. (2004). Atherosclerosis in the apolipoprotein-E-deficient mouse: a decade of progress. *Arterioscler. Thromb. Vasc. Biol.* 24, 1006–1014. doi: 10.1161/01.ATV.0000128849.12617.f4

Mulvany, M. J., and Aalkjaer, C. (1990). Structure and function of small arteries. *Physiol. Rev.* 70, 921–961. doi: 10.1152/physrev.1990.70.4.921

Mulvany, M. J., Hansen, O. K., and Aalkjaer, C. (1978). Direct evidence that the greater contractility of resistance vessels in spontaneously hypertensive rats is associated with a narrowed lumen, a thickened media, and an increased number of smooth muscle cell layers. *Circ. Res.* 43, 854–864. doi: 10.1161/01.res.43.6.854

Nielsen, G., Wandall-Frostholm, C., Sadda, V., Oliván-Viguera, A., Lloyd, E. E., Bryan, R. M., et al. (2013). Alterations of N-3 polyunsaturated fatty acid-activated K2P channels in hypoxia-induced pulmonary hypertension. *Basic Clin. Pharmacol. Toxicol.* 113, 250–258. doi: 10.1111/bcpt.12092

Nossum, V., Hjelde, A., and Brubakk, A. O. (2002). Small amounts of venous gas embolism cause delayed impairment of endothelial function and increase polymorphonuclear neutrophil infiltration. *Eur. J. Appl. Physiol.* 86, 209–214. doi: 10.1007/s00421-001-0531-y

Nossum, V., Koteng, S., and Brubakk, A. O. (1999). Endothelial damage by bubbles in the pulmonary artery of the pig. *Undersea Hyperb. Med.* 26, 1–8.

Obad, A., Palada, I., Valic, Z., Ivancev, V., Bakovic, D., Wisloff, U., et al. (2007). The effects of acute oral antioxidants on diving-induced alterations in human cardiovascular function. *J. Physiol.* 578(Pt 3), 859–870. doi: 10.1113/jphysiol.2006.122218

Okon, E. B., Szado, T., Laher, I., McManus, B., and van Breemen, C. (2003). Augmented contractile response of vascular smooth muscle in a diabetic mouse model. *J. Vasc. Res.* 40, 520–530. doi: 10.1159/000075238

Plump, A. S., Smith, J. D., Hayek, T., Aalto-Setala, K., Walsh, A., Verstuyft, J. G., et al. (1992). Severe hypercholesterolemia and atherosclerosis in apolipoprotein E-deficient mice created by homologous recombination in ES cells. *Cell* 71, 343–353. doi: 10.1016/0092-8674(92)90362-g

Pontier, J. M., Vallee, N., and Bourdon, L. (2009). Bubble-induced platelet aggregation in a rat model of decompression sickness. *J. Appl. Physiol.* 107, 1825–1829. doi: 10.1152/japplphysiol.91644.2008

Rocco, M., Pelaia, P., Di Benedetto, P., Conte, G., Maggi, L., Fiorelli, S., et al. (2019). Inert gas narcosis in scuba diving, different gases different reactions. *Eur. J. Appl. Physiol.* 119, 247–255. doi: 10.1007/s00421-018-4020-y

Rosenfeld, M. E., Kauser, K., Martin-McNulty, B., Polinsky, P., Schwartz, S. M., and Rubanyi, G. M. (2002). Estrogen inhibits the initiation of fatty streaks throughout the vasculature but does not inhibit intra-plaque hemorrhage and the progression of established lesions in apolipoprotein E deficient mice. *Atherosclerosis* 164, 251–259. doi: 10.1016/s0021-9150(02)00178-8

Rune, I., Rolin, B., Lykkesfeldt, J., Nielsen, D. S., Krych, L., Kanter, J. E., et al. (2018). Long-term Western diet fed apolipoprotein E-deficient rats exhibit only modest early atherosclerotic characteristics. *Sci. Rep.* 8:5416. doi: 10.1038/s41598-018-23835-z

Terraz, S., Baechtold, F., Renard, D., Barsi, A., Rosselet, A., Gnaegi, A., et al. (1999). Hypoxic contraction of small pulmonary arteries from normal and endotoxemic rats: fundamental role of NO. *Am. J. Physiol.* 276, H1207–H1214. doi: 10.1152/ajpheart.1999.276.4.H1207

Van Assche, T., Fransen, P., Guns, P. J., Herman, A. G., and Bult, H. (2007). Altered Ca2+ handling of smooth muscle cells in aorta of apolipoprotein E-deficient mice before development of atherosclerotic lesions. *Cell Calcium* 41, 295–302. doi: 10.1016/j.ceca.2006.06.010

Villar, I. C., Hobbs, A. J., and Ahluwalia, A. (2008). Sex differences in vascular function: implication of endothelium-derived hyperpolarizing factor. *J. Endocrinol.* 197, 447–462. doi: 10.1677/joe-08-070

Wei, S., Zhang, Y., Su, L., He, K., Wang, Q., Zhang, Y., et al. (2015). Apolipoprotein E-deficient rats develop atherosclerotic plaques in partially ligated carotid arteries. *Atherosclerosis* 243, 589–592. doi: 10.1016/j.atherosclerosis.2015.10.093

Wingelaar, T. T., van Ooij, P. A. M., and van Hulst, R. A. (2017). Oxygen toxicity and special operations forces diving: hidden and dangerous. *Front. Psychol.* 8:1263. doi: 10.3389/fpsyg.2017.01263

Conflict of Interest: The authors declare that the research was conducted in the absence of any commercial or financial relationships that could be construed as a potential conflict of interest.

The reviewer AM declared a past co-authorship with one of the authors VM.

frontiers in Physiology

ORIGINAL RESEARCH
published: 20 April 2020
doi: 10.3389/fphys.2020.00342

Lower Body Weight in Rats Under Hypobaric Hypoxia Exposure Would Lead to Reduced Right Ventricular Hypertrophy and Increased AMPK Activation

Karen Flores[1,2], Patricia Siques[1,2], Julio Brito[1,2], Stefany Ordenes[1,2], Karem Arriaza[1,2], E. Pena[1,2], Fabiola León-Velarde[3], Rosario López[4], Ángel L. López de Pablo[5] and Silvia Arribas[5]*

[1] Institute of Health Studies, University Arturo Prat, Iquique, Chile, [2] Institute DECIPHER, German-Chilean Institute for Research on Pulmonary Hypoxia and Its Health Sequelae, Iquique, Chile, [3] Department of Biological and Physiological Sciences, Facultad de Ciencias y Filosofía/IIA, Cayetano Heredia University, Lima, Peru, [4] Department of Preventive Medicine and Public Health, University Autónoma of Madrid, Madrid, Spain, [5] Department of Physiology, Universidad Autónoma de Madrid, Madrid, Spain

OPEN ACCESS

Edited by:
Marc-Antoine Custaud, Université d'Angers, France

Reviewed by:
Jan Neckář, Institute of Physiology (ASCR), Czechia
Iman Momken, University of Évry Val d'Essonne, France

***Correspondence:**
Karen Flores
kfloresu@unap.cl;
karen.flores.urra@gmail.com

Specialty section:
This article was submitted to Environmental, Aviation and Space Physiology, a section of the journal Frontiers in Physiology

Received: *23 November 2019*
Accepted: *25 March 2020*
Published: *20 April 2020*

Citation:
Flores K, Siques P, Brito J, Ordenes S, Arriaza K, Pena E, León-Velarde F, López R, López de Pablo ÁL and Arribas S (2020) Lower Body Weight in Rats Under Hypobaric Hypoxia Exposure Would Lead to Reduced Right Ventricular Hypertrophy and Increased AMPK Activation. Front. Physiol. 11:342. doi: 10.3389/fphys.2020.00342

Background: Both chronic hypoxia (CH) and long-term chronic intermittent hypoxia (CIH) exposure lead to right ventricular hypertrophy (RVH). Weight loss is an effective intervention to improve cardiac function and energy metabolism in cardiac hypertrophy. Likewise, caloric restriction (CR) also plays an important role in this cardioprotection through AMPK activation. We aimed to determine the influence of body weight (BW) on RVH, AMPK and related variables by comparing rats exposed to both hypoxic conditions.

Methods: Sixty male adult rats were separated into two groups (n = 30 per group) according to their previous diet: a caloric restriction (CR) group and an ad libitum (AL) group. Rats in both groups were randomly assigned to 3 groups: a normoxic group (NX, n = 10), a CIH group (2 days hypoxia/2 days normoxia; n = 10) and a CH group (n = 10). The CR group was previously fed 10 g daily, and the other was fed ad libitum. Rats were exposed to simulated hypobaric hypoxia in a hypobaric chamber set to 428 Torr (the equivalent pressure to that at an altitude of 4,600 m above sea level) for 30 days. Measurements included body weight; hematocrit; serum insulin; glycemia; the degree of RVH (Fulton's index and histology); and AMPK, mTOR, and PP2C expression levels in the right ventricle determined by western blotting.

Results: A lower degree of RVH, higher AMPK activation, and no activation of mTOR were found in the CR groups exposed to hypobaric hypoxia compared to the AL groups ($p < 0.05$). Additionally, decreased glycemia and serum insulin levels were observed. Interestingly, PP2C expression showed an increase in the AL groups but not in the CR groups ($p < 0.05$).

Conclusion: Maintaining a low weight before and during exposure to high-altitude hypoxia, during either CH or CIH, could prevent a major degree of RVH. This cardioprotection would likely be due to the activation of AMPK. Thus, body weight is a factor that might contribute to RVH at high altitudes.

Keywords: right ventricle hypertrophy, hypobaric hypoxia, AMPK, body weight, high altitude

INTRODUCTION

Exposure to hypoxic environments under both chronic hypoxia and long-term chronic intermittent hypoxia induces cardiopulmonary changes that allow the maintenance of the circulatory demands and the homeostasis of tissues under conditions of limited oxygen availability (Ostadal et al., 1998). Under Long-term chronic intermittent hypoxia condition individuals work at a high altitude for days and rest at sea level for the same period (Richalet et al., 2002). Hypoxia exposure elevates pulmonary artery pressure by vasoconstriction (Von Euler and Liljestrand, 1946; Moudgil et al., 2005), and after a long period of exposure there is a remodeling of pulmonary vasculature leading to right ventricular hypertrophy (RVH) (Brito et al., 2007, 2018; Penaloza and Arias-Stella, 2007).

Cardiac hypertrophy is associated with increased cardiomyocyte cell volume, enhanced protein synthesis, and changes in gene transcription and translation (Glennon et al., 1995). Additionally, human studies and animal experimental models have identified that right ventricular dysfunction due to pressure overload is associated with metabolic derangements (Ryan and Archer, 2014). Because of its particular role, the heart requires high metabolic activity due to constant overloading (Noppe et al., 2014).

AMP-activated protein kinase (AMPK) is a heterotrimeric protein kinase composed of a catalytic α subunit and two regulatory subunits (β & ϒ). As an intracellular energy sensor, in the heart, AMPK is activated in response to an increase in the AMP/ATP ratio under stress conditions such as hypoxia, hypertrophy and hypoglycemia (Arad et al., 2007; Viollet et al., 2009). Studies in mice revealed that AMPK activation attenuates the development of cardiac hypertrophy by inhibiting protein synthesis and activating autophagy (Chan et al., 2004, 2008; Kang et al., 2011; Li et al., 2014). AMPK activation can also increase the uptake of glucose, enhance fatty acid oxidation (Dyck and Lopaschuk, 2006; Nagendran et al., 2013) and inhibit protein synthesis to reserve energy stores (Liu et al., 2006). Therefore, AMPK would have a protective role by restoring the energy balance and a key role against cardiovascular diseases and cellular stress (Dolinsky and Dyck, 2006). This role has been seen in humans under chronic hypoxia (CH) (Zhang et al., 2018) but has rarely been studied in hypobaric chronic intermittent hypoxia (CIH). The cardioprotective role of the AMPK pathway against cardiac hypertrophy involves mammalian target of rapamycin (mTOR), which is a major regulator of myocardial protein synthesis and a major driver of cardiac hypertrophy (Proud, 2004) whose activation regulates cell proliferation, apoptosis, cell migration and metabolism (Li et al., 2014). However, the inactivation of AMPK by dephosphorylation has been described to be attributed to PP2C (Davies et al., 1995; Marley et al., 1996; Steinberg, 2007). PP2C is a protein serine/threonine phosphatase that controls the specific dephosphorylation of thousands of phosphoprotein substrates (Shi, 2009). The primary function of PP2C appears to be the regulation of stress signaling, although it also plays a role in cell differentiation, growth, survival, apoptosis, and metabolism (Lu and Wang, 2008).

The impact of caloric restriction (CR) on inducing weight loss in cardiac hypertrophy has substantial clinical importance (Karwi et al., 2019). Recently, it has been reported in both humans and animal models that overweight and obesity influence high-altitude illness outcomes such as pulmonary hypertension (San Martin et al., 2017; Brito et al., 2018). Studies in mice show that CR is a potent dietary intervention to produce beneficial cardiac effects (Kobara et al., 2015; Melo et al., 2016) through AMPK activation, which plays an important role in cardioprotection (Shinmura et al., 2005, 2008; Chen et al., 2013).

The impact of a change in body weight before and during exposure to hypoxia at a high altitude, as well as the activation of AMPK in RVH, is not well known. Therefore, it is hypothesized that during high-altitude hypobaric hypoxia, a lower body weight would promote a reduced RVH through the activation of AMPK. Thus, the aim of this study was to determine the influence of body weight (BW) on RVH, through caloric restriction compared to an ad libitum food intake regimen, as well as its association with AMPK and related variables, by comparing rats exposed to both hypoxic conditions (CIH and CH).

MATERIALS AND METHODS

Animal Model

The model used for this experiment was largely described and validated previously in several studies (Siques et al., 2006). The study was performed on sixty male Wistar rats (12 weeks of age) obtained from the animal facility of the Institute of Health Studies of Arturo Prat University, Iquique, Chile. The rats were assigned to two groups according to the amount of food provided during the previous month of exposure (CR 10 g and AL daily). Then, it was obtained a CR group (body weight 251.6 ± 1.9 g; n = 30), which received 10 g/day of food (Corresponding to caloric restriction 70%), and an ad libitum (AL) group (body weight 434.6 ± 5.9 g; n = 30). This model of caloric restriction is based on the works in rats of Kobara et al. (2015) and Melo et al. (2016). Then, both groups were randomly divided into three groups: (1) a normobaric normoxia (NX) group (n = 10), which served as a sea-level control; (2) a chronic intermittent hypobaric hypoxia (CIH) group (n = 10),

which underwent 2 days of exposure to hypobaric hypoxia alternating with 2 days of exposure to normobaric normoxia; and (3) a chronic hypobaric hypoxia (CH) group (n = 10), which underwent permanent exposure to hypobaric hypoxia. All groups received water ad libitum and a standard balanced diet for laboratory rats (22.0% crude protein, 5.0% crude fat, 5.0% crude fiber, 9.0% ash and 12% moisture (5POO®, LabDiet®, Prolab RMH3000). Food intake was measured through the determination of the amount of residual food, and fasting times were accurately controlled. The exposure time of each group was 30 days, and hypobaric hypoxia was simulated in a chamber at 428 Torr (equivalent to an altitude of 4,600 m above sea level). The time of ascension from sea level to 4,600 m above sea level was 60 min.

The chamber conditions were as follows: internal flow of 3.14 L/min of air and humidity between 21 and 30%. NX groups were located in the same room at sea level (760 Torr) and housed under the same chamber conditions as the groups exposed to hypoxia. The rats were placed in individual cages at a temperature of 22 ± 2°C and a circadian rhythm of 12 h of light and 12 h of dark. Movement inside the cage was not restricted, but no exercise was performed. At the end of the exposure period, the rats were euthanized with an overdose of ketamine (0.9 mg/kg of weight), organs were collected and stored at −80°C, and specific variables were measured.

The animal protocol and experimental model were in accordance with Chilean Law No. 20380 regarding animal experimentation and were approved by the Research Ethics Committee of Arturo Prat University, Iquique, Chile.

Body Weight, Hematocrit, Blood Glucose, and Serum Insulin

Both biochemical and physiological parameters in all study groups were measured at day 0 under basal normoxic conditions and after 30 days immediately after removal from the chamber. The body weight and residual food were measured using an electronic scale (Acculab V-1200®, Chicago, IL, United States).

Blood extraction (1 mL) for biochemical measurements was performed via cardiac puncture under anesthesia (0.3 mg/kg body weight) after 10 h of fasting. The hematocrit (Hct) values, calculated as percentages, were measured using capillaries, which were centrifuged (5804 R Eppendorf AG®, Hamburg, Germany) at 5,000 rpm for 5 min. Glucose in blood was measured using a glucometer (CarenSensN®), and serum insulin was measured using a commercial kit (Reta Insulin ELISA Kit®, ALPCO, Salem, VT, United States).

Western Blot Analysis

For protein analysis, 50 mg of right ventricular cardiac muscle was obtained from each rat. Protein extraction was started by tissue homogenization (Stir-Pak®, Barrington, IL, United States) with 500 μL RIPA lysis buffer, which contains a mixture of phosphatase and protease inhibitors (4 mM PMSF, 10 μM leupeptin, 1 mM EDTA, 1 mM EGTA, 20 mM NaF, 20 mM HEPES and 1 mM DTT). Then, the homogenates were centrifuged (5804 R Eppendorf AG®, Hamburg, Germany) at 12,000 rpm for 20 min at 4°C, and the supernatant was extracted. For the quantification of the total protein extracted, the Bradford reaction was used (Bradford, 1976) with a BioPhotometer (Eppendorf AG®, Hamburg, Germany) at 590 nm, and samples were then stored at −80°C. For western blotting, the samples were previously diluted with 2X Laemmli buffer [0.125 M Tris-HCl, 4% SDS (p/v), 20% glycerol (v/v), 0.004% bromophenol blue, 10% β-mercaptoethanol (pH 6.8)]. Then, 50 μg of the protein were separated according to their molecular weight (MW) under an electric field via sodium dodecyl sulfate-polyacrylamide gel electrophoresis (SDS-PAGE) (30% bis-acrylamide (v/v), 150 mM Tris (pH 6.8 and 8.8), 1.0% TEMED (w/v), H_2O) at 6 and 12%. Electrophoretic separation was initiated with the application of direct current to 150 V over 80 min with a power supply (PolyScience®, EPS-300, Taipei, Taiwan, China), and the proteins were then transferred from the polyacrylamide gel to a polyvinylidene difluoride (PVDF) membrane at 180 mA for 90 min with a semidry electroblotting system (Owl™ HEP systems, Thermo Fisher Scientific®, United States).

To avoid nonspecific antibody binding, the PVDF membrane was blocked with bovine serum albumin (BSA) at a concentration range of 3–5% in TBS-T solution containing 10 mM HCl, 150 mM NaCl, and 0.05% Tween-20 at pH 7.4. The blocking time was 1 h at room temperature. Then, the membrane was incubated with the corresponding primary antibodies [AMPKα1/2 (sc-25792), p-AMPKα1/2 (sc-101630), mTOR (sc-517464), p-mTORC1 (sc-293133), PP2Cα (sc-517264), and β-actin (sc-130657)] at a dilution of 1:500 (Santa Cruz Biotechnology®, Santa Cruz, CA, United States) and incubated overnight at 4°C. Finally, the membrane was incubated with secondary antibodies (anti-goat, anti-rabbit and anti-mouse antibodies, Santa Cruz Biotechnology®, Santa Cruz, CA, United States) at a dilution of 1:2,000 in 3% BSA for 1 h at room temperature, washed with TBS-T and then imaged in a dark room with a chemiluminescence kit (Chemiluminescence West Pico®, Super Signal Substrate, Thermo Fisher Scientific®, Rockford, IL, United States). The density of the bands was measured with ImageJ software and normalized according to β-actin expression and Ponceau staining. The activity levels of AMPK and mTOR were determined by the ratio of phosphorylated protein to total protein.

Right Ventricular Hypertrophy and Histology

RVH was evaluated at the end of the exposure period (day 30) using Fulton's index [RV/LV+Septum (g/g)], as described previously (Kay, 1980). Also, total ventricles weight vs. body weight ratio was obtained (g/g). For morphological assessment under light microscopy, the ventricular tissue was cut transversally and fixed in 4% paraformaldehyde at room temperature overnight and then dehydrated and embedded in paraffin. Paraffin-embedded tissue slices (5 μm thick) were routinely stained with hematoxylin and eosin (H&E) and finally, the area was measured through ImageJ software.

Data Analysis

All data recorded were included in a database and analyzed using the SPSS program (IBM SPSS® V.21.0®, Armonk, NY, United States). The normality of the variables was established by the Kolmogorov-Smirnov test, and all variables had a normal distribution. The means and standard errors (SEs) were calculated for all variables. To determine differences in the measured variables over time, a paired-sample Student's t test was performed between the two groups. To establish the intergroup differences, repeated-measures analysis of variance (ANOVA) was used. For variables measured once, an independent Student's t test and one-way ANOVA followed by the least significant difference (LSD) *post hoc* test were performed. The level of significance was established at the 95% confidence level, with $p < 0.05$ considered indicative of significance.

RESULTS

Body Weight, Hematocrit, Blood Glucose, and Serum Insulin

Previous exposure body weight was decreased in CR compared to AL group ($p < 0.001$) (**Figure 1A**). The body weight was lower in both the AL and the CR hypoxia-exposed groups (CIH and CH) than in the NX group ($p < 0.001$) at the end of exposure day 30 (**Figure 1B**). Remarkably, the AL group lowered their weight by a greater proportion than the CR group ($p < 0.001$). Importantly, food intake under CH in both the AL and CR groups was similar (10 g), whereas under CIH, both groups showed reduced intake, with less intake in the AL group than in the CR group while they were in the chamber. Interestingly, CR group under chronic hypoxia did not further reduce the food intake. Despite this observation, the AL group showed a higher weight than the CR group at the end of the exposure.

Both the AL- and CR-exposed groups exhibited a decrease in blood glucose levels and serum insulin compared to the NX groups and basal levels ($p < 0.01$). Interestingly, the CR group exposed to CIH showed lower insulin levels than the AL group exposed to CIH ($p < 0.01$) (**Figures 1C,D**).

Under hypobaric hypoxic conditions (CIH and CH), both the AL and CR groups showed an increase in Hct compared to the NX groups and basal levels ($p < 0.001$), with values being higher in the CH groups ($p < 0.01$). Notably, this increase was less in the CR groups than in the AL groups exposed to CH ($p < 0.01$) (**Figure 1E**).

Right Ventricular Hypertrophy

RVH was observed in both the AL and CR groups under hypobaric hypoxic conditions compared to the NX groups ($p < 0.01$) and was higher in the CH groups than in the CIH groups. Remarkably, a lower degree of hypertrophy was observed in the CR group than in the AL group ($p < 0.05$), and the degree of hypertrophy observed in the CR group under CH was similar to that in the AL group under CIH (**Figure 2A**). Similar results were found with total ventricles weight vs. body weight ratio (**Figure 2B**). Representative images and the quantification of the area clearly show the enlargement of myocytes, which was coincident with the hypertrophy found in the CR and AL groups (**Figures 2C,D**). Interestingly, the weights of both ventricles (RV and LV) in rats of the AL group were higher than those in the CR group, as expected.

AMPK, mTOR, and PP2C Expression Levels

AMPK activation was increased only in the CR groups under both CIH and CH ($p < 0.05$), while the AL groups showed no AMPK activation. Interestingly, in this latter group, a decrease in AMPK under CH was found ($p < 0.05$) (**Figures 3A,D**).

Conversely, in the CR groups under both CIH and CH, there was no mTOR activation and no overexpression of PP2Cα, while in the AL group, there was a higher activation and expression of both proteins under CH than under CIH ($p < 0.05$) (**Figures 3B–D**).

DISCUSSION

This research on long-term CIH and CH right ventricular hypertrophy revealed important and novel findings. Caloric restriction results in: (1) reduced RVH; (2) activation of AMPK; and (3) no activation of mTOR and PP2Cα was seen.

This research is in line with other studies and calls attention to the importance of a low body weight to decrease cardiac risk (Riordan et al., 2008; Derumeaux et al., 2017) with ventricular hypertrophy (Karwi et al., 2019). However, the influence of body weight on AMPK activation in RVH induced by CH and long-term CIH exposure has received little attention.

In this study, both the AL and CR groups lost body weight and had lower blood glucose and serum insulin levels due to the metabolic effects of hypoxia, as has been reported with hypobaric and hypoxic hypoxia models (Chiu et al., 2004; Gamboa et al., 2011; Siques et al., 2018). Moreover, the CR group not only lost body weight under hypoxia but also began exposure with a lower body weight than did the AL group. These results call attention to the importance of maintaining a low body weight before and during exposure to long-term hypobaric hypoxia.

Interestingly, regarding hematocrit, the CR group had a lower hematocrit before the exposure, with no difference among the groups. This result is consistent with those of some authors, who explain that this lower hematocrit is the effect of decreased intake of dietary energy and of blood-forming nutrients (Faris et al., 2012; Gasmi et al., 2018). Despite the possible influence of CR in the hematocrit level, it is important to highlight that the all exposed to hypoxia groups had elevated hematocrit at day 30.

On the other hand, the model of this study is effectively an unusual model of exposure that is scarcely known. Food intake clearly has an effect on insulin level, but the regimen and degree of hypoxia are also extremely important, which is in agreement with the results of Debevec and Millet (1985), who demonstrated that the regimen and the degree of hypoxia can lead to variation in the results. In our results, the degree of hypoxia was the most important variable because it determined the amount of food intake, although the difference was not significant between the

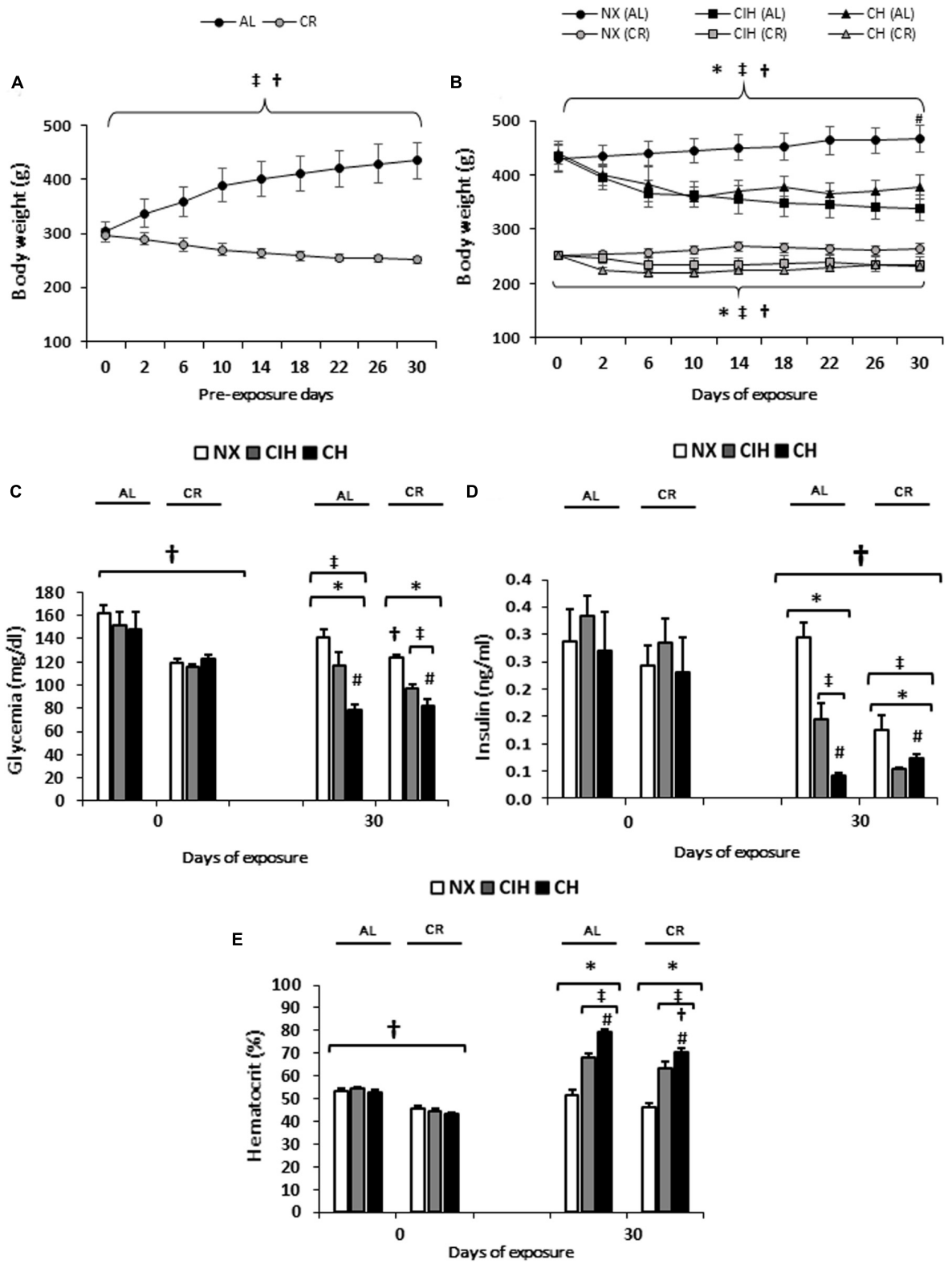

FIGURE 1 | Physiological and biochemical parameters: Ad libitum (AL) and caloric restriction (CR) groups on days 0 and 30: normoxic group (NX), chronic intermittent hypoxia group (CIH), and chronic hypoxia group (CH). **(A)** Body weight (g) previous to exposure, **(B)** Body weight (g) during exposure, **(C)** Blood glucose (mg/dl) and **(D)** Serum insulin (ng/ml) **(E)** Hematocrit (%). The values are the mean ($\bar{x}$) ± standard error (SE). $^{*}p < 0.05$: hypoxia-exposed vs. NX; $^{\#}p < 0.05$: CIH vs. CH. $^{\dagger}p < 0.05$: AL vs. CR; ‡Day 30 vs. Day 0 for each group NX, CIH and CH of AL and CR groups.

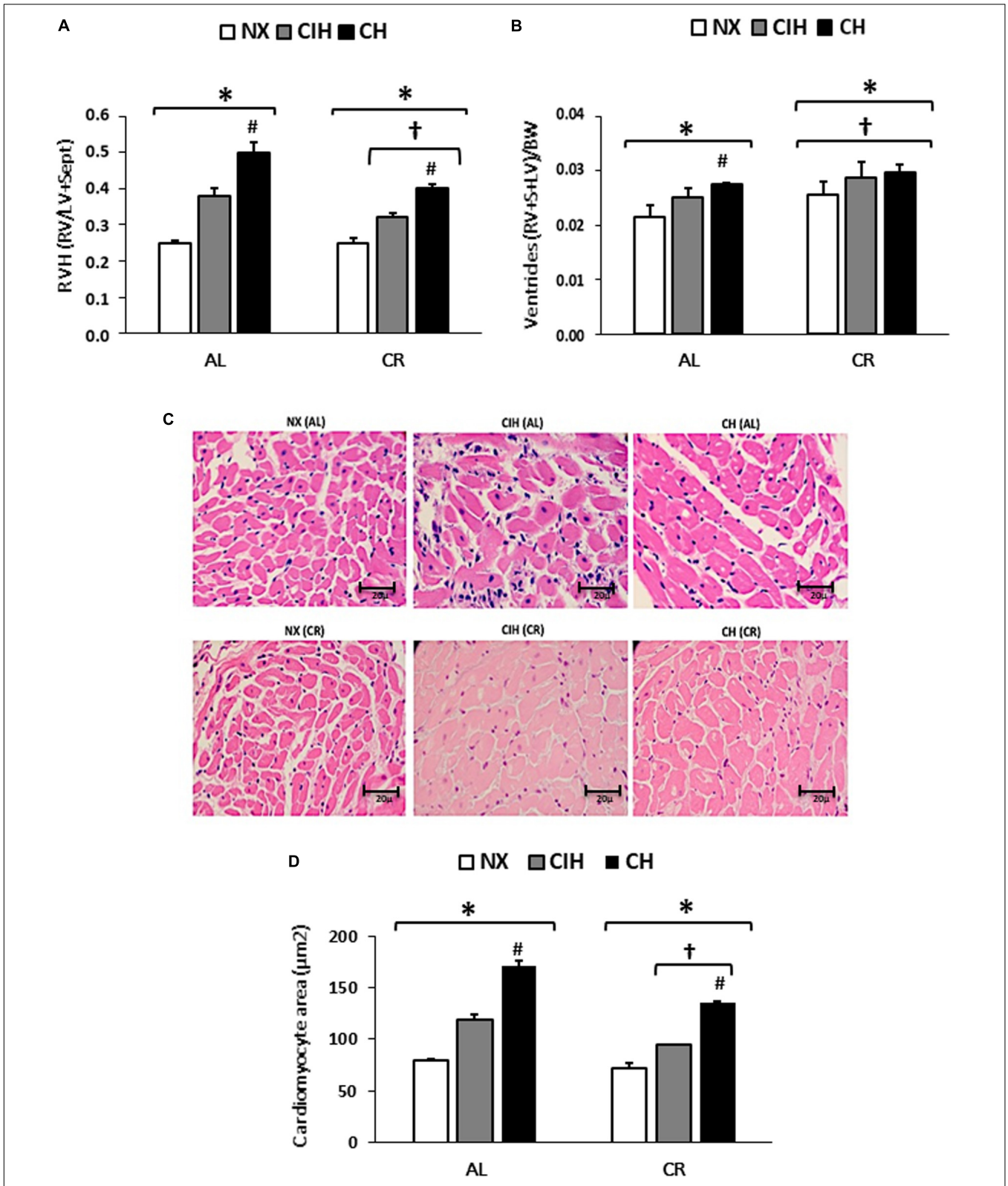

FIGURE 2 | Grade of right ventricular hypertrophy (RVH): Ad libitum (AL) and caloric restriction (CR) groups on day 30: normoxic group (NX), chronic intermittent hypoxia group (CIH), and chronic hypoxia group (CH). **(A)** Expressed as Fulton's index [right ventricle (RV) weight/(left ventricle (LV) weight + septum weight)]. **(B)** Ventricles (RV+S+LV)/BW ratio. **(C)** Hematoxylin and eosin staining of the slices of the RV and **(D)** of the cardiomyocyte area of the RV. The values are the mean ($\bar{x}$) ± standard error (SE). $^{*}p < 0.05$: hypoxia-exposed vs. NX; $^{\#}p < 0.05$: CIH vs. CH. $^{\dagger}p < 0.05$: AL vs. CR.

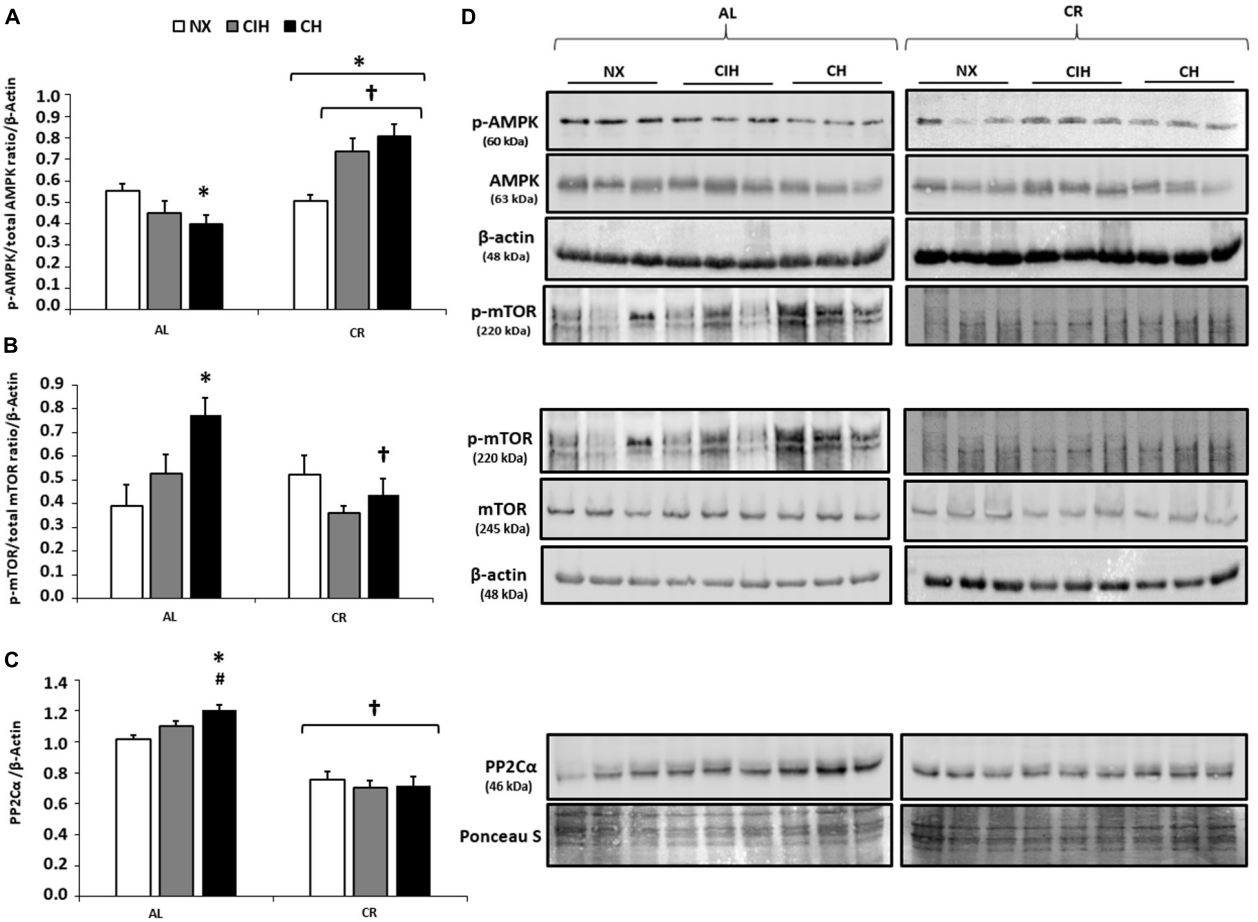

FIGURE 3 | Protein expression levels in the right ventricle (RV): Ad libitum (AL) and caloric restriction (CR) groups at day 30: normoxic group (NX), chronic intermittent hypoxia group (CIH), and chronic hypoxia group (CH). **(A)** Activation of AMPK (p-AMPK/total AMPK ratio); **(B)** Activation of mTOR (p-mTOR/total mTOR ratio) normalized by β-actin; **(C)** PP2Cα expression levels, normalized by Ponceau staining; and **(D)** Representative bands are shown. Values are means (X) ± standard errors (SEs). $^{*}p < 0.05$: hypoxia-exposed vs. NX; $^{\#}p < 0.05$: CIH vs. CH. $^{\dagger}p < 0.05$: AL vs. CR.

CR and the AL in CH groups. Interestingly, AL groups, in both hypoxia conditions show a decrease of food-intake and a possible explanation could be attributed to the hypoxic stressor and its side effects (San Martin et al., 2017).

Conversely, the CIH groups eat differently under hypoxic stimuli. Those fed ad libitum eat 4.5 g; however, the CR group eat an average of 7.9 g. The AL groups could have been affected by anorexia and general malaise, as occurs in humans (acute mountain sickness), and particularly so when just slightly over a healthy body weight (as described by San Martin et al., 2017). Furthermore, the AL group maintained a substantial amount of fat tissue, which has an influence in insulin. Additionally, insulin sensitivity has been demonstrated to be increased in hypoxia (Chiu et al., 2004; Gamboa et al., 2011). Therefore, both food intake and hypoxia regimen would contribute to determine insulin levels, highlighting that the kind and degree of hypoxia might be the most critical.

Ventricular hypertrophy) is characterized by increased cardiomyocyte size, a higher degree of sarcomere organization and enhanced protein synthesis levels, all of which are closely associated with energy metabolism (Tham et al., 2015). Human studies in the same model of CIH showed that this hypertrophy is associated with cardiometabolic factors, among others (Brito et al., 2018). Our results demonstrate RVH in those exposed to hypoxia, and importantly, that RVH in CR is lesser than in AL. Although, in this study does not seems to be restricted to the latter, because CR rats eat more food than AL inside the chamber in CIH condition; and the CR rats did developed RVH as well but at a lesser, only under hypoxic conditions, where AMPK pathway might play a major role as is discussed below. However, in the current study, it is clear that with CR, the hypoxia regimen increased the AMPK activity and inhibited mTOR, which might explain the degree of RVH that was found. The weights of both ventricles, including LV, in rats of the AL group were higher than those in the CR group, as expected because of the pre-exposure weight.

AMPK is known as an energy sensor and a regulator of cardiac energy metabolism under normal and stress conditions. Additionally, AMPK has been shown to inhibit cardiac hypertrophy (Sung et al., 2015) and to have a role beyond

metabolic regulation. It also plays a critical role in an ample variety of cellular processes, such as regulating protein synthesis, transcriptional activity and energy supply (Baskin and Taegtmeyer, 2011; Cates et al., 2018; Feng et al., 2018). Additionally, CR-induced relative energy deficits, such as hypoxia, hypertrophy and hypoglycemia, result in increased intracellular levels of the AMP/ATP ratio, activating AMPK (Arad et al., 2007; Viollet et al., 2009). Our study (caused by pressure overload as a consequence of hypoxia) presents all of the above stressors; however, only CR groups that began with a lower body weight prior to exposure and maintained it exhibited the activation of AMPK activation and lower RVH. Similarly, other studies demonstrate other pathways that involve AMPK, showing nutrient deprivation produce an increase of AMPK activity, and this activation decreases the cardiac remodeling through degradation of hypertrophic proteins mediated by AMPK-induced transcription factors, such as MEF2 (Baskin and Taegtmeyer, 2011). However, in our study the hypoxic stressor appears to play a clear role. Another kind of RVH induction in rats showed that the activation of AMPK by metformin significantly reduced RVH, highlighting the importance of AMPK in clinical treatments for RVH (Li et al., 2016). Other evidence has demonstrated that pharmacological AMPK activation attenuates the development of cardiac hypertrophy by inhibiting protein synthesis through the inactivation of the mammalian target of rapamycin (mTOR) signaling pathway (Chan et al., 2004, 2008; Kang et al., 2011).

Thus, in the process of regulating ventricular hypertrophy mTOR is involved. mTOR is the key sensor of nutrient status, consisting of two distinct complexes, mTORC1 and mTORC2, and its activation contributes to cell survival in cardiomyocytes and regulates cell proliferation, apoptosis, cell migration and metabolism. Moreover, the protective effects of AMPK on PO-induced cardiac hypertrophy were recently shown to be partially mediated by the inhibition of mTORC1 signaling but not mTORC2 signaling (Li et al., 2014). This study, focused on mTORC1, showed that only the CR group demonstrated no activation of mTOR, which supports the role of the activation of AMPK as a protector against RVH in high-altitude hypoxia (hypobaric hypoxia).

Conversely, in the AL group exposed to CH, increased mTOR activation and decreased AMPK activation showed an inverse regulation between the two kinases. Further support for our findings comes from reports demonstrating that the inhibition of mTOR under chronic hypobaric hypoxic conditions resulted in the prevention of RVH in an animal model (Paddenberg et al., 2007) and that increased AMPK activity and decreased mTOR activity attenuated RVH in pulmonary-artery-hypertension-induced rats (Deng et al., 2017).

In this study, we have shown that the modification of body weight through diet leads to reduced RVH under high-altitude exposure. CR has been established as a potent dietary intervention that produces beneficial cardiac effects (Kobara et al., 2015; Melo et al., 2016) through AMPK activation, which plays an important role in cardioprotection, as has been demonstrated in the left ventricle (Shinmura et al., 2005, 2008; Chen et al., 2013).

On the other hand, it was interesting to observe that the PP2Cα expression level was increased in the AL group after CH exposure but not in the CR group. This finding further supports the lack of AMPK activation. Notably, the time of hypoxia exposure in the CIH group was lower than that in the CH group. This fact, could explain the reason to have a remarkably RVH in AL's chronic groups.

Many authors have described that AMPK inactivation by dephosphorylation is attributed to PP2C (Davies et al., 1995; Marley et al., 1996; Steinberg, 2007). This dephosphorylation is enhanced under nutrient-rich conditions (the AL group of this study) but deranged under nutrient-poor conditions (Davies et al., 1995; Sanders et al., 2007; Hardie et al., 2012). The finding of a lack of expression of this phosphatase would be another way to explain the reduced hypertrophy in the CR group allowing AMPK activation.

The aim of this study was to evaluate RVH in different regimens of long-term hypoxia and not the degree of pulmonary hypertension, which is well known that hypoxemia induce an increase in pulmonary artery pressure and all the involved mechanisms leading to RVH. Given that we cannot correlate both proteins (AMPK and mTOR) with the actual degree of PAP at any stage, this would be a limitation. However, in that sense, the literature supports and describes that CR could decrease PAP and RVH (Ding et al., 2015). Thence, in the current study, it is clear that with CR, and the hypoxia regimen increased the AMPK activity and inhibited mTOR, which might explain the RVH that was found.

In addition, Wang and Unger (2005) suggested that AMPK activity was reduced and the expression of PP2C was increased significantly in the hearts of obese rats, which is rather in agreement with the histological findings of more fat between myocytes in the AL group, although the rats in these groups were not obese. This study also has the limitation that obese rats were not included, since the inclusion of obese rats raises the concern of introducing a bias, and the main aim was just to analyze CR in the development of RVH. Another limitation of this study is the lack of assessment of the cardiac functional status because the focus was more for cardiac morphology.

CONCLUSION

This study contributes to a better understanding of the possible relationship between body weight and AMPK activation in the development of RVH under hypoxia. Caloric restriction, either under CH or CIH, would be contributory to a decreased degree of high-altitude-induced RVH through the activation of AMPK. Nonetheless, further research is necessary to corroborate this finding and whether it can be translated to clinical grounds.

DATA AVAILABILITY STATEMENT

All data sets for this study are included in the manuscript.

ETHICS STATEMENT

The animal study was reviewed and approved by the Research Ethics Committee of Arturo Prat University, Iquique, Chile.

AUTHOR CONTRIBUTIONS

KF, PS, and JB conceived and designed the study, performed the experiments, analyzed and interpreted the data, drafted the manuscript, critically revised important intellectual content in the manuscript, and provided overall supervision. ÁL and SA contributed to the interpretation of the results and assisted in critical decisions and revision. FL-V, KA, SO, EP, and RL contributed to critical revisions of the manuscript. All authors approved the final manuscript and agreed to be accountable for all aspects of the work.

FUNDING

This study was supported by grants from projects GORE FIC Tarapacá BIP30477541-0 and Internal Project VRIIP0098-18, UNAP.

ACKNOWLEDGMENTS

We would like to thank Gabriela Lamas and Daniel Aguayo for their technical assistance in the laboratory.

REFERENCES

Arad, M., Seidman, C. E., and Seidman, J. G. (2007). AMP-activated protein kinase in the heart: role during health and disease. *Circ. Res.* 100, 474–488. doi: 10.1161/01.res.0000258446.23525.37

Baskin, K. K., and Taegtmeyer, H. (2011). AMP-activated protein kinase regulates E3 ligases in rodent heart. *Circ. Res.* 109, 1153–1161. doi: 10.1161/circresaha.111.252742

Bradford, M. M. (1976). A rapid and sensitive method for the quantitation of microgram quantities of protein utilizing the principle of protein-dye binding. *Anal. Biochem.* 72, 248–254. doi: 10.1016/0003-2697(76)90527-3

Brito, J., Siqués, P., León-Velarde, F., De La Cruz, J. J., López, V., and Herruzo, R. (2007). Chronic intermittent hypoxia at high altitude exposure for over 12 years: assessment of hematological, cardiovascular, and renal effects. *High Alt. Med. Biol.* 8, 236–244. doi: 10.1089/ham.2007.8310

Brito, J., Siques, P., Lopez, R., Romero, R., Leon-Velarde, F., Flores, K., et al. (2018). Long-term intermittent work at high altitude: right heart functional and morphological status and associated cardiometabolic factors. *Front. Physiol.* 9:248. doi: 10.3389/fphys.2018.00248

Cates, C., Rousselle, T., Wang, J., Quan, N., Wang, L., Chen, X., et al. (2018). Activated protein C protects against pressure overload-induced hypertrophy through AMPK signaling. *Biochem. Biophys. Res. Commun.* 495, 2584–2594. doi: 10.1016/j.bbrc.2017.12.125

Chan, A. Y., Dolinsky, V. W., Soltys, C. L., Viollet, B., Baksh, S., Light, P. E., et al. (2008). Resveratrol inhibits cardiac hypertrophy via AMP-activated protein kinase and akt. *J. Biol. Chem.* 283, 24194–24201. doi: 10.1074/jbc.M802869200

Chan, A. Y., Soltys, C. L., Young, M. E., Proud, C. G., and Dyck, J. R. (2004). Activation of AMP-activated protein kinase inhibits protein synthesis associated with hypertrophy in the cardiac myocyte. *J. Biol. Chem.* 279, 32771–32779. doi: 10.1074/jbc.M403528200

Chen, K., Kobayashi, S., Xu, X., Viollet, B., and Liang, Q. (2013). AMP activated protein kinase is indispensable for myocardial adaptation to caloric restriction in mice. *PLoS One* 8:e59682. doi: 10.1371/journal.pone.0059682

Chiu, L. L., Chou, S. W., Cho, Y. M., Ho, H. Y., Ivy, J. L., Hunt, D., et al. (2004). Effect of prolonged intermittent hypoxia and exercise training on glucose tolerance and muscle GLUT4 protein expression in rats. *J. Biomed. Sci.* 11, 838–846. doi: 10.1007/bf02254369

Davies, S. P., Helps, N. R., Cohen, P. T., and Hardie, D. G. (1995). 5'-AMP inhibits dephosphorylation, as well as promoting phosphorylation, of the AMP-activated protein kinase. Studies using bacterially expressed human protein phosphatase-2C alpha and native bovine protein phosphatase-2AC. *FEBS Lett.* 377, 421–425. doi: 10.1016/0014-5793(95)01368-7

Debevec, T., and Millet, G. P. (1985). Discerning normobaric and hypobaric hypoxia: significance of exposure duration. *J. Appl. Physiol.* 116:1255. doi: 10.1152/japplphysiol.00873.2013

Deng, Y., Wu, W., Guo, S., Chen, Y., Liu, C., Gao, X., et al. (2017). Altered mTOR and Beclin-1 mediated autophagic activation during right ventricular remodeling in monocrotaline-induced pulmonary hypertension. *Respir. Res.* 18:53. doi: 10.1186/s12931-017-0536-7

Derumeaux, G., Ernande, L., and Sawaki, D. (2017). Weight loss to rejuvenate the heart. *Eur. Heart J. Cardiovasc. Imaging* 19, 143–144. doi: 10.1093/ehjci/jex318

Ding, M., Lei, J., Qu, Y., Zhang, H., Xin, W., Ma, F., et al. (2015). Calorie restriction attenuates monocrotaline-induced pulmonary arterial hypertension in rats. *J. Cardiovasc. Pharmacol.* 65, 562–570. doi: 10.1097/FJC.0000000000000224

Dolinsky, V. W., and Dyck, J. R. (2006). Role of AMP-activated protein kinase in healthy and diseased hearts. *Am. J. Physiol. Heart Circ. Physiol.* 291, H2557–H2569. doi: 10.1152/ajpheart.00329.2006

Dyck, J. R., and Lopaschuk, G. D. (2006). AMPK alterations in cardiac physiology and pathology: enemy or ally? *J. Physiol.* 574, 95–112. doi: 10.1113/jphysiol.2006.109389

Faris, M. A.-I. E., Hussein, R. N., Ai-Kurd, R. A., Al-Fararjeh, M. A., Bustanji, Y. K., and Mohammand, M. K. (2012). Impact of ramadan intermittent fasting on oxidative stress measured by urinary 15-f(2 t)-isoprostane. *J Nutr Metab.* 2012:802924.

Feng, Y., Zhang, Y., and Xiao, H. (2018). AMPK and cardiac remodelling. *Sci. China Life Sci.* 61, 14–23. doi: 10.1007/s11427-017-9197-5

Gamboa, J. L., Garcia-Cazarin, M. L., and Andrade, F. H. (2011). Chronic hypoxia increases insulin-stimulated glucose uptake in mouse soleus muscle. *Am. J. Physiol. Regul. Integr. Comp. Physiol.* 300, R85–R91. doi: 10.1152/ajpregu.00078.2010

Gasmi, M., Sellami, M., Denham, J., Padulo, J., Kuvacic, G., Selmi, W., et al. (2018). Time-restricted feeding influences immune responses without compromising muscle performance in older men. *Nutrition.* 5, 29–37. doi: 10.1016/j.nut.2017.12.014

Glennon, P. E., Sugden, P. H., and Poole-Wilson, P. A. (1995). Cellular mechanisms of cardiac hypertrophy. *Br. Heart J.* 73, 496–499. doi: 10.1136/hrt.73.6.496

Hardie, D. G., Ross, F. A., and Hawley, S. A. (2012). AMPK: a nutrient and energy sensor that maintains energy homeostasis. *Nat. Rev. Mol. Cell Biol.* 13, 251–262. doi: 10.1038/nrm3311

Kang, S., Chemaly, E. R., Hajjar, R. J., and Lebeche, D. (2011). Resistin promotes cardiac hypertrophy via the AMP-activated protein kinase/mammalian target of rapamycin (AMPK/mTOR) and c-Jun N-terminal kinase/insulin receptor substrate 1 (JNK/IRS1) pathways. *J. Biol. Chem.* 286, 18465–18473. doi: 10.1074/jbc.M110.200022

Karwi, Q. G., Zhang, L., Altamimi, T. R., Wagg, C. S., Patel, V., Uddin, G. M., et al. (2019). Weight loss enhances cardiac energy metabolism and function in heart failure associated with obesity. *Diabetes Obes. Metab.* 21, 1944–1955. doi: 10.1111/dom.13762

Kay, J. M. (1980). Effect of intermittent normoxia on chronic hypoxic pulmonary hypertension, right ventricular hypertrophy, and polycythemia in rats. *Am. Rev. Respir. Dis.* 121, 993–1001. doi: 10.1164/arrd.1980.121.6.993

Kobara, M., Furumori-Yukiya, A., Kitamura, M., Matsumura, M., Ohigashi, M., Toba, H., et al. (2015). Short-term caloric restriction suppresses cardiac oxidative stress and hypertrophy caused by chronic pressure overload. *J. Card. Fail* 21, 656–666. doi: 10.1016/j.cardfail.2015.04.016

Li, S., Han, D., Zhang, Y., Xie, X., Ke, R., Zhu, Y., et al. (2016). Activation of AMPK prevents monocrotaline-induced extracellular matrix remodeling of pulmonary artery. *Med. Sci. Monit. Basic Res.* 22, 27–33. doi: 10.12659/msmbr.897505

Li, Y., Chen, C., Yao, F., Su, Q., Liu, D., Xue, R., et al. (2014). AMPK inhibits cardiac hypertrophy by promoting autophagy via mTORC1. *Arch. Biochem. Biophys.* 558, 79–86. doi: 10.1016/j.abb.2014.06.023

Liu, L., Cash, T. P., Jones, R. G., Keith, B., Thompson, C. B., and Simon, M. C. (2006). Hypoxia-induced energy stress regulates mRNA translation and cell growth. *Mol. Cell* 21, 521–531. doi: 10.1016/j.molcel.2006.01.010

Lu, G., and Wang, Y. (2008). Functional diversity of mammalian type 2C protein phosphataseisoforms: new tales from an old family. *Clin. Exp. Pharmacol. Physiol.* 35, 107–112. doi: 10.1111/j.1440-1681.2007.04843.x

Marley, A. E., Sullivan, J. E., Carling, D., Abbott, W. M., Smith, G. J., Taylor, I. W., et al. (1996). Biochemical characterization and deletion analysis of recombinant human protein phosphatase 2C alpha. *Biochem. J.* 320, 801–806. doi: 10.1042/bj3200801

Melo, D. S., Costa-Pereira, L. V., Santos, C. S., Mendes, B. F., Costa, K. B., Santos, C. F., et al. (2016). Severe calorie restriction reduces cardiometabolic risk factors and protects rat hearts from ischemia/reperfusion injury. *Front. Physiol.* 7:106. doi: 10.3389/fphys.2016.00106

Moudgil, R., Michelakis, E. D., and Archer, S. L. (2005). Hypoxic pulmonary vasoconstriction. *J. Appl. Physiol.* 98, 390–403.

Nagendran, J., Waller, T. J., and Dyck, J. R. (2013). AMPK signalling and the control of substrate use in the heart. *Mol. Cell Endocrinol.* 366, 180–193. doi: 10.1016/j.mce.2012.06.015

Noppe, G., Dufeys, C., Buchlin, P., Marquet, N., Castanares-Zapatero, D., Balteau, M., et al. (2014). Reduced scar maturation and contractility lead to exaggerated left ventricular dilation after myocardial infarction in mice lacking AMPKalpha1. *J. Mol. Cell Cardiol.* 74, 32–43. doi: 10.1016/j.yjmcc.2014.04.018

Ostadal, B., Ostadalova, I., Kolar, F., Pelouch, V., and Dhalla, N. (1998). "Cardiac adaptation to chronic hypoxia," in *Myocardial Preservation and Cellular Adaptation*, eds E. E. Bittar and D. K. Das (London: Press INC), 43–60. doi: 10.1016/s1569-2590(08)60007-5

Paddenberg, R., Stieger, P., von Lilien, A. L., Faulhammer, P., Goldenberg, A., Tillmanns, H. H., et al. (2007). Rapamycin attenuates hypoxia-induced pulmonary vascular remodeling and right ventricular hypertrophy in mice. *Respir. Res.* 8:15. doi: 10.1186/1465-9921-8-15

Penaloza, D., and Arias-Stella, J. (2007). The heart and pulmonary circulation at high altitudes: healthy highlanders and chronic mountain sickness. *Circulation* 115, 1132–1146. doi: 10.1161/circulationaha.106.624544

Proud, C. G. (2004). Ras, PI3-kinase and mTOR signaling in cardiac hypertrophy. *Cardiovasc. Res.* 63, 403–413. doi: 10.1016/j.cardiores.2004.02.003

Richalet, J.-P., Donoso, M. V., Jiménez, D., Antezana, A.-M., Hudson, C., Cortès, G., et al. (2002). Chilean miners commuting from sea level to 4500 m: a prospective study. *High Alt. Med. Biol.* 3, 159–166. doi: 10.1089/15270290260131894

Riordan, M. M., Weiss, E. P., Meyer, T. E., Ehsani, A. A., Racette, S. B., Villareal, D. T., et al. (2008). The effects of caloric restriction- and exercise-induced weight loss on left ventricular diastolic function. *Am. J. Physiol. Heart Circ. Physiol.* 294, H1174–H1182. doi: 10.1152/ajpheart.01236.2007

Ryan, J. J., and Archer, S. L. (2014). The right ventricle in pulmonary arterial hypertension: disorders of metabolism, angiogenesis and adrenergic signaling in right ventricular failure. *Circ. Res.* 115, 176–188. doi: 10.1161/circresaha.113.301129

San Martin, R., Brito, J., Siques, P., and Leon-Velarde, F. (2017). Obesity as a conditioning factor for high-altitude diseases. *Obes. Facts* 10, 363–372. doi: 10.1159/000477461

Sanders, M. J., Grondin, P. O., Hegarty, B. D., Snowden, M. A., and Carling, D. (2007). Investigating the mechanism for AMP activation of the AMP-activated protein kinase cascade. *Biochem. J.* 403, 139–148. doi: 10.1042/bj20061520

Shi, Y. (2009). Serine/threonine phosphatases: mechanism through structure. *Cell* 139, 468–484. doi: 10.1016/j.cell.2009.10.006

Shinmura, K., Tamaki, K., and Bolli, R. (2005). Short-term caloric restriction improves ischemic tolerance independent of opening of ATP-sensitive K+ channels in both young and aged hearts. *J. Mol. Cell Cardiol.* 39, 285–296. doi: 10.1016/j.yjmcc.2005.03.010

Shinmura, K., Tamaki, K., and Bolli, R. (2008). Impact of 6-mo caloric restriction on myocardial ischemic tolerance: possible involvement of nitric oxide-dependent increase in nuclear Sirt1. *Am. J. Physiol. Heart Circ. Physiol.* 295, H2348–H2355. doi: 10.1152/ajpheart.00602.2008

Siques, P., Brito, J., Flores, K., Ordenes, S., Arriaza, K., Pena, E., et al. (2018). Long-term chronic intermittent hypobaric hypoxia induces glucose transporter (GLUT4) translocation through AMP-activated protein kinase (AMPK) in the soleus muscle in lean rats. *Front. Physiol.* 9:799. doi: 10.3389/fphys.2018.00799

Siques, P., Brito, J., León-Velarde, F., Barrios, L., Cruz, J. J. D. L., López, V., et al. (2006). Time course of cardiovascular and hematological responses in rats exposed to chronic intermittent hypobaric hypoxia (4600 m). *High Alt. Med. Biol.* 7, 72–80. doi: 10.1089/ham.2006.7.72

Steinberg, G. R. (2007). Inflammation in obesity is the common link between defects in fatty acid metabolism and insulin resistance. *Cell Cycle* 6, 888–894. doi: 10.4161/cc.6.8.4135

Sung, M. M., Zordoky, B. N., Bujak, A. L., Lally, J. S., Fung, D., Young, M. E., et al. (2015). AMPK deficiency in cardiac muscle results in dilated cardiomyopathy in the absence of changes in energy metabolism. *Cardiovasc. Res.* 107, 235–245. doi: 10.1093/cvr/cvv166

Tham, Y. K., Bernardo, B. C., Ooi, J. Y., Weeks, K. L., and McMullen, J. R. (2015). Pathophysiology of cardiac hypertrophy and heart failure: signaling pathways and novel therapeutic targets. *Arch. Toxicol.* 89, 1401–1438. doi: 10.1007/s00204-015-1477-x

Viollet, B., Athea, Y., Mounier, R., Guigas, B., Zarrinpashneh, E., Horman, S., et al. (2009). AMPK: lessons from transgenic and knockout animals. *Front. Biosci.* 14:19–44. doi: 10.2741/3229

Von Euler, U. S., and Liljestrand, G. (1946). Observations on the pulmonary arterial blood pressure in the cat. *Acta Physiol. Scand.* 12, 301–320. doi: 10.1111/j.1748-1716.1946.tb00389.x

Wang, M. Y., and Unger, R. H. (2005). Role of PP2C in cardiac lipid accumulation in obese rodents and its prevention by troglitazone. *Am. J. Physiol. Endocrinol. Metab.* 288, E216–E221. doi: 10.1152/ajpendo.00004.2004

Zhang, H., Liu, B., Li, T., Zhu, Y., Luo, G., Jiang, Y., et al. (2018). AMPK activation serves a critical role in mitochondria quality control via modulating mitophagy in the heart under chronic hypoxia. *Int. J. Mol. Med.* 41, 69–76. doi: 10.3892/ijmm.2017.3213

Conflict of Interest: The authors declare that the research was conducted in the absence of any commercial or financial relationships that could be construed as a potential conflict of interest.

frontiers in Physiology

ORIGINAL RESEARCH
published: 18 January 2021
doi: 10.3389/fphys.2020.540591

Mechanical Stretch Induces Smooth Muscle Cell Dysfunction by Regulating ACE2 via P38/ATF3 and Post-transcriptional Regulation by miR-421

*Xiaolin Liu, Xinxin Liu, Mengmeng Li, Yu Zhang, Weijia Chen, Meng Zhang, Cheng Zhang and Mei Zhang**

The Key Laboratory of Cardiovascular Remodeling and Function Research, The State and Shandong Province Joint Key Laboratory of Translational Cardiovascular Medicine, Chinese Ministry of Education, Chinese National Health Commission and Chinese Academy of Medical Sciences, Qilu Hospital of Shandong University, Jinan, China

OPEN ACCESS

Edited by:
Olga Vinogradova, Russian Academy of Sciences, Russia

Reviewed by:
Mario Kassmann, Charité – Universitätsmedizin Berlin, Germany
Masanori Yoshizumi, Nara Medical University, Japan

***Correspondence:**
Mei Zhang
qiluzhangmei@126.com

Specialty section:
This article was submitted to Vascular Physiology, a section of the journal Frontiers in Physiology

Received: *05 March 2020*
Accepted: *08 December 2020*
Published: *18 January 2021*

Citation:
Liu X, Liu X, Li M, Zhang Y, Chen W, Zhang M, Zhang C and Zhang M (2021) Mechanical Stretch Induces Smooth Muscle Cell Dysfunction by Regulating ACE2 via P38/ATF3 and Post-transcriptional Regulation by miR-421. Front. Physiol. 11:540591. doi: 10.3389/fphys.2020.540591

Mechanical stretch promotes deregulation of vascular smooth muscle cell (VSMC) functions during hypertension-induced vascular remodeling. ACE2 has a wide range of cardiovascular and renal protective effects. Loss of ACE2 is associated with cardiovascular disease, but little is known about the regulation of its expression, especially by abnormal mechanical stretch during hypertension. The present study was designed to investigate the contribution of ACE2 to vascular remodeling under mechanical stretch and to assess the possible underlying mechanisms. The abdominal aortic constriction model was established to mimic the environment *in vivo*. FX-5000T Strain Unit provided mechanical stretch *in vitro*. Overexpression was used to analyze the role of ACE2 played in the proliferation, migration, apoptosis, and collagen metabolism of the VSMCs. RT-qPCR, Western blot, luciferase assay, and ChIP assay were used to elucidate the molecular mechanism of ACE2 expression regulated by stretch. We found that mechanical stretch modulated the expression of the ACE2/Ang-(1–7) and ACE/AngII axis. ACE2 was mechanically sensitive and was involved in the stretch-induced dysfunction of VSMCs. The p38 MAPK/ATF3 pathway and miR-421 participated in the regulation of ACE2. Thus, ACE2 may contribute to the development of vascular remodeling under conditions of mechanical stretch.

Keywords: angiotensin-converting enzyme 2, mechanical stretch, vascular smooth muscle cells, P38 MAPK, ATF3, miR-421

INTRODUCTION

Hypertension is a major risk factor for cardiovascular disease (CVD) and can cause vascular structural and functional abnormalities. During this process, vascular remodeling is a characteristic pathological feature of hypertensive vascular disease (Shi et al., 2018). Hypertension is often accompanied by an increase in the mechanical stretch of the blood vessel wall. As a consequence,

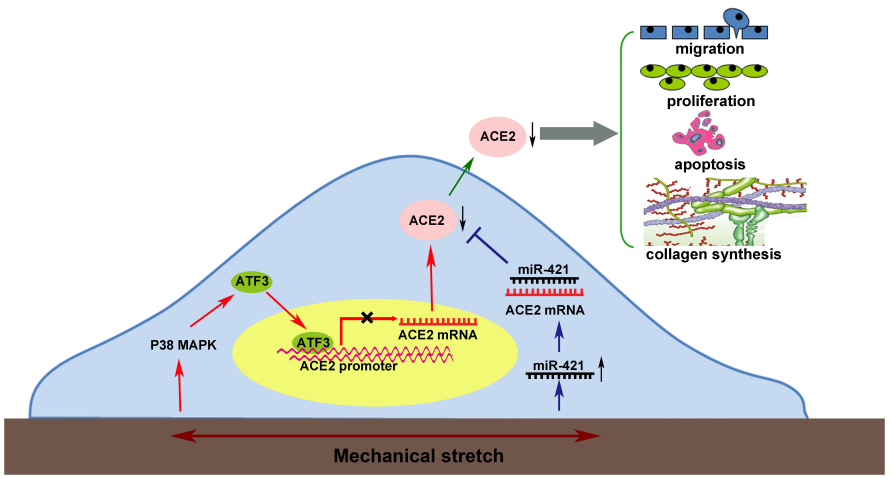

GRAPHICAL ABSTRACT | Mechanical stretch may decrease the level of the protective factor ACE2 via the p38 MAPK/ATF3 pathway by prompting ATF3 translocation into the nucleus, which could directly bind to the ACE2 promoter via post-transcriptional regulation by miR-421.

excess mechanical stretch affects vascular cells, such as endothelial cells (ECs), vascular smooth muscle cells (VSMCs), and adventitial fibroblasts, and causes the dysfunction of these cells (Hahn and Schwartz, 2009), thus resulting in abnormal vascular structure and function. While stretch can affect all vascular cells, VSMCs located in the media of vascular wall are the main target cells. Under physiological conditions, VSMCs rarely proliferate and migrate, usually performing contractile phenotype (Hu et al., 2014). However, under abnormal mechanical stretch, VSMCs undergo phenotypic transformation, characterized by increased proliferation, migration, and extracellular matrix synthesis, thus resulting in the thickening and stiffening of the arterial wall (Qi et al., 2016; Wang et al., 2019).

The renin angiotensin system (RAS) is closely related to cardiovascular disease. ACE2 is a homolog of ACE but differs from ACE in substrate specificity (Riviere et al., 2005), which is able to cleave Ang II and produce the vasodilating peptide Ang-(1–7) (Gallagher et al., 2006). A wealth of evidence has been uncovered regarding the involvement of ACE2 in cardiovascular disease, including heart failure (Patel et al., 2016), abdominal aortic aneurysms (Thatcher et al., 2014), and atherosclerosis (Zhang et al., 2010). The atheroprotective actions of ACE2 have been shown in a variety of studies. This enzyme is expressed in both normal and diseased vessels of human (Zulli et al., 2008) and animals including rat (Zhang et al., 2019) and mouse (Sahara et al., 2014). It is abundant in different cell types, such as ECs, VSMCs, and macrophages (Zhang et al., 2010, 2019).

It is widely recognized that the RAS system is closely associated with mechanical stimulus (Malhotra et al., 1999; Hu et al., 2014; Abdul-Muneer et al., 2018). Mechanical stretch promoted vascular damage by up-regulating AT1 receptor in SMCs of rats (Hitomi et al., 2006). Others have proved that exposure of endothelial cells to shear stress was reported to decrease the expression of ACE via p53 and the post-transcriptional regulation of miR-143/145 (Kohlstedt et al., 2013). Our team previously demonstrated that ACE could mediate the mechanical stretch-induced phenotype modulation of SMCs (Hu et al., 2014). However, relatively little is known about the mechanisms that regulate ACE2 expression in vascular cells, especially by mechanical stimulus. There was one study finding claiming that ACE2 was strongly abundant in low shear stress-induced carotid plaques (Fraga-Silva et al., 2015), so it is reasonable to speculate that ACE2 is also mechanoresponsive and is possibly involved in mechanical stretch-induced vascular remodeling.

In the current study, the abdominal aortic constriction model was established to investigate the role of ACE2 in vascular modeling *in vivo*. As for *in vitro* studies, VSMCs were exposed to mechanical stretch for the indicated time. The aim of our study is to explore the role of ACE2 played in the functions of VSMCs under mechanical stretch as well as the possible mechanisms that underlie this process. A better understanding of the role that ACE2 plays in the development of vascular remodeling may provide clinicians with opportunities to develop new therapies for treatment.

MATERIALS AND METHODS

Cell Culture and *in vitro* Mechanical Stretch System

Vascular smooth muscle cells of human aorta were purchased from the Sciencell Company (United States) and cultured in smooth muscle cell medium with 5% CO_2 at 37°C. To apply cyclic mechanical stretch to smooth muscle cells, flexible-bottomed six-well culture plates from Flexcell International Corporation were used. First, the VSMCs were starved for 24 h with serum-free medium. Then, the medium was replaced, and the cells were stimulated with cyclic mechanical stretch. A Flexcell Tension Plus FX-5000T system (Flexcell International Corp.,

Hillsborough, NC) was used to apply 18% mechanical stretch (pathological) at 1 Hz.

Abdominal Aortic Constriction of Rats

The abdominal aortic constriction model was performed on rats to induce pressure overload (Cheng et al., 2012). Thirty Wistar rats (male, 200–250 g) were obtained from Beijing University Animal Research Center. The rats were anesthetized with 2% isoflurane. A midline abdominal incision was used to separate the skin, subcutaneous tissue, muscle, and peritoneum. The spleen, stomach, and part of the intestine were pulled to the right of the abdominal cavity and protected with saline gauze. The suprarenal level of the abdominal aorta above the kidneys was tied with 6-0 silk to a polyethylene catheter (PE10), and then the catheter was immediately removed. The sham surgery animals underwent the same procedure without abdominal aortic constriction. The animal experimental protocol conformed to the Guide for the Care and Use of Laboratory Animals published by the US National Institutes of Health and was approved by the ethics committee of Shandong University.

RNA Extraction and Quantitative Real-Time PCR

TRIzol reagent was used to extract total RNA from the VSMCs. We used spectrophotometry to quantify the concentration of RNA. Then, RNA was reverse-transcribed into cDNA. The SYRB Premix Ex Taq kit (TaKaRa Bio, Japan) was used for real-time PCR. The relative mRNA expression levels of ACE2 and ACE were assessed by the $2^{-\Delta\Delta Ct}$ method.

Western Blot Analysis

Protein was extracted from the VSMCs and rat aortas. Total cell lysates were separated with 10% sodium dodecyl sulfate–polyacrylamide gel electrophoresis and transferred to polyvinylidene fluoride membranes. The membranes were incubated with 5% non-fat milk for 2 h and then overnight at 4℃ with the corresponding primary antibodies for ACE2 (1:1,000; Abcam, Cambridge, United Kingdom), ACE (1:1,000; Abcam, Cambridge, United Kingdom), activating transcription factor 3 (ATF3; 1:1,000; Abcam, Cambridge, United Kingdom), collagen I (1:1,000; Abcam, Cambridge, United Kingdom), collagen III (1:1,000; Abcam, Cambridge, United Kingdom), total p38 and phosphorylated-p38 (Thr180/Tyr182) (p-p38) (1:1,000; Cell Signaling Technology, MA, United States), total JNK and phosphorylated-JNK (Thr183/Tyr185) (p-JNK) (1:1,000; Cell Signaling Technology, MA, United States), total Erk1/2 and phosphorylated-Erk1/2 (Thr202/Tyr204) (p-Erk1/2) (1:1,000; Cell Signaling Technology, MA, United States), GAPDH (1:1,000; ProteinTech, Wuhan, China), and appropriate secondary antibodies (1:5,000; Abcam, Cambridge, United Kingdom) for 1 h at room temperature. Visualization involved enhanced chemiluminescence plus reagents. Band densities were analyzed by the use of Adobe Photoshop CS6.

ACE2 Activity Assay

The ACE2 and ACE activity of the VSMCs exposed to cyclic mechanical stretch was determined as described previously (Liu et al., 2011). A reagent, 7-Mca-YVADAPK (Dnp) (R&D Systems, Minneapolis, United States), which is cleaved by ACE2, was used as a fluorogenic substrate. Ten μg total protein extracts were incubated with 1.0 μmol/L 7-Mca-YVADAPK (Dnp) in a final volume of 100 μL reaction buffer at room temperature. EDTA (1 mmol/L) and human ACE2 (25 ng) (R&D Systems, Minneapolis, MN, United States) were designed as negative and positive controls, respectively. Fluorescence kinetics was measured for 4 h by the use of Varioskan Flash (Thermo Fisher Scientific, Worcester, MA, United States) at an excitation wavelength of 320 nm and an emission wavelength of 400 nm. ACE2 activity was defined as the difference in fluorescence with or without the ACE2 inhibitor DX600 (1 μmol/L, Phoenix Pharmaceuticals, Belmont, CA, United States). Data were calculated from triplicate wells and presented as fluorescence unit per hour and normalized to milligram tissue protein.

ELISA

The VSMCs were subjected to mechanical stretch at the indicated time points and then harvested. The cytoplasmic proteins were extracted using a commercial kit (Pierce), and the protein concentration was determined by bicinchoninic acid assay. The cytoplasmic proteins from each well were stored at −80°C. AngII and Ang-(1–7) levels were evaluated by commercial ELISA kits (AngII-SPI-BIO, France, and Ang 1–7-Bachem, United States, respectively).

Construction of Adenovirus Vector

To achieve adenovirus-mediated ACE2 overexpression, the adenoviral vector was purchased from GenePharma Co. Ltd. (Shanghai, China), and the full-length coding sequence of human ACE2 C-terminally tagged with green fluorescent protein (GFP) was cloned into the vector. A vector cloned with GFP alone was used as the negative control (NC).

Bromodeoxyuridine Incorporation Assay

Bromodeoxyuridine (BrdU) incorporation assays were used to determine VSMC proliferation. Cells at passages 4–7 were seeded onto six-well Bioflex plates coated with collagen I and underwent different levels of mechanical stretch. The cells were treated with BrdU labeling medium for 6 h and were fixed with an ethanol fixative at -20°C, incubated at 4°C with anti-BrdU working solution overnight, and then stained with anti-mouse-Ig-fluorescein antibody for 30 min and DAPI for 8 min to label the nuclei. Then, the cells were examined using a microscope.

Cell Scratch Test

Scratch tests were performed to evaluate the effect of mechanical stretch on VSMC migration. Cells transfected with Ad-ACE2 or Ad-GFP were plated directly onto silicone membranes of Flexcell six-well plates. After reaching confluence, a line of cells was removed with a sterile 100 μL pipette tip across the layer. The culture media were replaced with serum-free medium, and then

the VSMCs were exposed to 18% mechanical stretch for 12 h. Then, cells were fixed by incubation with 90% ethanol for 20 min, and the migrated distance was measured along the wound edge using Photoshop CS6 software.

Transient Transfection

VSMCs were transfected with negative control siRNA or ATF3 siRNA (GenePharma, Shanghai). For miR-421 over-expression and inhibition, miR-421 mimics, and inhibitor (GenePharma, Shanghai) were transfected into the VSMCs. Lipofectamine 3000 was used for transfection.

Histopathology

The constricted abdominal aortas of rats were dissected and immediately fixed in 4% formalin. The tissue was embedded in paraffin. Successive transverse paraffin sections were cut at a thickness of 5 μm and underwent immunohistochemical incubation with antibodies for ACE2 (1:50) and ACE (1:50) (Abcam, United Kingdom) overnight, followed by incubation with the appropriate secondary antibodies. Signals were amplified with the use of 3,3-diaminobenzidine, counterstained with hematoxylin and analyzed by the use of Image-Pro Plus 6.0 (Media Cybernetics, United States).

Dual Luciferase Reporter Assay

The 3′-UTR fragments of ACE2 mRNA were cloned into the pmirGLO vector (GenePharma, China). Site-specific mutants were generated using PCR. HEK-293T cells were cultured in DMEM in an atmosphere of 5% CO_2 at 37°C. Cells at 50–60% confluence were cotransfected with 100 ng of the 3′-UTR luciferase reporter vector and 50 pmol miR-421 mimics (GenePharma, China) using Lipofectamine 3000 transfection reagent (Invitrogen, United States) following the manufacturer's instructions. After 48 h, firefly and Renilla luciferase activities were detected on a microplate reader (Biotek, United States) using the Dual-Luciferase Reporter Assay System (Promega, United States). To determine the luciferase activity, the ratio of firefly luciferase to Renilla luciferase was calculated for each well.

A series of DNA fragments upstream of the transcription initiation site in the ACE2 promoter [P (-2,000 to -1 bp), P0 (-1,510 to -1 bp), P1 (-227 to 1 bp), P2 (-441 to -218 bp), P3 (-655 to -432 bp), P4 (-868 to -646 bp), P5 (-1,082 to -859 bp), P6 (-1,296 to -1,073 bp) and P7 (-1,510 to -1,289 bp)] were constructed using the pGL3.10-Basic vector. The constructs were transfected into HEK-293T cells with Lipofectamine 3000 transfection reagent (Invitrogen, United States), and the Renilla vector (Promega) was cotransfected to normalize the transfection efficiency, with or without transfection of pcDNA 3.1(+)/ATF3 plasmid. After 48 h, the firefly and Renilla luciferase activities were detected on a microplate reader (Biotek, United States) using the Dual-Luciferase Reporter Assay System (Promega, United States). To determine the luciferase activity, the ratio of firefly luciferase to Renilla luciferase was calculated for each well.

Chromatin Immunoprecipitation Assay

ChIP was performed using VSMCs (density, 1×10^6 cells). The ChIP assay was performed using the SimpleChIP® Enzymatic Chromatin IP Kit (Magnetic Beads) (CST, United States). The chromatin solution was immunoprecipitated using 5 μg anti-ATF3 (CST, United States) antibody or normal anti-IgG antibody, followed by overnight incubation with magnetic beads at 4°C. Next, the beads were washed multiple times, and the antibody–protein–DNA complexes were eluted. Protein and RNA were removed by treatment with proteinase K and RNase, respectively. Next, PCR was performed using the immunoprecipitated genomic DNA and primers specific for the ATF3 binding site upstream of the transcription start site in the ACE2 promoter. The PCR products obtained were electrophoresed on 1% agarose gel.

Flow Cytometry

We used the Annexin V-FITC Apoptosis Detection Kit (BIPEC, United States) to determine the apoptotic cells. In brief, cells with or without stretch treatment were resuspended with 400 mL binding buffer at 10^6 cells/mL, underwent 15 min annexin V-FITC labeling, then 5 min PI labeling, and then were analyzed by flow cytometry in 1 h. In total, 10,000 cells were counted in each assay.

Statistical Analysis

Each experiment was performed for at least three times, and all data were presented as mean ± SEM. Student's *t*-test was used to analyze two group comparisons. A comparison among multiple groups was conducted by one-way ANOVA. All statistical tests were calculated using GraphPad Prism 5.00 (GraphPad Software). In this study, a *P*-value less than 0.05 was considered to be statistically significant.

RESULTS

In vivo Abdominal Aortic Constriction in Rats Influences the Expression of ACE2 and ACE

The abdominal aortic constriction model was performed in rats to induce pressure overload, which could result in elevated mechanical stretch. We found that the levels of ACE2 time-dependently decreased in the abdominal aorta after aortic constriction by RT-qPCR (**Figure 1A**), Western blot (**Figure 1B**), and immunohistochemical staining (**Figure 1D**) analyses. In contrast, the expression of ACE was up-regulated in the aorta after abdominal aortic constriction compared to the sham group ($P < 0.05$; **Figures 1A,C,D**). These results showed that both ACE2 and ACE are responsive to mechanical stretch induced by blood pressure. We collected paracancerous tissues from patients with colorectal cancer combining hypertension or not. A total of 12 patients with colorectal cancer were collected, including six patients with a history of hypertension. Representative photomicrographs of immunohistochemical staining showed significant thickening of the arterial wall in patients with hypertension. Our results showed that the expression of ACE2 in smooth muscle cells significantly decreased in those patients with hypertension, including different sizes of arteries (**Figure 1E**).

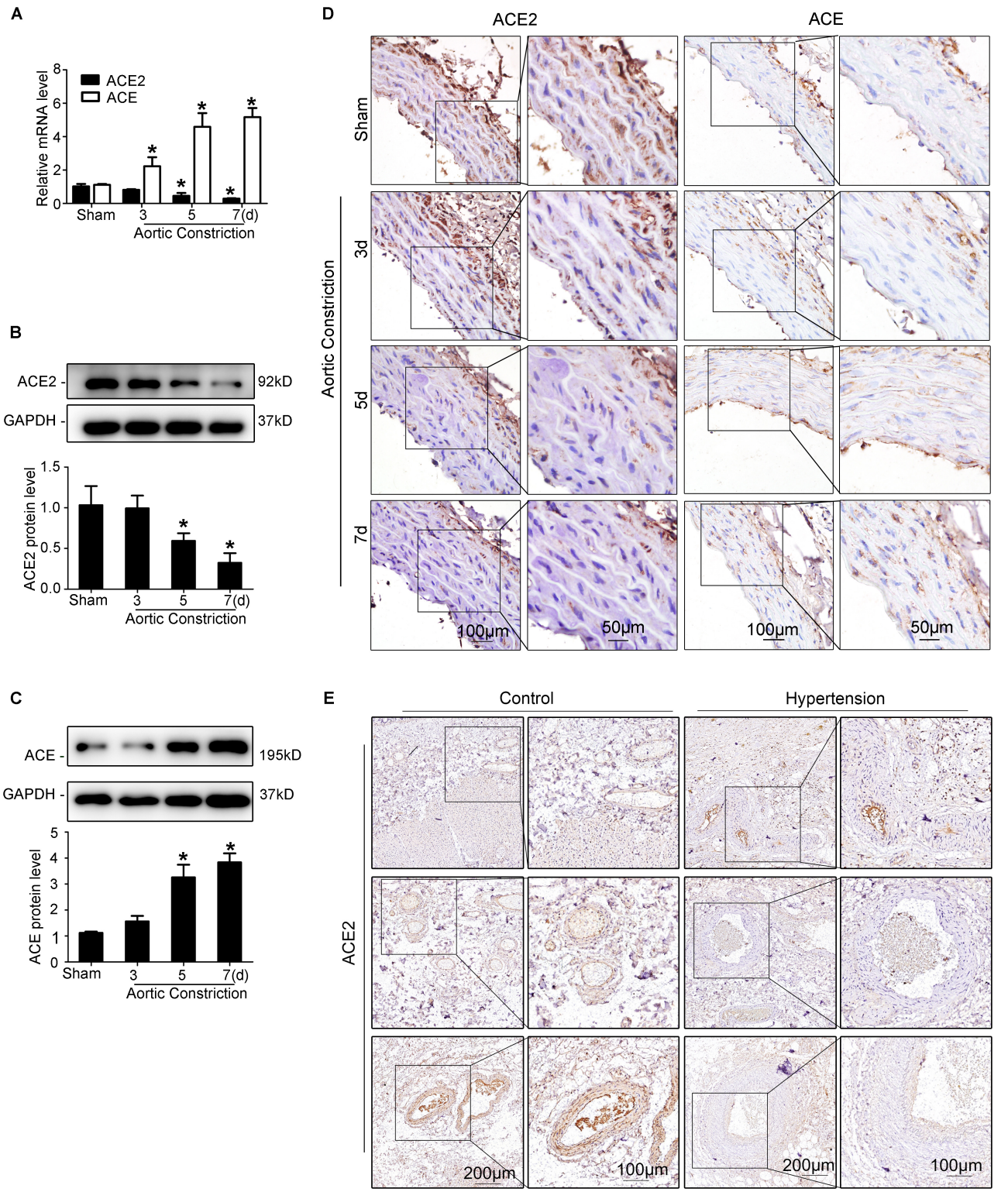

FIGURE 1 | Elevated mechanical stretch suppresses ACE2 and increases ACE expression in the aorta *in vivo*. **(A)** ACE2 and ACE mRNA expression in the aortas of the aortic constriction group and the sham group by RT-qPCR. **(B,C)** ACE2 and ACE protein levels in the aortas of the aortic constriction group and the sham group by Western blot. **(D)** Representative immunohistochemical staining of ACE2 and ACE in sections from the aortas of the aortic constriction group and the sham operation group. **(E)** Representative photomicrographs of immunohistochemical staining of ACE2 in the paracancerous tissues of patients with hypertension or without. Values are expressed as means ± SEM. $^*P < 0.05$ vs. sham ($n = 4$).

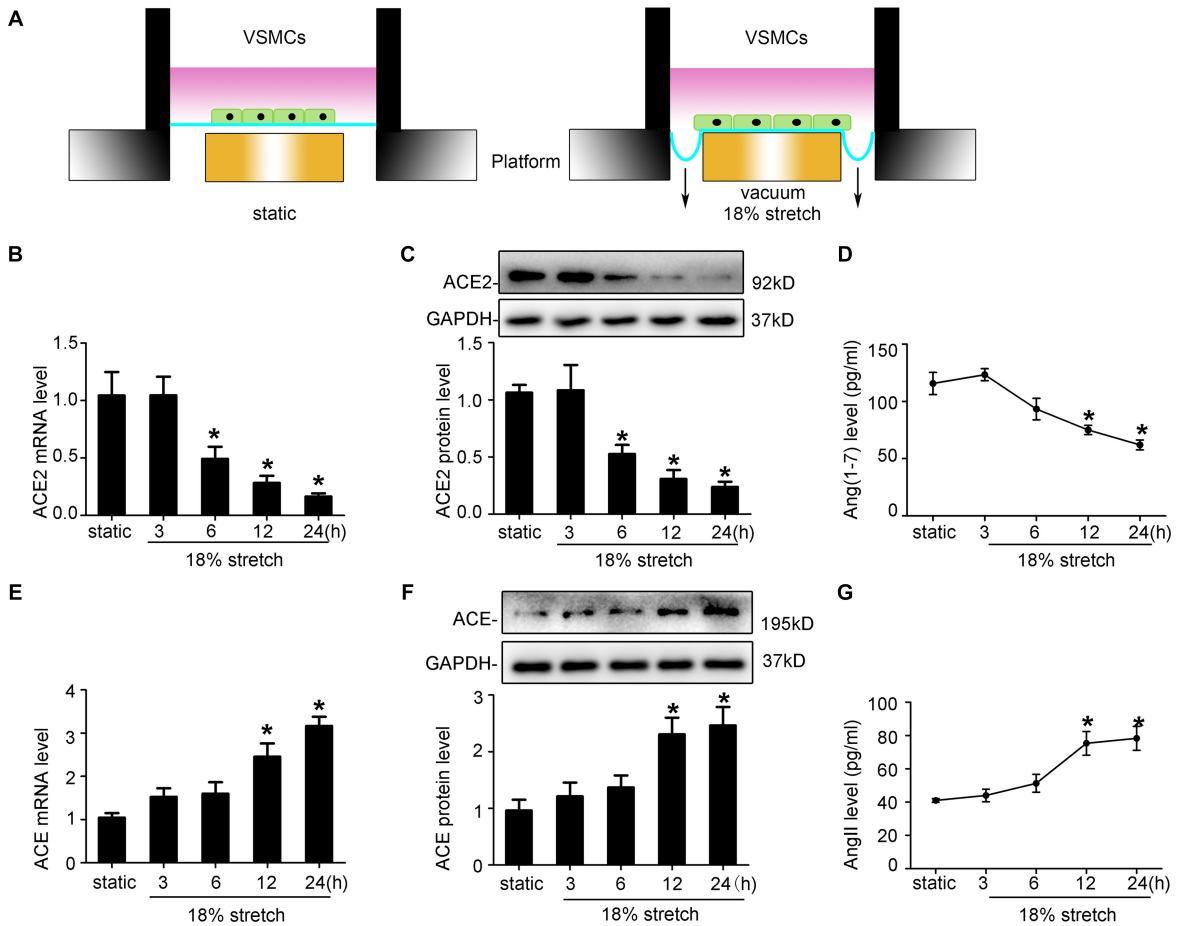

FIGURE 2 | Mechanical stretch modulates ACE2, ACE, Ang-(1–7), and Ang II expression in vascular smooth muscle cells (VSMCs) *in vitro*. **(A)** Schematic diagrams of the mechanical stretch loading system in the current study. VSMCs were subjected to 18% 1 Hz mechanical stretch for the indicated time. **(B,E)** RT-qPCR analysis of ACE2 and ACE mRNA in VSMCs under mechanical stretch for the indicated time. **(C,F)** Western blot analysis of ACE2 and ACE protein expression in VSMCs under mechanical stretch for the indicated time. **(D,G)** Levels of AngII and Ang-(1-7) in VSMCs after exposure to mechanical stretch were assayed by ELISA. Values are expressed as means ± SEM. *$P < 0.05$ vs. static ($n = 4$).

Mechanical Stretch Modulates ACE2/Ang-(1–7) and ACE/AngII Expression in VSMCs *in vitro*

ACE2 is widely expressed in the human aorta, including intima and media. Thus, endothelial cells may also play an important role in stretch-induced vascular remodeling. As VSMCs are the main target cells of elevated mechanical stretch, we focused on the functions of VSMCs in the present study. Here, using a mechanical stretch loading system (**Figure 2A**), we found that VSMCs subjected to mechanical stretch for the indicated time showed decreased ACE2 expression at both mRNA and protein levels, with a significant decrease from 6 h ($P < 0.05$; **Figures 2B,C**), while the expression of ACE was increased ($P < 0.05$; **Figures 2E,F**). ACE2 enzyme activity also declined under stretch ($P < 0.05$; **Supplementary Figure 1**). The protective effects of ACE2 were related to its ability to degrade a vasoconstrictor (AngII) and produce a vasodilator [Ang-(1–7)], so we also assessed the levels of Ang-(l–7) and AngII of cytoplasmic protein. The levels of Ang-(l–7) decreased, while the levels of AngII time-dependently increased under stretch ($P < 0.05$; **Figures 2D,G**).

ACE2 is widely expressed in the human aorta, including intima and media. Thus, endothelial cells may also play an important role in stretch-induced vascular remodeling. As VSMCs are the main target cells of elevated mechanical stretch, we focused on the functions of VSMCs in the present study. By using FX-5000T Strain Unit, which provided mechanical stretch (**Figure 2A**), we found that VSMCs exposed to mechanical stretch for the indicated time showed a decreased ACE2 expression at both mRNA and protein levels, with a significant decrease from 12 h ($P < 0.05$; **Figures 2B,C**), while the expression of ACE was increased ($P < 0.05$; **Figures 2E,F**). ACE2 enzyme activity also declined under stretch ($P < 0.05$; **Supplementary Figure 1**). The protective effects of ACE2 were related to its ability to degrade a vasoconstrictor (AngII) and produce a vasodilator [Ang-(1–7)] (Thatcher et al., 2014), so we also assessed the levels of Ang-(l–7) and AngII of cytoplasmic protein. The levels of Ang-(l–7)

decreased, while the levels of AngII time-dependently increased under stretch ($P < 0.05$; **Figures 2D,G**).

Considering smaller arteries and arterioles (e.g., mesenteric, kidney arteries) that play a quite important role in regulating systemic blood pressure, we purchased smooth muscle cells isolated from superior mesenteric artery (SMA) and then compared them with the aortic smooth muscle cells that we used before. Our results showed that there was no difference in morphology between the two kinds of cells, nor was there any difference in α-SMA expression. Furthermore, after applying FX-5000T Strain Unit, we found that both types of SMCs exposed to mechanical stretch for the indicated time showed a decreased ACE2 expression (**Supplementary Figure 7**).

The Effect of ACE2 on Mechanical Stretch-Induced VSMC Proliferation, Migration, Apoptosis, and Collagen Metabolism

Mechanical stretch may modulate the functions of VSMCs, such as process of proliferation, migration, and phenotypic transformation; 18% mechanical stretch for 12 h markedly promoted the proliferation of VSMCs compared to static control, and overexpression of ACE2 partly rescued the proliferation increased by stretch ($P < 0.05$; **Figures 3A,B**). The efficiency of ACE2 overexpression is shown in **Supplementary Figure 2**. A cell scratch test indicated that the migration distance of VSMCs was obviously stimulated under conditions of stretch, and the promotive effect of mechanical stretch on migration was partly abolished by ACE2 overexpression ($P < 0.01$; **Figures 3C,D**). Moreover, the overexpression of ACE2 reversed the apoptosis and collagen synthesis induced by mechanical stretch ($P < 0.05$; **Figures 3E–H**).

Taken together, our results revealed that ACE2 was involved in mechanical stretch-induced VSMC dysfunction.

The p38 MAPK/ATF3 Pathway Participates in the Expression of ACE2 Under Mechanical Stretch

Previous studies found that mechanical stretch caused the sustained activation of MAPK family members in VSMCs (Haga et al., 2007). A recent study demonstrated that Ang II downregulates ACE2 via the AT1-ERK/p38 MAP kinase pathway (Koka et al., 2008). We found that mechanical stretch induced the phosphorylation of p38 MAPK, JNK, and ERK1/2 ($P < 0.05$, **Figure 4A**). To validate these results, VSMCs were pretreated with the p38 MAPK inhibitor SB203580, JNK inhibitor SP600125, or ERK1/2 inhibitor PD98059 for 1 h, and then the cells underwent 18% stretch for 12 h. The result showed that SB203580 significantly attenuated the stretch-induced downregulation of ACE2 ($P < 0.05$, **Figure 4B**). When exposed to 18% mechanical stretch, the expression of ATF3 was increased, and SB203580 blocked the induction ($P < 0.05$, **Figure 4D**). This result was consistent with previous research claiming that the activation of ATF3 was via the p38 MAPK pathway (Song et al., 2016). Then, we transfected VSMCs with ATF3 siRNA and found that the knockdown of ATF3 reversed the ACE2 level downregulated by mechanical stretch ($P < 0.05$, **Figure 4C**). The efficiency of silence of ATF3 is shown in **Supplementary Figure 3**. Immunofluorescence revealed an increased level of ATF3 in the nuclear region under 18% stretch, which indicated that mechanical stretch modulated the expression of ACE2 by promoting the translocation of ATF3 into the nucleus (**Figure 4E**). Thus, we have full reason to conclude that mechanical stretch may modulate the expression via the p38 MAPK/ATF3 pathway.

ACE2 Is a Direct Transcriptional Target of ATF3

As the results above have shown, the expression of ACE2 may be regulated by stretch via modulating the expression and the location of ATF3. To further identify whether ATF3 could regulate ACE2, we used the JASPAR database (jaspar.genereg.net) to analyze the potential ATF3 binding site in the ACE2 promoter sequence (**Figure 5A**). Different lengths of the ACE2 promoter, named P-P7, were cloned and inserted into the pGL3.10-Basic vector. Then, these derivatives were, respectively, transfected in HEK-293T cells. The relative luciferase activity of P and P0 were almost 30-fold higher than that of the pGL3.10-Basic vector, and those of P1 to P7 were approximately 10-fold higher ($P < 0.05$, **Figure 5B**). An analysis of the luciferase activity indicated that these ACE2 promoter fragments were transcriptionally active. Full-length promoter P and Renilla were co-transfected in VSMCs, and then the VSMCs were exposed to stretch for 6 h. The dual luciferase reporter assay showed that stretch significantly suppressed the activity of ACE2 promoter ($P < 0.05$, **Figure 5C**), which further illustrated that ACE2 is a mechanically sensitive gene. We then co-transfected P and pcDNA-ATF3 (or ATF3 siRNA) in HEK-293T cells and found that overexpression of ATF3 decreased the transcriptional activity of ACE2 promoter ($P < 0.05$, **Figure 5D**), while ATF3 siRNA significantly enhanced the activity ($P < 0.05$, **Figure 5E**), which suggested that ATF3 supressed the expression of ACE2. Next, we intended to find the binding site of ATF3 in the promoter of ACE2. Cotransfection with pcDNA–ATF3 significantly decreased the transcriptional activities of the P and P0 derivatives of the ACE2 promoter ($P < 0.05$, **Figure 5G**), which indicated that the binding site of ATF3 in the promoter of ACE2 was in the region from -1,510 to -1 bp. We then constructed seven fragments of this region (truncated promoter P0) and then cotransfected these fragments with pcDNA-ATF3 into HEK-293T cells. The luciferase activity of P6 significantly decreased ($P < 0.01$, **Figure 5H**), suggesting that -1,296 to -1,073 bp of the ACE2 promoter may contain the binding site of ATF3. ChIP assays were used to verify whether ATF3 interacted with the -1,296- to -1,073-bp region of the ACE2 promoter. The VSMCs were formaldehyde-crosslinked, and chromatin was prepared and digested to fragments (**Supplementary Figure 4**). Chromatin was immunoprecipitated using anti-ATF3 antibody or normal anti-IgG antibody. The results of the ChIP assay further verified that ATF3 binds to this transcriptional area of the ACE2 gene

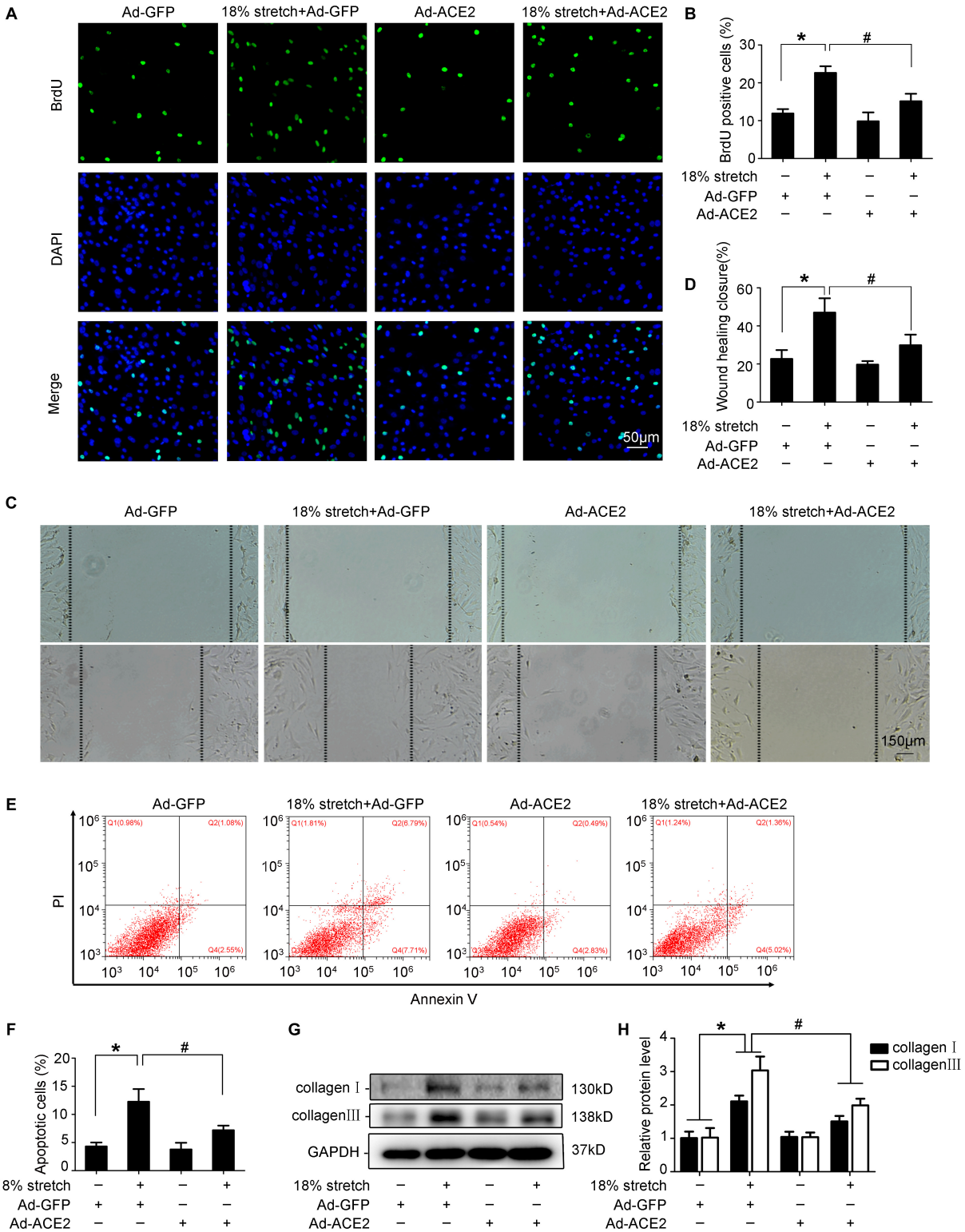

FIGURE 3 | ACE2 was involved in mechanical stretch-induced vascular smooth muscle cells (VSMC) dysfunction. VSMCs were transfected with Ad-ACE2 or Ad-GFP for 24 h and then exposed to mechanical stretch (18% elongation, 1 Hz) for 12 h or not. **(A,B)** Representative views of BrdU-positive cells in different conditions and the percentage of BrdU-positive cells out of total cells. **(C,D)** Representative views of migration distance in different conditions. **(E,F)** Summarized data showing cell apoptosis as determined by flow cytometry analysis in VSMCs. **(G,H)** Western blot analysis of collagen I and collagen III in VSMCs with or without overexpression of ACE2. Values are expressed as means ± SEM. $^{*}P < 0.05$ vs. Ad-GFP; $^{\#}P < 0.05$ vs. 18% stretch + Ad-GFP ($n = 4$).

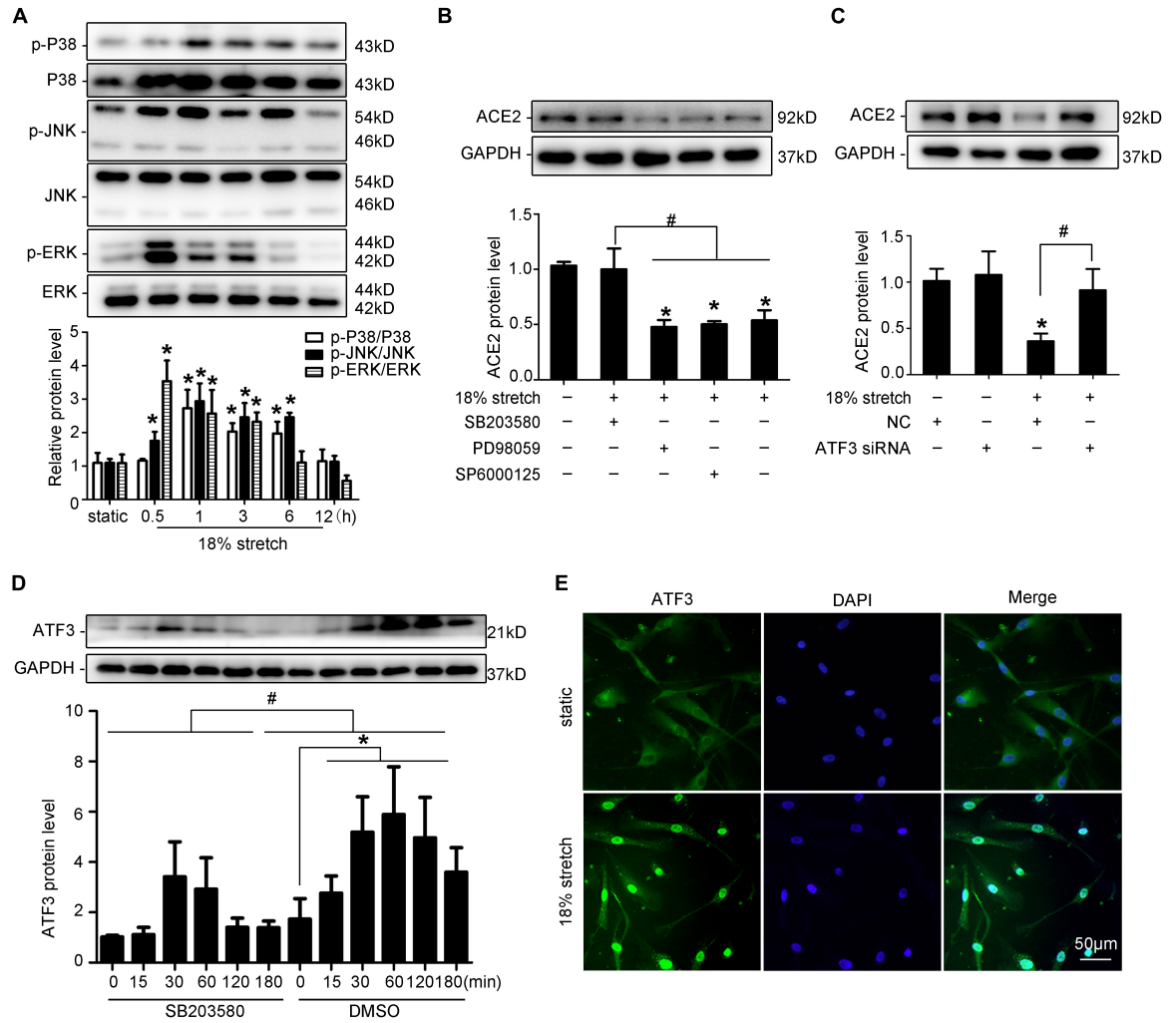

FIGURE 4 | p38 MAPK/ATF3 is involved in ACE2 expression in vascular smooth muscle cells (VSMCs) under 18% mechanical stretch. **(A)** Western blot analysis of the phosphorylation of MAPKs under 18% mechanical stretch for 0–12 h. $^{*}P < 0.05$ vs. static group. **(B)** Western blot analysis of ACE2 in VSMCs under mechanical stretch pretreated with SB203580, SP600125, or PD98059. $^{*}P < 0.05$ vs. static control. $^{\#}P < 0.05$ vs. 18% stretch control. **(C)** Western blot analysis of ACE2 in VSMCs under 18% stretch or not after transfecting with negative control or ATF3 siRNA. $^{*}P < 0.05$ vs. NC group, $^{\#}P < 0.05$ vs. 18% stretch with NC group. **(D)** Western blot analysis of ATF3 in VSMCs under 18% mechanical stretch with or without pretreatment of SB203580. **(E)** Immunofluorescence using anti-ATF3 was performed under stretch or not.

(**Figure 5F**). Taken together, these data suggest that ACE2 is a direct transcriptional target of ATF3.

miR-421 Is Involved in the Expression of ACE2 Under Mechanical Stretch

Kassiri et al. (2009) found that the ACE2 mRNA expression and protein levels did not match in rat myocardial infarction, suggesting that there may be post-transcriptional regulation. To verify whether miRNAs are involved in the regulation of ACE2 expression, Dicer siRNA was used to interfere with the expression of the Dicer enzyme to block the synthesis of miRNAs. RT-qPCR and Western blot results indicated that ACE2 expression was increased after Dicer interference compared with the control group ($P < 0.05$; **Figures 6A,B**). We used prediction software (TargetScan, miRD, and microRNA.org) to search for putative miRNAs. The three libraries predicted 256, 50, and 21 microRNAs, respectively, and two microRNAs (miR-421 and miR-203) were predicted among all three libraries (**Figure 6C**). In our research, the levels of miR-421 increased under 18% mechanical stretch ($P < 0.05$, **Figure 6D**), while the levels of miR-203 decreased (**Supplementary Figure 5**). Thus, we focused on miR-421 in the following experiments, which were harbored in the binding sites of ACE2 3′-UTR (**Figure 6E**).

To verify whether miR-421 binds to ACE2-3′-UTR, miR-421 mimics and luciferase reporters containing wild-type (WT) or mutant (Mut) sequences of ACE2-3′-UTR were transfected into HEK-293T cells. Compared with the control group, the miR-421 mimics significantly reduced the ACE2-3′-UTR-WT

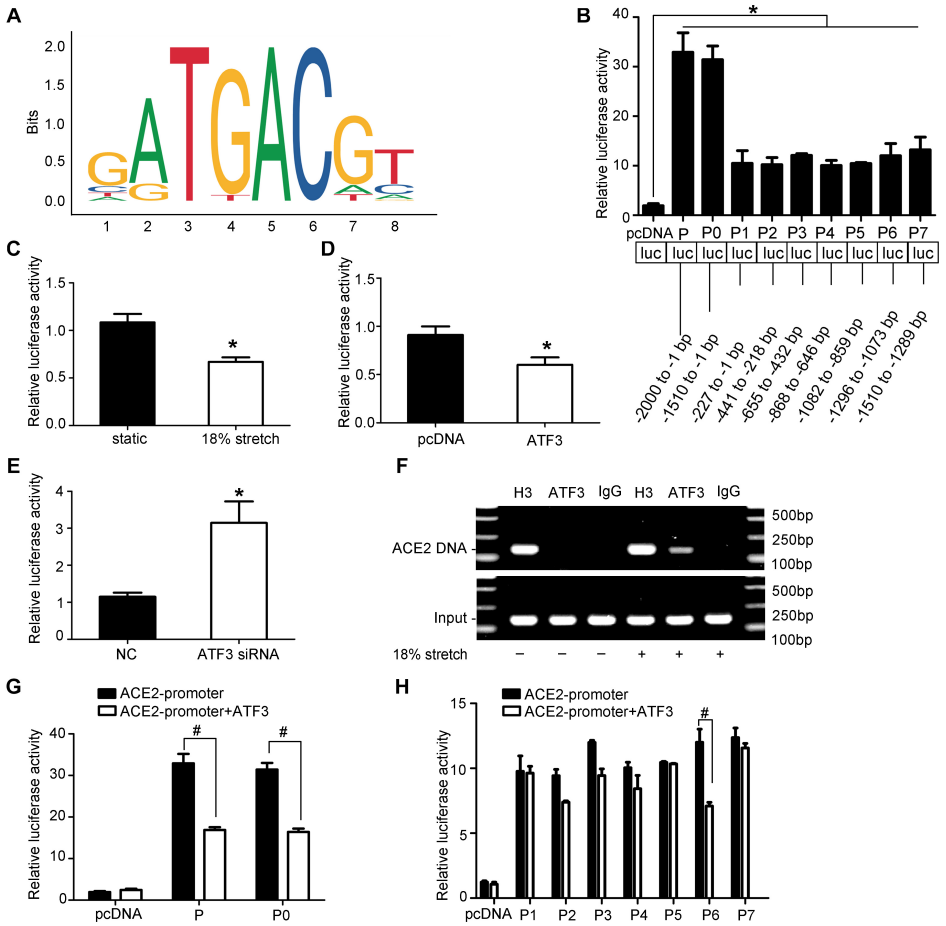

FIGURE 5 | ACE2 is a direct transcriptional target of ATF3. **(A)** The sequence logo of a potential ATF3 binding site in JASPAR. **(B)** The relative luciferase activities of the full ACE2 promoter and the truncated constructs in HEK-293T cells. *$P < 0.05$ vs. pGL3.10-Basic vector. **(C)** The relative luciferase activities of the full ACE2 promoter P in vascular smooth muscle cells under mechanical stretch for 6 h or not. *$P < 0.05$ vs. static control. **(D,E)** The relative luciferase activities of the full ACE2 promoter P co-transfected with pcDNA-ATF3 (or ATF3 siRNA). *$P < 0.05$ vs. control. **(F)** ChIP assay showing ATF3 directly bound to the ACE2 promoter (P6, at the -1,296 to -1,073 bp region). IgG, negative control; H3, positive control; ATF3, ATF3 antibody. **(G,H)** Luciferase activity analysis of P-P7 promoter with or without co-transfection of ATF3. #$P < 0.05$ vs. the corresponding promoter without co-transfection of ATF3 ($n = 4$).

luciferase activity but had no effect on the ACE2-3′-UTR-Mut luciferase activity ($P > 0.05$, **Figure 6H**), indicating that miR-421 directly targets ACE2-3′-UTR. To further validate the effect of miR-421 on the expression of ACE2, VSMCs were transfected with miR-421 mimics, inhibitor, or NC sequence. The efficiency of mimics and inhibitor was detected (**Supplementary Figure 6**). We found that miR-421 mimics significantly reduced the expression of ACE2 in VSMCs ($P < 0.05$; **Figures 6F,I**), while the miR-421 inhibitor significantly increased the expression of ACE2 ($P < 0.05$; **Figures 6G,J**). Taken together, the results above suggested that miR-421 negatively regulated the expression of ACE2 by directly binding to the 3′-UTR. However, whether miR-421 is involved in stretch-regulated ACE2 is still unknown. After the VSMCs were transfected with the miR-421 inhibitor, we assessed the expression of ACE2 under mechanical stretch. The miR-421 inhibitor significantly attenuated the stretch-induced downregulation of ACE2 expression ($P < 0.01$, **Figure 6K**). These results indicated that miR-421 was involved in the regulation of mechanical stretch on ACE2 expression.

DISCUSSION

From the present findings and those in the literature, **Graphical Abstract** summarizes a network of molecular events leading to the dysfunction of VSMCs by mechanical stretch. Mechanical stretch may decrease the level of the protective factor ACE2 via the p38 MAPK/ATF3 pathway by prompting ATF3 translocation into the nucleus, which could directly bind to the ACE2 promoter, and via post-transcriptional regulation by miR-421. Downregulation of ACE2 by mechanical stretch leads to vascular remodeling by being involved in the process of VSMC proliferation, migration, apoptosis, and collagen metabolism.

Hypertension is often accompanied by an increase in mechanical stretch of the vascular wall. It is one of the most

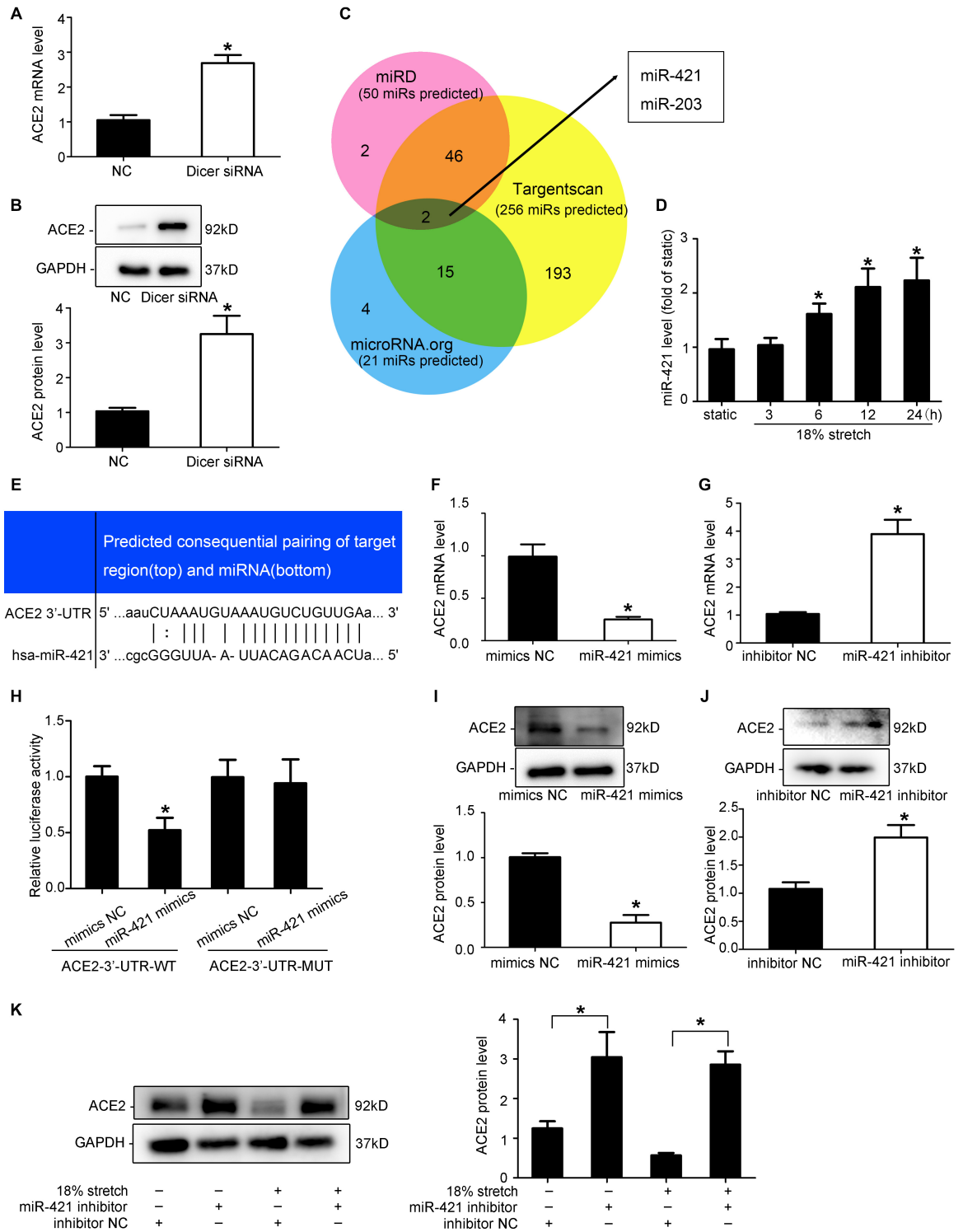

FIGURE 6 | miR-421 is involved in the expression of ACE2 under mechanical stretch. **(A,B)** RT-qPCR and Western blot analysis of ACE2 mRNA and protein expression in vascular smooth muscle cells (VSMCs) transfected with Dicer siRNA. **(C)** Venn diagram of the number of transcription factors in three libraries. **(D)** RT-qPCR analysis of the levels of miR-421 under 18% mechanical stretch for the indicated time. **(E)** Sequence alignment between miR-421 and putative binding sites in the 3′-UTR of ACE2 mRNA. **(H)** Effects of the miR-421 mimics on the activities of the luciferase reporter plasmids with the full-length (Wild) and mutated (Mut) ACE2-3′-UTR. HEK-293T cells were transfected with the ACE2-3′-UTR-WT and ACE2-3′-UTR-mut, together with miR-421 mimics, for 48 h. **(F,G,I,J)** RT-qPCR and Western blot analysis of ACE2 mRNA and protein expression in VSMCs transfected with miR-421 mimics (or inhibitor). **(K)** Western blot analysis of ACE2 protein expression in VSMCs under stretch for 12 h transfected with miR-421 inhibitor. Values are expressed as means ± SEM. *$P < 0.05$ vs. NC group ($n = 4$).

common factors that cause cardiovascular remodeling, including cardiac and vascular remodeling. Vascular remodeling, often in the aorta, refers to the changes in the structure and function of the arterial wall, which is accompanied by increased stiffness, loss of compliance, and increased inflammatory response in the vascular wall (Galderisi and de Divitiis, 2008; Alghamri et al., 2013). Elevated mechanical stretch promotes proliferation, migration, and collagen synthesis of vascular cells, which causes thickening and stiffness of the vascular wall (Shah et al., 2013; Jufri et al., 2015). As main target of mechanical stretch, VSMCs play a pivotal role in vascular remodeling.

Accumulating evidence demonstrated that "ACE2 is a tissue-specific negative feedback regulator of activated RAS, and the ACE2/Ang-(1–7)-Mas receptor axis plays an important role in regulating blood pressure and cardiovascular remodeling" (Turner and Hooper, 2002; Yamamoto et al., 2006; Zhong et al., 2010; Pan et al., 2018). ACE2 has been shown to reduce hypertension, myocardial hypertrophy, and fibrosis due to Ang II and heart failure induced by pressure overload (Gurley et al., 2006; Grobe et al., 2007; Mercure et al., 2008). Multiple studies have shown that ACE2 plays important roles in VSMC function exposed to various stimuli, including high glucose (Lavrentyev and Malik, 2009), Ang II, Ang II (Patel et al., 2014), and hypoxia (Zhang et al., 2009). In our study, vascular remodeling in a hypertensive model caused by abdominal aortic constriction is associated with a significantly decreased expression of ACE2. As for *in vitro* experiments, the levels of ACE2/Ang-(1–7) and ACE/Ang II in VSMCs showed different trends under the stimulation of mechanical stretch. Stretch promoted the dysfunction of VSMCs, including proliferation, migration, apoptosis, and collagen synthesis. By carrying out gain-of-function experiments, we found that the overexpression of ACE2 by adenovirus significantly reduced the influence of mechanical stretch on SMCs, which suggests a possible role for ACE2 in stretch-induced vascular remodeling. It may seem contradictory that proliferation and apoptosis were simultaneously induced under mechanical stretch in our study. However, we are not the first to report this phenomenon as Professor Li (Ping et al., 2017) and Professor Yan (Cai et al., 2012) also found the same in their research. Although the reason remains largely unclear, there is one explanation that may help. Professor Li found in their study that "dying apoptotic cells were surrounded by the proliferating cells, forming a "dead cell-inducing apoptosis, apoptotic cell-inducing proliferation" vicious circle, leading to accelerated vascular remodeling and eventually diseases" (Ping et al., 2017).

Although ACE2 is profoundly protective in different diseases, it is still difficult in clinical administration due to its instability and degradability. Therefore, we focused on the underlying mechanisms in the hope of finding a new mediator to increase the expression or activity of ACE2. Many signaling pathways have been indicated to be mechano-responsive, which could be influenced by mechanical stretch, including the PI3K/Akt10, PKC11, NFκB12, Rho family GTPases13, and MAPK pathways (Bao et al., 2019). P38 is one of the main members of the MAPK family participating in various cell activities such as cell proliferation, migration, and apoptosis. In our study, we found that stretch increased the phosphorylation level of p38, and the repression of mechanical stretch on ACE2 expression can be weakened by the inhibition of p38. ATF3 is a member of the ATF/CREB gene family, which is an immediate-early gene. Lv et al. (2011) proved that ATF3 can regulate the proliferation and migration of VSMCs. Recent studies have found that ATF3 plays a key role in hypertensive cardiac remodeling (Li et al., 2017). These studies indicate that ATF3 is a mechanically induced gene. Thus, we proposed that p38 MAPK may link the activation of ATF3 with the decreased expression of ACE2 in VSMCs under mechanical stretch. In our study, we confirmed that mechanical stretch downregulated the expression of ACE2 via the p38 MAPK/ATF3 pathway by promoting the expression and translocation of ATF3 into the nucleus. Using dual-luciferase reporter assay and ChIP assays, we demonstrated a new regulatory mechanism of ACE2 expression in which ATF3 binds directly to the promoter and inhibits its expression. These results strongly indicated the pivotal roles of the p38/ATF3 pathway in mechanical stretch-induced ACE2 in VSMCs.

It is known that modulation of gene expression involves various steps, including transcriptional regulation, post-transcriptional regulation, protein synthesis, and degradation. A large number of studies have demonstrated that mechano-miRNAs may also play a role in the progression of vascular remodeling. For example, Professor Zhou found that endothelium-derived miR-126, in response to shear stress, can be delivered to VSMCs and prevent VSMC turnover (Zhou et al., 2013). Lamin A/C negatively regulated by miR-124-3p modulates the apoptosis of vascular smooth muscle cells during cyclic stretch (Bao et al., 2019). We knocked down the expression of the Dicer enzyme to block the synthesis of miRNAs and verified that miRNAs are involved in the regulation of ACE2 expression. By using the prediction softwares (TargetScan, miRD, and microRNA.org), two microRNAs (miR-421 and miR-203) were predicted among all three libraries. In our research, the levels of miR-421 increased under mechanical stretch, while the levels of miR-203 decreased, so we focused on miR-421 in the following experiments. Several studies have revealed that miR-421 is very important for proliferation, apoptosis, and tumorigenesis (Meng et al., 2019; Xiao et al., 2019). However, whether miR-421 can be induced by mechanical stretch and whether it is involved in stretch-regulated ACE2 in SMCs are still unknown. In our research, the levels of miR-421 increased under mechanical stretch. Using dual-luciferase reporter assay, ACE2 was validated as a direct target of miR-421, which was consistent with a previous study (Lambert et al., 2014). By performing both gain-of-function experiments, we confirmed that stretch could regulate ACE2 expression via post-transcriptional pathway by miR-421.

In summary, our data revealed that pathological mechanical stretch suppresses the expression of ACE2 via the p38 MAPK/ATF3 pathway and post-transcriptional regulation by miR-421, contributing to promote VSMC dysfunction and vascular remodeling in the hypertension process. A better

understanding of the role that ACE2 plays in the development of vascular remodeling may provide clinicians with opportunities to develop new therapies for treatment.

A few limitations need to be mentioned. First, we did not study the mechanisms of how ACE2 influences the functions of VSMCs. Second, the role of ACE2 would be better supported by its overexpression *in vivo*.

DATA AVAILABILITY STATEMENT

All datasets generated for this study are included in the article/**Supplementary Material**.

ETHICS STATEMENT

The study was approved by the Medical Ethics Committee of Qilu Hospital of Shandong University (KYLL-202011-121).

AUTHOR CONTRIBUTIONS

XLL, XXL, and ML designed the experiments. XLL, YZ, and WC performed the experiments. MenZ and CZ analyzed the data. XLL and MeiZ wrote the manuscript. All authors approved the final version of the manuscript.

FUNDING

This work was supported by the National Natural Science Foundation of China (Nos. 81270404 and 81770439).

SUPPLEMENTARY MATERIAL

The Supplementary Material for this article can be found online at: https://www.frontiersin.org/articles/10.3389/fphys.2020.540591/full#supplementary-material

REFERENCES

Abdul-Muneer, P. M., Bhowmick, S., and Briski, N. (2018). Angiotensin II causesneuronal damage in stretch-injured neurons: protective effects of losartan, an angiotensin T1 receptor blocker. *Mol. Neurobiol.* 55, 5901–5912. doi: 10.1007/s12035-017-0812-z

Alghamri, M. S., Weir, N. M., Anstadt, M. P., Elased, K. M., Gurley, S. B., and Morris, M. (2013). Enhanced angiotensin II-induced cardiac and aortic remodeling in ACE2 knockout mice. *J. Cardiovasc. Pharmacol. Ther.* 18, 138–151. doi: 10.1177/1074248412460124

Bao, H., Li, H. P., Shi, Q., Huang, K., Chen, X. H., Chen, Y. X., et al. (2019). Lamin A/C negatively regulated by miR-124-3p modulates apoptosis of vascular smooth muscle cells during cyclic stretch application in rats. *Acta Physiol.* 228:e13374. doi: 10.1111/apha.13374

Cai, Y., Knight, W. E., Guo, S., Li, J. D., Knight, P. A., and Yan, C. (2012). Vinpocetine suppresses pathological vascular remodeling by inhibiting vascular smooth muscle cell proliferation and migration. *J. Pharmacol. Exp. Ther.* 343, 479–488. doi: 10.1124/jpet.112.195446

Cheng, W. P., Wang, B. W., Chen, S. C., Chang, H., and Shyu, K. G. (2012). Mechanical stretch induces the apoptosis regulator PUMA in vascular smooth muscle cells. *Cardiovasc. Res.* 93, 181–189. doi: 10.1093/cvr/cvr280

Fraga-Silva, R. A., Montecucco, F., Costa-Fraga, F. P., Nencioni, A., Caffa, I., Bragina, M. E., et al. (2015). Diminazene enhances stability of atherosclerotic plaques in ApoE-deficient mice. *Vascul Pharmacol.* 74, 103–113. doi: 10.1016/j.vph.2015.08.014

Galderisi, M., and de Divitiis, O. (2008). Risk factor-induced cardiovascular remodeling and the effects of angiotensin-converting enzyme inhibitors. *J. Cardiovasc. Pharmacol.* 51, 523–531. doi: 10.1097/FJC.0b013e31817751a7

Gallagher, P. E., Chappell, M. C., Ferrario, C. M., and Tallant, E. A. (2006). Distinct roles for ANG II and ANG-(1-7) in the regulation of angiotensin-converting enzyme 2 in rat astrocytes. *Am. J. Physiol. Cell Physiol.* 290, C420–C426. doi: 10.1152/ajpcell.00409.2004

Grobe, J. L., Mecca, A. P., Lingis, M., Shenoy, V., Bolton, T. A., Machado, J. M., et al. (2007). Prevention of angiotensin II-induced cardiac remodeling by angiotensin-(1-7). *Am. J. Physiol. Heart Circ. Physiol.* 292, H736–H742. doi: 10.1152/ajpheart.00937.2006

Gurley, S. B., Allred, A., Le, T. H., Griffiths, R., Mao, L., Philip, N., et al. (2006). Altered blood pressure responses and normal cardiac phenotype in ACE2-null mice. *J. Clin. Invest.* 116, 2218–2225. doi: 10.1172/JCI16980

Haga, J. H., Li, Y. S., and Chien, S. (2007). Molecular basis of the effects of mechanical stretch on vascular smooth muscle cells. *J. Biomech.* 40, 947–960. doi: 10.1016/j.jbiomech.2006.04.011

Hahn, C., and Schwartz, M. A. (2009). Mechanotransduction in vascular physiology and atherogenesis. *Nat. Rev. Mol. Cell Biol.* 10, 53–62. doi: 10.1038/nrm2596

Hitomi, H., Fukui, T., Moriwaki, K., Matsubara, K., Sun, G. P., Rahman, M., et al. (2006). Synergistic effect of mechanical stretch and angiotensin II on superoxide production via NADPH oxidase in vascular smooth muscle cells. *J. Hypertens* 24, 1089–1095. doi: 10.1097/01.hjh.0000226199.51805.88

Hu, B., Song, J. T., Qu, H. Y., Bi, C. L., Huang, X. Z., Liu, X. X., et al. (2014). Mechanical stretch suppresses microRNA-145 expression by activating extracellular signal-regulated kinase 1/2 and upregulating angiotensin-converting enzyme to alter vascular smooth muscle cell phenotype. *PLoS One* 9:e96338. doi: 10.1371/journal.pone.0096338

Jufri, N. F., Mohamedali, A., Avolio, A., and Baker, M. S. (2015). Mechanical stretch: physiological and pathological implications for human vascular endothelial cells. *Vasc. Cell* 7:8. doi: 10.1186/s13221-015-0033-z

Kassiri, Z., Zhong, J., Guo, D., Basu, R., Wang, X., Liu, P. P., et al. (2009). Loss of angiotensin-converting enzyme 2 accelerates maladaptive left ventricular remodeling in response to myocardial infarction. *Circ. Heart Fail* 2, 446–455. doi: 10.1161/CIRCHEARTFAILURE.108.840124

Kohlstedt, K., Trouvain, C., Boettger, T., Shi, L., Fisslthaler, B., and Fleming, I. (2013). AMP-activated protein kinase regulates endothelial cell angiotensin-converting enzyme expression via p53 and the post-transcriptional regulation of microRNA-143/145. *Circ. Res.* 112, 1150–1158. doi: 10.1161/CIRCRESAHA.113.301282

Koka, V., Huang, X. R., Chung, A. C., Wang, W., Truong, L. D., and Lan, H. Y. (2008). Angiotensin II up-regulates angiotensin I-converting enzyme (ACE), but down-regulates ACE2 via the AT1-ERK/p38 MAP kinase pathway. *Am. J. Pathol.* 172, 1174–1183. doi: 10.2353/ajpath.2008.070762

Lambert, D. W., Lambert, L. A., Clarke, N. E., Hooper, N. M., Porter, K. E., and Turner, A. J. (2014). Angiotensin-converting enzyme 2 is subject to post-transcriptional regulation by miR-421. *Clin. Sci.* 127, 243–249. doi: 10.1042/CS20130420

Lavrentyev, E. N., and Malik, K. U. (2009). High glucose-induced Nox1-derived superoxides downregulate PKC-βII, which subsequently decreases ACE2 expression and ANG(1-7) formation in rat VSMCs. *Am. J. Physiol. -Heart Circ. Physiol.* 296, H106–H118. doi: 10.1152/ajpheart.00239.2008

Li, Y., Li, Z., Zhang, C., Li, P., Wu, Y., Wang, C., et al. (2017). Cardiac fibroblast-specific activating transcription factor 3 protects against heart failure by suppressing MAP2K3-p38 signaling. *Circulation* 135, 2041–2057. doi: 10.1161/CIRCULATIONAHA.116.024599

Liu, C. X., Hu, Q., Wang, Y., Zhang, W., Ma, Z. Y., Feng, J. B., et al. (2011). Angiotensin-converting enzyme (ACE) 2 overexpression ameliorates

glomerular injury in a rat model of diabetic nephropathy: a comparison with ACE inhibition. *Mol. Med.* 17, 59–69. doi: 10.2119/molmed.2010.00111

Lv, D., Meng, D., Zou, F. F., Fan, L., Zhang, P., Yu, Y., et al. (2011). Activating transcription factor 3 regulates survivability and migration of vascular smooth muscle cells. *IUBMB Life* 63, 62–69. doi: 10.1002/iub.416

Malhotra, R., Sadoshima, J., Brosius, F. C. III, and Izumo, S. (1999). Mechanical stretch and angiotensin II Differentially upregulate the renin-angiotensin system in cardiac myocytes in vitro. *Circ. Res.* 85, 137–146.

Meng, Q., Li, S., Liu, Y., Zhang, S., Jin, J., Zhang, Y., et al. (2019). Circular RNA circSCAF11 accelerates the glioma tumorigenesis through the miR-421/SP1/VEGFA Axis. *Mol. Ther. Nucleic Acids* 17, 669–677. doi: 10.1016/j.omtn.2019.06.022

Mercure, C., Yogi, A., Callera, G. E., Aranha, A. B., Bader, M., Ferreira, A. J., et al. (2008). Angiotensin(1-7) blunts hypertensive cardiac remodeling by a direct effect on the heart. *Circ Res* 103, 1319–1326. doi: 10.1161/CIRCRESAHA.108.184911

Pan, X., Shao, Y., Wu, F., Wang, Y., Xiong, R., Zheng, J., et al. (2018). FGF21 prevents angiotensin ii-induced hypertension and vascular dysfunction by activation of ACE2/Angiotensin-(1-7) Axis in Mice. *Cell Metab.* 27, 1323.e5–1337.e5. doi: 10.1016/j.cmet.2018.04.002

Patel, V. B., Zhong, J. C., Fan, D., Basu, R., Morton, J. S., Parajuli, N., et al. (2014). Angiotensin-converting enzyme 2 is a critical determinant of angiotensin II-induced loss of vascular smooth muscle cells and adverse vascular remodeling. *Hypertension* 64, 157–164. doi: 10.1161/HYPERTENSIONAHA.114.03388

Patel, V. B., Zhong, J. C., Grant, M. B., and Oudit, G. Y. (2016). Role of the ACE2/Angiotensin 1-7 axis of the renin-angiotensin system in heart failure. *Circ. Res.* 118, 1313–1326. doi: 10.1161/CIRCRESAHA.116.307708

Ping, S., Liu, S., Zhou, Y., Li, Z., Li, Y., Liu, K., et al. (2017). Protein disulfide isomerase-mediated apoptosis and proliferation of vascular smooth muscle cells induced by mechanical stress and advanced glycosylation end products result in diabetic mouse vein graft atherosclerosis. *Cell Death Dis.* 8:e2818. doi: 10.1038/cddis.2017.213

Qi, Y. X., Yao, Q. P., Huang, K., Shi, Q., Zhang, P., Wang, G. L., et al. (2016). Nuclear envelope proteins modulate proliferation of vascular smooth muscle cells during cyclic stretch application. *Proc. Natl. Acad. Sci. U.S.A.* 113, 5293–5298. doi: 10.1073/pnas.1604569113

Riviere, G., Michaud, A., Breton, C., VanCamp, G., Laborie, C., Enache, M., et al. (2005). Angiotensin-converting enzyme 2 (ACE2) and ACE activities display tissue-specific sensitivity to undernutrition-programmed hypertension in the adult rat. *Hypertension* 46, 1169–1174. doi: 10.1161/01.HYP.0000185148.27901.fe

Sahara, M., Ikutomi, M., Morita, T., Minami, Y., Nakajima, T., Hirata, Y., et al. (2014). Deletion of angiotensin-converting enzyme 2 promotes the development of atherosclerosis and arterial neointima formation. *Cardiovasc. Res.* 101, 236–246. doi: 10.1093/cvr/cvt245

Shah, M. R., Wedgwood, S., Czech, L., Kim, G. A., Lakshminrusimha, S., Schumacker, P. T., et al. (2013). Cyclic stretch induces inducible nitric oxide synthase and soluble guanylate cyclase in pulmonary artery smooth muscle cells. *Int. J. Mol. Sci.* 14, 4334–4348. doi: 10.3390/ijms14024334

Shi, L., Tian, C., Sun, L., Cao, F., and Meng, Z. (2018). The lncRNA TUG1/miR-145-5p/FGF10 regulates proliferation and migration in VSMCs of hypertension. *Biochem. Biophys. Res. Commun.* 501, 688–695. doi: 10.1016/j.bbrc.2018.05.049

Song, H. M., Park, G. H., Eo, H. J., and Jeong, J. B. (2016). Naringenin-mediated ATF3 expression contributes to apoptosis in human colon cancer. *Biomol. Ther.* 24, 140–146. doi: 10.4062/biomolther.2015.109

Thatcher, S. E., Zhang, X., Howatt, D. A., Yiannikouris, F., Gurley, S. B., Ennis, T., et al. (2014). Angiotensin-converting enzyme 2 decreases formation and severity of angiotensin II-induced abdominal aortic aneurysms. *Arterioscler. Thromb. Vasc. Biol.* 34, 2617–2623. doi: 10.1161/ATVBAHA.114.304613

Turner, A. J., and Hooper, N. M. (2002). The angiotensin-converting enzyme gene family: genomics and pharmacology. *Trends Pharmacol. Sci.* 23, 177–183. doi: 10.1016/s0165-6147(00)01994-5

Wang, W. B., Li, H. P., Yan, J., Zhuang, F., Bao, M., Liu, J. T., et al. (2019). CTGF regulates cyclic stretch-induced vascular smooth muscle cell proliferation via microRNA-19b-3p. *Exp. Cell Res.* 376, 77–85. doi: 10.1016/j.yexcr.2019.01.015

Xiao, W., Zheng, S., Zou, Y., Yang, A., Xie, X., Tang, H., et al. (2019). CircAHNAK1 inhibits proliferation and metastasis of triple-negative breast cancer by modulating miR-421 and RASA1. *Aging* 11, 12043–12056. doi: 10.18632/aging.102539

Yamamoto, K., Ohishi, M., Katsuya, T., Ito, N., Ikushima, M., Kaibe, M., et al. (2006). Deletion of angiotensin-converting enzyme 2 accelerates pressure overload-induced cardiac dysfunction by increasing local angiotensin II. *Hypertension* 47, 718–726. doi: 10.1161/01.HYP.0000205833.89478.5b

Zhang, C., Zhao, Y. X., Zhang, Y. H., Zhu, L., Deng, B. P., Zhou, Z. L., et al. (2010). Angiotensin-converting enzyme 2 attenuates atherosclerotic lesions by targeting vascular cells. *Proc. Natl. Acad. Sci. U.S.A.* 107, 15886–15891. doi: 10.1073/pnas.1001253107

Zhang, R., Su, H., Ma, X., Xu, X., Liang, L., Ma, G., et al. (2019). MiRNA let-7b promotes the development of hypoxic pulmonary hypertension by targeting ACE2. *Am. J. Physiol. Lung Cell Mol. Physiol.* 316, L547–L557. doi: 10.1152/ajplung.00387.2018

Zhang, R., Wu, Y., Zhao, M., Liu, C., Zhou, L., Shen, S., et al. (2009). Role of HIF-1alpha in the regulation ACE and ACE2 expression in hypoxic human pulmonary artery smooth muscle cells. *Am. J. Physiol. Lung Cell Mol. Physiol.* 297, L631–L640. doi: 10.1152/ajplung.90415.2008

Zhong, J., Basu, R., Guo, D., Chow, F. L., Byrns, S., Schuster, M., et al. (2010). Angiotensin-converting enzyme 2 suppresses pathological hypertrophy, myocardial fibrosis, and cardiac dysfunction. *Circulation* 122, 717–728. doi: 10.1161/CIRCULATIONAHA.110.955369 718 p following 728,

Zhou, J., Li, Y. S., Nguyen, P., Wang, K. C., Weiss, A., Kuo, Y. C., et al. (2013). Regulation of vascular smooth muscle cell turnover by endothelial cell-secreted microRNA-126: role of shear stress. *Circ. Res.* 113, 40–51. doi: 10.1161/CIRCRESAHA.113.280883

Zulli, A., Burrell, L. M., Buxton, B. F., and Hare, D. L. (2008). ACE2 and AT4R are present in diseased human blood vessels. *Eur. J. Histochem.* 52, 39–44. doi: 10.4081/1184

Conflict of Interest: The authors declare that the research was conducted in the absence of any commercial or financial relationships that could be construed as a potential conflict of interest.

Advantages of publishing in Frontiers

OPEN ACCESS
Articles are free to read for greatest visibility and readership

FAST PUBLICATION
Around 90 days from submission to decision

HIGH QUALITY PEER-REVIEW
Rigorous, collaborative, and constructive peer-review

TRANSPARENT PEER-REVIEW
Editors and reviewers acknowledged by name on published articles

Frontiers
Avenue du Tribunal-Fédéral 34
1005 Lausanne | Switzerland

Visit us: www.frontiersin.org
Contact us: frontiersin.org/about/contact

REPRODUCIBILITY OF RESEARCH
Support open data and methods to enhance research reproducibility

DIGITAL PUBLISHING
Articles designed for optimal readership across devices

FOLLOW US
@frontiersin

IMPACT METRICS
Advanced article metrics track visibility across digital media

EXTENSIVE PROMOTION
Marketing and promotion of impactful research

LOOP RESEARCH NETWORK
Our network increases your article's readership